University of Nevada, Reno

Detrital zircon uranium-lead geochronology and hafnium-isotope analyses of passive margin and Roberts Mountains allochthon strata: Interpreting the Early Paleozoic tectonic evolution of western Laurentia

A dissertation submitted in partial fulfillment of the requirements for the degree of Doctor of Philosophy in Geology

By
Gwen M. Linde

Dr. James H. Trexler, Jr./Dissertation Advisor

May, 2016

THE GRADUATE SCHOOL

We recommend that the dissertation
prepared under our supervision by

GWEN MARGARET LINDE

Entitled

Detrital zircon uranium-lead geochronology and hafnium isotope analyses of passive margin and Roberts Mountains allochthon strata: Interpreting the Early Paleozoic tectonic evolution of western Laurentia

be accepted in partial fulfillment of the
requirements for the degree of

DOCTOR OF PHILOSOPHY

James H. Trexler, Jr., Ph.D., Advisor

Patricia H. Cashman, Ph.D., Committee Member

Stacia M. Gordon, Ph.D., Committee Member

Michael Ressel, Ph.D., Committee Member

Paul A. Neill, Ph.D., Graduate School Representative

David W. Zeh, Ph.D., Dean, Graduate School

May, 2016

ABSTRACT

This dissertation investigated Neoproterozoic–Devonian units of the western Laurentian passive margin and Roberts Mountains allochthon (RMA) and determined U-Pb detrital ages and Hf isotope zircon analyses that provide new insights into the early Paleozoic tectonics of western Laurentia. The three chapters investigate several difficult questions and contradictions in the understanding of early Paleozoic tectonism in western Laurentia through analysis of sedimentary units. The provenance, depositional histories, and tectonic evolution of the lower Paleozoic sedimentary strata of north-central Nevada have long been subjects of speculation and debate. Detrital zircon U-Pb geochronology and Hf-isotope analyses indicate the provenance, sedimentary distribution patterns, and tectonic evolution of Upper Neoproterozoic–Cambrian passive margin strata and Ordovician – Devonian strata of the RMA, with a special emphasis on the enigmatic Harmony Formation.

The study reported in Chapter 1 uses detrital zircon U-Pb geochronology to determine whether or not the Upper Neoproterozoic–Lower Cambrian Osgood Mountain Quartzite and the Upper Cambrian–Lower Ordovician Preble Formation in the Osgood Mountains of northern Nevada were units of the western Laurentian passive margin. Within the Osgood Mountain Quartzite, U-Pb age populations of the detrital zircons shift with stratal age. This shift indicates that the zircons were shed in different proportions from the source terranes, which suggests a change in provenance within the Osgood Mountain Quartzite. These changes are consistent across a Great Basin transect of coeval passive margin strata. The change in provenance is due to a shift in sedimentary transport patterns, which was caused by the Late Neoproterozoic-Early Cambrian uplift of the

Transcontinental Arch. This study provided independent corroboration of the existence of the Transcontinental Arch and better precision for the timing at which the Arch uplifted. The study also recorded the impact of the uplifted Arch on continent-wide sediment dispersal patterns—the change in predominant source terranes—and confirmed the Arch as a sediment source for passive-margin strata. Regional coeval changes in detrital zircon U-Pb age patterns provide a correlative tool in unfossiliferous sediments and could be useful in future studies.

Chapter 2 describes how detrital zircon U-Pb geochronology and Hf-isotope analyses were used to determine the provenance, sedimentary transport, and tectonic evolution of RMA strata. Workers have speculated for decades, with little agreement, on the origin, depositional basin(s), and subsequent tectonic transport of the RMA. Zircon grains from six Ordovician to Devonian arenite samples were analyzed for U-Pb ages; approximately one-quarter of these grains were further analyzed for Hf isotope ratios. Five of the studied units have similar U-Pb age poulations and Hf-isotope ratios, while the U-Pb ages and Hf-ratios of the Ordovician lower Vinini Formation are significantly different. Comparison of these data with known analyses of igneous basement rocks and other sedimentary units of Laurentia reveals that the lower Vinini Formation originated in the north-central Laurentian craton. The other five units, as well as Ordovician passive margin sandstones of the western Laurentian margin, had a common source in the Peace River Arch region of western Canada. All of the RMA strata were deposited near the Peace River Arch region and subsequently tectonically transported south along the Laurentian margin, from where they were emplaced onto the craton during the Antler orogeny. This study determined the origin, location of the depositional basin, and

proposed a subsequent tectonic evolution that accounts for origin, deposition, and current location of the RMA strata.

Chapter 3 describes the origin, age, and tectonic development of the Harmony Formation. The Harmony Formation has always been difficult to explain—it is mostly an immature feldspathic arenite, which would argue for minimal transport from origin to deposition. However, its general position as the top thrust plate in the RMA stack argues for deposition oceanward of other more texturally mature RMA strata. The age of the Harmony Formation is equally contentious—published age determinations range from Cambrian to Mississippian. Zircon grains from ten arenite samples were analyzed for U-Pb ages; grains from eight of these samples were further analyzed for Hf-isotope ratios. Seven of the arenite units have similar U-Pb age peaks and Hf isotope ratios, whereas three differ significantly. The data confirmed the subdivision of the Harmony Formation into two petrofacies, quartzose (Harmony A) and feldspathic (Harmony B). Harmony A originated in the central Laurentian craton. Harmony B had a common source in eastern Alberta–western Saskatchewan, north of the source of the Harmony A. All of the Harmony Formation strata were deposited near eastern Alberta in Late Neoproterozoic through Cambrian time and subsequently tectonically interleaved with the Roberts Mountains allochthon strata. The entire package was tectonically transported south along the Laurentian margin. Subsequently, it was emplaced eastward onto the craton during the Late Devonian to Early Mississippian Antler orogeny. This study proposed a reasonable solution to one of the longest enduring and most puzzling conundrums of the western Cordillera—the origin, age, and transport of the Harmony Formation.

These three studies demonstrated the utility of detrital zircon U-Pb geochronology and Hf-isotope analyses in better understanding difficult sedimentary and tectonic problems. The studies also provided new insights into the Early Paleozoic tectonic evolution of western Laurentia.

DEDICATION

I dedicate this dissertation to the glory of the Holy Trinity, Father, Son, and Holy Spirit, who make all such efforts possible.

And Jesus came and said to them, "All authority in heaven and on earth has been given to me. Go therefore and make disciples of all nations, baptizing them in the name of the Father and of the Son and of the Holy Spirit, teaching them to observe all that I have commanded you; and behold, I am with you always, to the close of the age."

Matthew 28:18-20 (Revised Standard Version)

ACKNOWLEDGMENTS

I would first like to acknowledge the essential role that Bill Dickinson played in all of our Roberts Mountains allochthon and Harmony Formation studies. He had thought much about the difficult puzzle of the Harmony Formation over several decades and was always enthusiastic about hearing new ideas and sharing his perspective. Bill was an incomparable mentor and model for all of us and his loss to the entire geoscience community is profound. *Requiem aeternam dona ei, Domine, et requiescat in pace.*

I thank George Gehrels, director of the Arizona LaserChron center, for supporting my work. Without his help and creative funding ideas, I would not have had a research project. I thank Paul Link, Tim Lawton, and Scott Johnston for sharing their data and providing valuable input to my passive margin investigations. I thank the researchers and staff at the Arizona LaserChron center, especially Mark Pecha and Nicole Giesler and volunteer laboratory assistants Dan Sturmer of the University of Nevada, Reno and later Shell Oil Company and UNR graduate students Connor Newman and Kyle Basler-Reeder for critical help in Tucson. I thank Daniel Sturmer and Ross Miller, both graduate students at UNR, for their assistance with field work.

Detrital zircon analyses of the Osgood Mountains Quartzite, the Preble Formation, and some Harmony Formation samples were funded by NSF EAR-0510915 to Pat Cashman. Detrital zircon analyses of the Roberts Mountains allochthon samples and some Harmony Formation samples were funded by under Arizona LaserChron NSF grants EAR-1338583 to Gehrels. The original collecting effort for these RMA and Harmony Formation samples was supported by EAR-9116000 and EAR-9416933.

I also thank the following for supporting my graduate studies: the National Science Foundation Graduate Research fellowship program, the Rocky Mountain Association of Geologists Veterans Memorial Scholarship, the Nevada Petroleum and Geothermal Society, Raytheon Corporation's Student Veterans Scholarship, the Nevada Petroleum and Geothermal Society, the Graduate Student Association of the University of Nevada Reno, the Cordilleran Section of the Geological Society of America, and the U.S. Veterans Administration Post-9/11 GI Bill.

I thank Pat Cashman, always a source of humor, encouragement, structural geology wisdom, and writing expetise par excellence. Pat is always there for her students, and always willing to help anyone who calls upon her. She is a superb model of the dedicated teacher. I thank Jim Trexler, my advisor for both Masters and PhD studies. Jim was always ready to put my work at the top of his stack, whether it was writing letters of recommendations, editing grant proposals, or giving sage advice. He taught me how to be a field geologist, and I cannot imagine a better mentor. I especially thank Jim for supporting my work on detrital zircons and isotope geochemistry—an area totally new to him, yet he was always ready to forge ahead.

TABLE OF CONTENTS

ABSTRACT i

DEDICATION v

ACKNOWLEDGMENTS vi

TABLE OF CONTENTS viii

LIST OF TABLES xii

LIST OF FIGURES xiii

INTRODUCTION 1

References Cited 7

CHAPTER 1 – STRATIGRAPHIC TRENDS IN DETRITAL ZIRCON GEOCHRONOLOGY OF UPPER NEOPROTEROZOIC AND CAMBRIAN STRATA, OSGOOD MOUNTAINS, NEVADA AND ELSEWHERE IN THE CORDILLERAN MIOGEOCLINE: EVIDENCE FOR EARLY CAMBRIAN UPLIFT OF THE TRANSCONTINENTAL ARCH 10

1. Abstract 10

2. Introduction 11

3. Geologic setting 16

4. Methods 20

5. Detrital zircon geochronology results 24

a. Osgood Mountain Quartzite 24

b. Preble Formation 24

6. Discussion 25

a. Osgood Mountain Quartzite 25

b. Preble Formation 26

7. Regional Correlation 26

a. Nevada-Utah Border 26

b. Central Utah 27

c. Northeastern Utah 29

d. Southeastern Utah 29

e. Implications of the regional correlation 30

8. Summary and Conclusions 33

9. References Cited 35

CHAPTER 2 – DETRITAL ZIRCON U-PB GEOCHRONOLOGY AND HF ISOTOPE GEOCHEMISTRY OF THE ROBERTS MOUNTAINS ALLOCHTHON: NEW INSIGHTS INTO THE EARLY PALEOZOIC TECTONICS OF WESTERN NORTH AMERICA 39

1. Abstract 39

2. Introduction 40

3. Geologic setting 44

a. Regional tectonostratigraphic framework 44

b. Roberts Mountains allochthon strata 48

4. Methods 50

a. Uranium-Lead geochronology 52

b. Hafnium isotope analyses 52

5. Results: U-Pb ages and Hf-isotope analyses 54
6. Provenance of the Roberts Mountains allochthon.....55
a. Provenance of the RMA exclusive of the lower Vinini Formation 55
b. Provenance of the lower Vinini Formation 59
7. Discussion: Sedimentological and Paleogeographic implications 62
8. Summary and Conclusions.....66
9. References Cited 68
CHAPTER 3 – DETRITAL ZIRCON GEOCHRONOLOGY AND HF ISOTOPE GEOCHEMISTRY OF THE HARMONY FORMATION OF NEVADA: NEW INSIGHTS INTO PROVENANCE, TRANSPORT, AND AGE.....77
1. Abstract 77
2. Introduction 78
3. Geologic setting.....83
a. Regional tectonostratigraphic framework.....83
b. The Harmony Formation 86
4. Methods.....93
5. Results: U-Pb ages and Hf-isotope analyses 95
6. Discussion: Provenance and age of the Harmony Formation 101
a. Provenance of the Harmony A 101
b. Provenance of the Harmony B 108

c. Age of the Harmony Formation 108

7. Paleogeographic implications 109

8. Conclusions 112

9. References Cited 114

CONCLUSIONS.....126

1. Summary and conclusions.....126

2. Recommendations for future work.....128

3. References Cited 130

APPENDIX A: STATISTICAL ANALYSIS OF OSGOOD MOUNTAIN QUARTZITE SAMPLES 131

APPENDIX B: U-PB GEOCHRONLOGIC ANALYSES OF SELECTED OSGOOD MOUNTAINS QUARTZITE AND PREBLE FORMATION STRATA 132

APPENDIX C: U-PB GEOCHRONLOGIC ANALYSES OF SELECTED ROBERTS MOUNTAINS ALLOCHTHON STRATA 140

APPENDIX D: HAFNIUM ISOTOPE DATA OF SELECTED ROBERTS MOUNTAINS ALLOCHTHON STRATA 155

APPENDIX E: U-PB GEOCHRONLOGIC ANALYSES OF SELECTED HARMONY FORMATION STRATA 160

APPENDIX F: HAFNIUM ISOTOPE DATA OF SELECTED HARMONY FORMATION STRATA 174

APPENDIX REFERENCES CITED 179

LIST OF TABLES

Table 1: Locations and sample numbers of passive margin samples referenced to UTM locations 16

Table 2: Locations of samples analyzed in Roberts Mountains allocthon study referenced to UTM locations 48

Table 3: K-S statistical analysis results for Roberts Mountains allocthon samples 54

Table 4: Locations of samples analyzed in Harmony Formation study referenced to UTM locations 92

Table 5: K-S statistical analysis results for Harmony Formation samples 100

LIST OF FIGURES

Figure 1. Main age provinces in North America that are potential source terranes for the Late Neoproterozoic-Early Cambrian western Laurentian passive margin 12

Figure 2. Location of passive margin study areas in the vicinity of the Osgood Mountains, and location of the study areas within the Great Basin region 15

Figure 3. Stratigraphic column of Osgood Mountain Quartzite and Preble Formation ...18

Figure 4. Normalized probability plots of units sampled in and around the Osgood Mountains 22

Figure 5. Plots of detrital zircon age of each passive margin Neoproperozoic - Cambrian unit organized by locality 23

Figure 6. Stratigraphic columns of the passive margin strata discussed 28

Figure 7. Plots of compilations of passive margin units showing the distribution of detrital zircon ages 31

Figure 8. Locations of the main age provinces in North America that are potential source terranes for western Laurentian Roberts Mountains allocthon strata 41

Figure 9. Map of north-central Nevada, showing Roberts Mountains allocthon sample locations and the traces of the Roberts Mountains and Golconda thrusts 43

Figure 10. Early Devonian "Northwest Passage" between Laurentia, Baltica, and Siberia), with possible origin of Roberts Mountains allocthon strata 44

Figure 11. Tectonostratigraphic diagram of units of the Roberts Mountains allocthon in north-central Nevada mountain ranges, showing locations of detrital zircon samples 46

Figure 12. Normalized probability plots showing U-Pb ages of Roberts Mountains allocthon strata sampled 51

Figure 13. U-Pb ages and Hf isotope data for Roberts Mountains allocthon strata 53

Figure 14. Map of western Canada showing the Cordilleran accreted terranes, the Cordilleran passive margin, the basement provinces of the Canadian Shield, and proposed provenance of Roberts Mountains allocthon strata. 57

Figure 15. U-Pb ages and Hf isotope data of Roberts Mountains allocthon and coeval passive margin strata 58

Figure 16. Normalized probability plot of Roberts Mountains allocthon strata from this study, exclusive of the lower Vinini Formation 59

Figure 17. Compilation plots showing the distribution of detrital zircon ages in upper Neoproterozoic–Cambrian western Laurentian passive margin units 61

Figure 18. U-Pb ages and Hf isotope data for Roberts Mountains allocthon and select Laurentian passive margin strata 63

Figure 19. Paleogeographic maps of Laurentia from Middle Ordovician through Mississippian time, with tectonic evolution of Roberts Mountains allocthon strata 65

Figure 20. Map of north-central Nevada, showing sample locations, extent of the Harmony Formation, and the traces of the Roberts Mountains and Golconda thrusts 79

Figure 21. Contrasting tectonic models proposed to explain the source and transport of the Harmony Formation, shown in Early Devonian time 80

Figure 22. Locations of the main age provinces in North America that are potential source terranes for western Laurentian Harmony Formation strata 82

Figure 23. The Harmony Formation in Little Cottonwood Canyon, Galena Range, Nevada (photos).....87

Figure 24. Tectonostratigraphic diagram of units of the Roberts Mountains allochthon, including the Harmony Formation, in selected north-central Nevada mountain ranges, showing locations of detrital zircon samples.....88

Figure 25. The Devonian Scott Canyon Formation with Harmony Formation clast inclusion, in Galena Canyon, Galena Range, Nevada (photo) 90

Figure 26. Normalized probability plots showing U-Pb ages of Harmony Formation strata sampled 96

Figure 27. U-Pb ages and Hf isotope data for Harmony Formation 98

Figure 28. U-Pb ages and Hf-isotope data for Harmony A samples and selected western Laurentian passive margin strata 99

Figure 29. Map of western Canada showing the Cordilleran accreted terranes, the Cordilleran passive margin, the basement provinces of the Canadian Shield, and proposed provenance of Harmony Formation strata 103

Figure 30. U-Pb ages and Hf isotope data for Harmony B samples and select Laurentian passive margin strata 107

Figure 31. Paleogeographic maps of Laurentia for Early Cambrian through Mississippian time, with tectonic evolution of Harmony Formation strata 111

Detrital zircon uranium-lead geochronology and hafnium-isotope analyses of passive margin and Roberts Mountains allochthon strata:
Interpreting the Early Paleozoic tectonic evolution of western Laurentia

Gwen M. Linde
Ph.D. dissertation

Introduction

The sedimentary units of the Lower Paleozoic passive margin and Roberts Mountains allochthon in north-central Nevada are well studied, but their provenance, depositional histories, and tectonic evolution have long been subjects of speculation and debate (e.g., Schuchert, 1923; Kay, 1951; Roberts et al., 1958; Hotz and Willden, 1964; Burchfiel and Davis, 1972; Speed and Sleep, 1982; Madrid, 1987; Burchfiel et al., 1992; Poole et al., 1992; Gehrels et al., 2000). This dissertation uses detrital zircon uranium-lead geochronology and hafnium-isotope analyses to investigate the origin, sedimentary distribution patterns, and tectonic evolution of the Upper Neoproterozoic – Cambrian passive margin strata and Ordovician – Devonian strata of the Roberts Mountains allochthon, with a special emphasis on the enigmatic Harmony Formation.

Early Paleozoic time along the western Laurentian margin has commonly been interpreted as a quiescent interval (e.g., Poole et al., 1992; Dickinson, 2009, and references cited therein). The final Neoproterozoic rifting that separated the Rodinian supercontinent lasted from ca. 570-520 Ma and was followed by a drift phase and the deposition of passive-margin sediments through mid-Devonian time (Poole et al., 1992; Dickinson, 2009; Yonkee et al., 2014). The quiescent interval came to an end with the Antler orogeny, during which the Roberts Mountains allochthon (RMA) was emplaced

onto the western Laurentian margin (Dickinson, 2006). The RMA is an internally disrupted package of Cambrian – Devonian oceanic sediments, primarily composed of chert, argillite, quartzose turbidites, and some pillow basalts and volcanogenic debris flows (Doebrich, 1994; Dickinson, 2006; Dickinson, 2009).

Chapter 1 tests the hypothesis that the uplift of the Transcontinental Arch can be discerned from changes in provenance of western Laurentian passive margin strata, which in turn reflect changing drainage patterns that resulted from the uplift of the arch. Sedimentary strata of the Lower Paleozoic passive margin were investigated; these strata are mostly quartzite, with some siltstone, argillite, and phyllite and carbonate intervals (e.g., Stewart, 1991; Poole et al., 1992). These units have been correlated across a broad region of western North America (e.g., Poole et al., 1992). Detrital zircon U-Pb geochronology of the Upper Neoproterozoic – Lower Cambrian Osgood Mountain Quartzite and the Upper Cambrian – Lower Ordovician Preble Formation in the Osgood Mountains of northern Nevada records a provenance change within the Osgood Mountain Quartzite. Detrital zircons from the samples of the Osgood Mountain Quartzite collected lower in the stratigraphic section are predominantly Mesoproterozoic. Detrital zircons from the samples collected higher in the stratigraphic section and all of the Preble Formation samples are predominantly Upper Mesoproterozoic – Paleoproterozoic. Comparison of these data with previous work (Lawton et al., 2010; Gehrels and Pecha, 2014; Yonkee et al., 2014) reveals that the same change in U-Pb age populations and provenance occurred in correlative strata throughout an east–west transect of the Great Basin. This regional shift in provenance records the uplift of the Transcontinental Arch by Early Cambrian time. The uplifted arch forced a change in sedimentation and

drainage patterns, restricting the transport of sediment from the eastern Laurentian to western Laurentia craton. The uplift of the arch also exposed basement rocks and provided new sources for western Laurentian passive-margin sediments.

Sedimentary units of the Roberts Mountains allochthon were investigated to determine the provenance, sedimentary transport, and tectonic history of the strata (Chapter 2). The RMA consists of internally deformed Cambrian through Devonian rocks that structurally overlie coeval passive margin strata in northeastern and north-central Nevada (Schuchert, 1923; Kay, 1951; Roberts et al., 1958; Madrid, 1987; Burchfiel et al., 1992). RMA rocks include chert, argillite, arenite, quartzite, limestone, and mafic volcanic rocks. The RMA is often thought to have been deposited in an ocean basin outboard of coeval passive-margin strata in western Laurentia and to have been tectonically emplaced onto the passive margin during the Late Devonian to Early Mississippian Antler orogeny (e.g., Roberts et al., 1958; Burchfiel and Davis, 1972; Madrid, 1987).

Zircon grains from six Ordovician to Devonian arenite samples were analyzed for U-Pb ages; these grains were further analyzed for Hf-isotope ratios. Five of the units sampled have similar U-Pb age peaks and Hf-isotope ratios, whereas the data from the Ordovician lower Vinini Formation are significantly different. Comparison of these data with previous U-Pb and Hf analyses of igneous basement rocks and other coeval sedimentary units reveals that the lower Vinini Formation originated in the north-central Laurentian craton (Bickford et al., 1986; Hoffman, 1989; Ross, 1991; Anderson and Morrison, 1992; Bickford and Anderson, 1993; Van Schmus et al., 1993; Lund et al., 2010; Todt and Link, 2013). The other five units sampled, as well as Ordovician passive margin sandstones of the western Laurentian margin, have detrital-zircon ages similar to

the timing of magmatic activity and terrane accretion in the Peace River Arch region of western Canada (Hoffman, 1989; Ross, 1991; Villeneuve et al., 1993). All of the RMA strata were likely deposited near the Peace River Arch region, and subsequently tectonically transported south along the western Laurentian margin to where they were emplaced onto the craton during the Antler orogeny.

Chapter 3 focuses on a similar study but focused on the Harmony Formation (Chapter 3). The Harmony Formation is primarily a texturally immature feldspathic arenite. It has been interpreted as a turbidite deposit (Roberts, 1964; Suczek, 1979) and is often interpreted as a part of the RMA (Hotz and Willden, 1964; Suczek, 1979; Madrid, 1987). The age of the Harmony Formation has long been controversial. When first mapped, the unit was interpreted as no younger than Mississippian (Ferguson et al., 1951). The Harmony Formation was later interpreted as Cambrian, based on trilobite fauna (Hotz and Willden, 1964). Jones (1997a; 1997b) interpreted the Harmony Formation as Devonian, based on a single conodont.

Zircon grains from ten arenite samples were analyzed for U-Pb ages and Hf-isotope ratios. Seven of the arenite units sampled have similar U-Pb age peaks and Hf-isotope ratios, while the remaining three samples differ significantly. The data confirm the previous subdivision of the Harmony Formation into two petrofacies, quartzose (Harmony A) and feldspathic (Harmony B) (Gehrels et al., 2000). Comparison of these data with U-Pb and Hf analyses of igneous basement rocks and other sedimentary units reveals that Harmony A samples originated in the central Laurentian craton (Gehrels and Pecha, 2014; Yonkee et al., 2014; Linde et al., 2014). In comparison, Harmony B had a common source in eastern Alberta – western Saskatchewan, north of the source of the

Harmony A (Collerson et al., 1988; Villenueve et al., 1993; Gehrels and Ross, 1998; Gehrels and Pecha, 2014; Peterson et al., 2015). Harmony Formation strata were transported from sources in central Laurentia or eastern Alberta – western Saskatchewan, deposited near eastern Alberta in Late Neoproterozoic through Cambrian time, and subsequently tectonically interleaved with the RMA strata. The entire package was tectonically transported south along the Laurentian margin and was subsequently emplaced eastward onto the craton during the Late Devonian to Early Mississippian Antler orogeny.

These three studies interpreted the provenance of passive margin and Roberts Mountains allochthon strata and thus provided new insights into the Early Paleozoic sedimentary dispersal patterns and tectonic evolution of western Laurentia. These studies also demonstrated the utility of detrital zircon U-Pb geochronology and Hf-isotope analyses to better understand difficult sedimentary and tectonic problems concerning the tectonic evolution of western Laurentia.

References Cited

Amato, J.M., and Mack, G.H., 2012, Detrital zircon geochronology from the Cambrian-Ordovician Bliss Sandstone, New Mexico: Evidence for contrasting Grenville-age and Cambrian sources on opposite sides of the Transcontinental Arch: Geological Society of America Bulletin, v. 124, p. 1826-1840.

Bahlburg, H., Vervoort, J.D., DuFrane, S.A., Carlotto, V., Reimann, C., and Cardenas, J., 2011, The U–Pb and Hf isotope evidence of detrital zircons of the Ordovician Ollantaytambo Formation, southern Peru, and the Ordovician provenance and paleogeography of southern Peru and northern Bolivia: Journal of South American Earth Sciences, v. 32, p. 196–209.

Burchfiel, B.C., Cowan, D.S., and Davis, G.A., 1992, Tectonic overview of the Cordilleran orogeny in the western United States, *in* Burchfiel, B.C., Lipman, P.W., and Zoback, M.L., eds., The Cordilleran Orogen: Conterminous U.S.: Boulder, Colorado, Geological Society of America, The Geology of North America, v. G-3, p. 407–480.

Colpron, M., and Nelson, J., 2009, A Palaeozoic Northwest Passage: Incursion of Caledonian, Baltican and Siberian terranes into eastern Panthalassa, and the early evolution of the North American Cordillera, *in* Cawood, P.A. and Kroner, A., eds., Earth Accretionary Systems in Space and Time: Geological Society of London Special Publication 318, p. 273–307.

Dickinson, W.R., 2006, Geotectonic evolution of the Great Basin: Geosphere, v. 2, p. 353-368.

Dickinson, W.R., 2009, Anatomy and global context of the North American Cordillera: Geological Society of America Memoirs, v. 204, p. 1-29.

Doebrich, J.L., 1994, Preliminary geologic map of the Galena Canyon quadrangle, Lander county, Nevada: U.S. Geological Survey Open File Report 94-664, scale 1:24,000: Boulder, CO, U.S. Geological Survey.

Fedo, C.M., Sircombe, K., and Rainbird, R., 2003, Detrital zircon analysis of the sedimentary record, *in* Hanchar J.M., and Hoskin, P.W.O., eds., Zircon: Reviews in Mineralogy and Geochemistry, v. 53, p. 277–303.

Ferguson, H.G., Roberts, R.J., and Muller, S.W., 1951, Geology of the Winnemucca Quadrangle, Nevada: U.S. Geological Survey Geologic Quadrangle Map GQ-11, scale 1:125,000: Boulder, CO, U.S. Geological Survey.

Gehrels, G.E., 2000, Introduction to detrital zircon studies of Paleozoic and Triassic strata in western Nevada and northern California, *in* Soreghan, M.J., and Gehrels, G.E.,

eds., Paleozoic and Triassic Paleogeography and Tectonics of Western Nevada and Northern California: Geological Society of America Special Paper 347, p.1–17.

Gehrels, G.E., 2012, Detrital zircon U-Pb geochronology: Current methods and new opportunities, *in* Busby, C., and Azor, A., eds., Recent Advances in Tectonics of Sedimentary Basins: Hoboken, New Jersey, Blackwell Publishing, p. 47-62.

Gehrels, G.E., 2014, Detrital zircon U-Pb geochronology applied to tectonics: Annual Review of Earth and Planetary Sciences, v. 42, p. 127-149.

Gehrels, G.E., and Pecha, M., 2014, Detrital zircon U-Pb geochronology and Hf isotope geochemistry of Paleozoic and Triassic passive margin strata of western North America: Geosphere, v. 10, p. 49-65.

Gehrels, G.E., Dickinson, W.R., Riley, B.C.D., Finney, S.C., Smith, M.T., 2000, Detrital zircon geochronology of the Roberts Mountains allochthon, Nevada, *in* Gehrels, G.E., and Soreghan, M.J., eds., Paleozoic and Triassic Paleogeography and Tectonics of Western Nevada and Northern California: Boulder, Colorado, Geological Society of America, Special Paper 347, p. 19–42.

Guynn, J., and Gehrels, G.E., 2006, Comparison of detrital zircon age distribution using the K-S test: online manual published by the University of Arizona LaserChron Center.

Hotz, P.F., and Willden, R., 1964, Geology and mineral deposits of the Osgood Mountains quadrangle: U.S. Geological Survey Professional Paper 431, 128 p.

Jones, A.E., 1997a, Geologic map of the Delvada Spring quadrangle Nevada: Nevada Bureau of Mines and Geology Field Studies Map FS-13, scale 1:24,000, Reno, NV: Nevada Bureau of Mines and Geology.

Jones, A.E., 1997b, Geologic map of the Hot Springs Peak quadrangle and the southeastern part of the Little Poverty quadrangle, Nevada: Nevada Bureau of Mines and Geology Field Studies Map FS-14, scale 1:24,000, Reno, NV: Nevada Bureau of Mines and Geology.

Kay, M., 1951, North American geosynclines: Geological Society of America Memoir 48.

Ketner, K.B, Crafford, A.E.J., Harris, A.G., Repetski, J.E., and Wardlaw, B.R., 2005, Late Devonian to Mississippian arkosic rock derived from a granitic terrane in northwestern Nevada adds a new dimension to the Antler orogeny, *in* Rhoden, H.N., Steininger, R.C., and Vikre, P.G., eds., Symposium 2005: Window to the World: Geological Society of Nevada Symposium Proceedings, v. 1, p. 135-145.

Lawton, T.F., Hunt, G.J., and Gehrels, G.E., 2010, Detrital zircon record of thrust belt unroofing in Lower Cretaceous synorogenic conglomerates, central Utah: Geology, v. 38, p. 463-466.

Madrid, R.J., 1987, Stratigraphy of the Roberts Mountains allochthon in north-central Nevada [PhD dissertation]: Stanford, California, Stanford University, 336 p.

Poole, F.G., Stewart, J.H., Palmer, A.R., Sandberg, C.A., Madrid, R.A., Ross, R.J., Jr., Hintze, L.F., Miller, M.M., and Wrucke, C.T., 1992, Latest Precambrian to latest Devonian time; development of a continental margin: *in* Burchfiel, B.C., Lipman, P.W., and Zoback, M.L., eds., The Cordilleran Orogen: Conterminous U.S.: Boulder, CO, Geological Society of America, the Geology of North America, v. G-3.

Roberts, R.J., 1964, Stratigraphy and structure of the Antler Peak quadrangle, Humboldt and Lander counties Nevada: U.S. Geological Survey Professional Paper 459A, 93 p.

Roberts, R.J., Hotz, P.E., Gilluly, J., and Ferguson, H.G., 1958, Paleozoic rocks of north-central Nevada: American Association of Petroleum Geologists Bulletin, v. 42. p. 2813-2857.

Schuchert, C., 1923, Sites and natures of the North American geosynclines: Bulletin of the Geological Society of America, v. 34, p. 151-230.

Speed, R.C., and Sleep, N.H., 1982, Antler orogeny and foreland basin: A model: Geological Society of America Bulletin, v. 93, p. 815-828.

Stewart, J.H., 1972, Initial deposits in the Cordilleran geosyncline: Evidence of a Late Precambrian (<850 m.y.) continental separation. Geological Society of America Bulletin, v. 83, p. 1345-1360.

Stewart, J.H., 1991, Latest Proterozoic and Cambrian rocks of the western United States—An overview, in Cooper, J.D., and Stevens, C.H., eds., 1991, Paleozoic paleogeography of the western United States—II: Pacific Section Society of Economic Paleontologists and Mineralogists, v. 67, p. 13-38.

Suczek, C.A., 1977, Tectonic relations of the Harmony Formation, northern Nevada [PhD dissertation]: Stanford University, 96 p.

Villeneuve, M.E., Ross, G.M., Theriault, R.J., Miles, W., Parrish, R.R., and Broome, J., 1993, Tectonic subdivision and U-Pb geochronology of the crystalline basement of the Alberta basin, western Canada: Geological Survey of Canada, Bulletin 447, 86 p.

Wright, J., and Wyld, S., 2006, Gondwana, Iapetan, Cordilleran interactions: A geodynamic model for the Paleozoic tectonic evolution of the North American Cordillera, *in* Haggart, J., Enkin, R., and Monger, J., eds., Paleogeography of the North American Cordillera: Evidence For and Against Large-Scale Displacements: Geological Association of Canada Special Paper 46, p. 377–408.

Yonkee, W.A., Dehler, C.D., Link, P.K., Balgord, E.A., Keeley, J.A., Hayes, D.S., Wells, M.L., Fanning, C.M., Johnston, S.M., 2014, Tectono-stratigraphic framework of Neoproterozoic to Cambrian strata, west-central U.S.: Protracted rifting, glaciation, and evolution of the North American Cordilleran margin, Earth Science Reviews, v.136, p. 59-95.

Chapter 1

Stratigraphic trends in detrital zircon geochronology of Upper Neoproterozoic and Cambrian strata, Osgood Mountains, Nevada and elsewhere in the Cordilleran miogeocline: Evidence for Early Cambrian uplift of the Transcontinental Arch

This chapter was published: Linde, G.M., Cashman, P.H., Trexler, J.H., Jr., and Dickinson, W.R., 2014, Stratigraphic trends in detrital zircon geochronology of Upper Neoproterozoic and Cambrian strata, Osgood Mountains, Nevada and elsewhere in the Cordilleran miogeocline: Evidence for Early Cambrian uplift of the Transcontinental Arch: Geosphere, v. 10, p. 1-9.

1. Abstract

U-Pb detrital zircon geochronology provides insight into the provenance of the Upper Neoproterozoic-Lower Cambrian Osgood Mountain Quartzite and the Upper Cambrian – Lower Ordovician Preble Formation in the Osgood Mountains of northern Nevada. A total of 535 detrital zircon grains from six samples of quartz arenite were analyzed by laser-ablation-multicollector-inductively coupled plasma-mass spectrometry (LA-MC-ICP-MS). The detrital zircon age data of these Neoproterozoic-Lower Paleozoic passive margin units record a provenance change within the Osgood Mountain Quartzite. Comparison of these data with the work of others reveals that this change in provenance occurred in correlative strata throughout an East-West transect of the Great Basin. From latest Neoproterozoic through earliest Cambrian time, most grains were shed from the

1.0-1.2 Ga Grenville orogen. After that time, drainage patterns changed and most grains were derived from the 1.6-1.8 Ga Yavapai and Mazatzal provinces; very few grains from the Grenville orogen were found in the younger strata. We suggest that this shift records the uplift, in Early Cambrian time, of the Transcontinental Arch. Our data also support our interpretation that the Osgood Mountain Quartzite and the Preble Formation are correlative to other contemporaneous passive margin strata in western Laurentia.

2. Introduction

The Transcontinental Arch, a region of uplift that extends from the southwestern U.S. to south-central Ontario, Canada (Fig. 1), is a fundamental feature of the Lower Paleozoic Laurentian craton. It was first recognized from broad structures and Phanerozoic sedimentation patterns in the mid-continent (Fig. 1) (Keith, 1928). Sloss (1963; 1988) noted the deposition of the Middle and lowermost Upper Cambrian Sauk II sequence onlapping from the craton margin onto the Transcontinental Arch (Fig. 1). Carlson (1999) proposed, instead of a discrete arch, a platform—a discontinuous zone with highs and lows and flanking basins that give the appearance of an arch (Fig. 1).

In recent U-Pb detrital zircon geochronology studies, researchers have proposed the Transcontinental Arch as a barrier to sediment delivery from the central Laurentian craton to its western margin in early Paleozoic time (Amato and Mack, 2012; Gehrels and Pecha, 2014; Yonkee et al., 2014). Amato and Mack (2012) document evidence from the Bliss Sandstone for the existence of the Transcontinental Arch by at least the Late Cambrian. They explain the differences in detrital zircon populations between the Tapeats Sandstone west of the arch and the Cambrian sandstones east of the arch, with

the uplift of the arch possibly as early as Early Cambrian time (Amato and Mack, 2012). Gehrels and Pecha (2014) estimated the uplift of the arch by Early Cambrian time. Others note the possibility of Early Cambrian uplift of the arch as the cause of the differences in detrital zircon age peaks and groups in passive margin strata in Utah (Yonkee et al., 2014).

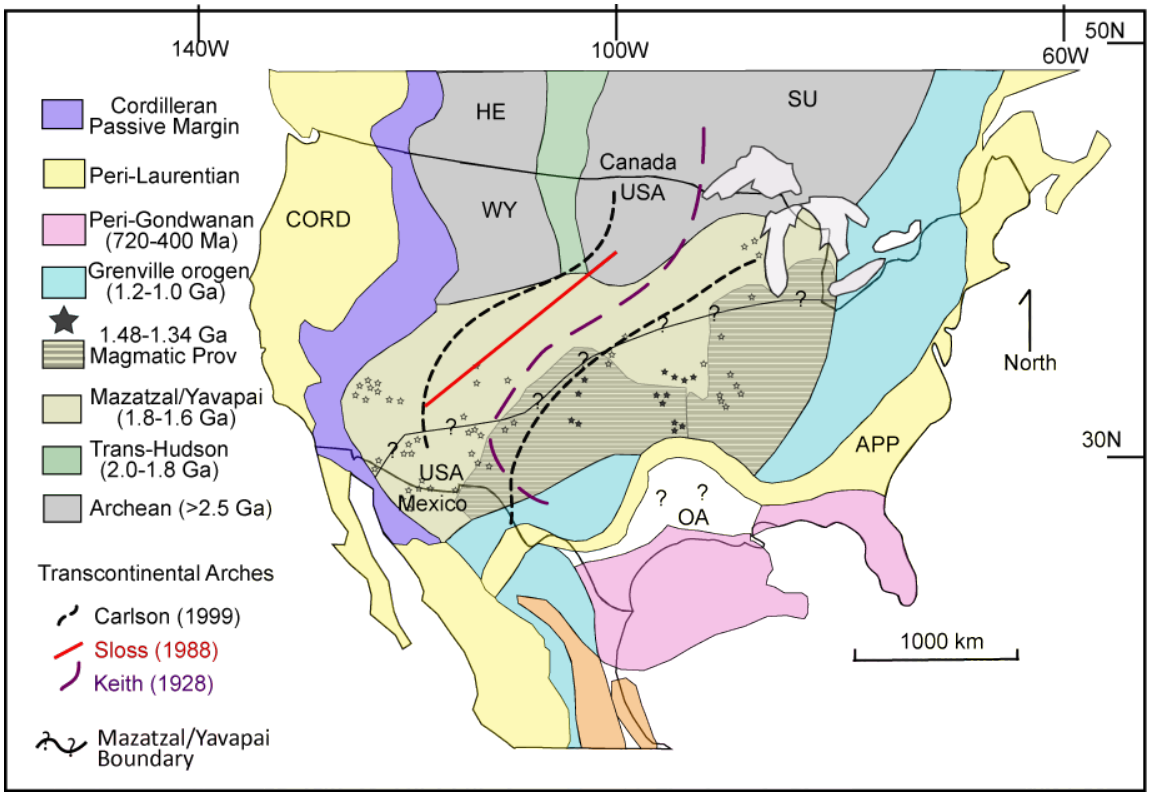

Figure 1: Location of the main age provinces in North America that are potential source terranes for the Late Neoproterozoic-Early Cambrian western Laurentian passive margin. Hypothesized Transcontinental Arches are superimposed (Keith, 1928; Sloss, 1988; Carlson, 1999). WY: Wyoming province; HE: Hearn province; SU: Superior province; CORD: Cordilleran; APP: Appalachian; OA: Ouachita-Marathon. Figure is after Gehrels et al. (2011) and adapted from Anderson and Morrison (1992), Bickford et al. (1986), Hoffman (1989), Burchfiel et al. (1992), Bickford and Anderson (1993), Van Schmus et al. (1993), Dickinson and Lawton (2001), and Dickinson and Gehrels (2009).

Upper Neoproterozoic – Lower Cambrian siliciclastic rocks on the western Laurentian passive margin record sedimentation that initiated after rifting and continental separation (e.g., Stewart, 1972; Poole et al., 1992). These passive margin rocks were deposited on a discontinuously exposed succession of diamictite and volcanic strata that reflect initial rifting (e.g., Poole et al., 1992; Yonkee et al., 2014, and references cited therein). These strata are mostly quartzite, with some siltstone, argillite, and phyllite; carbonate intervals are present in some locations (e.g., Stewart, 1991; Poole et al., 1992). These units have been correlated across a broad region of western North America (e.g., Poole et al., 1992).

Previous detrital zircon studies of Upper Neoproterozoic – Lower Paleozoic passive margin strata record similar changes in detrital zircon age peaks and groups and therefore possibly similar changes in provenance. Zircon ages in Upper Neoproterozoic – Lower Cambrian strata in Utah (Lawton et al., 2010; Gehrels and Pecha, 2014; Yonkee et al., 2014), Idaho (Yonkee et al., 2014), and Nevada (Gehrels and Pecha, 2014; Yonkee et al., 2014) change from predominantly Mesoproterozoic in the older strata to Upper Mesoproterozoic – Paleoproterozoic in the younger strata.

The only previous detrital zircon study of the Osgood Mountain Quartzite was Gehrels and Dickinson (1995); they sampled from the upper part of the formation. The Preble Formation has never been the subject of a published detrital zircon study.

We dated detrital zircons from three localities of the Upper Neoproterozoic – Lower Cambrian Osgood Mountain Quartzite and three localities of the Upper Cambrian – Lower Ordovician Preble Formation in the Osgood Mountains and near Edna Mountain, north-central Nevada (Fig. 2b and Table 1). We show that the detrital zircon ages shift within the Osgood Mountain Quartzite; detrital zircons from the older samples are

predominantly Mesoproterozoic, while detrital zircons from the younger sample, and all of the Preble Formation samples, are predominantly Upper Mesoproterozoic – Paleoproterozoic. Coeval passive margin strata in other studies throughout the Great Basin (e.g., Lawton et al., 2010; Gehrels and Pecha, 2014; Yonkee et al., 2014) show the same shift in ages. This suggests that a change in provenance in these passive margin strata is widely recorded in this region of western Laurentia.

In this paper, we present new U-Pb zircon ages from the Osgood Mountain Quartzite and the Preble Formation. The dates were obtained using laser-ablation-multicollector-inductively coupled plasma-mass spectrometry (LA-MC-ICP-MS). We compare these new data with the detrital zircon ages of coeval passive margin strata throughout the Great Basin to evaluate provenance and sediment transport patterns, and the possibility that these patterns were altered by the uplift of the Transcontinental Arch.

Several unsolved problems are addressed in this study. (1) What is the provenance of the Osgood Mountain Quartzite and the Preble Formation? (2) Are the Osgood Mountain Quartzite and Preble Formation passive margin units, as others have interpreted? (3) Within the Osgood Mountain Quartzite, there is a significant change in detrital zircon grain ages. Are there similar patterns of detrital zircon grain ages varying with time among other coeval passive margin units? (4) If a consistent stratigraphic pattern of detrital zircon ages exists in all Neoproterozoic-Cambrian sections, what caused a widespread change in detrital zircon ages with time in these units?

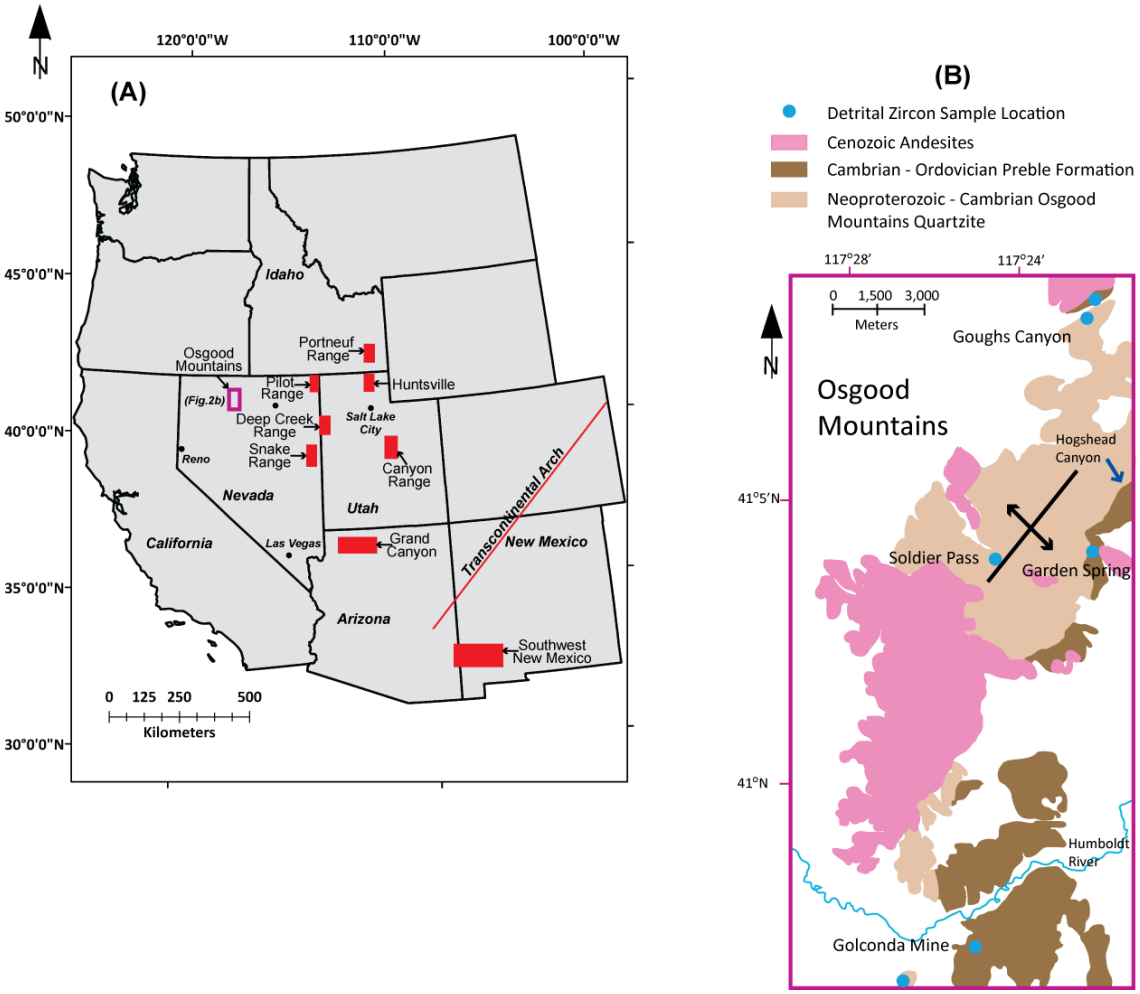

Figure 2. (a) Location of study areas in the vicinity of the Osgood Mountains, and location of the study areas within the Great Basin region. Transcontinental Arch is after Sloss (1988). (b) Geologic map of the Osgood Mountains. The six sample locations are shown. Broad northeast-trending anticline of the range is shown with location of Soldier Pass sample in the core of the anticline and Preble Formation on both flanks of the anticline. Hogshead Canyon, location of unit thickness estimate of the Preble Formation, is shown. Northern part of the map is after Hotz and Willden, 1964. Southern part is after Erickson and Marsh, 1974.

Cambrian - Ordovician Preble Formation

	Sample	Easting	Northing
Golconda Mine	GOL-02-CP	0465271	4533874
Garden Spring	GS-01-CP	0470302	4548660
Gough's Canyon	GC-01-CP	0468513	4554509

Neoproterozoic - Cambrian Osgood Mountains Quartzite

	Sample	Easting	Northing
Golconda Mine	GOL-01-COM	0462354	4531791
Goughs Canyon	GC-03-COM	0468951	4554410
Soldier Pass	SP-01-COM	0463750	4548029

NAD 83 UTM 11N

Table 1. Locations and sample numbers of samples referenced to UTM locations.

3. Geologic Setting

The North American craton contains several Proterozoic and Archean age provinces, thus providing geographically distinguishable crustal provinces that are source terranes for the Upper Proterozoic and Lower Paleozoic continental margin sedimentary section (e.g., Gehrels et al., 2011 and references cited therein) (Fig. 1). The Yavapai/Mazatzal Province (1.8-1.6 Ga) forms the core of the craton in the U.S. (Fig.1). It is bounded on the northwest by the Trans-Hudson orogenic terrane (2.0-1.8 Ga) and Archean rocks (> 2.5 Ga) of the Wyoming and Superior Provinces (Fig. 1). It is bounded on the east and southeast by the terranes of the Grenville orogen (1.2-1.0 Ga) (Fig. 1).

The 1.2-1.0 Ga Grenville orogen of southern and eastern North America (Fig. 1) was the dominant sediment source for western Laurentia throughout the Neoproterozoic (Rainbird et al., 1997; 2012), including the Upper Proterozoic passive margin section from the northwest U.S. to Sonora, Mexico (e.g., Lawton et al., 2010; Gehrels and Pecha, 2014; Yonkee et al., 2014). In contrast, the 1.8-1.6 Ga Yavapai-Mazatzal and 1.48-1.34 Ga mid-continent granite rhyolite provinces within the North America craton (Fig. 1) were the dominant sediment sources higher in the passive margin section (e.g., Lawton et al., 2010; Gehrels and Pecha, 2014, Yonkee et al., 2014).

In northern Nevada, the Osgood Mountain Quartzite and Preble Formation have been interpreted as passive margin strata. The Osgood Mountain Quartzite and Preble Formation have an interesting position and tectonic and metamorphic history. They are far to the west of most other passive margin units and are overthrust by both the Roberts Mountains allochthon and the Golconda allochthon (Burchfiel et al., 1992; Poole et al., 1992). The Preble Formation is metamorphosed to greenschist facies, and has refolded folds (Cashman et al., 2011). The Preble Formation has been interpreted as being in conformable stratigraphic succession with the Osgood Mountain Quartzite (Fig. 3), based on map relationships and compositional similarity of an upper member of the Osgood Mountain Quartzite to the Preble Formation (Hotz and Willden, 1964).

Structurally, the Osgood Mountains comprise a large, northeast-trending anticline with a sub-horizontal axis (Fig. 2b). The Preble Formation is exposed only on the flanks of the anticline (Fig. 2b). Late Paleozoic rocks are thrust over the anticline in the northern and western parts of the range, and the southern extent of the Osgood Mountains is overlain by Cenozoic andesite flows (Fig. 2b) (Hotz and Willden, 1964). The Osgood

Mountain Quartzite and Preble Formation are primarily exposed in the central and southern portions of the range (Fig. 2b).

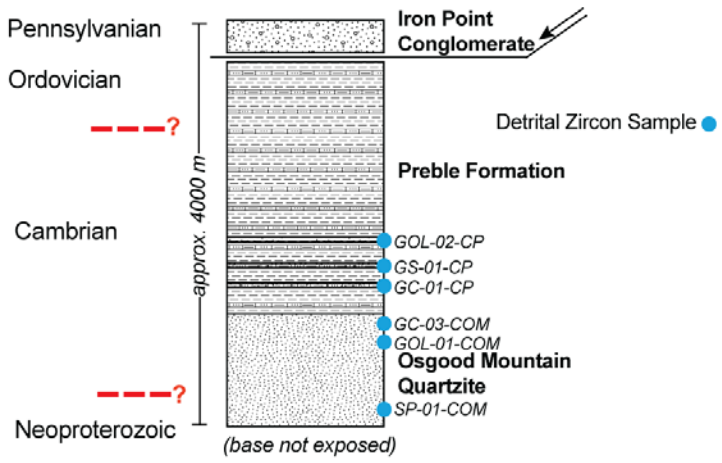

Figure 3: Stratigraphic column of the Osgood Mountain Quartzite and Preble Formation. Subjacent strata are not shown. Red dashed lines are approximate system boundaries. The fault is the Iron Point fault, a mid-Pennsylvanian normal fault. Structural relationships are after Cashman et al. (2011); unit ages are after Hotz and Willden (1964) and Madden-McGuire (1991).

The Osgood Mountain Quartzite consists mostly of fine- to medium-grained quartz arenite, with some silty and shaly beds (Fig. 3). The formation crops out in the Osgood Mountains in an outcrop belt 14 km long, from the northwestern Osgood Mountains near Goughs Canyon, to the Golconda Mine area in the northwestern part of Edna Mountain (Fig. 2b). Goughs Canyon and the Golconda Mine, where two samples were taken, are on opposite flanks of an anticline and are relatively high in the stratigraphic section (Figs. 2b and 3). Soldier Pass, where a third sample was collected, is closer to the core of the anticline and is thus lower in the stratigraphic section (Figs. 2b and 3). The base of the

Osgood Mountain Quartzite is not exposed; the thickness has been estimated at more than 1524 m (5000 ft) (Hotz and Willden, 1964). The upper part of the Osgood Mountain Quartzite is the Twin Canyon Member, which crops out only on the east side of the range, and consists of more silty and shaly material than the rest of the formation. This member has been interpreted as a transition between the Osgood Mountain Quartzite and the overlying Preble Formation (Hotz and Willden, 1964). The Osgood Mountain Quartzite is barren of fossils (Hotz and Willden, 1964). Based on the age of the overlying Preble Formation, the Osgood Mountain Quartzite is Late Neoproterozoic to Early Cambrian in age (Madden-McGuire, 1991).

The Preble Formation consists of phyllite and shale, interbedded limestone, and quartz arenite. The Preble Formation crops out over an area approximately 50 km in length, from the northwestern Osgood Mountain near Goughs Canyon, south to the Sonoma Range. The thickness of the Preble Formation has been estimated at approximately 2350 m (7700 ft) (Ferguson et al., 1952) based upon the estimated thicknesses of the subunits, though the same workers suggested that the structural thickness may exceed 4572m (15,000 ft), due to isoclinal folding. The thickness was estimated at approximately 1524 m (5000 ft) near Hogshead Canyon (Fig. 2b), where both upper and lower contacts are faults (Hotz and Willden, 1964). However, these authors noted that tight folding and lack of distinctive bedding precluded them from making detailed studies of the thickness and stratigraphy of the unit. Based on middle Early Cambrian trilobite fauna collected in the lower part of the Preble Formation, the base of the unit is of Early Cambrian age (Madden-McGuire, 1991). The fossils occur approximately 400 m above the upper contact of the pure quartz arenite Osgood Mountain Quartzite, consistent with a Late

Neoproterozoic age for most of the Osgood Mountain Quartzite (Madden-McGuire, 1991). Graptolites near the youngest subunit of the Preble Formation indicate that the top of the unit is Early Ordovician in age (Madden-McGuire, 1991).

4. Methods

Quartz arenite samples were collected from six locations and stratigraphic intervals (Figs. 2b and 3 and Table 1). Three samples were analyzed from the Upper Neoproterozoic – Lower Cambrian Osgood Mountain Quartzite and three samples were analyzed from the Lower Cambrian – Lower Ordovician Preble Formation.

Zircon grains were separated and analyzed at the University of Arizona LaserChron facility using standard techniques described by Gehrels (2000, 2011), Gehrels et al. (2006, 2008) and Johnston et al. (2009), to yield a best age distribution reflective of the true distribution of detrital zircon ages in each sample. A split of zircons representative of the final sample yield was mounted in a 1" (2.54 cm) diameter epoxy plug, with the laboratory's SL (Sri Lanka) zircon standard (563.5 ±3.2 Ma, Gehrels et al., 2008). Approximately 100 randomly selected grains were analyzed for each sample. Analyses were conducted by LA-MC-ICP-MS using the New Wave UP193HE laser connected to the Nu Plasma high resolution inductively coupled plasma-mass spectrometry (NU HR ICP-MS).

Analytical results are displayed graphically on normalized probability plots (Figs. 4 and 5). On our plots, we did not include analyses with greater than 10% uncertainty in age. We also discarded analyses with greater than 30% discordance (70% concordance) and greater than 5% reverse discordance (105% concordance). Normalized probability

plots (Figs. 4 and 5) allow visual comparison between zircon populations and display the data from this study and the research of others. The normalized probability plots are generated by summing the ages and uncertainties and normalizing the graphs so that all curves on the same plot have the same area under the curve.

We compared detrital zircon age distributions both visually and statistically. Our initial appraisal was visual comparison of the probability plots. We also compared many age distributions using the Kolmogorov-Smirnov (K-S) statistic (Guynn and Gehrels, 2006). The K-S statistic estimates the probability (P value) that two sample populations could have been derived from the same parent population. P>.05 indicates >95% probability that two U-Pb distributions are not statistically different and could have been derived from the same parent (P=1.0 reflecting effective statistical identity). The K-S statistic is sensitive to proportions of ages present, and a low P value may indicate that the proportions of ages are different, even though the ages are similar (Gehrels, 2012).

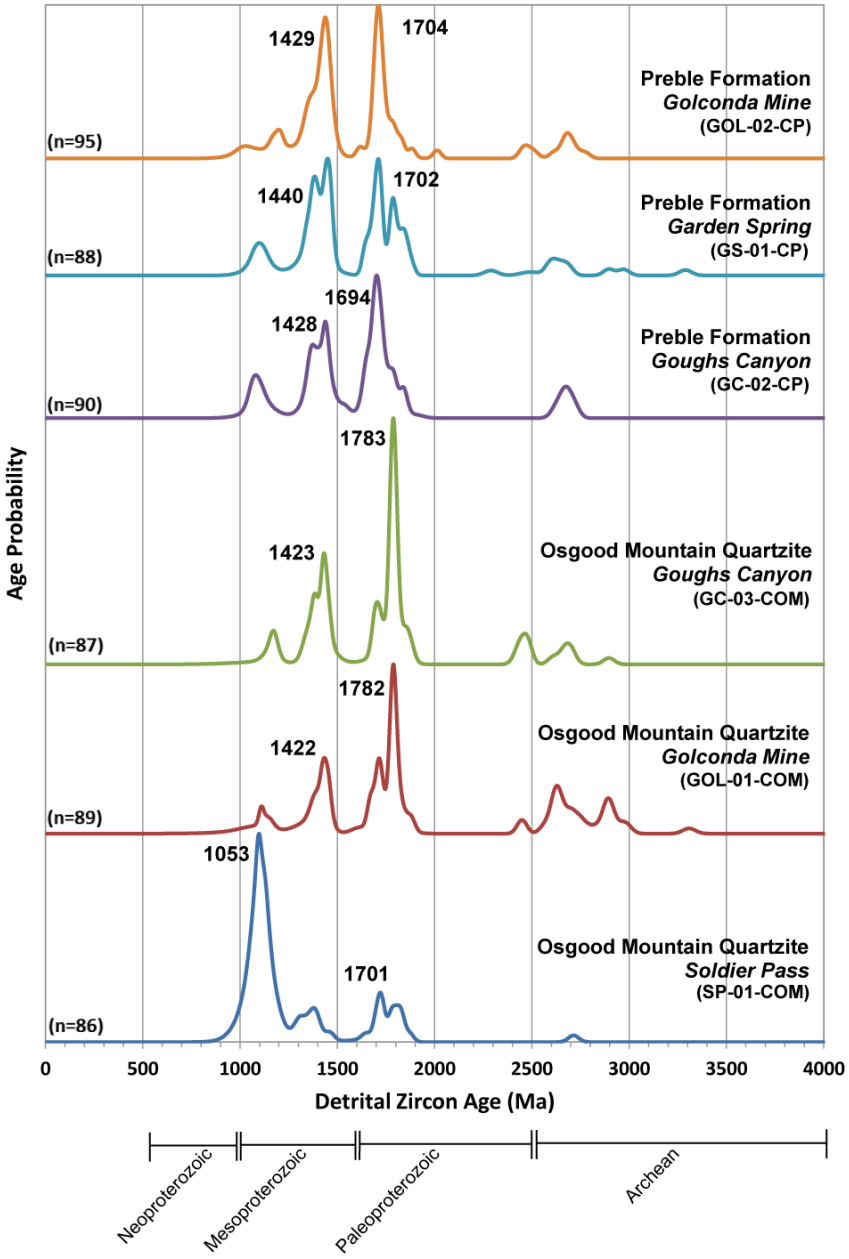

Figure 4: Normalized probability plots of units sampled in and around the Osgood Mountains. The curves contain all analyses for each unit and are normalized such that the area is the same under each curve. Within each location the older units are on the bottom. Horizontal axis is age in millions of years. Number of concordant detrital zircons in each sample is shown in parentheses.

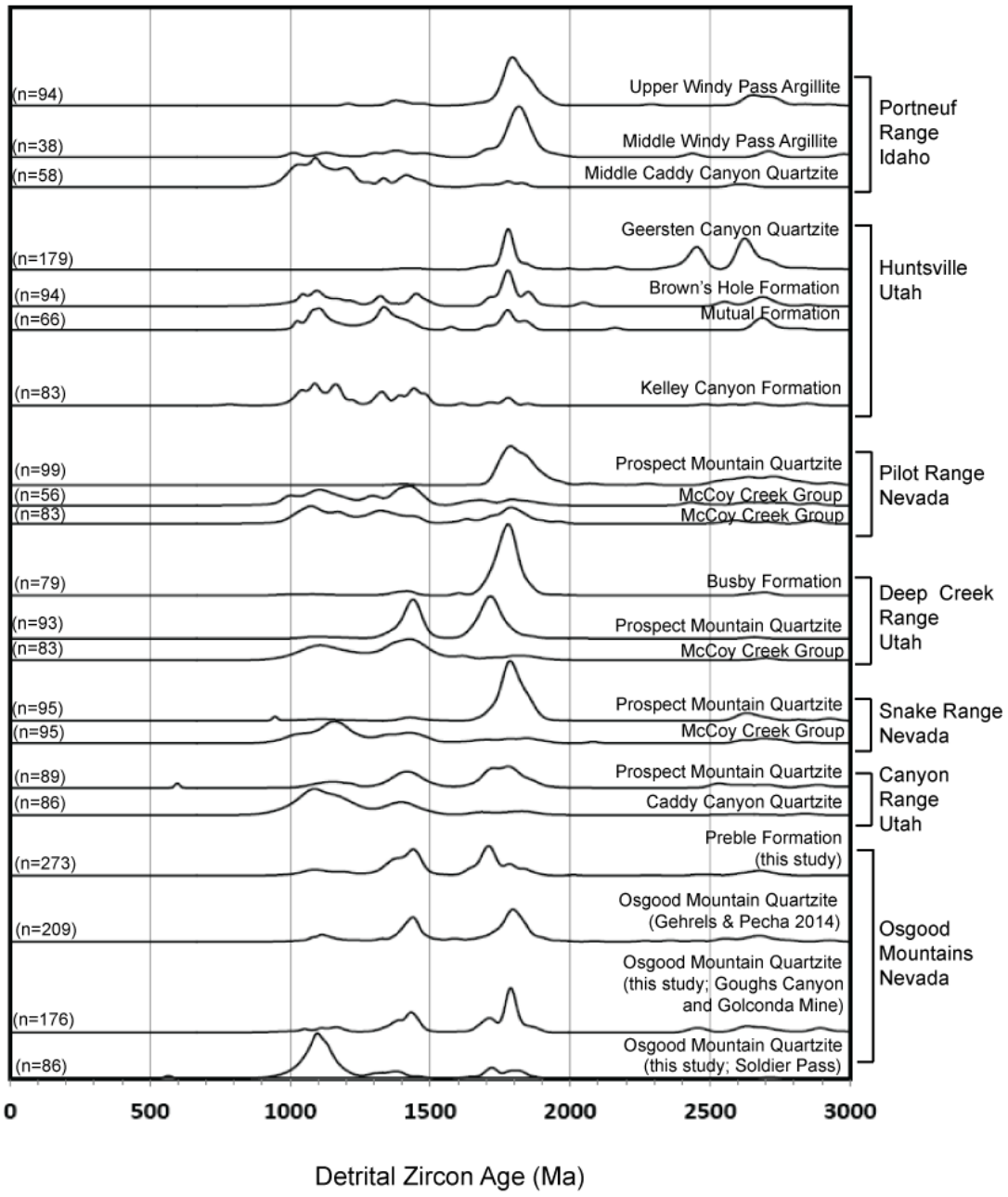

Figure 5. Plots of detrital zircon age of each Neoproperozoic - Cambrian unit organized by locality (see map, Fig. 1) showing the distribution of detrital zircon ages. Curves are normalized probability plots. The number of detrital zircon grains comprising each analysis is shown on the left. Within each location the older units are on the bottom. Canyon Range: Lawton et al., 2010; Snake, Deep Creek, and Pilot Ranges: Yonkee et al., 2014; Huntsville: Yonkee et al., 2014; Portneuf Range: Yonkee et al., 2014; Osgood Mountains: Linde et al., 2012; Gehrels and Pecha, 2014.

5. Detrital Zircon Geochronology Results

a. Osgood Mountain Quartzite (Upper Neoproterozoic – Lower Cambrian)

Two samples from near the top of the Osgood Mountain Quartzite, collected at Goughs Canyon and Golconda Mine (Figs. 2b and 3 and Table 1), and one sample from approximately 400 meters below the top of the unit, collected at Soldier Pass (Figs. 2b and 3 and Table 1), were analyzed. Our visual and statistical analyses indicate that the Mesoproterozoic and Paleoproterozoic detrital zircon age groups of the two younger samples are similar to one another, though the proportions of ages are somewhat different (see Appendix A for statistical analysis discussion). The detrital zircon age groups from these two samples are quite different; the older sample is dominated by Mesoproterozoic grains, while the younger sample is dominated by Paleoproterozoic grains (Fig. 4). K-S test results confirm that these detrital zircon grain populations are dissimilar: P is less than 0.05.

b. Preble Formation (Lower Cambrian – Lower Ordovician)

The three Preble Formation samples were collected low in the formation (Fig. 3) at Goughs Canyon, Garden Spring and Golconda Mine (Fig. 2b and Table 1). The samples all contained Paleoproterozoic and Mesoproterozoic age peaks (Fig. 4). Applying the K-S test, we found that within the Preble Formation, the three different sample pairs have P values of 0.849, 0.881, and 0.937. All sample pairs of the Preble Formation and Osgood Mountain Quartzite have P values less than 0.05.

6. Discussion

a. Osgood Mountain Quartzite

The source of the detrital zircon grains in the Osgood Mountain Quartzite samples is Laurentian, and the samples have two distinct provenances. The change in detrital zircon ages from the older Soldier Pass sample to the younger Goughs Canyon and Golconda Mine samples indicates a significant change in provenance during the deposition of the Osgood Mountain Quartzite. The grains from Soldier Pass are predominantly Mesoproterozoic (Fig. 4) and we interpret that their source was the 1.2-1.0 Ga Grenville orogen (Fig. 1). There are also some Paleoproterozoic grains which we interpret to have been derived from the 1.8–1.7 Ga Yavapai province and the 2.0–1.8 Ga Trans-Hudson orogen (Fig. 1). There are a few Mesoproterozoic grains; these are interpreted to have been shed from the 1.48-1.34 Ga mid-continent granite-rhyolite provinces (Fig. 1). In contrast, the detrital zircon ages in the Goughs Canyon and Golconda Mine samples (Fig. 4) share age peaks with one another, and these peaks are different from those of the Solider Pass sample (Fig. 4). The Paleoproterozoic grains in these samples are interpreted to have been shed from the 1.8-1.7 Ga Yavapai Province and the 1.7-1.62 Ga Mazatzal Province (Fig. 1). Mesoproterozoic grains are interpreted to have been shed from the 1.48-1.34 Ga mid-continent granite-rhyolite provinces (Fig. 1). Archean grains are interpreted to have been sourced from the Archean craton (Fig. 1). A few Mesoproterozoic grains are interpreted to have been derived from the 1.2-1.0 Ga Grenville orogen (Fig. 1).

b. Preble Formation

The detrital zircon ages in all three Preble Formation samples are similar (Fig. 4). We interpret that these three Preble Formation samples share a common Laurentian source. Mesoproterozoic grains predominate in all three samples (Fig. 4) and are interpreted to have been shed from the 1.48-1.34 mid-continent granite-rhyolite provinces (Fig. 1). There are a large number of Paleoproterozoic grains which are interpreted to have been derived from the 1.7-1.62 Ga Mazatzal Province and the 1.8-1.7 Ga Yavapai Province (Fig 1). A smaller number of Mesoproterozoic grains are interpreted as having their source in the 1.2-1.0 Ga Grenville orogen (Fig. 1). The remaining grains are Archean and their source is interpreted as the Archean craton (Fig. 1).

7. Regional Correlation

Detrital zircon ages in passive margin strata across a transect of the Great Basin vary stratigraphically in a manner similar to that which we documented within the Osgood Mountain Quartzite, recording a major regional change in provenance.

a. Nevada-Utah Border: Deep Creek Range, Pilot Range, and Snake Range

Detrital zircons from rocks in the Deep Creek, Pilot, and Snake Ranges (Fig. 2a) record a similar shift of ages as detrital zircons analyzed in the Osgood Mountains. The older strata are the Neoproterozoic McCoy Creek Group (Fig. 6). In all three ranges, the McCoy Creek group has similar Mesoproterozoic age groups and peaks (Fig. 5) (Yonkee et al., 2014). We interpret these grains as primarily shed from the 1.2-1.0 Ga Grenville orogen and the 1.48-1.34 Ga mid-continent granite-rhyolite province (Fig. 1). This is

quite similar to the older Osgood Mountain Quartzite (Soldier Pass) sample, which we interpreted to be sourced in these same terranes. The younger strata in all three ranges are the Cambrian Prospect Mountain Quartzite, and in the Deep Creek Range, the Cambrian Busby Formation (Fig. 6). In all three ranges, the detrital zircons in these younger strata have similar Paleoproterozoic and Mesoproterozoic age groups and peaks (Fig. 5) (Yonkee et al., 2014). We interpret these grains as shed from the 1.80-1.70 Ga Yavapai Province and the 1.34-1.48 Ga mid-continent granite-rhyolite province (Fig. 1), very similar to the younger Osgood Mountain Quartzite samples.

b. <u>Central Utah: Canyon Range</u>

Detrital zircons in Canyon Range strata (Fig. 2a) indicate a similar shift of ages as those analyzed in the Osgood Mountains. The older unit analyzed in the Canyon Range is the Neoproterozoic Caddy Canyon Quartzite (Fig. 6). This unit has Mesoproterozoic age groups and peaks (Fig. 5) (Lawton, et al. 2010) which we interpret as primarily shed from the 1.2-1.0 Ga Grenville orogen and the 1.48-1.34 Ga mid-continent granite-rhyolite province (Fig. 1). These age peaks and our source area interpretation are very similar to those of the older Osgood Mountain Quartzite sample. The younger unit in the Canyon Range is the Cambrian Prospect Mountain Quartzite (Fig. 6). This unit has Paleoproterozoic and Mesoproterozoic age groups and peaks (Fig. 5) (Lawton, et al., 2010). We interpret these detrital zircons as shed from the 1.80-1.70 Ga Yavapai Province and the 1.48-1.34 Ga mid-continent granite-rhyolite province (Fig. 1), quite similar to the younger Osgood Mountain Quartzite samples.

Figure 6: Stratigraphic columns of the passive margin strata discussed. Subjacent strata are not shown. Neoproterozoic-Cambrian boundary at 540 Ma is approximated for each location. Strata in the Osgood Mountains are shown in stratigraphic succession and correlative with regional passive margin strata. Only the detrital zircon samples referenced in the text are shown.

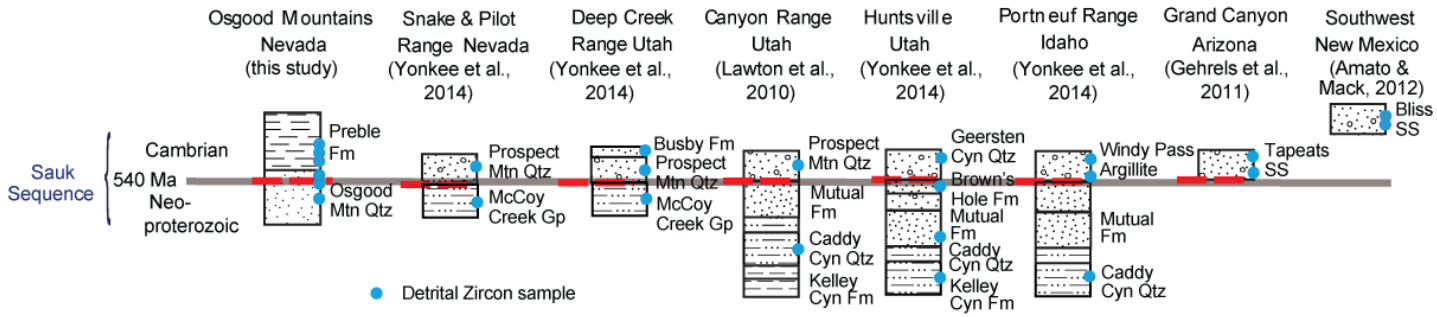

c. Northeastern Utah: Huntsville

Detrital zircons from Huntsville samples (Fig. 2a) record a comparable shift of ages to those analyzed in the Osgood Mountains. The older units in the Huntsville section are the Neoproterozoic Kelley Canyon and Mutual Formations and the Neoproterozoic – Cambrian Brown's Hole Formation (Fig. 6). The Kelley Canyon Formation (Yonkee et al., 2014), the Mutual Formation (Stewart, et al. 2001; Yonkee et al., 2014), and the Brown's Hole Formation (Yonkee et al., 2014) have similar Mesoproterozoic age groups and peaks (Fig. 5). We interpret these grains as primarily derived from the 1.2-1.0 Ga Grenville orogen and the 1.48-1.34 Ga mid-continent granite-rhyolite province (Fig. 1)—very similar to that of our older Osgood Mountain Quartzite sample. The younger unit in the Huntsville section is the Cambrian Geersten Canyon Quartzite (Fig. 6). The Geersten Canyon Quartzite (Stewart et al., 2001; Yonkee et al., 2014) has Mesoproterozoic, Paleoproterozoic, and Archean age groups and peaks (Fig. 5). We interpret these grains as derived primarily from the 1.80-1.70 Ga Yavapai Province and secondarily from the 1.2-1.0 Ga Grenville orogen and the > 2.5 Ga Archean craton (Fig. 1). These age peaks and our interpreted provenance are similar to that for our younger Osgood Mountain Quartzite samples.

d. Southeastern Idaho: Portneuf Range

Detrital zircons from rocks in the Portneuf Range (Fig. 2a), record a shift of ages similar to those analyzed in the Osgood Mountains. In the Portneuf Range, the older unit is the Neoproterozoic Middle Caddy Canyon Quartzite (Fig. 6). The Middle Caddy Canyon Quartzite has Mesoproterozoic age groups and peaks (Fig. 5) (Yonkee et al.,

2014). We interpret these grains as primarily shed from the 1.2-1.0 Ga Grenville orogen (Fig. 1). These age peaks and our source area interpretation are very similar to that of the older Osgood Mountain Quartzite sample. The younger unit in the Portneuf Range is the Windy Pass Argillite, comprising upper and middle members (Fig. 6). Both members have Paleoproterozoic age peaks and groups (Fig. 5) (Yonkee et al., 2014). We interpret these grains as shed from the 1.80-1.70 Ga Yavapai Province (Fig. 1). This is very similar to the younger Osgood Mountain Quartzite sample.

e. Implications of the regional correlation

In the five areas of the passive margin examined, the detrital zircon age patterns change in a systematic way (Fig. 7). The detrital zircons of the older strata are predominantly the age of the Grenville orogen and the detrital zircons of the younger strata are predominantly the age of the Yavapai province basement rocks.

The shift in detrital zircon age across the region implies a provenance change across the region at approximately the same time. Continent-spanning river systems carried sands from the Grenville orogenic terrane across the Laurentian continent to the western passive margin in Late Neoproterozoic to Early Cambrian time (e.g., Rainbird et al., 1997; Cawood and Nemchin, 2001; Mueller et al., 2007; Dehler et al., 2010; Kingsbury-Stewart et al., 2013). By Early to Middle Cambrian time, as this study has found, river systems were carrying relatively very few Grenville-aged detrital zircons to the passive margin in the areas that we investigated.

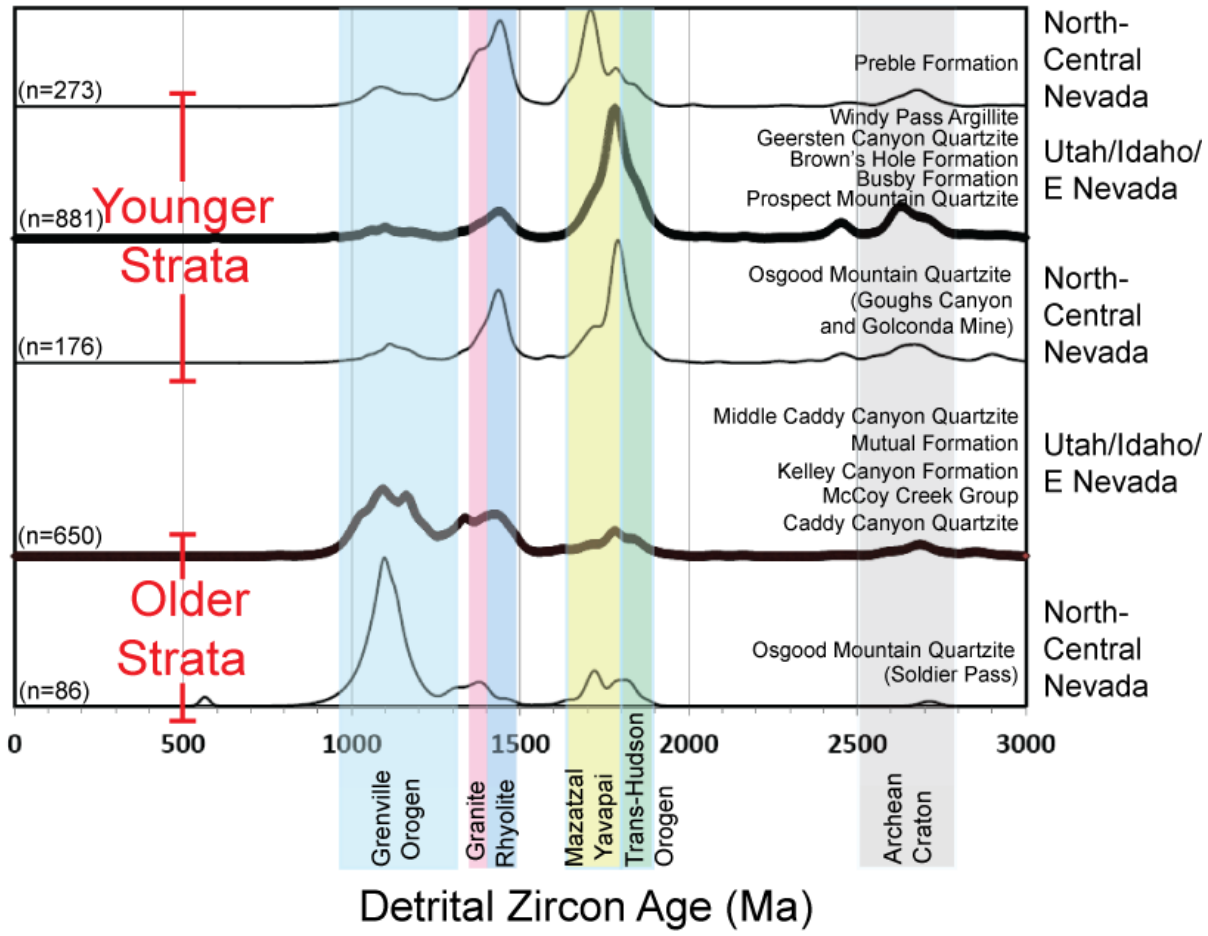

Figure 7. Plots of compilations of units showing the distribution of detrital zircon ages. Curves on the upper part of the figure are compilations of the younger strata throughout the region, compared with the younger strata in our pilot study. Curves on the lower part of the figure are compilations of the older strata throughout the region, compared with the older strata in our pilot study. Curves are normalized probability plots. The number of detrital zircon grains comprising each analysis is shown on the left. The thinner lines are from our pilot study; the thicker lines are the composites of data from elsewhere in the Basin and Range. The color bars indicate the ages of magmatic activity and terrane accretion in Laurentia; the colors are the same as Fig. 1. Canyon Range: Lawton et al., 2010; Snake, Deep Creek, and Pilot Ranges: Yonkee et al., 2014; Huntsville: Yonkee et al., 2014; Portneuf Range: Yonkee et al., 2014; Osgood Mountains: Linde et al., 2012; Gehrels and Pecha, 2012.

Our data support the proposal that the Transcontinental Arch, a continent-scale crustal feature that was not present in the Middle Neoproterozoic, was uplifted in the latest Neoproterozoic or earliest Cambrian. The uplifted arch provided vertical relief, and forced a change in sedimentation and drainage patterns, restricting the transport of sediment from the Grenville orogenic terrane to western Laurentia. This gradual change in drainage patterns caused the observed dearth of Grenville-age zircons. The uplift of the arch also would have exposed basement rocks of the Archean craton, the Trans-Hudson orogen, the Yavapai and Mazatzal terranes, and the mid-continent anorgenic granites (Fig. 1). Sloss (1963) demonstrated the onlap of the Sauk sequence onto basement rocks by Middle Cambrian time; this onlap requires that the basement rocks were exposed. These uplifted and exposed basement rocks became the sources for the sediments draining from the western flank of the Transcontinental Arch to the western Laurentian margin. The uplift of the arch caused the preponderance of zircons of the age of the Trans-Hudson orogen, Yavapai/Mazatal, and mid-continent granite province in the younger passive margin strata investigated in this study.

Across the Great Basin transect investigated for this study, the definitive shift in detrital zircon age spectra records a tectonic event that caused a coeval change in sediment transport patterns. This detrital zircon age shift therefore could be a useful correlation tool. Such a tool would be particularly helpful in quartz arenites, which are often lacking in biostratigraphic markers and thus difficult to date with confidence. We suggest that stratigraphic sections documented by our work and others can be correlated based on this consistent change in detrital zircon age peaks, and that other sections in the region can also be correlated in this way.

8. Summary and conclusions

U-Pb analyses of detrital zircons from the Osgood Mountain Quartzite and the Preble Formation in northern Nevada demonstrate that these units were shed from sources within the North American craton, and that the sources changed with time. The oldest sample of the Osgood Mountain Quartzite, taken near Soldier Pass, was derived primarily from the Grenville orogen. The younger Osgood Mountain Quartzite samples were derived primarily from the Yavapai and Mazatzal provinces. The stratigraphically overlying Preble Formation was also derived primarily from the Yavapai and Mazatzal provinces.

The shift in age peaks and groups of detrital zircons within the Osgood Mountain Quartzite section is also recorded in other passive margin strata in Nevada, Utah, and Idaho. This shift indicates a widespread change in provenance; the older passive margin units were derived primarily from the Grenville orogen and the younger units were derived primarily from the more proximal Yavapai and Mazatzal provinces.

Our data support the proposal that the widespread and time-correlative shift in provenance of passive margin strata across the Great Basin records the uplift of the Transcontinental Arch. In Late Neoproterozoic time, these passive margin units were sourced primarily in the Grenville orogen; by Early Cambrian most passive margin units were sourced primarily from the Yavapai and Mazatzal provinces with very little input from the Grenville orogen. The predominantly east-to-west paleocurrents (Seeland, 1968) carried Grenville sands from the eastern third of the craton to the western passive margin until Early Cambrian time, when the Transcontinental Arch was uplifted and blocked this sediment dispersal pattern, and also provided a new sediment source for

western Laurentia. Our results corroborate previous suggestions that the Transcontinental Arch blocked the transport of sediments in the Early Paleozoic (Mack and Amato, 2012; Gehrels and Pecha, 2014; Yonkee et al., 2014). This study substantiates the previous interpretations by demonstrating coeval shifts in provenance across a broad transect of the Great Basin and confirms that the uplift of the arch was sufficient to change drainage patterns by Early Cambrian time.

We propose that analysis and comparison of detrital zircon age signatures can be used to support other chronostratigraphic correlation tools, especially in fossil-poor and notoriously hard-to-date quartz arenites. When used in conjunction with other correlation methods, shifts in detrital zircon age spectra can provide important information where other stratigraphic techniques are unavailable.

9. References Cited

Amato, J.M., and Mack, G.H., 2012, Detrital zircon geochronology from the Cambrian-Ordovician Bliss Sandstone, New Mexico: Evidence for contrasting Grenville-age and Cambrian sources on opposite sides of the Transcontinental Arch: Geological Society of America Bulletin, v. 124, p. 1826-1840.

Anderson, J.L., and Morrison, J., 1992, The role of anorogenic granites in the Proterozoic crustal development of North America, in Condie, K.C., ed., Proterozoic Crustal Evolution: New York, Elsevier, p. 263-299.

Bickford, M.E., Van Schmus, R., and Zietz, I., 1986, Proterozoic history of the midcontinent region of North America: Geology, v. 14, no. 6, p. 492–496.

Bickford, M.E., and Anderson, J.L., 1993, Middle Proterozoic magmatism, in Reed, J.C., Bickford, M.E., Houston, R.S., Link, P.K., Rankin, D.W., Sims, P.K., and Van Schmus, W.R., eds., Precambrian Conterminous U.S.: Boulder, Colorado, Geological Society of America, The Geology of North America, v. C-2, p. 281–292.

Burchfiel, B.C., Cowan, D.S., and Davis, G.A., 1992, Tectonic overview of the Cordilleran orogeny in the western United States, in Burchfiel, B.C., Lipman, P.W., and Zoback, M.L., eds, The Cordilleran Orogen: Conterminous U.S.: Boulder, Colorado, Geological Society of America, The Geology of North America, v. G-3, p. 407–480.

Carlson, M.P., 1999, Transcontinental Arch—a pattern formed by rejuvenation of local features across central North America: Tectonophysics, v. 305, p. 224-233.

Cashman, P.H., Villa, D.E., Taylor, W.J., Davydov, V.I., and Trexler, J.H., Jr., 2011, Paleozoic contractional and extensional deformation at Edna Mountain, Nevada: Geological Society of America Bulletin, v. 123, p. 651–668.

Cawood, P.A. and Nemchin, A.A., 2001, Paleogeographic development of the east Laurentian margin: Constraints from U-Pb dating of detrital zircons in the Newfoundland Appalachians: Geological Society of America Bulletin, v. 113, p. 1234-1246.

Dehler, C.M., Fanning, C.M., Link, P.K., Kingsbury, E.M., and Rybcynski, D., 2010, Maximum depositional age and provenance of the Uinta Mountain Group and Big Cottonwood Formation, northern Utah: Paleogeography of rifting western Laurentia: Geological Society of America Bulletin, v. 122, p. 1689-1699.

Dickinson, W.R., and Gehrels, G.E., 2009, U-Pb ages of detrital zircons in Jurassic eolian and associated sandstones of the Colorado Plateau: Evidence for transcontinental

dispersal and intraregional recycling of sediment: Geological Society of America Bulletin, v. 121, p. 408–433.

Dickinson, W.R., and Lawton, T.F., 2001, Carboniferous to Cretaceous assembly and fragmentation of Mexico: Geological Society of America Bulletin, v. 113, p. 1142–1160.

Erickson, R.L., and Marsh, S.P., 1974, Geologic map of the Golconda Quadrangle, Humboldt County, Nevada: U.S. Geological Survey Geologic Quadrangle Map GQ-1174, 1:24,000.

Ferguson, H.G., Roberts, R.J., and Muller, S.W., 1952, Geology of the Golconda Quadrangle, Nevada: U.S. Geological Survey Geologic Quadrangle Map GQ-15, scale 1:125,000: Boulder, CO, U.S. Geological Survey.

Gehrels, G.E., 2000, Introduction to detrital zircon studies of Paleozoic and Triassic strata in western Nevada and northern California, in Soreghan, M.J., and Gehrels, G.E., eds., Paleozoic and Triassic Paleogeography and Tectonics of Western Nevada and Northern California: Geological Society of America Special Paper 347, p.1–17.

Gehrels, G.E., 2012, Detrital zircon U-Pb geochronology: Current methods and new opportunities, in Busby, C., and Azor, A., eds., Recent Advances in Tectonics of Sedimentary Basins: Hoboken, New Jersey, Blackwell Publishing.

Gehrels, G.E., and Pecha, M., 2014, Detrital zircon U-Pb geochronology and Hf isotope geochemistry of Paleozoic and Triassic passive margin strata of western North America: Geosphere, v. 10, p. 49-65.

Gerhrels, G.E., and Dickinson, W.R., 1995, Detrital zircon provenance of Cambrian to Triassic miogeoclinal and eugeoclinal strata in Nevada: American Journal of Science, v. 295, p. 18-48.

Gehrels, G.E., Valencia, V., and Pullen, A., 2006, Detrital zircon geochronology by laser-ablation multicollector ICPMS at the Arizona LaserChron Center: in Lozweski, T., and Huff, W., eds., Geochronology: Emerging Opportunities, Paleontology Society Short Course: Paleontology Society Paper 11, 10 p.

Gehrels, G.E., Valencia, V.A., and Ruiz, J., 2008, Enhanced precision, accuracy, efficiency, and spatial resolution of U-Pb ages by laser ablation-multicollector-inductively coupled plasma-mass spectrometry: Geochemistry, Geophysics, Geosystems, v.9, p. 1-13.

Gehrels, G.E., Blakey, R., Karlstrom, K.E., Timmons, J.M., Dickinson, B., and Pecha, M., 2011, Detrital zircon U-Pb geochronology of Paleozoic strata in the Grand Canyon, Arizona: Lithosphere, v. 3, p. 183-200.

Guynn, J., and Gehrels, G.E., 2006, Comparison of detrital zircon age distribution using the K-S test: online manual published by the University of Arizona LaserChron Center:https://docs.google.com/file/d/0B9ezu34P5h8eZWZmOWUzOTItZDgyZi00NDRiLWI4ZTctNTljNTM5OTU1MGUz/edit?hl=enandpli=1

Hoffman, P.F., 1989, Precambrian geology and tectonic history of North America in Bally, A.W., and Palmer, A.R., eds., The Geology of North America—An Overview: Boulder, Colorado, Geological Society of America, The Geology of North America, v. A, p. 447–512.

Hotz, P.E. and Willden, P., 1964, Geology and mineral deposits of the Osgood Mountains quadrangle Humboldt County, Nevada: U.S. Geological Survey Professional Paper 431, 127 p.; scale 1:62,500.

Johnston, S., Gehrels, G., Valencia, V., and Ruiz, J., 2009, Small-volume U-Pb geochronology by laser ablation-multicollector-ICP mass spectrometry: Chemical Geology, v. 259, p. 218–229, doi:10.1016/j.chemgeo .2008.11.004.

Keith, A., 1928, Structural symmetry in North America: Geological Society of America Bulletin, v. 39, p. 321-385.

Kingsbury-Stewart, E.M., Osterhout, S.L., Link, P.K., and Dehler, C.M., 2013, Sequence stratigraphy and formalization of the Middle Uinta Mountain Group (Neoproterozoic), central Uinta Mountains, Utah: a closer look at the western Laurentian seaway at ca. 750 Ma: Precambrian Research, v. 236, p. 65-84

Lawton, T.F., Hunt, G.J., and Gehrels, G.E., 2010, Detrital zircon record of thrust belt unroofing in Lower Cretaceous synorogenic conglomerates, central Utah: Geology, v. 38, p. 463-466.

Madden-McGuire, Dawn, 1991, Stratigraphy of the limestone-bearing part of the Lower Cambrian to Lower Ordovician Preble Formation near its type locality, Humboldt County, North-Central Nevada, in Raines, G.L., Lisle, R.E., Schaefer, R.W., and Wilkinson, W.H., eds., Geology and ore deposits of the Great Basin, Geological Society of Nevada symposium proceedings, p. 875-839.

Mueller, P.A., Foster, D.A., Mogk, D.W., Wooden, J.L, Kamenov, G.D., and Vogl, J.J., 2007, Detrital mineral chronology of the Uinta Mountain Group: Implications for the Grenville flood in southwestern Laurentia: Geology, v. 35, p. 431-434.

Poole, F.G., Stewart, J.H., Palmer, A.R., Sandberg, C.A., Madrid, R.A., Ross, R.J., Jr., Hintze, L.F., Miller, M.M., and Wrucke, C.T., 1992, Latest Precambrian to latest Devonian time; development of a continental margin: *in* Burchfiel, B.C., Lipman, P.W., and Zoback, M.L., eds., The Cordilleran Orogen: Conterminous U.S.: Boulder, Colorado, Geological Society of America, the Geology of North America, v. G-3.

Rainbird, R.H., McNicoll, J., Theriault, R.J., Heaman, L.M., Abbott, J.G., Long, D.G.F., and Thorkelson, D.J., 1997, Pan-continental river system draining Grenville orogeny recorded by U-Pb and Sm-Nd geochronology of Neoproterozoic quartzarenites and mudrocks, northwestern Canada: The Journal of Geology, v. 105, p. 1-17.

Rainbird, R.H., Cawood, P., and Gehrels, G., 2012, The great Grenvillian sedimentation episode: record of supercontinent Rodinia's assembly, *in* Busby, C. and Azor, A., eds., Tectonics of sedimentary basins: recent advances. Blackwell Publishing Ltd, p. 583-601.

Seeland, D.A., 1968, Paleocurrents of the Late Precambrian to Early Ordovician (Basal Sauk) transgressive clastics of the western and northern United States with a review of the stratigraphy [PhD dissertation]: University of Utah, 276 p.

Sloss, L.L., 1963, Sequences in the cratonic interior of North America: Geological Society of America Bulletin, v. 74, p. 93-114.

Sloss, L.L. (Ed.), 1988, Tectonic evolution of the craton in Phanerozoic time, *in* Sloss, L.L., ed., Sedimentary Cover—North American Craton: U.S.: Boulder, Colorado, Geological Society of America, The Geology of North America, v. D-2.

Stewart, J.H., 1972, Initial deposits in the Cordilleran geosyncline: Evidence of a Late Precambrian (<850 m.y.) continental separation. Geological Society of America Bulletin, v. 83, p. 1345-1360.

Stewart, J.H., 1991, Latest Proterozoic and Cambrian rocks of the western United States—An overview, in Cooper, J.D., and Stevens, C.H., eds., 1991, Paleozoic paleogeography of the western United States—II: Pacific Section Society of Economic Paleontologists and Mineralogists, v. 67, p. 13-38.

Stewart, J.H., Gehrels, G.E., Barth, A.P., Link. P.K., Christie-Blick, N., and Wrucke, C.T., 2001, Detrital zircon provenance of Mesoproterozoic to Cambrian arenites in the western United States and northwestern Mexico: Geological Society of America Bulletin, v. 113, p. 1343-1356.

Van Schmus, W.R., Bickford, M.E., Sims, P.K., Anderson, J.L., Shearer, C.K., and Treves, S.B., 1993, Proterozoic geology of the western midcontinent region, in Reed, J.C., Bickford, M.E., Houston, R.S., Link, P.K., Rankin, D.W., Sims, P.K., and Van Schmus, W.R., eds., Precambrian Conterminous U.S.: Boulder, Colorado, Geological Society of America, The Geology of North America, v. C-2, p. 239–259.

Yonkee, W.A., Dehler, C.D., Link, P.K., Balgord, E.A., Keeley, J.A., Hayes, D.S., Wells, M.L., Fanning, C.M., Johnston, S.M., 2014, Tectono-stratigraphic framework of Neoproterozoic to Cambrian strata, west-central U.S.: Protracted rifting, glaciation, and evolution of the North American Cordilleran margin, Earth Science Reviews, v.136, p. 59-95.

Chapter 2

Detrital zircon U-Pb geochronology and Hf isotope geochemistry of the Roberts Mountains allochthon: New insights into the Early Paleozoic tectonics of western North America

This chapter was published: Linde, G.M., Trexler, J.H., Jr., Cashman, P.H., Gehrels, G., and Dickinson, W.R., 2016, Detrital zircon U-Pb geochronology and Hf isotope geochemistry of the Roberts Mountains allochthon: New insights into the Early Paleozoic tectonics of western North America: Geosphere, v. 12, p. 1-16.

1. Abstract

Detrital zircon U-Pb geochronology and Hf isotope geochemistry provide new insights into the provenance, sedimentary transport, and tectonic evolution of the Roberts Mountains allochthon strata of north-central Nevada. Using laser-ablation inductively coupled plasma mass spectrometry, a total of 1151 zircon grains from six Ordovician to Devonian arenite samples were analyzed for U-Pb ages; of these, 228 grains were further analyzed for Hf isotope ratios. Five of the units sampled have similar U-Pb age peaks and Hf isotope ratios, while the ages and ratios of the Ordovician lower Vinini Formation are significantly different. Comparison of our data with that of igneous basement rocks and other sedimentary units supports our interpretation that the lower Vinini Formation originated in the north-central Laurentian craton. The other five units sampled, as well as Ordovician passive margin sandstones of the western Laurentian margin, had a common source in the Peace River Arch region of western Canada. We propose that the Roberts Mountains allochthon strata were deposited near the Peace River Arch region, and

subsequently tectonically transported south along the Laurentian margin, from where they were emplaced onto the craton during the Antler orogeny.

2. Introduction

The Roberts Mountains allochthon (RMA) consists of internally deformed Cambrian through Devonian rocks, and structurally overlies coeval passive margin strata in northeastern and north-central Nevada (Schuchert, 1923; Kay, 1951; Roberts et al., 1958; Madrid, 1987; Burchfiel et al., 1992) (Figs. 8 and 9). Roberts Mountains allochthon rocks include chert, argillite, arenite, quartzite, limestone, and mafic volcanic rocks. The RMA is often thought to have been deposited in an ocean basin outboard of coeval passive margin strata in western Laurentia and to have been tectonically emplaced onto this margin during the Late Devonian to Early Mississippian Antler orogeny (e.g., Roberts et al., 1958; Burchfiel and Davis, 1972; Madrid, 1987). Various workers have suggested wildly disparate sources for the RMA strata. Some workers (e.g., Roberts et al., 1958; Burchfiel and Davis, 1972; Poole et al., 1992) suggested that the RMA strata originated in western Laurentia (Fig. 8) and deposited in an ocean basin to the west. Speed and Sleep (1982) hypothesized that the RMA strata are the accretionary prism of a far-traveled arc. Gehrels et al. (2000a) proposed that the RMA originated in the Peace River Arch region of western Canada. Wright and Wyld (2006) suggested that the RMA was deposited as far afield as Avalonia or Gondwana and subsequently was tectonically transported to western Laurentia along its southern margin (Fig. 10). Colpron and Nelson (2009) proposed that RMA strata could have originated in the northern Baltica–southern Caledonides region and been tectonically transported along the northwest margin of

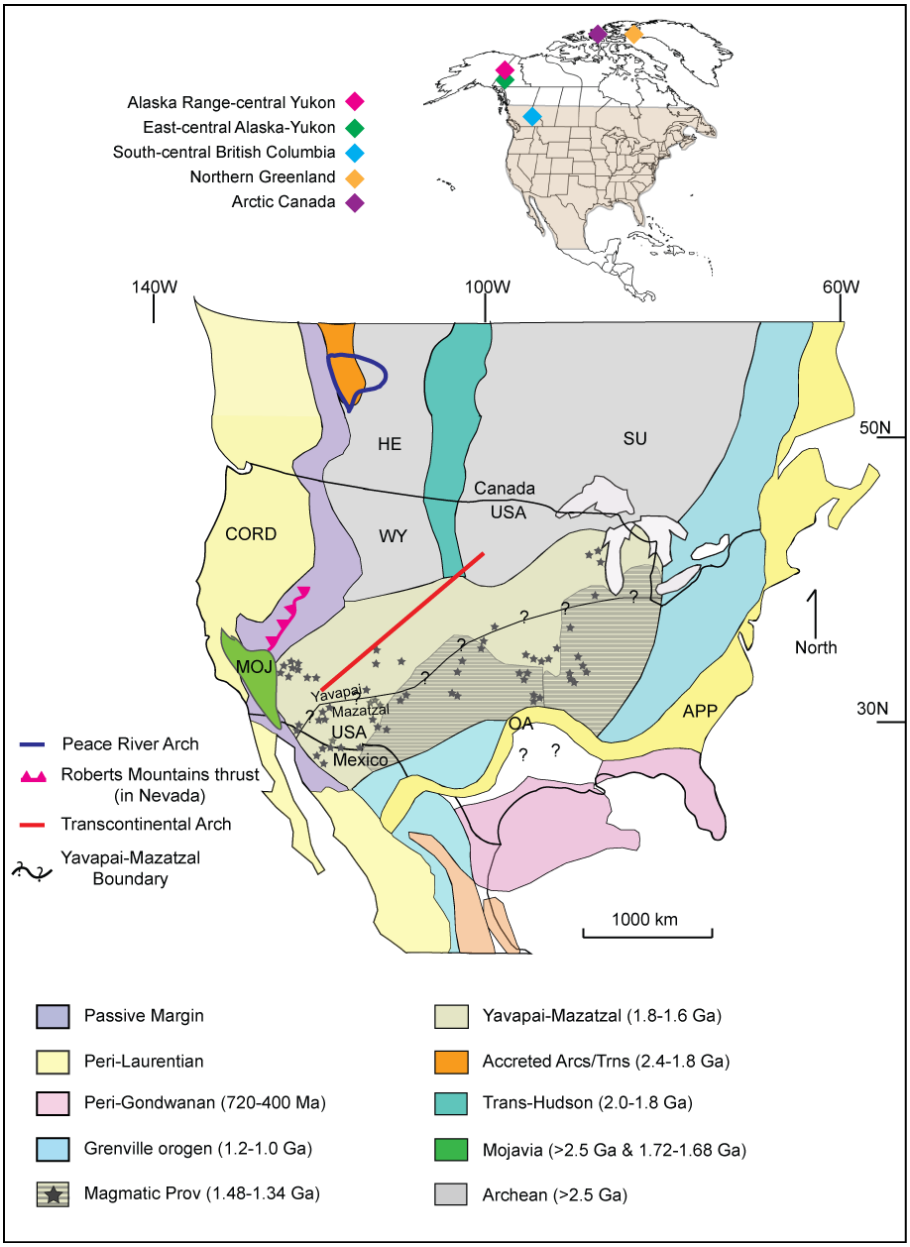

Figure 8. Locations of the main age provinces in North America that are potential source terranes for western Laurentian strata. The location of Transcontinental Arch is shown as a red line (Sloss, 1988); the Peace River Arch is shown as a blue line. The trace of the Roberts Mountains thrust is shown. WY—Wyoming province; HE—Hearn province; SU—Superior province; CORD—Cordilleran; APP—Appalachian; OA—Ouachita-Marathon; MOJ—Mojavia. Figure is after Gehrels et al. (2011) and compiled from Bickford et al. (1986), Hoffman (1989), Ross (1991), Burchfiel et al. (1992), Anderson and Morrison (1992), Bickford and Anderson (1993), Van Schmus et al. (1993), Villeneuve et al. (1993), Dickinson and Lawton (2001), Whitmeyer and Karlstrom (2007), and Dickinson and Gehrels (2009). An inset map of North America shows other locations referred to in the text.

Laurentia (Fig. 10). Determining the provenance of the RMA units will unravel this puzzle and provide new insight into early Paleozoic tectonics in the western Cordillera.

The gaps in understanding about the RMA strata—their provenance, sedimentary transport to depositional basin, and possible subsequent tectonic transport—can be addressed using detrital zircon analyses. We analyzed detrital zircons to obtain both uranium-lead ages and hafnium isotope ratios. U-Pb ages are important for identifying and then characterizing the provenance of sedimentary strata, and for comparison between sedimentary units (Gehrels et al., 2000b; Fedo et al., 2003; Gehrels, 2012, 2014). Hafnium isotope compositions are used to determine the geochemical character of the magma in which the zircons crystallized. When combined with U-Pb ages, Hf isotope composition provides a powerful complement for interpreting sedimentary provenance (Bahlburg et al., 2011; Gehrels and Pecha, 2014).

In this study, we determined the U-Pb ages and Hf isotope compositions of detrital zircons in six samples of RMA strata in north-central Nevada. We use these data to interpret provenance, sedimentary transport to depositional basins, possible subsequent tectonic transport, and relationships between RMA units. Our study builds on an earlier analysis of RMA samples that determined U-Pb ages using isotope-dilution–thermal ionization mass spectrometry (ID-TIMS) (Gehrels et al., 2000a, 2000b). Using detrital zircons from the same samples, the original data set was enlarged and enhanced. We analyzed a significantly larger number of grains per sample, changed and updated grain selection methods, and added Hf isotope composition analyses. We used laser-ablation–inductively coupled plasma mass spectrometry (LA-ICPMS) for all analyses. We report

here 1151 new U-Pb ages and 228 new Hf isotope analyses. Detrital zircon analyses allow us to resolve the original sources of these units. We show that some RMA units in some cases share an origin, while others units do not.

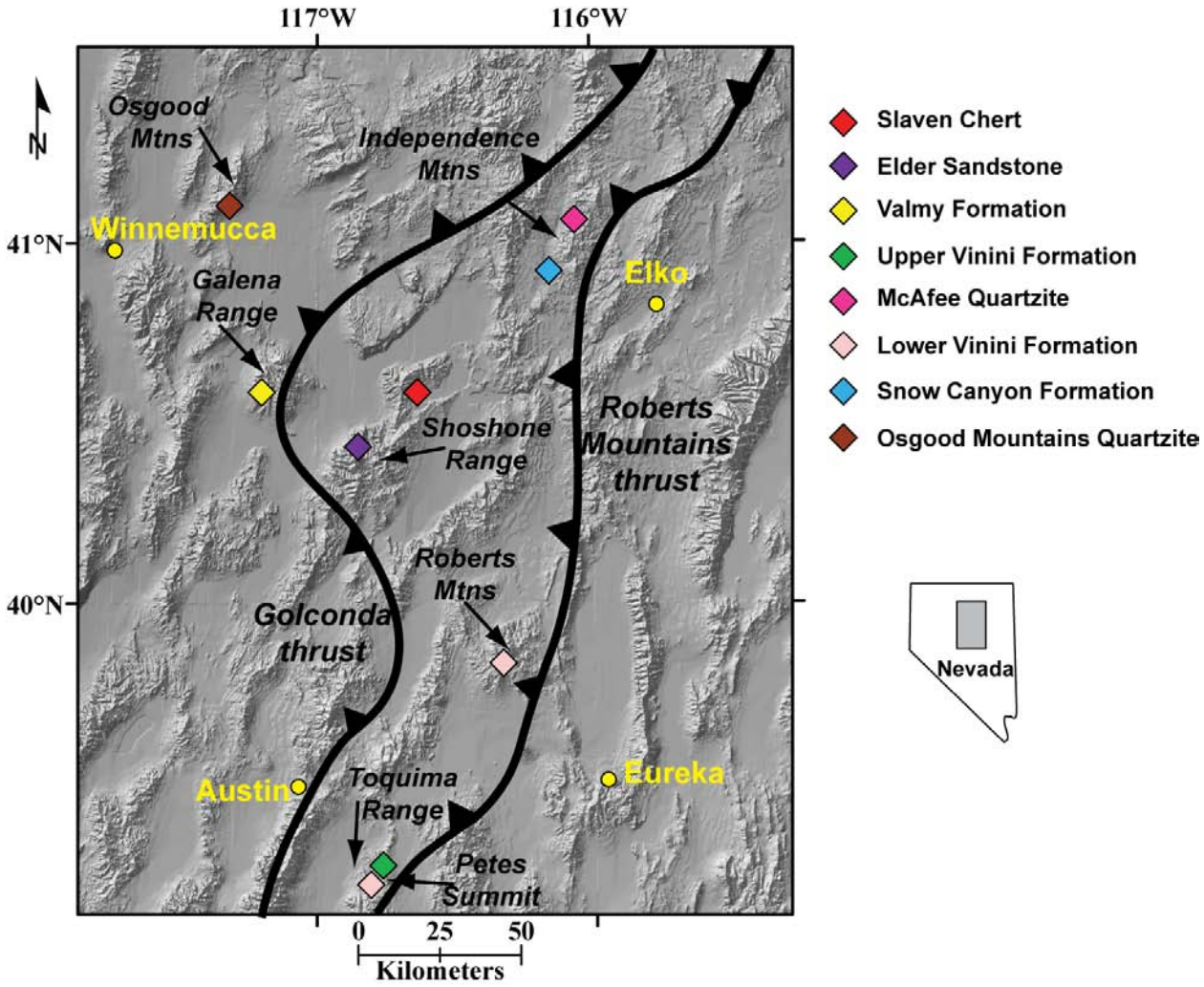

Figure 9. Map of north-central Nevada, showing sample locations (colored symbols) and the traces of the Roberts Mountains and Golconda thrusts. Some Roberts Mountains allochthon (RMA) rocks crop out to the west of the Golconda thrust in tectonic windows through the allochthon. Antler orogenic highlands are the map area to the west of the Roberts Mountains thrust; Antler Foreland Basin is the map area to the east of the Roberts Mountains thrust. Thrust traces are after Dickinson (2006); Antler highlands and basin are after Poole (1974).

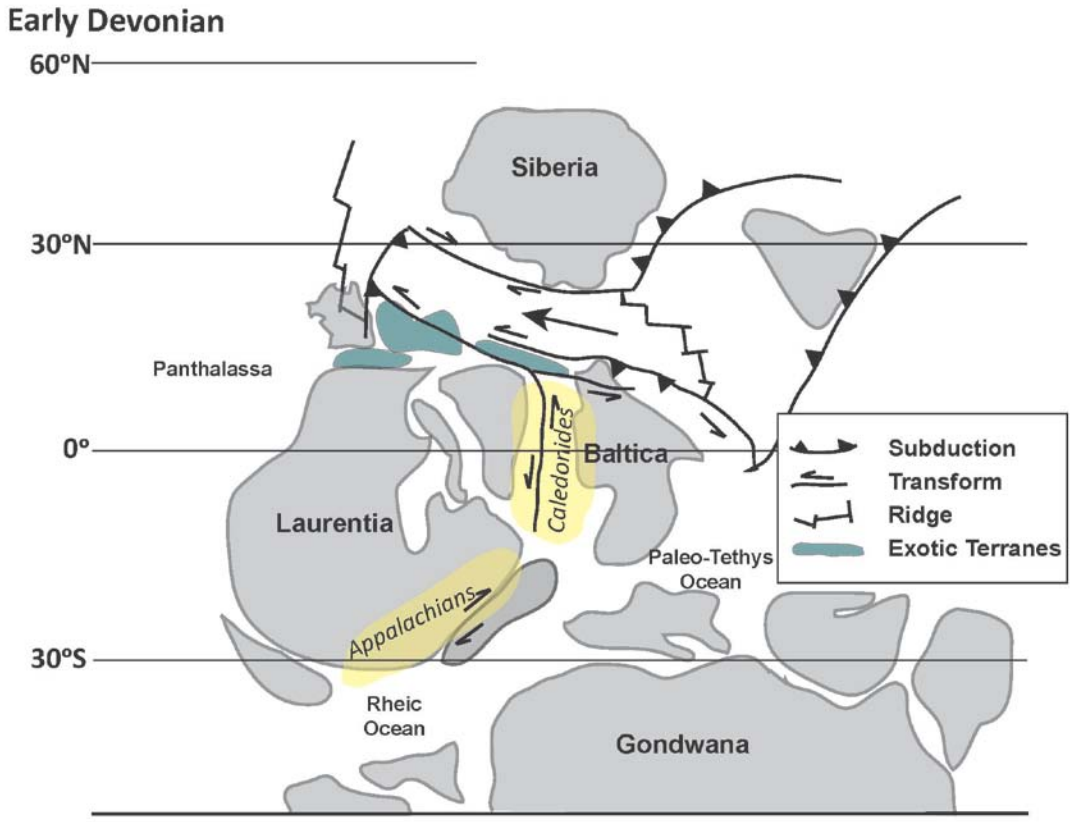

Figure 10. Early Devonian "Northwest Passage" between Laurentia, Baltica, and Siberia proposed by Colpron and Nelson (2009). Exotic terranes include the Alexander, Klamath, and northern Sierran terranes. Map is after Colpron and Nelson (2009).

3. Geologic Setting

a. Regional Tectonostratigraphic Framework

The North American craton contains several Proterozoic and Archean age provinces, thus providing geologically distinguishable crustal provinces that are source terranes for the upper Proterozoic and lower Paleozoic continental margin sedimentary section (e.g., Gehrels et al., 2011, and references cited therein) (Fig. 8). The Yavapai-Mazatzal Province (1.8–1.6 Ga) extends across central North America (Fig.1). It is bounded on the

north and northwest by the Trans-Hudson orogenic terrane (2.0–1.8 Ga) and Archean rocks (>2.5 Ga) of the Wyoming and Superior Provinces (Fig. 8). It is bounded on the south and east by the terranes of the Grenville orogen (1.2–1.0 Ga) and on the west by the Mojavia terrane (>2.5 Ga with 1.6–1.7 Ga granitoids) (Fig. 8).

Detrital zircon sources for the passive margin section changed in the upper Proterozoic–Lower Cambrian (Linde et al., 2014, and references cited therein). The 1.2–1.0 Ga Grenville orogen of southern and eastern North America (Fig. 8) was a significant sediment source for western Laurentia throughout the Neoproterozoic (Rainbird et al., 1997, 2012), including the upper Proterozoic passive margin section from the northwest United States to Sonora, Mexico (e.g., Lawton et al., 2010; Gehrels and Pecha, 2014; Yonkee et al., 2014; Linde et al., 2014). In contrast, the 1.8–1.6 Ga Yavapai-Mazatzal and 1.48–1.34 Ga mid-continent granite-rhyolite provinces within the North America craton (Fig. 8) were the more predominant sediment sources for strata higher in the passive margin section (e.g., Lawton et al., 2010; Gehrels and Pecha, 2014; Yonkee et al., 2014; Linde et al., 2014).

The RMA is often interpreted as a package of oceanic sediments emplaced structurally eastward onto the western Laurentian craton during the Late Devonian– Early Mississippian Antler orogeny (Roberts et al., 1958; Poole et al., 1992). Roberts Mountains allochthon strata are exposed in north-central Nevada between the Golconda thrust on the west and the Roberts Mountains thrust on the east; some units crop out west of the Golconda thrust in tectonic windows (Fig. 9). Rocks of the allochthon structurally overlie coeval rocks of the western Laurentian passive margin (e.g., Schuchert, 1923; Kay, 1951; Roberts et al., 1958; Madrid, 1987) (Fig. 11). Roberts Mountains allochthon

strata are highly deformed, and include imbricated older-over-younger thrust sheets (Evans and Theodore, 1978; Oldow, 1984; Noble and Finney, 1999). The metamorphic grade of the strata is generally greenschist facies or lower (Gehrels et al., 2000a). The RMA was emplaced along the Roberts Mountains thrust during the Late Devonian to Early Mississippian Antler orogeny (Roberts et al., 1958). The Antler foreland basin, west of the Laurentian craton and east of the Antler orogen, was filled between Devonian and Early Mississippian time by sediments shed from the uplifting Antler highlands (Poole, 1974; Trexler et al., 2003) (Fig. 9).

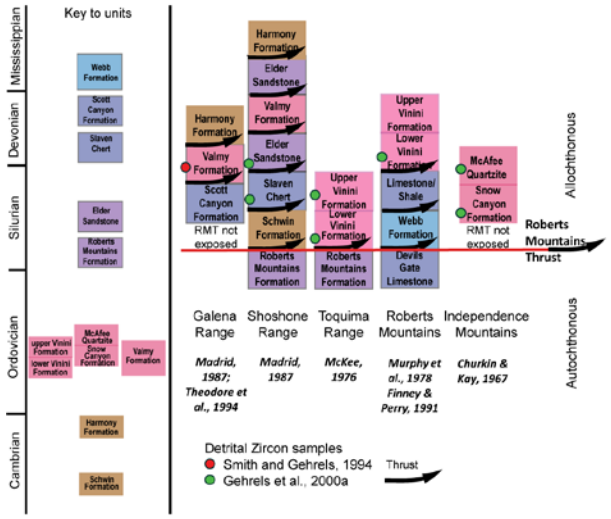

Figure 11. Tectonostratigraphic diagram of units of the Roberts Mountains allochthon (RMA) in selected north-central Nevada mountain ranges, showing locations of detrital zircon samples. Units are shown in their physical, structurally superimposed, order. Most units are internally disrupted with multiple imbricate thrusts not shown on this chart. Units are color coded for geologic period as indicated on left margin of chart.

The plate tectonic setting of the Antler orogeny has been variously interpreted as continent-continent collision, continent-arc collision, backarc thrusting, and polarity reversal of a subduction zone (e.g., Nilsen and Stewart, 1980; Speed and Sleep, 1982;

Dickinson et al., 1983). The RMA is often interpreted as an accretionary prism formed due to plate convergence at the continental margin (Speed and Sleep, 1982; Oldow, 1984; Dickinson, 2000).

Evidence for Antler-age tectonism has been reported along the western Laurentian margin, in Alaska and Canada (e.g., Nilsen and Stewart, 1980; Gehrels and Smith, 1987; Dusel-Bacon et al., 2006; Nelson et al., 2006; Paradis et al., 2006; Piercey et al., 2006; Colpron et al., 2007). Middle to Late Devonian continental arc magmatism occurred in the Alaska Range and central Yukon (Piercey et al., 2006) (Fig. 8). Upper Devonian–Early Mississippian felsic igneous and metaigneous rocks record bimodal volcanism in east-central Alaska and the Yukon (Dusel-Bacon et al., 2006) (Fig. 8). In south-central British Columbia (Fig. 8), a Late Devonian continental arc and backarc developed (Paradis et al., 2006).

Colpron et al. (2007) and Colpron and Nelson (2009) have proposed a direct link between the Antler orogeny and coeval tectonism of western Laurentia. They propose that a “Northwest Passage” opened in mid-Paleozoic time between Laurentia and Siberia, and a Scotia-style arc developed along the northern Laurentian margin in the Early Devonian (Fig. 10). The Alexander terrane, and other fragments such as the eastern Klamath and northern Sierran terranes, were transported from a Baltica origin to northwestern Laurentia through the Northwest Passage via the westward migration of the arc’s subduction zone (Fig. 10). By Middle Devonian time, a sinistral transform fault developed at the southern end of this passage and extended southward along western Laurentia. This system transported these terranes and fragments south along the margin. Colpron and Nelson (2009) note progressively younger deformation southward along the

Laurentian margin, from Alaska and the Yukon to Nevada, and suggest that this records the southward propagation of the transpressional system. They propose that this fault system could have provided the weakness along which Devonian subduction initiated.

b. **Roberts Mountains Allochthon Strata**

The RMA strata sampled (Figs. 9 and 11; Table 2) are arenite beds within units that are predominantly chert and argillite with some limestone and mafic volcanic rocks. Most contacts between and within units are structural, and the stratigraphic bases and tops of units are not known. The strata of the RMA are described briefly below, as evidence of their depositional environments.

Sample Location UTM: NAD 83	Easting	Northing
Ordovician Snow Canyon Formation Snow Canyon; Independence Mtns	0579760	4585698 *(UTM 11T)*
Ordovician lower Vinini Formation Petes Summit; Toquima Range	0518089	4337111 *(UTM 11S)*
Ordovician McAfee Quartzite McAfee Peak; Independence Mtns	0590637	4599583 *(UTM 11T)*
Ordovician upper Vinini Formation Petes Summit; Toquima Range	0518089	4337111 *(UTM 11S)*
Silurian Elder Sandstone Elder Creek; Shoshone Range	0516196	4460270 *(UTM 11T)*
Devonian Slaven Chert Slaven Canyon; Shoshone Range	0519428	4479302 *(UTM 11T)*

Table 2: Locations of samples analyzed in this study referenced to UTM locations.

The Snow Canyon Formation and the McAfee Quartzite in the Independence Mountains (Figs. 9 and 11; Table 2) are the equivalent of the upper Vinini and Valmy formations, respectively (Holm-Denoma et al., 2011). Both units are Middle Ordovician

based on graptolite fauna (Churkin and Kay, 1967). The Snow Canyon Formation is predominantly chert with arenite, shale, and siltstone layers, and basaltic lavas with interbedded limestone (Churkin and Kay, 1967). The McAfee Quartzite is predominantly massive cliff-forming quartzite with intervals of shale and siltstone and bedded chert (Churkin and Kay, 1967). The arenite intervals in these formations are interpreted as turbidites (Miller and Larue, 1983).

The Vinini Formation (Figs. 9 and 11; Table 2) was first mapped in the Roberts Mountains by Merriam and Anderson (1942) along Vinini Creek. Merriam and Anderson (1942) recognized two informal units (upper and lower) based on lithology and graptolite fauna and described the extreme structural disruption of these rocks. In later work, Noble and Finney (1999) used precise radiolarian biostratigraphy to demonstrate a high degree of structural imbrication both within the Vinini Formation and within Devonian cherts. In the Toquima Range, near Petes Summit (Fig. 9), the Vinini Formation is divided into two informal units (upper and lower), which are mapped in depositional contact, and the extreme structural complexity and repetition of thrust slices is also mapped (McKee, 1976). We observed the depositional contact at Petes Summit, where the quartz arenite of the upper Vinini rests on shale of the lower Vinini. The lower Vinini Formation is predominantly quartz arenite, with siltstone, shale, chert, and limestone (Finney et al., 1993). The lower Vinini Formation is Upper Lower to Lower Middle Ordovician in age, based on graptolite and conodont fauna (Finney et al., 1993). The arenite intervals in the lower Vinini Formation are interpreted as turbidites (Finney et al., 1993). The upper Vinini Formation is predominantly shale and bedded chert, with some siltstone and arenite (Finney et al., 1993). The unit is Middle Middle to Upper Ordovician, based on

graptolites and conodonts (Finney et al., 1993). Graptolites and conodonts of the lower Vinini Formation are similar to those found in coeval Laurentian shelf carbonate deposits (Finney and Ethington, 1992; Finney, 1998). At Petes Summit, we observed low-angle cross lamination and hummocky cross stratification in the arenite of the upper Vinini Formation. We therefore interpret the upper Vinini as having been deposited in a high-energy environment at a depth above storm wave base on the continental shelf and probably at less than 100 m depth.

The Elder Sandstone (Figs. 9 and 11; Table 2) is predominantly fine-grained sandstone and siltstone, with some cherty shale and quartzite (Gilluly and Gates, 1965). Fossils are sparse in the unit; the age is Lower Silurian based on graptolites (Gilluly and Gates, 1965). The Elder Sandstone is interpreted as a turbidite deposit (Madrid, 1987).

The Slaven Chert (Figs. 9 and 11; Table 2) is predominantly black, bedded chert with shale beds and some limey sandstone and siltstone (Gilluly and Gates, 1965). The unit is Middle Devonian based on a variety of fossils (Gilluly and Gates, 1965). The arenite intervals in the Slaven Chert are interpreted as turbidites (Madrid, 1987).

4. Methods

Zircon grains from six arenite samples were analyzed for U-Pb ages and Hf isotope ratios (Figs. 9 and 11; Table 2). A small number of zircon grains from these samples were previously analyzed for U-Pb ages by Gehrels et al. (2000a), using ID-TIMS (Fig. 5). Zircon grains were separated and analyzed at the University of Arizona LaserChron facility using standard techniques described by Gehrels and Pecha (2014) to yield a best age distribution reflective of the true distribution of detrital zircon ages in each sample.

Approximately 200 randomly selected grains were analyzed in each sample for U-Pb ages. Approximately 50 of these grains were subsequently analyzed for Hf isotopes. Hf analyses were conducted on top of the pits left after U-Pb analysis, to ensure that Hf isotope data were collected from the same domain as the U-Pb age. Analyses were conducted by LA-ICPMS using the Photon Machines Anlyte G2 excimer laser connected to the Nu Plasma high-resolution inductively coupled plasma-mass spectrometer, using methods identical to those described by Gehrels and Pecha (2014).

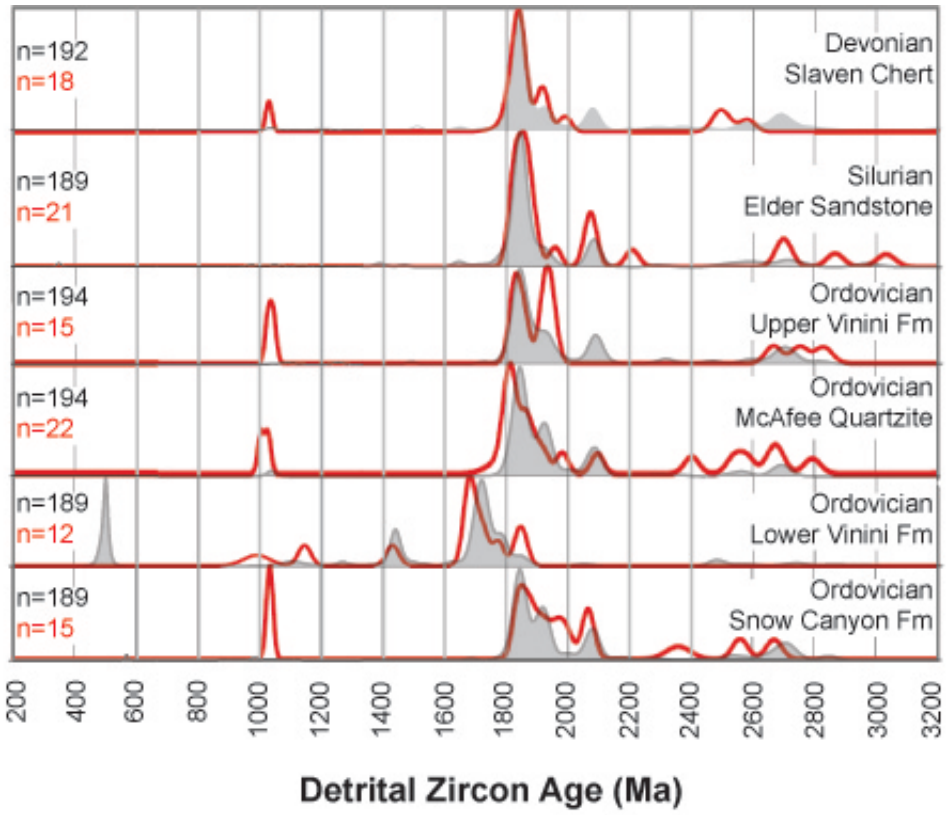

Figure 12. Normalized probability plots showing U-Pb ages of strata sampled. Red lines show the data from isotope-dilution thermal ionization mass spectrometry (Gehrels et al., 2000a); grayfilled curves are the data from laser-ablation inductively coupled plasma mass spectrometry (this study). Numbers of grains analyzed are shown (n =).

a. Uranium-Lead Geochronology

Analytical results are displayed graphically on normalized probability plots (Figs. 12 and 13), which allow visual comparison between zircon populations. U-Pb geochronology results are displayed in Figure 12, which contains both data from the original ID-TIMS analyses of these samples (Gehrels et al., 2000a) and the LA-ICPMS analyses of the current study, and in Figure 13, which displays the U-Pb results and Hf isotope analyses of the current study on the same chart. The essential U-Pb isotope information and ages are reported in Appendix C.

We compared detrital zircon age distributions both visually and statistically. Our initial appraisal was visual comparison of the probability plots. We also compared age distributions using the Kolmogorov-Smirnov (K-S) statistic (Guynn and Gehrels, 2006) (Table 3). The K-S statistic calculates whether a statistically significant difference exists between two distributions. $P<0.05$ indicates >95% probability that two U-Pb distributions are not the same. The K-S statistic is sensitive to proportions of ages present, and a low-P value may indicate that the proportions of age peaks are different, even though the ages are similar (Gehrels, 2012).

b. Hafnium Isotope Analysis

Hafnium isotope data are shown on Hf-evolution diagrams (Fig. 13) that display epsilon Hf(t) (eHf(t)) values at the time of crystallization. The essential Hf isotope information is reported in Appendix D.

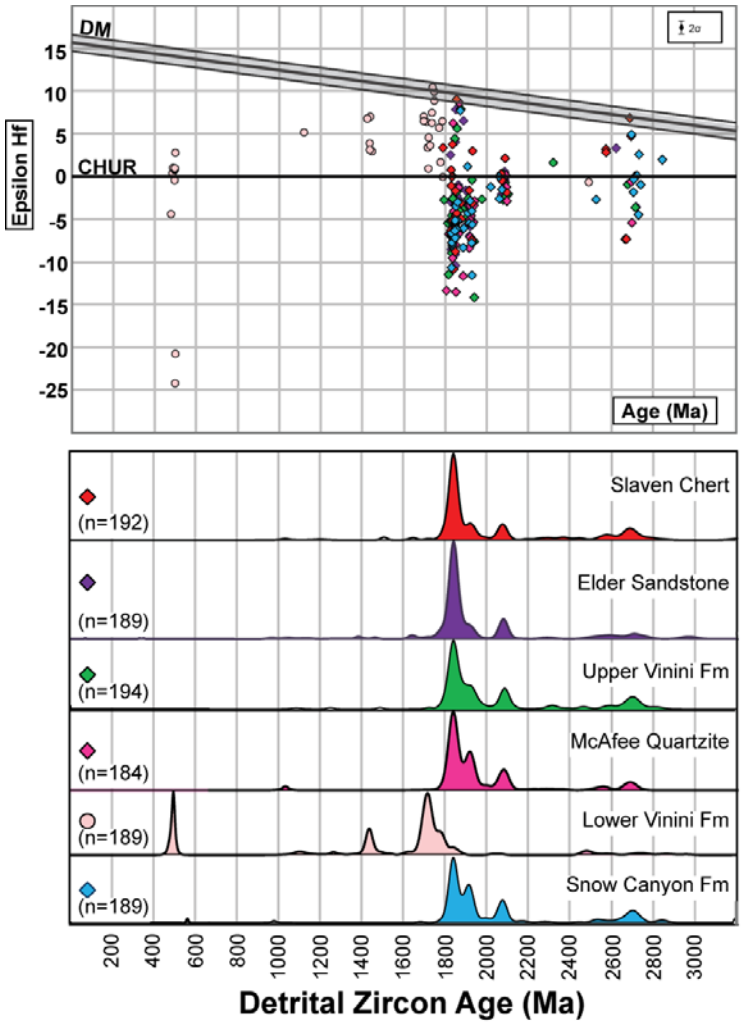

Figure 13. U-Pb ages and Hf isotope data for Roberts Mountains allochthon strata. U-Pb dates were run for all sample grains; approximately one-fourth of these grains were analyzed for hafnium isotopes. The upper graph shows εHf(t) (epsilon Hf) values for each sample. The average measurement uncertainty for all hafnium analyses is shown in the upper right at the 2σ of the values. Reference lines on the Hf plot are as follows: Depleted mantle (DM) is calculated using 176Hf/177Hf =0.283225; 176Lu/177Hf = 0.038513 (Vervoort and Blichert-Toft, 1999); CHUR—chondritic uniform reservoir, is calculated using 176Hf/177Hf = 0.282785 and 176Lu/177Hf = 0.0336 (Bouvier et al., 2008).

	Slaven Chert	Elder Sandstone	Valmy Formation	Upper Vinini Formation	McAfee Quartzite	Snow Cyn Formation	Eureka Quartzite	Kinnikinic Quartzite	Mt Wilson Formation
Slaven Chert		0.130	0.156	0.402	0.103	0.069	0.064	0.239	0.010
Elder Sandstone	0.130		0.001	0.001	0.013	0.000	0.000	0.000	0.000
Valmy Formation	0.156	0.001		0.330	0.018	0.458	0.118	0.010	0.050
Upper Vinini Formation	0.402	0.001	0.330		0.203	0.872	0.748	0.307	0.348
McAfee Quartzite	0.103	0.013	0.018	0.203		0.318	0.433	0.990	0.020
Snow Canyon Formation	0.069	0.000	0.458	0.872	0.318		0.786	0.313	0.200
Eureka Quartzite	0.064	0.000	0.118	0.748	0.433	0.786		0.948	0.768
Kinnikinic Quartzite	0.239	0.000	0.010	0.307	0.990	0.313	0.948		0.104
Mt Wilson Formation	0.010	0.000	0.050	0.348	0.020	0.200	0.768	0.104	

Table 3: K-S statistical analysis results. The RMA strata are shown with green highlights, and the passive margin strata are shown with blue highlights. Comparisons between units with values greater than 0.05 are highlighted in yellow. $P<0.05$ indicates >95% probability that two U-Pb distributions are not the same.

5. Results: U-Pb Ages and Hf Isotope Ratios

Although the ID-TIMS data (Gehrels et al., 2000a) are similar to the new LA-ICPMS data (Fig. 12), there are variations in the proportions of age groups. The two studies used different grain-selection procedures. For the ID-TIMS study, zircon crystals were selected from color and morphology groups, without regard to the number of grains in each group. For our LA-ICPMS study, we attempted to select grains at random from the entire population of grains. This procedure resulted in a more representative age distribution because the grains are chosen randomly. The results and interpretations that follow are all based upon LA-ICPMS ages from our current study.

U-Pb geochronology and Hf isotope analyses reveal that the RMA strata are in two distinct groups. Five of the six samples (the Snow Canyon Formation, the McAfee Quartzite, the upper Vinini Formation, the Elder Sandstone, and the Slaven Chert) yield similar U-Pb age spectra, while the remaining sample, the lower Vinini Formation, yields significantly different U-Pb age spectra (Figs. 12 and 13). The Hf data from the five samples with similar U-Pb ages are similar, while the lower Vinini Formation sample, because of its different age spectra, yields significantly different Hf ratios (Fig. 13).

6. Provenance of the Roberts Mountains Allochthon

To interpret provenance, we compared the data from our study to known U-Pb ages and Hf isotope data from Laurentian basement provinces and other sedimentary units.

a. Provenance of the Roberts Mountains Allochthon Exclusive of the Lower Vinini

The detrital zircon age spectra of the Snow Canyon Formation, the McAfee Quartzite, the upper Vinini Formation, the Elder Sandstone, and the Slaven Chert are consistent with provenance in the Peace River Arch (PRA) region of western Canada (Fig. 14). The 1820–1960 Ma grains are similar in age to magmatic arcs in the PRA region, including the Fort Simpson, the Rimbey, the Ksituan, and the Great Bear arcs (Hoffman, 1989; Ross, 1991; Villeneuve et al., 1993) (Fig. 14). The 2060–2120 Ma grains are similar in age to accreted terranes in the PRA region, including the Buffalo Head and Chincaga terranes (Hoffman, 1989; Ross, 1991; Villeneuve et al., 1993) (Fig. 14). The 2650–2750 Ma grains are similar in age to Archean terranes in the PRA region, including the Nova and Hearne terranes (Hoffman, 1989; Ross, 1991; Villeneuve et al., 1993) (Fig. 14).

The Hf isotope data are consistent with provenance in the PRA region. The 1820–1960 Ma grains have a wide range of values, from juvenile and moderately juvenile through evolved (eHf(t) +10 to –15), similar to those of other units interpreted to originate in the PRA region (Gehrels and Pecha, 2014). The 2060–2120 Ma grains are more narrowly grouped, with moderately juvenile to evolved values of eHf(t) +3 to –6, compatible with other units originating in the PRA region (Gehrels and Pecha, 2014).

The 2560–2750 Ma grains have juvenile, moderately juvenile, and evolved values of eHf(t) +6 to –15, also compatible with PRA origin (Gehrels and Pecha, 2014). The ages of basement terranes that comprise the PRA region (Fig. 7) are all represented in the age spectra of the RMA samples (exclusive of the lower Vinini Formation).

The detrital zircon U-Pb ages and Hf isotope data from these RMA strata are similar to selected passive margin strata and RMA strata analyzed in other studies (Fig. 15). The RMA strata sampled in this study (exclusive of the lower Vinini) have U-Pb age spectra similar to those of the Ordovician Valmy Formation of the RMA (Gehrels and Pecha, 2014), as well as the Eureka Quartzite and the Mount Wilson Formation (Gehrels and Pecha, 2014), and the Kinnikinic Quartzite (Barr, 2009), Ordovician units of the western Laurentian passive margin (Figs. 15 and 16). The K-S analyses of the RMA and the Ordovician passive margin units discussed above do not contradict our interpretation that the RMA strata have a common provenance with the Ordovician passive margin sandstones (Table 3). These RMA strata also show similar Hf isotope ratios to the Valmy Formation (Gehrels and Pecha, 2014) and to the Eureka Quartzite and the Mount Wilson Formation (Gehrels and Pecha, 2014) (Fig. 15).

The Peace River Arch region of western Canada is the source for the RMA units in this study, exclusive of the lower Vinini Formation, and for the Ordovician passive margin sandstones. The Peace River Arch region was an uplifted region from late Neoproterozoic through Middle Devonian time (Cant, 1988; Cant and O'Connell, 1988; Cecile et al., 1997). Igneous bodies in the PRA region have ages similar to the U-Pb ages of zircons in the RMA rocks sampled (Figs. 14 and 15). The U-Pb age spectra of the RMA rocks sampled are not consistent with derivation from the central Laurentian

craton; the Yavapai-Mazatzal terranes are 1.6–1.8 Ga and cannot serve as a source of the 1.8–2.0 Ga grains in the samples.

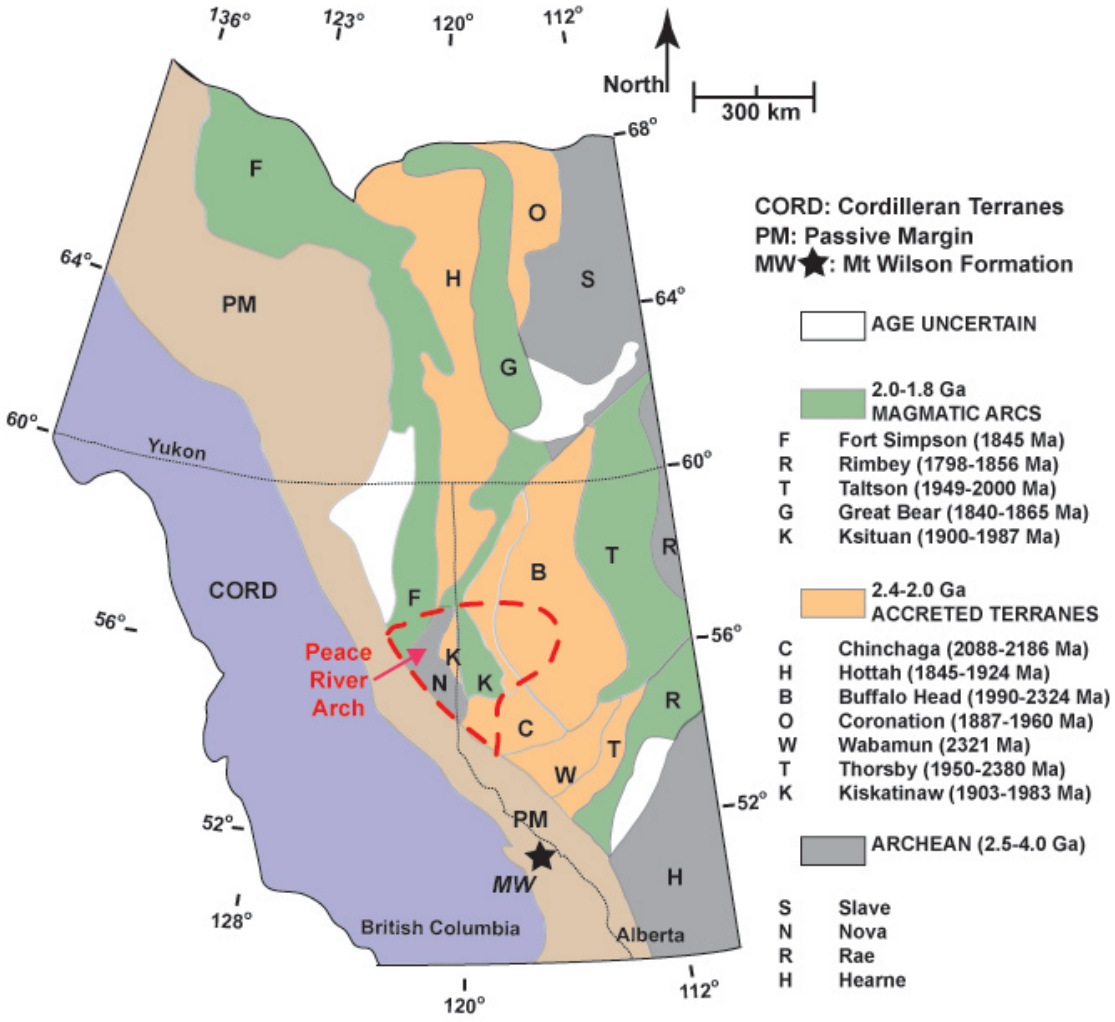

Figure 14. Map of western Canada showing the Cordilleran accreted terranes, the Cordilleran passive margin, and the basement provinces of the Canadian Shield. The Peace River Arch region is outlined by the red dashed line. The location of the Mount Wilson Formation sample (Gehrels and Pecha, 2014) is shown. The map is after Gehrels and Ross (1998); the basement provinces are compiled from Hoffman (1989), Ross (1991), and Villeneuve et al. (1993). WY Wyoming province; HE— Hearn province; SU—Superior province; CORD—Cordilleran; APP—Appalachian; OA—Ouachita-Marathon; MOJ—Mojavia.

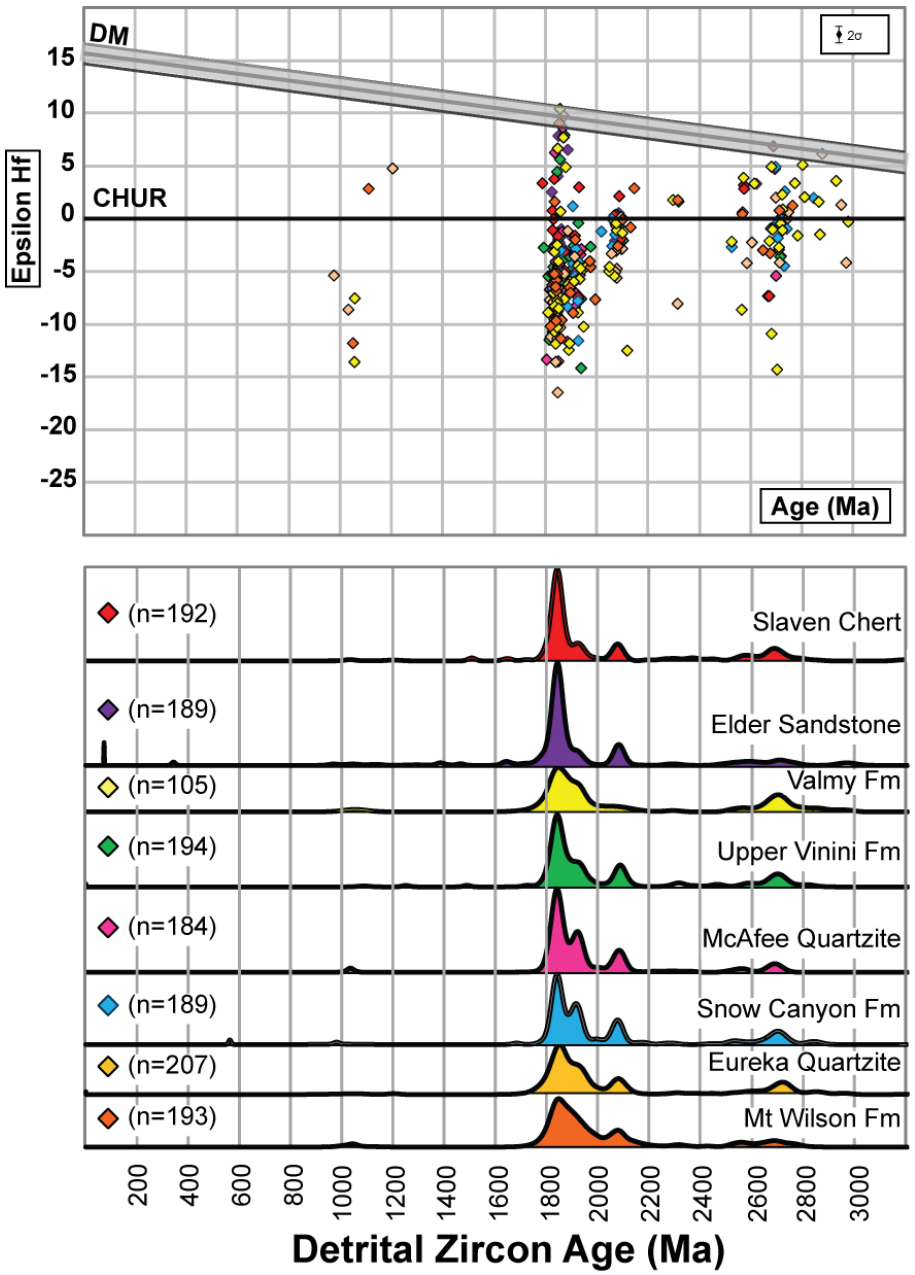

Figure 15. U-Pb ages and Hf isotope data of RMA and coeval passive margin strata. The data from the Mount Wilson Formation, the Eureka Quartzite, and the Valmy Formation are from Gehrels and Pecha (2014). Diagrams and symbols are as in Figure 13.

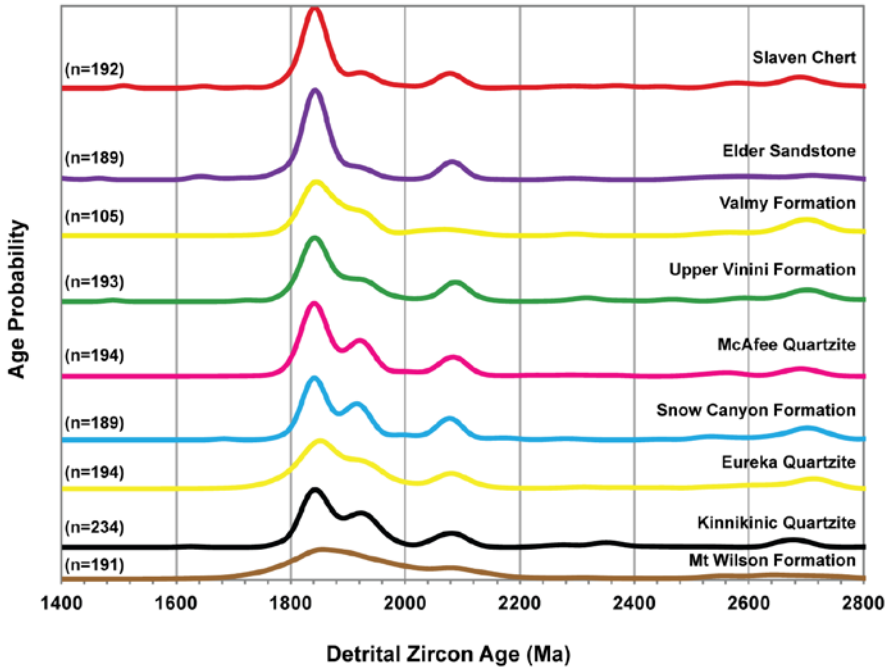

Figure 16. Normalized probability plot of Roberts Mountains allochthon (RMA) strata from this study, exclusive of the lower Vinini Formation. The plot includes the Valmy Formation of the RMA, analyzed by Gehrels and Pecha (2014). The plot also includes select Ordovician passive margin strata: the Mount Wilson Formation and Eureka Quartzite (Gehrels and Pecha, 2014) and the Kinnikinic Quartzite (Barr, 2009). No Hf isotope data are available for the Kinnikinic Quartzite, so only a normalized probability plot is shown.

b. Provenance of the Lower Vinini Formation

The U-P age spectra of the lower Vinini Formation are consistent with provenance in north-central Laurentia. The 490–500 Ma grains are similar in age to plutonic suites in roof pendants and inliers within the Challis volcanic-plutonic complex and the Idaho batholith (Lund et al., 2010). The 1110–1120 Ma grains are consistent with the Grenville orogen; the 1420 Ma grains are consistent with the central Laurentian anorogenic granites; the 1660–1800 Ma grains are consistent with the Yavapai-Mazatzal terranes; and the 2470–2750 Ma grains are consistent with the Archean craton (Bickford et al., 1986; Hoffman, 1989; Ross, 1991; Anderson and Morrison, 1992; Bickford and

Anderson, 1993; Van Schmus et al., 1993) (Fig. 8). River systems traversing the north-central craton from east to west transported sediments from these crystalline bedrock sources—or from sediments recycled from them—and subsequently deposited them off the western Laurentian margin as the lower Vinini Formation.

The Hf isotope data of the lower Vinini grains are also consistent with origin in north-central Laurentia. The 490–500 Ma grains have mostly moderately juvenile to evolved values (eHf(t) +3 to –5), with two grains highly evolved (eHf(t) –20 to –25). The moderately juvenile to evolved grains are compatible with the plutonic suites in Idaho; however, the highly evolved grains are unlike any analyzed in these suites (Todt and Link, 2013). The 1110–1120 Ma grains have moderately juvenile values (eHf(t) +4 to +6), similar to those of the Grenville orogen (Mueller et al., 2008; Bickford et al., 2010). The 1420 Ma grains have juvenile to moderately juvenile values (eHf(t) +7 to +3), compatible with the anorogenic granitoids of the mid-Laurentian craton (Goodge and Vervoort, 2006). The 1660–1800 Ma grains have juvenile to moderately juvenile values (eHf(t) +10–0), similar to the Yavapai-Mazatzal terranes (Bickford et al., 2008). The 2470–2750 Ma grains have moderately juvenile to evolved values (eHf(t) +6 to –6), compatible with those in northern Greenland and Arctic Canada (Rohr et al., 2008, 2010) (Fig. 8).

The Early Cambrian uplift of the Transcontinental Arch altered the drainage patterns in western Laurentia; this change is recorded in the changing detrital zircon age patterns between upper Neoproterozoic and Lower Cambrian passive margin strata (Linde et al., 2014, and references cited therein) (Fig. 17). The uplift of the arch blocked the transport of Grenville-age grains and created, on the west flank of the arch itself, a new highland

and source of sand, consisting of Yavapai-Mazatzal basement rocks and sedimentary rocks recycled from this basement. In many older passive margin strata that predate the uplift of the arch, Grenville-age grains predominate (Fig. 17). These grains were transported by continent-spanning rivers that drained the central cratonand Grenville orogenic terrane to the western Laurentian margin through the late Neoproterozoic (Rainbird et al., 1997, 2012). In many younger passive margin strata, deposited after the uplift of the arch, Yavapai-Mazatzal–age grains dominate (Fig. 17). Rivers originating in the central craton were blocked from flowing to the west by the uplifted arch, which blocked the transport of many Grenville-age grains (Amato and Mack, 2012; Gehrels and Pecha, 2014; Linde et al., 2014; Yonkee et al., 2014).

The detrital zircon U-Pb ages and Hf isotope data of the lower Vinini Formation resemble those of the younger, post–Transcontinental Arch uplift, passive margin strata, such as the Geersten Quartzite of Utah and the Osgood Mountains Quartzite of Nevada (Fig. 18). These are the only post–arch uplift passive margin data sets for which we have both U-Pb ages and Hf isotope data. The lower Vinini Formation U-Pb age spectra and Hf isotope ratios are similar to those of the younger passive margin strata. The provenance of the lower Vinini Formation is central Laurentian, shed from the western flanks of the Transcontinental Arch and the regions to the west of the arch, after the uplift of the arch (Fig 8).

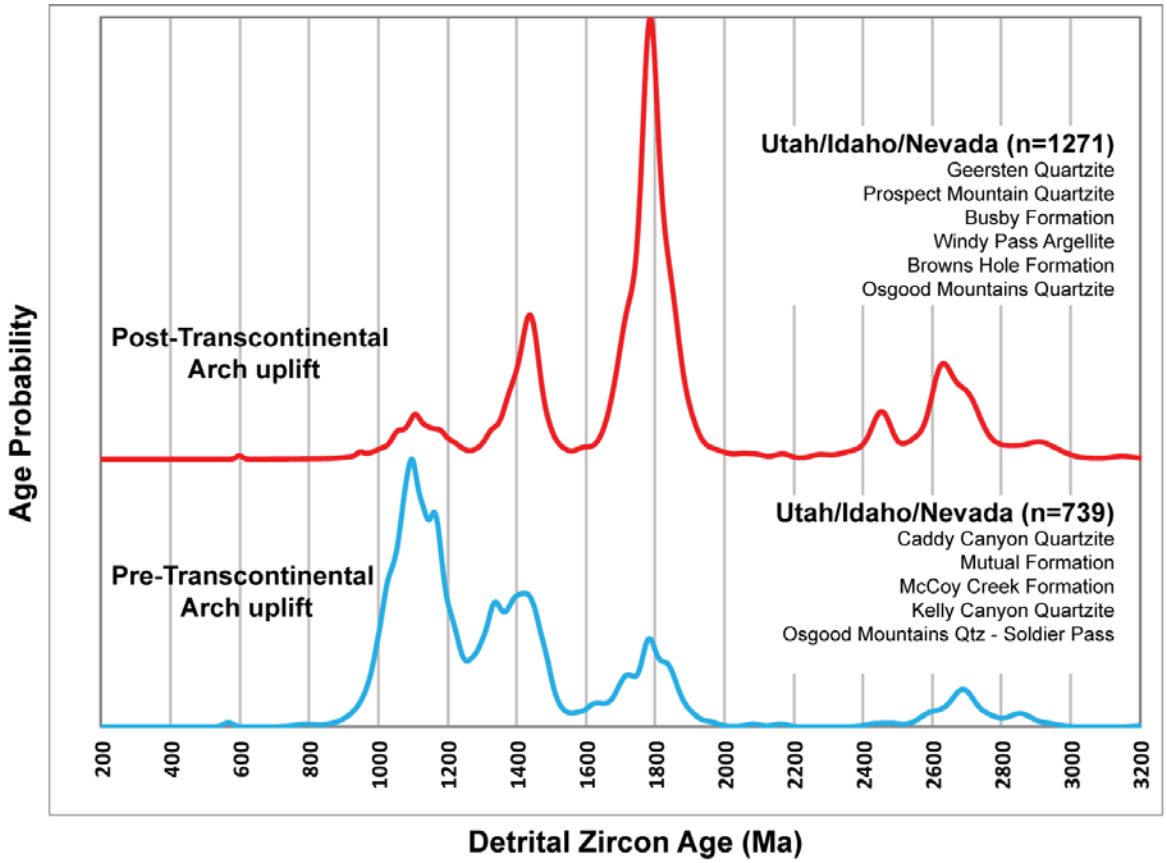

Figure 17. Compilation plots of units showing the distribution of detrital zircon ages in upper Neoproterozoic–Cambrian western Laurentian passive margin units (after Linde et al., 2014). The upper curve (red) is a compilation of ages of the relatively younger strata throughout the region. The lower curve (blue) is a compilation of ages of the relatively older strata throughout the region. The curves are normalized probability plots. The number of detrital zircon grains comprising each compilation is shown on the right. Osgood Mountains Quartzite (Linde et al., 2014); Kelley Canyon Quartzite, Caddy Canyon Quartzite, Brown's Hole Formation, Geersten Canyon Quartzite, Mutual Formation, Prospect Mountain Quartzite, McCoy Creek Group,
Busby Formation, and Windy Pass Argillite (Yonkee et al., 2014); Kelley Canyon Quartzite, Caddy Canyon Quartzite, Mutual Formation, and Prospect Mountain Quartzite (Lawton et al., 2010).

7. Discussion: Sedimentology and Paleogeographic Implications

Sedimentological analyses provide a further constraint and suggest that the Ordovician passive margin sandstones are not the source of the RMA strata, but rather that these strata have a common source. Finney and Perry (1991) proposed that the Eureka

Quartzite (an extensive Ordovician passive margin unit) was the source of the sandstones in the younger sections of the Vinini and Valmy formations of the RMA. However, the grains of the Ordovician passive margin sandstones are more texturally mature than those of the RMA strata, whose grains are coarser, larger, and more poorly sorted (Ketner, 1966). The more mature shelf sands such as the Eureka Quartzite and Mount Wilson Formation could not be the source of the more immature RMA sandstones. The RMA and passive margin sandstones have similar U-Pb age spectra and Hf isotope ratios (Fig. 14) and share a common source in the PRA region.

The Ordovician passive margin sands and the RMA strata sampled have different depositional histories (Fig. 19). The Mount Wilson Formation was deposited in a nearshore to shelf environment immediately outboard of the Peace River Arch (Kent, 1994). Other Ordovician passive margin sandstones, now preserved as the Eureka Quartzite and the Kinnikinic Quartzite, were shed from the Peace River Arch, and subsequently moved southward along the western Laurentian margin via longshore transport to the depositional basin (Ketner, 1968) (Fig. 19B). The evidence for this transport is that grain size decreases and sorting improves in Ordovician arenites from near the PRA source (the Mount Wilson Formation) southward through Idaho (the Kinnikinic Quartzite) and into Nevada and California (the Eureka Quartzite) (Ketner, 1968). The texturally immature arenites of the RMA did not undergo the extensive reworking of this longshore transport. Sediments of the RMA strata, other than the lower Vinini Formation, were deposited as turbidites (Miller and Larue, 1983; Madrid, 1987; Finney et al., 1993) offshore of the Peace River Arch (Figs. 19A–19C). To reach their current geographic location, the RMA strata were *tectonically* transported south along the

western Laurentian margin, in Latest Devonian time (Fig. 19E). This is consistent with a sinistral transpressional fault system, as proposed by Colpron and Nelson (2009) (Figs. 19D and 19E). Subsequent shortening moved the RMA up onto the craton in the Antler orogeny of Latest Devonian–Earliest Mississippian time (Figs. 19E and 19F).

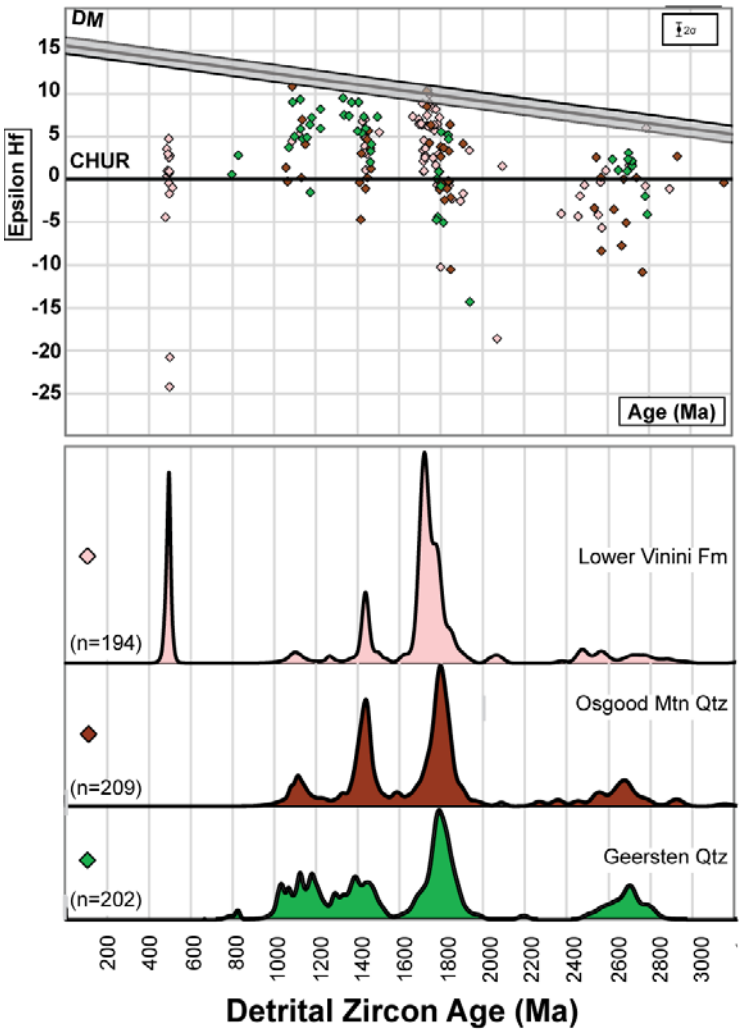

Figure 18. U-Pb ages and Hf isotope data for Roberts Mountains allochthon (RMA) and select Laurentian passive margin strata. The data from the Osgood Mountains Quartzite and the Geersten Canyon Quartzite are from Gehrels and Pecha (2014). The lower Vinini data includes those from this study (n = 189) and from Gehrels and Pecha (2014) (n = 105). Diagrams and symbols are as in Figure 13.

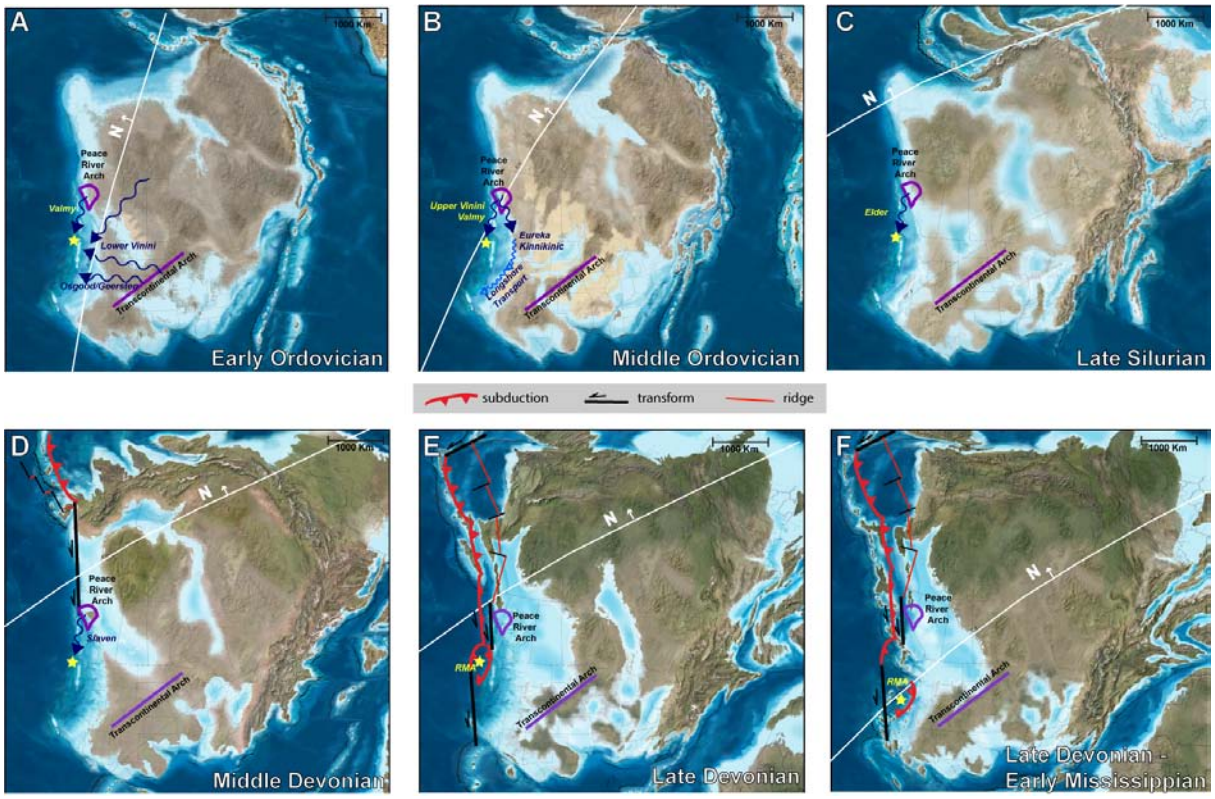

Figure 19. Paleogeographic maps of Laurentia from Middle Ordovician through Mississippian time (Blakey, 2013). Stars represent the depositional basin of Roberts Mountains allochthon (RMA) strata. White lines show the approximate position of the paleoequator. Blue wavy lines show approximate depositional pathways of units discussed. Transcontinental Arch (Sloss, 1988) and Peace River Arch (Ross, 1991) are superimposed. (A) Early Ordovician time. The lower Vinini is derived from the central craton and Transcontinental Arch; the Valmy Formation is derived from the Peace River Arch. (B) Middle Ordovician time. The upper Vinini and Valmy formations are shed from the Peace River Arch into an oceanic basin. The Eureka Quartzite is also derived from the Peace River Arch and transported via longshore current along the western Laurentian margin. (C) Late Silurian time. The Elder Sandstone is shed from the Peace River Arch region. (D) Middle Devonian time. The Slaven Chert is derived from the Peace River Arch. A Scotia-style arc has moved to the western margin of northern Laurentia, and a sinistral transpressional fault system has developed along the western margin. RMA strata are tectonically transported south along the margin by this fault system. (E) Late Devonian time. Subduction has initiated along much of the western margin of Laurentia, moving the RMA strata onto the craton. (F) Early Mississippian time. The Antler orogeny has uplifted the RMA strata into a highland on the western Laurentian margin.

8. Conclusions

Sedimentological analyses provide a further constraint and suggest that the Ordovician passive margin sandstones are not the source of the RMA strata, but rather that these strata have a common source. Finney and Perry (1991) proposed that the Eureka Quartzite (an extensive Ordovician passive margin unit) was the source of the sandstones in the younger sections of the Vinini and Valmy formations of the RMA. However, the grains of the Ordovician passive margin sandstones are more texturally mature than those of the RMA strata, whose grains are coarser, larger, and more poorly sorted (Ketner, 1966). The more mature shelf sands such as the Eureka Quartzite and Mount Wilson Formation could not be the source of the more immature RMA sandstones. The RMA and passive margin sandstones have similar U-Pb age spectra and Hf isotope ratios (Fig. 14) and share a common source in the PRA region.

The Ordovician passive margin sands and the RMA strata sampled have different depositional histories (Fig. 19). The Mount Wilson Formation was deposited in a nearshore to shelf environment immediately outboard of the Peace River Arch (Kent, 1994). Other Ordovician passive margin sandstones, now preserved as the Eureka Quartzite and the Kinnikinic Quartzite, were shed from the Peace River Arch, and subsequently moved southward along the western Laurentian margin via longshore transport to the depositional basin (Ketner, 1968) (Fig. 19B). The evidence for this transport is that grain size decreases and sorting improves in Ordovician arenites from near the PRA source (the Mount Wilson Formation) southward through Idaho (the

Kinnikinic Quartzite) and into Nevada and California (the Eureka Quartzite) (Ketner, 1968). The texturally immature arenites of the RMA did not undergo the extensive reworking of this longshore transport. Sediments of the RMA strata, other than the lower Vinini Formation, were deposited as turbidites (Miller and Larue, 1983; Madrid, 1987; Finney et al., 1993) offshore of the Peace River Arch (Figs. 19A–19C). To reach their current geographic location, the RMA strata were *tectonically* transported south along the western Laurentian margin, in Latest Devonian time (Fig. 19E). This is consistent with a sinistral transpressional fault system, as proposed by Colpron and Nelson (2009) (Figs. 19D and 19E). Subsequent shortening moved the RMA up onto the craton in the Antler orogeny of Latest Devonian–Earliest Mississippian time (Figs. 19E and 19F).

9. References cited

Amato, J.M., and Mack, G.H., 2012, Detrital zircon geochronology from the Cambrian-Ordovician Bliss Sandstone, New Mexico: Evidence for contrasting Grenville-age and Cambrian sources on opposite sides of the Transcontinental Arch: Geological Society of America Bulletin, v. 124, p. 1826-1840.

Anderson, J.L., and Morrison, J., 1992, The role of anorogenic granites in the Proterozoic crustal development of North America, *in* Condie, K.C., ed., Proterozoic Crustal Evolution: New York, Elsevier, p. 263-299.

Bahlburg, H., Vervoort, J.D., DuFrane, S.A., Carlotto, V., Reimann, C., and Cardenas, J., 2011, The U–Pb and Hf isotope evidence of detrital zircons of the Ordovician Ollantaytambo Formation, southern Peru, and the Ordovician provenance and paleogeography of southern Peru and northern Bolivia: Journal of South American Earth Sciences, v. 32, p. 196–209.

Barr, E.E., 2009, Determining the regional-scale detrital zircon provenance of the Middle-Late Ordovician Kinnikinic (Eureka) Quartzite, east-central Idaho, U.S. [Master's thesis]: Pullman, Washington, Washington State University, 134 p.

Bickford, M.E., and Anderson, J.L., 1993, Middle Proterozoic magmatism, in Reed, J.C., Bickford, M.E., Houston, R.S., Link, P.K., Rankin, D.W., Sims, P.K., and Van Schmus, W.R., eds., Precambrian Conterminous U.S.: Boulder, Colorado, Geological Society of America, The Geology of North America, v. C-2, p. 281–292.

Bickford, M.E., Van Schmus, R., and Zietz, I., 1986, Proterozoic history of the midcontinent region of North America: Geology, v. 14, no. 6, p. 492–496.

Bickford, M.E., Mueller, P.A., Kamenov, G.D., and Hill, B.M., 2008, Crustal evolution of southern Laurentia during the Paleoproterozoic: Insights from zircon isotopic studies of ca. 1.75 Ga rocks in central Colorado: Geology, v. 36, p. 555–558.

Bickford, M.E., McLelland, J.M., Mueller, P.A., Kamenov, G.D., and Neadle, M., 2010, Hafnium isotopic compositions of zircon from Adirondack AMCG suites: Implications for the petrogenesis of anorthosites, gabbros, and granitic members of the suites: Canadian Mineralogist, v. 48, p. 751–761.

Blakey, R., 2013, Key Time Slices of North American Geologic History: cpgeosystems.com/nam.html

Bouvier, A., Vervoort, J.D., and Patchett, J.D., 2008, The Lu-Hf and Sm-Nd isotopic composition of CHUR: Constraints from unequilibrated chondrites and implications

for the bulk composition of terrestrial planets: Earth and Planetary Science Letters, v. 273, p. 48–57.

Burchfiel, B.C., and Davis, G.A., 1972, Structural framework and evolution of the southern part of the Cordilleran orogen, western United States: American Journal of Science, v. 272, p. 97-118.

Burchfiel, B.C., Cowan, D.S., and Davis, G.A., 1992, Tectonic overview of the Cordilleran orogen in the western United States, *in* Burchfiel, B.C., Lipman, P.W., and Zoback, M.L., eds., The Cordilleran Orogen: Conterminous U.S.: Boulder, Colorado, Geological Society of America, The Geology of North America, v. G-3, p. 407–480.

Cant, D. J., 1988, Regional structure and development of the Peace River Arch, Alberta: A Paleozoic failed-rift system?: Bulletin of Canadian Petroleum Geology, v. 36, p. 284-295.

Cant, D. and O'Connell, S., 1988, The Peace River Arch: Its structure and origin, *in,* James, D.P. and Leckie, D.A., eds., Sequences, Stratigraphy, Sedimentology: Surface and Subsurface: Canadian Society of Petroleum Geologists, Memoir 15, p. 537-542.

Cecile, M.P., Morrow, D.W., and Williams, G.K., 1997, Early Paleozoic (Cambrian to Early Devonian) tectonic framework, Canadian Cordillera: Bulletin of Canadian Petroleum Geology, v. 45, p. 54-74.

Churkin, M., Jr., and Kay, M., 1967, Graptolite-bearing Ordovician siliceous and volcanic rocks, northern Independence Range, Nevada: Geological Society of America Bulletin, v. 78, p. 651-668.

Colpron, M., and Nelson, J., 2009, A Palaeozoic Northwest Passage: Incursion of Caledonian, Baltican and Siberian terranes into eastern Panthalassa, and the early evolution of the North American Cordillera, *in* Cawood, P.A., and Kroner, A., eds., Earth Accretionary Systems in Space and Time: Geological Society of London Special Publication 318, p. 273–307.

Colpron, M., Nelson, J.L., and Murphy, D.C., 2007, Northern Cordilleran terranes and their interactions through time: GSA Today, v. 17, p. 4–10.

Dickinson, W.R., 2000, Geodynamic interpretation of Paleozoic tectonic trends oriented oblique to the Mesozoic Klamath-Sierran continental margin in California, *in* Soreghan, M.J., and Gehrels, G.E., eds., Paleozoic and Triassic Paleogeography and Tectonics of Western Nevada and Northern California: Geological Society of America Special Paper 347, p.209-245.

Dickinson, W.R., 2006, Geotectonic evolution of the Great Basin: Geosphere, v. 2, p. 353-368.

Dickinson, W.R., and Lawton, T.F., 2001, Carboniferous to Cretaceous assembly and fragmentation of Mexico: Geological Society of America Bulletin, v. 113, p. 1142–1160.

Dickinson, W.R., and Gehrels, G.E., 2009, U-Pb ages of detrital zircons in Jurassic eolian and associated sandstones of the Colorado Plateau: Evidence for transcontinental dispersal and intraregional recycling of sediment: Geological Society of America Bulletin, v. 121, p. 408–433.

Dickinson, W.R., Harbaugh, D.W., Saller, A.H., Heller, P.L., and Snyder, W.S., 1983, Detrital modes of upper Paleozoic sandstones derived from Antler orogen in Nevada: Implications for the nature of the Antler orogeny: American Journal of Science. v. 282, p. 481-509.

Dusel-Bacon, C., Hopkins, M.J., Mortensen, J.K., Dashevsky, S.S., Bressler, J.R., and Day, W.C., 2006, Paleozoic tectonic and metallogenic evolution of the pericratonic rocks of east–central Alaska and adjacent Yukon, *in* Colpron, M., and Nelson, J.L., eds., Paleozoic Evolution and Metallogeny of Pericratonic Terranes at the Ancient Pacific Margin of North America, Canadian and Alaskan Cordillera: Geological Association of Canada, Special Paper 45, p. 25–74.

Evans, J.G., and Theodore, T.G., 1978, Deformation of the Roberts Mountains Allochthon in North-Central Nevada: U.S. Geological Survey Professional Paper 1060, 18 p.

Fedo, C.M., Sircombe, K., and Rainbird, R., 2003, Detrital zircon analysis of the sedimentary record, *in* Hanchar J.M., and Hoskin, P.W.O., eds., Zircon: Reviews in Mineralogy and Geochemistry, v. 53, p. 277–303.

Finney, S.C., 1998, The Laurentian affinity of the Roberts Mountains allochthon: Abstracts with Programs, Geological Society of America, v. 30, n. 7.

Finney, S.C., and Perry, B.D., 1991, Depositional setting and paleogeography of Ordovician Vinini Formation, central Nevada, *in* Cooper, J.D., and Stevens. C.H., eds., Paleozoic paleography of the western United States-II, Volume 2: Pacific Section, Society of Economic Paleontologists and Mineralogists book 67, p. 747-766.

Finney, S.C. and Ethington, R.L., 1992, Graptolite and conodont faunas in Ordovician Vinini Formation, Roberts Mountains, central Nevada, demonstrate that the Roberts Mountains allochthon is not an exotic terrane: Fifth North American Paleontological Convention, abstracts and program, Field Museum of Natural History, v. 6, p. 97.

Finney, S.C., Perry, B.D., Emsbo, P., and Madrid, R.J., 1993, Stratigraphy of the Roberts Mountains allochthon, Roberts Mountains and Shoshone Range, Nevada, *in* Lahren, M.M., Trexler, J.H., Jr., and Spinosa, C., eds., Crustal Evolution of the Great Basin

and Sierra Nevada: Cordilleran/Rocky Mountain Section, Geological Society of America Guidebook, p. 197-230.

Gehrels, G.E., 2000, Introduction to detrital zircon studies of Paleozoic and Triassic strata in western Nevada and northern California, in Soreghan, M.J., and Gehrels, G.E., eds., Paleozoic and Triassic Paleogeography and Tectonics of Western Nevada and Northern California: Geological Society of America Special Paper 347, p.1–17.

Gehrels, G.E., 2012, Detrital zircon U-Pb geochronology: Current methods and new opportunities, *in* Busby, C., and Azor, A., eds., Recent Advances in Tectonics of Sedimentary Basins: Hoboken, New Jersey, Blackwell Publishing, p. 47-62.

Gehrels, G.E., 2014, Detrital zircon U-Pb geochronology applied to tectonics: Annual Review of Earth and Planetary Sciences, v. 42, p. 127-149.

Gehrels, G.E., and Smith, M.T., 1987, "Antler" allochthon in the Kootenay arc?: Geology, v. 15, p. 769-770.

Gerhrels, G.E., and Dickinson, W.R., 1995, Detrital zircon provenance of Cambrian to Triassic miogeoclinal and eugeoclinal strata in Nevada: American Journal of Science, v. 295, p. 18-48.

Gehrels, G.E., and Ross, G.M., 1998, Detrital zircon geochronology of Neoproterozoic to Permian miogeoclinal strata in British Columbia and Alberta: Canadian Journal of Earth Sciences, v. 35, p. 1380–1401.

Gehrels, G.E., and Pecha, M., 2014, Detrital zircon U-Pb geochronology and Hf isotope geochemistry of Paleozoic and Triassic passive margin strata of western North America: Geosphere, v. 10, p. 49-65.

Gehrels, G.E., Dickinson, W.R., Riley, B.C.D., Finney, S.C., Smith, M.T., 2000a, Detrital zircon geochronology of the Roberts Mountains allochthon, Nevada, *in* Gehrels, G.E., and Soreghan, M.J., eds., Paleozoic and Triassic Paleogeography and Tectonics of Western Nevada and Northern California: Boulder, Colorado, Geological Society of America, Special Paper 347, p. 19–42.

Gehrels, G.E., and 13 others, 2000b, Tectonic implications of detrital zircon data from Paleozoic and Triassic strata in western Nevada and northern California, *in* Gehrels, G.E., and Soreghan, M.J., eds., Paleozoic and Triassic Paleogeography and Tectonics of Western Nevada and Northern California: Boulder, Colorado, Geological Society of America, Special Paper 347, p. 133–150.

Gehrels, G.E., Valencia, V.A., and Ruiz, J., 2008, Enhanced precision, accuracy, efficiency, and spatial resolution of U-Pb ages by laser ablation-multicollector-inductively coupled plasma-mass spectrometry: Geochemistry, Geophysics, Geosystems, v.9, p. 1-13.

Gehrels, G.E., Blakey, R., Karlstrom, K.E., Timmons, J.M., Dickinson, B., and Pecha, M., 2011, Detrital zircon U-Pb geochronology of Paleozoic strata in the Grand Canyon, Arizona: Lithosphere, v. 3, p. 183-200.

Gilluly, J., and Gates, O., 1965, Geology of the northern Shoshone Range, Nevada: U.S. Geological Survey Professional Paper 465, 153 p.

Goodge, J.W., and Vervoort, J.D., 2006, Origin of Mesoproterozoic A-type granites in Laurentia: Hf isotopic evidence: Earth and Planetary Science Letters, v. 243, p. 711–731.

Guynn, J., and Gehrels, G.E., 2006, Comparison of detrital zircon age distribution using the K-S test: online manual published by the University of Arizona LaserChron Center: https://docs.google.com/file/d/0B9ezu34P5h8eZWZmOWUzOTItZDgyZi00NDRiLWI4ZTctNTljNTM5OTU1MGUz/edit?hl=enandpli=1

Holm-Denoma, C.S., Hofstra, A.H., Noble, P.J., and Leslie, S.A., 2011, Paleozoic stratigraphy and kinematics of the Roberts Mountains allochthon in the Independence Mountains, northern Nevada: *in* Steininger, R. and Pennell, B., eds., Great Basin evolution and metallogeny, Geological Society of Nevada 2010 symposium, p. 1039-1054.

Hoffman, P.F., 1989, Precambrian geology and tectonic history of North America in Bally, A.W., and Palmer, A.R., eds., The Geology of North America—An Overview: Boulder, Colorado, Geological Society of America, The Geology of North America, v. A, p. 447–512.

Kay, M., 1951, North American geosynclines: Geological Society of America Memoir 48, 143 p.

Kent, D.M., 1994, Paleogeographic evolution of the cratonic platform—Cambrian to Triassic, *in* Mossop, G.D. and Shetsen, I., eds., Geological atlas of the Western Canadian sedimentary basin, p. 69-86.

Ketner, K.B., 1966, Comparison of Ordovician eugeosynclinal and miogeosynclinal quartzites of the Cordilleran geosyncline: U.S. Geological Survey Professional Paper 550-C, p. C54-C60.

Ketner, K.B., 1968, Origin of Ordovician quartzite in the Cordilleran miogeosyncline: U.S. Geological Survey Professional Paper 600-B, p. 69-177.

Lawton, T.F., Hunt, G.J., and Gehrels, G.E., 2010, Detrital zircon record of thrust belt unroofing in Lower Cretaceous synorogenic conglomerates, central Utah: Geology, v. 38, p. 463-466.

Linde, G.M., Cashman, P.H., Trexler, J.H., Jr., and Dickinson, W.R., 2014, Stratigraphic trends in detrital zircon geochronology of upper Neoproterozoic and Cambrian strata, Osgood Mountains, Nevada and elsewhere in the Cordilleran miogeocline: Evidence for early Cambrian uplift of the Transcontinental Arch: Geosphere, v. 10., p. 1402-1410.

Lund, K., Aleinikoff, J.N., Evans, K.V., duBray, E.A., Dewitt, E.H., and Unruh, D.M., 2010, SHRIMP U-PB dating of recurrent Cryogenian and Late Cambrian-Early Ordovician alkalic magmatism in central Idaho: Implication for Rodinian rift tectonics: Geological Society of America Bulletin, v. 122, p. 430-453.

Madrid, R.J., 1987, Stratigraphy of the Roberts Mountains allochthon in north-central Nevada [PhD dissertation]: Stanford, California, Stanford University, 336 p.

McKee, E.H., 1976, Geology of the northern part of the Toquima Range, Lander, Eureka, and Nye counties, Nevada: U.S. Geological Survey Professional Paper 931, 49 p.

Merriam, C.W., and Anderson, C.A., 1942, Reconnaissance survey of the Roberts Mountains, Nevada: Geological Society of America Bulletin, v. 53, p. 1675-1727.

Miller, E.L, and Larue, D.K., 1983, Ordovician quartzite in the Roberts Mountains allochthon, Nevada: Deep sea fan deposits derived from cratonal North America, *in* Stevens, C.H., ed., Pre-Jurassic rocks in western North American suspect terranes: Society of Economic Paleontologists and Mineralogists, Pacific Section, 1983 convention, p. 91-102.

Mueller, P.A., Kamenov, G.D., Heatherington, A.L., and Richards, J., 2008, Crustal evolution in the southern Appalachian orogen: Evidence from Hf isotopes in detrital zircons: The Journal of Geology, v. 116, p. 414–422.

Murphy, M.A., McKee, E.H., Winterer, E.L., Matti, J.C., and Dunham, J.B., 1978, Preliminary geologic map of the Roberts Creek Mountain quadrangle, Nevada: US Geological Survey Open-File Report 78-376, 2 sheets.

Nelson, J.L., Colpron, M., Piercey, S.J., Dusel-Bacon, C., Murphy, D.C., and Roots, C.F., 2006, Paleozoic tectonic and metallogenetic evolution of pericratonic terranes in Yukon, northern British Columbia and eastern Alaska, *in* Colpron, M. and Nelson, J.L., eds., Paleozoic Evolution and Metallogeny of Pericratonic Terranes at the Ancient Pacific Margin of North America, Canadian and Alaskan Cordillera: Geological Association of Canada, Special Paper 45, p. 323-360.

Nilsen, T.H., and Stewart, J.H., 1980, The Antler orogeny-Mid-Paleozoic tectonism in western North America (Penrose Conference Report): Geology, v. 8. p. 298-302.

Noble, P.J., and Finney, S.C., 1999, Recognition of fine-scale imbricate thrusts in lower Paleozoic orogenic belts—An example from the Roberts Mountains allochthon, Nevada: Geology, v. 27, p. 543–546.

Oldow, J.S., 1984, Evolution of a late Mesozoic back-arc fold and thrust belt, northwestern Great Basin, U.S.A.: Tectonophysics. v. 102. p. 245-274.

Paradis, S., Bailey, S.L., Creaser, R.A., Piercey, S. J., and Schiarraza, P., 2006, Paleozoic magmatism and syngenetic massive sulphide deposits of the Eagle Bay assemblage, Kootenay terrane, southern British Columbia, *in* Colpron, M., and Nelson, J.L., eds., Paleozoic Evolution and Metallogeny of Pericratonic Terranes at the Ancient Pacific Margin of North America, Canadian and Alaskan Cordillera: Geological Association of Canada, Special Paper 45, p. 383–414.

Piercey, S.J., Nelson, J.L., Colpron, M., Dusel-Bacon, C., Roots, C.F., and Simard, R.L., 2006, Paleozoic magmatism and crustal recycling along the ancient Pacific margin of North America, northern Cordillera, *in* Colpron, M., and Nelson, J.L., eds., Paleozoic Evolution and Metallogeny of Pericratonic Terranes at the Ancient Pacific Margin of North America, Canadian and Alaskan Cordillera: Geological Association of Canada, Special Paper 45, p. 281–322.

Poole, E.G., 1974, Flysch deposits of Antler foreland basin, western United States, *in* Dickinson. W.R., ed., Tectonics and sedimentation: Society of Economic Paleontologists and Mineralogists Special Publication 22, p. 58-82.

Poole, F.G., Stewart, J.H., Palmer, A.R., Sandberg, C.A., Madrid, R.A., Ross, R.J., Jr., Hintze, L.F., Miller, M.M., and Wrucke, C.T., 1992, Latest Precambrian to latest Devonian time; development of a continental margin: *in* Burchfiel, B.C., Lipman, P.W., and Zoback, M.L., eds., The Cordilleran Orogen: Conterminous U.S.: Boulder, Colorado, Geological Society of America, the Geology of North America, v. G-3.

Rainbird, R.H., McNicoll, J., Theriault, R.J., Heaman, L.M., Abbott, J.G., Long, D.G.F., and Thorkelson, D.J., 1997, Pan-continental river system draining Grenville orogeny recorded by U-Pb and Sm-Nd geochronology of Neoproterozoic quartz arenites and mudrocks, northwestern Canada: The Journal of Geology, v. 105, p. 1-17.

Rainbird, R.H., Cawood, P., and Gehrels, G., 2012, The great Grenvillian sedimentation episode: record of supercontinent Rodinia's assembly, *in* Busby, C. and Azor, A., eds., Tectonics of sedimentary basins: recent advances. Blackwell Publishing Ltd., p. 583-601.

Roberts, R.J., Hotz, P.E., Gilluly, J., and Ferguson, H.G., 1958, Paleozoic rocks of north-central Nevada: American Association of Petroleum Geologists Bulletin, v. 42. p. 2813-2857.

Rohr, T.S., Andersen, T., and Dypvik, H., 2008, Provenance of Lower Cretaceous sediments in the Wandel Sea Basin, North Greenland: Journal of the Geological Society, v. 165, p. 755–767.

Rohr, T.S., Andersen, T., Dypvik, H., and Embry, A.F., 2010, Detrital zircon characteristics of the Lower Cretaceous Isachsen Formation, Sverdrup Basin: Source constraints from age and Hf isotope data: Canadian Journal of Earth Sciences, v. 47, p. 255–271.

Ross, G.M., 1991, Precambrian basement in the Canadian Cordillera: An introduction: Canadian Journal of Earth Sciences. v. 28. p. 1133-1139.

Schuchert, C, 1923, Sites and nature of the North American geosynclines: Geological Society of America Bulletin, v. 34, p. 151-230.

Sloss, L.L. (Ed.), 1988, Tectonic evolution of the craton in Phanerozoic time, *in* Sloss, L.L., ed., Sedimentary Cover—North American Craton: U.S.: Boulder, Colorado, Geological Society of America, The Geology of North America, v. D-2.

Smith, M., and Gehrels, G., 1994, Detrital zircon geochronology and the provenance of the Harmony and Valmy Formations, Roberts Mountains allochton, Nevada: Geological Society of America Bulletin, v. 106, p. 968-979.

Speed, R.C., and Sleep, N.H., 1982, Antler orogeny and foreland basin: A model: Geological Society of America Bulletin, v. 93, p. 815-828.

Theodore, T.G., Murchey, B.L., Hanger, R.A., Strong, E.E., and Ashinhurst, R.T., 1994, To accompany the preliminary geologic map of the Snow Gulch quadrangle, Humboldt and Lander Counties, Nevada: U.S. Geological Survey Open File Report 94-436, 31 p.

Todt, M. K., and Link, P.K., 2013, Sedimentary provenance of the Upper Cambrian Worm Creek Quartzite, Idaho, using U-Pb and Lu-Hf isotopic analysis of zircon grains: Northwest Geology, v. 42, p. 293-298.

Trexler, J.H., Jr., Cashman, P.H., Cole, J.C., Snyder, W.S., Tosdal, R.M., Davydov, V.I., 2003, Widespread effects of middle Mississippian deformation in the Great Basin of western North America: Geological Society of America Bulletin, v. 115, p. 1278-1288.

Van Schmus, W.R., Bickford, M.E., Sims, P.K., Anderson, J.L., Shearer, C.K., and Treves, S.B., 1993, Proterozoic geology of the western midcontinent region, *in* Reed, J.C., Bickford, M.E., Houston, R.S., Link, P.K., Rankin, D.W., Sims, P.K., and Van Schmus, W.R., eds., Precambrian Conterminous U.S.: Boulder, Colorado, Geological Society of America, The Geology of North America, v. C-2, p. 239–259.

Vervoort, J.D., and Blichert-Toft, J., 1999, Evolution of the depleted mantle: Hf isotope evidence from juvenile rocks through time: Geochimica et Cosmochimica Acta, v. 63, p. 533–556.

Villeneuve, M.E., Ross, G.M., Theriault, R.J., Miles, W., Parrish, R.R., and Broome, J., 1993, Tectonic subdivision and U-Pb geochronology of the crystalline basement of the Alberta basin, western Canada: Geological Survey of Canada, Bulletin 447, 86 p.

Whitmeyer, S.J. and Karlstrom, K.E., Tectonic model for the Proterozoic growth of North America: Geosphere, v. 3, p. 220-259.

Wright, J., and Wyld, S., 2006, Gondwana, Iapetan, Cordilleran interactions: A geodynamic model for the Paleozoic tectonic evolution of the North American Cordillera, *in* Haggart, J., Enkin, R., and Monger, J., eds., Paleogeography of the North American Cordillera: Evidence For and Against Large-Scale Displacements: Geological Association of Canada Special Paper 46, p. 377–408.

Yonkee, W.A., Dehler, C.D., Link, P.K., Balgord, E.A., Keeley, J.A., Hayes, D.S., Wells, M.L., Fanning, C.M., Johnston, S.M., 2014, Tectono-stratigraphic framework of Neoproterozoic to Cambrian strata, west-central U.S.: Protracted rifting, glaciation, and evolution of the North American Cordilleran margin, Earth Science Reviews, v.136, p. 59-95.

Chapter 3

Detrital zircon geochronology and HF isotope geochemistry of the Harmony Formation of Nevada: New insights into provenance, transport, and age

Gwen M. Linde[1], James H. Trexler, Jr.[1], Patricia H. Cashman[1], George Gehrels[2], and William R. Dickinson*

This chapter was submitted to Geosphere and was in review at the time of the publication of this dissertation as: Linde, G.M., Trexler, J.H., Jr., Cashman, P.H., Gehrels, G., and Dickinson, W.R., 2016, Detrital zircon geochronology and HF isotope geochemistry of the Harmony Formation of Nevada: New insights into provenance, transport, and age.

1. Abstract

U-Pb geochronology and Hf-isotope geochemistry of detrital zircons provide new insights into the origin, age, and tectonic evolution of the enigmatic Harmony Formation, commonly considered a unit of the Roberts Mountains allochthon of north-central Nevada. Using laser-ablation inductively coupled plasma mass spectrometry, ten arenite samples were analyzed for U-Pb ages, and eight of these samples were further analyzed for Hf-isotope ratios. Three of the sampled arenite units have similar U-Pb age peaks and Hf-isotope ratios, including a 1.0-1.4 Ga peak with εHf values of +12 to -3 and a 2.5-2.7 Ga peak with εHf values of +7 to -5. The remaining seven samples differ significantly; each of these has age peaks of 1.7-1.9 Ga with εHf of +10 to -20 and age peaks of 2.3-2.7 Ga with εHf of +6 to -8. The data confirm the subdivision of the Harmony Formation into two petrofacies: quartzose (Harmony A) and feldspathic (Harmony B) (Gehrels et al., 2000a). The three samples that revealed the 1.0–1.4 and 2.5–2.7 Ga peaks are the

Harmony A, which originated in the central Laurentian craton. The other seven units sampled are the Harmony B, which was sourced from eastern Alberta-western Saskatchewan, north of the Harmony A source. We propose that all of the Harmony Formation strata were deposited near eastern Alberta and subsequently tectonically interleaved with the Roberts Mountains allochthon strata. The entire package was tectonically transported south along the Laurentian margin and then emplaced eastward onto the craton during the Late Devonian-Early Mississippian Antler orogeny.

2. Introduction

Early Paleozoic time along the western Laurentian margin has commonly been interpreted as a quiescent interval (e.g., Poole et al., 1992; Dickinson, 2009, and references cited therein). The final Neoproterozoic rifting that separated the Rodinian supercontinent lasted from ca. 570-520 Ma and was followed by the deposition of passive margin sediments through mid-Devonian time (Poole et al., 1992; Dickinson, 2009; Yonkee et al., 2014). The quiescent interval came to an end with the Antler orogeny, during which the Roberts Mountains allochthon (RMA) was emplaced onto the western Laurentian margin (Dickinson, 2006). The RMA is an internally disrupted package of Cambrian–Devonian oceanic sediments, primarily composed of chert, argillite, quartzose turbidites, and some pillow basalts and volcanogenic debris flows (Doebrich, 1994; Dickinson, 2006; Dickinson, 2009) (Fig. 20).

The Harmony Formation of north-central Nevada presents an opportunity to investigate the tectonic evolution of western Laurentia. It is an enigmatic, fault-bounded,

feldspathic arenite mapped as a unit of the RMA (Madrid, 1987; Doebrich, 1994; Theodore, et al., 1994; Dickinson, 2006) (Fig. 20). Its age, provenance, and stratigraphic relationship with other RMA strata have long been controversial. It is primarily a texturally immature feldspathic arenite, which indicates minimal reworking and therefore minimal transport to the basin of deposition.

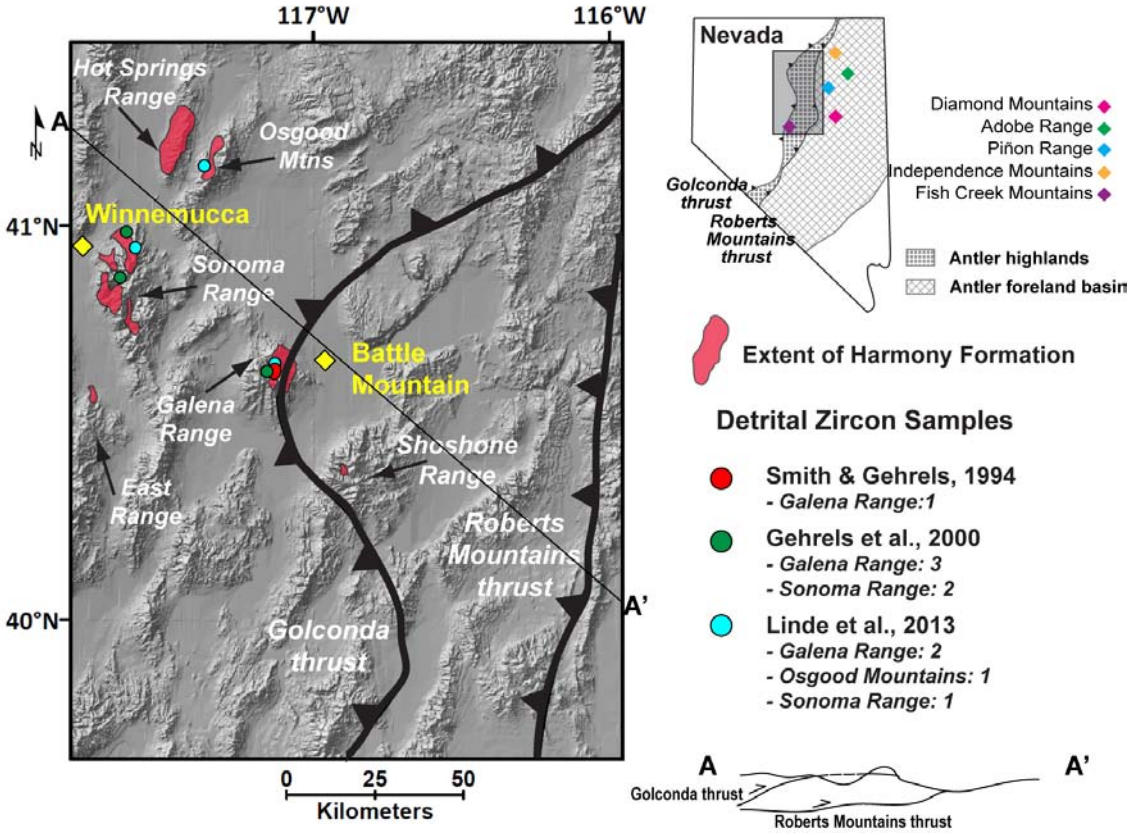

Figure 20. Map of north-central Nevada, showing sample locations (colored symbols), number of samples in each range, and the traces of the Roberts Mountains and Golconda thrusts. Some RMA rocks crop out to the west of the Golconda thrust in tectonic windows through the allochthon as shown in a notional, not-to-scale cross-section. The Antler orogenic highlands and Antler Foreland Basin are shown on the inset state map, with other Nevada locations mentioned in the text. Thrust traces are after Dickinson (2006); Antler highlands and basin are after Poole (1974). (Harmony Formation mapping: Ferguson et al., 1951; Roberts, 1964; Hotz and Willden, 1964; Gilluly, 1967; Madrid, 1987; Doebrich, et al., 1994; Theodore et al., 1994; Jones 1997a, 1997b). An inset map of Nevada shows where the larger scale map is located, as well as the location of other mountain ranges mentioned in the text. UTM coordinates of Harmony Formation samples are compiled in Table 4.

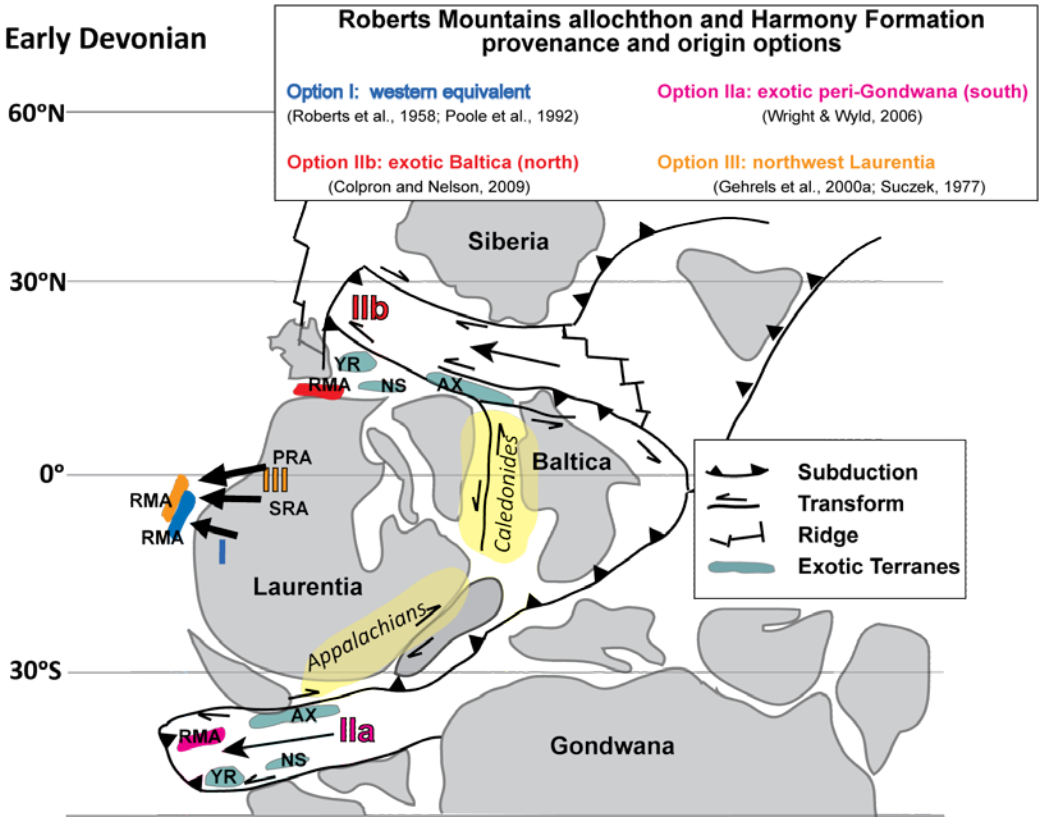

Figure 21: Contrasting tectonic models proposed to explain the source and tectonic transport of the Roberts Mountains allochthon and Harmony Formation, shown in Early Devonian time. Exotic terranes include the Alexander, Klamath, and Northern Sierran terranes. AX—Alexander Terrane; YR—Yreka Terrane; NS—Northern Sierra Terrane; RMA—Roberts Mountains allochthon; PRA—Peace River Arch; SRA—Salmon River Arch. Map is after Colpron and Nelson (2009).

Three general models have been invoked to explain the source, deposition, and transport of the RMA and the Harmony Formation (Fig. 21). The first model proposes that the oceanic sediments of the RMA and Harmony Formation are the coeval deep marine equivalent of the autochthonous passive margin strata of eastern Nevada (e.g., Roberts et al., 1958; Burchfiel and Davis, 1972; Poole et al., 1992) (Fig. 21, option I). This model is based upon the similar ages of the autochthonous and allochthonous strata, and the relative physical proximity of the proposed basin of deposition, directly offshore

the eventual location of the emplaced strata. The second model calls for an exotic, extra-Laurentian origin for the RMA and Harmony Formation and subsequent tectonic transport to a location offshore the emplacement. Two such models were proposed; one infers a peri-Gondwanan origin for the RMA and Harmony Formation with subsequent transport around the southern margin of Laurentia (Wright and Wyld, 2006) (Fig. 21, option IIa). The other model invokes origin in Baltica and subsequent tectonic transport around the northern margin of Laurentia (Colpron and Nelson, 2009) (Fig. 21, option IIb). These models are based on similarity of detrital-zircon ages and geologic history between the RMA and Harmony Formation and other terranes interpreted to be exotic and far traveled (Wright and Wyld, 2006; Colpron and Nelson, 2009). The third model calls for a distant, though still Laurentian, origin for the RMA and Harmony Formation and subsequent sedimentary transport to a location offshore western Laurentia with subsequent emplacement (Fig. 21, option III). Gehrels et al. (2000a) interpreted a source for the RMA in the Peace River Arch region of eastern Canada, based on similarity of detrital zircon U-Pb ages. Suczek (1977) suggested that the Harmony Formation originated in the Salmon River Arch region of Idaho, due to lithological similarity between the Harmony Formation and potential sedimentary sources (Fig. 22).

The age of the Harmony Formation has long been controversial. The earliest mappers interpreted the unit as Mississippian, based on Pennsylvanian limestone deposited unconformably on the Harmony Formation (Ferguson et al., 1951). Later workers interpreted the Harmony Formation as Cambrian, based on Cambrian trilobites found in the unit (Hotz and Willden, 1964). Jones (1997a) extracted a single conodont interpreted as Devonian and thus interpreted a Devonian age. Based on Jones (1997a) and

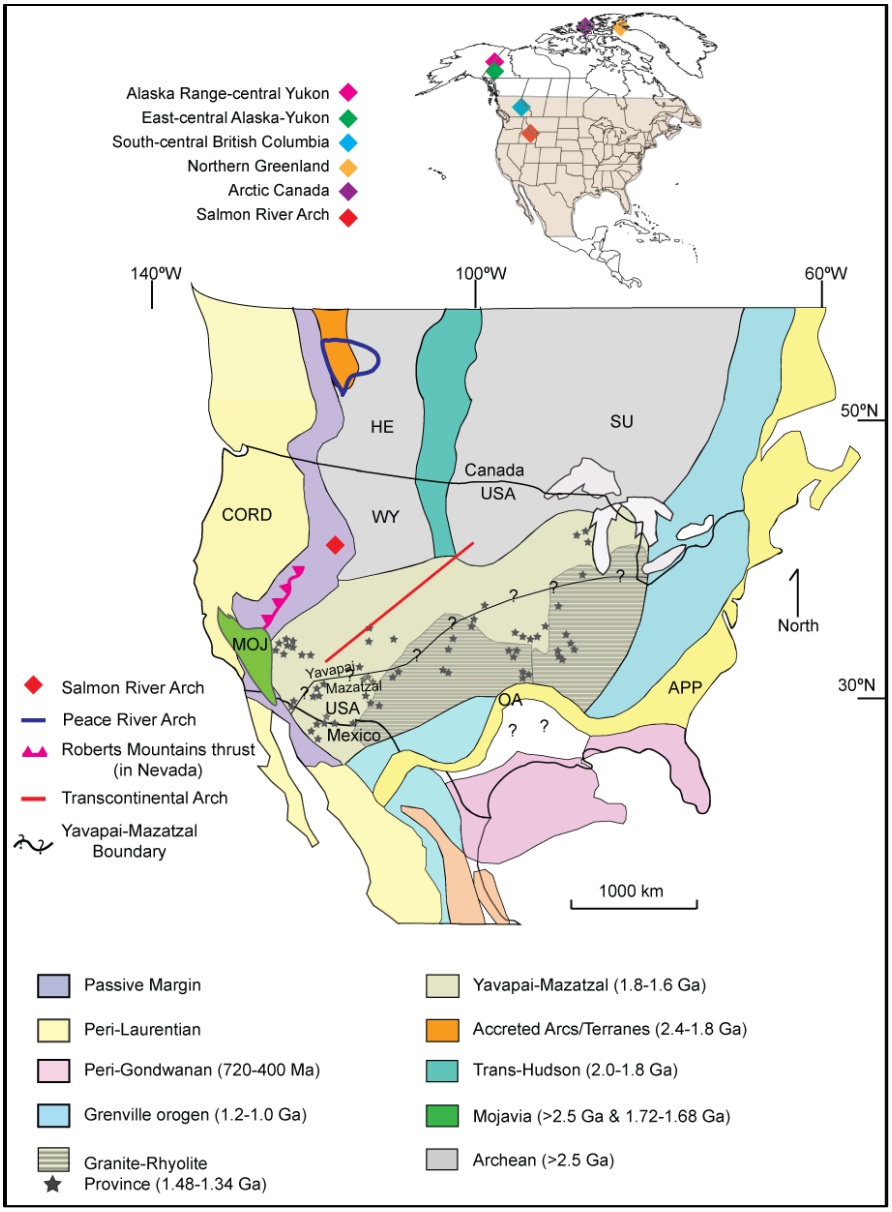

Figure 22: Locations of the main age provinces in North America that are potential source terranes for western Laurentian strata. The location of Transcontinental Arch is shown as a red line (Sloss, 1988); the Peace River Arch is shown as a blue line and the Salmon River Arch is a red diamond. The trace of the Roberts Mountains thrust in Nevada is shown. WY—Wyoming province; HE—Hearn province; SU—Superior province; CORD—Cordilleran; APP—Appalachian; OA—Ouachita-Marathon. Figure is after Gehrels et al. (2011) and compiled from Bickford et al. (1986), Hoffman (1989), Ross (1991), Burchfiel et al. (1992), Anderson and Morrison (1992), Bickford and Anderson (1993), Van Schmus et al. (1993), Villeneuve et al. (1993), Dickinson and Lawton (2001), and Dickinson and Gehrels (2009). An inset map of North America shows other locations referred to in the text.

interpreted geological relationships, Ketner et al. (2005) interpreted a Devonian-Mississippian age.

Analysis of detrital-zircon provenance is a useful method for understanding links between sedimentary units and source terranes (e.g. Fedo et al., 2003; Cawood, et al., 2007). To investigate the source, depositional history, and tectonic evolution of the Harmony Formation, we analyzed detrital zircons to obtain U-Pb ages and Hf-isotope ratios. U-Pb ages are important for identifying and then characterizing the provenance of sedimentary strata, and for comparison among sedimentary units (Gehrels, 2000; Fedo et al., 2003; Gehrels, 2012; Gehrels, 2014). Hf-isotope compositions can be used to determine the geochemical character of the magma in which the zircons crystallized (Bahlburg et al., 2011; Gehrels and Pecha, 2014). Using our new detrital-zircon data, we interpret that the Harmony Formation is from western Laurentia and not exotic. We propose that all of the Harmony Formation strata were deposited near eastern Alberta and subsequently tectonically interleaved with the remainder of the RMA strata. The entire package was tectonically transported south along the Laurentian margin and subsequently emplaced eastward onto the craton during the Late Devonian-Early Mississippian Antler orogeny.

3. Geologic Setting

a. Regional Tectonostratigraphic Framework

The North American craton contains several Proterozoic and Archean crustal provinces that are geologically distinct source terranes for the upper Proterozoic and lower Paleozoic Laurentian strata (e.g., Gehrels et al., 2011 and references cited therein)

(Fig. 22). The Yavapai-Mazatzal Province (1.8-1.6 Ga) extends across central North America (Hoffman, 1989; Whitmeyer and Karlstrom, 2007) (Fig. 22). The granite-rhyolite province crops out within the Yavapai-Mazatzal Province (Bickford, et al., 1986; Anderson and Morrison, 1992). The Yavapai-Mazatzal Province is bounded on the north and northwest by the Trans-Hudson orogenic terrane (Whitmeyer and Karlstrom, 2007) (2.0-1.8 Ga) and Archean rocks (> 2.5 Ga) of the Wyoming and Superior provinces (Fig. 22), on the east and southeast by the terranes of the Grenville orogen (1.2-1.0 Ga) (Hoffman, 1989), and on the west by the Mojavia terrane (> 2.0-2.4 Ga with 1.7-1.8 Ga arcs) (Whitmeyer and Karlstrom, 2007; Nelson et al., 2011) (Fig. 22).

Detrital-zircon data demonstrate that sources for the upper Neoproterozoic-lower Paleozoic western Laurentian passive margin changed between upper Proterozoic and Lower Cambrian time (Linde et al., 2014a, and references cited therein). A significant sediment source for the upper Proterozoic Laurentian passive margin strata from the northwest U.S. to Sonora, Mexico was the 1.2–1.0 Ga Grenville orogen of southern and eastern North America (e.g., Rainbird et al., 1997; Lawton et al., 2010; Rainbird et al., 2012; Gehrels and Pecha, 2014; Yonkee et al., 2014; Linde et al., 2014a) (Fig. 22). In contrast, the 1.8–1.6 Ga Yavapai-Mazatzal and 1.48-1.34 Ga mid-continent granite-rhyolite provinces are the more predominant sediment sources of many strata higher in the passive-margin section (e.g., Lawton et al., 2010; Gehrels and Pecha, 2014; Linde et al., 2014a; Yonkee et al., 2014) (Fig. 22).

The Roberts Mountains allochthon is commonly interpreted as a sequence of Cambrian through Devonian oceanic sedimentary rocks emplaced structurally eastward onto the western Laurentian craton during the Late Devonian-Early Mississippian Antler

orogeny (Roberts et al., 1958; Poole et al., 1992). The Antler orogeny may be linked to tectonism that is inferred along the western margin of Laurentia from Late Devonian through Early Mississippian time; a model that explains this tectonism may also explain possible tectonic transport and emplacement of the RMA. This tectonism is recorded from Alaska to British Columbia and is younger to the south. Middle to Late Devonian continental arc magmatism occurred in the Alaska Range and central Yukon (Piercey et al., 2006) (Fig. 22). Upper Devonian – Lower Mississippian felsic igneous and meta-igneous rocks record bimodal volcanism in east-central Alaska and the Yukon (Dusel-Bacon et al., 2006) (Fig. 22), and in south-central British Columbia, a Late Devonian continental arc and backarc developed (Paradis et al., 2006) (Fig. 22).

Colpron and Nelson (2009) proposed a model that links the Antler orogeny and Devonian-Mississippian tectonism of the western Laurentian margin. They propose a "Northwest Passage" opened between Laurentia and Siberia in mid-Paleozoic time, within which an arc developed along the northern Laurentian margin in the Early Devonian (Colpron et al., 2007; Colpron and Nelson, 2009) (Fig. 21). The Alexander terrane, and other fragments such as the eastern Klamath and northern Sierran terranes commonly interpreted as exotic to Laurentia (e.g., Bazard et al., 1995; Gehrels et al., 1996; Grove et al., 2008; Colpron and Nelson, 2009; Beranek et al., 2013), were transported from their origin in Baltica to northwestern Laurentia through the “Northwest Passage” by means of the westward migration of the subduction zone (Fig. 21). By Middle Devonian time, a sinistral transpressional system developed at the southern end of this passage. The transform fault gradually propagated southward along western

Laurentia and transported the terranes and fragments south along the margin. Colpron and Nelson (2009) inferred that the progressively younger tectonism southward along the Laurentian margin records the southward propagation of the transpressional system. They propose that this fault system could have provided the weakness along which Devonian shortening initiated, resulting in the emplacement of the RMA (Colpron and Nelson, 2009).

RMA strata crop out in north-central Nevada between the Roberts Mountains thrust on the east and the Golconda thrust on the west, though some units are exposed in tectonic windows west of the Golconda thrust (Fig. 20). Strata of the allochthon structurally overlie coeval rocks of the western Laurentian passive margin (e.g., Schuchert, 1923; Kay, 1951; Roberts et al., 1958; Madrid, 1987). RMA strata are highly deformed, and include imbricated older over younger thrust sheets (Evans and Theodore, 1978; Oldow, 1984; Noble and Finney, 1999). The metamorphic grade of RMA rocks is generally greenschist facies or lower (Gehrels et al., 2000a). Sediments shed from the rising Antler highlands filled the Antler foreland basin, east of the Antler orogen and west of the Laurentian craton, between Devonian and Early Mississippian time (Poole, 1974; Trexler et al., 2003) (Fig. 20).

b. The Harmony Formation

The Harmony Formation is primarily a texturally immature feldspathic arenite; it is often interpreted as a part of the RMA, due to its structural imbrication with, and position above, RMA units (Madrid, 1987). The Harmony Formation was first described in Harmony Canyon of the Sonoma Range as a coarse micaceous and feldspathic sandstone

(Ferguson et al., 1951) (Figs. 20 and 23). Interbedded shale and limestone and graded beds are common (Ferguson et al., 1951; Roberts, 1964) (Fig. 23). Ferguson et al. (1951) estimated the thickness of the unit as up to 1524m (5,000 ft). The contact between the exposed base of the Harmony Formation and other units are faults (Fig. 24); therefore, the true thickness of the Harmony Formation is unknown (Ferguson et al., 1951; Ferguson et al., 1952; Roberts, 1964; Hotz and Willden, 1964).

Figure 23. The Harmony Formation in Little Cottonwood Canyon, Galena Range, Nevada. Left photo: the red bar shows a 1m trekking pole. Right photo: the scale totals 15cm. Photos by Gwen Linde.

The Harmony Formation has been interpreted as a turbidite deposit. Roberts (1964) observed the extensive graded bedding, fragments of marine fossils, and lack of cross-beds and ripple marks, and concluded that the Harmony was deposited by density currents. In comparison, Hotz and Willden (1964) suggested that the Harmony

Formation was deposited in an ocean basin by turbidity currents, based on its textural and mineralogical immaturity. Suczek (1977) documented features typical of turbidites, including sole marks, graded beds, plane beds, and interbedded marine shales. Suczek (1977) also documented facies A, B, and C of the classic Bouma (1963) sequence and interpreted the depositional environment of the Harmony Formation as turbidites deposited on inner and middle submarine fans.

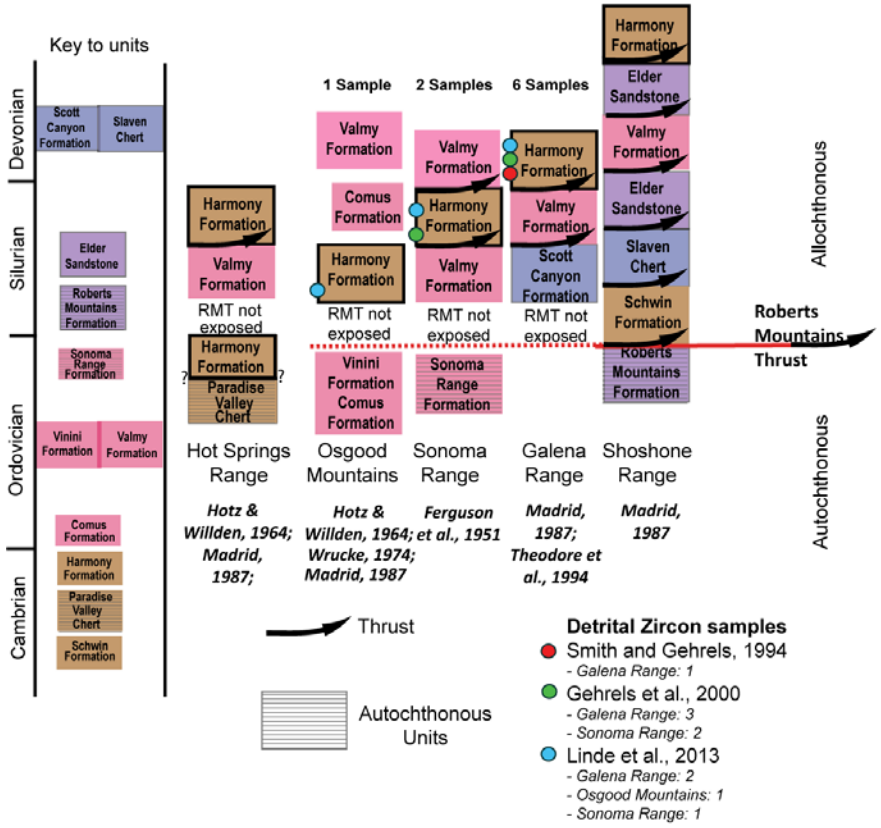

Figure 24. Tectonostratigraphic diagram of units of the Roberts Mountains allochthon in north-central Nevada mountain ranges in which the Harmony Formation crops out, showing locations of detrital zircon samples. Units are shown in their physical, structurally superimposed, and not chronostratigraphic order. Most units are internally disrupted with multiple imbricate thrusts not shown on this chart. Autochthonous units are shown with crosshatching. RMT—Roberts Mountains Thrust, as mapped by Ferguson et al. (1951); Hotz and Willden (1964); Wrucke (1974); Madrid (1987); and Theodore et al. (1994).

The Harmony Formation crops out in several ranges in north-central Nevada (Fig. 20). In the Hot Springs Range the Harmony Formation rests on the Cambrian Paradise Valley Chert with a contact that is interpreted as depositional (Hotz and Willden, 1964), structural (Madrid, 1987), or obscured (Jones, 1997a) (Figs. 20 and 24). In the other locations where the Harmony Formation is exposed, it is mapped as the top thrust in the RMA strata, except in the Sonoma Range where it is found both structurally above and below the Valmy Formation, which consists primarily of arenite, chert, and greenstone (Ferguson et al., 1951; Roberts, 1964; Hotz and Willden, 1964; Gilluly, 1967; Madrid, 1987) (Figs. 20 and 24). In the Sonoma Range, the Pennsylvanian-Permian Antler Peak Limestone was deposited on the Harmony Formation (Ferguson et al., 1951), and in the Galena Range, the Pennsylvanian Battle Formation, a conglomerate, was deposited on the Harmony Formation (Roberts, 1964). In both cases, the contact is an angular unconformity.

The Harmony Formation is inferred to have been exposed as part of the advancing Antler orogen, because clasts of the unit are found in Mississippian strata of the Antler foreland basin, which is interpreted to have filled from detritus shed from the Antler highlands (Dickinson, 2009). These Harmony Formation clasts are found in strata in the Diamond Mountains (Harbaugh, 1980), the Adobe Range (Ketner and Ross, 1990), the Independence Mountains, the Piñon Range, the East Range, and the Fish Creek Mountains (Ketner, 1998) (Fig. 20). Clasts and olistoliths of Cambrian trilobite-bearing Harmony Formation strata are in the Devonian Scott Canyon Formation in the Galena Range (Theodore, et al., 1994; Doebrich, 1994; this study) (Figs. 21 and 25). Because of the contained clasts and olistoliths of Harmony rocks, Doebrich (1994) speculated that

the Scott Canyon Formation was deposited in a volcanogenic debris flow sourced from a highland and/or the advancing allochthon that contained Harmony rocks.

The age of the Harmony Formation has long been controversial. The Harmony Formation was first mapped in the Sonoma (Ferguson et al., 1951) and Galena Ranges (Roberts 1951) and interpreted to be no younger than Mississippian because Pennsylvanian strata were deposited on the Harmony beds. Hotz and Willden (1964) interpreted the age of the Harmony Formation as Late Cambrian, based on trilobite faunas of Laurentian affinity that are resedimented in Harmony limestone lenses in the

Figure 25. The Devonian Scott Canyon Formation with Harmony Formation clast inclusion, in Galena Canyon, Galena Range, Nevada. The red arrow points to the Harmony Formation clast. Photo by Gwen Linde.

Hot Springs Range and the Osgood Mountains (Fig.20). The Harmony Formation is therefore no older than Cambrian. Doebrich et al. (1994) and Theodore (1994) interpreted the Harmony Formation as Cambrian based on both the trilobites and their field observation of clasts and olistoliths of Harmony Formation in the Devonian Scott Canyon Formation in the Galena Range (Figs. 20 and 25). Jones (1997a and 1997b) processed limestone from the Harmony Formation in the Hot Springs Range and reported a single conodont interpreted as Devonian. Later workers interpreted the Harmony Formation as Upper Devonian–Lower Mississippian, based on Jones, 1997a and 1997b) (Ketner et al., 2005; Ketner, 2008). These studies interpreted the limestone beds which contain the Cambrian trilobites as resedimented mélange blocks (in the Osgood Mountains; Jones, 1997a and 1997b) or a separate unit which they mapped as "Cambrian Limestone" (in the Hot Springs Range; Jones, 1997a and 1997b).

Though it had been mapped as one lithostratigraphic formation (e.g. Roberts, 1951; Gilluly, 1967; Doebrich, 1994), the Harmony Formation comprises two distinct sub-units that can be distinguished by their detrital-zircon spectra and with less clarity, by composition (Fig. 26). Gehrels et al. (2000a) designated these as petrofacies, and called the generally more quartzose, more texturally mature "Harmony A" and the generally more feldspathic, more texturally immature "Harmony B" (Gehrels et al., 2000a). The Harmony B crops out everywhere the Harmony Formation is found, while the Harmony A has been described only in Little Cottonwood Canyon of the Galena Range (Fig. 20). Dickinson and Gehrels (2000) interpreted the contact between the Harmony A and B in Little Cottonwood Canyon as sharp, but concordant, and proposed that the two petrofacies recorded two successive submarine fan deposits.

The provenance of the Harmony Formation has also been much debated. Some workers proposed that the Harmony Formation was derived from a possible western land mass, because they could not find an eastern feldspathic granitoid source (Ferguson et al., 1951; Ketner, 1977). Several studies have interpreted the Salmon River Arch of western Idaho as the source of Harmony Formation sands, based on lithological similarities between potential granitic sources and the Harmony B (Rowell et al., 1979; Schweickert and Snyder, 1981; Suczek, 1977; Stewart and Suczek, 1977). Based on early U-Pb analyses of detrital zircons, Wallin (1990) and Smith and Gehrels (1994) thought the source was south of the present position of Harmony Formation outcrops. Based on more

SAMPLE LOCATION UTM: NAD 83 (11N)	**Easting**	**Northing**	**Sample from**	**Harmony A/B**	**Hf?**
Elbow Canyon *Sonoma Range*	441026	4514450	Gehrels et al., 2000	B	yes
Harmony Canyon *Sonoma Range*	446225	4533064	Gehrels et al., 2000	B	yes
Kluncy Canyon *Sonoma Range*	0447927	4531085	Linde et al., 2013	B	no
Gough's Canyon *Osgood Mountains*	0471723	4556266	Linde et al., 2013	B	no
Little Cottonwood Canyon #10 *Galena Range*	0490510	4495682	Linde et al., 2013	A	yes
Little Cottonwood Canyon #9 *Galena Range*	0491232	4495602	Linde et al., 2013	B	yes
Little Cottonwood Canyon #4 *Galena Range*	0490623	4494977	Gehrels et al., 2000	B	yes
Little Cottonwood Canyon #3 *Galena Range*	490459	4494916	Gehrels et al., 2000	B	yes
Little Cottonwood Canyon #2 *Galena Range*	490529	4495008	Gehrels et al., 2000	A	yes
Little Cottonwood Canyon #1 *Galena Range*	490600	4494792	Smith & Gehrels, 1994	A	yes

Table 4: Locations of samples analyzed in this study referenced to UTM locations.

extensive U-Pb analyses of detrital zircons (Fig. 26), Gehrels et al. (2000a), proposed that the Harmony A originated in central or southern Laurentia, and the Harmony B was derived from northern Laurentia (Fig.22). Later workers suggested that the Harmony Formation was an exotic accreted terrane, based on the inability to find any local source terranes (Ketner et al., 2005; Jones-Crafford 2008).

4. Methods

This study describes U-Pb and Hf-isotope zircon analyses from ten arenite samples of the Harmony Formation (Figs. 20 and. 24; Table 4). Zircons from six of these samples were previously analyzed by ID-TIMS (Smith and Gehrels, 1994; Gehrels et al, 2000a) (Figs. 20 and 26; Table 4). This study reports ~200 additional U-Pb analyses and ~50 new Hf-isotope analyses of zircons from these same six samples by LA-ICPMS (Fig. 26). Moreover, ~100 LA-ICPMS U-Pb zircon analyses were performed from four additional arenite samples; these samples are previously described in Linde et al. (2013). On two of these samples, ~25 of the grains were further analyzed by LA-ICPMS for Hf-isotope ratios. The re-analysis of the original six arenite samples incorporated new methodology. Grains were selected randomly rather than by color or morphology, we increased the sample size to 200 grains for the U-Pb ages to obtain a more statistically significant sample size, and we incorporated Hf-isotope analyses. The sampling in the 2000s was accomplished to broaden the geographic scope into new drainages in the Sonoma Range and the Osgood Mountains and to test the finding by Gehrels et al. (2000a) of two distinct petrofacies in the Galena Range. A smaller number of grains were analyzed for these

samples in 2009; reduced cost and increased speed of analyses since that time has made analyses of greater numbers of grains more affordable and practical.

We separated and analyzed zircon at the University of Arizona LaserChron facility using standard techniques to yield a best age distribution reflective of the true distribution of detrital-zircon ages in each sample (Gehrels and Pecha, 2014). We selected zircon grains at random, choosing from all areas of the sample mount and not biasing selection by size, crystal shape, or color. We excluded grains with fractures, inclusions, or zonation. We positioned the analyses in the zircon cores to reduce the chance of analyzing overgrowths that might be compromised by Pb loss. Hf analyses were not conducted on every arenite sample due to cost constraints. Hf analyses were positioned on top of the U-Pb ablated pits to ensure that Hf-isotope data were collected from the same growth domain as the U-Pb ages. The data was collected over multiple trips. LA-ICPMS analyses in 2009 used a New Wave UP193 HE excimer laser, and in 2013-2014, the analyses were performed using a Photon Machines Analyte G2 excimer laser. In all analyses, the laser was connected to a Nu Plasma multi-collector high resolution ICPMS, using methods described in Gehrels and Pecha (2014). For both U-Pb and Hf analyses, we used a beam diameter of 35 μm; for a few very small zircon grains we used a beam diameter of 30 μm.

Analytical results are displayed graphically on normalized-probability plots and Hf-evolution diagrams for visual comparison among zircon populations (Figs. 26, 27, 28, and 30). Hf-evolution diagrams display epsilon Hf ($\varepsilon Hf_{(t)}$) values at the time of zircon crystallization (Figs. 27, 28, and 30). For U-Pb analyses, measured ion intensities from the Nu HR ICPMS are imported into a data reduction program, "agecalc," which reduces

data, calculates ages, applies corrections and filters, and creates data tables, concordia diagrams, histograms, and normalized-probability plots (Gehrels and Pecha, 2014). For Hf analyses, a data-reduction program, "hfcalc," reduces data, calculates Hf ratios, applies corrections, and creates data tables and Hf-evolution charts (Gehrels and Pecha, 2014). We rejected U-Pb analyses for which uncertainties are greater than 10%, discordance is greater than 20%, and reverse discordance is greater than 5%. For Hf analyses, we applied a 2-sigma filter (Gehrels and Pecha, 2014).

In addition to visual evaluation, we also compared age distributions using the Kolmogorov-Smirnov (K-S) statistic (Guynn and Gehrels, 2006) (Table 5). The K-S calculates whether a statistically significant difference exists between two distributions. P (probability) <0.05 indicates >95% probability that two U-Pb distributions are not the same. The K-S statistic is sensitive to proportions of ages present, and a low P value may not indicate statistical difference between the ages of populations but rather that the proportions of age peaks are different (Gehrels, 2012).

5. Results: Uranium-Lead Agesand Hf-isotope ratios

Although the ID-TIMS data are similar to our new LA-ICPMS data, there are variations in the proportions of age groups (Fig. 26). Different grain selection procedures were used in the two studies. In the ID-TIMS study, zircon crystals were selected based on color and morphology (Gehrels et al., 2000a). For the current LA-ICPMS study, we attempted to select grains randomly from the entire population of grains, to obtain a more representative age distribution. The results and interpretations that follow are based upon the LA-ICPMS ages.

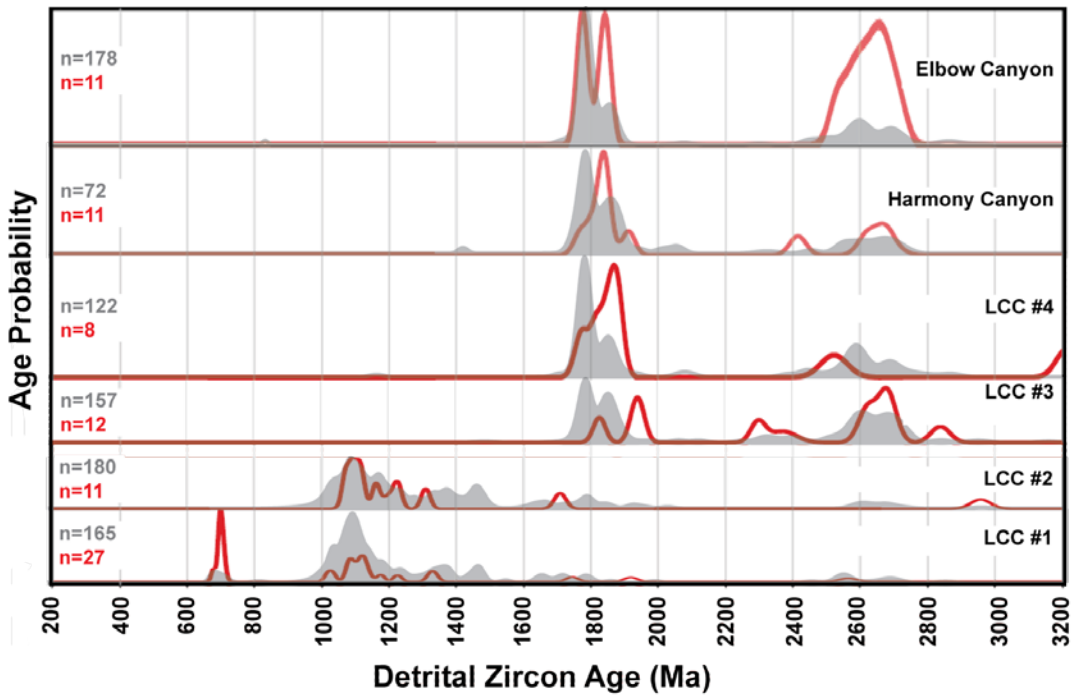

Figure 26. Normalized probability plots showing U-Pb ages of strata sampled. These data are analyses of the six samples collected and first analyzed in the 1990s and reanalyzed for this study. Red lines show the data from isotope-dilution thermal ionization mass spectrometry (Gehrels et al., 2000a); grey-filled curves are the data from laser-ablation inductively coupled plasma mass spectrometry (this study). Numbers of grains analyzed are shown.

The three Harmony A samples, LCC #1, #2, and #10, have similar U-Pb ages and Hf-isotope ratios and differ significantly from Harmony B (Figs. 26 and 27). In Harmony A samples, there is a major age peak at ca. 1.0-1.2 Ga, which includes 45-62% of the analyses from each sample (Figs. 26 and 27). These grains yielded $\varepsilon Hf_{(t)}$ ratios of +10 to -8 (Fig.27). Smaller age populations from ca. 1.2-1.5 Ga, ca. 1.6-1.8 Ga, and ca. 2.5-2.8 Ga each comprise up to 15% of the zircons (Figs. 26 and 27). The age populations of 1.2-1.5 Ga yielded $\varepsilon Hf_{(t)}$ ratios of +12 to -1, the age populations of 1.6-1.8 Ga yielded $\varepsilon Hf_{(t)}$ ratios of +10 to -13, and the age populations of 2.5-2.8 Ga yielded $\varepsilon Hf_{(t)}$ ratios of +7 to -2

(Fig. 27). The LCC#1 sample also has a small (n = 7) peak at ca. 685 Ma, consisting of 4% of the total analyses.

In comparison, the seven Harmony B samples, LCC #3, #4, and #9, and Kluncy, Gough's, Harmony, and Elbow Canyons, revealed a major age peak at ca. 1.7-1.9 Ga, consisting of 60-65% of the analyses (Figs. 26 and 27). These grains yielded $\varepsilon Hf_{(t)}$ ratios of +1- to -20 (Fig. 27). The samples also yield smaller age populations at ca. 2.4-2.8 Ga, representative of 20% of the sample (Figs. 26 and 27). The age populations of 2.4-2.7 Ga yielded $\varepsilon Hf_{(t)}$ ratios of +5 to -5 and the age populations of 2.7-2.8 Ga yielded $\varepsilon Hf_{(t)}$ ratios of +7 to -9 (Fig. 27).

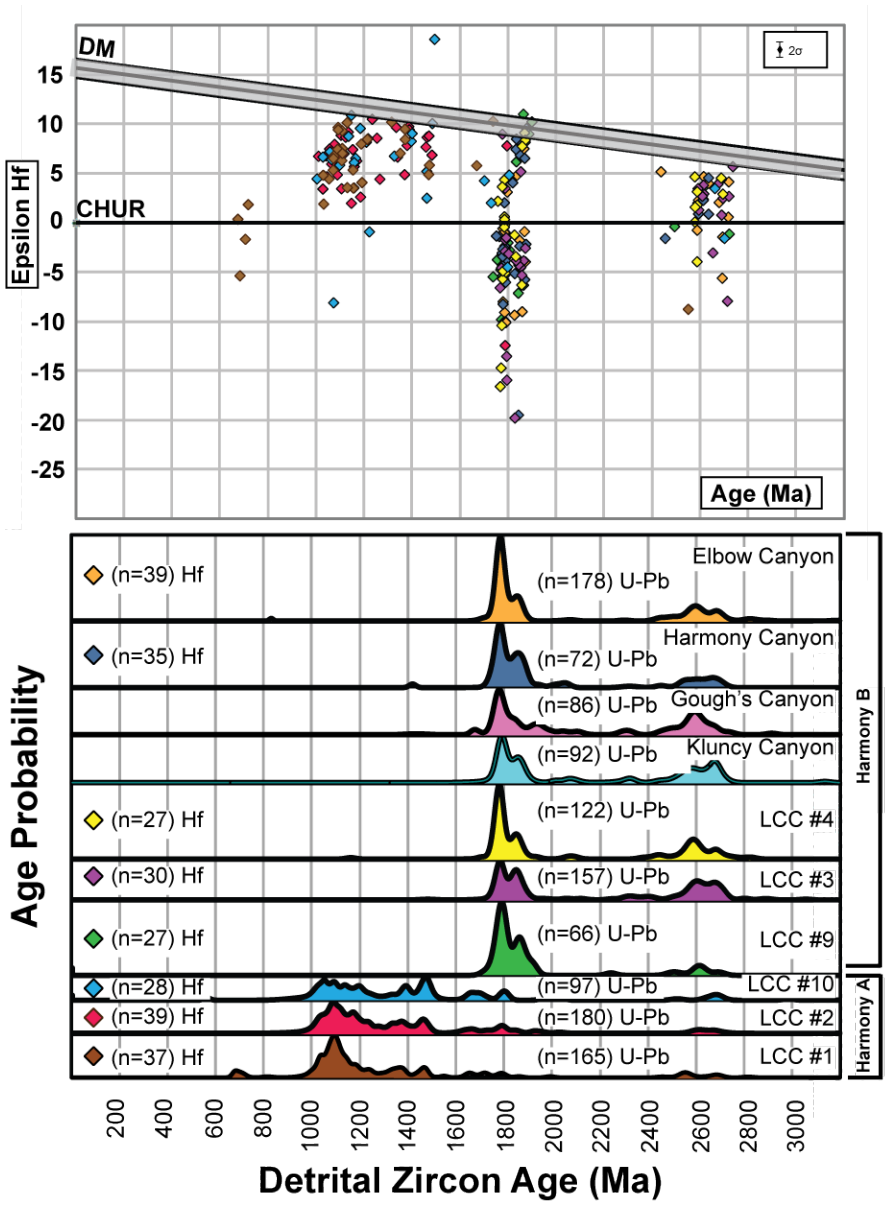

Figure 27. U-Pb ages and Hf isotope data for Harmony Formation. U-Pb dates were run for all sample grains; approximately ¼ of these grains were analyzed for hafnium isotopes. The lower graph shows the normalized probability plots of U-Pb ages. The subdivision of Harmony A and B is indicated. The number of grains analyzed for U-Pb ages and Hf isotopes is shown. The upper graph shows Epsilon Hf values at the time of zircon crystallization ($\varepsilon Hf_{(t)}$) vs. age for each sample. The average measurement uncertainty for all hafnium analyses on this chart in ± epsilion units is shown in the upper right at the 2σ level. Reference lines on the Hf plot are as follows: Depleted mantle (DM) is calculated using $^{176}Hf/^{177}Hf=0.283225$; $^{176}Lu/^{177}Hf=0.038513$ (Vervoort and Blichert-Toft, 1999); Chondritic uniform reservoir, CHUR, is calculated using $^{176}Hf/^{177}Hf=0.282785$ and $^{176}Lu/^{177}Hf=0.0336$ (Bouvier et al., 2008).

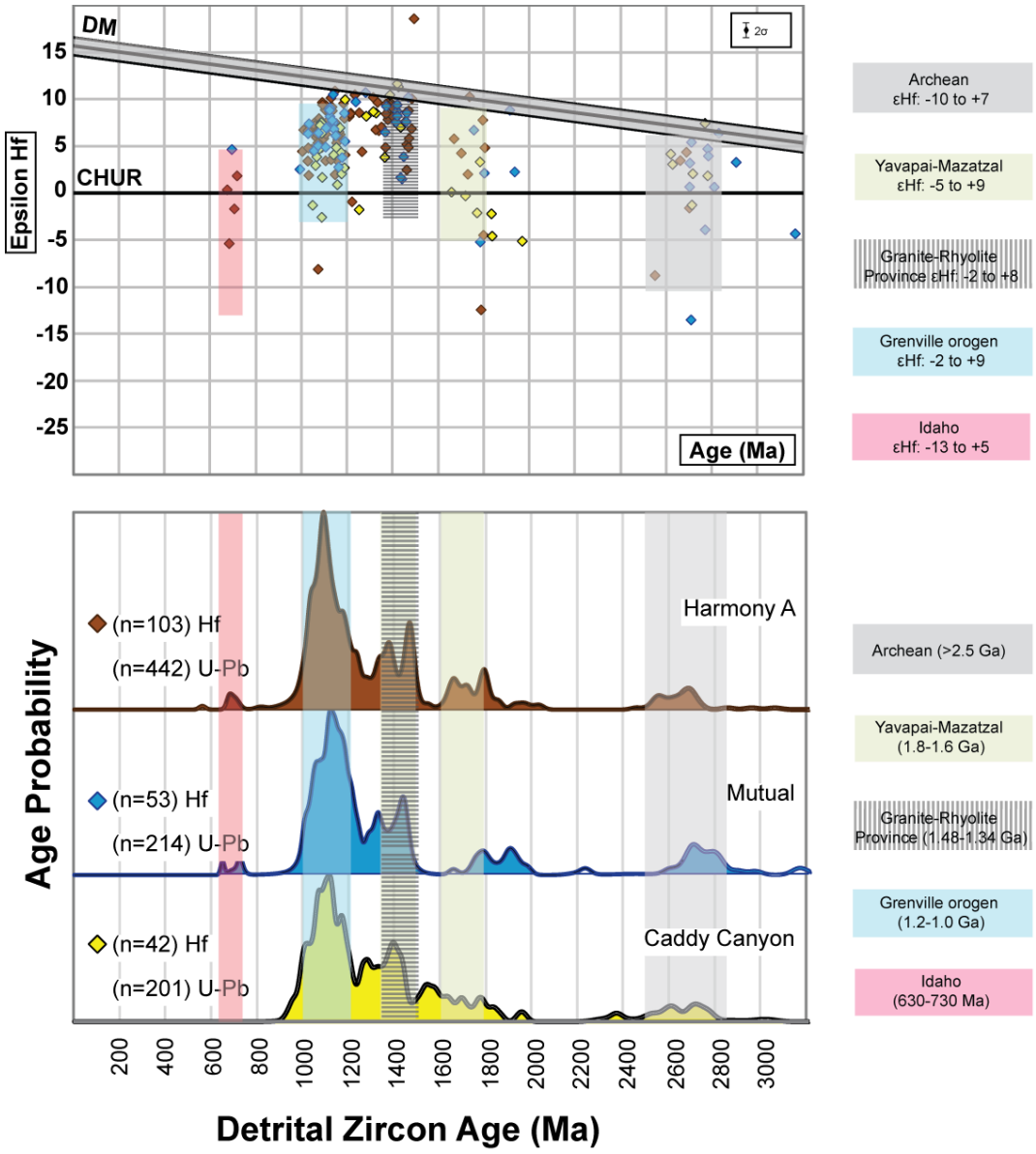

Figure 28. U-Pb ages and Hf isotope data for Harmony A samples and selected western Laurentian passive margin strata, showing the similarities between the U-Pb ages and Hf isotope analyses of the Harmony A and these passive margin strata. Data from the Neoproterozoic Mutual Formation and Caddy Canyon Quartzite are from Gehrels and Pecha (2014). Colored age bars that correspond to Laurentian basement terrane ages are superimposed over the U-Pb ages on the normalized probability plots. The ages are from references cited in Fig. 3. Colored Hf-isotope range bars that correspond to the same Laurentian terranes are shown on the Hf evolution diagram (Grenville: Bickford et al., 2010; Mueller et al., 2008. Granite-Rhyolite province: Goodge and Vervoort, 2006; Mueller et al., 2008. Yavapai-Mazatzal: Holm et al., 2013. Achaean: Rohr et al., 2008; Rohr et al., 2010. Idaho: Gaschnig, et al., 2013). Diagrams and symbols are as in Figure 27.

Table 5: K-S statistical analysis results. The Harmony A samples are shown with green highlights, central Laurentian passive margin strata are shown with blue highlights, Harmony B samples are shown with orange highlights, and southern British Columbia-northeastern Washington samples are shown with red highlights. Comparisons between units with values greater than 0.05 are highlighted in yellow. P<0.05 indicates >95% probability that two U-Pb distributions are not the same.

	LCC #1	LCC #2	LCC #10	Caddy Cyn Quartzite	Mutual Formation	LCC #9	LCC #3	LCC #4	Kluncy Canyon	Gough's Canyon	Harmony Canyon	Elbow Canyon	Horsethief Creek Group	Hamill Group	Addy Quartzite
LCC #1		0.077	0.010	0.013	0.007	0.000	0.000	0.000	0.000	0.000	0.000	0.000	0.000	0.000	0.000
LCC #2	0.077		0.196	0.838	0.357	0.000	0.000	0.000	0.000	0.000	0.000	0.000	0.000	0.000	0.000
LCC #10	0.010	0.196		0.588	0.227	0.000	0.000	0.000	0.000	0.000	0.000	0.000	0.000	0.000	0.000
Caddy Canyon Quartzite	0.013	0.838	0.588		0.689	0.000	0.000	0.000	0.000	0.000	0.000	0.000	0.000	0.000	0.000
Mutual Formation	0.007	0.357	0.227	0.689		0.000	0.000	0.000	0.000	0.000	0.000	0.000	0.000	0.000	0.000
LCC #9	0.000	0.000	0.000	0.000	0.000		0.000	0.033	0.000	0.000	0.745	0.090	0.041	0.061	0.006
LCC #3	0.000	0.000	0.000	0.000	0.000	0.000		0.018	0.942	0.199	0.001	0.000	0.009	0.000	0.000
LCC #4	0.000	0.000	0.000	0.000	0.000	0.033	0.018		0.085	0.154	0.376	0.982	0.028	0.005	0.003
Kluncy Canyon	0.000	0.000	0.000	0.000	0.000	0.000	0.942	0.085		0.722	0.024	0.011	0.139	0.004	0.000
Gough's Canyon	0.000	0.000	0.000	0.000	0.000	0.000	0.199	0.154	0.722		0.014	0.010	0.092	0.022	0.000
Harmony Canyon	0.000	0.000	0.000	0.000	0.000	0.745	0.001	0.376	0.024	0.014		0.642	0.147	0.065	0.010
Elbow Canyon	0.000	0.000	0.000	0.000	0.000	0.090	0.000	0.982	0.011	0.010	0.642		0.001	0.001	0.003
Horsethief Creek Group	0.000	0.000	0.000	0.000	0.000	0.041	0.009	0.028	0.139	0.092	0.147	0.001		0.000	0.000
Hamill Group	0.000	0.000	0.000	0.000	0.000	0.061	0.000	0.005	0.004	0.022	0.065	0.001	0.000		0.008
Addy Quartzite	0.000	0.000	0.000	0.000	0.000	0.006	0.000	0.003	0.000	0.000	0.010	0.003	0.000	0.008	

6. Discussion: Provenance and Age of the Harmony Formation

To understand the tectonic evolution of the Harmony Formation, we must first understand its provenance. To interpret provenance, we compared the data from our study to known U-Pb ages and Hf-isotope data from other coeval sedimentary units, as well as Laurentian basement provinces.

a. Provenance of the Harmony A

The Harmony A arenites are composed of detrital zircons that have potential sources in the Laurentian craton. We can account for these age spectra as follows: the 1.0-1.2 Ga grains are consistent with provenance in the Grenville orogen (Hoffman, 1989; Bickford and Anderson, 1993; Van Schmus et al., 1993) (Figs. 22 and 28), and the 1.3-1.5 Ga grains are similar to those with origin in the granite-rhyolite province of central Laurentia (Bickford et al., 1986; Hoffman, 1989; Anderson and Morrison, 1992; Bickford and Anderson, 1993; Van Schmus et al., 1993) (Figs. 22 and 28). The 1.6-1.8 Ga grains are consistent with provenance in the Yavapai-Mazatzal terranes and the 2.5-2.8 Ga grains are comparable with those origininating in the Archean craton (Bickford et al., 1986; Hoffman, 1989; Ross, 1991; Van Schmus et al., 1993) (Figs. 22 and 28). The seven zircons from 673-716 Ma in sample LCC#1 sample have a potential source in Idaho. Several workers have reported zircon ages that fall within this range in igneous suites in Idaho: 684 ± 4 Ma and 685 ± 7 Ma (Lund et al., 2003), 667 ± 5 Ma, 717 ± 4 Ma, and 709 ± 5 Ma (Fanning and Link, 2004), and 680-706 Ma (Durk et al., 2007). The U-Pb ages of the Harmony A are compatible with provenance in the central Laurentian craton. The

grains in the Harmony A arenites could have been derived from the igneous terranes or from recycled sediments originally derived from these terranes. The Hf-isotope ratios of the Harmony A samples are also similar to those in potential source terranes in central Laurentia. The 1.0-1.2 Ga grains have juvenile to intermediate values ($\varepsilon Hf_{(t)}$ +10 to -8), similar to those of the Grenville orogen (Bickford et al., 2010; Mueller et al., 2008), and the 1.4-1.5 Ga grains have juvenile to moderately juvenile values ($\varepsilon Hf_{(t)}$ +10 to +2.5), compatible with the granitoids of the mid-Laurentian craton (Goodge and Vervoort, 2006) (Figs. 22 and 28). The 1.6-1.8 Ga grains have juvenile to intermediate values ($\varepsilon Hf_{(t)}$ +10 to -6), similar to the Yavapai orogenic terrane (Holm et al., 2013). The 2.5-2.8 Ga grains have moderately juvenile to intermediate values ($\varepsilon Hf_{(t)}$ +7 to -2), compatible with those in northern Greenland and Arctic Canada of the Northeast Canadian shield (Rohr et al., 2008; Rohr et al., 2010) (Figs. 22 and 28). The 673-716 Ma grains have intermediate to evolved values ($\varepsilon Hf_{(t)}$ +1.9 to -5.3), within the range of 630-730 Ma zircons in the Idaho batholith, interpreted as inherited from the Windermere Supergroup volcanics (Gaschnig et al., 2013).

The Harmony A U-Pb ages and Hf-isotope ratios are similar to those of coeval passive margin sedimentary units of western Laurentia (Fig. 28). The upper Neoproterozoic-Lower Cambrian Mutual Formation and Caddy Canyon Quartzite are interpreted as originating in central Laurentia prior to the uplift of the Transcontinental Arch (Gehrels and Pecha, 2014; Linde et al., 2014a; Yonkee et al., 2014) (Fig. 28). The K-S analyses of these units support an interpretation of a common provenance for these units; the Mutual Formation and Caddy Canyon Quartzite have P-values of > 0.25 with one another and Harmony A samples (Table 5). We interpret that the sediments comprising the Harmony

A, the Mutual Formation, and the Caddy Canyon Quartzite were derived from sources in the central Laurentian craton prior to the uplift of the Transcontinental Arch, and were transported to the western Laurentian margin by continent-spanning rivers.

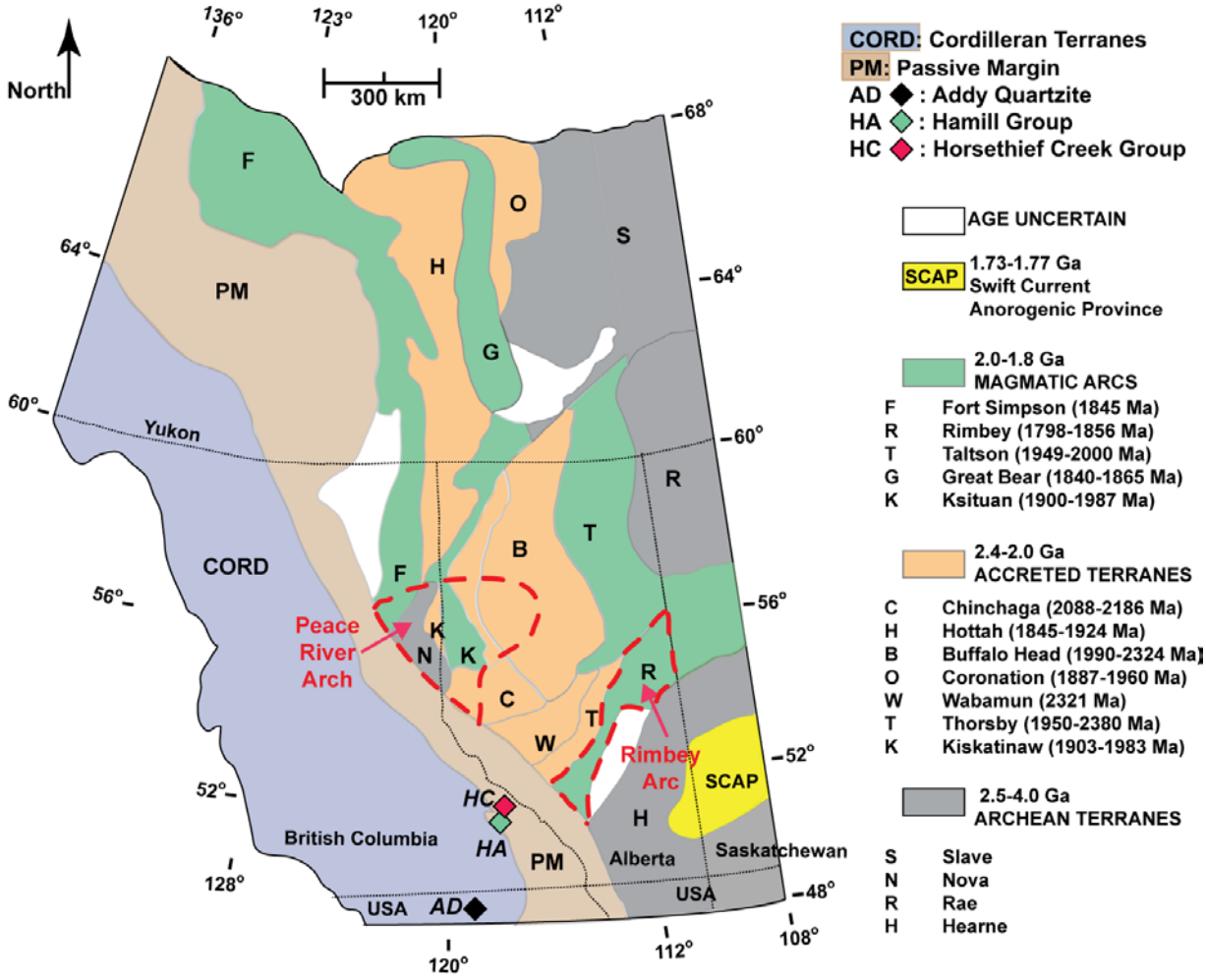

Figure 29. Map of western Canada showing the Cordilleran accreted terranes, the Cordilleran passive margin, and the basement provinces of the Canadian Shield. The Peace River Arch and Rimbey arc regions are outlined by red dashed lines. The Swift Current anorogenic province (SCAP) is highlighted in yellow. The location of the Hamill Group and Horsethief Creek Group samples (Gehrels and Pecha, 2014) are shown. Sample locations are shown by colored diamonds; Horsethief Creek Group (HC) and Hamill Group (HA) are from Gehrels and Pecha (2014); Addy Quartzite (AD) is from Linde et al. (2014b). Map is after Gehrels and Ross (1998); the basement provinces are compiled from Collerson et al. (1988), Hoffman (1989), Ross (1991), Villeneuve et al. (1993), and Peterson et al. (2015).

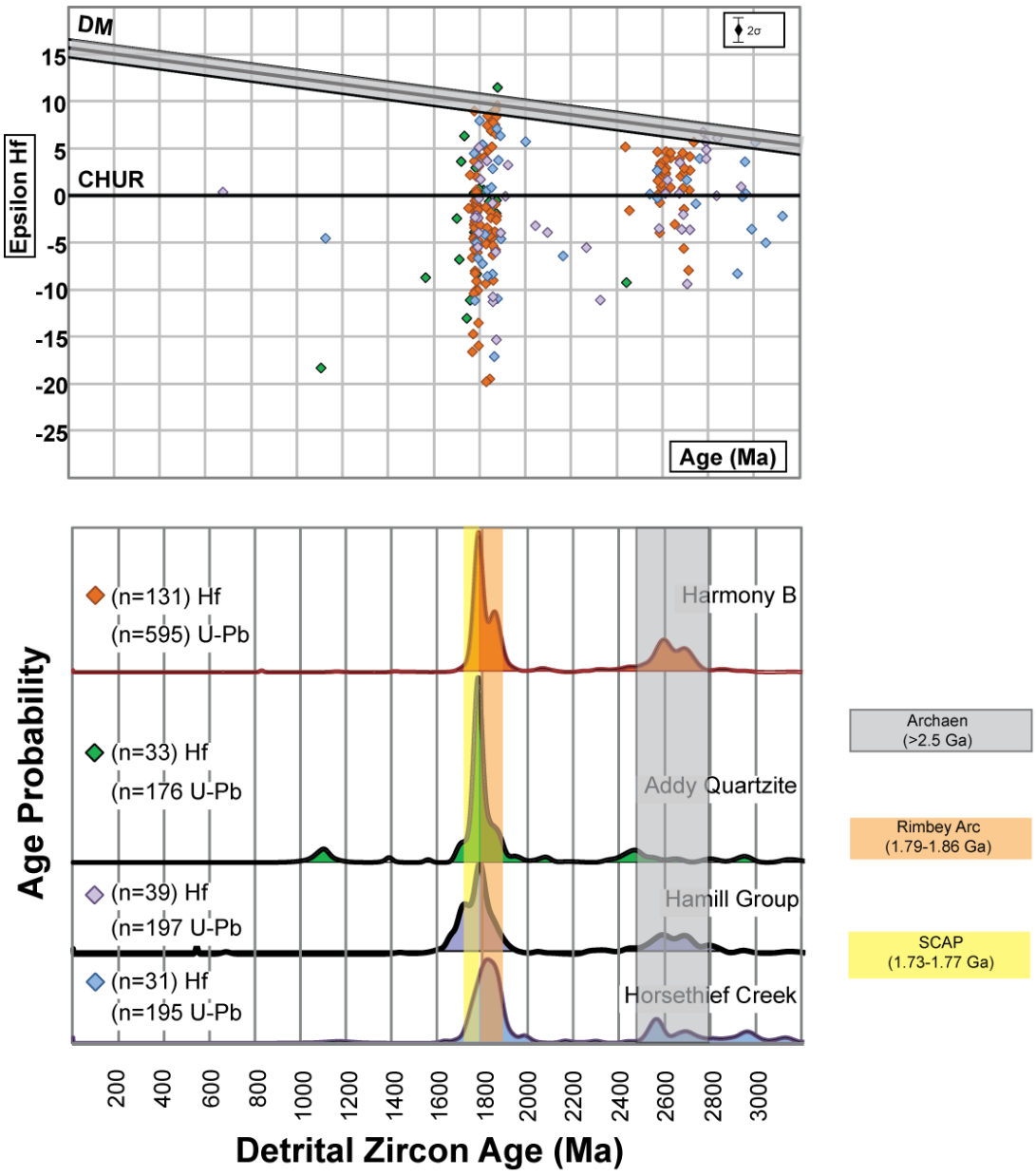

Figure 30. U-Pb ages and Hf isotope data for Harmony B samples and select Laurentian passive margin strata, showing the similarities between the U-Pb ages and Hf isotope analyses of the Harmony B and these passive margin strata. Colored age bars that correspond to Peace River Arch region basement terrane ages are superimposed over the U-Pb ages on the normalized probability plots. Data from the Horsethief Creek Group and the Hamill Group are from Gehrels and Pecha (2014). U-Pb analyses of the Addy Quartzite are from Linde et al. (2014b); Hf analyses of the Addy Quartzite are Linde's unpublished work. Diagrams and symbols are as in Figure 27.

b. <u>Provenance of the Harmony B</u>

The Harmony B arenites are composed of detrital zircons that have potential sources in igneous terranes of eastern Alberta and western Saskatchewan. The Harmony B primary age populations of 1.75-1.9 Ga are within the zircon ages of two igneous provinces: the 1.73-1.77 Ga Swift Current anorogenic province of the Kivalliq Igneous Suite of western Saskatchewan (Collerson et al., 1988; Peterson et al., 2015) and the 1.79-1.86 Ga Rimbey arc of eastern Alberta (Villenueve et al., 1993; Gehrels and Ross, 1998) (Figs. 29 and 30). The Harmony B age populations of ca. 2.4-2.7 Ga and 2.7-2.8 Ga are similar to those of Archean terranes in the same region (Figs. 29 and 30). Hf-isotope analyses have not been accomplished on the igneous provinces of eastern Alberta and western Sasketchewan; therefore, no direct comparison between the Hf ratios of the Harmony B samples and these potential source terranes is possible. However, the Harmony B grains have a range of U-Pb ages and $\varepsilon Hf_{(t)}$ values similar to those of the Horsethief Creek and Hamill Groups and the Addy Quartzite, passive margin units interpreted to have originated in eastern Alberta-western Saskatchewan (Linde et al., 2013; Gehrels and Pecha, 2014) (Fig. 30).

We considered other potential source terranes for the Harmony B: the Belt Supergroup, the Trans-Hudson orogen, and the Yavapai-Mazatzal terrane, and considered the possibility that the Harmony Formation shared provenance with the strata of the Roberts Mountains allochthon. The Belt Supergroup and Harmony B sediments share many detrital zircon age populations, but approximately 20% of the Belt Supergroup zircons are ca 1.4-1.7 Ga, younger than the youngest (ca. 1.75 Ga) Harmony B zircons (Link et al., 2013). If the Belt Supergroup was the source of the Harmony B, we would

expect to find some of these 1.4-1.7 Ga zircons in the Harmony B, but do not. The Trans-Hudson orogen and the Harmony B sediments also share many age populations; however, the 1.8-2.0 Ga Trans-Hudson orogen (Whitmeyer and Karlstrom, 2007) could not have supplied the 1.75-1.8 Ga zircons which comprise nearly 35% of the Harmony B. The Yavapai-Mazatzal terrane also shares many age populations with the Harmony B; however, Harmony B samples are missing grains of the age of the other major provinces in central Laurentia, including the Grenville orogenic terrane and the granite-rhyolite magmatic province; the later is located within the Yavapai-Mazatzal terrane (Figs. 22 and 30). It is not likely that river systems would flow across the Yavapai-Mazatzal terrane and transport only grains of that age, without also entraining Grenville or granite-rhyolite province aged grains. We therefore conclude that it is unlikely that the Harmony B originated in central Laurentia. The RMA strata and the Harmony B share some age populations, but dissimilarities preclude a common source. The RMA strata have major age populations from 1.80-1.95 Ga, with no grains < ca. 1.8 Ga (Linde et al., 2016); however, the Harmony B has a significant age population < ca. 1.8 Ga. We interpret that the Harmony B sediments did not originate in the same source as or from the RMA strata.

The detrital zircon U-Pb age spectra and Hf-isotope ratios of the Harmony B are consistent with origin in eastern Alberta and western Saskatchewan (Figs. 29 and 30). This region was exposed throughout Cambrian time and submerged from Ordovician through Mississippian time (Cant, 1988; Cant and O'Connell, 1988; Kent, 1994). We interpret that the provenance of the sediments of the Harmony B, the Horsethief Creek Group, the Hamill Group, and the Addy Quartzite is the Rimbey arc of eastern Alberta and the Swift Current anorogenic province of western Saskatchewan (Figs. 29 and 30).

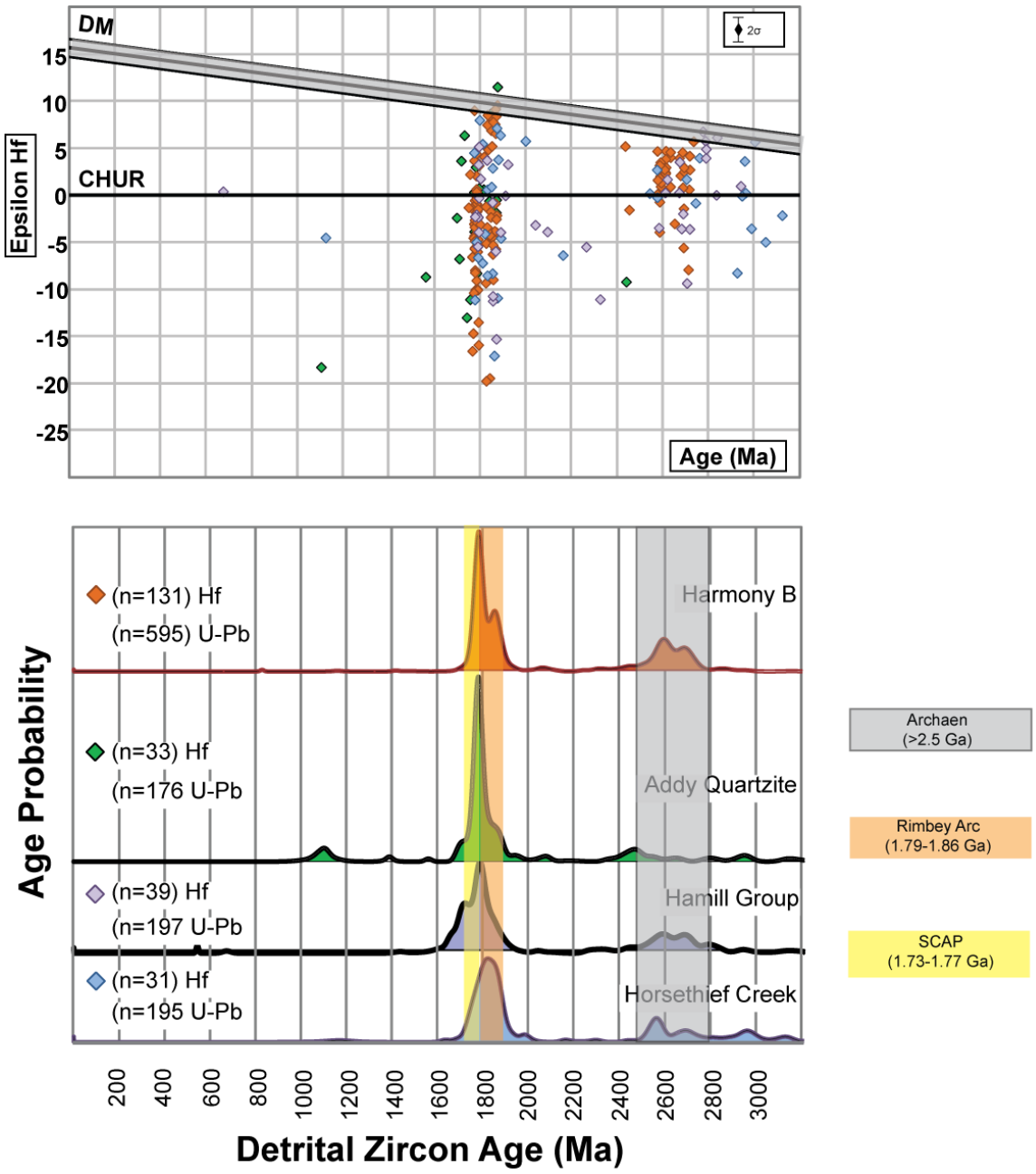

Figure 30. U-Pb ages and Hf isotope data for Harmony B samples and select Laurentian passive margin strata, showing the similarities between the U-Pb ages and Hf isotope analyses of the Harmony B and these passive margin strata. Colored age bars that correspond to Peace River Arch region basement terrane ages are superimposed over the U-Pb ages on the normalized probability plots. Data from the Horsethief Creek Group and the Hamill Group are from Gehrels and Pecha (2014). U-Pb analyses of the Addy Quartzite are from Linde et al. (2014b); Hf analyses of the Addy Quartzite are Linde's unpublished work. Diagrams and symbols are as in Figure 27.

c. Age of the Harmony Formation

The depositional age of the Harmony Formation has been interpreted variously as Cambrian, Devonian, and Devonian-Mississippian. We considered several lines of evidence to interpret the age of the unit. 1) Late Cambrian fossils of North American affinity have been identified in Harmony Formation outcrops in two mountain ranges (Hotz and Willden, 1964). 2) Clasts and olistoliths of the Harmony B have been observed in the Devonian Scott Canyon Formation, near the mouth of Galena Canyon in the Galena Range (Doebrich, 1994; Theodore et al., 1994; Theodore pers. comm. 2015), and confirmed by our field work (Fig. 25). 3) By Mississippian time, the Harmony B strata were subaerally exposed on the craton as a part of the Antler highlands. We deduce this because clasts of the Harmony B were shed from the Antler highlands and transported eastward into the Antler foreland basin where they have been documented in many Mississippian Antler foreland basin units (Harbaugh, 1980; Ketner and Ross, 1990; Ketner, 1998) (Fig. 20). 4) Analysis of deposits interpreted as back- and forebulge deposits overlying the autochthonous passive margin indicates that the RMA was approaching the western Laurentian margin by early Late Devonian time (Goebel, 1991; Dickinson, 2000). 5) The Rimbey arc and Swift Current anorogenic province—the most likely sources of the zircons in the Harmony B—were submerged during the Devonian, not subaerially exposed (Cant, 1988; Cant and O'Connell, 1988; Kent, 1994) (Fig. 31). This region was the site of deposition of shallow shelf carbonates in the Devonian (Kent, 1994). 6) Though there are no fossils in the Harmony A, the similarity of Harmony A U-Pb detrital zircon age spectra and Hf-isotope ratios with those of late Neoproterozoic – Early Cambrian passive margin units, such as the Mutual Formation and the Caddy

Canyon Quartzite, strongly suggest deposition at the same time as these units and before the uplift of the Transcontinental Arch.

We also considered the evidence for a Devonian-Mississippian age of the Harmony Formation. The only datum supporting a Devonian or younger age for the Harmony Formation is a single conodont interpreted as Devonian (Jones, 1997a; 1997b). Ketner et al. (2005) cited this datum in arguing for a Late Devonian-Early Mississippian age for the Harmony Formation. Ketner et al. (2005) also cited additional sampling, but no sample numbers or photos are available or have been published. Weighing the unrepeated nature of the single occurrence against the other evidence presented, we conclude that the Harmony Formation is Cambrian.

7. Paleogeographic Implications

The Harmony A and B are two distinct units with different provenance and depositional history. We prefer the interpretation that the sediments of the Harmony A originated in the central Laurentian craton, before the uplift of the Transcontinental Arch, and were deposited as turbidites in a basin off the western margin in late Neoproterozoic or Early Cambrian time (Fig. 31A). We propose that the sediments of the Harmony B originated in eastern Alberta-western Saskatchewan and were deposited as turbidites in a basin off the northwestern Laurentian margin in Late Cambrian time (Fig. 31B). It is likely that passive-margin arenites such as the Horsethief Creek Group, Hamill Group, and Addy Quartzite also originated in eastern Alberta – western Saskatchewan and were deposited in southern British Columbia and northeastern Washington (Figs. 31A and 31B). These units are the nearshore and shallow shelf equivalents of the deeper marine

Harmony B (Lindsey and Gaylord, 1992; Gehrels and Ross, 1998). From Ordovician through Devonian time, other RMA strata were deposited in the region (Linde et al., 2016).

We propose that some of the models considered above can now be excluded as reasonable explanations for the origin and transport of the Harmony Formation. The first model proposed that the RMA and the Harmony Formation were the deep marine equivalents of coeval allochthonous passive margin strata. The source of the Harmony A sediments is the central Laurentian craton, but the source of the Harmony B sediments is not. Additionally, the RMA strata, exclusive of the lower Vinini Formation, do not share age populations or a source with coeval sediments of the passive margin (Linde et al., 2016). The second model proposed that the RMA and Harmony Formation were extra-Laurentian and were tectonically transported to the western Laurentian margin along with known exotic terranes such as the Alexander terrane. The Harmony Formation has similar age populations and Hf-isotope ratios as western Laurentian terranes. While an exotic source might be possible, a Laurentian source is the simpler solution. The Harmony B also contains trilobite faunas of North American affinity, precluding an exotic origin (Hotz and Willden, 1964). The third model proposed a source in western Laurentia, in the Peace River Arch (PRA) for the RMA and the Salmon River Arch (SRA) for the Harmony Formation. The SRA can be ruled out, as there are no potential source terranes with appropriate age populations. However, the PRA region is a good candidate as a source for RMA sediments, and the Rimbey arc-Swift Current Anorogenic province to the southeast of the PRA is the likely source for Harmony B sediments.

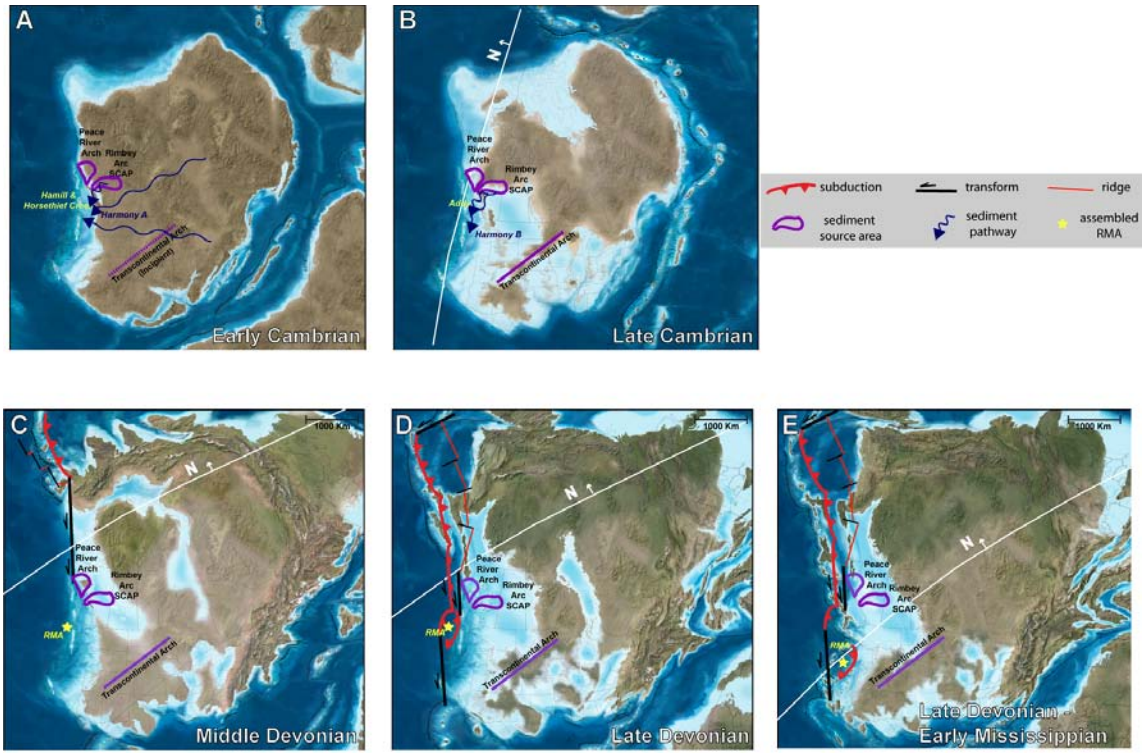

Figure 31: Paleogeographic maps of Laurentia for Early Cambrian through Mississippian time (Blakey, 2013). White lines show the approximate position of the paleoequator. Blue wavy lines show approximate sediment transport pathways of units discussed. The Transcontinental Arch (Sloss, 1988) and Peace River Arch (Ross, 1991) are superimposed. (A) Early Cambrian time. The Harmony A is derived from the central Laurentia, before the uplift of the Transcontinental Arch. The Horsethief Creek Group and Hamill Group are deposited near southeast British Columbia (B) Late Cambrian Time. The Transcontinental Arch has been uplifted. The Harmony B is shed from the Rimbey arc of eastern Alberta and the Swift Current Anorogenic Province of western Saskatchewan (C) Middle Devonian time. An arc has moved westward around the north edge of Laurentia, from northern Baltica to the western margin of northern Laurentia, and a sinistral transpressional fault system has developed along the western margin of Laurentia. The Harmony A and B, and remaining Roberts Mountains allochthon (RMA) strata, are tectonically transported south along the margin by this fault system. (D) Late Devonian time. Shortening and development of an accretionary prism has initiated along much of the western margin of Laurentia, moving the Harmony Formation and RMA strata onto the craton. (E) Early Mississippian time. The Antler orogeny has uplifted the accretionary prism of the Harmony Formation and RMA strata into a highland on the western Laurentian margin.

To reach their current position, we propose that the Harmony A and B were tectonically transported south along the western Laurentian margin in latest Devonian time (Fig. 31D) along with the other RMA strata (Linde et al., 2016). This is consistent with the sinistral transpressional fault system along the western Laurentian margin proposed by Colpron and Nelson (2009) (Figs 31C and 31D). Subsequent shortening emplaced the RMA up onto the western Laurentian craton in the Antler orogeny of latest Devonian-earliest Mississippian time (Fig. 12E). The Harmony Formation strata were imbricated with the rest of the RMA strata during the southward transport, or during emplacement onto the craton, or both.

8. Conclusions

These U-Pb geochronology and Hf-isotope analyses of the Harmony Formation strata give new insight on its provenance, age, and tectonic history. We confirmed previous U-Pb detrital zircon geochronology that had proposed two distinct sub-units of the Harmony Formation, and we interpret different sources for these sub-units (Gehrels et al., 2000a; Gehrels, et al., 2000b). We also confirm that the Harmony Formation is distinct from the strata of the RMA. Our new data indicate that the provenance of the Harmony A was likely in central Laurentia, prior to the uplift of the Transcontinental Arch, and that the provenance of the Harmony B was probably in eastern Alberta-western Saskatchewan. We propose that the Harmony A and B were deposited off the western Laurentian margin of British Columbia in late Neoproterozoic-Cambrian time. The remainder of the RMA was deposited in the same general area, from Ordovician through Devonian time.

Our preferred model is that the Harmony A and B, and the other RMA strata, were tectonically transported in late Devonian time southward along the western Laurentian margin on a sinistral transpressional fault system. The entire RMA package, including the Harmony Formation, was subsequently emplaced eastward onto the craton during the Late Devonian-Early Mississippian Antler orogeny. The Harmony Formation strata were imbricated with the rest of the RMA strata during the tectonic transport to the south or during structural emplacement onto the craton.

9. References Cited

Anderson, J.L., and Morrison, J., 1992, The role of anorogenic granites in the Proterozoic crustal development of North America, *in* Condie, K.C., ed., Proterozoic Crustal Evolution: New York, Elsevier, p. 263-299.

Bahlburg, H., Vervoort, J.D., DuFrane, S.A., Carlotto, V., Reimann, C., and Cardenas, J., 2011, The U–Pb and Hf isotope evidence of detrital zircons of the Ordovician Ollantaytambo Formation, southern Peru, and the Ordovician provenance and paleogeography of southern Peru and northern Bolivia: Journal of South American Earth Sciences, v. 32, p. 196–209.

Bazard, D.R., Butler, R.F., Gehrels, G.E., and Soja, C.M., 1995, Early Devonian paleomagnetic data from the Lower Devonian Karheen Formation suggest Laurentia-Baltica connection for the Alexander terrane: Geology, v. 23, p. 707-710.

Beranek, L.P., Van Stall, C.R., McClelland, W.C., Israel, S, and Mihalynuk, M.G., 2013, Baltican crustal provenance for Cambrian-Ordovician sandstones of the Alexander terrane, North American Cordillera: evidence from detrital zircon U-Pb geochronology and Hf isotope geochemistry: Journal of the Geological Society, London, v. 170, p. 7-18.

Bickford, M.E., and Anderson, J.L., 1993, Middle Proterozoic magmatism, *in* Reed, J.C., Bickford, M.E., Houston, R.S., Link, P.K., Rankin, D.W., Sims, P.K., and Van Schmus, W.R., eds., Precambrian Conterminous U.S.: Boulder, Colorado, Geological Society of America, The Geology of North America, v. C-2, p. 281–292.

Bickford, M.E., Van Schmus, R., and Zietz, I., 1986, Proterozoic history of the midcontinent region of North America: Geology, v. 14, no. 6, p. 492–496.

Bickford, M.E., McLelland, J.M., Mueller, P.A., Kamenov, G.D., and Neadle, M., 2010, Hafnium isotopic compositions of zircon from Adirondack AMCG suites: Implications for the petrogenesis of anorthosites, gabbros, and granitic members of the suites: Canadian Mineralogist, v. 48, p. 751–761.

Blakey, R., 2013, Key Time Slices of North American Geologic History: cpgeosystems.com/nam.html

Bouma, A.H., 1963, Sedimentology of some flysch deposits: A graphic approach to facies interpretation: Elsevier, Amsterdam, 168 p.

Bouvier, A., Vervoort, J.D., and Patchett, J.D., 2008, The Lu-Hf and Sm-Nd isotopic composition of CHUR: Constraints from unequilibrated chondrites and implications

for the bulk composition of terrestrial planets: Earth and Planetary Science Letters, v. 273, p. 48–57.

Burchfiel, B.C. and Davis, G.A., 1972, Structural framework and evolution of the southern part of the Cordilleran Orogen, Western United States: American Journal of Science, v. 272, p. 97-118.

Burchfiel, B.C., Cowan, D.S., and Davis, G.A., 1992, Tectonic overview of the Cordilleran orogeny in the western United States, *in* Burchfiel, B.C., Lipman, P.W., and Zoback, M.L., eds., The Cordilleran Orogen: Conterminous U.S.: Boulder, Colorado, Geological Society of America, The Geology of North America, v. G-3, p. 407–480.

Cant, D. J., 1988, Regional structure and development of the Peace River Arch, Alberta: A Paleozoic failed-rift system?: Bulletin of Canadian Petroleum Geology, v. 36, p. 284-295.

Cant, D. and O'Connell, S., 1988, The Peace River Arch: Its structure and origin, *in*, James, D.P. and Leckie, D.A., eds., Sequences, Stratigraphy, Sedimentology: Surface and Subsurface: Canadian Society of Petroleum Geologists, Memoir 15, p. 537-542.

Cawood, P.A., Nemchin, A.A., Strachan, R., Prave, T., and Krabbendam, M., 2007, Sedimentary basin and detrital zircon record along East Laurentia and Baltica during assembly and breakup of Rodinia: Journal of the Geological Society, London, p. 257-275.

Collerson, K.D., Van Schmus, R.W., Lewry, J.F., and Bickford, M.E., 1988, Buried Precambrian basement in south-central Saskatchewan: Provisional results from Sm-Nd model ages and U-Pb zircon geochronology; *in* Summary of investigations 1988, Saskatchewan Geological Survey, Saskatchewan Energy and Mines, Miscellaneous Report 88-4, p. 141-150.

Colpron, M., and Nelson, J., 2009, A Palaeozoic Northwest Passage: Incursion of Caledonian, Baltican and Siberian terranes into eastern Panthalassa, and the early evolution of the North American Cordillera, *in* Cawood, P.A. and Kroner, A., eds., Earth Accretionary Systems in Space and Time: Geological Society of London Special Publication 318, p. 273–307.

Colpron, M., Nelson, J.L., and Murphy, D.C., 2007, Northern Cordilleran terranes and their interactions through time: GSA Today, v. 17, p. 4–10.

Dickinson, W.R., 2000, Geodynamic interpretation of Paleozoic tectonic trends oriented oblique to the Mesozoic Klamath-Sierran continental margin in California, *in* Soreghan, M.J., and Gehrels, G.E., eds., Paleozoic and Triassic Paleogeography and Tectonics of Western Nevada and Northern California: Geological Society of America Special Paper 347, p. 209-245.

Dickinson, W.R., 2006, Geotectonic evolution of the Great Basin: Geosphere, v.2, p. 353-368.

Dickinson, W.R., 2009, Anatomy and global context of the North American Cordillera: Geological Society of America Memoirs, v. 204, p. 1-29.

Dickinson, W.R., and Gehrels, G.E., 2000, Sandstone petrofacies of detrital zircon samples from Paleozoic and Triassic strata is suspect terranes of northern Nevada and California, *in* Gehrels, G.E., and Soreghan, M.J., eds., Paleozoic and Triassic Paleogeography and Tectonics of Western Nevada and Northern California: Boulder, Colorado, Geological Society of America, Special Paper 347, p. 151-171.

Dickinson, W.R., and Lawton, T.F., 2001, Carboniferous to Cretaceous assembly and fragmentation of Mexico: Geological Society of America Bulletin, v. 113, p. 1142–1160.

Dickinson, W.R., and Gehrels, G.E., 2009, U-Pb ages of detrital zircons in Jurassic eolian and associated sandstones of the Colorado Plateau: Evidence for transcontinental dispersal and intraregional recycling of sediment: Geological Society of America Bulletin, v. 121, p. 408–433.

Doebrich, J.L., 1994, Preliminary geologic map of the Galena Canyon quadrangle, Lander county, Nevada: U.S. Geological Survey Open File Report 94-664, scale 1:24,000: Boulder, CO, U.S. Geological Survey.

Dusel-Bacon, C., Hopkins, M.J., Mortensen, J.K., Dashevsky, S.S., Bressler, J.R., and Day, W.C., 2006, Paleozoic tectonic and metallogenic evolution of the pericratonic rocks of east–central Alaska and adjacent Yukon, *in* Colpron, M. and Nelson, J.L., eds., Paleozoic Evolution and Metallogeny of Pericratonic Terranes at the Ancient Pacific Margin of North America, Canadian and Alaskan Cordillera: Geological Association of Canada, Special Paper 45, p. 25–74.

Durk, K.M., Link, P.K, and Fanning, C.M., 2007, Neoproterozoic 695 Ma felsic orthogneiss, Wildhorse Creek, Pioneer Mountains, south-central Idaho: New tie point in reconstruction of Rodinian Rifting: Geological Society of America Abstracts with Programs, v. 39, n.6.

Evans, J.G., and Theodore, T.G., 1978, Deformation of the Roberts Mountains Allochthon in North-Central Nevada: U.S. Geological Survey Professional Paper 1060, 18 p.

Fanning, C.M., and Link, P.K., 2004, U-Pb SHRIMP ages of Neoproterozoic (Sturtian) glaciogenic Pocatello Formation, southeastern Idaho: Geology, v. 32, p. 881-884.

Fedo, C.M., Sircombe, K., and Rainbird, R., 2003, Detrital zircon analysis of the sedimentary record, *in* Hanchar J.M., and Hoskin, P.W.O., eds., Zircon: Reviews in Mineralogy and Geochemistry, v. 53, p. 277–303.

Ferguson, H.G., Roberts, R.J., and Muller, S.W., 1951, Geology of the Winnemucca Quadrangle, Nevada: U.S. Geological Survey Geologic Quadrangle Map GQ-11, scale 1:125,000: Boulder, CO, U.S. Geological Survey.

Ferguson, H.G., Roberts, R.J., and Muller, S.W., 1952, Geology of the Golconda Quadrangle, Nevada: U.S. Geological Survey Geologic Quadrangle Map GQ-15, scale 1:125,000: Boulder, CO, U.S. Geological Survey.

Gaschnig, R.M., Vervoort, J.D., Lewis, R.S, and Tikoff, B., 2013, Probing for Proterozoic and Archean crust in the northern U.S. Cordillera with inherited zircon from the Idaho batholith: Geological Society of America Bulletin, v. 125, p. 73-88.

Gehrels, G.E., 2000, Introduction to detrital zircon studies of Paleozoic and Triassic strata in western Nevada and northern California, *in* Soreghan, M.J., and Gehrels, G.E., eds., Paleozoic and Triassic Paleogeography and Tectonics of Western Nevada and Northern California: Geological Society of America Special Paper 347, p.1–17.

Gehrels, G.E., 2012, Detrital zircon U-Pb geochronology: Current methods and new opportunities, *in* Busby, C., and Azor, A., eds., Recent Advances in Tectonics of Sedimentary Basins: Hoboken, New Jersey, Blackwell Publishing, p. 47-62.

Gehrels, G.E., 2014, Detrital zircon U-Pb geochronology applied to tectonics: Annual Review of Earth and Planetary Sciences, v. 42, p. 127-149.

Gehrels, G.E., and Ross, G.M., 1998, Detrital zircon geochronology of Neoproterozoic to Permian miogeoclinal strata in British Columbia and Alberta: Canadian Journal of Earth Sciences, v. 35, p. 1380–1401.

Gehrels, G.E., and Pecha, M., 2014, Detrital zircon U-Pb geochronology and Hf isotope geochemistry of Paleozoic and Triassic passive margin strata of western North America: Geosphere, v. 10, p. 49-65.

Gehrels, G.E., Butler, R.F., and Bazard, D.R., 1996, Detrital Zircon geochronology of the Alexander terrane, southeastern Alaska: Geological Society of America Bulletin, v. 108, p. 722-734.

Gehrels, G.E., Dickinson, W.R., Riley, B.C.D., Finney, S.C., Smith, M.T., 2000a, Detrital zircon geochronology of the Roberts Mountains allochthon, Nevada, *in* Gehrels, G.E., and Soreghan, M.J., eds., Paleozoic and Triassic Paleogeography and Tectonics of Western Nevada and Northern California: Boulder, Colorado, Geological Society of America, Special Paper 347, p. 19–42.

Gehrels, G.E., Dickinson, W.R., Darby, B.J., Harding, J.P., Manuszak, J.D., Riley, B.C.D., Spurlin, M.S., Finney, S.C., Girty, G.H., Harwood, D.S., Miller, M.M., Satterfield, J.I., Smith, M.T., Snyder, W.S., Wallin, E.T., and Wyld, S.J., 2000b,Tectonic implications of detrital zircon data from Paleozoic and Triassic strata in western Nevada and northern California, *in* Gehrels, G.E., and Soreghan, M.J., eds., Paleozoic and Triassic Paleogeography and Tectonics of Western Nevada and Northern California: Boulder, Colorado, Geological Society of America, Special Paper 347, p. 133–150.

Gehrels, G.E., Valencia, V.A., and Ruiz, J., 2008, Enhanced precision, accuracy, efficiency, and spatial resolution of U-Pb ages by laser ablation-multicollector-inductively coupled plasma-mass spectrometry: Geochemistry, Geophysics, Geosystems, v.9, p. 1-13.

Gehrels, G.E., Blakey, R., Karlstrom, K.E., Timmons, J.M., Dickinson, B., and Pecha, M., 2011, Detrital zircon U-Pb geochronology of Paleozoic strata in the Grand Canyon, Arizona: Lithosphere, v. 3, p. 183-200.

Gilluly, J., 1967, Geologic Map of the Winnemucca quadrangle, Pershing and Humboldt counties, Nevada: U.S. Geological Survey Geologic Quadrangle Map GQ-656, scale 1:62,500: Boulder, CO, U.S. Geological Survey.

Goebel, K.A., 1991, Paleogeographic setting of Late Devonian to Early Mississippian transition from passive to collisional margin, Antler foreland, eastern Nevada and western Utah, *in* Cooper, J.D., and Stevens, C.H., eds., Paleozoic paleogeography of the western United States—II: Pacific Section, SEPM (Society for Sedimentary Geology) book 67, p. 401-418.

Goodge, J.W., and Vervoort, J.D., 2006, Origin of Mesoproterozoic A-type granites in Laurentia: Hf isotopic evidence: Earth and Planetary Science Letters, v. 243, p. 711–731.

Grove, M., Gehrels, G.E., Cotkin, S.J., Wright, J.E., and Zou, H., 2008, Non-Laurentian cratonal provenance of Late Ordovician eastern Klamath blueschists and a link to the Alexander terrane, *in* Wright, J.E., and Shervais, J.W., eds., Ophiolites, Arcs, and Batholiths: A tribute to Cliff Hopon: Geological Society of America Special Paper 438, p. 223-250.

Guynn, J., and Gehrels, G.E., 2006, Comparison of detrital zircon age distribution using the K-S test: online manual published by the University of Arizona LaserChron Center:https://docs.google.com/file/d/0B9ezu34P5h8eZWZmOWUzOTItZDgyZi00NDRiLWI4ZTctNTljNTM5OTU1MGUz/edit?hl=enandpli=1

Harbaugh, D.W., 1980, Depositional facies and provenance of the Mississippian Chainman Shale and Diamond Peak Formation, Central Diamond Mountains, Nevada [M.S. Thesis]: Stanford University, 81 p.

Hoffman, P.F., 1989, Precambrian geology and tectonic history of North America *in* Bally, A.W., and Palmer, A.R., eds., The Geology of North America—An Overview: Boulder, Colorado, Geological Society of America, The Geology of North America, v. A, p. 447–512.

Holm, D.K., Hull, A., Vervoort, J.D., and Schneier, D.A., 2013, Origin of 1700-1800 Ma rocks in the central Yavapai and Penokean Provinces: insights from zircon Hf isotope data: Abstracts with Programs—Geological Society of America, v. 45, n. 7, p. 309.

Hotz, P.F., and Willden, R., 1964, Geology and mineral deposits of the Osgood Mountains quadrangle: U.S. Geological Survey Professional Paper 431, 128 p.

Jones, A.E., 1997a, Geologic map of the Delvada Spring quadrangle Nevada: Nevada Bureau of Mines and Geology Field Studies Map FS-13, scale 1:24,000, Reno, NV: Nevada Bureau of Mines and Geology.

Jones, A.E., 1997b, Geologic map of the Hot Springs Peak quadrangle and the southeastern part of the Little Poverty quadrangle, Nevada: Nevada Bureau of Mines and Geology Field Studies Map FS-14, scale 1:24,000, Reno, NV: Nevada Bureau of Mines and Geology.

Jones-Crafford, A.E., 2008, Paleozoic tectonic domains of Nevada: An interpretive discussion to accompany the geologic map of Nevada: Geosphere, v.4, p. 260-291.

Kay, M., 1951, North American geosynclines: Geological Society of America Memoir 48.

Kent, D.M., 1994, Paleogeographic evolution of the cratonic platform—Cambrian to Triassic, *in* Mossop, G.D. and Shetsen, I., eds., Geological atlas of the Western Canadian sedimentary basin, p. 69-86.

Ketner, K.B., 1977, Deposition and deformation of Lower Paleozoic western facies rocks, northern Nevada *in* Stewart, J.H., Stevens, C.H., and Fitsche, A.E., eds., Paleozoic paleogeography of the western United States, Pacific Coast Paleogeography Symposium I: Society of Economic Paleontologists and Mineralogists, p. 251-258.

Ketner, K.B., 1998, The nature and timing of tectonism in the western facies terrane of Nevada and California—An outlilne of evidence and interpretations derived from geologic maps of key areas: U.S. Geological Survey Professional Paper 1592.

Ketner, K.B., 2008, The Inskip Formation, the Harmony Formation, and the Havallah Sequence of northwestern Nevada—An interrelated Paleozoic assemblage in the home of the Sonoma Orogeny: U.S. Geological Survey Professional Paper 1757.

Ketner, K.B., Jones-Crafford, A.E., Harris, A.G., Repetski, J.E., and Wardlaw, B.R., 2005, Late Devonian to Mississippian arkosic rock derived from a granitic terrane in

northwestern Nevada adds a new dimension to the Antler orogeny, *in* Rhoden, H.N., Steinniger, R.C., and Vikre, P.G., eds., Geological Society of Nevada Symposium 2005: Window to the World, Reno, Nevada, May 2005, p. 133-145.

Ketner, K.B., and Ross, R.J., Jr., 1990, Geologic Map of the Northern Adobe Range, Elko County, Nevada: United States Geological Survey Miscellaneous Investigations Series Map I-2081, scale 1:24,000: Boulder, CO, U.S. Geological Survey.

Ketner, K.B, Crafford, A.E.J., Harris, A.G., Repetski, J.E., and Wardlaw, B.R., 2005, Late Devonian to Mississippian arkosic rock derived from a granitic terrane in northwestern Nevada adds a new dimension to the Antler orogeny, *in* Rhoden, H.N., Steininger, R.C., and Vikre, P.G., eds., Symposium 2005: Window to the World: Geological Society of Nevada Symposium Proceedings, v. 1, p. 135-145.

Lawton, T.F., Hunt, G.J., and Gehrels, G.E., 2010, Detrital zircon record of thrust belt unroofing in Lower Cretaceous synorogenic conglomerates, central Utah: Geology, v. 38, p. 463-466.

Linde, G.M., Cashman, P., Dickinson, W., and Trexler, J.H., 2013, The Provenance challenge of the Harmony Formation in central Nevada: an enigmatic piece of the Cordilleran jigsaw puzzle: Geological Society of America Abstracts with Programs, v. 66.

Linde, G.M., Cashman, P.H., Trexler, J.H., Jr., and Dickinson, W.R., 2014a, Stratigraphic trends in detrital zircon geochronology of upper Neoproterozoic and Cambrian strata, Osgood Mountains, Nevada and elsewhere in the Cordilleran miogeocline: Evidence for early Cambrian uplift of the Transcontinental Arch: Geosphere, v. 10., p. 1402-1410.

Linde, G.M., Cashman, P.H., Trexler, J.H., Jr., and Dickinson, W.R., 2014b, The provenance of the Cambrian Addy Quartzite, northeast Washington: connections between British Columbia and central Nevada: Geological Society of America Abstracts with Programs, v. 46, n.3.

Linde, G.M., Cashman, P.H., Trexler, J.H., Jr., Gehrels, G., and Dickinson, W.R., 2016, Detrital zircon U-Pb geochronology and Hf isotope geochemistry of the Roberts Mountains allochthon: New insights into the Early Paleozoic tectonics of western North America: Geosphere, v. 12, p. 1-16.

Lindsey, K.A. and Gaylord, D.R., 1992. Fluvial, coastal, nearshore, and shelf deposits in the Upper Proterozoic (?) to Lower Cambrian Addy Quartzite, northeastern Washington: Sedimentary Geology, v. 77, p. 15-35.

Link, P.K., Steel, T., Stewart, E.S., Sherwin, J., Hess, L.R., and McDonald, C, 2013, Detrital zircons in the Mesoproterozoic upper Belt Supergroup in the Beaverhead and Lemhi ranges, Montana and Idaho: Northwest Geology, p. 39-44.

Lund, K., Aleinikoff, J.N., Evans, K.V., and Fanning, C.M., 2003, SHRIMP U-Pb geochronology of Neoproterozoic Windermere Supergroup, central Idaho: Implications for rifting of western Laurentia and synchroneity of Sturtian glacial deposits: Bulletin of the Geological Society of America, v. 115, p. 349-372.

Ludwig, K.R., 2008, Isoplot 3.6, Berkeley Geochronology Center Special Publication 4, 77 p.

Madrid, R.J., 1987, Stratigraphy of the Roberts Mountains allochthon in north-central Nevada [Ph.D. dissertation]: Stanford, California, Stanford University, 336 p.

Mueller, P.A., Kamenov, G.D., Heatherington, A.L., and Richards, J., 2008, Crustal evolution in the southern Appalachian orogen: Evidence from Hf isotopes in detrital zircons: The Journal of Geology, v. 116, p. 414–422.

Nelson, S.T., hart, G.L., and Frost, C.D., 2011, A reassessment of Mojavia and a new Cheyenne Belt alignment in the eastern Great Basin: Geosphere, p. 513-527.

Nilsen, T.H., and Stewart, J.H., 1980, The Antler orogeny—Mid-Paleozoic tectonism in western North America (Penrose Conference Report): Geology, v. 8. p. 298-302.

Noble, P.J., and Finney, S.C., 1999, Recognition of fine-scale imbricate thrusts in lower Paleozoic orogenic belts—An example from the Roberts Mountains allochthon, Nevada: Geology, v. 27, p. 543–546.

Oldow, J.S., 1984, Evolution of a late Mesozoic back-arc fold and thrust belt, northwestern Great Basin. U.S.A.: Tectonophysics, v. 102. p. 245-274.

Paradis, S., Bailey, S.L., Creaser, R.A., Piercey, S. J., and Schiarraza, P., 2006, Paleozoic magmatism and syngenetic massive sulphide deposits of the Eagle Bay assemblage, Kootenay terrane, southern British Columbia, *in* Colpron, M. and Nelson, J.L., eds., Paleozoic Evolution and Metallogeny of Pericratonic Terranes at the Ancient Pacific Margin of North America, Canadian and Alaskan Cordillera: Geological Association of Canada, Special Paper 45, p. 383–414.

Patchett, P.J., 1983, Importance of the Lu-Hf isotopic system in studies of planetary chronology and chemical evolution: Geochimica et Cosmochimica Acta, v. 47, p. 81-91.

Patchett, P.J., and Tatsumoto, M., 1980, A routine high-precision method for Lu-Hf isotope geochemistry and chronology: Contributions to Mineralogy and Petrology, v. 75, 263-267.

Peterson, T. D., Scott, J.M.J., LeCheminant, A.N., Jefferson, C.W., and Pehrsson, S.J., 2015, The Kivalliq Igneous Suite: Anorogenic bimodal magmatism at 1.75 Ga in the western Churchill Province, Canada: Precambrian Research, v. 262, p. 101-119.

Piercey, S.J., Nelson, J.L., Colpron, M., Dusel-Bacon, C., Roots, C.F., and Simard, R.L., 2006, Paleozoic magmatism and crustal recycling along the ancient Pacific margin of North America, northern Cordillera, *in* Colpron, M. and Nelson, J.L., eds., Paleozoic Evolution and Metallogeny of Pericratonic Terranes at the Ancient Pacific Margin of North America, Canadian and Alaskan Cordillera: Geological Association of Canada, Special Paper 45, p. 281–322.

Poole, E.G., 1974, Flysch deposits of Antler foreland basin, western United States, *in* Dickinson, W.R., ed., Tectonics and sedimentation: Society of Economic Paleontologists and Mineralogists Special Publication 22, p. 58-82.

Poole, F.G., Stewart, J.H., Palmer, A.R., Sandberg, C.A., Madrid, R.A., Ross, R.J., Jr., Hintze, L.F., Miller, M.M., and Wrucke, C.T., 1992, Latest Precambrian to latest Devonian time; development of a continental margin: *in* Burchfiel, B.C., Lipman, P.W., and Zoback, M.L., eds., The Cordilleran Orogen: Conterminous U.S.: Boulder, CO, Geological Society of America, the Geology of North America, v. G-3.

Rainbird, R.H., McNicoll, J., Theriault, R.J., Heaman, L.M., Abbott, J.G., Long, D.G.F., and Thorkelson, D.J., 1997, Pan-continental river system draining Grenville orogeny recorded by U-Pb and Sm-Nd geochronology of Neoproterozoic quartz arenites and mudrocks, northwestern Canada: The Journal of Geology, v. 105, p. 1-17.

Rainbird, R.H., Cawood, P., and Gehrels, G., 2012, The great Grenvillian sedimentation episode: record of supercontinent Rodinia's assembly, *in* Busby, C. and Azor, A., eds., Tectonics of sedimentary basins: recent advances. Blackwell Publishing Ltd, p. 583-601.

Roberts, R.J., 1951, Geology of the Antler Peak Quadrangle, Nevada: U.S. Geological Survey Geologic Quadrangle Map GQ-10, scale 1:62,500: Boulder, CO, U.S. Geological Survey.

Roberts, R.J., 1964, Stratigraphy and structure of the Antler Peak quadrangle, Humboldt and Lander counties Nevada: U.S. Geological Survey Professional Paper 459A, 93 p.

Roberts, R.J., Hotz, P.E., Gilluly, J., and Ferguson, H.G., 1958, Paleozoic rocks of north-central Nevada: American Association of Petroleum Geologists Bulletin, v. 42. p. 2813-2857.

Rohr, T.S., Andersen, T., and Dypvik, H., 2008, Provenance of Lower Cretaceous sediments in the Wandel Sea Basin, North Greenland: Journal of the Geological Society, v. 165, p. 755–767.

Rohr, T.S., Andersen, T., Dypvik, H., and Embry, A.F., 2010, Detrital zircon characteristics of the Lower Cretaceous Isachsen Formation, Sverdrup Basin: Source constraints from age and Hf isotope data: Canadian Journal of Earth Sciences, v. 47, p. 255–271.

Ross, G.M., 1991, Precambrian basement in the Canadian Cordillera: An introduction: Canadian Journal of Earth Sciences, v. 28, p. 1133-1139.

Rowell, A.J., Rees, M.N., and Suczek, C.A., 1979, Margin of the North American continent in Nevada during Late Cambrian time: American Journal of Science, v. 279, p. 1-18.

Scherer, E., Munker, C., and Mezger, K., 2001, Calibrating the Lu-Hf clock: Science, v. 293, p. 683–686,

Schuchert, C., 1923, Sites and natures of the North American geosynclines: Bulletin of the Geological Society of America, v. 34, p. 151-230.

Schweickert, R.A., and Snyder, W.S., 1981, Paleozoic plate tectonics of the Sierra Nevada and adjacent regions: The geotectonic development of California, Rubey Volume 1, p. 182-201.

Sloss, L.L. (Ed.), 1988, Tectonic evolution of the craton in Phanerozoic time, *in* Sloss, L.L., ed., Sedimentary Cover—North American Craton: U.S.: Boulder, Colorado, Geological Society of America, The Geology of North America, v. D-2.

Smith, M., and Gehrels, G., 1994, Detrital zircon geochronology and the provenance of the Harmony and Valmy Formations, Roberts Mountains allochton, Nevada: Geological Society of America Bulletin, v. 106, p. 968-979.

Söderlund, U., Patchett, P.J., Vervoort, J.D., and Isachsen, C.E., 2004, The ^{176}Lu decay constant determined by Lu-Hf and U-Pb isotope systematics of Precambrian mafic intrusions: Earth and Planetary Science Letters, v. 219, p. 311-324.

Stacey, J.S., and Kramers, J.D., 1975, Approximation of terrestrial lead isotope evolution by a two stage model: Earth and Planetary Science Letters, v. 26, p. 207-221.

Stewart, J.H. and Suczek, C.A., 1977, Cambrian and latest Precambrian paleogeography and tectonics in the western United States, *in* Stewart, J.H., Stevens, C.H., and Fitsche, A.E., eds. Paleozoic paleogeography of the western United States, Pacific Coast Paleogeography Symposium I: Society of Economic Paleontologists and Mineralogists, p. 1-17.

Suczek, C.A., 1977, Tectonic relations of the Harmony Formation, northern Nevada [Ph.D. dissertation]: Stanford University, 96 p.

Theodore, T.G., Murchey, B.L., Hanger, R.A., Strong, E.E., and Ashinhurst, R.T., 1994, To accompany the preliminary geologic map of the Snow Gulch quadrangle, Humboldt and Lander Counties, Nevada: U.S. Geological Survey Open File Report 94-436, 31 p.

Trexler, J.H., Jr., Cashman, P.H., Cole, J.C., Snyder, W.S., Tosdal, R.M., Davydov, V.I., 2003, Widespread effects of middle Mississippian deformation in the Great Basin of western North America: Geological Society of America Bulletin, v. 115, p. 1278-1288.

Van Schmus, W.R., Bickford, M.E., Sims, P.K., Anderson, J.L., Shearer, C.K., and Treves, S.B., 1993, Proterozoic geology of the western midcontinent region, *in* Reed, J.C., Bickford, M.E., Houston, R.S., Link, P.K., Rankin, D.W., Sims, P.K., and Van Schmus, W.R., eds., Precambrian Conterminous U.S.: Boulder, Colorado, Geological Society of America, The Geology of North America, v. C-2, p. 239–259.

Vervoort, J.D., and Patchett, P.J., 1996, Behavior of hafnium and neodymium isotopes in the crust: Constraints from crustally derived granites: Geochimica et Cosmochimica Acta, v. 60, p. 3717–3733.

Vervoort, J.D., and Blichert-Toft, J., 1999, Evolution of the depleted mantle: Hf isotope evidence from juvenile rocks through time: Geochimica et Cosmochimica Acta, v. 63, p. 533–556.

Vervoort, J.D., Patchett, P.J., Blichert-Toft, J., and Albarede, F., 1999, Relationships between Lu-Hf and Sm-Nd isotopic systems in the global sedimentary system: Earth and Planetary Science Letters, v. 168, p. 79–99.

Vervoort, J.D., Patchett, P.J., Soderlund, U., and Baker, M., 2004, Isotopic composition of Yb and the determination of Lu concentrations and Lu/Hf ratios by isotope dilution using MC-ICPMS: Geochemistry Geophysics Geosystems, v. 5, Q11002.

Villeneuve, M.E., Ross, G.M., Theriault, R.J., Miles, W., Parrish, R.R., and Broome, J., 1993, Tectonic subdivision and U-Pb geochronology of the crystalline basement of the Alberta basin, western Canada: Geological Survey of Canada, Bulletin 447, 86 p.

Wallin, E.T., 1990, Provenance of selected lower Paleozoic siliclastic rocks in the Roberts Mountains allochthon, Nevada, *in* Harwood, D.S., and Miller, M.M., eds., Paleozoic and early Mesozoic paleogeographic relations; Sierra Nevada, Klamath Mountains, and related terranes: Boulder, Colorado, Geological Society of America Special Paper 255, p. 17-32.

Whitmeyer, S.J., and Karlstrom, K.E., 2007, Tectonic model for the Proterozoic growth of North America: Geosphere, p. 220-259.

Woodhead, J.D., and Hergt, J.M., 2004, A preliminary appraisal of seven natural zircon reference materials for in situ Hf isotope determination: Geostandards and Geoanalytical Research, v. 29 (2), p. 183-195.

Woodhead, J., Hergt, J., Shelley, M., Eggins, S., and Kemp, R., 2004, Zircon Hf-isotope analysis with an excimer laser, depth profiling, ablation of complex geometries, and concomitant age estimation: Chemical Geology, v. 209, p. 121-135.

Wright, J., and Wyld, S., 2006, Gondwana, Iapetan, Cordilleran interactions: A geodynamic model for the Paleozoic tectonic evolution of the North American Cordillera, *in* Haggart, J., Enkin, R., and Monger, J., eds., Paleogeography of the North American Cordillera: Evidence For and Against Large-Scale Displacements: Geological Association of Canada Special Paper 46, p. 377–408.

Wrucke, C.T., 1974, Geologic map of the Gold Acres – Tenabo area, Shoshone Range, Lander County, Nevada: U.S. Geological Survey Miscellaneous Field Studies Map MF-647, scale 1:15,840: Boulder, CO, U.S. Geological Survey.

Yonkee, W.A., Dehler, C.D., Link, P.K., Balgord, E.A., Keeley, J.A., Hayes, D.S., Wells, M.L., Fanning, C.M., Johnston, S.M., 2014, Tectono-stratigraphic framework of Neoproterozoic to Cambrian strata, west-central U.S.: Protracted rifting, glaciation, and evolution of the North American Cordilleran margin, Earth Science Reviews, v.136, p. 59-95.

Conclusions

1. Summary and Conclusions

This dissertation investigated Neoproterozoic–Devonian units of the western Laurentian passive margin and Roberts Mountains allochthon (RMA) and determined new U-Pb detrital ages and Hf isotope zircon analyses. From these analyses, this study reports new interpretations of the early Paleozoic tectonics of western Laurentia.

The study reported in Chapter 1 used detrital zircon U-Pb geochronology to confirm that the Upper Neoproterozoic–Lower Cambrian Osgood Mountain Quartzite and the Upper Cambrian–Lower Ordovician Preble Formation in the Osgood Mountains of northern Nevada are units of the western Laurentian passive margin. This also found that U-Pb age populations of the detrital zircons shift with stratal age within the Osgood Mountain Quartzite, indicating a change in provenance within the Osgood Mountain Quartzite. This shift in U-Pb age populations and change in provenance is similar in coeval passive margin strata across the Great Basin. This was a result of the Late Neoproterozoic-Early Cambrian uplift of the Transcontinental Arch, which changed sedimentary transport patterns, and resulted in the observed shift in provenance. This study provided independent corroboration of the existence of the Transcontinental Arch and better precision for the timing at which the Arch uplifted. The study also recorded the impact of the uplifted Arch on continent-wide sediment dispersal patterns—the change in predominant source terranes—and confirmed the Arch as a sediment source for passive margin strata.

The study reported in Chapter 2 used detrital zircon U-Pb geochronology and Hf-isotope analyses to study Roberts Mountains allochthon strata. Zircon grains from six Ordovician to Devonian arenite samples were analyzed for U-Pb ages and some were further analyzed for Hf-isotope ratios. Five of the units have similar U-Pb age populations and Hf-isotope ratios, while those of the Ordovician lower Vinini Formation differ significantly. The lower Vinini Formation originated in the north-central Laurentian craton. The other five units, as well as Ordovician passive-margin sandstones of the western Laurentian margin, had a common source in the Peace River Arch region of western Canada. All of the RMA strata were deposited near the Peace River Arch region and then tectonically transported south along the Laurentian margin, where they were emplaced onto the craton during the Antler orogeny.

Chapter 3 used detrital zircon U-Pb geochronology and Hf-isotope analyses to investigate the Harmony Formation, an enigmatic unit in the RMA. Zircon grains from ten arenite samples were analyzed. Three of the arenite units (Harmony A) have similar U-Pb age peaks and Hf isotope ratios, whereas seven (Harmony B) differ significantly. The data confirmed the subdivision of the Harmony Formation into two petrofacies: quartzose (Harmony A) and feldspathic (Harmony B). Harmony A originated in the central Laurentian craton. Harmony B had a common source in eastern Alberta–western Saskatchewan, north of the source of the Harmony A. All of the Harmony Formation strata were deposited near eastern Alberta in Late Neoproterozoic through Cambrian time and subsequently imbricated tectonically with other Roberts Mountains allochthon strata. The entire package was tectonically transported south along the Laurentian margin and

then emplaced eastward onto the craton during the Late Devonian to Early Mississippian Antler orogeny.

These three studies demonstrated the utility of detrital zircon U-Pb geochronology and Hf isotope analyses to better understand difficult sedimentary and tectonic problems. The studies also provided new insights into the Early Paleozoic tectonic evolution of western Laurentia.

2. Recommendations for Future Work

Future work could use detrital zircons to analyze units that are suspected to be, or are correlated with, Roberts Mountains allochthon strata. Several such units described below are good candidates for future work.

- Intriguing U-Pb analyses of metasediments in Sierran roof pendants are a starting point for further work. The May Lake pendant has some detrital-zircon ages quite similar to the Harmony B (Memeti et al., 2010); limited sampling should be expanded and Hf-isotope analyses added.
- The El Paso terrane of the southern Sierra/northern Mojave Desert region has been correlated with the Roberts Mountains allochthon, and limited detrital zircon geochronology shows that the ages are similar (Chapman et al., 2015). This initial sampling of the El Paso terrane should be expanded and Hf isotope analyses included.
- The Middle to Upper Ordovician Palmetto Formation of the Toquima, Toiyabe, and Monitor Ranges, and in Esmeralda county, Nevada, has been interpreted as an

allochthonous sequence of the Roberts Mountains allochthon (Ross, 1967; Kleinhampl and Ziony, 1985; McKee, 1968). The Palmetto Formation has also been interpreted as autochthonous and not part of the RMA (Stewart, 1980).

- Units of the Roberts Mountains allochthon in Northeastern Nevada (e.g., McFarlane, 1997; McFarlane, 2001) are ideal candidates for detrital zircon geochronology and Hf isotope studies, to determine if the same age and Hf isotope patterns found in this study are repeated.
- The Roberts Mountains thrust is interpreted in strata in Idaho (e.g., Coats, 1980; Link and Geslin, 1999), and detrital zircon geochronology and Hf isotope studies would determine if these rocks are Roberts Mountains allochthon strata.

3. References Cited

Chapman, A.D., Ernst, W.G., Gottlieb, E., Powerman, V., and Metzger, E.P., 2015, Detrital zircon geochronology of Neoproterozoic – Lower Cambrian passive-margin strata of the White-Inyo Range, east-central California: Implications for the Mojave-Snow Lake fault hypothesis: Geological Society of America Bulletin, v. 127, p. 926-944.

Coats, R.R., 1980, The Roberts Mountains thrust in central Twin Falls County, Idaho: Abstracts with programs – Geological Society of America, v. 12, p. 270.

Kleinhampl, F.J., and Ziony, J.E., 1967, Preliminary geologic map of northern Nye County, Nevada: U.S. Geological Survey Open-file Map, OF-67-129.

Link, P.K., and Geslin, J.K., 1999, Upper Paleozoic basins in southern Idaho and their relationship to emplacement and reactivation of the Roberts Mountains Allochthon: Abstracts with programs – Geological Society of America, v. 31, p. 22.

McFarlane, M.J., 1997, The Roberts Mountains thrust in the Snake Mountains, Elko county, Nevada: fNevada Petroleum Society 1997 Field Trip Guidebook, p.17-34.

McFarlane, M.J., 2001, Late Paleozoic tectonism in the northern Snake Mountains, Elko county, Nevada [PhD dissertation]: Reno, Nevada, University of Nevada, 297 p.

McKee, E.H., 1968, Geologic map of southwestern part of Lander county, Nevada: U.S. Geologic Survey, Open-File Map.

Ross, R.J., Jr., 1967, Some Middle Ordovician brachiopods and trilobites from the Basin Ranges, Western United States: U.S. Geological Survey Professional Paper 523D.

Stewart, J.H., 1980, Geology of Nevada – a discussion to accompany the Geologic Map of Nevada: Nevada bureau of Mines and Geology Special Publication 4.

Memeti, V., Gehrels, G.E., Paterson, S.R., Thompson, J.M., Mueller, R.M., and Pignotta, G.S., 2010, Evaluating the Mojave-Snow Lake fault hypothesis and origins of central Sierran metasedimentary pendant strata using detrital zircon provenance analyses: Lithosphere, v. 2, p. 341-36

APPENDIX A

Statistical Analysis of Osgood Mountain Quartzite Samples

A visual scan of the Goughs Canyon and Golconda Mine relative probability graphs (Figs. 6 and 7) reveals similar age peaks, with similar numbers of grains, at ca. 1700 Ma. Both of these graphs also show peaks at ca. 2500 Ma and 2900 Ma, though with different numbers of grains forming the peaks. The K-S statistical test found very low correlation ($P<0.05$) between these two samples, when we compared the entire data set for each sample. However, the K-S test is very sensitive to proportions of ages, and as with these samples, will indicate no or low correlation, though a visual examination coupled with geologic understanding indicates the contrary—a high likelihood of common sources (Gehrels, 2012). Within the Osgood Mountain Quartzite, we used the K-S statistical test to compare the distinct Neoproterozoic and Archean grain subpopulations. The correlation between the Goughs Canyon and Golconda Mine Neoproterozoic subpopulations was 0.957, while the correlation between these two samples' Archean subpopulations was 0.174. This comparison of subpopulations allows us to account the different proportions of grains of similar ages that would otherwise indicate no correlation.

APPENDIX B

U-Pb geochronologic analyses of selected Osgood Mountain Quartzite and Preble Formation strata

Table notes are at the end of the appendix.

Isotope ratios											Apparent ages (Ma)								
Analysis	U	206Pb	U/Th	206Pb*	±	207Pb*	±	206Pb*	±	error	206Pb*	±	207Pb*	±	206Pb*	±	Best age	±	Conc
	(ppm)	204Pb		207Pb*	(%)	235U*	(%)	238U	(%)	corr.	238U*	(Ma)	235U	(Ma)	207Pb*	(Ma)	(Ma)	(Ma)	(%)
SAMPLE: Osgood Mountain Quartzite GC-03-COM LOCATION: Goughs Canyon, Osgood Mountains 0468951 4554410 (NAD 83 UTM 11N)																			
GC-03-COMB-2	39	5019	1.6	13.3082	7.0	1.9400	7.3	0.1873	2.3	0.31	1106.5	23.2	1095.0	49.1	1072.3	139.8	1072.3	139.8	103.2
GC03OEM-99	227	2831	1.4	12.8138	2.6	1.7529	3.3	0.1629	2.0	0.60	972.9	18.1	1028.2	21.4	1147.9	52.3	1147.9	52.3	84.8
GC03OEM-85	79	12349	1.6	12.7692	1.6	2.0042	3.4	0.1856	3.0	0.88	1097.6	30.1	1116.9	23.1	1154.8	32.8	1154.8	32.8	95.0
GC03OEM-88	116	60376	2.6	12.7043	1.5	2.1192	3.0	0.1953	2.6	0.87	1149.8	27.0	1155.1	20.4	1164.9	29.1	1164.9	29.1	98.7
GC03OEM-34	137	58888	3.0	12.6600	0.9	2.1557	2.2	0.1979	2.0	0.91	1164.2	21.0	1166.9	15.0	1171.9	17.7	1171.9	17.7	99.3
GC03OEM-37	38	6599	2.2	12.6355	9.2	2.1072	9.5	0.1931	2.2	0.23	1138.2	22.9	1151.2	65.5	1175.7	183.3	1175.7	183.3	96.8
GC03OEM-74	87	28506	2.3	12.6005	1.1	2.0615	3.6	0.1884	3.4	0.95	1112.7	34.5	1136.1	24.3	1181.2	21.9	1181.2	21.9	94.2
GC03OEM-14	137	5688	1.1	11.6434	1.2	2.7830	2.9	0.2350	2.6	0.91	1360.7	31.9	1351.0	21.3	1335.6	22.6	1335.6	22.6	101.9
GC03OEM-36	123	15944	1.2	11.5991	1.7	2.2045	3.5	0.1854	3.0	0.87	1096.7	30.6	1182.5	24.3	1343.0	33.0	1343.0	33.0	81.7
GC-03-COMB-15	69	12589	4.2	11.5051	1.4	2.8992	2.1	0.2419	1.6	0.76	1396.6	20.2	1381.7	16.0	1358.7	26.7	1358.7	26.7	102.8
GC-03-COMB-4	85	16572	1.1	11.4792	1.6	2.9036	2.7	0.2417	2.2	0.81	1395.7	27.4	1382.8	20.3	1363.0	30.1	1363.0	30.1	102.4
GC03OEM-40	91	72904	1.4	11.3947	1.5	2.8545	2.5	0.2359	2.0	0.79	1365.4	24.0	1370.0	18.5	1377.2	28.7	1377.2	28.7	99.1
GC03OEM-32	178	90171	2.1	11.3817	1.0	2.7877	1.7	0.2301	1.4	0.81	1335.1	16.4	1352.3	12.5	1379.4	18.8	1379.4	18.8	96.8
GC-03-COMB-17	58	10200	3.8	11.3592	2.0	2.9652	2.9	0.2443	2.0	0.71	1408.9	25.7	1398.7	21.8	1383.2	39.1	1383.2	39.1	101.9
GC03OEM-61	117	46256	2.7	11.3553	0.6	2.9245	1.9	0.2409	1.8	0.94	1391.1	22.8	1388.3	14.6	1383.9	12.4	1383.9	12.4	100.5
GC03OEM-54	123	43469	0.9	11.3012	1.2	2.9874	1.7	0.2449	1.3	0.75	1411.9	16.5	1404.4	13.3	1393.0	22.2	1393.0	22.2	101.4
GC03OEM-50	120	67158	1.8	11.2873	1.5	3.0835	3.4	0.2524	3.0	0.89	1451.0	38.8	1428.6	25.7	1395.4	29.2	1395.4	29.2	104.0
GC03OEM-53	78	23155	2.0	11.1918	1.1	3.0536	2.3	0.2479	2.1	0.88	1427.5	26.3	1421.1	17.8	1411.7	21.2	1411.7	21.2	101.1
GC03OEM-19	194	10573	1.1	11.1409	1.3	2.5264	3.1	0.2041	2.8	0.91	1197.5	30.7	1279.7	22.5	1420.4	24.4	1420.4	24.4	84.3
GC03OEM-13	261	16815	2.1	11.0933	0.4	2.9720	2.1	0.2391	2.0	0.98	1382.1	25.4	1400.5	15.7	1428.6	7.1	1428.6	7.1	96.7
GC03OEM-26	257	58196	1.9	11.0899	0.4	3.0205	2.4	0.2429	2.3	0.98	1402.0	29.5	1412.8	18.2	1429.2	8.5	1429.2	8.5	98.1
GC03OEM-17	328	140166	1.9	11.0829	0.3	3.0727	1.8	0.2470	1.8	0.98	1422.9	23.1	1425.9	14.1	1430.4	6.4	1430.4	6.4	99.5
GC-03-COMB-13	132	22326	5.1	11.0637	0.9	3.1578	2.9	0.2534	2.7	0.95	1455.9	35.7	1446.9	22.2	1433.7	17.0	1433.7	17.0	101.6
GC03OEM-11	133	33704	2.5	11.0538	0.4	3.1250	2.2	0.2505	2.2	0.98	1441.2	27.8	1438.9	16.8	1435.4	7.4	1435.4	7.4	100.4
GC-03-COMB-7	53	9842	2.5	11.0367	3.8	2.9531	4.2	0.2364	1.7	0.41	1367.9	20.9	1395.6	31.5	1438.3	72.4	1438.3	72.4	95.1
GC03OEM-78	258	71339	1.3	11.0227	0.8	3.1213	3.2	0.2495	3.1	0.97	1436.1	39.7	1438.0	24.6	1440.8	15.6	1440.8	15.6	99.7
GC03OEM-79	64	16660	3.2	11.0090	2.2	3.1663	6.2	0.2528	5.8	0.94	1453.0	75.9	1449.0	48.2	1443.1	42.0	1443.1	42.0	100.7
GC03OEM-56	77	25088	1.5	10.9914	1.6	3.1966	2.0	0.2548	1.2	0.61	1463.3	16.2	1456.3	15.8	1446.2	31.0	1446.2	31.0	101.2
GC03OEM-59	211	53488	1.7	10.9415	0.7	3.0655	1.9	0.2433	1.8	0.93	1403.7	22.1	1424.1	14.4	1454.8	13.1	1454.8	13.1	96.5
GC03OEM-60	205	46982	3.2	10.8966	0.7	3.1786	1.9	0.2512	1.7	0.92	1444.7	22.4	1452.0	14.6	1462.6	14.1	1462.6	14.1	98.8
GC03OEM-82	112	85617	2.4	10.8362	1.9	3.0915	3.6	0.2430	3.1	0.86	1402.1	38.9	1430.6	27.6	1473.2	35.2	1473.2	35.2	95.2
GC03OEM-6	34	22175	6.0	10.6891	4.3	3.2104	4.6	0.2489	1.4	0.31	1432.7	18.1	1459.7	35.3	1499.1	81.9	1499.1	81.9	95.6
GC-03-COMB-8	43	5216	0.9	9.7865	2.3	3.2668	4.1	0.2319	3.4	0.83	1344.3	41.1	1473.2	31.9	1664.1	42.9	1664.1	42.9	80.8
GC03OEM-76	305	8984	1.4	9.6557	0.8	3.7015	7.0	0.2592	7.0	0.99	1485.8	92.8	1571.7	56.3	1689.0	14.5	1689.0	14.5	88.0
GC03OEM-7	129	43009	4.0	9.6507	0.6	4.2113	2.4	0.2948	2.3	0.96	1665.3	33.9	1676.2	19.6	1689.9	11.6	1689.9	11.6	98.5
GC-03-COMB-18	49	10308	1.7	9.5933	1.5	4.2623	2.2	0.2966	1.6	0.73	1674.2	24.2	1686.1	18.4	1700.9	27.9	1700.9	27.9	98.4
GC03OEM-63	163	53730	3.6	9.5676	0.6	4.3672	2.3	0.3030	2.3	0.97	1706.4	34.2	1706.2	19.4	1705.9	10.5	1705.9	10.5	100.0
GC03OEM-72	191	108859	1.8	9.5480	0.5	4.4355	2.2	0.3071	2.1	0.97	1726.7	31.7	1719.0	17.9	1709.6	9.6	1709.6	9.6	101.0
GC-03-COMB-12	149	24932	2.4	9.5405	0.6	4.3513	1.0	0.3011	0.8	0.79	1696.7	12.4	1703.1	8.7	1711.1	11.8	1711.1	11.8	99.2
GC-03-COMB-10	34	7849	0.4	9.4460	1.7	4.4494	2.4	0.3048	1.8	0.72	1715.2	26.7	1721.6	20.3	1729.4	31.0	1729.4	31.0	99.2
GC03OEM-98	210	171831	2.6	9.4323	0.5	4.2438	2.1	0.2903	2.0	0.96	1643.1	29.2	1682.5	17.2	1732.0	10.1	1732.0	10.1	94.9
GC03OEM-52	225	47789	2.2	9.4147	0.6	4.6787	2.0	0.3195	2.0	0.96	1787.1	30.5	1763.4	17.1	1735.5	11.1	1735.5	11.1	103.0
GC03OEM-9	79	41900	1.5	9.2316	1.1	4.8444	2.0	0.3243	1.7	0.85	1810.9	26.7	1792.6	16.8	1771.4	19.2	1771.4	19.2	102.2
GC03OEM-24	230	85672	0.7	9.2312	0.4	4.6750	1.4	0.3130	1.4	0.96	1755.4	20.9	1762.8	11.8	1771.5	7.1	1771.5	7.1	99.1
GC03OEM-90	398	29867	2.1	9.2141	0.3	4.4033	2.2	0.2943	2.2	0.99	1662.8	31.9	1713.0	18.2	1774.9	5.3	1774.9	5.3	93.7
GC03OEM-30	94	60580	2.1	9.1982	0.9	4.7791	2.3	0.3188	2.1	0.92	1784.0	32.5	1781.2	19.1	1778.0	16.6	1778.0	16.6	100.3
GC03OEM-8	116	79078	2.0	9.1850	0.9	4.8060	2.1	0.3202	1.9	0.89	1790.5	28.9	1785.9	17.5	1780.6	17.3	1780.6	17.3	100.6
GC03OEM-31	274	226840	2.0	9.1826	0.4	4.8687	4.0	0.3242	3.9	1.00	1810.4	62.2	1796.9	33.4	1781.1	6.9	1781.1	6.9	101.6
GC-03-COMB-16	191	39374	2.0	9.1809	0.5	4.7562	1.9	0.3167	1.9	0.97	1773.6	29.0	1777.2	16.3	1781.5	9.2	1781.5	9.2	99.6
GC03OEM-91	70	31319	1.5	9.1776	1.0	4.8327	2.3	0.3217	2.1	0.91	1797.9	32.8	1790.6	19.4	1782.1	17.9	1782.1	17.9	100.9
GC03OEM-22	294	69402	3.9	9.1728	0.6	4.5721	3.7	0.3042	3.6	0.99	1712.0	54.7	1744.2	30.7	1783.0	10.4	1783.0	10.4	96.0
GC03OEM-46	278	77460	2.6	9.1616	0.8	4.6066	1.3	0.3061	1.0	0.76	1721.4	14.4	1750.5	10.5	1785.3	14.9	1785.3	14.9	96.4
GC03OEM-77	101	31274	1.4	9.1516	1.1	4.7773	3.3	0.3171	3.1	0.94	1775.5	48.2	1780.9	27.7	1787.3	20.3	1787.3	20.3	99.3
GC03OEM-75	166	63747	2.5	9.1512	0.4	4.8189	2.7	0.3198	2.7	0.99	1788.9	41.9	1788.2	22.9	1787.3	7.6	1787.3	7.6	100.1
GC03OEM-87	200	40045	3.4	9.1501	0.3	4.8520	2.8	0.3220	2.8	0.99	1799.4	44.2	1794.0	23.8	1787.6	5.7	1787.6	5.7	100.7
GC-03-COMB-6	200	45059	1.5	9.1495	0.5	4.6647	2.2	0.3095	2.2	0.98	1738.4	33.3	1760.9	18.7	1787.7	8.6	1787.7	8.6	97.2
GC03OEM-64	340	117457	3.4	9.1478	0.4	4.6108	1.0	0.3059	1.0	0.93	1720.5	14.6	1751.2	8.6	1788.0	6.9	1788.0	6.9	96.2
GC03OEM-33	227	195016	1.2	9.1449	0.4	4.7385	2.5	0.3143	2.5	0.99	1761.7	38.7	1774.1	21.3	1788.6	6.8	1788.6	6.8	98.5
GC03OEM-2	473	34046	2.2	9.1410	0.3	4.4344	2.5	0.2940	2.5	0.99	1661.4	36.1	1718.8	20.6	1789.4	5.2	1789.4	5.2	92.8
GC03OEM-89	287	96458	1.6	9.1316	0.4	4.6338	4.1	0.3069	4.0	0.99	1725.4	61.0	1755.4	33.9	1791.2	7.7	1791.2	7.7	96.3
GC03OEM-18	145	72271	2.8	9.1160	0.6	4.8525	2.9	0.3208	2.8	0.98	1793.8	43.5	1794.1	24.0	1794.4	11.5	1794.4	11.5	100.0
GC03OEM-21	151	65310	1.0	9.1136	1.1	4.8168	1.6	0.3184	1.2	0.75	1781.8	18.8	1787.8	13.5	1794.9	19.4	1794.9	19.4	99.3
GC-03-COMB-9	520	118162	8.0	9.1044	0.3	4.8092	1.8	0.3176	1.8	0.99	1777.8	27.3	1786.5	15.0	1796.7	5.1	1796.7	5.1	98.9
GC03OEM-92	1071	54860	6.6	9.0999	0.2	4.7391	2.1	0.3128	2.1	1.00	1754.3	32.2	1774.2	17.6	1797.6	3.1	1797.6	3.1	97.6
GC03OEM-96	286	215082	1.8	9.0986	0.6	4.8961	2.7	0.3231	2.7	0.97	1804.8	42.0	1801.6	23.1	1797.8	11.6	1797.8	11.6	100.4

U-Pb geochronologic analyses of the Osgood Mountain Quartzite and Preble Formation

Isotope ratios											Apparent ages (Ma)								
Analysis	U	206Pb	U/Th	206Pb*	±	207Pb*	±	206Pb*	±	error	206Pb*	±	207Pb*	±	206Pb*	±	Best age	±	Conc
	(ppm)	204Pb		207Pb*	(%)	235U*	(%)	238U	(%)	corr.	238U*	(Ma)	235U	(Ma)	207Pb*	(Ma)	(Ma)	(Ma)	(%)
SAMPLE: Osgood Mountain Quartzite GC-03-COM LOCATION: Goughs Canyon, Osgood Mountains 0468951 4554410 (NAD 83 UTM 11N)																			
GC03OEM-62	169	84340	2.7	9.0977	0.8	4.8988	2.5	0.3232	2.4	0.94	1805.5	37.4	1802.0	21.3	1798.0	15.4	1798.0	15.4	100.4
GC03OEM-68	317	85489	3.1	9.0924	0.3	4.9351	3.8	0.3254	3.8	1.00	1816.2	59.4	1808.3	31.8	1799.1	6.1	1799.1	6.1	101.0
GC03OEM-95	407	112318	3.5	9.0844	0.2	4.8573	1.3	0.3200	1.3	0.99	1789.9	19.8	1794.9	10.8	1800.7	3.7	1800.7	3.7	99.4
GC03OEM-27	172	61107	2.9	9.0039	0.4	4.8839	1.3	0.3189	1.3	0.96	1784.5	19.6	1799.5	11.0	1816.9	6.5	1816.9	6.5	98.2
GC03OEM-20	477	290763	2.8	8.9754	0.3	5.0916	2.9	0.3314	2.9	0.99	1845.4	46.9	1834.7	25.0	1822.6	5.7	1822.6	5.7	101.2
GC03OEM-38	163	90863	6.0	8.8549	0.4	5.1698	1.5	0.3320	1.4	0.97	1848.1	23.2	1847.7	12.7	1847.1	6.8	1847.1	6.8	100.1
GC03OEM-93	135	78186	2.3	8.8384	1.1	5.2158	1.8	0.3343	1.5	0.80	1859.4	23.7	1855.2	15.6	1850.5	19.7	1850.5	19.7	100.5
GC03OEM-73	124	17769	2.9	8.7728	1.0	4.9347	3.9	0.3140	3.8	0.96	1760.2	58.0	1808.2	33.0	1863.9	18.9	1863.9	18.9	94.4
GC03OEM-81	45	11611	6.8	8.7620	1.9	4.9462	3.3	0.3143	2.7	0.82	1761.9	41.8	1810.2	27.8	1866.2	33.7	1866.2	33.7	94.4
GC03OEM-23	90	54496	7.3	8.6767	0.7	5.4207	2.0	0.3411	1.9	0.93	1892.1	31.1	1888.1	17.4	1883.8	13.3	1883.8	13.3	100.4
GC03OEM-16	300	224669	2.4	6.3516	1.7	9.1419	2.5	0.4211	1.9	0.76	2265.6	36.8	2352.3	23.3	2428.3	28.2	2428.3	28.2	93.3
GC03OEM-43	314	20734	1.9	6.3106	0.6	9.8417	2.2	0.4504	2.1	0.96	2397.2	42.4	2420.1	20.3	2439.3	10.4	2439.3	10.4	98.3
GC-03-COMB-11	32	8231	0.8	6.2967	1.7	10.0435	3.0	0.4587	2.5	0.83	2433.7	51.3	2438.8	28.1	2443.0	28.5	2443.0	28.5	99.6
GC03OEM-47	128	49917	2.9	6.1750	0.5	10.2161	2.5	0.4575	2.4	0.98	2428.7	48.6	2454.5	22.7	2476.0	8.9	2476.0	8.9	98.1
GC03OEM-5	289	207482	2.3	6.1693	0.3	10.5546	1.5	0.4723	1.5	0.98	2493.4	30.9	2484.7	14.1	2477.6	4.7	2477.6	4.7	100.6
GC03OEM-49	159	89144	2.4	6.1616	0.4	10.5095	3.1	0.4696	3.1	0.99	2482.0	62.8	2480.8	28.6	2479.7	7.2	2479.7	7.2	100.1
GC03OEM-28	409	17300	1.9	5.7087	0.6	10.0832	4.4	0.4175	4.3	0.99	2249.0	81.8	2442.4	40.2	2607.7	10.0	2607.7	10.0	86.2
GC03OEM-29	202	62420	2.6	5.5469	0.2	11.2570	2.3	0.4529	2.3	1.00	2408.0	45.7	2544.6	21.3	2655.5	3.3	2655.5	3.3	90.7
GC-03-COMB-19	103	37380	2.2	5.4778	0.5	12.9928	1.7	0.5162	1.6	0.95	2683.0	35.8	2679.1	16.2	2676.2	8.8	2676.2	8.8	100.3
GC03OEM-39	84	85566	2.0	5.3987	0.3	13.4200	2.2	0.5255	2.2	0.99	2722.3	48.1	2709.7	20.7	2700.2	5.6	2700.2	5.6	100.8
GC03OEM-84	242	54946	1.5	5.3938	0.6	12.4797	1.8	0.4882	1.7	0.95	2562.9	35.3	2641.2	16.5	2701.7	9.1	2701.7	9.1	94.9
GC-03-COMB-5	157	53140	1.3	4.7877	0.2	16.1005	1.1	0.5591	1.1	0.98	2862.8	24.8	2882.8	10.5	2896.8	3.5	2896.8	3.5	98.8
SAMPLE: Osgood Mountain Quartzite GOL-01-COM LOCATION: Golconda Mine, Edna Mountain 0462354 4531791 (NAD 83 UTM 11N)																			
GOL-01COM-51	26	3924	2.4	13.6577	9.4	1.8193	10.0	0.1802	3.4	0.34	1068.1	33.8	1052.4	65.6	1020.0	190.5	1020.0	190.5	104.7
GOL-01COM-46	45	6990	1.6	13.5514	5.3	1.8252	5.6	0.1794	1.8	0.31	1063.7	17.2	1054.6	36.8	1035.8	107.5	1035.8	107.5	102.7
GOL-01COM-12	45	8099	1.1	13.3101	3.8	1.8621	4.4	0.1798	2.1	0.48	1065.6	20.5	1067.7	28.8	1072.0	77.0	1072.0	77.0	99.4
GOL-01COM-72	86	10775	1.5	13.2350	3.3	1.9576	4.1	0.1879	2.3	0.57	1110.0	23.7	1101.1	27.3	1083.4	66.6	1083.4	66.6	102.5
GOL-01COM-45	318	49259	2.5	13.0614	0.6	1.9557	2.0	0.1853	2.0	0.95	1095.7	19.7	1100.4	13.8	1109.8	12.5	1109.8	12.5	98.7
GOL-01COM-95	143	33160	4.3	12.8660	1.7	2.0924	3.5	0.1952	3.1	0.88	1149.7	32.8	1146.3	24.4	1139.9	34.0	1139.9	34.0	100.9
GOL-01COM-86	150	21622	3.4	12.8372	1.3	2.0823	3.5	0.1939	3.2	0.92	1142.3	33.8	1143.0	24.0	1144.3	26.5	1144.3	26.5	99.8
GOL-01COM-10	77	6732	1.8	12.0043	3.1	2.3690	4.3	0.2063	2.9	0.69	1208.8	32.4	1233.3	30.4	1276.3	60.2	1276.3	60.2	94.7
GOL-01COM-29	39	10467	1.9	11.6034	2.9	2.7822	3.2	0.2341	1.4	0.44	1356.2	17.3	1350.8	24.2	1342.2	56.2	1342.2	56.2	101.0
GOL-01COM-16	47	11262	2.0	11.5760	2.7	2.7672	4.1	0.2323	3.0	0.74	1346.7	36.9	1346.7	30.4	1346.8	52.6	1346.8	52.6	100.0
GOL-01COM-49	99	13817	1.7	11.4196	1.2	2.9033	3.9	0.2405	3.7	0.95	1389.1	45.8	1382.8	29.3	1373.0	24.0	1373.0	24.0	101.2
GOL-01COM-57	26	5978	1.8	11.3486	3.1	2.9455	4.5	0.2424	3.3	0.73	1399.4	41.1	1393.7	33.9	1385.0	58.8	1385.0	58.8	101.0
GOL-01COM-38	117	23756	2.0	11.3376	1.1	2.8013	2.9	0.2303	2.7	0.93	1336.3	32.7	1355.9	21.8	1386.9	20.6	1386.9	20.6	96.4
GOL-01COM-42	103	25635	1.4	11.3318	2.1	2.8660	2.5	0.2355	1.4	0.56	1363.5	17.2	1373.0	18.9	1387.8	39.9	1387.8	39.9	98.2
GOL-01COM-73	159	27780	2.2	11.2095	1.4	2.8957	7.1	0.2354	7.0	0.98	1362.8	85.6	1380.8	53.6	1408.7	26.5	1408.7	26.5	96.7
GOL-01COM-47	72	13207	1.3	11.1517	2.2	2.9964	3.3	0.2423	2.5	0.75	1398.9	31.0	1406.7	25.1	1418.5	42.0	1418.5	42.0	98.6
GOL-01COM-93	607	25552	1.4	11.1105	0.3	2.7594	1.5	0.2224	1.4	0.98	1294.3	16.9	1344.6	11.0	1425.6	6.0	1425.6	6.0	90.8
GOL-01COM-40	429	78412	4.4	11.1026	0.4	3.0786	3.0	0.2479	3.0	0.99	1427.6	37.9	1427.4	22.9	1427.0	8.2	1427.0	8.2	100.0
GOL-01COM-79	100	19216	1.7	11.0673	1.5	3.1435	2.4	0.2523	1.9	0.80	1450.5	25.1	1443.4	18.7	1433.0	28.1	1433.0	28.1	101.2
GOL-01COM-31	94	15195	1.2	11.0484	1.5	3.1237	4.1	0.2503	3.8	0.93	1440.0	49.1	1438.5	31.6	1436.3	29.1	1436.3	29.1	100.3
GOL-01COM-36	60	13627	3.0	11.0460	2.5	3.1292	3.8	0.2507	2.8	0.74	1442.1	36.1	1439.9	28.9	1436.7	47.9	1436.7	47.9	100.4
GOL-01COM-53	186	42046	3.4	11.0139	1.1	3.1526	3.9	0.2518	3.7	0.96	1447.9	48.2	1445.6	29.8	1442.3	20.4	1442.3	20.4	100.4
GOL-01COM-62	228	36186	11.1	10.9886	0.8	3.1181	2.6	0.2485	2.5	0.95	1430.8	31.8	1437.2	20.0	1446.7	15.1	1446.7	15.1	98.9
GOL-01COM-70	181	40113	1.8	10.9321	1.1	3.1373	2.2	0.2487	1.9	0.86	1432.0	24.8	1441.9	17.3	1456.5	21.8	1456.5	21.8	98.3
GOL-01COM-71	232	21681	1.6	10.9250	0.7	3.0729	1.3	0.2435	1.1	0.84	1404.8	13.5	1426.0	9.8	1457.7	13.2	1457.7	13.2	96.4
GOL-01COM-80	84	21050	1.6	10.0944	2.0	3.7886	3.3	0.2774	2.6	0.78	1578.1	35.9	1590.3	26.3	1606.6	38.0	1606.6	38.0	98.2
GOL-01COM-98	197	19607	2.5	9.7650	0.5	3.5698	0.6	0.2528	0.4	0.58	1453.0	4.7	1542.8	4.9	1668.2	9.4	1668.2	9.4	87.1
GOL-01COM-64	388	45114	0.9	9.7465	0.4	3.3658	8.4	0.2379	8.3	1.00	1375.9	103.4	1496.5	65.5	1671.7	7.7	1671.7	7.7	82.3
GOL-01COM-58	40	11025	3.1	9.7348	3.0	4.2986	4.2	0.3035	2.9	0.70	1708.6	44.2	1693.1	34.7	1673.9	55.8	1673.9	55.8	102.1
GOL-01COM-25	120	14129	2.4	9.6798	1.5	4.0620	3.6	0.2852	3.3	0.91	1617.4	47.5	1646.7	29.7	1684.4	27.6	1684.4	27.6	96.0
GOL-01COM-89	81	19013	2.9	9.5914	1.3	4.3599	3.6	0.3033	3.4	0.93	1707.6	50.6	1704.8	29.8	1701.3	23.6	1701.3	23.6	100.4
GOL-01COM-77	106	35024	3.6	9.5661	1.2	4.3757	3.1	0.3036	2.8	0.93	1709.1	42.5	1707.8	25.3	1706.1	21.3	1706.1	21.3	100.2
GOL-01COM-48	106	24655	2.6	9.5334	0.8	4.3393	2.1	0.3000	1.9	0.92	1691.5	28.6	1700.9	17.3	1712.4	15.3	1712.4	15.3	98.8
GOL-01COM-55	194	33259	4.2	9.5260	0.9	4.3526	2.3	0.3007	2.2	0.92	1694.9	32.1	1703.4	19.4	1713.9	17.2	1713.9	17.2	98.9
GOL-01COM-6	200	37784	3.5	9.5108	0.7	4.0840	4.5	0.2817	4.4	0.99	1600.0	63.0	1651.1	36.7	1716.8	13.0	1716.8	13.0	93.2
GOL-01COM-61	295	71681	3.3	9.4933	0.2	4.2777	5.8	0.2945	5.8	1.00	1664.1	85.3	1689.1	47.9	1720.2	4.1	1720.2	4.1	96.7
GOL-01COM-50	92	13088	2.5	9.4850	1.8	4.4356	2.8	0.3051	2.2	0.78	1716.7	33.2	1719.0	23.3	1721.8	32.3	1721.8	32.3	99.7
GOL-01COM-14	346	26661	4.1	9.4333	0.4	4.4248	3.2	0.3027	3.2	0.99	1704.8	47.7	1717.0	26.6	1731.8	8.0	1731.8	8.0	98.4
GOL-01COM-13	87	8200	3.1	9.3500	1.5	4.4807	3.0	0.3038	2.6	0.86	1710.4	38.9	1727.4	25.0	1748.1	28.2	1748.1	28.2	97.8
GOL-01COM-1	191	49405	2.1	9.2508	0.8	4.7369	1.3	0.3178	1.1	0.80	1779.0	16.7	1773.8	11.2	1767.6	14.5	1767.6	14.5	100.6
GOL-01COM-60	1098	100584	10.1	9.1853	0.2	4.7137	2.6	0.3140	2.6	1.00	1760.4	40.0	1769.7	21.8	1780.6	3.9	1780.6	3.9	98.9
GOL-01COM-20	157	36797	3.1	9.1772	0.7	4.7845	1.5	0.3185	1.4	0.89	1782.2	21.3	1782.2	13.0	1782.2	13.1	1782.2	13.1	100.0
GOL-01COM-52	151	31456	1.6	9.1641	0.7	4.8427	3.1	0.3219	3.0	0.98	1798.9	47.5	1792.4	26.1	1784.8	12.4	1784.8	12.4	100.8
GOL-01COM-37	304	64050	8.8	9.1641	0.3	4.8812	3.1	0.3244	3.1	1.00	1811.3	49.2	1799.0	26.4	1784.8	5.6	1784.8	5.6	101.5
GOL-01COM-24	94	9641	23.1	9.1611	1.0	4.8677	2.3	0.3234	2.1	0.90	1806.4	32.7	1796.7	19.3	1785.4	17.9	1785.4	17.9	101.2
GOL-01COM-2	267	81434	3.7	9.1610	0.7	4.9452	2.7	0.3286	2.6	0.97	1831.4	42.1	1810.0	23.0	1785.4	12.3	1785.4	12.3	102.6
GOL-01COM-39	1358	139130	7.2	9.1581	0.2	4.5830	4.4	0.3044	4.4	1.00	1713.1	65.9	1746.2	36.6	1786.0	3.9	1786.0	3.9	95.9
GOL-01COM-33	368	79653	3.6	9.1512	0.3	4.6900	2.7	0.3113	2.6	0.99	1747.0	40.5	1765.5	22.3	1787.3	5.3	1787.3	5.3	97.7
GOL-01COM-5	344	89812	2.9	9.1465	0.3	4.8894	1.9	0.3243	1.9	0.99	1810.9	30.3	1800.4	16.4	1788.3	5.5	1788.3	5.5	101.3
GOL-01COM-34	1393	152492	5.7	9.1356	0.3	4.6173	2.6	0.3059	2.6	0.99	1720.6	39.7	1752.4	22.0	1790.5	4.8	1790.5	4.8	96.1
GOL-01COM-11	297	54714	3.2	9.1301	0.3	4.7411	2.9	0.3139	2.9	1.00	1760.1	44.3	1774.5	24.2	1791.6	5.0	1791.6	5.0	98.2
GOL-01COM-44	354	81105	2.4	9.1239	0.2	4.8558	2.3	0.3213	2.3	1.00	1796.2	36.3	1794.6	19.6	1792.8	3.0	1792.8	3.0	100.2
GOL-01COM-92	109	22473	3.8	9.1197	1.2	4.6546	1.7	0.3079	1.3	0.74	1730.2	19.4	1759.1	14.4	1793.6	21.1	1793.6	21.1	96.5

U-Pb geochronologic analyses of the Osgood Mountain Quartzite and Preble Formation

Isotope ratios											Apparent ages (Ma)								
Analysis	U	206Pb	U/Th	206Pb*	±	207Pb*	±	206Pb*	±	error	206Pb*	±	207Pb*	±	206Pb*	±	Best age	±	Conc
	(ppm)	204Pb		207Pb*	(%)	235U*	(%)	238U	(%)	corr.	238U*	(Ma)	235U	(Ma)	207Pb*	(Ma)	(Ma)	(Ma)	(%)
SAMPLE: Osgood Mountain Quartzite GOL-01-COM LOCATION: Golconda Mine, Edna Mountain 0462354 4531791 (NAD 83 UTM 11N)																			
GOL-01COM-99	1025	121561	3.2	9.1197	0.2	4.8393	0.8	0.3201	0.7	0.95	1790.1	11.5	1791.8	6.5	1793.6	4.5	1793.6	4.5	99.8
GOL-01COM-21	278	71135	2.8	9.1111	0.5	4.7199	1.4	0.3119	1.3	0.94	1750.0	19.5	1770.8	11.4	1795.4	8.7	1795.4	8.7	97.5
GOL-01COM-9	470	67337	2.0	9.0910	0.3	4.7369	1.9	0.3123	1.9	0.99	1752.1	28.6	1773.8	15.9	1799.4	5.9	1799.4	5.9	97.4
GOL-01COM-68	114	33334	0.9	9.0140	0.8	5.1006	2.4	0.3335	2.2	0.93	1855.1	35.4	1836.2	20.0	1814.8	15.4	1814.8	15.4	102.2
GOL-01COM-69	96	33488	3.9	8.9502	0.9	4.9969	2.4	0.3244	2.2	0.92	1811.0	34.2	1818.8	20.0	1827.7	17.0	1827.7	17.0	99.1
GOL-01COM-91	247	24013	7.9	8.9118	0.7	4.8931	9.4	0.3163	9.4	1.00	1771.4	145.2	1801.1	79.4	1835.5	13.6	1835.5	13.6	96.5
GOL-01COM-54	23	3297	207.7	8.9059	3.2	5.1609	4.0	0.3334	2.4	0.59	1854.6	38.0	1846.2	34.1	1836.7	58.7	1836.7	58.7	101.0
GOL-01COM-88	154	44121	2.2	8.7748	0.5	5.1831	2.2	0.3299	2.1	0.98	1837.7	33.6	1849.8	18.3	1863.5	8.3	1863.5	8.3	98.6
GOL-01COM-8	56	27209	10.4	8.6638	1.0	5.4374	2.6	0.3417	2.4	0.92	1894.7	39.8	1890.8	22.7	1886.5	18.9	1886.5	18.9	100.4
GOL-01COM-87	46	16005	0.7	6.3038	1.2	9.8794	2.1	0.4517	1.7	0.81	2402.7	34.6	2423.6	19.6	2441.1	21.1	2441.1	21.1	98.4
GOL-01COM-76	172	48370	2.7	6.2451	0.6	10.0210	3.2	0.4539	3.2	0.98	2412.5	63.8	2436.7	29.8	2457.0	10.3	2457.0	10.3	98.2
GOL-01COM-81	259	100137	1.0	5.8698	0.3	11.4287	2.9	0.4865	2.9	0.99	2555.7	61.7	2558.8	27.5	2561.2	5.7	2561.2	5.7	99.8
GOL-01COM-41	201	65965	1.1	5.6262	0.3	12.3932	2.4	0.5057	2.4	0.99	2638.3	51.5	2634.7	22.5	2631.9	4.7	2631.9	4.7	100.2
GOL-01COM-19	124	21437	1.0	5.6213	0.4	12.4133	1.3	0.5061	1.3	0.96	2639.9	27.5	2636.2	12.4	2633.3	6.4	2633.3	6.4	100.2
GOL-01COM-17	627	44578	6.8	5.5828	0.9	10.5440	2.0	0.4269	1.8	0.90	2291.9	34.0	2483.8	18.3	2644.7	14.5	2644.7	14.5	86.7
GOL-01COM-15	137	61474	1.1	5.5788	0.6	12.7109	2.9	0.5143	2.9	0.98	2674.9	63.1	2658.5	27.6	2645.9	9.4	2645.9	9.4	101.1
GOL-01COM-66	469	97806	2.4	5.4487	0.3	12.5770	3.0	0.4970	3.0	1.00	2601.0	65.0	2648.5	28.7	2685.0	4.2	2685.0	4.2	96.9
GOL-01COM-18	281	78230	2.3	5.4179	0.2	13.3935	1.4	0.5263	1.4	0.99	2725.8	31.6	2707.8	13.6	2694.4	3.6	2694.4	3.6	101.2
GOL-01COM-100	41	16993	2.3	5.3891	1.4	12.7942	2.3	0.5001	1.9	0.81	2614.1	41.0	2664.6	22.0	2703.2	22.4	2703.2	22.4	96.7
GOL-01COM-27	47	10243	2.5	5.2954	0.9	13.1530	2.4	0.5052	2.3	0.94	2635.9	49.1	2690.7	22.9	2732.1	14.1	2732.1	14.1	96.5
GOL-01COM-3	36	16902	3.0	5.2576	1.4	14.5856	2.3	0.5562	1.9	0.80	2850.8	43.3	2788.6	22.3	2743.9	23.1	2743.9	23.1	103.9
GOL-01COM-63	158	47721	0.9	5.1538	0.8	10.0810	3.0	0.3768	2.9	0.96	2061.4	50.7	2442.2	27.6	2776.6	13.5	2776.6	13.5	74.2
GOL-01COM-22	436	15206	0.5	4.9970	1.3	9.9982	7.9	0.3623	7.8	0.99	1993.3	134.4	2434.6	73.4	2827.2	21.0	2827.2	21.0	70.5
GOL-01COM-59	99	53930	5.6	4.8216	0.3	16.0083	2.2	0.5598	2.2	0.99	2865.8	51.5	2877.3	21.5	2885.3	4.8	2885.3	4.8	99.3
GOL-01COM-26	90	42028	1.5	4.8168	0.4	15.9893	1.9	0.5586	1.9	0.98	2860.8	43.7	2876.2	18.4	2886.9	6.1	2886.9	6.1	99.1
GOL-01COM-90	445	190198	1.9	4.8033	0.2	16.2707	2.0	0.5668	1.9	0.99	2894.7	45.2	2892.8	18.7	2891.5	3.6	2891.5	3.6	100.1
GOL-01COM-35	139	61928	1.7	4.8020	0.3	16.7150	1.6	0.5821	1.6	0.98	2957.5	37.6	2918.6	15.5	2891.9	5.2	2891.9	5.2	102.3
GOL-01COM-4	213	87181	1.3	4.7856	0.1	16.4807	1.8	0.5720	1.8	1.00	2916.1	41.8	2905.1	17.1	2897.5	2.4	2897.5	2.4	100.6
GOL-01COM-56	165	24965	1.4	4.7325	0.4	15.0154	0.8	0.5154	0.7	0.89	2679.5	16.0	2816.2	7.8	2915.6	6.0	2915.6	6.0	91.9
GOL-01COM-83	141	54482	2.5	4.5839	0.4	17.5685	2.2	0.5841	2.2	0.99	2965.4	51.3	2966.4	21.0	2967.1	5.9	2967.1	5.9	99.9
GOL-01COM-28	137	58113	2.7	4.5212	0.3	17.5811	1.8	0.5765	1.8	0.98	2934.5	41.3	2967.1	17.1	2989.3	5.1	2989.3	5.1	98.2
GOL-01COM-65	119	86632	1.5	3.6976	0.6	25.2440	2.8	0.6770	2.8	0.98	3332.7	72.3	3317.7	27.7	3308.6	9.2	3308.6	9.2	100.7
SAMPLE: Osgood Mountain Quartzite SP-01-COM LOCATION: Soldier Pass, Osgood Mountains 0463750 4548029 (NAD 83 UTM 11N)																			
SP-01COM-24	41	4488	1.9	13.6778	4.6	1.7684	5.2	0.1754	2.6	0.49	1041.9	24.6	1033.9	34.1	1017.0	92.9	1017.0	92.9	102.4
SP-01COM-82	62	12554	2.6	13.6665	3.1	1.8008	3.6	0.1785	1.7	0.48	1058.7	16.9	1045.7	23.4	1018.7	63.4	1018.7	63.4	103.9
SP-01COM-82	62	12554	2.6	13.6665	3.1	1.8008	3.6	0.1785	1.7	0.48	1058.7	16.9	1045.7	23.4	1018.7	63.4	1018.7	63.4	103.9
SP-01COM-84	92	15305	2.8	13.4667	2.7	1.8274	3.3	0.1785	2.0	0.59	1058.7	19.3	1055.4	21.9	1048.5	54.3	1048.5	54.3	101.0
SP-01COM-54	81	13785	2.4	13.4638	3.9	1.8647	5.5	0.1821	3.9	0.71	1078.4	38.8	1068.6	36.5	1048.9	78.5	1048.9	78.5	102.8
SP-01COM-65	64	6863	1.3	13.3954	2.5	1.7676	2.7	0.1717	1.2	0.45	1021.6	11.7	1033.7	17.8	1059.2	49.3	1059.2	49.3	96.5
SP-01COM-95	87	13398	2.3	13.3840	2.6	1.8458	3.6	0.1792	2.5	0.69	1062.5	24.0	1061.9	23.5	1060.9	52.2	1060.9	52.2	100.1
SP-01COM-70	122	26481	2.0	13.3639	1.8	1.8977	3.1	0.1839	2.4	0.80	1088.4	24.4	1080.3	20.3	1063.9	37.1	1063.9	37.1	102.3
SP-01COM-101	80	17510	2.7	13.3586	3.5	1.9207	4.3	0.1861	2.5	0.58	1100.1	25.6	1088.3	29.0	1064.7	71.1	1064.7	71.1	103.3
SP-01COM-98	88	16706	2.7	13.3409	3.5	1.8659	4.0	0.1805	1.8	0.46	1069.9	18.0	1069.1	26.4	1067.4	71.2	1067.4	71.2	100.2
SP-01COM-81	92	19617	2.7	13.3374	2.1	1.8916	3.2	0.1830	2.3	0.74	1083.2	23.3	1078.1	21.1	1067.9	43.1	1067.9	43.1	101.4
SP-01COM-93	115	14418	2.0	13.3334	3.1	1.9031	3.6	0.1840	1.8	0.50	1089.0	17.7	1082.2	23.7	1068.5	62.3	1068.5	62.3	101.9
SP-01COM-57	195	32750	2.6	13.3310	1.5	1.9747	4.0	0.1909	3.7	0.93	1126.4	38.1	1106.9	26.8	1068.9	29.8	1068.9	29.8	105.4
SP-01COM-72	181	33236	2.3	13.3267	2.1	1.8680	3.0	0.1806	2.2	0.72	1070.0	21.8	1069.8	20.1	1069.5	42.2	1069.5	42.2	100.0
SP-01COM-21	79	10158	2.4	13.3058	2.6	1.9438	4.5	0.1876	3.7	0.83	1108.3	38.1	1096.3	30.4	1072.7	51.4	1072.7	51.4	103.3
SP-01COM-8	135	20259	2.7	13.3052	1.2	1.9122	2.7	0.1845	2.4	0.90	1091.6	24.4	1085.3	18.1	1072.8	24.1	1072.8	24.1	101.8
SP-01COM-50	110	20289	2.0	13.2992	1.6	1.9350	2.4	0.1866	1.8	0.76	1103.1	18.5	1093.3	16.2	1073.7	31.7	1073.7	31.7	102.7
SP-01COM-86	208	33550	3.1	13.2880	1.1	1.8420	2.3	0.1775	2.0	0.88	1053.4	19.7	1060.6	15.2	1075.4	22.3	1075.4	22.3	98.0
SP-01COM-58	105	17841	2.4	13.2828	4.1	1.8981	4.6	0.1829	2.1	0.45	1082.6	20.7	1080.4	30.5	1076.2	82.2	1076.2	82.2	100.6
SP-01COM-39	59	22120	1.2	13.2599	4.0	1.8495	4.2	0.1779	1.5	0.35	1055.3	14.3	1063.3	27.8	1079.6	79.4	1079.6	79.4	97.8
SP-01COM-61	124	24044	2.0	13.2461	2.1	1.9353	3.9	0.1859	3.3	0.84	1099.2	32.9	1093.4	26.0	1081.7	42.3	1081.7	42.3	101.6
SP-01COM-41	76	18468	2.2	13.2360	3.1	1.9867	3.3	0.1907	1.0	0.29	1125.3	9.9	1111.0	22.0	1083.2	62.5	1083.2	62.5	103.9
SP-01COM-35	135	25863	1.2	13.1930	2.0	1.9453	2.8	0.1861	1.9	0.69	1100.4	19.5	1096.8	18.8	1089.7	40.6	1089.7	40.6	101.0
SP-01COM-5	106	19010	3.2	13.1887	1.8	1.9889	2.1	0.1902	0.9	0.46	1122.7	9.8	1111.7	13.9	1090.4	36.5	1090.4	36.5	103.0
SP-01COM-48	144	30952	2.4	13.1677	1.1	1.8919	2.0	0.1807	1.6	0.83	1070.7	16.1	1078.3	13.1	1093.6	22.1	1093.6	22.1	97.9
SP-01COM-76	127	23297	1.9	13.1664	2.9	1.9275	4.1	0.1841	2.9	0.71	1089.1	29.1	1090.7	27.4	1093.8	58.0	1093.8	58.0	99.6
SP-01COM-16	62	15291	2.8	13.1603	4.9	1.8337	5.5	0.1750	2.6	0.47	1039.7	24.6	1057.6	36.1	1094.7	97.4	1094.7	97.4	95.0
SP-01COM-63	261	42681	2.4	13.1542	0.6	1.9690	2.2	0.1879	2.1	0.96	1109.7	21.2	1105.0	14.5	1095.7	11.9	1095.7	11.9	101.3
SP-01COM-17	219	36061	3.3	13.1482	1.2	1.9416	2.1	0.1852	1.7	0.82	1095.1	17.5	1095.6	14.2	1096.5	24.2	1096.5	24.2	99.9
SP-01COM-85	185	24561	2.9	13.1434	0.9	1.9099	2.9	0.1821	2.8	0.95	1078.2	27.7	1084.5	19.5	1097.3	17.5	1097.3	17.5	98.3
SP-01COM-44	294	81733	3.0	13.1380	0.8	1.9415	3.8	0.1850	3.7	0.98	1094.2	37.6	1095.5	25.6	1098.1	15.1	1098.1	15.1	99.6
SP-01COM-13	107	17831	3.1	13.1326	2.4	1.8868	3.6	0.1797	2.6	0.74	1065.4	25.9	1076.5	23.8	1098.9	48.4	1098.9	48.4	96.9
SP-01COM-55	178	40286	3.8	13.1288	0.9	1.9072	1.6	0.1816	1.4	0.83	1075.7	13.4	1083.6	10.9	1099.5	18.5	1099.5	18.5	97.8
SP-01COM-67	78	18111	2.1	13.1248	2.5	1.9487	4.3	0.1855	3.5	0.82	1096.9	35.6	1098.0	29.0	1100.1	49.9	1100.1	49.9	99.7
SP-01COM-40	59	13207	2.5	13.1169	5.3	1.9614	5.4	0.1866	1.3	0.24	1102.9	13.3	1102.4	36.7	1101.3	105.9	1101.3	105.9	100.1
SP-01COM-53	54	7901	1.0	13.0861	4.7	1.9605	5.5	0.1861	3.0	0.54	1100.1	30.5	1102.1	37.3	1106.0	93.0	1106.0	93.0	99.5
SP-01COM-31	106	19723	2.7	13.0660	1.3	1.9525	3.4	0.1850	3.1	0.92	1094.4	31.2	1099.3	22.7	1109.1	26.8	1109.1	26.8	98.7
SP-01COM-75	158	28681	4.0	13.0645	1.4	1.9589	2.1	0.1856	1.7	0.77	1097.6	16.7	1101.5	14.4	1109.3	27.1	1109.3	27.1	98.9
SP-01COM-26	230	29484	4.9	13.0231	0.9	2.0967	5.7	0.1980	5.6	0.99	1164.8	59.6	1147.7	39.0	1115.6	18.9	1115.6	18.9	104.4
SP-01COM-9	70	17003	1.6	13.0116	2.1	2.0311	2.7	0.1917	1.7	0.62	1130.4	17.7	1126.0	18.7	1117.4	42.9	1117.4	42.9	101.2
SP-01COM-80	144	33202	2.5	13.0016	1.9	2.0364	7.7	0.1920	7.5	0.97	1132.3	77.4	1127.8	52.4	1119.0	37.1	1119.0	37.1	101.2
SP-01COM-12	164	22606	6.5	12.9995	1.9	2.0342	2.2	0.1918	1.0	0.46	1131.0	10.2	1127.0	14.6	1119.3	38.2	1119.3	38.2	101.1

U-Pb geochronologic analyses of the Osgood Mountain Quartzite and Preble Formation

Isotope ratios											Apparent ages (Ma)								
Analysis	U (ppm)	206Pb 204Pb	U/Th	206Pb* 207Pb*	± (%)	207Pb* 235U*	± (%)	206Pb* 238U	± (%)	error corr.	206Pb* 238U*	± (Ma)	207Pb* 235U	± (Ma)	206Pb* 207Pb*	± (Ma)	Best age (Ma)	± (Ma)	Conc (%)
SAMPLE: Osgood Mountain Quartzite SP-01-COM LOCATION: Soldier Pass, Osgood Mountains 0463750 4548029 (NAD 83 UTM 11N)																			
SP-01COM-18	106	23522	1.6	12.9363	2.1	2.0377	3.5	0.1912	2.8	0.81	1127.8	29.3	1128.2	23.9	1129.0	41.5	1129.0	41.5	99.9
SP-01COM-14	82	22652	2.0	12.9306	2.7	1.9805	3.5	0.1857	2.2	0.62	1098.2	21.9	1108.9	23.5	1129.9	54.5	1129.9	54.5	97.2
SP-01COM-62	424	57530	8.7	12.9266	0.6	2.0362	2.3	0.1909	2.2	0.96	1126.2	22.7	1127.7	15.6	1130.5	12.6	1130.5	12.6	99.6
SP-01COM-10	133	32834	3.4	12.9249	1.8	1.9608	2.8	0.1838	2.2	0.78	1087.7	22.4	1102.2	19.2	1130.7	35.2	1130.7	35.2	96.2
SP-01COM-30	150	24825	2.1	12.9204	2.0	1.9777	3.0	0.1853	2.3	0.76	1096.0	23.2	1107.9	20.3	1131.5	39.0	1131.5	39.0	96.9
SP-01COM-45	108	22766	3.2	12.9050	1.5	2.0024	3.8	0.1874	3.5	0.91	1107.4	35.2	1116.3	25.7	1133.8	30.8	1133.8	30.8	97.7
SP-01COM-34	328	41054	2.0	12.8879	0.8	2.1380	2.8	0.1998	2.7	0.96	1174.5	28.7	1161.2	19.4	1136.5	16.2	1136.5	16.2	103.3
SP-01COM-3	123	22900	2.3	12.8770	1.4	1.9750	2.0	0.1844	1.5	0.74	1091.2	15.0	1107.0	13.7	1138.2	27.4	1138.2	27.4	95.9
SP-01COM-19	120	24221	2.5	12.8273	2.0	1.9097	3.8	0.1777	3.2	0.85	1054.2	31.0	1084.5	25.1	1145.8	39.6	1145.8	39.6	92.0
SP-01COM-37	211	42890	5.0	12.7819	0.9	2.1304	2.0	0.1975	1.7	0.88	1161.8	18.3	1158.7	13.6	1152.8	18.7	1152.8	18.7	100.8
SP-01COM-78	199	6061	2.6	12.7549	3.8	2.0154	4.8	0.1864	3.0	0.62	1102.0	30.1	1120.7	32.8	1157.0	75.6	1157.0	75.6	95.2
SP-01COM-90	79	14112	1.5	12.6955	3.1	2.2832	4.3	0.2102	3.0	0.69	1230.0	33.2	1207.1	30.5	1166.3	62.4	1166.3	62.4	105.5
SP-01COM-59	80	32635	2.0	12.6526	2.4	2.0926	3.6	0.1920	2.7	0.75	1132.3	28.1	1146.4	24.9	1173.0	47.7	1173.0	47.7	96.5
SP-01COM-99	376	74969	4.5	12.5662	1.3	2.2287	5.2	0.2031	5.0	0.97	1192.1	54.5	1190.1	36.3	1186.6	25.8	1186.6	25.8	100.5
SP-01COM-60	63	9690	2.2	12.5195	2.2	2.3172	2.7	0.2104	1.5	0.58	1231.0	17.3	1217.6	19.0	1193.9	43.3	1193.9	43.3	103.1
SP-01COM-88	53	3684	1.2	12.4120	5.5	1.8531	9.0	0.1668	7.1	0.79	994.5	65.2	1064.5	59.4	1210.9	109.2	1210.9	109.2	82.1
SP-01COM-74	68	12974	2.0	12.3664	5.5	1.9849	16.1	0.1780	15.1	0.94	1056.2	147.5	1110.4	109.1	1218.1	107.5	1218.1	107.5	86.7
SP-01COM-79	100	13006	2.1	11.8504	1.3	2.6118	1.4	0.2245	0.6	0.42	1305.5	6.9	1304.0	10.3	1301.4	24.7	1301.4	24.7	100.3
SP-01COM-23	118	33356	1.9	11.7955	1.6	2.5846	3.3	0.2211	2.8	0.87	1287.8	33.2	1296.3	23.8	1310.5	30.6	1310.5	30.6	98.3
SP-01COM-47	64	11686	1.2	11.6103	2.1	2.7367	4.1	0.2304	3.6	0.87	1336.8	43.2	1338.5	30.7	1341.1	40.0	1341.1	40.0	99.7
SP-01COM-91	82	14759	2.1	11.5216	2.4	2.7454	3.9	0.2294	3.0	0.78	1331.4	36.5	1340.9	28.9	1355.9	46.6	1355.9	46.6	98.2
SP-01COM-25	70	18994	1.5	11.4371	2.0	2.7028	2.6	0.2242	1.5	0.60	1304.0	18.1	1329.2	18.9	1370.1	39.4	1370.1	39.4	95.2
SP-01COM-92	79	14776	1.3	11.4171	1.6	2.8655	3.3	0.2373	2.9	0.88	1372.5	36.1	1372.9	24.9	1373.4	29.9	1373.4	29.9	99.9
SP-01COM-96	65	11764	2.1	11.4133	3.6	2.7556	5.3	0.2281	3.9	0.73	1324.5	46.9	1343.6	39.8	1374.1	69.7	1374.1	69.7	96.4
SP-01COM-15	101	18535	2.5	11.3596	1.5	2.9901	3.5	0.2463	3.2	0.91	1419.6	40.8	1405.1	26.8	1383.1	28.4	1383.1	28.4	102.6
SP-01COM-52	109	51476	0.9	11.3049	1.2	2.9897	2.4	0.2451	2.1	0.88	1413.3	27.2	1405.0	18.6	1392.4	22.6	1392.4	22.6	101.5
SP-01COM-28	87	15887	0.9	10.8949	1.3	3.2267	2.4	0.2550	2.1	0.85	1464.0	27.1	1463.6	18.8	1462.9	23.9	1462.9	23.9	100.1
SP-01COM-94	195	27235	2.1	10.0082	4.5	3.2864	9.6	0.2386	8.5	0.88	1379.2	105.7	1477.8	75.1	1622.5	83.6	1622.5	83.6	85.0
SP-01COM-1	95	21643	1.4	9.8616	1.4	4.0563	3.0	0.2901	2.6	0.88	1642.1	37.8	1645.6	24.1	1650.0	25.8	1650.0	25.8	99.5
SP-01COM-64	203	38127	3.8	9.6270	0.4	4.2076	1.8	0.2938	1.7	0.97	1660.4	25.4	1675.5	14.6	1694.5	7.8	1694.5	7.8	98.0
SP-01COM-71	239	77679	3.9	9.5299	0.5	4.3175	4.9	0.2984	4.9	0.99	1683.4	72.7	1696.7	40.7	1713.1	9.4	1713.1	9.4	98.3
SP-01COM-77	225	97962	1.7	9.5244	0.6	4.4156	2.1	0.3050	2.0	0.95	1716.1	29.7	1715.3	17.1	1714.2	11.3	1714.2	11.3	100.1
SP-01COM-27	410	27054	4.3	9.4716	0.2	4.0280	2.5	0.2767	2.5	1.00	1574.7	34.7	1639.9	20.3	1724.4	4.4	1724.4	4.4	91.3
SP-01COM-38	268	56645	3.9	9.4428	0.5	4.5997	1.7	0.3150	1.6	0.95	1765.3	25.0	1749.2	14.2	1730.0	9.8	1730.0	9.8	102.0
SP-01COM-36	242	46769	3.2	9.4069	0.3	4.4365	1.2	0.3027	1.2	0.97	1704.6	17.7	1719.2	10.1	1737.0	5.7	1737.0	5.7	98.1
SP-01COM-7	108	22966	3.5	9.2424	0.9	4.8327	2.7	0.3239	2.6	0.95	1809.0	41.0	1790.6	23.1	1769.3	16.1	1769.3	16.1	102.2
SP-01COM-83	237	44995	4.5	9.1897	0.4	4.7346	2.3	0.3156	2.3	0.99	1768.0	35.8	1773.4	19.7	1779.7	6.8	1779.7	6.8	99.3
SP-01COM-4	346	75753	3.5	9.1351	0.4	4.7975	1.9	0.3179	1.8	0.97	1779.2	28.4	1784.5	15.7	1790.6	7.6	1790.6	7.6	99.4
SP-01COM-43	165	89167	4.2	9.0598	0.4	4.8364	1.9	0.3178	1.8	0.97	1778.9	28.5	1791.3	15.9	1805.6	7.9	1805.6	7.9	98.5
SP-01COM-49	574	27141	2.5	9.0038	0.2	4.1659	2.7	0.2720	2.7	1.00	1551.2	37.7	1667.3	22.5	1816.9	3.6	1816.9	3.6	85.4
SP-01COM-89	219	80385	1.7	8.9469	0.4	5.1578	2.6	0.3347	2.6	0.99	1861.1	41.5	1845.7	22.1	1828.4	7.4	1828.4	7.4	101.8
SP-01COM-87	108	17381	3.4	8.9142	0.6	5.1129	1.6	0.3306	1.4	0.92	1841.1	23.1	1838.3	13.4	1835.0	11.4	1835.0	11.4	100.3
SP-01COM-29	48	21377	2.9	8.7328	1.2	5.3921	3.1	0.3415	2.8	0.92	1894.0	46.0	1883.6	26.2	1872.2	21.8	1872.2	21.8	101.2
SP-01COM-11	36	19263	1.6	5.3524	0.9	13.1036	3.0	0.5087	2.9	0.96	2651.0	63.1	2687.1	28.6	2714.5	14.5	2714.5	14.5	97.7
SAMPLE: Preble Formation GS-01-CP LOCATION: Garden Spring, Osgood Mountains 0470302 4548660 (NAD 83 UTM 11N)																			
GS-01CP-25	99	10357	1.1	13.3338	3.1	1.6203	4.4	0.1567	3.2	0.72	938.4	28.0	978.1	27.9	1068.5	62.0	1068.5	62.0	87.8
GS-01CP-50	168	25130	1.7	13.3220	1.7	1.9273	3.4	0.1862	2.9	0.87	1100.9	29.6	1090.6	22.5	1070.2	33.3	1070.2	33.3	102.9
GS-01CP-63	153	37815	1.8	13.2444	1.2	1.9350	3.5	0.1859	3.3	0.94	1098.9	33.5	1093.3	23.6	1081.9	24.3	1081.9	24.3	101.6
GS-01CP-39	136	56330	1.5	13.0935	1.5	1.8890	4.1	0.1794	3.8	0.93	1063.6	37.5	1077.2	27.3	1104.9	30.4	1104.9	30.4	96.3
GS-01CP-86	64	8160	1.9	13.0511	3.3	2.0664	3.8	0.1956	2.0	0.52	1151.6	20.7	1137.7	26.1	1111.3	65.3	1111.3	65.3	103.6
GS-01CP-03	57	7458	2.0	13.0010	4.5	1.9581	5.4	0.1846	3.0	0.55	1092.2	29.7	1101.2	36.2	1119.1	89.6	1119.1	89.6	97.6
GS-01CP-19	119	21877	2.4	12.9944	1.3	1.9596	2.2	0.1847	1.7	0.80	1092.5	17.6	1101.7	14.7	1120.1	26.0	1120.1	26.0	97.5
GS-01CP-72	132	25545	2.0	12.9306	1.9	1.9306	2.6	0.1811	1.8	0.69	1072.7	17.9	1091.8	17.5	1129.9	37.7	1129.9	37.7	94.9
GS-01CP-59	37	4896	2.3	12.9228	3.7	2.0715	4.3	0.1942	2.3	0.52	1143.8	23.6	1139.4	29.7	1131.1	73.6	1131.1	73.6	101.1
GS-01CP-46	73	14997	1.1	11.8136	2.7	2.7489	2.9	0.2355	1.0	0.34	1363.4	12.0	1341.8	21.4	1307.5	52.5	1307.5	52.5	104.3
GS-01CP-13	60	10768	1.2	11.7710	4.7	2.6394	5.1	0.2253	1.9	0.38	1310.0	22.9	1311.7	37.4	1314.5	91.0	1314.5	91.0	99.7
GS-01CP-66	69	6183	1.7	11.6233	3.0	2.7596	3.3	0.2326	1.3	0.40	1348.3	15.7	1344.7	24.4	1338.9	58.1	1338.9	58.1	100.7
GS-01CP-47	114	32535	2.3	11.5984	0.8	2.8339	3.0	0.2384	2.9	0.96	1378.3	36.2	1364.5	22.7	1343.1	15.8	1343.1	15.8	102.6
GS-01CP-91	40	6655	1.1	11.5726	2.7	2.7108	3.4	0.2275	2.2	0.63	1321.5	25.7	1331.4	25.3	1347.4	51.2	1347.4	51.2	98.1
GS-01CP-24	54	18099	0.7	11.4864	1.9	2.8214	3.3	0.2350	2.7	0.82	1360.9	33.7	1361.2	25.1	1361.8	36.8	1361.8	36.8	99.9
GS-01CP-97	121	20019	1.5	11.4740	1.7	2.8312	2.8	0.2356	2.3	0.79	1363.8	27.8	1363.8	21.4	1363.9	33.3	1363.9	33.3	100.0
GS-01CP-98	97	13061	1.8	11.4705	2.4	2.8816	3.6	0.2397	2.7	0.74	1385.3	33.3	1377.1	27.2	1364.5	46.8	1364.5	46.8	101.5
GS-01CP-35	164	11281	0.9	11.4635	1.5	2.2818	4.4	0.1897	4.1	0.94	1119.8	42.2	1206.7	30.8	1365.6	28.2	1365.6	28.2	82.0
GS-01CP-11	101	23332	1.5	11.4206	2.1	2.8495	3.3	0.2360	2.5	0.77	1366.0	31.1	1368.7	24.5	1372.9	39.8	1372.9	39.8	99.5
GS-01CP-54	188	38945	1.0	11.4115	0.8	2.9124	1.6	0.2410	1.4	0.88	1392.1	17.7	1385.1	12.1	1374.4	14.4	1374.4	14.4	101.3
GS-01CP-71	188	34048	2.2	11.4059	0.9	2.8387	2.8	0.2348	2.6	0.95	1359.7	31.9	1365.8	20.7	1375.3	17.1	1375.3	17.1	98.9
GS-01CP-37	368	57766	3.4	11.3863	0.4	2.8787	2.7	0.2377	2.6	0.99	1374.9	32.6	1376.4	20.0	1378.6	7.5	1378.6	7.5	99.7
GS-01CP-21	43	6648	0.8	11.3667	3.6	2.8038	4.2	0.2311	2.1	0.51	1340.5	26.0	1356.5	31.7	1382.0	70.1	1382.0	70.1	97.0
GS-01CP-79	127	8247	1.9	11.3360	2.2	2.7132	2.5	0.2231	1.2	0.49	1298.1	14.5	1332.1	18.8	1387.1	42.5	1387.1	42.5	93.6
GS-01CP-60	89	17756	1.7	11.3337	1.5	2.9323	2.5	0.2410	1.9	0.79	1392.1	24.4	1390.3	18.6	1387.5	28.7	1387.5	28.7	100.3
GS-01CP-22	195	35025	1.1	11.2788	0.7	2.8307	2.6	0.2316	2.5	0.97	1342.6	30.1	1363.7	19.3	1396.9	12.7	1396.9	12.7	96.1
GS-01CP-64	121	5066	2.2	11.2689	1.5	2.8824	2.8	0.2356	2.4	0.85	1363.7	29.4	1377.3	21.1	1398.5	27.9	1398.5	27.9	97.5
GS-01CP-29	273	84802	2.4	11.2475	0.5	2.9468	1.7	0.2404	1.6	0.95	1388.7	19.9	1394.0	12.7	1402.2	10.1	1402.2	10.1	99.0
GS-01CP-77	68	12781	1.6	11.1405	1.9	3.0452	3.8	0.2460	3.3	0.87	1418.1	41.9	1419.0	29.0	1420.5	36.2	1420.5	36.2	99.8
GS-01CP-90	454	6490	1.7	11.0885	1.3	2.6106	7.6	0.2099	7.5	0.99	1228.5	83.7	1303.6	55.8	1429.4	23.9	1429.4	23.9	85.9

U-Pb geochronologic analyses of the Osgood Mountain Quartzite and Preble Formation

Isotope ratios											Apparent ages (Ma)								
Analysis	U (ppm)	206Pb 204Pb	U/Th	206Pb* 207Pb*	± (%)	207Pb* 235U*	± (%)	206Pb* 238U	± (%)	error corr.	206Pb* 238U*	± (Ma)	207Pb* 235U	± (Ma)	206Pb* 207Pb*	± (Ma)	Best age (Ma)	± (Ma)	Conc (%)
SAMPLE: Preble Formation GS-01-CP LOCATION: Garden Spring, Osgood Mountains 0470302 4548660 (NAD 83 UTM 11N)																			
GS-01CP-100	119	35401	1.4	11.0702	0.9	3.2529	1.3	0.2612	1.0	0.76	1495.8	13.4	1469.9	10.3	1432.6	16.6	1432.6	16.6	104.4
GS-01CP-36	185	25447	1.0	11.0463	0.7	2.9381	3.0	0.2354	2.9	0.97	1362.7	35.9	1391.8	22.8	1436.7	13.7	1436.7	13.7	94.8
GS-01CP-53	101	18801	2.2	11.0317	1.2	3.2046	3.0	0.2564	2.8	0.92	1471.4	36.6	1458.3	23.4	1439.2	22.3	1439.2	22.3	102.2
GS-01CP-51	85	19617	1.2	10.9874	1.6	3.2288	3.4	0.2573	3.1	0.89	1476.0	40.3	1464.1	26.7	1446.9	30.0	1446.9	30.0	102.0
GS-01CP-38	130	27153	1.6	10.9823	1.1	3.1621	3.7	0.2519	3.6	0.96	1448.1	46.4	1448.0	28.8	1447.7	20.5	1447.7	20.5	100.0
GS-01CP-08	133	31769	2.6	10.9637	1.1	3.2434	2.1	0.2579	1.8	0.86	1479.1	24.2	1467.6	16.4	1451.0	20.4	1451.0	20.4	101.9
GS-01CP-31	235	39440	1.2	10.9311	0.9	3.1570	2.0	0.2503	1.8	0.88	1440.0	22.8	1446.7	15.5	1456.6	17.9	1456.6	17.9	98.9
GS-01CP-94	234	88414	2.0	10.9244	1.2	3.1610	3.2	0.2504	2.9	0.93	1440.8	38.0	1447.7	24.4	1457.8	22.3	1457.8	22.3	98.8
GS-01CP-41	87	9900	2.3	10.9220	1.1	3.1119	3.8	0.2465	3.6	0.96	1420.4	45.8	1435.6	28.9	1458.2	20.8	1458.2	20.8	97.4
GS-01CP-65	183	37569	2.9	10.9151	0.7	3.1724	2.0	0.2511	1.8	0.93	1444.4	23.9	1450.5	15.2	1459.4	13.5	1459.4	13.5	99.0
GS-01CP-85	103	23975	1.6	10.9144	0.8	3.1469	2.2	0.2491	2.1	0.93	1433.9	26.4	1444.2	17.1	1459.5	15.8	1459.5	15.8	98.2
GS-01CP-10	83	34693	1.7	10.8904	2.0	3.1760	3.9	0.2509	3.3	0.85	1442.9	43.1	1451.3	30.1	1463.7	38.5	1463.7	38.5	98.6
GS-01CP-73	166	17043	1.5	10.8498	0.8	3.2494	2.7	0.2557	2.5	0.95	1467.8	33.4	1469.0	20.7	1470.8	15.5	1470.8	15.5	99.8
GS-01CP-67	111	6575	1.8	10.8075	3.2	3.2162	3.5	0.2521	1.5	0.42	1449.3	19.2	1461.1	27.0	1478.2	59.8	1478.2	59.8	98.0
GS-01CP-12	258	30683	4.0	9.9184	0.7	3.7924	2.0	0.2728	1.9	0.94	1555.0	25.9	1591.1	15.9	1639.3	12.1	1639.3	12.1	94.9
GS-01CP-02	336	15353	1.3	9.9010	0.6	2.9804	2.0	0.2140	1.9	0.96	1250.2	21.8	1402.6	15.2	1642.6	10.6	1642.6	10.6	76.1
GS-01CP-52	475	19821	1.7	9.8064	0.4	3.3968	2.2	0.2416	2.2	0.99	1395.0	27.7	1503.7	17.6	1660.4	7.1	1660.4	7.1	84.0
GS-01CP-16	110	17675	2.5	9.7623	0.9	4.0445	2.5	0.2864	2.4	0.93	1623.3	34.1	1643.2	20.7	1668.7	16.7	1668.7	16.7	97.3
GS-01CP-84	190	19260	2.6	9.7005	0.8	3.8262	1.9	0.2692	1.7	0.90	1536.7	23.2	1598.3	15.2	1680.4	15.3	1680.4	15.3	91.4
GS-01CP-89	247	118384	3.8	9.6313	0.5	4.2425	1.3	0.2963	1.2	0.93	1673.2	17.9	1682.3	10.7	1693.6	8.8	1693.6	8.8	98.8
GS-01CP-80	383	18114	3.2	9.6253	0.5	4.1416	3.3	0.2891	3.3	0.99	1637.1	47.1	1662.5	26.9	1694.8	9.1	1694.8	9.1	96.6
GS-01CP-42	203	21933	4.2	9.6161	0.7	4.0759	1.4	0.2843	1.3	0.89	1612.8	18.3	1649.5	11.8	1696.6	12.1	1696.6	12.1	95.1
GS-01CP-70	77	14166	1.7	9.5685	1.1	4.2266	4.5	0.2933	4.4	0.97	1658.1	64.1	1679.2	37.0	1705.7	19.5	1705.7	19.5	97.2
GS-01CP-07	245	88480	3.7	9.5542	0.4	4.2824	4.2	0.2967	4.2	0.99	1675.1	62.1	1690.0	34.9	1708.4	7.8	1708.4	7.8	98.1
GS-01CP-18	133	24880	3.7	9.5322	1.0	4.1195	1.7	0.2848	1.4	0.80	1615.5	19.9	1658.2	14.2	1712.7	19.1	1712.7	19.1	94.3
GS-01CP-96	311	11420	2.8	9.5205	0.5	4.0071	3.4	0.2767	3.3	0.99	1574.7	46.6	1635.6	27.5	1714.9	10.1	1714.9	10.1	91.8
GS-01CP-87	283	107158	2.7	9.5162	0.4	4.5231	1.2	0.3122	1.1	0.94	1751.4	17.6	1735.2	10.2	1715.8	7.9	1715.8	7.9	102.1
GS-01CP-76	116	12014	1.3	9.5149	2.5	4.4488	4.0	0.3070	3.2	0.79	1726.0	48.0	1721.5	33.4	1716.0	45.8	1716.0	45.8	100.6
GS-01CP-45	310	79524	2.1	9.5130	0.4	4.4290	3.3	0.3056	3.2	0.99	1718.9	48.8	1717.8	27.0	1716.4	6.5	1716.4	6.5	100.1
GS-01CP-28	469	59047	1.3	9.4960	0.2	4.2203	1.3	0.2907	1.3	0.98	1644.8	18.2	1678.0	10.5	1719.7	4.2	1719.7	4.2	95.6
GS-01CP-06	87	27765	1.1	9.4826	0.9	4.3558	2.7	0.2996	2.6	0.94	1689.2	38.4	1704.0	22.7	1722.3	17.4	1722.3	17.4	98.1
GS-01CP-04	159	50814	1.7	9.4757	0.5	4.4583	3.4	0.3064	3.3	0.99	1722.9	50.5	1723.2	28.0	1723.6	8.6	1723.6	8.6	100.0
GS-01CP-27	290	103177	2.3	9.4724	0.4	4.4854	2.1	0.3082	2.1	0.98	1731.6	31.4	1728.3	17.5	1724.2	7.4	1724.2	7.4	100.4
GS-01CP-61	430	48448	2.5	9.2261	0.5	4.8871	2.6	0.3270	2.5	0.98	1823.9	40.4	1800.0	21.8	1772.5	8.5	1772.5	8.5	102.9
GS-01CP-57	500	136252	3.3	9.1801	0.2	4.9260	2.0	0.3280	1.9	0.99	1828.5	30.9	1806.7	16.5	1781.6	4.1	1781.6	4.1	102.6
GS-01CP-95	139	33330	2.0	9.1781	0.6	4.7749	2.2	0.3178	2.2	0.96	1779.2	33.5	1780.5	18.9	1782.0	11.6	1782.0	11.6	99.8
GS-01CP-01	333	121268	2.2	9.1763	0.3	4.7919	3.1	0.3189	3.1	1.00	1784.4	47.7	1783.5	25.8	1782.4	5.4	1782.4	5.4	100.1
GS-01CP-78	305	68002	2.3	9.1515	0.5	4.7183	2.7	0.3132	2.7	0.98	1756.3	41.0	1770.5	22.7	1787.3	8.7	1787.3	8.7	98.3
GS-01CP-69	267	64348	2.2	9.1435	0.2	4.7588	2.8	0.3156	2.8	1.00	1768.1	43.9	1777.7	23.9	1788.9	4.1	1788.9	4.1	98.8
GS-01CP-88	555	120816	3.5	9.1154	0.5	4.9925	4.1	0.3301	4.1	0.99	1838.7	65.5	1818.1	34.9	1794.5	9.0	1794.5	9.0	102.5
GS-01CP-20	199	62338	3.6	9.0830	0.5	4.7635	3.3	0.3138	3.3	0.99	1759.4	50.1	1778.5	27.6	1801.0	8.7	1801.0	8.7	97.7
GS-01CP-55	380	46290	1.9	8.9806	0.5	4.6418	1.5	0.3023	1.4	0.94	1702.9	21.6	1756.8	12.9	1821.6	9.7	1821.6	9.7	93.5
GS-01CP-81	208	85830	0.8	8.9501	0.5	5.0251	2.1	0.3262	2.1	0.97	1819.9	32.5	1823.6	17.8	1827.7	8.6	1827.7	8.6	99.6
GS-01CP-83	535	99813	4.1	8.9097	0.3	5.0028	1.1	0.3233	1.1	0.96	1805.7	17.1	1819.8	9.6	1835.9	5.9	1835.9	5.9	98.4
GS-01CP-75	142	18385	2.1	8.8476	0.8	4.9499	3.4	0.3176	3.3	0.97	1778.1	51.7	1810.8	28.9	1848.6	14.8	1848.6	14.8	96.2
GS-01CP-17	120	29448	3.4	8.8410	0.5	5.0998	2.6	0.3270	2.6	0.98	1823.8	40.6	1836.1	22.0	1849.9	8.2	1849.9	8.2	98.6
GS-01CP-99	285	24331	1.7	8.7883	0.3	4.4771	1.1	0.2854	1.0	0.95	1618.3	14.3	1726.7	8.8	1860.8	6.2	1860.8	6.2	87.0
GS-01CP-92	269	68081	4.0	8.6789	0.5	5.2985	1.6	0.3335	1.5	0.94	1855.4	23.4	1868.6	13.3	1883.3	9.9	1883.3	9.9	98.5
GS-01CP-23	478	23962	2.5	6.8886	2.1	7.3711	4.0	0.3683	3.4	0.85	2021.2	58.4	2157.5	35.4	2289.8	35.8	2289.8	35.8	88.3
GS-01CP-32	617	49511	3.0	6.1105	3.0	9.6403	5.7	0.4272	4.8	0.85	2293.2	92.5	2401.0	52.2	2493.7	51.1	2493.7	51.1	92.0
GS-01CP-56	409	113804	1.5	5.7766	0.1	11.8377	2.1	0.4960	2.1	1.00	2596.4	45.0	2591.7	19.8	2587.9	2.5	2587.9	2.5	100.3
GS-01CP-62	445	24465	1.2	5.7061	0.3	9.8035	2.5	0.4057	2.4	0.99	2195.3	45.3	2416.5	22.6	2608.4	5.8	2608.4	5.8	84.2
GS-01CP-26	447	21996	1.9	5.6219	0.7	9.6921	4.8	0.3952	4.8	0.99	2146.8	86.8	2406.0	44.3	2633.1	12.2	2633.1	12.2	81.5
GS-01CP-34	237	65637	1.0	5.5164	0.2	11.1885	3.5	0.4476	3.5	1.00	2384.7	68.8	2539.0	32.2	2664.6	3.0	2664.6	3.0	89.5
GS-01CP-44	65	36641	1.4	5.4257	0.5	12.9959	2.2	0.5114	2.1	0.97	2662.6	45.6	2679.4	20.3	2692.0	8.6	2692.0	8.6	98.9
GS-01CP-14	200	38071	1.2	4.7923	0.4	14.7942	3.8	0.5142	3.8	0.99	2674.6	83.7	2802.1	36.6	2895.2	7.1	2895.2	7.1	92.4
GS-01CP-09	161	42489	1.6	4.5683	0.3	17.4065	2.9	0.5767	2.9	1.00	2935.3	68.9	2957.5	28.2	2972.6	4.4	2972.6	4.4	98.7
GS-01CP-49	104	54313	1.6	3.7424	0.4	24.0357	2.2	0.6524	2.1	0.98	3237.5	54.0	3269.8	21.1	3289.7	6.4	3289.7	6.4	98.4
SAMPLE: Preble Formation GOL-02-CP LOCATION: Golconda Mine, Edna Mountain 0465271 4533874 (NAD 83 UTM 11N)																			
GOL-02CP-54	128	8820	3.3	13.6763	1.8	1.5939	2.6	0.1581	1.9	0.72	946.2	16.3	967.8	16.1	1017.2	36.2	1017.2	36.2	93.0
GOL-02CP-46	89	5780	2.1	13.6416	2.8	1.6629	3.4	0.1645	2.0	0.57	981.9	17.8	994.5	21.9	1022.4	57.5	1022.4	57.5	96.0
GOL-02CP-37	44	6824	2.3	13.4026	6.2	1.9228	6.7	0.1869	2.6	0.38	1104.6	26.1	1089.1	45.1	1058.1	125.7	1058.1	125.7	104.4
GOL-02CP-20	60	10305	0.6	13.1984	5.1	1.9044	5.7	0.1823	2.5	0.44	1079.5	25.3	1082.6	38.3	1088.9	103.2	1088.9	103.2	99.1
GOL-02CP-57	77	8546	1.3	13.0262	3.9	1.9945	4.7	0.1884	2.7	0.57	1112.8	27.7	1113.6	31.9	1115.2	77.2	1115.2	77.2	99.8
GOL-02CP-21	73	9127	4.0	12.9392	3.9	2.0318	4.0	0.1907	1.2	0.29	1125.0	11.9	1126.2	27.5	1128.6	77.2	1128.6	77.2	99.7
GOL-02CP-7	256	21995	2.2	12.6592	1.1	2.1983	3.1	0.2018	2.9	0.93	1185.1	31.8	1180.5	21.9	1172.0	22.2	1172.0	22.2	101.1
GOL-02CP-14	182	30256	3.2	12.5747	1.5	2.2415	3.6	0.2044	3.3	0.91	1199.0	35.8	1194.1	25.1	1185.2	28.8	1185.2	28.8	101.2
GOL-02CP-96	31	3482	4.4	12.4676	7.2	2.1316	7.5	0.1927	2.3	0.31	1136.2	24.3	1159.1	52.2	1202.1	141.6	1202.1	141.6	94.5
GOL-02CP-60	550	40729	2.7	12.4669	1.9	2.0371	2.6	0.1842	1.8	0.68	1089.8	18.1	1128.0	18.0	1202.2	38.1	1202.2	38.1	90.7
GOL-02CP-38	367	35749	2.5	12.4339	0.9	2.2545	2.0	0.2033	1.9	0.91	1193.1	20.3	1198.2	14.4	1207.4	16.7	1207.4	16.7	98.8
GOL-02CP-82	81	15514	1.7	12.0992	1.8	2.4887	4.1	0.2184	3.7	0.89	1273.4	42.2	1268.8	29.7	1261.0	36.1	1261.0	36.1	101.0
GOL-02CP-86	180	25338	2.8	11.6471	1.6	2.7227	3.0	0.2300	2.6	0.85	1334.4	31.1	1334.7	22.4	1335.0	30.6	1335.0	30.6	100.0
GOL-02CP-93	93	16506	3.1	11.6214	1.3	2.7266	2.7	0.2298	2.3	0.87	1333.5	27.9	1335.7	19.8	1339.2	25.6	1339.2	25.6	99.6
GOL-02CP-99	67	11748	1.6	11.5391	1.2	2.7435	2.4	0.2296	2.1	0.87	1332.4	24.9	1340.3	17.8	1353.0	23.0	1353.0	23.0	98.5
GOL-02CP-85	78	15894	0.7	11.5218	2.6	2.9196	3.0	0.2440	1.4	0.47	1407.3	17.6	1387.0	22.6	1355.9	50.9	1355.9	50.9	103.8

U-Pb geochronologic analyses of the Osgood Mountain Quartzite and Preble Formation

Isotope ratios											Apparent ages (Ma)								
Analysis	U (ppm)	206Pb 204Pb	U/Th	206Pb* 207Pb*	± (%)	207Pb* 235U*	± (%)	206Pb* 238U	± (%)	error corr.	206Pb* 238U*	± (Ma)	207Pb* 235U	± (Ma)	206Pb* 207Pb*	± (Ma)	Best age (Ma)	± (Ma)	Conc (%)
SAMPLE: Preble Formation GOL-02-CP LOCATION: Golconda Mine, Edna Mountain 0465271 4533874 (NAD 83 UTM 11N)																			
GOL-02CP-98	60	13554	1.9	11.5077	3.3	2.7890	4.3	0.2328	2.7	0.63	1349.0	33.3	1352.6	32.2	1358.2	64.2	1358.2	64.2	99.3
GOL-02CP-71	94	13760	2.9	11.4941	2.2	2.8500	3.0	0.2376	2.0	0.68	1374.1	25.3	1368.8	22.5	1360.5	42.0	1360.5	42.0	101.0
GOL-02CP-70	82	13267	2.1	11.4669	2.8	2.8581	3.8	0.2377	2.5	0.66	1374.7	31.0	1370.9	28.4	1365.1	54.5	1365.1	54.5	100.7
GOL-02CP-19	87	13061	0.8	11.4572	1.5	2.7783	2.6	0.2309	2.2	0.83	1339.0	26.7	1349.7	19.8	1366.7	28.1	1366.7	28.1	98.0
GOL-02CP-6	96	14881	2.3	11.4096	1.6	2.8485	2.3	0.2357	1.6	0.72	1364.4	19.9	1368.4	17.0	1374.7	30.3	1374.7	30.3	99.2
GOL-02CP-13	95	14093	2.0	11.4007	1.8	2.7702	5.6	0.2291	5.3	0.95	1329.6	63.8	1347.5	41.9	1376.2	34.8	1376.2	34.8	96.6
GOL-02CP-16	184	39901	2.8	11.3737	1.4	2.9025	3.1	0.2394	2.7	0.90	1383.7	34.1	1382.6	23.1	1380.8	26.1	1380.8	26.1	100.2
GOL-02CP-66	81	13331	1.3	11.3435	1.7	2.8970	3.1	0.2383	2.6	0.84	1378.0	32.2	1381.1	23.2	1385.9	31.8	1385.9	31.8	99.4
GOL-02CP-63	66	10675	2.4	11.3133	4.2	2.7702	4.6	0.2273	1.8	0.39	1320.3	21.2	1347.5	34.3	1391.0	81.5	1391.0	81.5	94.9
GOL-02CP-30	13	3078	2.4	11.3112	11.7	3.0118	12.0	0.2471	2.7	0.23	1423.4	34.8	1410.6	91.9	1391.3	225.4	1391.3	225.4	102.3
GOL-02CP-88	106	18521	2.3	11.2712	1.7	2.8732	2.5	0.2349	1.8	0.73	1360.0	22.6	1374.9	19.1	1398.1	33.2	1398.1	33.2	97.3
GOL-02CP-17	84	4318	1.3	11.2024	4.4	2.8828	5.6	0.2342	3.5	0.62	1356.6	42.5	1377.4	42.2	1409.9	83.9	1409.9	83.9	96.2
GOL-02CP-75	187	24157	1.1	11.1826	0.9	2.9993	2.2	0.2433	2.0	0.91	1403.6	25.6	1407.4	16.9	1413.3	17.6	1413.3	17.6	99.3
GOL-02CP-48	77	9608	0.9	11.1472	1.6	3.0849	4.2	0.2494	3.8	0.92	1435.4	49.5	1428.9	32.0	1419.3	31.0	1419.3	31.0	101.1
GOL-02CP-56	98	15044	0.9	11.1324	1.4	3.0539	2.4	0.2466	2.0	0.83	1420.8	25.5	1421.2	18.5	1421.9	26.1	1421.9	26.1	99.9
GOL-02CP-58	133	19875	2.9	11.1057	1.1	3.1100	2.6	0.2505	2.4	0.91	1441.0	30.3	1435.2	19.9	1426.4	20.6	1426.4	20.6	101.0
GOL-02CP-11	131	22755	1.8	11.1034	0.7	3.1260	1.4	0.2517	1.3	0.88	1447.4	16.4	1439.1	11.1	1426.8	13.1	1426.8	13.1	101.4
GOL-02CP-67	340	7541	1.4	11.0749	1.1	2.7976	3.5	0.2247	3.3	0.95	1306.7	39.4	1354.9	26.3	1431.7	21.3	1431.7	21.3	91.3
GOL-02CP-40	98	20386	1.2	11.0659	1.5	3.1236	2.3	0.2507	1.7	0.76	1442.1	22.3	1438.5	17.5	1433.3	28.4	1433.3	28.4	100.6
GOL-02CP-49	121	16321	1.5	11.0557	1.1	3.1738	4.0	0.2545	3.9	0.96	1461.6	51.0	1450.8	31.2	1435.1	20.5	1435.1	20.5	101.8
GOL-02CP-8	62	13504	2.3	11.0449	1.6	3.2916	2.3	0.2637	1.7	0.73	1508.6	22.4	1479.1	17.8	1436.9	29.8	1436.9	29.8	105.0
GOL-02CP-45	96	14724	2.8	11.0413	1.9	3.1164	2.9	0.2496	2.2	0.76	1436.2	28.6	1436.8	22.4	1437.5	35.9	1437.5	35.9	99.9
GOL-02CP-22	156	24532	2.3	11.0354	1.3	3.0671	2.1	0.2455	1.7	0.81	1415.1	22.0	1424.5	16.5	1438.6	24.3	1438.6	24.3	98.4
GOL-02CP-91	102	16431	1.7	11.0284	1.8	3.1329	2.1	0.2506	1.1	0.52	1441.5	14.3	1440.8	16.4	1439.8	34.5	1439.8	34.5	100.1
GOL-02CP-9	288	48627	1.5	11.0271	0.6	3.1570	3.3	0.2525	3.3	0.99	1451.3	42.4	1446.7	25.5	1440.0	10.7	1440.0	10.7	100.8
GOL-02CP-39	114	15557	1.7	11.0203	2.2	3.2222	2.7	0.2575	1.6	0.58	1477.2	20.9	1462.5	21.1	1441.2	42.1	1441.2	42.1	102.5
GOL-02CP-28	402	75182	1.3	10.9893	0.5	3.2052	3.5	0.2555	3.5	0.99	1466.6	45.3	1458.4	27.0	1446.5	9.7	1446.5	9.7	101.4
GOL-02CP-64	121	19495	1.6	10.9667	1.3	3.1578	3.7	0.2512	3.4	0.93	1444.5	44.5	1446.9	28.4	1450.4	25.0	1450.4	25.0	99.6
GOL-02CP-18	230	42276	1.8	10.9364	0.5	3.1297	2.4	0.2482	2.3	0.97	1429.4	29.6	1440.0	18.3	1455.7	10.4	1455.7	10.4	98.2
GOL-02CP-44	215	33775	2.5	10.9144	1.1	3.2384	3.8	0.2563	3.7	0.95	1471.1	48.3	1466.4	29.9	1459.5	21.8	1459.5	21.8	100.8
GOL-02CP-27	90	17093	0.9	10.9079	2.1	3.2022	3.6	0.2533	2.9	0.81	1455.6	37.6	1457.7	27.6	1460.7	40.1	1460.7	40.1	99.7
GOL-02CP-65	125	15211	1.6	10.8753	1.3	3.2250	3.3	0.2544	3.0	0.91	1461.0	39.2	1463.2	25.4	1466.4	25.3	1466.4	25.3	99.6
GOL-02CP-89	131	16339	1.3	10.8738	1.2	3.2286	2.1	0.2546	1.7	0.82	1462.3	22.7	1464.0	16.4	1466.6	23.1	1466.6	23.1	99.7
GOL-02CP-94	114	15076	1.7	10.8728	2.3	3.2507	3.1	0.2563	2.0	0.65	1471.1	26.6	1469.4	24.0	1466.8	44.5	1466.8	44.5	100.3
GOL-02CP-25	199	29410	2.8	10.8526	1.1	3.2369	2.1	0.2548	1.8	0.86	1463.1	23.7	1466.0	16.3	1470.3	20.1	1470.3	20.1	99.5
GOL-02CP-83	118	25794	2.4	10.0389	1.0	3.8563	3.0	0.2808	2.8	0.94	1595.3	39.8	1604.6	24.2	1616.8	19.1	1616.8	19.1	98.7
GOL-02CP-43	45	9704	1.2	9.7928	2.0	4.2478	2.5	0.3017	1.5	0.59	1699.7	22.0	1683.3	20.4	1662.9	37.0	1662.9	37.0	102.2
GOL-02CP-87	103	18643	2.3	9.6623	0.8	4.3084	1.2	0.3019	1.0	0.77	1700.8	14.3	1695.0	10.3	1687.7	14.7	1687.7	14.7	100.8
GOL-02CP-5	170	34880	1.8	9.6617	0.8	4.3796	1.4	0.3069	1.1	0.81	1725.4	17.4	1708.5	11.7	1687.8	15.3	1687.8	15.3	102.2
GOL-02CP-36	83	15655	3.1	9.6526	1.1	4.4956	3.2	0.3147	3.0	0.94	1763.9	46.6	1730.2	26.8	1689.6	20.9	1689.6	20.9	104.4
GOL-02CP-81	68	15520	3.4	9.6019	1.7	4.3154	2.6	0.3005	2.0	0.77	1693.9	29.5	1696.3	21.3	1699.3	30.6	1699.3	30.6	99.7
GOL-02CP-1	232	21177	2.3	9.5847	0.4	4.2648	1.8	0.2965	1.7	0.97	1673.8	25.1	1686.6	14.4	1702.6	8.1	1702.6	8.1	98.3
GOL-02CP-100	322	15116	2.5	9.5826	1.3	3.4675	4.9	0.2410	4.7	0.97	1391.9	59.3	1519.9	38.7	1703.0	23.2	1703.0	23.2	81.7
GOL-02CP-12	282	29515	3.2	9.5706	0.5	4.4041	2.9	0.3057	2.8	0.99	1719.5	42.7	1713.1	23.7	1705.3	8.9	1705.3	8.9	100.8
GOL-02CP-10	290	69506	1.9	9.5656	0.7	4.5368	2.6	0.3147	2.5	0.97	1764.0	39.1	1737.7	21.8	1706.2	12.1	1706.2	12.1	103.4
GOL-02CP-72	469	49364	4.3	9.5655	0.5	4.1149	8.4	0.2855	8.4	1.00	1618.8	119.8	1657.3	68.6	1706.3	9.6	1706.3	9.6	94.9
GOL-02CP-65	137	17659	1.0	9.5603	1.4	4.3318	2.7	0.3004	2.3	0.86	1693.1	34.9	1699.4	22.5	1707.3	25.8	1707.3	25.8	99.2
GOL-02CP-53	113	13025	3.5	9.5462	1.1	3.9456	2.1	0.2732	1.8	0.86	1556.9	24.7	1623.1	16.9	1710.0	19.9	1710.0	19.9	91.0
GOL-02CP-55	162	32982	3.2	9.5421	0.9	4.4099	4.4	0.3052	4.3	0.98	1717.0	64.9	1714.2	36.4	1710.8	16.5	1710.8	16.5	100.4
GOL-02CP-69	118	21234	1.7	9.5339	1.0	4.4538	2.7	0.3080	2.5	0.92	1730.7	38.2	1722.4	22.6	1712.4	19.2	1712.4	19.2	101.1
GOL-02CP-90	224	52317	1.5	9.5246	1.0	4.4689	1.9	0.3087	1.6	0.84	1734.4	24.0	1725.2	15.5	1714.1	18.5	1714.1	18.5	101.2
GOL-02CP-26	216	46815	4.7	9.5222	0.5	4.4045	3.1	0.3042	3.1	0.99	1712.0	46.8	1713.2	26.1	1714.6	9.0	1714.6	9.0	99.8
GOL-02CP-84	152	34159	1.8	9.5138	0.6	4.4714	2.1	0.3085	2.0	0.95	1733.5	30.2	1725.7	17.3	1716.2	11.8	1716.2	11.8	101.0
GOL-02CP-4	153	27283	2.1	9.4951	0.9	4.5074	1.7	0.3104	1.4	0.86	1742.7	21.8	1732.3	13.8	1719.9	15.8	1719.9	15.8	101.3
GOL-02CP-61	132	33675	1.7	9.4436	1.0	4.3538	2.1	0.2982	1.9	0.88	1682.4	27.7	1703.6	17.5	1729.8	18.2	1729.8	18.2	97.3
GOL-02CP-95	96	17639	2.7	9.4422	1.0	4.5463	2.4	0.3113	2.2	0.90	1747.3	33.7	1739.5	20.2	1730.1	19.0	1730.1	19.0	101.0
GOL-02CP-79	120	25839	2.9	9.4175	0.8	4.5515	3.4	0.3109	3.3	0.97	1745.0	51.1	1740.4	28.7	1734.9	15.3	1734.9	15.3	100.6
GOL-02CP-24	169	38576	2.3	9.4134	0.6	4.4807	1.9	0.3059	1.8	0.95	1720.5	27.5	1727.4	15.9	1735.7	11.0	1735.7	11.0	99.1
GOL-02CP-62	108	20485	1.4	9.3606	1.7	4.3343	3.5	0.2943	3.0	0.86	1662.8	44.1	1699.9	28.7	1746.0	32.0	1746.0	32.0	95.2
GOL-02CP-51	105	23012	2.2	9.3436	1.4	4.4725	3.2	0.3031	2.9	0.90	1706.6	43.0	1725.9	26.3	1749.4	24.8	1749.4	24.8	97.6
GOL-02CP-41	347	27483	1.7	9.2404	0.3	4.4788	2.6	0.3002	2.6	0.99	1692.1	38.4	1727.0	21.6	1769.7	5.9	1769.7	5.9	95.6
GOL-02CP-92	81	2937	2.1	9.2379	5.3	4.8849	5.3	0.3273	0.9	0.16	1825.2	13.5	1799.7	45.0	1770.2	96.3	1770.2	96.3	103.1
GOL-02CP-68	96	21166	3.2	9.2375	1.3	4.7998	2.4	0.3216	2.0	0.85	1797.4	32.0	1784.9	20.3	1770.2	23.4	1770.2	23.4	101.5
GOL-02CP-97	123	26701	1.6	9.1442	0.7	4.9225	2.2	0.3265	2.1	0.95	1821.2	33.5	1806.1	18.7	1788.7	12.5	1788.7	12.5	101.8
GOL-02CP-52	140	28978	3.0	9.1066	0.7	4.8205	3.4	0.3184	3.3	0.98	1781.8	51.7	1788.5	28.5	1796.2	11.9	1796.2	11.9	99.2
GOL-02CP-80	420	13454	1.7	8.9706	0.5	4.0362	2.0	0.2626	1.9	0.96	1503.1	26.1	1641.5	16.4	1823.6	9.7	1823.6	9.7	82.4
GOL-02CP-33	214	64848	5.5	8.9209	0.5	5.0991	3.7	0.3299	3.6	0.99	1838.0	57.9	1836.0	31.1	1833.7	9.0	1833.7	9.0	100.2
GOL-02CP-74	114	28014	0.9	8.6726	0.9	5.1874	3.6	0.3263	3.5	0.97	1820.4	55.7	1850.6	30.9	1884.6	16.6	1884.6	16.6	96.6
GOL-02CP-78	85	22485	1.3	8.0676	1.1	6.3128	3.1	0.3694	2.9	0.93	2026.4	50.6	2020.2	27.4	2013.9	20.1	2013.9	20.1	100.6
GOL-02CP-59	413	127844	3.4	6.2630	0.4	9.6973	2.9	0.4405	2.9	0.99	2352.8	56.6	2406.5	26.6	2452.1	6.1	2452.1	6.1	96.0
GOL-02CP-29	270	34309	1.1	6.1792	0.4	9.9985	3.2	0.4481	3.1	0.99	2386.8	62.7	2434.6	29.2	2474.9	6.4	2474.9	6.4	96.4
GOL-02CP-32	28	9118	1.0	6.0417	1.4	10.7817	3.0	0.4724	2.7	0.88	2494.2	55.7	2504.5	28.3	2512.8	24.1	2512.8	24.1	99.3
GOL-02CP-77	169	53574	2.3	5.6828	0.3	12.6150	3.0	0.5199	2.9	1.00	2698.9	64.9	2651.3	27.8	2615.2	4.3	2615.2	4.3	103.2
GOL-02CP-76	137	49291	0.9	5.4838	0.4	12.9061	2.7	0.5133	2.7	0.99	2670.7	58.2	2672.8	25.3	2674.4	6.1	2674.4	6.1	99.9
GOL-02CP-50	260	59633	1.4	5.4777	0.2	12.8567	3.6	0.5108	3.6	1.00	2659.9	78.2	2669.2	33.9	2676.2	2.9	2676.2	2.9	99.4
GOL-02CP-23	84	29706	3.2	5.4754	0.8	13.2406	4.6	0.5258	4.5	0.98	2723.8	99.7	2697.0	43.1	2676.9	13.8	2676.9	13.8	101.7

U-Pb geochronologic analyses of the Osgood Mountain Quartzite and Preble Formation

Isotope ratios											Apparent ages (Ma)								
Analysis	U	206Pb	U/Th	206Pb*	±	207Pb*	±	206Pb*	±	error	206Pb*	±	207Pb*	±	206Pb*	±	Best age	±	Conc
	(ppm)	204Pb		207Pb*	(%)	235U*	(%)	238U	(%)	corr.	238U*	(Ma)	235U	(Ma)	207Pb*	(Ma)	(Ma)	(Ma)	(%)
SAMPLE: Preble Formation GOL-02-CP LOCATION: Golconda Mine, Edna Mountain 0465271 4533874 (NAD 83 UTM 11N)																			
GOL-02CP-31	174	46215	4.4	5.3994	0.4	13.0579	4.1	0.5113	4.0	0.99	2662.4	88.0	2683.8	38.3	2700.0	7.4	2700.0	7.4	98.6
GOL-02CP-47	49	12873	0.5	5.3403	0.6	12.9992	2.4	0.5035	2.4	0.97	2628.7	51.2	2679.6	23.0	2718.2	9.2	2718.2	9.2	96.7
GOL-02CP-34	134	30130	2.1	5.1674	0.4	14.2616	0.9	0.5345	0.8	0.90	2760.3	17.4	2767.3	8.2	2772.3	6.3	2772.3	6.3	99.6
SAMPLE: Preble Formation GC-01-CP LOCATION: Goughs Canyon, Osgood Mountains 0468513 4554509 (NAD 83 UTM 11N)																			
GC-01CP-99	67	7864	0.9	13.3853	4.2	1.9362	4.5	0.1880	1.7	0.39	1110.4	17.8	1093.7	30.2	1060.7	83.8	1060.7	83.8	104.7
GC-01CP-42	374	7922	2.8	13.3562	1.0	1.6731	2.2	0.1621	1.9	0.88	968.3	17.1	998.4	13.8	1065.1	21.1	1065.1	21.1	90.9
GC-01CP-35	126	12881	3.2	13.3228	1.3	1.8839	2.8	0.1820	2.4	0.88	1078.1	24.2	1075.4	18.5	1070.1	26.9	1070.1	26.9	100.7
GC-01CP-1	82	6225	1.1	13.3174	1.8	1.8699	2.0	0.1806	0.8	0.43	1070.3	8.3	1070.5	13.0	1070.9	35.7	1070.9	35.7	99.9
GC-01CP-54	92	9626	1.9	13.2099	2.0	1.9456	2.3	0.1864	1.1	0.50	1101.9	11.5	1096.9	15.3	1087.2	39.5	1087.2	39.5	101.4
GC-01CP-39	254	33601	2.8	13.1546	1.7	1.9956	2.8	0.1904	2.3	0.81	1123.5	23.5	1114.0	19.1	1095.6	33.4	1095.6	33.4	102.5
GC-01CP-70	241	26616	2.3	13.1206	1.3	1.9557	3.3	0.1861	3.0	0.92	1100.2	30.8	1100.4	22.2	1100.7	25.6	1100.7	25.6	100.0
GC-01CP-41	66	7593	1.5	12.8284	6.1	2.1988	6.5	0.2046	2.3	0.35	1199.9	24.8	1180.7	45.3	1145.7	120.9	1145.7	120.9	104.7
GC-01CP-33	86	7658	1.5	11.5874	2.1	2.7403	4.4	0.2303	3.9	0.88	1336.0	46.8	1339.5	32.8	1344.9	40.7	1344.9	40.7	99.3
GC-01CP-14	94	10628	3.6	11.5536	1.4	2.7866	2.4	0.2335	1.9	0.81	1352.8	23.1	1352.0	17.6	1350.6	26.8	1350.6	26.8	100.2
GC-01CP-36	100	12913	1.4	11.5343	2.3	2.8680	4.3	0.2399	3.6	0.84	1386.3	45.1	1373.5	32.2	1353.8	44.2	1353.8	44.2	102.4
GC-01CP-10	106	9003	1.8	11.4787	1.0	2.8828	3.1	0.2400	2.9	0.94	1386.7	36.6	1377.4	23.5	1363.1	20.0	1363.1	20.0	101.7
GC-01CP-76	96	12962	2.7	11.4763	2.4	2.9075	3.3	0.2420	2.2	0.68	1397.1	27.8	1383.9	24.6	1363.5	46.2	1363.5	46.2	102.5
GC-01CP-89	153	15603	1.7	11.4563	1.0	2.7335	5.1	0.2271	5.0	0.98	1319.4	60.0	1337.6	38.2	1366.8	19.8	1366.8	19.8	96.5
GC-01CP-62	165	28978	2.9	11.4391	1.3	2.7267	1.8	0.2262	1.3	0.71	1314.6	15.3	1335.7	13.4	1369.7	24.5	1369.7	24.5	96.0
GC-01CP-31	84	4346	1.9	11.4310	3.6	2.6653	3.7	0.2210	0.8	0.21	1287.0	9.0	1318.9	27.2	1371.1	69.4	1371.1	69.4	93.9
GC-01CP-59	109	12825	2.6	11.4108	1.0	2.9356	1.4	0.2429	1.0	0.72	1402.0	13.1	1391.1	10.9	1374.5	19.3	1374.5	19.3	102.0
GC-01CP-50	115	8845	1.2	11.3600	1.9	2.7880	2.9	0.2297	2.2	0.76	1332.9	26.6	1352.3	21.8	1383.1	36.4	1383.1	36.4	96.4
GC-01CP-26	115	14427	2.7	11.3268	1.4	2.7298	2.1	0.2243	1.6	0.75	1304.3	18.9	1336.6	15.9	1388.7	27.3	1388.7	27.3	93.9
GC-01CP-43	557	14007	4.2	11.2330	0.5	2.3215	3.2	0.1891	3.1	0.99	1116.7	32.2	1218.9	22.6	1404.6	9.7	1404.6	9.7	79.5
GC-01CP-24	145	2814	3.8	11.2240	3.8	2.4936	6.9	0.2030	5.8	0.83	1191.4	62.8	1270.2	50.3	1406.2	73.4	1406.2	73.4	84.7
GC-01CP-65	83	9995	2.1	11.1861	1.6	2.8973	2.4	0.2351	1.8	0.73	1361.0	21.6	1381.2	18.1	1412.6	31.1	1412.6	31.1	96.3
GC-01CP-21	93	10864	1.2	11.1224	2.8	3.1118	4.1	0.2510	3.0	0.73	1443.7	38.3	1435.6	31.3	1423.6	53.3	1423.6	53.3	101.4
GC-01CP-29	166	26944	1.4	11.1110	2.0	2.8894	2.7	0.2328	1.8	0.68	1349.4	22.5	1379.2	20.6	1425.5	38.4	1425.5	38.4	94.7
GC-01CP-64	464	18751	3.7	11.0575	0.5	2.7383	1.6	0.2196	1.5	0.95	1279.8	17.5	1338.9	11.8	1434.7	9.1	1434.7	9.1	89.2
GC-01CP-38	211	18810	2.7	11.0570	1.3	3.0858	2.2	0.2475	1.8	0.81	1425.3	22.8	1429.2	16.8	1434.8	24.4	1434.8	24.4	99.3
GC-01CP-67	98	11381	1.6	11.0432	1.5	3.1627	2.3	0.2533	1.7	0.76	1455.5	22.7	1448.1	17.7	1437.2	28.3	1437.2	28.3	101.3
GC-01CP-72	97	14360	1.7	11.0299	2.3	3.2547	2.4	0.2604	0.9	0.38	1491.7	12.2	1470.3	18.9	1439.5	42.9	1439.5	42.9	103.6
GC-01CP-94	255	37775	2.2	11.0263	0.8	3.2311	2.6	0.2584	2.5	0.95	1481.6	32.8	1464.6	20.2	1440.1	15.1	1440.1	15.1	102.9
GC-01CP-71	233	32667	3.2	11.0141	0.4	3.0656	1.8	0.2449	1.7	0.97	1412.1	21.7	1424.1	13.4	1442.2	7.8	1442.2	7.8	97.9
GC-01CP-34	108	19907	1.2	10.9687	1.0	3.0783	1.9	0.2449	1.6	0.85	1412.0	20.6	1427.3	14.6	1450.1	18.8	1450.1	18.8	97.4
GC-01CP-90	55	7827	1.5	10.9655	3.7	3.1771	4.2	0.2527	2.0	0.48	1452.2	26.4	1451.6	32.5	1450.7	70.2	1450.7	70.2	100.1
GC-01CP-44	124	20276	1.3	10.9306	1.5	3.1568	2.8	0.2503	2.3	0.85	1439.8	30.2	1446.7	21.3	1456.7	27.8	1456.7	27.8	98.8
GC-01CP-81	54	8473	2.0	10.8660	2.7	3.1817	3.6	0.2507	2.4	0.66	1442.3	30.8	1452.7	28.1	1468.0	52.2	1468.0	52.2	98.3
GC-01CP-17	75	11068	2.4	10.8580	2.1	3.0557	3.8	0.2406	3.1	0.83	1390.0	38.8	1421.7	28.7	1469.4	40.0	1469.4	40.0	94.6
GC-01CP-5	72	18148	1.6	10.8498	2.0	3.0802	3.1	0.2424	2.3	0.75	1399.1	29.3	1427.8	23.7	1470.8	38.4	1470.8	38.4	95.1
GC-01CP-92	265	10446	4.0	10.4561	1.3	2.9013	5.3	0.2200	5.2	0.97	1282.0	60.2	1382.3	40.3	1540.6	24.0	1540.6	24.0	83.2
GC-01CP-51	52	6556	1.9	9.9760	2.6	3.9491	5.0	0.2857	4.3	0.85	1620.2	61.4	1623.8	40.7	1628.5	48.7	1628.5	48.7	99.5
GC-01CP-22	51	8637	2.1	9.9705	2.3	4.0989	3.3	0.2964	2.5	0.74	1673.5	36.2	1654.1	27.3	1629.6	42.1	1629.6	42.1	102.7
GC-01CP-20	318	20120	3.3	9.9617	1.0	3.0599	22.0	0.2211	21.9	1.00	1287.5	256.2	1422.7	169.7	1631.2	18.9	1631.2	18.9	78.9
GC-01CP-19	539	12548	2.9	9.8920	0.5	3.1051	4.8	0.2228	4.8	1.00	1296.5	56.4	1433.9	37.1	1644.2	8.7	1644.2	8.7	78.9
GC-01CP-55	340	9070	2.2	9.8518	0.5	3.0216	9.1	0.2159	9.1	1.00	1260.2	103.8	1413.1	69.4	1651.8	9.3	1651.8	9.3	76.3
GC-01CP-13	161	18614	2.2	9.8037	0.5	3.8386	1.0	0.2729	0.9	0.88	1555.7	12.8	1600.9	8.4	1660.9	9.0	1660.9	9.0	93.7
GC-01CP-40	120	21740	4.9	9.7596	1.3	4.1653	2.8	0.2948	2.4	0.87	1665.6	35.5	1667.2	22.7	1669.2	24.8	1669.2	24.8	99.8
GC-01CP-85	167	7494	3.6	9.6775	1.7	3.4897	2.7	0.2449	2.1	0.77	1412.3	26.0	1524.9	21.0	1684.8	31.2	1684.8	31.2	83.8
GC-01CP-60	69	10401	2.1	9.6750	1.4	4.2454	3.1	0.2979	2.7	0.88	1680.9	40.4	1682.9	25.3	1685.3	26.5	1685.3	26.5	99.7
GC-01CP-73	134	16995	5.1	9.6560	1.0	3.7830	3.4	0.2649	3.2	0.96	1515.0	43.2	1589.1	26.9	1688.9	18.3	1688.9	18.3	89.7
GC-01CP-56	81	14357	4.6	9.6522	1.9	4.3534	2.9	0.3048	2.2	0.75	1714.8	33.1	1703.5	24.1	1689.6	35.4	1689.6	35.4	101.5
GC-01CP-9	118	18378	1.6	9.6459	1.0	4.3890	1.6	0.3070	1.3	0.78	1726.2	19.4	1710.3	13.5	1690.8	18.8	1690.8	18.8	102.1
GC-01CP-57	443	6826	3.2	9.6453	0.8	3.8147	1.1	0.2669	0.8	0.73	1524.8	11.0	1595.8	8.9	1690.9	13.9	1690.9	13.9	90.2
GC-01CP-27	248	31181	6.2	9.6352	0.6	4.3402	1.6	0.3033	1.5	0.94	1707.6	23.1	1701.0	13.5	1692.9	10.3	1692.9	10.3	100.9
GC-01CP-48	93	13474	3.3	9.6253	1.6	4.3247	3.1	0.3019	2.7	0.87	1700.7	40.7	1698.1	25.8	1694.8	28.6	1694.8	28.6	100.4
GC-01CP-15	158	30220	3.4	9.6202	0.7	4.2466	2.1	0.2963	2.0	0.94	1672.9	29.2	1683.1	17.3	1695.8	13.1	1695.8	13.1	98.7
GC-01CP-88	86	6794	2.4	9.6080	1.4	3.9232	3.9	0.2734	3.6	0.94	1557.9	50.4	1618.5	31.4	1698.1	25.0	1698.1	25.0	91.7
GC-01CP-11	270	54004	4.1	9.5764	0.8	4.3452	2.5	0.3018	2.3	0.94	1700.2	34.9	1702.0	20.4	1704.2	15.1	1704.2	15.1	99.8
GC-01CP-97	62	12157	2.5	9.5716	1.5	4.2770	1.7	0.2969	0.9	0.53	1676.0	13.3	1688.9	14.1	1705.1	26.8	1705.1	26.8	98.3
GC-01CP-8	156	24418	3.3	9.5690	1.0	4.4036	2.0	0.3056	1.8	0.88	1719.1	27.1	1713.0	16.8	1705.6	17.5	1705.6	17.5	100.8
GC-01CP-45	84	16910	1.8	9.5609	1.5	4.3604	2.3	0.3024	1.8	0.76	1703.0	26.6	1704.9	19.3	1707.1	28.0	1707.1	28.0	99.8
GC-01CP-49	254	37117	5.8	9.5456	0.6	4.3928	2.9	0.3041	2.8	0.98	1711.7	41.9	1711.0	23.6	1710.1	11.4	1710.1	11.4	100.1
GC-01CP-3	544	20771	3.7	9.4957	0.2	3.8012	1.4	0.2618	1.3	0.98	1499.0	17.8	1593.0	10.9	1719.7	4.3	1719.7	4.3	87.2
GC-01CP-95	213	40101	3.9	9.4920	0.9	4.3479	1.6	0.2993	1.3	0.82	1687.9	18.9	1702.5	12.8	1720.4	16.2	1720.4	16.2	98.1
GC-01CP-79	191	8452	2.0	9.4731	1.2	4.3974	2.8	0.3021	2.6	0.91	1701.8	38.7	1711.9	23.5	1724.1	21.2	1724.1	21.2	98.7
GC-01CP-82	246	29955	5.6	9.4702	0.8	4.5915	1.8	0.3154	1.7	0.91	1767.0	26.0	1747.7	15.4	1724.7	13.9	1724.7	13.9	102.5
GC-01CP-74	197	41893	2.9	9.4604	1.0	4.4568	3.4	0.3058	3.2	0.95	1720.0	49.0	1723.0	28.3	1726.6	19.3	1726.6	19.3	99.6
GC-01CP-69	546	90522	2.8	9.4061	0.4	4.6073	3.0	0.3143	2.9	0.99	1761.9	45.2	1750.6	24.7	1737.1	7.6	1737.1	7.6	101.4
GC-01CP-84	187	40470	4.7	9.3679	0.7	4.6292	1.4	0.3145	1.3	0.88	1762.9	19.6	1754.5	12.1	1744.6	12.6	1744.6	12.6	101.0
GC-01CP-68	109	20910	2.0	9.2893	0.9	4.5937	1.8	0.3095	1.5	0.85	1738.2	22.9	1748.1	14.8	1760.0	17.2	1760.0	17.2	98.8
GC-01CP-53	190	9623	4.9	9.2691	1.8	4.3075	3.7	0.2896	3.3	0.88	1639.4	47.3	1694.8	30.7	1764.0	32.4	1764.0	32.4	92.9
GC-01CP-16	524	25336	3.9	9.2366	0.4	4.1291	2.1	0.2766	2.0	0.98	1574.3	28.5	1660.1	17.0	1770.4	7.2	1770.4	7.2	88.9
GC-01CP-25	184	42749	2.9	9.1878	0.6	4.7623	2.5	0.3173	2.5	0.97	1776.7	38.2	1778.3	21.3	1780.1	11.5	1780.1	11.5	99.8
GC-01CP-30	396	58353	7.1	9.1301	0.3	4.5582	2.6	0.3018	2.6	0.99	1700.4	38.2	1741.7	21.4	1791.6	4.8	1791.6	4.8	94.9
GC-01CP-66	346	58174	4.0	9.0981	0.4	4.9536	3.5	0.3269	3.4	0.99	1823.2	54.6	1811.4	29.3	1797.9	7.9	1797.9	7.9	101.4

U-Pb geochronologic analyses of the Osgood Mountain Quartzite and Preble Formation

Isotope ratios											Apparent ages (Ma)								
Analysis	U	206Pb	U/Th	206Pb*	±	207Pb*	±	206Pb*	±	error	206Pb*	±	207Pb*	±	206Pb*	±	Best age	±	Conc
	(ppm)	204Pb		207Pb*	(%)	235U*	(%)	238U	(%)	corr.	238U*	(Ma)	235U	(Ma)	207Pb*	(Ma)	(Ma)	(Ma)	(%)
SAMPLE: Preble Formation GC-01-CP LOCATION: Goughs Canyon, Osgood Mountains 0468513 4554509 (NAD 83 UTM 11N)																			
GC-01CP-47	92	15847	4.7	9.0776	1.2	4.9457	2.5	0.3256	2.2	0.87	1817.1	34.3	1810.1	21.0	1802.1	22.2	1802.1	22.2	100.8
GC-01CP-7	102	15599	9.9	8.8955	1.1	5.0375	2.2	0.3250	1.9	0.86	1814.1	29.5	1825.6	18.4	1838.8	20.1	1838.8	20.1	98.7
GC-01CP-63	218	41428	10.7	8.8852	0.5	5.0193	2.9	0.3234	2.8	0.98	1806.6	44.4	1822.6	24.3	1840.9	9.3	1840.9	9.3	98.1
GC-01CP-86	96	13285	6.2	8.8626	1.1	5.1343	2.7	0.3300	2.4	0.91	1838.5	39.1	1841.8	22.9	1845.5	20.6	1845.5	20.6	99.6
GC-01CP-6	51	9705	1.8	8.6385	2.5	5.4723	3.8	0.3428	2.8	0.74	1900.4	46.1	1896.3	32.4	1891.7	45.4	1891.7	45.4	100.5
GC-01CP-77	222	20999	1.5	5.6427	2.0	10.7180	2.6	0.4386	1.7	0.65	2344.5	32.9	2499.0	24.0	2627.0	32.7	2627.0	32.7	89.2
GC-01CP-52	208	25549	1.8	5.6363	0.5	10.9378	1.2	0.4471	1.1	0.91	2382.4	22.3	2517.9	11.4	2628.9	8.3	2628.9	8.3	90.6
GC-01CP-4	125	52373	1.2	5.5033	0.5	13.0332	2.0	0.5202	2.0	0.97	2700.0	43.9	2682.1	19.3	2668.5	7.8	2668.5	7.8	101.2
GC-01CP-98	212	69019	1.2	5.5013	0.4	12.6590	1.5	0.5051	1.4	0.96	2635.6	30.6	2654.6	13.9	2669.1	6.8	2669.1	6.8	98.7
GC-01CP-75	154	50100	1.2	5.4968	0.4	12.6644	3.1	0.5049	3.1	0.99	2634.8	66.3	2655.0	29.1	2670.5	6.7	2670.5	6.7	98.7
GC-01CP-58	290	27914	2.8	5.4287	0.9	10.5648	3.3	0.4160	3.2	0.96	2242.1	61.0	2485.6	31.0	2691.1	14.7	2691.1	14.7	83.3
GC-01CP-18	105	20755	1.1	5.3618	0.4	12.4128	4.2	0.4827	4.1	1.00	2539.0	87.0	2636.1	39.1	2711.6	6.3	2711.6	6.3	93.6
GC-01CP-80	106	39471	2.3	5.3240	0.4	14.2995	1.0	0.5522	0.8	0.88	2834.1	19.2	2769.8	9.0	2723.2	7.4	2723.2	7.4	104.1
GC-01CP-93	359	44185	2.3	5.2510	0.3	13.4855	1.5	0.5136	1.5	0.98	2671.9	32.7	2714.3	14.3	2746.0	4.4	2746.0	4.4	97.3

Notes:

1. Analyses with >10% uncertainty (1-sigma) in 206Pb/238U age are not included.
2. Analyses with >10% uncertainty (1-sigma) in 206Pb/207Pb age are not included, unless 206Pb/238U age is <500 Ma.
3. Best age is determined from 206Pb/238U age for analyses with 206Pb/238U age <1000 Ma and from 206Pb/207P.
4. Concordance is based on 206Pb/238U age / 206Pb/207Pb age. Value is not reported for 206Pb/238U ages <500
5. Analyses with 206Pb/238U age > 500 Ma and with >30% discordance (<70% concordance) are not included.
6. Analyses with 206Pb/238U age > 500 Ma and with >5% reverse discordance (<105% concordance) are not included.
7. All uncertainties are reported at the 1-sigma level, and include only measurement errors.
8. Systematic errors are as follows (at 2-sigma level): [sample 1: 2.5% (206Pb/238U) & 1.4% (206Pb/207Pb)] These values are reported on cells U1 and W1 of NUagecalc.
9. Analyses conducted by LA-MC-ICPMS, as described by Gehrels et al. (2008).
10. U concentration and U/Th are calibrated relative to Sri Lanka zircon standard and are accurate to ~20%.
11. Common Pb correction is from measured 204Pb with common Pb composition interpreted from Stacey and Kramers (1975).
12. Common Pb composition assigned uncertainties of 1.5 for 206Pb/204Pb, 0.3 for 207Pb/204Pb, and 2.0 for 208Pb/204Pb.
13. U/Pb and 206Pb/207Pb fractionation is calibrated relative to fragments of a large Sri Lanka zircon of 563.5 ± 3.2 Ma (2-sigma).
14. U decay constants and composition as follows: 238U = 9.8485 x 10-10, 235U = 1.55125 x 10-10, 238U/235U = 137.88.
15. Weighted mean and concordia plots determined with Isoplot (Ludwig, 2008).

APPENDIX C

U-Pb geochronologic anlayses of selected Roberts Mountains allochthon strata

Table notes are at the end of the appendix.

						Isotope ratios							Apparent ages (Ma)							
	U	206Pb	U/Th	206Pb*	±	207Pb*	±	206Pb*	±	error	206Pb*	±	207Pb*	±	206Pb*	±	Best age	±	Conc.	Discord.
	(ppm)	204Pb		207Pb*	(%)	235U*	(%)	238U	(%)	corr.	238U*	(Ma)	235U	(Ma)	207Pb*	(Ma)	(Ma)	(Ma)	(%)	(%)
Sample: Snow Canyon Formation. Location: Snow Canyon, Independence Mountains; 0579760 4585698 (NAD 83 UTM 11T)																				
SNOW-CYN-171	530	103043	4.4	16.9299	0.8	0.7446	1.2	0.0914	0.9	0.76	564.0	5.1	565.1	5.4	569.6	17.5	564.0	5.1	99.0	1.0 0.9, 0.8
SNOW-CYN-182	221	138508	1.1	13.9234	0.6	1.6320	1.2	0.1648	1.0	0.87	983.4	9.3	982.6	7.4	980.9	11.6	980.9	11.6	100.3	-0.3
SNOW-CYN-75	40	18372	1.4	13.8037	3.3	1.7128	3.6	0.1715	1.5	0.41	1020.2	14.0	1013.3	23.0	998.4	66.2	998.4	66.2	102.2	-2.2
SNOW-CYN-92	92	61584	1.0	9.6861	0.8	4.2147	1.1	0.2961	0.8	0.73	1671.9	12.1	1676.9	9.3	1683.2	14.4	1683.2	14.4	99.3	0.7
SNOW-CYN-118	228	22936	4.3	9.1736	0.3	4.1335	3.1	0.2750	3.1	0.99	1566.2	42.8	1660.9	25.3	1782.9	5.7	1782.9	5.7	87.8	12.2
SNOW-CYN-61	38	34156	0.7	9.1307	1.7	4.9244	3.1	0.3261	2.6	0.85	1819.5	41.5	1806.4	26.2	1791.4	30.2	1791.4	30.2	101.6	-1.6
SNOW-CYN-98	59	33444	0.8	9.0275	0.6	4.8745	1.2	0.3192	1.0	0.85	1785.6	15.4	1797.9	9.8	1812.1	10.9	1812.1	10.9	98.5	1.5
SNOW-CYN-87	55	60278	1.1	9.0027	1.0	4.8071	1.7	0.3139	1.4	0.81	1759.7	21.2	1786.1	14.3	1817.1	18.0	1817.1	18.0	96.8	3.2
SNOW-CYN-63	29	74802	0.7	8.9658	1.3	4.9828	2.2	0.3240	1.8	0.82	1809.3	28.8	1816.4	18.8	1824.6	23.2	1824.6	23.2	99.2	0.8
SNOW-CYN-9	62	32646	0.6	8.9568	0.9	5.1270	2.4	0.3331	2.2	0.93	1853.2	35.9	1840.6	20.3	1826.4	15.6	1826.4	15.6	101.5	-1.5
SNOW-CYN-30	53	42708	0.9	8.9538	0.8	4.9671	1.2	0.3226	0.9	0.76	1802.2	14.9	1813.7	10.5	1827.0	14.6	1827.0	14.6	98.6	1.4
SNOW-CYN-196	64	59693	0.7	8.9475	1.0	5.0527	1.6	0.3279	1.3	0.80	1828.1	20.8	1828.2	13.9	1828.3	17.9	1828.3	17.9	100.0	0.0
SNOW-CYN-113	61	77813	0.6	8.9453	0.6	5.0860	1.3	0.3300	1.1	0.88	1838.2	18.3	1833.8	11.0	1828.7	11.2	1828.7	11.2	100.5	-0.5
SNOW-CYN-38	40	62208	0.8	8.9424	1.5	4.9646	1.7	0.3220	0.8	0.47	1799.4	12.2	1813.3	14.1	1829.3	26.8	1829.3	26.8	98.4	1.6
SNOW-CYN-32	257	74199	1.0	8.9331	0.3	4.9875	0.8	0.3231	0.8	0.93	1805.0	12.0	1817.2	6.9	1831.2	5.3	1831.2	5.3	98.6	1.4
SNOW-CYN-27	38	25786	0.7	8.9315	1.4	4.9938	1.7	0.3235	0.9	0.55	1806.7	14.4	1818.3	14.1	1831.5	25.3	1831.5	25.3	98.6	1.4
SNOW-CYN-14	41	40359	0.9	8.9305	1.7	5.1028	2.3	0.3305	1.5	0.68	1840.8	24.6	1836.6	19.2	1831.7	30.2	1831.7	30.2	100.5	-0.5
SNOW-CYN-141	42	34914	1.2	8.9287	1.0	5.1209	1.9	0.3316	1.6	0.85	1846.2	26.3	1839.6	16.4	1832.1	18.5	1832.1	18.5	100.8	-0.8
SNOW-CYN-36	22	21333	1.4	8.9287	2.3	4.9182	2.8	0.3185	1.5	0.53	1782.3	22.9	1805.4	23.3	1832.1	42.3	1832.1	42.3	97.3	2.7
SNOW-CYN-121	59	43360	1.3	8.9282	1.1	5.0217	1.4	0.3252	0.9	0.65	1815.0	14.4	1823.0	11.8	1832.2	19.1	1832.2	19.1	99.1	0.9
SNOW-CYN-144	44	51830	1.5	8.9251	1.0	5.0984	2.2	0.3300	1.9	0.88	1838.5	31.1	1835.8	18.7	1832.8	18.7	1832.8	18.7	100.3	-0.3
SNOW-CYN-70	244	279260	0.9	8.9240	0.2	5.1293	1.4	0.3320	1.4	0.98	1848.0	21.7	1841.0	11.7	1833.0	4.3	1833.0	4.3	100.8	-0.8
SNOW-CYN-77	69	122422	1.0	8.9221	0.8	4.9495	1.2	0.3203	1.0	0.79	1791.1	15.3	1810.7	10.4	1833.4	13.7	1833.4	13.7	97.7	2.3
SNOW-CYN-22	28	27707	1.2	8.9195	2.0	5.0542	2.5	0.3270	1.4	0.58	1823.6	23.0	1828.5	21.1	1833.9	36.7	1833.9	36.7	99.4	0.6
SNOW-CYN-179	41	29085	0.8	8.9153	0.9	5.1042	1.6	0.3300	1.3	0.83	1838.6	21.2	1836.8	13.6	1834.8	16.3	1834.8	16.3	100.2	-0.2
SNOW-CYN-78	35	49548	0.8	8.9141	1.0	5.0933	1.6	0.3293	1.3	0.80	1834.9	20.7	1835.0	13.7	1835.0	17.7	1835.0	17.7	100.0	0.0
SNOW-CYN-142	35	24716	1.0	8.9133	1.4	5.1169	1.9	0.3308	1.3	0.67	1842.2	20.2	1838.9	15.9	1835.2	25.2	1835.2	25.2	100.4	-0.4
SNOW-CYN-126	138	84479	0.7	8.9119	0.4	4.9794	1.0	0.3218	0.9	0.91	1798.7	14.5	1815.8	8.5	1835.5	7.5	1835.5	7.5	98.0	2.0
SNOW-CYN-191	51	36556	1.7	8.9117	1.0	5.0967	1.3	0.3294	0.9	0.66	1835.6	13.6	1835.6	10.9	1835.5	17.4	1835.5	17.4	100.0	0.0
SNOW-CYN-169	79	42642	1.1	8.9099	1.0	4.7323	2.1	0.3058	1.9	0.89	1720.0	28.7	1773.0	17.9	1835.9	17.9	1835.9	17.9	93.7	6.3
SNOW-CYN-132	51	53246	1.6	8.9013	1.0	5.0986	1.2	0.3292	0.7	0.55	1834.3	10.6	1835.9	10.3	1837.6	18.3	1837.6	18.3	99.8	0.2
SNOW-CYN-118	32	36028	0.7	8.9007	1.1	5.0476	1.8	0.3258	1.5	0.81	1818.2	23.1	1827.4	15.3	1837.8	19.2	1837.8	19.2	98.9	1.1
SNOW-CYN-151	79	97830	1.2	8.8996	0.5	5.1611	1.1	0.3331	1.0	0.90	1853.5	15.4	1846.2	9.0	1838.0	8.4	1838.0	8.4	100.8	-0.8
SNOW-CYN-135	115	155050	1.3	8.8940	0.4	5.1009	1.7	0.3290	1.7	0.97	1833.7	26.8	1836.3	14.6	1839.1	7.0	1839.1	7.0	99.7	0.3
SNOW-CYN-164	111	106505	0.9	8.8935	0.4	5.1512	0.9	0.3323	0.9	0.91	1849.3	13.8	1844.6	8.0	1839.2	6.9	1839.2	6.9	100.5	-0.5
SNOW-CYN-10	63	56602	1.7	8.8918	0.7	5.1925	1.3	0.3349	1.1	0.86	1861.9	18.1	1851.4	11.0	1839.6	11.9	1839.6	11.9	101.2	-1.2
SNOW-CYN-170	77	174559	1.1	8.8910	0.5	5.0152	1.1	0.3234	1.0	0.88	1806.3	15.6	1821.9	9.5	1839.7	9.6	1839.7	9.6	98.2	1.8
SNOW-CYN-172	20	30578	1.4	8.8891	1.8	5.1124	2.6	0.3296	1.8	0.71	1836.4	29.4	1838.2	21.9	1840.1	32.8	1840.1	32.8	99.8	0.2
SNOW-CYN-107	36	78308	1.1	8.8882	0.5	5.0762	1.2	0.3272	1.1	0.90	1824.9	17.7	1832.1	10.5	1840.3	9.8	1840.3	9.8	99.2	0.8
SNOW-CYN-89	43	63599	1.0	8.8864	0.9	4.9870	1.2	0.3214	0.8	0.65	1796.6	11.9	1817.1	9.9	1840.7	16.1	1840.7	16.1	97.6	2.4
SNOW-CYN-31	89	73950	1.2	8.8863	0.5	5.1486	4.2	0.3318	4.2	0.99	1847.2	67.3	1844.2	35.9	1840.7	9.4	1840.7	9.4	100.4	-0.4
SNOW-CYN-116	112	142250	1.7	8.8851	0.4	5.0449	1.9	0.3251	1.8	0.98	1814.6	29.0	1826.9	15.9	1840.9	6.9	1840.9	6.9	98.6	1.4
SNOW-CYN-200	115	109959	1.2	8.8846	0.5	5.0839	1.2	0.3276	1.1	0.92	1826.7	17.7	1833.4	10.3	1841.0	8.8	1841.0	8.8	99.2	0.8
SNOW-CYN-166	21	23371	0.8	8.8836	1.7	5.0960	2.1	0.3283	1.3	0.60	1830.3	20.2	1835.4	17.8	1841.3	30.2	1841.3	30.2	99.4	0.6
SNOW-CYN-185	117	105425	1.0	8.8826	0.4	5.1330	1.1	0.3307	1.0	0.93	1841.7	16.0	1841.6	9.1	1841.5	7.3	1841.5	7.3	100.0	0.0
SNOW-CYN-67	159	213593	2.3	8.8809	0.4	5.1590	1.3	0.3323	1.2	0.95	1849.5	19.3	1845.9	10.7	1841.8	6.9	1841.8	6.9	100.4	-0.4
SNOW-CYN-147	97	119246	1.5	8.8803	0.7	5.1142	1.1	0.3294	0.8	0.73	1835.4	12.5	1838.5	9.1	1841.9	13.1	1841.9	13.1	99.6	0.4
SNOW-CYN-58	106	142558	1.4	8.8795	0.2	5.0922	0.8	0.3279	0.8	0.96	1828.4	12.8	1834.8	7.1	1842.1	4.3	1842.1	4.3	99.3	0.7
SNOW-CYN-153	120	161045	1.5	8.8774	0.6	5.1887	1.9	0.3341	1.8	0.96	1858.1	29.4	1850.8	16.2	1842.5	10.0	1842.5	10.0	100.8	-0.8
SNOW-CYN-162	73	160747	1.9	8.8767	0.6	5.2203	1.3	0.3361	1.1	0.88	1867.8	18.3	1855.9	10.9	1842.7	10.8	1842.7	10.8	101.4	-1.4
SNOW-CYN-45	145	153135	1.4	8.8719	0.4	5.1497	1.0	0.3314	1.0	0.93	1845.0	15.6	1844.3	8.9	1843.6	7.0	1843.6	7.0	100.1	-0.1
SNOW-CYN-97	51	75488	0.9	8.8689	1.0	5.0177	1.5	0.3228	1.1	0.75	1803.2	17.2	1822.3	12.3	1844.2	17.4	1844.2	17.4	97.8	2.2
SNOW-CYN-48	45	74407	0.7	8.8670	0.6	5.0794	2.3	0.3267	2.2	0.97	1822.1	34.8	1832.7	19.2	1844.6	10.4	1844.6	10.4	98.8	1.2
SNOW-CYN-53	59	50868	0.9	8.8657	0.7	5.1750	1.5	0.3328	1.3	0.89	1851.7	21.3	1848.5	12.6	1844.9	12.1	1844.9	12.1	100.4	-0.4
SNOW-CYN-102	105	91204	1.2	8.8506	0.4	4.6709	3.2	0.2998	3.2	0.99	1690.5	47.4	1762.0	26.9	1848.0	7.5	1848.0	7.5	91.5	8.5
SNOW-CYN-195	142	293159	1.8	8.8469	0.3	5.1931	1.4	0.3332	1.3	0.98	1853.9	21.5	1851.5	11.6	1848.7	5.1	1848.7	5.1	100.3	-0.3
SNOW-CYN-181	52	51405	1.4	8.8439	0.6	5.1351	1.5	0.3294	1.3	0.90	1835.4	21.2	1841.9	12.5	1849.3	11.3	1849.3	11.3	99.2	0.8
SNOW-CYN-110	29	18187	0.6	8.8431	1.2	5.1409	2.2	0.3297	1.8	0.83	1837.0	29.0	1842.9	18.6	1849.5	22.1	1849.5	22.1	99.3	0.7
SNOW-CYN-186	32	5844	1.3	8.8378	2.1	5.1393	2.5	0.3294	1.2	0.49	1835.5	19.2	1842.6	20.9	1850.6	38.6	1850.6	38.6	99.2	0.8
SNOW-CYN-138	105	64442	1.0	8.8370	0.4	5.0873	1.0	0.3261	0.9	0.92	1819.2	14.4	1834.0	8.4	1850.8	6.9	1850.8	6.9	98.3	1.7
SNOW-CYN-122	35	38370	1.0	8.8355	1.2	4.9485	2.4	0.3171	2.1	0.88	1775.6	33.1	1810.6	20.6	1851.1	21.3	1851.1	21.3	95.9	4.1
SNOW-CYN-80	61	36852	1.0	8.8280	0.9	5.1081	2.1	0.3271	1.9	0.90	1824.1	30.1	1837.5	18.0	1852.6	17.1	1852.6	17.1	98.5	1.5
SNOW-CYN-57	32	17759	0.7	8.8266	1.5	5.1974	2.1	0.3327	1.4	0.70	1851.5	23.1	1852.2	17.6	1852.9	26.7	1852.9	26.7	99.9	0.1
SNOW-CYN-108	38	60111	0.5	8.8246	1.4	5.1563	2.3	0.3300	1.9	0.81	1838.5	30.3	1845.4	19.9	1853.3	24.9	1853.3	24.9	99.2	0.8
SNOW-CYN-106	38	32659	1.3	8.8223	1.3	5.1253	2.6	0.3279	2.3	0.86	1828.4	35.9	1840.3	22.3	1853.8	24.1	1853.8	24.1	98.6	1.4
SNOW-CYN-2	80	117742	1.3	8.8218	0.7	5.3102	1.8	0.3398	1.6	0.92	1885.5	26.6	1870.5	15.1	1853.9	12.6	1853.9	12.6	101.7	-1.7

U-Pb geochronologic anlayses of selected Roberts Mountains allochthon strata

						Isotope ratios							Apparent ages (Ma)							
	U	206Pb	U/Th	206Pb*	±	207Pb*	±	206Pb*	±	error	206Pb*	±	207Pb*	±	206Pb*	±	Best age	±	Conc.	Discord.
	(ppm)	204Pb		207Pb*	(%)	235U*	(%)	238U	(%)	corr.	238U*	(Ma)	235U	(Ma)	207Pb*	(Ma)	(Ma)	(Ma)	(%)	(%)
Sample: Snow Canyon Formation. Location: Snow Canyon, Independence Mountains; 0579760 4585698 (NAD 83 UTM 11T)																				
SNOW-CYN-117	28	46056	0.4	8.8209	0.8	5.0624	2.1	0.3239	1.9	0.93	1808.6	30.7	1829.8	17.8	1854.1	14.4	1854.1	14.4	97.5	2.5
SNOW-CYN-43	63	96847	1.6	8.8191	0.8	5.1893	1.5	0.3319	1.2	0.82	1847.7	19.3	1850.9	12.5	1854.4	15.2	1854.4	15.2	99.6	0.4
SNOW-CYN-190	96	79453	1.0	8.8049	0.5	5.2493	1.2	0.3352	1.0	0.88	1863.6	16.7	1860.7	10.0	1857.3	9.8	1857.3	9.8	100.3	-0.3
SNOW-CYN-129	207	322649	4.7	8.8048	0.4	5.1065	1.5	0.3261	1.5	0.96	1819.4	23.1	1837.2	12.9	1857.4	7.4	1857.4	7.4	98.0	2.0
SNOW-CYN-7	90	95659	2.1	8.8007	0.7	5.2804	1.3	0.3370	1.1	0.86	1872.4	18.1	1865.7	11.0	1858.2	11.8	1858.2	11.8	100.8	-0.8
SNOW-CYN-15	143	160011	1.5	8.7858	0.3	5.2873	1.1	0.3369	1.0	0.96	1871.8	16.7	1866.8	9.1	1861.3	5.3	1861.3	5.3	100.6	-0.6
SNOW-CYN-198	84	67128	2.8	8.7442	0.7	5.3116	1.5	0.3369	1.3	0.87	1871.5	21.4	1870.7	12.9	1869.8	13.3	1869.8	13.3	100.1	-0.1
SNOW-CYN-173	101	187975	1.5	8.7147	1.9	5.3476	9.5	0.3380	9.3	0.98	1877.0	151.0	1876.5	81.1	1875.9	33.7	1875.9	33.7	100.1	-0.1
SNOW-CYN-49	155	236451	1.5	8.7019	0.3	5.3935	1.5	0.3404	1.5	0.98	1888.6	24.7	1883.8	13.3	1878.6	6.1	1878.6	6.1	100.5	-0.5
SNOW-CYN-161	20	14401	0.7	8.6899	3.0	5.3032	3.4	0.3342	1.7	0.49	1858.9	27.1	1869.4	29.1	1881.1	53.4	1881.1	53.4	98.8	1.2
SNOW-CYN-184	33	14196	0.8	8.6771	1.0	5.3435	1.4	0.3363	0.9	0.67	1868.7	15.1	1875.9	11.9	1883.7	18.6	1883.7	18.6	99.2	0.8
SNOW-CYN-193	47	51193	1.8	8.6649	1.1	5.3317	1.5	0.3351	1.0	0.68	1862.9	16.2	1874.0	12.5	1886.2	19.2	1886.2	19.2	98.8	1.2
SNOW-CYN-85	67	48040	0.6	8.6331	0.8	5.4444	1.5	0.3409	1.3	0.84	1891.0	20.9	1891.9	13.1	1892.9	15.0	1892.9	15.0	99.9	0.1
SNOW-CYN-163	50	19275	0.7	8.6250	1.0	5.4224	2.2	0.3392	2.0	0.90	1882.8	32.3	1888.4	18.9	1894.6	17.3	1894.6	17.3	99.4	0.6
SNOW-CYN-131	51	97967	0.7	8.6054	0.7	5.4474	1.0	0.3400	0.7	0.73	1886.6	11.5	1892.3	8.2	1898.6	11.8	1898.6	11.8	99.4	0.6
SNOW-CYN-17	41	19804	1.8	8.6010	1.4	5.5060	1.7	0.3435	0.9	0.53	1903.3	14.5	1901.5	14.4	1899.6	25.5	1899.6	25.5	100.2	-0.2
SNOW-CYN-44	263	143112	3.3	8.5768	0.2	5.5014	1.1	0.3422	1.1	0.99	1897.3	18.6	1900.8	9.8	1904.6	2.8	1904.6	2.8	99.6	0.4
SNOW-CYN-119	41	49974	1.2	8.5763	0.7	5.4997	1.2	0.3421	1.0	0.80	1896.7	15.7	1900.5	10.2	1904.7	12.7	1904.7	12.7	99.6	0.4
SNOW-CYN-66	46	64039	0.9	8.5736	0.9	5.5461	1.7	0.3449	1.5	0.85	1910.0	24.3	1907.8	14.9	1905.3	16.6	1905.3	16.6	100.2	-0.2
SNOW-CYN-24	24	26300	1.0	8.5711	1.8	5.5083	2.4	0.3424	1.6	0.67	1898.3	26.7	1901.9	20.7	1905.8	32.1	1905.8	32.1	99.6	0.4
SNOW-CYN-93	174	270312	1.3	8.5637	0.3	5.3319	1.1	0.3312	1.0	0.96	1844.0	16.4	1874.0	9.2	1907.4	5.5	1907.4	5.5	96.7	3.3
SNOW-CYN-197	73	17621	0.9	8.5621	0.7	5.2005	0.9	0.3229	0.6	0.66	1804.1	9.5	1852.7	7.8	1907.7	12.3	1907.7	12.3	94.6	5.4
SNOW-CYN-81	53	72976	0.8	8.5612	0.8	5.5731	2.4	0.3460	2.2	0.94	1915.7	36.6	1911.9	20.3	1907.9	15.0	1907.9	15.0	100.4	-0.4
SNOW-CYN-5	51	120427	0.9	8.5565	0.8	5.5541	2.1	0.3447	1.9	0.93	1909.1	32.2	1909.0	18.0	1908.9	13.9	1908.9	13.9	100.0	0.0
SNOW-CYN-73	64	43049	1.8	8.5523	0.8	5.4394	1.3	0.3374	1.1	0.81	1874.1	17.8	1891.1	11.6	1909.8	14.1	1909.8	14.1	98.1	1.9
SNOW-CYN-155	25	48093	0.9	8.5510	1.6	5.5469	2.2	0.3440	1.5	0.67	1905.9	24.1	1907.9	18.6	1910.0	28.7	1910.0	28.7	99.8	0.2
SNOW-CYN-120	52	68253	1.0	8.5493	0.8	5.4796	1.6	0.3398	1.3	0.87	1885.5	22.0	1897.4	13.4	1910.4	13.9	1910.4	13.9	98.7	1.3
SNOW-CYN-94	31	21928	0.7	8.5442	1.8	5.5028	2.3	0.3410	1.4	0.63	1891.5	23.7	1901.0	19.6	1911.5	31.8	1911.5	31.8	99.0	1.0
SNOW-CYN-12	178	265794	0.8	8.5365	0.2	5.6221	0.9	0.3481	0.9	0.98	1925.4	14.2	1919.5	7.5	1913.1	2.7	1913.1	2.7	100.6	-0.6
SNOW-CYN-139	153	165091	0.9	8.5273	0.3	5.4565	0.7	0.3375	0.6	0.92	1874.4	10.1	1893.8	5.8	1915.0	4.6	1915.0	4.6	97.9	2.1
SNOW-CYN-84	137	86779	1.4	8.5210	0.4	4.8362	1.7	0.2989	1.7	0.98	1685.7	24.6	1791.2	14.3	1916.4	6.5	1916.4	6.5	88.0	12.0
SNOW-CYN-42	78	96370	1.0	8.5178	0.3	5.5566	1.1	0.3433	1.1	0.96	1902.4	17.4	1909.4	9.5	1917.0	5.5	1917.0	5.5	99.2	0.8
SNOW-CYN-71	77	73803	1.3	8.5136	0.6	5.5132	1.2	0.3404	1.1	0.88	1888.7	17.6	1902.7	10.5	1917.9	10.3	1917.9	10.3	98.5	1.5
SNOW-CYN-52	102	104843	0.7	8.5122	0.6	5.6229	1.6	0.3471	1.5	0.92	1920.9	24.5	1919.6	13.8	1918.2	11.0	1918.2	11.0	100.1	-0.1
SNOW-CYN-91	163	95427	1.0	8.5103	0.3	5.5469	1.0	0.3424	1.0	0.96	1898.1	16.2	1907.9	8.8	1918.6	4.8	1918.6	4.8	98.9	1.1
SNOW-CYN-82	89	172417	1.1	8.4982	0.5	5.7182	1.8	0.3524	1.7	0.96	1946.2	28.7	1934.1	15.5	1921.2	9.5	1921.2	9.5	101.3	-1.3
SNOW-CYN-176	21	16687	0.9	8.4967	1.2	5.5232	1.9	0.3404	1.5	0.78	1888.4	24.5	1904.2	16.6	1921.5	21.8	1921.5	21.8	98.3	1.7
SNOW-CYN-56	84	70209	1.5	8.4947	0.6	5.6662	1.4	0.3491	1.3	0.89	1930.3	20.9	1926.2	12.1	1921.9	11.2	1921.9	11.2	100.4	-0.4
SNOW-CYN-167	133	111624	2.1	8.4863	0.3	5.5587	3.1	0.3421	3.1	1.00	1896.9	50.6	1909.7	26.6	1923.7	5.2	1923.7	5.2	98.6	1.4
SNOW-CYN-125	45	97694	1.2	8.4827	0.8	5.5844	1.4	0.3436	1.2	0.83	1903.8	19.1	1913.7	12.1	1924.4	14.1	1924.4	14.1	98.9	1.1
SNOW-CYN-60	68	36343	0.5	8.4825	0.5	5.5416	1.6	0.3409	1.5	0.96	1891.1	24.4	1907.1	13.4	1924.5	8.2	1924.5	8.2	98.3	1.7
SNOW-CYN-160	37	69009	0.8	8.4800	0.9	5.5747	1.6	0.3429	1.3	0.82	1900.4	21.8	1912.2	13.9	1925.0	16.7	1925.0	16.7	98.7	1.3
SNOW-CYN-8	21	22966	0.8	8.4799	2.5	5.5882	2.8	0.3437	1.2	0.45	1904.4	20.4	1914.3	23.8	1925.0	44.3	1925.0	44.3	98.9	1.1
SNOW-CYN-199	51	33912	1.2	8.4780	0.8	5.2437	2.1	0.3224	1.9	0.92	1801.6	30.2	1859.7	17.9	1925.4	14.9	1925.4	14.9	93.6	6.4
SNOW-CYN-51	68	129535	1.1	8.4745	0.7	5.6710	1.5	0.3486	1.4	0.90	1927.7	22.8	1927.0	13.2	1926.2	12.1	1926.2	12.1	100.1	-0.1
SNOW-CYN-16	61	65104	1.3	8.4678	1.0	5.6441	2.3	0.3466	2.1	0.91	1918.5	35.3	1922.9	20.1	1927.6	17.2	1927.6	17.2	99.5	0.5
SNOW-CYN-150	80	101032	1.0	8.4644	0.4	5.7295	1.2	0.3517	1.1	0.94	1942.9	18.4	1935.8	10.1	1928.3	6.9	1928.3	6.9	100.8	-0.8
SNOW-CYN-171	101	114861	1.0	8.4521	0.3	5.6969	1.1	0.3492	1.1	0.95	1930.9	17.9	1930.9	9.7	1930.9	6.1	1930.9	6.1	100.0	0.0
SNOW-CYN-130	185	400942	2.5	8.4329	0.3	5.5471	1.1	0.3393	1.0	0.95	1883.1	17.1	1907.9	9.5	1935.0	6.1	1935.0	6.1	97.3	2.7
SNOW-CYN-158	296	152000	3.1	8.4303	0.1	5.8503	1.6	0.3577	1.6	1.00	1971.3	26.3	1953.9	13.5	1935.5	2.4	1935.5	2.4	101.8	-1.8
SNOW-CYN-105	160	165134	1.1	8.4184	0.3	5.7095	1.4	0.3486	1.4	0.97	1927.9	23.2	1932.8	12.3	1938.0	5.7	1938.0	5.7	99.5	0.5
SNOW-CYN-76	42	42216	1.2	8.4155	1.0	5.6969	1.4	0.3477	0.9	0.69	1923.7	15.6	1930.9	11.8	1938.7	17.8	1938.7	17.8	99.2	0.8
SNOW-CYN-111	24	16024	0.4	8.3638	1.9	5.7827	2.8	0.3508	2.0	0.72	1938.3	33.4	1943.8	24.0	1949.7	34.4	1949.7	34.4	99.4	0.6
SNOW-CYN-20	140	189553	1.0	8.2253	0.2	6.0233	1.6	0.3593	1.6	0.99	1979.0	27.7	1979.2	14.3	1979.5	3.6	1979.5	3.6	100.0	0.0
SNOW-CYN-101	84	24275	1.6	8.1606	0.5	6.0538	0.9	0.3583	0.7	0.81	1974.1	12.4	1983.6	7.9	1993.5	9.5	1993.5	9.5	99.0	1.0
SNOW-CYN-145	112	168637	1.1	8.1305	0.6	6.2179	1.6	0.3667	1.5	0.93	2013.7	26.1	2007.0	14.1	2000.1	10.2	2000.1	10.2	100.7	-0.7
SNOW-CYN-175	29	26832	1.3	8.1279	1.3	6.0692	2.8	0.3578	2.5	0.89	1971.6	42.2	1985.8	24.4	2000.7	23.1	2000.7	23.1	98.5	1.5
SNOW-CYN-137	29	19947	1.0	8.0567	1.3	6.2843	3.8	0.3672	3.6	0.94	2016.2	62.8	2016.3	33.6	2016.3	22.2	2016.3	22.2	100.0	0.0
SNOW-CYN-149	17	31838	1.6	7.8987	2.3	6.6467	3.4	0.3808	2.5	0.73	2079.9	44.3	2065.6	30.1	2051.3	41.1	2051.3	41.1	101.4	-1.4
SNOW-CYN-55	22	29334	0.9	7.8764	1.2	6.6872	2.6	0.3820	2.3	0.89	2085.6	41.3	2070.9	23.1	2056.3	21.3	2056.3	21.3	101.4	-1.4
SNOW-CYN-103	140	191427	1.0	7.8757	0.3	6.5152	0.6	0.3722	0.6	0.89	2039.5	9.7	2048.0	5.5	2056.5	5.0	2056.5	5.0	99.2	0.8
SNOW-CYN-180	17	21370	0.6	7.8676	1.4	6.5746	2.1	0.3752	1.5	0.73	2053.6	26.6	2056.0	18.1	2058.3	24.6	2058.3	24.6	99.8	0.2
SNOW-CYN-68	33	41028	0.9	7.8558	0.9	6.6908	2.3	0.3812	2.2	0.93	2081.9	38.8	2071.4	20.7	2060.9	15.1	2060.9	15.1	101.0	-1.0
SNOW-CYN-143	47	98075	2.3	7.8195	1.1	6.6754	2.2	0.3786	1.8	0.85	2069.6	32.2	2069.4	19.0	2069.1	20.2	2069.1	20.2	100.0	0.0
SNOW-CYN-174	79	110194	1.4	7.8145	0.4	6.7721	1.9	0.3838	1.9	0.98	2094.1	33.2	2082.1	16.8	2070.2	6.7	2070.2	6.7	101.2	-1.2
SNOW-CYN-168	48	41454	1.8	7.8088	0.8	6.5249	2.3	0.3695	2.2	0.94	2027.2	37.8	2049.3	20.3	2071.5	13.8	2071.5	13.8	97.9	2.1
SNOW-CYN-133	100	157286	1.9	7.8081	0.4	6.5668	0.8	0.3719	0.7	0.86	2038.2	11.6	2054.9	6.8	2071.7	6.9	2071.7	6.9	98.4	1.6
SNOW-CYN-136	72	125174	1.5	7.7845	0.7	6.6245	1.5	0.3740	1.3	0.89	2048.3	23.1	2062.6	13.1	2077.0	12.0	2077.0	12.0	98.6	1.4
SNOW-CYN-159	44	23361	0.4	7.7819	1.0	6.7898	1.8	0.3832	1.5	0.84	2091.3	26.3	2084.4	15.5	2077.6	16.8	2077.6	16.8	100.7	-0.7
SNOW-CYN-79	38	40014	0.9	7.7792	1.1	6.7149	1.7	0.3789	1.3	0.76	2070.9	23.5	2074.6	15.4	2078.2	20.0	2078.2	20.0	99.7	0.3
SNOW-CYN-35	36	96347	1.0	7.7782	1.0	6.5640	1.3	0.3703	0.8	0.64	2030.8	14.1	2054.5	11.2	2078.4	17.2	2078.4	17.2	97.7	2.3
SNOW-CYN-90	48	137843	1.7	7.7692	0.6	6.6163	1.0	0.3728	0.8	0.81	2042.6	14.3	2061.5	8.9	2080.4	10.3	2080.4	10.3	98.2	1.8
SNOW-CYN-47	36	46409	1.2	7.7680	0.9	6.8556	1.9	0.3862	1.6	0.87	2105.4	29.1	2092.9	16.5	2080.7	16.3	2080.7	16.3	101.2	-1.2
SNOW-CYN-28	114	109106	1.9	7.7640	0.3	6.3333	3.4	0.3566	3.4	1.00	1966.2	57.7	2023.1	30.0	2081.6	5.6	2081.6	5.6	94.5	5.5
SNOW-CYN-148	55	100102	1.1	7.7586	0.8	6.8005	1.3	0.3827	1.0	0.78	2088.8	17.7	2085.8	11.3	2082.9	14.0	2082.9	14.0	100.3	-0.3
SNOW-CYN-40	85	56626	1.3	7.7557	0.6	6.5800	1.0	0.3701	0.8	0.81	2030.0	13.9	2056.7	8.6	2083.5	10.1	2083.5	10.1	97.4	2.6
SNOW-CYN-37	17	27848	0.8	7.7555	1.7	6.6059	2.3	0.3716	1.5	0.66	2036.8	26.4	2060.1	20.2	2083.6	30.2	2083.6	30.2	97.8	2.2
SNOW-CYN-39	327	296998	1.7	7.7505	0.1	6.6438	0.8	0.3735	0.8	0.99	2045.7	13.3	2065.2	6.7	2084.7	1.3	2084.7	1.3	98.1	1.9
SNOW-CYN-59	47	66031	1.0	7.7478	0.8	6.7059	1.1	0.3768	0.7	0.62	2061.4	11.8	2073.4	9.5	2085.3	14.7	2085.3	14.7	98.9	1.1
SNOW-CYN-194	41	23020	1.6	7.7450	0.9	6.7494	1.4	0.3791	1.0	0.74	2072.2	18.3	2079.1	12.4	2085.9	16.7	2085.9	16.7	99.3	0.7
SNOW-CYN-146	48	83544	1.8	7.7395	0.6	6.7863	1.9	0.3809	1.8	0.95	2080.6	31.6	2083.9	16.6	2087.2	10.4	2087.2	10.4	99.7	0.3
SNOW-CYN-140	74	83165	1.1	7.7327	0.4	6.4127	2.3	0.3596	2.3	0.98	1980.5	39.3	2034.0	20.6	2088.8	7.4	2088.8	7.4	94.8	5.2
SNOW-CYN-115	68	54519	1.1	7.7280	0.5	6.7785	1.1	0.3799	1.0	0.90	2075.9	16.9	2082.9	9.3	2089.8	8.1	2089.8	8.1	99.3	0.7
SNOW-CYN-88	138	143188	1.2	7.4955	0.2	7.1449	0.7	0.3884	0.6	0.95	2115.5	11.5	2129.7	6.0	2143.4	3.8	2143.4	3.8	98.7	1.3

U-Pb geochronologic anlayses of selected Roberts Mountains allochthon strata

					Isotope ratios						Apparent ages (Ma)								
	U	206Pb	U/Th	206Pb*	±	207Pb*	±	206Pb*	±	error	206Pb*	±	207Pb*	±	206Pb*	±	Best age	±	Conc.	Discord.
	(ppm)	204Pb		207Pb*	(%)	235U*	(%)	238U	(%)	corr.	238U*	(Ma)	235U	(Ma)	207Pb*	(Ma)	(Ma)	(Ma)	(%)	(%)
Sample: Snow Canyon Formation. Location: Snow Canyon, Independence Mountains; 0579760 4585698 (NAD 83 UTM 11T)																				
SNOW-CYN-187	22	6820	1.0	7.3431	1.4	7.4295	3.0	0.3957	2.6	0.88	2149.1	48.3	2164.5	26.9	2179.2	25.0	2179.2	25.0	98.6	1.4
SNOW-CYN-33	78	97913	1.0	7.3383	0.6	7.4187	2.1	0.3948	2.0	0.96	2145.2	37.1	2163.2	18.9	2180.3	9.8	2180.3	9.8	98.4	1.6
SNOW-CYN-50	48	44805	1.3	6.9949	0.5	8.2642	1.2	0.4193	1.1	0.91	2257.1	21.3	2260.4	11.2	2263.4	9.0	2263.4	9.0	99.7	0.3
SNOW-CYN-100	22	50899	1.4	6.8541	1.0	8.4369	2.5	0.4194	2.3	0.92	2257.8	43.6	2279.2	22.6	2298.4	16.6	2298.4	16.6	98.2	1.8
SNOW-CYN-177	52	61826	0.8	6.2895	0.4	10.1238	1.6	0.4618	1.5	0.97	2447.5	30.8	2446.1	14.4	2445.0	6.4	2445.0	6.4	100.1	-0.1
SNOW-CYN-69	56	63570	1.6	6.0064	0.3	11.0800	0.9	0.4827	0.9	0.93	2538.9	18.3	2529.9	8.7	2522.6	5.6	2522.6	5.6	100.6	-0.6
SNOW-CYN-46	276	284199	1.9	6.0006	0.6	11.0102	1.7	0.4792	1.6	0.94	2523.6	33.4	2524.0	15.8	2524.3	9.8	2524.3	9.8	100.0	0.0
SNOW-CYN-4	137	142690	1.1	5.9847	0.4	9.6794	4.6	0.4201	4.5	1.00	2261.1	86.7	2404.7	42.0	2528.7	6.3	2528.7	6.3	89.4	10.6
SNOW-CYN-6	32	61997	1.3	5.9371	0.3	11.3035	1.3	0.4867	1.2	0.96	2556.5	25.9	2548.5	11.9	2542.1	5.8	2542.1	5.8	100.6	-0.6
SNOW-CYN-96	65	69104	1.3	5.8166	0.4	11.5934	1.1	0.4891	1.0	0.94	2566.7	22.2	2572.1	10.5	2576.4	6.6	2576.4	6.6	99.6	0.4
SNOW-CYN-124	31	54605	1.4	5.8076	0.5	11.3933	1.2	0.4799	1.1	0.93	2526.8	23.6	2555.9	11.4	2579.0	7.7	2579.0	7.7	98.0	2.0
SNOW-CYN-178	42	11830	0.6	5.6477	0.8	11.9939	3.0	0.4913	2.9	0.96	2576.2	61.4	2603.9	28.1	2625.5	13.2	2625.5	13.2	98.1	1.9
SNOW-CYN-21	31	94305	1.2	5.6435	0.7	11.0815	1.6	0.4536	1.5	0.91	2411.1	29.7	2530.0	15.1	2626.8	11.0	2626.8	11.0	91.8	8.2
SNOW-CYN-72	101	95097	1.4	5.5658	0.3	12.2453	0.8	0.4943	0.8	0.92	2589.3	16.0	2623.4	7.7	2649.8	5.4	2649.8	5.4	97.7	2.3
SNOW-CYN-134	63	87523	0.6	5.5329	0.4	12.5376	1.3	0.5031	1.3	0.95	2627.2	27.5	2645.6	12.7	2659.6	7.2	2659.6	7.2	98.8	1.2
SNOW-CYN-54	101	158945	0.9	5.5320	0.1	12.5754	1.3	0.5045	1.3	1.00	2633.3	27.8	2648.4	12.2	2659.9	2.0	2659.9	2.0	99.0	1.0
SNOW-CYN-114	127	179368	1.8	5.4575	0.4	12.8436	1.8	0.5084	1.7	0.98	2649.6	37.4	2668.2	16.6	2682.4	6.3	2682.4	6.3	98.8	1.2
SNOW-CYN-156	27	49994	0.6	5.4306	0.9	13.0700	1.5	0.5148	1.2	0.78	2677.0	25.8	2684.7	14.2	2690.5	15.5	2690.5	15.5	99.5	0.5
SNOW-CYN-86	25	36023	1.2	5.4221	1.0	12.9442	1.3	0.5090	0.8	0.65	2652.5	17.8	2675.6	11.9	2693.1	15.9	2693.1	15.9	98.5	1.5
SNOW-CYN-25	115	205883	2.4	5.4168	0.2	13.2727	1.3	0.5214	1.3	0.99	2705.2	28.7	2699.2	12.4	2694.7	3.1	2694.7	3.1	100.4	-0.4
SNOW-CYN-65	57	55824	0.7	5.4016	0.5	13.2284	1.6	0.5182	1.6	0.96	2691.7	34.3	2696.1	15.4	2699.4	7.9	2699.4	7.9	99.7	0.3
SNOW-CYN-154	160	212749	1.7	5.3971	0.2	13.4276	1.0	0.5256	1.0	0.98	2722.9	21.9	2710.2	9.5	2700.7	3.4	2700.7	3.4	100.8	-0.8
SNOW-CYN-127	67	106148	0.4	5.3965	0.3	12.9554	1.0	0.5071	0.9	0.95	2644.1	20.0	2676.4	9.1	2700.9	5.0	2700.9	5.0	97.9	2.1
SNOW-CYN-104	91	192420	1.0	5.3937	0.2	13.6249	2.4	0.5330	2.4	1.00	2754.0	52.8	2724.0	22.4	2701.8	3.9	2701.8	3.9	101.9	-1.9
SNOW-CYN-13	116	242807	1.2	5.3870	0.2	13.3988	1.3	0.5235	1.3	0.99	2714.0	27.8	2708.2	12.0	2703.8	3.4	2703.8	3.4	100.4	-0.4
SNOW-CYN-41	58	98319	0.4	5.3824	0.4	13.2352	1.0	0.5167	0.9	0.89	2685.0	18.7	2696.6	9.1	2705.2	7.3	2705.2	7.3	99.3	0.7
SNOW-CYN-95	122	200709	0.4	5.3772	0.2	13.0938	1.1	0.5106	1.0	0.99	2659.4	22.7	2686.4	9.9	2706.8	2.5	2706.8	2.5	98.2	1.8
SNOW-CYN-112	22	31369	0.6	5.3767	0.7	13.3170	1.9	0.5193	1.8	0.93	2696.2	40.1	2702.4	18.4	2707.0	11.5	2707.0	11.5	99.6	0.4
SNOW-CYN-3	134	267317	1.1	5.3708	0.2	13.5939	1.2	0.5295	1.2	0.99	2739.4	27.2	2721.8	11.7	2708.8	3.0	2708.8	3.0	101.1	-1.1
SNOW-CYN-165	69	52575	0.7	5.3288	0.2	13.6884	1.9	0.5290	1.9	1.00	2737.4	42.3	2728.4	18.0	2721.7	2.7	2721.7	2.7	100.6	-0.6
SNOW-CYN-34	67	77982	0.9	5.3074	0.2	13.5090	0.8	0.5200	0.7	0.96	2699.2	15.8	2715.9	7.1	2728.4	3.7	2728.4	3.7	98.9	1.1
SNOW-CYN-192	85	137048	1.0	5.2992	0.3	13.7156	0.9	0.5271	0.9	0.95	2729.4	20.0	2730.3	8.9	2730.9	4.7	2730.9	4.7	99.9	0.1
SNOW-CYN-26	203	367278	0.8	5.2736	0.1	13.8384	0.5	0.5293	0.5	0.96	2738.5	10.2	2738.7	4.5	2738.9	2.3	2738.9	2.3	100.0	0.0
SNOW-CYN-152	50	103476	0.6	5.2493	0.4	14.0412	2.0	0.5346	2.0	0.98	2760.7	44.7	2752.5	19.4	2746.5	7.4	2746.5	7.4	100.5	-0.5
SNOW-CYN-23	34	83229	1.2	4.9896	0.5	15.1884	3.0	0.5496	2.9	0.98	2823.6	67.0	2827.1	28.4	2829.6	8.8	2829.6	8.8	99.8	0.2
SNOW-CYN-123	63	216756	1.3	4.9483	0.3	15.2936	0.8	0.5489	0.8	0.92	2820.5	17.2	2833.7	7.8	2843.1	5.1	2843.1	5.1	99.2	0.8
SNOW-CYN-157	85	109893	60.7	4.9314	0.2	15.7985	1.0	0.5651	0.9	0.97	2887.5	21.7	2864.7	9.1	2848.7	3.7	2848.7	3.7	101.4	-1.4
SNOW-CYN-128	33	44308	0.7	4.9293	0.2	15.0765	0.7	0.5390	0.6	0.95	2779.2	14.0	2820.1	6.2	2849.4	3.5	2849.4	3.5	97.5	2.5
SNOW-CYN-183	48	296306	1.3	3.2593	0.2	30.3488	1.4	0.7174	1.4	0.99	3486.4	36.6	3498.2	13.6	3504.9	3.4	3504.9	3.4	99.5	0.5
Sample: McAfee Quartzite. Location:McAfee Creek, Independence Mountains; 0590637 4599583 (NAD 83 UTM 11T)																				
McAfee-97SF1-70	148	54632	1.8	13.6151	1.3	1.7270	1.8	0.1705	1.2	0.66	1015.1	11.1	1018.6	11.5	1026.3	26.9	1026.3	26.9	98.9	1.1
McAfee-97SF1-8	365	133119	1.1	13.5575	0.4	1.7968	0.6	0.1767	0.4	0.66	1048.8	3.7	1044.3	3.8	1034.9	8.7	1034.9	8.7	101.3	-1.3
McAfee-97SF1-22	256	49041	1.2	13.5242	0.9	1.7693	1.3	0.1735	1.0	0.76	1031.6	9.4	1034.2	8.4	1039.8	17.2	1039.8	17.2	99.2	0.8
McAfee-97SF1-123	22	18308	0.7	9.4113	3.4	4.6400	3.8	0.3167	1.8	0.46	1773.6	27.3	1756.5	32.0	1736.1	62.3	1736.1	62.3	102.2	-2.2
McAfee-97SF1-196	100	55987	14.5	9.0724	0.6	4.8917	0.9	0.3219	0.7	0.74	1798.9	10.7	1800.8	7.7	1803.1	11.2	1803.1	11.2	99.8	0.2
McAfee-97SF1-118	125	79313	1.6	9.0669	0.4	5.0574	0.6	0.3326	0.5	0.80	1850.8	8.3	1829.0	5.5	1804.2	7.1	1804.2	7.1	102.6	-2.6
McAfee-97SF1-39	26	16134	0.4	9.0410	1.6	5.2194	2.3	0.3422	1.6	0.72	1897.4	26.7	1855.8	19.2	1809.4	28.4	1809.4	28.4	104.9	-4.9
McAfee-97SF1-132	39	20055	1.5	9.0232	1.7	5.1813	2.1	0.3391	1.2	0.56	1882.2	19.1	1849.5	17.9	1813.0	31.7	1813.0	31.7	103.8	-3.8
McAfee-97SF1-138	60	28368	0.8	9.0139	1.8	5.0199	3.3	0.3282	2.7	0.84	1829.5	43.6	1822.7	27.6	1814.8	32.4	1814.8	32.4	100.8	-0.8
McAfee-97SF1-105	41	18612	0.9	8.9972	1.6	5.1451	2.5	0.3357	2.0	0.78	1866.1	31.9	1843.6	21.5	1818.2	28.6	1818.2	28.6	102.6	-2.6
McAfee-97SF1-37	55	26707	0.4	8.9772	1.3	5.1850	2.0	0.3376	1.4	0.73	1875.1	23.3	1850.2	16.7	1822.3	24.2	1822.3	24.2	102.9	-2.9
McAfee-97SF1-88	47	19442	1.3	8.9765	1.4	5.0823	1.6	0.3309	0.9	0.54	1842.6	14.0	1833.1	13.8	1822.4	24.9	1822.4	24.9	101.1	-1.1
McAfee-97SF1-69	38	26642	0.6	8.9759	1.5	5.0202	2.0	0.3268	1.2	0.63	1822.9	19.6	1822.7	16.6	1822.5	27.7	1822.5	27.7	100.0	0.0
McAfee-97SF1-55	40	25808	0.6	8.9653	0.9	5.1478	1.3	0.3347	1.0	0.75	1861.2	15.7	1844.0	11.0	1824.7	15.7	1824.7	15.7	102.0	-2.0
McAfee-97SF1-67	193	230751	1.8	8.9651	0.4	5.0628	0.8	0.3292	0.7	0.84	1834.5	10.4	1829.9	6.6	1824.7	7.6	1824.7	7.6	100.5	-0.5
McAfee-97SF1-46	77	24989	1.1	8.9645	0.7	5.1457	1.1	0.3346	0.9	0.78	1860.4	14.0	1843.7	9.5	1824.8	12.7	1824.8	12.7	102.0	-2.0
McAfee-97SF1-73	46	32729	1.5	8.9609	1.1	4.9831	1.6	0.3239	1.1	0.72	1808.5	17.9	1816.5	13.4	1825.6	20.1	1825.6	20.1	99.1	0.9
McAfee-97SF1-59	51	29910	1.1	8.9555	1.0	5.1569	1.5	0.3349	1.0	0.70	1862.3	16.6	1845.5	12.4	1826.7	18.9	1826.7	18.9	102.0	-2.0
McAfee-97SF1-48	104	44482	1.4	8.9519	0.5	5.2185	0.7	0.3388	0.4	0.61	1881.0	6.7	1855.6	5.7	1827.4	9.6	1827.4	9.6	102.9	-2.9
McAfee-97SF1-57	82	32122	0.6	8.9452	1.1	5.1135	1.4	0.3317	0.9	0.64	1846.8	14.4	1838.4	11.9	1828.7	19.6	1828.7	19.6	101.0	-1.0
McAfee-97SF1-24	160	77284	1.0	8.9366	0.4	5.0418	0.8	0.3268	0.7	0.88	1822.8	11.3	1826.4	6.9	1830.5	7.1	1830.5	7.1	99.6	0.4
McAfee-97SF1-72	54	60708	1.0	8.9356	0.9	5.0992	1.2	0.3305	0.8	0.69	1840.6	13.5	1836.0	10.3	1830.7	15.8	1830.7	15.8	100.5	-0.5
McAfee-97SF1-34	52	52211	1.0	8.9343	1.3	5.2120	1.6	0.3377	1.0	0.61	1875.7	16.3	1854.6	14.0	1831.0	23.5	1831.0	23.5	102.4	-2.4
McAfee-97SF1-81	59	25202	1.0	8.9306	1.5	5.1926	2.0	0.3363	1.3	0.64	1869.0	20.9	1851.4	17.1	1831.7	27.8	1831.7	27.8	102.0	-2.0
McAfee-97SF1-167	35	19921	0.9	8.9280	1.5	5.1622	1.7	0.3343	0.8	0.45	1859.0	12.4	1846.4	14.5	1832.2	27.7	1832.2	27.7	101.5	-1.5
McAfee-97SF1-32	179	83322	1.8	8.9265	0.3	5.1293	0.5	0.3321	0.4	0.82	1848.4	7.1	1841.0	4.6	1832.5	5.5	1832.5	5.5	100.9	-0.9
McAfee-97SF1-60	124	92284	1.2	8.9247	0.6	5.1803	1.2	0.3353	1.1	0.89	1864.1	17.3	1849.4	10.2	1832.9	10.1	1832.9	10.1	101.7	-1.7
McAfee-97SF1-63	104	85678	0.8	8.9200	0.7	5.1371	1.0	0.3323	0.7	0.72	1849.7	11.6	1842.3	8.6	1833.8	12.7	1833.8	12.7	100.9	-0.9
McAfee-97SF1-29	73	60341	1.3	8.9199	1.1	5.1561	1.5	0.3336	1.1	0.70	1855.6	17.2	1845.4	13.0	1833.9	19.8	1833.9	19.8	101.2	-1.2
McAfee-97SF1-99	69	49911	1.2	8.9163	0.8	5.1807	1.3	0.3350	1.1	0.81	1862.7	17.2	1849.4	11.2	1834.6	14.0	1834.6	14.0	101.5	-1.5
McAfee-97SF1-182	40	18121	1.0	8.9152	1.2	5.1575	1.4	0.3335	0.7	0.54	1855.2	12.0	1845.6	11.8	1834.8	21.2	1834.8	21.2	101.1	-1.1
McAfee-97SF1-165	52	38529	1.1	8.9141	1.3	5.1820	1.5	0.3350	0.8	0.52	1862.7	12.3	1849.7	12.5	1835.0	22.8	1835.0	22.8	101.5	-1.5
McAfee-97SF1-4	81	40878	2.1	8.9140	0.7	5.1712	1.7	0.3343	1.5	0.91	1859.3	24.9	1847.9	14.4	1835.1	12.8	1835.1	12.8	101.3	-1.3
McAfee-97SF1-199	49	53281	0.3	8.9138	1.2	5.2136	2.2	0.3371	1.8	0.84	1872.5	30.0	1854.8	18.6	1835.1	21.2	1835.1	21.2	102.0	-2.0
McAfee-97SF1-42	112	125173	1.6	8.9110	0.4	5.1226	0.8	0.3311	0.6	0.84	1843.6	10.3	1839.9	6.5	1835.7	7.5	1835.7	7.5	100.4	-0.4
McAfee-97SF1-141	83	41362	0.9	8.9033	0.6	5.1451	0.8	0.3322	0.6	0.71	1849.2	9.1	1843.6	6.8	1837.2	10.2	1837.2	10.2	100.7	-0.7
McAfee-97SF1-1	77	40488	1.4	8.9022	0.6	5.1027	0.9	0.3295	0.7	0.76	1835.7	10.8	1836.5	7.6	1837.5	10.5	1837.5	10.5	99.9	0.1
McAfee-97SF1-56	101	42070	2.0	8.9022	0.9	5.2329	1.7	0.3379	1.4	0.85	1876.4	23.2	1858.0	14.3	1837.5	16.0	1837.5	16.0	102.1	-2.1
McAfee-97SF1-171	65	7463	0.9	8.9011	1.0	5.1056	1.6	0.3296	1.3	0.79	1836.4	20.4	1837.0	13.7	1837.7	17.8	1837.7	17.8	99.9	0.1
McAfee-97SF1-10	97	75222	1.1	8.9003	0.5	5.1321	0.8	0.3313	0.6	0.79	1844.6	10.3	1841.4	6.9	1837.9	9.1	1837.9	9.1	100.4	-0.4
McAfee-97SF1-23	38	19317	1.2	8.8978	1.7	5.1908	2.5	0.3350	1.9	0.73	1862.5	30.2	1851.1	21.7	1838.4	31.3	1838.4	31.3	101.3	-1.3
McAfee-97SF1-147	128	89745	1.3	8.8964	0.5	5.2104	0.8	0.3362	0.7	0.81	1868.3	10.9	1854.3	7.0	1838.6	8.7	1838.6	8.7	101.6	-1.6
McAfee-97SF1-194	70	47880	1.1	8.8946	0.9	5.1989	1.2	0.3354	0.9	0.70	1864.4	13.8	1852.4	10.3	1839.0	15.6	1839.0	15.6	101.4	-1.4

1.0, 0.8

U-Pb geochronologic anlayses of selected Roberts Mountains allochthon strata

						Isotope ratios							Apparent ages (Ma)							
	U	206Pb	U/Th	206Pb*	±	207Pb*	±	206Pb*	±	error	206Pb*	±	207Pb*	±	206Pb*	±	Best age	±	Conc.	Discord.
	(ppm)	204Pb		207Pb*	(%)	235U*	(%)	238U	(%)	corr.	238U*	(Ma)	235U	(Ma)	207Pb*	(Ma)	(Ma)	(Ma)	(%)	(%)
Sample: McAfee Quartzite. Location:McAfee Creek, Independence Mountains; 0590637 4599583 (NAD 83 UTM 11T)																				
McAfee-97SF1-87	112	85370	0.9	8.8939	0.6	5.1227	1.4	0.3304	1.3	0.89	1840.5	20.5	1839.9	12.2	1839.1	11.7	1839.1	11.7	100.1	-0.1
McAfee-97SF1-26	64	47470	0.8	8.8926	1.3	5.1972	2.6	0.3352	2.2	0.85	1863.5	35.7	1852.2	22.0	1839.4	24.3	1839.4	24.3	101.3	-1.3
McAfee-97SF1-127	31	28519	0.6	8.8922	1.4	5.3107	1.6	0.3425	0.7	0.45	1898.7	11.7	1870.6	13.6	1839.5	25.8	1839.5	25.8	103.2	-3.2
McAfee-97SF1-104	41	39172	0.6	8.8915	1.2	5.3890	2.7	0.3475	2.4	0.90	1922.7	39.7	1883.1	22.8	1839.6	21.4	1839.6	21.4	104.5	-4.5
McAfee-97SF1-180	58	47141	1.0	8.8888	0.9	5.1972	1.1	0.3350	0.6	0.53	1862.8	9.0	1852.2	9.0	1840.2	16.3	1840.2	16.3	101.2	-1.2
McAfee-97SF1-54	58	68284	1.0	8.8887	1.2	5.1392	1.4	0.3313	0.7	0.49	1844.7	10.8	1842.6	11.7	1840.2	21.7	1840.2	21.7	100.2	-0.2
McAfee-97SF1-80	54	24511	0.9	8.8875	0.8	5.2569	1.5	0.3389	1.2	0.82	1881.1	19.7	1861.9	12.5	1840.5	15.1	1840.5	15.1	102.2	-2.2
McAfee-97SF1-191	221	112477	1.4	8.8869	0.3	5.2600	0.5	0.3390	0.4	0.83	1882.0	7.0	1862.4	4.4	1840.6	5.1	1840.6	5.1	102.3	-2.3
McAfee-97SF1-140	143	92852	1.1	8.8855	0.9	5.3309	1.0	0.3435	0.6	0.56	1903.7	9.7	1873.8	8.9	1840.9	15.7	1840.9	15.7	103.4	-3.4
McAfee-97SF1-151	70	37149	0.9	8.8840	1.0	5.1835	1.3	0.3340	0.8	0.61	1857.7	12.6	1849.9	11.0	1841.2	18.5	1841.2	18.5	100.9	-0.9
McAfee-97SF1-130	82	30133	0.9	8.8816	0.7	5.1574	1.0	0.3322	0.7	0.71	1849.1	11.4	1845.6	8.5	1841.7	12.7	1841.7	12.7	100.4	-0.4
McAfee-97SF1-152	208	172847	1.4	8.8792	0.3	5.2894	0.6	0.3406	0.5	0.88	1889.7	8.7	1867.1	5.2	1842.1	5.3	1842.1	5.3	102.6	-2.6
McAfee-97SF1-65	112	62750	0.9	8.8774	0.5	5.2189	1.3	0.3360	1.2	0.92	1867.5	19.3	1855.7	11.0	1842.5	9.3	1842.5	9.3	101.4	-1.4
McAfee-97SF1-30	64	45044	0.9	8.8749	1.0	5.3672	1.5	0.3455	1.1	0.73	1912.9	17.7	1879.6	12.6	1843.0	18.2	1843.0	18.2	103.8	-3.8
McAfee-97SF1-129	106	109727	0.9	8.8734	0.5	5.2001	1.6	0.3347	1.5	0.94	1860.9	23.8	1852.6	13.3	1843.3	9.3	1843.3	9.3	101.0	-1.0
McAfee-97SF1-41	32	15171	0.8	8.8724	1.5	5.1290	1.7	0.3300	0.8	0.46	1838.6	12.6	1840.9	14.5	1843.5	27.5	1843.5	27.5	99.7	0.3
McAfee-97SF1-142	56	33815	1.0	8.8717	1.2	5.2151	2.2	0.3356	1.8	0.83	1865.3	29.9	1855.1	19.0	1843.7	22.5	1843.7	22.5	101.2	-1.2
McAfee-97SF1-2	48	36525	1.0	8.8696	1.5	5.2986	2.8	0.3408	2.3	0.84	1890.8	38.3	1868.6	23.7	1844.1	27.2	1844.1	27.2	102.5	-2.5
McAfee-97SF1-181	71	47991	1.2	8.8685	0.6	5.2031	0.8	0.3347	0.6	0.73	1860.9	9.9	1853.1	7.2	1844.3	10.4	1844.3	10.4	100.9	-0.9
McAfee-97SF1-95	43	24711	1.5	8.8684	1.2	5.2165	1.4	0.3355	0.7	0.52	1865.1	11.8	1855.3	11.9	1844.4	21.5	1844.4	21.5	101.1	-1.1
McAfee-97SF1-76	23	18357	0.5	8.8658	1.6	5.1964	2.9	0.3341	2.4	0.83	1858.4	39.1	1852.0	24.9	1844.9	29.8	1844.9	29.8	100.7	-0.7
McAfee-97SF1-85	46	33107	1.0	8.8658	1.4	5.1648	1.9	0.3321	1.3	0.66	1848.5	20.3	1846.8	16.3	1844.9	26.2	1844.9	26.2	100.2	-0.2
McAfee-97SF1-9	41	29173	0.8	8.8614	1.3	5.1313	1.8	0.3298	1.2	0.69	1837.3	19.5	1841.3	15.0	1845.8	23.1	1845.8	23.1	99.5	0.5
McAfee-97SF1-7	147	73596	1.8	8.8605	0.5	5.2193	0.6	0.3354	0.4	0.60	1864.5	5.9	1855.8	5.1	1846.0	8.7	1846.0	8.7	101.0	-1.0
McAfee-97SF1-75	55	45823	0.7	8.8590	1.0	5.1183	1.2	0.3289	0.7	0.61	1832.9	11.8	1839.2	10.3	1846.3	17.4	1846.3	17.4	99.3	0.7
McAfee-97SF1-21	29	38684	0.8	8.8559	1.6	5.1432	2.1	0.3303	1.3	0.63	1840.0	21.0	1843.3	17.8	1846.9	29.5	1846.9	29.5	99.6	0.4
McAfee-97SF1-15	141	135061	0.9	8.8552	0.4	5.2298	0.8	0.3359	0.7	0.86	1866.8	11.5	1857.5	7.0	1847.0	7.6	1847.0	7.6	101.1	-1.1
McAfee-97SF1-119	31	25016	0.8	8.8529	1.4	5.1270	1.5	0.3292	0.6	0.37	1834.5	9.0	1840.6	12.9	1847.5	25.4	1847.5	25.4	99.3	0.7
McAfee-97SF1-185	172	119121	1.4	8.8499	0.5	5.3336	0.6	0.3423	0.4	0.64	1897.9	6.5	1874.3	5.3	1848.1	8.5	1848.1	8.5	102.7	-2.7
McAfee-97SF1-179	148	175958	1.4	8.8479	0.4	5.2897	1.0	0.3394	1.0	0.94	1884.0	15.8	1867.2	8.8	1848.5	6.4	1848.5	6.4	101.9	-1.9
McAfee-97SF1-149	69	48868	0.8	8.8473	0.7	5.2416	1.3	0.3363	1.0	0.83	1869.0	17.0	1859.4	10.7	1848.7	12.6	1848.7	12.6	101.1	-1.1
McAfee-97SF1-170	350	260291	2.6	8.8434	0.2	5.3104	0.7	0.3406	0.7	0.95	1889.5	11.6	1870.5	6.4	1849.5	4.1	1849.5	4.1	102.2	-2.2
McAfee-97SF1-158	130	52699	0.7	8.8409	0.3	5.3466	0.6	0.3428	0.6	0.90	1900.3	9.2	1876.4	5.3	1850.0	4.9	1850.0	4.9	102.7	-2.7
McAfee-97SF1-121	95	17877	0.5	8.8303	0.6	5.2411	0.7	0.3357	0.4	0.57	1865.7	6.9	1859.3	6.4	1852.1	11.1	1852.1	11.1	100.7	-0.7
McAfee-97SF1-101	58	27385	0.9	8.8271	1.0	5.3236	2.3	0.3408	2.1	0.91	1890.6	34.7	1872.7	19.9	1852.8	17.2	1852.8	17.2	102.0	-2.0
McAfee-97SF1-114	122	65540	1.4	8.8252	0.8	5.2906	1.0	0.3386	0.7	0.63	1880.1	10.7	1867.3	8.9	1853.2	14.7	1853.2	14.7	101.5	-1.5
McAfee-97SF1-31	37	11541	1.0	8.8242	3.3	5.1687	3.4	0.3308	0.8	0.24	1842.2	13.1	1847.5	29.0	1853.4	59.7	1853.4	59.7	99.4	0.6
McAfee-97SF1-43	62	41289	0.8	8.8219	0.8	5.2456	1.1	0.3356	0.8	0.73	1865.6	13.1	1860.1	9.4	1853.9	13.6	1853.9	13.6	100.6	-0.6
McAfee-97SF1-134	42	50744	0.9	8.8111	1.3	5.2838	1.7	0.3377	1.1	0.65	1875.4	18.5	1866.3	14.9	1856.1	23.9	1856.1	23.9	101.0	-1.0
McAfee-97SF1-174	51	51900	0.6	8.8078	1.4	5.2234	1.7	0.3337	1.0	0.58	1856.2	16.0	1856.4	14.6	1856.7	25.2	1856.7	25.2	100.0	0.0
McAfee-97SF1-156	27	31386	0.7	8.8017	1.9	5.3535	2.1	0.3417	0.9	0.44	1895.1	14.8	1877.5	17.7	1858.0	33.5	1858.0	33.5	102.0	-2.0
McAfee-97SF1-11	42	55871	1.1	8.7904	1.0	5.1715	1.5	0.3297	1.1	0.73	1836.9	17.0	1847.9	12.4	1860.3	18.0	1860.3	18.0	98.7	1.3
McAfee-97SF1-97	58	9808	1.0	8.7848	2.4	5.1379	2.5	0.3274	0.5	0.22	1825.5	8.6	1842.4	21.2	1861.5	44.0	1861.5	44.0	98.1	1.9
McAfee-97SF1-148	133	60532	0.9	8.7816	0.4	5.3854	0.9	0.3430	0.8	0.88	1901.1	12.4	1882.5	7.4	1862.1	7.5	1862.1	7.5	102.1	-2.1
McAfee-97SF1-186	167	76118	0.5	8.7801	0.4	5.2625	0.8	0.3351	0.7	0.85	1863.1	11.0	1862.8	6.8	1862.4	7.7	1862.4	7.7	100.0	0.0
McAfee-97SF1-188	209	102704	2.1	8.7798	0.2	5.2888	1.3	0.3368	1.3	0.99	1871.1	21.1	1867.1	11.2	1862.5	3.6	1862.5	3.6	100.5	-0.5
McAfee-97SF1-135	71	27589	2.7	8.7796	0.9	5.4060	1.3	0.3442	0.9	0.74	1907.0	15.6	1885.8	10.9	1862.5	15.5	1862.5	15.5	102.4	-2.4
McAfee-97SF1-198	70	28156	1.8	8.7636	0.8	5.3948	1.0	0.3429	0.7	0.65	1900.6	11.0	1884.0	8.8	1865.8	14.1	1865.8	14.1	101.9	-1.9
McAfee-97SF1-74	138	29020	1.4	8.7609	1.3	5.1648	1.5	0.3282	0.8	0.51	1829.5	12.4	1846.8	12.9	1866.4	23.5	1866.4	23.5	98.0	2.0
McAfee-97SF1-68	130	27610	7.9	8.7590	0.5	5.3800	0.9	0.3418	0.8	0.82	1895.2	12.4	1881.7	7.9	1866.8	9.6	1866.8	9.6	101.5	-1.5
McAfee-97SF1-173	78	94259	0.9	8.7368	0.8	5.3305	1.1	0.3378	0.7	0.66	1875.9	11.4	1873.8	9.1	1871.3	14.4	1871.3	14.4	100.2	-0.2
McAfee-97SF1-168	23	13340	0.6	8.7152	2.7	5.5348	2.9	0.3498	1.1	0.38	1933.9	18.7	1906.0	25.0	1875.8	48.5	1875.8	48.5	103.1	-3.1
McAfee-97SF1-200	58	6394	1.6	8.7032	3.5	5.1737	3.6	0.3266	0.9	0.25	1821.8	14.1	1848.3	30.6	1878.3	62.8	1878.3	62.8	97.0	3.0
McAfee-97SF1-84	288	215283	2.2	8.6776	0.2	5.5389	1.4	0.3486	1.4	0.99	1927.9	23.5	1906.7	12.2	1883.6	3.1	1883.6	3.1	102.3	-2.3
McAfee-97SF1-82	51	46336	0.5	8.6595	1.0	5.6460	1.8	0.3546	1.5	0.84	1956.5	25.1	1923.2	15.2	1887.4	17.1	1887.4	17.1	103.7	-3.7
McAfee-97SF1-137	81	56270	1.0	8.6204	0.6	5.5716	0.7	0.3483	0.4	0.56	1926.7	6.3	1911.7	5.8	1895.5	10.0	1895.5	10.0	101.6	-1.6
McAfee-97SF1-50	20	15094	0.8	8.6202	2.5	5.4126	2.6	0.3384	0.9	0.36	1878.9	15.4	1886.8	22.6	1895.5	44.3	1895.5	44.3	99.1	0.9
McAfee-97SF1-62	84	63835	0.8	8.6101	0.9	5.6019	1.2	0.3498	0.7	0.60	1933.7	11.7	1916.4	10.1	1897.7	16.8	1897.7	16.8	101.9	-1.9
McAfee-97SF1-133	217	135144	2.3	8.5868	0.3	5.5672	0.4	0.3467	0.3	0.67	1918.9	4.4	1911.0	3.4	1902.5	5.3	1902.5	5.3	100.9	-0.9
McAfee-97SF1-83	130	92765	1.5	8.5802	0.3	5.7164	1.1	0.3557	1.1	0.96	1961.9	18.1	1933.8	9.6	1903.9	5.7	1903.9	5.7	103.0	-3.0
McAfee-97SF1-71	51	15293	0.8	8.5602	1.4	5.5355	1.5	0.3437	0.4	0.30	1904.3	7.2	1906.1	12.5	1908.1	24.9	1908.1	24.9	99.8	0.2
McAfee-97SF1-16	40	19096	0.9	8.5525	0.6	5.5807	1.0	0.3462	0.8	0.77	1916.2	12.8	1913.1	8.6	1909.7	11.3	1909.7	11.3	100.3	-0.3
McAfee-97SF1-64	77	48194	0.9	8.5457	0.9	5.6943	1.1	0.3529	0.7	0.60	1948.6	11.0	1930.5	9.4	1911.2	15.7	1911.2	15.7	102.0	-2.0
McAfee-97SF1-111	152	96908	1.1	8.5447	0.4	5.6370	1.5	0.3493	1.4	0.97	1931.4	23.7	1921.8	12.7	1911.4	6.9	1911.4	6.9	101.0	-1.0
McAfee-97SF1-139	35	39976	0.6	8.5403	1.4	5.6529	1.8	0.3501	1.2	0.66	1935.3	20.3	1924.2	15.9	1912.3	24.9	1912.3	24.9	101.2	-1.2
McAfee-97SF1-197	112	66494	0.8	8.5368	0.5	5.6486	0.7	0.3497	0.5	0.75	1933.3	9.2	1923.6	6.3	1913.0	8.6	1913.0	8.6	101.1	-1.1
McAfee-97SF1-145	62	26251	0.7	8.5281	0.9	5.7204	1.1	0.3538	0.5	0.46	1952.8	8.2	1934.5	9.2	1914.9	16.9	1914.9	16.9	102.0	-2.0
McAfee-97SF1-90	108	65400	2.9	8.5237	0.5	5.6950	0.7	0.3521	0.5	0.74	1944.4	8.9	1930.6	6.2	1915.8	8.7	1915.8	8.7	101.5	-1.5
McAfee-97SF1-36	52	33789	0.5	8.5227	0.9	5.8348	1.7	0.3607	1.4	0.84	1985.3	24.3	1951.6	14.6	1916.0	16.3	1916.0	16.3	103.6	-3.6
McAfee-97SF1-164	35	43119	0.9	8.5208	1.7	5.6507	1.9	0.3492	0.9	0.47	1930.8	15.1	1923.9	16.6	1916.4	30.4	1916.4	30.4	100.8	-0.8
McAfee-97SF1-175	39	19451	0.4	8.5199	0.7	5.6605	1.3	0.3498	1.0	0.81	1933.5	17.0	1925.4	10.8	1916.6	13.0	1916.6	13.0	100.9	-0.9
McAfee-97SF1-12	25	12442	0.4	8.5165	2.6	5.7178	3.0	0.3532	1.5	0.50	1949.7	24.9	1934.1	25.5	1917.3	45.9	1917.3	45.9	101.7	-1.7
McAfee-97SF1-115	38	29072	0.7	8.5136	0.8	5.6029	1.4	0.3460	1.1	0.79	1915.3	17.6	1916.5	11.6	1917.9	14.9	1917.9	14.9	99.9	0.1
McAfee-97SF1-47	111	68543	1.2	8.5132	0.6	5.5935	0.8	0.3454	0.5	0.62	1912.4	8.3	1915.1	6.9	1918.0	11.2	1918.0	11.2	99.7	0.3
McAfee-97SF1-176	56	34747	0.8	8.5127	0.7	5.7570	0.9	0.3554	0.6	0.63	1960.5	10.0	1940.0	8.2	1918.1	13.2	1918.1	13.2	102.2	-2.2
McAfee-97SF1-195	89	109017	1.0	8.5050	0.4	5.7565	0.9	0.3551	0.8	0.90	1958.8	13.1	1939.9	7.5	1919.7	6.9	1919.7	6.9	102.0	-2.0
McAfee-97SF1-13	99	98019	1.4	8.5043	0.7	5.7256	0.9	0.3531	0.6	0.66	1949.6	10.1	1935.2	7.8	1919.9	12.2	1919.9	12.2	101.5	-1.5
McAfee-97SF1-53	208	144709	0.9	8.4968	0.2	5.5126	0.7	0.3397	0.6	0.93	1885.3	9.9	1902.6	5.6	1921.4	4.3	1921.4	4.3	98.1	1.9
McAfee-97SF1-110	27	30132	0.5	8.4966	2.3	5.7107	2.8	0.3519	1.6	0.57	1943.7	26.3	1933.0	23.9	1921.5	40.8	1921.5	40.8	101.2	-1.2
McAfee-97SF1-166	101	32116	1.2	8.4955	0.7	5.6914	0.9	0.3507	0.6	0.67	1937.8	10.1	1930.1	7.8	1921.7	12.0	1921.7	12.0	100.8	-0.8
McAfee-97SF1-91	32	46292	0.6	8.4954	1.0	5.6505	2.4	0.3482	2.2	0.91	1925.8	36.8	1923.8	20.9	1921.7	17.9	1921.7	17.9	100.2	-0.2
McAfee-97SF1-162	46	32452	0.6	8.4746	0.8	5.6264	1.4	0.3458	1.1	0.80	1914.6	18.0	1920.2	11.7	1926.1	14.6	1926.1	14.6	99.4	0.6
McAfee-97SF1-122	70	61040	0.7	8.4719	0.7	5.6365	1.0	0.3463	0.7	0.70	1917.0	11.4	1921.7	8.5	1926.7	12.6	1926.7	12.6	99.5	0.5
McAfee-97SF1-18	248	171512	0.8	8.4709	0.2	5.8558	0.4	0.3598	0.4	0.91	1981.1	6.5	1954.7	3.6	1926.9	3.1	1926.9	3.1	102.8	-2.8

U-Pb geochronologic anlayses of selected Roberts Mountains allochthon strata

						Isotope ratios							Apparent ages (Ma)							
	U	206Pb	U/Th	206Pb*	±	207Pb*	±	206Pb*	±	error	206Pb*	±	207Pb*	±	206Pb*	±	Best age	±	Conc.	Discord.
	(ppm)	204Pb		207Pb*	(%)	235U*	(%)	238U	(%)	corr.	238U*	(Ma)	235U	(Ma)	207Pb*	(Ma)	(Ma)	(Ma)	(%)	(%)
Sample: McAfee Quartzite. Location:McAfee Creek, Independence Mountains; 0590637 4599583 (NAD 83 UTM 11T)																				
McAfee-97SF1-125	172	82627	0.5	8.4678	0.3	5.8646	0.5	0.3602	0.4	0.82	1983.0	7.5	1956.0	4.6	1927.6	5.4	1927.6	5.4	102.9	-2.9
McAfee-97SF1-187	148	81397	0.6	8.4575	0.4	5.6862	0.6	0.3488	0.5	0.76	1928.8	7.6	1929.3	5.2	1929.7	7.0	1929.7	7.0	100.0	0.0
McAfee-97SF1-163	35	26329	1.4	8.4530	1.4	5.8284	2.5	0.3573	2.1	0.84	1969.5	35.7	1950.6	21.8	1930.7	24.5	1930.7	24.5	102.0	-2.0
McAfee-97SF1-100	198	173972	1.1	8.4528	0.4	5.7481	0.9	0.3524	0.8	0.91	1946.0	14.0	1938.6	7.9	1930.8	6.7	1930.8	6.7	100.8	-0.8
McAfee-97SF1-106	214	69591	1.4	8.4463	0.4	5.5636	1.6	0.3408	1.6	0.97	1890.6	26.1	1910.5	14.1	1932.1	6.8	1932.1	6.8	97.8	2.2
McAfee-97SF1-20	32	92931	0.3	8.4431	1.9	5.7755	2.4	0.3537	1.5	0.62	1952.1	25.1	1942.7	20.9	1932.8	34.0	1932.8	34.0	101.0	-1.0
McAfee-97SF1-103	177	90205	1.1	8.4409	0.4	5.8803	1.8	0.3600	1.8	0.98	1982.1	30.2	1958.3	15.7	1933.3	6.3	1933.3	6.3	102.5	-2.5
McAfee-97SF1-172	121	73267	1.9	8.4322	0.4	5.8590	1.0	0.3583	0.9	0.93	1974.2	16.1	1955.2	8.9	1935.1	6.9	1935.1	6.9	102.0	-2.0
McAfee-97SF1-98	47	19878	0.6	8.4262	1.1	5.7621	1.8	0.3521	1.4	0.78	1944.8	23.8	1940.7	15.7	1936.4	20.3	1936.4	20.3	100.4	-0.4
McAfee-97SF1-116	234	162236	1.5	8.4261	0.2	5.7291	0.6	0.3501	0.5	0.94	1935.1	8.9	1935.8	4.9	1936.4	3.3	1936.4	3.3	99.9	0.1
McAfee-97SF1-169	268	102378	1.2	8.4152	0.3	5.8655	0.6	0.3580	0.5	0.86	1972.6	9.0	1956.2	5.3	1938.7	5.6	1938.7	5.6	101.7	-1.7
McAfee-97SF1-155	65	48475	1.1	8.4013	0.7	5.8356	0.9	0.3556	0.6	0.63	1961.1	9.6	1951.7	7.8	1941.7	12.5	1941.7	12.5	101.0	-1.0
McAfee-97SF1-160	207	139323	0.6	8.3877	0.3	5.9517	0.5	0.3621	0.4	0.83	1991.9	7.6	1968.8	4.6	1944.6	5.3	1944.6	5.3	102.4	-2.4
McAfee-97SF1-143	31	20466	0.8	8.3693	1.3	5.8189	1.7	0.3532	1.1	0.66	1949.9	19.3	1949.2	15.1	1948.5	23.5	1948.5	23.5	100.1	-0.1
McAfee-97SF1-150	27	21294	1.1	8.1785	2.4	6.2373	2.6	0.3700	1.1	0.42	2029.3	19.1	2009.7	23.1	1989.6	42.7	1989.6	42.7	102.0	-2.0
McAfee-97SF1-79	166	190358	2.4	8.1658	1.0	6.1503	1.6	0.3642	1.3	0.80	2002.3	22.2	1997.4	14.0	1992.4	17.0	1992.4	17.0	100.5	-0.5
McAfee-97SF1-193	29	12644	1.2	8.1512	1.4	6.2774	1.9	0.3711	1.3	0.68	2034.6	22.5	2015.3	16.6	1995.6	24.5	1995.6	24.5	102.0	-2.0
McAfee-97SF1-190	49	56619	1.0	8.1233	1.1	6.2513	1.7	0.3683	1.4	0.78	2021.4	23.6	2011.7	15.3	2001.7	19.5	2001.7	19.5	101.0	-1.0
McAfee-97SF1-108	37	29947	1.2	8.0755	0.9	6.4587	4.0	0.3783	3.9	0.97	2068.2	69.1	2040.3	35.2	2012.1	16.1	2012.1	16.1	102.8	-2.8
McAfee-97SF1-61	28	21027	0.7	7.8837	1.6	6.7797	3.3	0.3876	2.9	0.88	2111.9	52.2	2083.1	29.2	2054.7	27.9	2054.7	27.9	102.8	-2.8
McAfee-97SF1-124	220	148907	1.5	7.8661	0.4	6.7456	0.7	0.3848	0.6	0.83	2098.8	10.3	2078.6	6.1	2058.6	6.8	2058.6	6.8	102.0	-2.0
McAfee-97SF1-3	131	122598	0.7	7.8628	0.4	6.6220	0.6	0.3776	0.5	0.83	2065.2	9.4	2062.3	5.6	2059.3	6.2	2059.3	6.2	100.3	-0.3
McAfee-97SF1-136	32	21139	1.0	7.8429	1.2	6.7060	1.7	0.3815	1.2	0.73	2083.1	22.2	2073.4	15.2	2063.8	20.8	2063.8	20.8	100.9	-0.9
McAfee-97SF1-17	34	48125	1.0	7.8174	1.3	6.7366	1.8	0.3819	1.2	0.68	2085.4	21.7	2077.4	16.0	2069.6	23.5	2069.6	23.5	100.8	-0.8
McAfee-97SF1-45	74	82299	1.6	7.8143	0.5	6.7425	0.9	0.3821	0.8	0.83	2086.2	13.8	2078.2	8.3	2070.3	9.3	2070.3	9.3	100.8	-0.8
McAfee-97SF1-44	32	23564	1.3	7.7902	1.4	6.7853	2.5	0.3834	2.1	0.84	2092.0	37.2	2083.8	22.0	2075.7	24.0	2075.7	24.0	100.8	-0.8
McAfee-97SF1-153	102	52342	1.6	7.7808	0.3	6.7569	0.5	0.3813	0.4	0.75	2082.4	6.9	2080.1	4.6	2077.8	6.1	2077.8	6.1	100.2	-0.2
McAfee-97SF1-159	92	59209	2.0	7.7772	0.3	6.8379	0.8	0.3857	0.7	0.91	2102.8	13.4	2090.6	7.3	2078.6	6.1	2078.6	6.1	101.2	-1.2
McAfee-97SF1-27	99	56650	1.9	7.7718	0.5	6.9050	1.7	0.3892	1.6	0.96	2119.2	28.6	2099.3	14.7	2079.9	8.6	2079.9	8.6	101.9	-1.9
McAfee-97SF1-128	35	28440	0.6	7.7635	1.3	6.7911	2.1	0.3824	1.6	0.78	2087.4	28.7	2084.6	18.2	2081.7	22.5	2081.7	22.5	100.3	-0.3
McAfee-97SF1-66	44	18261	1.3	7.7627	1.4	6.7588	1.7	0.3805	1.0	0.60	2078.7	18.2	2080.3	15.1	2081.9	23.9	2081.9	23.9	99.8	0.2
McAfee-97SF1-51	116	117902	1.5	7.7619	0.3	6.6816	0.7	0.3761	0.6	0.86	2058.2	10.5	2070.2	6.1	2082.1	6.1	2082.1	6.1	98.9	1.1
McAfee-97SF1-131	43	19453	1.3	7.7593	0.8	6.8678	1.3	0.3865	1.0	0.76	2106.6	17.4	2094.5	11.3	2082.7	14.5	2082.7	14.5	101.1	-1.1
McAfee-97SF1-96	37	41735	0.8	7.7519	1.3	6.7094	1.5	0.3772	0.7	0.47	2063.3	12.5	2073.9	13.2	2084.4	23.2	2084.4	23.2	99.0	1.0
McAfee-97SF1-92	77	54214	1.0	7.7501	0.4	6.9409	0.5	0.3901	0.4	0.68	2123.5	6.6	2103.9	4.8	2084.8	7.0	2084.8	7.0	101.9	-1.9
McAfee-97SF1-157	96	56520	1.1	7.7247	0.7	7.0197	1.0	0.3933	0.7	0.72	2138.0	12.5	2113.9	8.5	2090.6	11.7	2090.6	11.7	102.3	-2.3
McAfee-97SF1-144	191	227075	3.0	7.7211	0.4	6.9869	0.6	0.3913	0.4	0.71	2128.7	7.7	2109.8	5.3	2091.4	7.4	2091.4	7.4	101.8	-1.8
McAfee-97SF1-112	96	58312	1.5	7.7181	0.4	6.9698	1.0	0.3901	0.9	0.91	2123.5	15.7	2107.6	8.5	2092.1	6.8	2092.1	6.8	101.5	-1.5
McAfee-97SF1-161	122	43647	2.6	7.7062	0.7	6.9036	1.8	0.3858	1.7	0.93	2103.5	30.8	2099.1	16.4	2094.8	11.8	2094.8	11.8	100.4	-0.4
McAfee-97SF1-117	70	60328	0.7	7.7054	0.9	6.9660	1.0	0.3893	0.4	0.43	2119.6	7.7	2107.1	8.8	2095.0	15.6	2095.0	15.6	101.2	-1.2
McAfee-97SF1-102	158	182899	2.0	7.7030	0.3	6.9974	1.1	0.3909	1.1	0.97	2127.1	19.5	2111.1	9.9	2095.5	4.5	2095.5	4.5	101.5	-1.5
McAfee-97SF1-58	61	67169	1.2	7.7000	1.0	6.9792	1.2	0.3898	0.7	0.59	2121.7	13.0	2108.8	10.8	2096.2	17.1	2096.2	17.1	101.2	-1.2
McAfee-97SF1-77	14	14773	0.7	7.6688	2.7	6.8338	4.4	0.3801	3.4	0.79	2076.7	61.2	2090.1	38.7	2103.3	47.1	2103.3	47.1	98.7	1.3
McAfee-97SF1-192	141	38567	1.5	7.6612	0.8	7.0802	1.2	0.3934	0.9	0.74	2138.6	16.8	2121.6	11.1	2105.1	14.6	2105.1	14.6	101.6	-1.6
McAfee-97SF1-146	68	40942	0.9	7.4085	2.3	7.8361	4.6	0.4210	4.1	0.87	2265.2	77.5	2212.4	41.9	2163.7	39.6	2163.7	39.6	104.7	-4.7
McAfee-97SF1-177	42	26578	1.1	7.1380	1.3	7.7105	2.2	0.3992	1.7	0.78	2165.2	31.1	2197.8	19.4	2228.4	23.2	2228.4	23.2	97.2	2.8
McAfee-97SF1-184	130	122276	0.6	6.9412	0.3	8.5982	0.7	0.4329	0.6	0.91	2318.6	11.8	2296.4	6.1	2276.7	4.9	2276.7	4.9	101.8	-1.8
McAfee-97SF1-93	78	104977	1.4	6.7845	0.7	8.8264	0.9	0.4343	0.6	0.63	2325.1	11.4	2320.2	8.5	2315.9	12.4	2315.9	12.4	100.4	-0.4
McAfee-97SF1-14	199	163185	2.2	6.5797	0.3	8.8274	0.8	0.4213	0.7	0.90	2266.2	13.0	2320.3	6.9	2368.3	5.5	2368.3	5.5	95.7	4.3
McAfee-97SF1-120	93	98992	1.0	6.0245	1.0	10.3590	1.1	0.4526	0.6	0.55	2406.9	12.6	2467.4	10.6	2517.6	16.1	2517.6	16.1	95.6	4.4
McAfee-97SF1-178	19	12587	1.4	5.9860	2.2	11.0919	2.8	0.4815	1.7	0.60	2534.0	35.3	2530.9	26.1	2528.4	37.5	2528.4	37.5	100.2	-0.2
McAfee-97SF1-28	164	187219	0.6	5.9014	0.4	11.3514	1.7	0.4859	1.7	0.98	2552.7	35.6	2552.4	16.1	2552.2	6.0	2552.2	6.0	100.0	0.0
McAfee-97SF1-6	33	40639	0.6	5.8551	0.8	11.3933	1.1	0.4838	0.8	0.71	2543.9	17.0	2555.9	10.7	2565.4	13.4	2565.4	13.4	99.2	0.8
McAfee-97SF1-33	148	110900	1.8	5.8451	0.2	11.8935	2.4	0.5042	2.4	1.00	2631.8	51.8	2596.1	22.6	2568.3	4.0	2568.3	4.0	102.5	-2.5
McAfee-97SF1-78	340	59900	1.9	5.8064	0.1	11.6908	1.0	0.4923	1.0	0.99	2580.7	20.6	2580.0	9.1	2579.3	1.7	2579.3	1.7	100.1	-0.1
McAfee-97SF1-80	33	38888	3.0	5.5220	0.5	12.9720	1.8	0.5195	1.7	0.95	2697.2	37.0	2677.6	16.6	2662.9	8.7	2662.9	8.7	101.3	-1.3
McAfee-97SF1-109	39	40962	1.1	5.5156	0.7	13.2807	1.4	0.5313	1.2	0.86	2746.8	27.5	2699.8	13.5	2664.8	12.3	2664.8	12.3	103.1	-3.1
McAfee-97SF1-35	19	27922	0.9	5.4744	1.0	13.1879	1.4	0.5236	1.1	0.75	2714.5	23.8	2693.2	13.5	2677.2	15.7	2677.2	15.7	101.4	-1.4
McAfee-97SF1-19	56	126221	0.9	5.4678	0.4	13.3972	0.6	0.5313	0.4	0.71	2746.9	9.8	2708.1	5.8	2679.2	7.2	2679.2	7.2	102.5	-2.5
McAfee-97SF1-189	157	96959	1.8	5.4204	0.2	13.0515	0.8	0.5131	0.7	0.95	2669.8	16.1	2683.4	7.3	2693.6	4.1	2693.6	4.1	99.1	0.9
McAfee-97SF1-94	28	19434	0.9	5.4195	0.9	13.1407	1.5	0.5165	1.1	0.77	2684.3	25.0	2689.8	13.9	2693.9	15.4	2693.9	15.4	99.6	0.4
McAfee-97SF1-183	41	78148	1.0	5.4112	1.1	13.5632	3.3	0.5323	3.1	0.94	2751.1	68.7	2719.7	30.9	2696.4	18.4	2696.4	18.4	102.0	-2.0
McAfee-97SF1-5	37	40293	0.5	5.4103	0.7	13.2931	0.9	0.5216	0.6	0.67	2706.0	14.0	2700.7	9.0	2696.7	11.7	2696.7	11.7	100.3	-0.3
McAfee-97SF1-49	22	20687	1.3	5.4069	0.6	13.0958	1.3	0.5135	1.1	0.89	2671.7	25.0	2686.6	12.1	2697.7	9.6	2697.7	9.6	99.0	1.0
McAfee-97SF1-113	66	64099	0.6	5.4038	0.3	13.3857	0.8	0.5246	0.7	0.92	2718.7	16.4	2707.2	7.6	2698.7	5.3	2698.7	5.3	100.7	-0.7
McAfee-97SF1-154	39	38256	1.1	5.4034	0.6	13.3648	0.8	0.5238	0.6	0.70	2715.1	12.4	2705.8	7.5	2698.8	9.4	2698.8	9.4	100.6	-0.6
McAfee-97SF1-52	91	108653	1.2	5.3143	0.3	14.0089	0.5	0.5399	0.5	0.85	2783.2	10.4	2750.3	5.1	2726.2	4.6	2726.2	4.6	102.1	-2.1
Sample: lower Vinini Formation. Location: Petes Summit, Toquima Range; 0518089 4337111 (NAD 83 UTM 11T)																				
LOW VININI 97SF12-1	22	91427	1.5	4.9423	0.7	15.4578	3.1	0.5541	3.0	0.97	2842.2	69.4	2843.9	29.6	2845.1	12.0	2845.1	12.0	99.9	0.1 0.9, 0.8
LOW VININI 97SF12-1	97	100669	1.8	13.1829	0.9	1.9263	1.5	0.1842	1.2	0.81	1089.7	12.2	1090.3	10.1	1091.2	17.7	1091.2	17.7	99.9	0.1
LOW VININI 97SF12-21	49	17084	0.7	16.6120	7.7	0.6363	7.9	0.0767	1.7	0.21	476.2	7.7	500.0	31.2	610.7	167.1	476.2	7.7	78.0	22.0
LOW VININI 97SF12-19	29	6565	1.0	18.5323	12.6	0.5789	13.5	0.0778	4.7	0.35	483.0	22.1	463.8	50.3	369.4	285.6	483.0	22.1	130.8	-30.8
LOW VININI 97SF12-165	873	12611	0.6	17.4648	0.7	0.6177	2.4	0.0782	2.2	0.95	485.6	10.5	488.4	9.2	501.5	16.3	485.6	10.5	96.8	3.2
LOW VININI 97SF12-115	62	15413	0.9	17.6785	3.4	0.6107	5.6	0.0783	4.4	0.79	486.0	20.8	484.0	21.6	474.6	75.8	486.0	20.8	102.4	-2.4
LOW VININI 97SF12-155	472	105117	0.7	17.6423	0.9	0.6126	3.7	0.0784	3.6	0.97	486.5	17.1	485.2	14.4	479.2	19.2	486.5	17.1	101.5	-1.5
LOW VININI 97SF12-158	123	39022	1.1	17.6655	3.8	0.6134	5.3	0.0786	3.7	0.70	487.7	17.5	485.7	20.5	476.3	83.7	487.7	17.5	102.4	-2.4
LOW VININI 97SF12-145	48	8994	0.7	17.8375	9.3	0.6117	9.9	0.0791	3.2	0.33	490.9	15.3	484.6	38.1	454.8	207.4	490.9	15.3	107.9	-7.9
LOW VININI 97SF12-105	347	165325	0.9	17.4690	1.8	0.6246	2.4	0.0791	1.6	0.65	491.0	7.3	492.8	9.3	501.0	40.1	491.0	7.3	98.0	2.0
LOW VININI 97SF12-22	148	29467	1.9	17.7759	2.6	0.6170	3.2	0.0795	1.9	0.58	493.4	8.9	488.0	12.5	462.5	58.5	493.4	8.9	106.7	-6.7
LOW VININI 97SF12-123	17	6152	0.6	18.0976	30.1	0.6067	31.3	0.0796	8.5	0.27	493.9	40.2	481.5	120.4	422.6	685.8	493.9	40.2	116.9	-16.9
LOW VININI 97SF12-20	177	91938	1.9	17.6265	2.2	0.6233	2.6	0.0797	1.4	0.55	494.2	6.8	491.9	10.2	481.1	48.5	494.2	6.8	102.7	-2.7
LOW VININI 97SF12-127	123	13467	1.4	16.9458	4.9	0.6489	5.4	0.0798	2.1	0.40	494.7	10.2	507.8	21.5	567.5	107.6	494.7	10.2	87.2	12.8
LOW VININI 97SF12-176	244	30814	1.0	17.5565	1.5	0.6266	2.7	0.0798	2.3	0.84	494.8	11.0	494.0	10.7	489.9	32.4	494.8	11.0	101.0	-1.0

U-Pb geochronologic anlayses of selected Roberts Mountains allochthon strata

					Isotope ratios								Apparent ages (Ma)							
	U	206Pb	U/Th	206Pb*	±	207Pb*	±	206Pb*	±	error	206Pb*	±	207Pb*	±	206Pb*	±	Best age	±	Conc.	Discord
	(ppm)	204Pb		207Pb*	(%)	235U*	(%)	238U	(%)	corr.	238U*	(Ma)	235U	(Ma)	207Pb*	(Ma)	(Ma)	(Ma)	(%)	(%)
Sample: lower Vinini Formation. Location: Petes Summit, Toquima Range; 0518089 4337111 (NAD 83 UTM 11T)																				
LOW VININI 97SF12-190	359	140836	1.0	17.4780	1.1	0.6299	2.4	0.0799	2.2	0.89	495.2	10.3	496.0	9.6	499.8	24.8	495.2	10.3	99.1	0.9
LOW VININI 97SF12-50	39	9890	0.5	18.4533	7.2	0.5967	8.2	0.0799	3.8	0.47	495.3	18.3	475.2	31.0	379.0	162.5	495.3	18.3	130.7	-30.7
LOW VININI 97SF12-142	38	16456	2.0	17.6961	10.5	0.6223	10.6	0.0799	1.7	0.16	495.3	8.2	491.3	41.3	472.4	231.8	495.3	8.2	104.8	-4.8
LOW VININI 97SF12-10	98	21025	0.5	17.4708	3.6	0.6309	3.9	0.0799	1.6	0.40	495.7	7.5	496.6	15.4	500.7	79.4	495.7	7.5	99.0	1.0
LOW VININI 97SF12-130	214	73022	0.3	17.3277	1.2	0.6371	1.8	0.0801	1.4	0.77	496.5	6.7	500.5	7.2	518.8	25.6	496.5	6.7	95.7	4.3
LOW VININI 97SF12-179	565	144200	0.7	17.4762	0.7	0.6319	1.3	0.0801	1.1	0.85	496.6	5.4	497.3	5.2	500.1	15.3	496.6	5.4	99.3	0.7
LOW VININI 97SF12-152	211	114161	0.7	17.3700	1.3	0.6365	3.3	0.0802	3.0	0.92	497.3	14.6	500.2	13.1	513.4	28.2	497.3	14.6	96.8	3.2
LOW VININI 97SF12-35	207	191128	0.7	17.4577	2.1	0.6334	2.4	0.0802	1.1	0.48	497.3	5.5	498.2	9.3	502.4	45.7	497.3	5.5	99.0	1.0
LOW VININI 97SF12-106	319	101139	1.1	17.4367	1.4	0.6348	2.5	0.0803	2.1	0.83	497.8	9.8	499.1	9.7	505.0	29.8	497.8	9.8	98.6	1.4
LOW VININI 97SF12-166	52	14553	0.8	17.4661	3.7	0.6342	4.8	0.0803	3.0	0.62	498.1	14.2	498.7	18.7	501.3	81.9	498.1	14.2	99.4	0.6
LOW VININI 97SF12-33	65	35323	0.8	16.8624	6.0	0.6571	6.1	0.0804	0.8	0.14	498.3	4.0	512.8	24.4	578.3	130.4	498.3	4.0	86.2	13.8
LOW VININI 97SF12-191	125	58894	0.7	17.2369	1.5	0.6438	2.9	0.0805	2.4	0.85	499.0	11.6	504.6	11.4	530.3	33.4	499.0	11.6	94.1	5.9
LOW VININI 97SF12-25	125	66771	1.6	17.6443	2.2	0.6292	2.5	0.0805	1.2	0.47	499.2	5.6	495.6	9.7	478.9	48.5	499.2	5.6	104.2	-4.2
LOW VININI 97SF12-36	153	8697	1.3	17.2246	4.2	0.6468	4.9	0.0808	2.6	0.53	500.9	12.4	506.5	19.5	531.9	91.3	500.9	12.4	94.2	5.8
LOW VININI 97SF12-93	60	28077	0.8	17.2241	5.9	0.6475	7.2	0.0809	4.0	0.56	501.4	19.5	507.0	28.7	532.0	130.1	501.4	19.5	94.3	5.7
LOW VININI 97SF12-117	173	51629	1.1	17.4399	2.4	0.6396	2.9	0.0809	1.6	0.56	501.5	7.9	502.0	11.6	504.6	53.8	501.5	7.9	99.4	0.6
LOW VININI 97SF12-7	594	134712	0.5	17.5449	0.6	0.6375	1.6	0.0811	1.5	0.92	502.8	7.1	500.7	6.3	491.4	13.8	502.8	7.1	102.3	-2.3
LOW VININI 97SF12-157	20	10328	1.6	13.1682	6.4	1.8758	7.3	0.1792	3.5	0.47	1062.3	33.8	1072.6	48.5	1093.5	129.3	1093.5	129.3	97.1	2.9
LOW VININI 97SF12-129	42	39781	1.2	13.1076	3.4	2.0169	4.7	0.1917	3.2	0.69	1130.8	33.5	1121.2	31.7	1102.8	67.3	1102.8	67.3	102.5	-2.5
LOW VININI 97SF12-45	122	97560	1.2	13.0154	1.0	2.0010	1.7	0.1889	1.4	0.81	1115.4	14.2	1115.9	11.6	1116.9	19.9	1116.9	19.9	99.9	0.1
LOW VININI 97SF12-187	60	48933	0.9	13.0102	2.4	1.9910	4.5	0.1879	3.7	0.84	1109.8	38.0	1112.5	30.2	1117.7	48.8	1117.7	48.8	99.3	0.7
LOW VININI 97SF12-126	73	44396	1.2	13.0060	2.2	2.0029	2.8	0.1889	1.8	0.63	1115.6	18.2	1116.5	19.2	1118.3	44.1	1118.3	44.1	99.8	0.2
LOW VININI 97SF12-177	43	28465	1.5	12.9205	3.7	2.0120	4.0	0.1885	1.4	0.35	1113.5	14.0	1119.6	26.9	1131.4	74.2	1131.4	74.2	98.4	1.6
LOW VININI 97SF12-189	110	101253	1.6	12.1600	1.8	2.3227	2.0	0.2048	0.9	0.45	1201.3	9.9	1219.3	14.1	1251.2	34.7	1251.2	34.7	96.0	4.0
LOW VININI 97SF12-193	128	85570	1.6	12.0755	0.6	2.4356	2.0	0.2133	2.0	0.96	1246.4	22.2	1253.2	14.7	1264.8	10.9	1264.8	10.9	98.5	1.5
LOW VININI 97SF12-192	97	63131	2.1	11.9392	1.2	2.5747	1.7	0.2229	1.2	0.69	1297.4	13.7	1293.5	12.3	1286.9	23.6	1286.9	23.6	100.8	-0.8
LOW VININI 97SF12-111	64	36049	1.4	11.4601	1.6	2.8730	3.6	0.2388	3.3	0.90	1380.4	40.8	1374.9	27.5	1366.2	30.8	1366.2	30.8	101.0	-1.0
LOW VININI 97SF12-61	75	50496	0.9	11.1687	1.9	3.1573	2.3	0.2558	1.4	0.58	1468.1	17.8	1446.8	18.0	1415.6	36.2	1415.6	36.2	103.7	-3.7
LOW VININI 97SF12-2	158	111192	1.2	11.1327	0.6	3.0652	0.9	0.2475	0.7	0.75	1425.5	8.4	1424.0	6.8	1421.8	11.3	1421.8	11.3	100.3	-0.3
LOW VININI 97SF12-63	66	39255	1.5	11.1125	0.9	3.1780	4.7	0.2561	4.6	0.98	1470.0	60.5	1451.8	36.1	1425.3	16.3	1425.3	16.3	103.1	-3.1
LOW VININI 97SF12-55	134	199794	1.8	11.0726	0.8	3.1441	1.6	0.2525	1.4	0.86	1451.3	18.2	1443.6	12.5	1432.1	15.8	1432.1	15.8	101.3	-1.3
LOW VININI 97SF12-101	61	56680	0.8	11.0656	1.6	3.0774	2.7	0.2470	2.2	0.81	1422.9	27.7	1427.1	20.5	1433.4	29.7	1433.4	29.7	99.3	0.7
LOW VININI 97SF12-121	99	108276	1.4	11.0628	0.7	3.1419	2.1	0.2521	2.0	0.95	1449.3	26.2	1443.0	16.4	1433.8	12.5	1433.8	12.5	101.1	-1.1
LOW VININI 97SF12-69	143	11317	1.2	11.0543	0.7	2.9727	6.3	0.2383	6.3	0.99	1378.0	77.7	1400.7	47.9	1435.3	12.5	1435.3	12.5	96.0	4.0
LOW VININI 97SF12-27	149	173305	1.2	11.0536	0.6	3.1318	1.1	0.2511	1.0	0.87	1444.0	13.0	1440.5	8.8	1435.4	10.7	1435.4	10.7	100.6	-0.6
LOW VININI 97SF12-48	252	86501	0.8	11.0503	0.4	3.1161	2.3	0.2497	2.2	0.99	1437.1	28.9	1436.7	17.5	1436.0	7.5	1436.0	7.5	100.1	-0.1
LOW VININI 97SF12-168	83	62578	0.9	11.0488	0.9	3.0775	1.6	0.2466	1.3	0.82	1421.0	16.4	1427.1	12.0	1436.2	17.2	1436.2	17.2	98.9	1.1
LOW VININI 97SF12-32	107	97581	1.2	11.0430	0.5	3.1211	1.1	0.2500	1.0	0.89	1438.3	12.5	1437.9	8.4	1437.2	9.3	1437.2	9.3	100.1	-0.1
LOW VININI 97SF12-183	267	183766	1.6	11.0402	0.3	3.1989	1.7	0.2561	1.6	0.98	1470.1	21.5	1456.9	12.9	1437.7	6.6	1437.7	6.6	102.3	-2.3
LOW VININI 97SF12-R81	47	57046	1.2	11.0387	2.1	3.1189	3.7	0.2497	3.1	0.83	1436.9	39.5	1437.4	28.4	1438.0	39.1	1438.0	39.1	99.9	0.1
LOW VININI 97SF12-134	109	117842	1.2	11.0362	0.5	3.1392	1.4	0.2513	1.3	0.92	1445.0	16.3	1442.4	10.6	1438.4	10.4	1438.4	10.4	100.5	-0.5
LOW VININI 97SF12-17	89	98704	1.0	11.0322	0.7	3.1131	3.0	0.2491	2.9	0.97	1433.8	37.1	1435.9	22.9	1439.1	14.0	1439.1	14.0	99.6	0.4
LOW VININI 97SF12-12	163	206911	2.0	11.0321	0.3	3.1687	1.1	0.2535	1.1	0.95	1456.7	13.9	1449.6	8.7	1439.1	6.7	1439.1	6.7	101.2	-1.2
LOW VININI 97SF12-173	131	113400	1.5	11.0269	0.8	3.1387	2.0	0.2510	1.8	0.91	1443.7	23.0	1442.2	15.1	1440.0	15.7	1440.0	15.7	100.3	-0.3
LOW VININI 97SF12-180	144	114950	0.8	11.0037	0.7	3.1353	1.8	0.2502	1.7	0.92	1439.6	21.3	1441.4	13.8	1444.0	13.3	1444.0	13.3	99.7	0.3
LOW VININI 97SF12-87	130	106569	1.3	11.0013	0.5	3.1620	1.5	0.2523	1.4	0.94	1450.3	18.2	1447.9	11.5	1444.5	9.5	1444.5	9.5	100.4	-0.4
LOW VININI 97SF12-150	62	108335	1.5	11.0000	1.3	3.1422	2.0	0.2507	1.5	0.74	1442.0	18.9	1443.1	15.1	1444.7	24.9	1444.7	24.9	99.8	0.2
LOW VININI 97SF12-90	42	18328	0.7	10.9930	2.8	2.8573	5.3	0.2278	4.5	0.85	1323.0	53.5	1370.7	39.8	1445.9	53.6	1445.9	53.6	91.5	8.5
LOW VININI 97SF12-56	62	48211	0.9	10.9241	1.1	3.2460	1.9	0.2572	1.6	0.83	1475.4	20.6	1468.2	14.7	1457.9	20.2	1457.9	20.2	101.2	-1.2
LOW VININI 97SF12-89	72	29370	0.5	10.9006	1.1	3.1895	2.0	0.2522	1.7	0.85	1449.6	22.3	1454.6	15.6	1462.0	20.0	1462.0	20.0	99.2	0.8
LOW VININI 97SF12-181	81	94981	0.7	10.7807	1.2	3.2842	2.0	0.2568	1.6	0.81	1473.4	21.4	1477.3	15.6	1482.9	22.2	1482.9	22.2	99.4	0.6
LOW VININI 97SF12-119	472	441019	1.8	10.6830	0.2	3.3801	1.5	0.2619	1.5	0.99	1499.5	19.9	1499.8	11.8	1500.2	4.5	1500.2	4.5	100.0	0.0
LOW VININI 97SF12-103	117	25158	1.4	10.4723	0.8	3.4708	1.2	0.2636	0.8	0.70	1508.3	11.0	1520.6	9.2	1537.7	15.8	1537.7	15.8	98.1	1.9
LOW VININI 97SF12-5	42	38927	1.0	10.0734	1.4	4.0212	2.4	0.2938	1.9	0.80	1660.4	28.3	1638.5	19.6	1610.4	26.8	1610.4	26.8	103.1	-3.1
LOW VININI 97SF12-135	131	109421	1.4	10.0473	0.6	3.9296	1.8	0.2863	1.7	0.94	1623.3	23.8	1619.8	14.2	1615.3	11.1	1615.3	11.1	100.5	-0.5
LOW VININI 97SF12-116	294	330298	7.9	9.9426	0.2	4.0194	0.6	0.2898	0.6	0.96	1640.7	8.1	1638.1	4.8	1634.8	3.2	1634.8	3.2	100.4	-0.4
LOW VININI 97SF12-47	110	166222	1.0	9.8068	0.8	4.1807	2.0	0.2974	1.9	0.93	1678.2	27.7	1670.2	16.6	1660.3	14.0	1660.3	14.0	101.1	-1.1
LOW VININI 97SF12-95	30	47258	1.2	9.7673	2.1	3.9913	3.6	0.2827	2.9	0.82	1605.1	41.9	1632.4	29.2	1667.7	38.0	1667.7	38.0	96.2	3.8
LOW VININI 97SF12-6	63	47189	1.2	9.7480	0.9	4.2250	2.9	0.2987	2.8	0.96	1684.9	41.5	1678.9	24.0	1671.4	15.8	1671.4	15.8	100.8	-0.8
LOW VININI 97SF12-167	114	104360	1.0	9.6750	0.4	4.1960	2.3	0.2944	2.2	0.98	1663.6	32.7	1673.2	18.6	1685.3	7.6	1685.3	7.6	98.7	1.3
LOW VININI 97SF12-148	60	91295	1.0	9.6592	0.9	4.2926	1.2	0.3007	0.9	0.73	1694.9	13.4	1691.9	10.2	1688.3	15.7	1688.3	15.7	100.4	-0.4
LOW VININI 97SF12-132	298	236126	2.1	9.6490	0.1	4.1064	4.0	0.2874	4.0	1.00	1628.4	57.7	1655.6	32.8	1690.3	2.8	1690.3	2.8	96.3	3.7
LOW VININI 97SF12-60	83	59214	2.2	9.6398	1.0	4.3025	1.9	0.3008	1.6	0.85	1695.3	23.9	1693.8	15.5	1692.0	18.3	1692.0	18.3	100.2	-0.2
LOW VININI 97SF12-146	59	44536	1.3	9.6389	0.7	4.3923	1.7	0.3071	1.6	0.91	1726.2	24.0	1710.9	14.4	1692.2	13.5	1692.2	13.5	102.0	-2.0
LOW VININI 97SF12-28	92	91848	1.4	9.6317	0.7	4.3348	3.9	0.3028	3.9	0.99	1705.2	57.8	1700.0	32.3	1693.6	12.3	1693.6	12.3	100.7	-0.7
LOW VININI 97SF12-172	87	47953	1.8	9.6304	0.6	4.0123	2.6	0.2802	2.6	0.98	1592.6	36.3	1636.7	21.4	1693.8	10.2	1693.8	10.2	94.0	6.0
LOW VININI 97SF12-53	66	58887	1.0	9.6269	0.9	4.4491	2.0	0.3106	1.8	0.89	1743.9	27.0	1721.5	16.4	1694.5	16.5	1694.5	16.5	102.9	-2.9
LOW VININI 97SF12-151	146	160127	1.7	9.6247	0.4	4.3294	3.3	0.3022	3.3	0.99	1702.3	49.2	1699.0	27.4	1694.9	7.5	1694.9	7.5	100.4	-0.4
LOW VININI 97SF12-139	75	59932	1.4	9.6131	0.9	4.3475	1.8	0.3031	1.6	0.87	1706.7	24.0	1702.4	15.2	1697.1	16.9	1697.1	16.9	100.6	-0.6
LOW VININI 97SF12-156	131	106360	4.1	9.6117	0.4	4.2931	1.3	0.2993	1.2	0.95	1687.7	18.2	1692.0	10.6	1697.4	7.2	1697.4	7.2	99.4	0.6
LOW VININI 97SF12-30	95	152741	3.6	9.6079	0.6	4.3800	2.8	0.3052	2.7	0.97	1717.1	40.4	1708.6	22.8	1698.1	11.8	1698.1	11.8	101.1	-1.1
LOW VININI 97SF12-76	78	84321	1.2	9.5860	0.5	4.4140	1.3	0.3069	1.1	0.90	1725.3	17.3	1715.0	10.5	1702.3	9.9	1702.3	9.9	101.4	-1.4
LOW VININI 97SF12-70	236	59343	1.8	9.5823	0.4	4.0681	2.0	0.2827	2.0	0.98	1605.0	27.7	1647.9	16.3	1703.0	8.0	1703.0	8.0	94.2	5.8
LOW VININI 97SF12-178	86	47757	1.8	9.5767	0.7	4.4238	2.0	0.3073	1.9	0.93	1727.2	28.7	1716.8	16.9	1704.1	13.7	1704.1	13.7	101.4	-1.4
LOW VININI 97SF12-131	51	58244	1.0	9.5734	1.5	4.3633	2.0	0.3030	1.4	0.67	1706.0	20.3	1705.4	16.6	1704.7	27.3	1704.7	27.3	100.1	-0.1
LOW VININI 97SF12-41	97	87525	1.3	9.5571	0.3	4.4214	1.4	0.3065	1.4	0.97	1723.3	20.7	1716.3	11.6	1707.9	5.9	1707.9	5.9	100.9	-0.9
LOW VININI 97SF12-38	148	165761	2.9	9.5499	0.4	4.4103	1.3	0.3055	1.2	0.96	1718.4	18.5	1714.3	10.6	1709.3	6.9	1709.3	6.9	100.5	-0.5
LOW VININI 97SF12-160	76	47195	0.8	9.5452	0.7	4.3174	1.4	0.2989	1.2	0.85	1685.8	17.4	1696.7	11.4	1710.2	13.4	1710.2	13.4	98.6	1.4
LOW VININI 97SF12-88	129	93608	1.5	9.5438	0.5	4.4221	3.1	0.3061	3.0	0.99	1721.4	45.7	1716.5	25.4	1710.4	8.9	1710.4	8.9	100.6	-0.6
LOW VININI 97SF12-118	103	35592	0.9	9.5437	0.5	4.2815	2.8	0.2964	2.8	0.98	1673.2	40.5	1689.8	23.0	1710.5	8.9	1710.5	8.9	97.8	2.2
LOW VININI 97SF12-57	71	118652	1.7	9.5331	1.1	4.4891	2.1	0.3104	1.7	0.83	1742.6	26.1	1729.0	17.1	1712.5	21.0	1712.5	21.0	101.8	-1.8
LOW VININI 97SF12-R83	54	57871	1.4	9.5330	1.2	4.4460	2.3	0.3074	1.9	0.85	1727.9	29.4	1720.9	18.9	1712.5	22.2	1712.5	22.2	100.9	-0.9
LOW VININI 97SF12-169	94	84308	1.8	9.5323	0.8	4.4364	2.4	0.3067	2.3	0.94	1724.5	34.0	1719.2	19.8	1712.7	14.7	1712.7	14.7	100.7	-0.7
LOW VININI 97SF12-54	91	174484	1.9	9.5321	0.5	4.4344	2.1	0.3066	2.1	0.97	1723.8	31.2	1718.8	17.6	1712.7	9.4	1712.7	9.4	100.6	-0.6

U-Pb geochronologic anlayses of selected Roberts Mountains allochthon strata

					Isotope ratios						Apparent ages (Ma)								
	U	206Pb	U/Th	206Pb*	±	207Pb*	±	206Pb*	±	error	206Pb*	±	207Pb*	±	206Pb*	±	Best age	±	Conc.	Discord.
	(ppm)	204Pb		207Pb*	(%)	235U*	(%)	238U	(%)	corr.	238U*	(Ma)	235U	(Ma)	207Pb*	(Ma)	(Ma)	(Ma)	(%)	(%)
Sample: lower Vinini Formation. Location: Petes Summit, Toquima Range; 0518089 4337111 (NAD 83 UTM 11T)																				
LOW VININI 97SF12-44	112	81278	2.5	9.5312	0.5	4.4437	1.8	0.3072	1.7	0.96	1726.8	25.6	1720.5	14.6	1712.9	9.1	1712.9	9.1	100.8	-0.8
LOW VININI 97SF12-43	236	261263	1.6	9.5301	0.4	4.2598	3.2	0.2944	3.2	0.99	1663.7	47.0	1685.6	26.6	1713.1	7.0	1713.1	7.0	97.1	2.9
LOW VININI 97SF12-154	220	316270	1.5	9.5289	0.3	4.4350	2.0	0.3065	1.9	0.98	1723.5	29.4	1718.9	16.4	1713.3	6.3	1713.3	6.3	100.6	-0.6
LOW VININI 97SF12-77	187	223570	1.9	9.5282	0.3	4.3675	2.4	0.3018	2.4	0.99	1700.3	36.1	1706.2	20.1	1713.5	4.7	1713.5	4.7	99.2	0.8
LOW VININI 97SF12-113	84	83469	1.3	9.5258	0.5	4.3577	4.1	0.3011	4.0	0.99	1696.6	60.2	1704.4	33.7	1713.9	10.0	1713.9	10.0	99.0	1.0
LOW VININI 97SF12-78	153	466926	1.9	9.5191	0.6	4.4938	3.0	0.3102	3.0	0.98	1741.9	45.3	1729.8	25.1	1715.2	10.2	1715.2	10.2	101.6	-1.6
LOW VININI 97SF12-109	155	88586	3.1	9.5185	0.5	4.5485	1.8	0.3140	1.7	0.96	1760.4	26.7	1739.9	15.1	1715.3	9.7	1715.3	9.7	102.6	-2.6
LOW VININI 97SF12-23	126	226755	2.0	9.5150	0.7	4.4484	1.9	0.3070	1.8	0.92	1725.8	26.5	1721.4	15.8	1716.0	13.6	1716.0	13.6	100.6	-0.6
LOW VININI 97SF12-107	138	155516	2.2	9.5096	0.5	4.3644	2.0	0.3010	2.0	0.97	1696.3	29.3	1705.6	16.6	1717.0	8.5	1717.0	8.5	98.8	1.2
LOW VININI 97SF12-159	104	98128	1.3	9.5094	0.8	4.5069	2.9	0.3108	2.8	0.96	1744.8	42.2	1732.3	23.9	1717.1	15.3	1717.1	15.3	101.6	-1.6
LOW VININI 97SF12-8	131	212812	0.9	9.5075	0.4	4.4582	2.2	0.3074	2.1	0.98	1728.0	32.3	1723.2	18.0	1717.4	7.6	1717.4	7.6	100.6	-0.6
LOW VININI 97SF12-75	265	486407	2.8	9.5009	0.2	4.4980	1.1	0.3099	1.1	0.99	1740.4	16.2	1730.6	8.9	1718.7	3.3	1718.7	3.3	101.3	-1.3
LOW VININI 97SF12-R82	153	399910	2.4	9.4953	0.3	4.5315	2.3	0.3121	2.3	0.99	1750.9	35.1	1736.8	19.2	1719.8	5.5	1719.8	5.5	101.8	-1.8
LOW VININI 97SF12-18	121	128301	1.9	9.4950	0.4	4.4698	1.8	0.3078	1.7	0.98	1729.9	26.3	1725.4	14.7	1719.9	6.6	1719.9	6.6	100.6	-0.6
LOW VININI 97SF12-175	155	180329	2.0	9.4932	0.4	4.4681	1.7	0.3076	1.7	0.98	1729.1	25.1	1725.1	14.1	1720.2	6.9	1720.2	6.9	100.5	-0.5
LOW VININI 97SF12-102	123	105962	2.4	9.4903	0.4	4.4650	4.1	0.3073	4.1	1.00	1727.5	62.6	1724.5	34.4	1720.8	6.9	1720.8	6.9	100.4	-0.4
LOW VININI 97SF12-125	200	245331	2.7	9.4902	0.3	4.4033	2.9	0.3031	2.9	1.00	1706.6	43.0	1713.0	23.8	1720.8	5.0	1720.8	5.0	99.2	0.8
LOW VININI 97SF12-16	97	118590	1.8	9.4880	0.7	4.4611	1.4	0.3070	1.2	0.87	1725.8	18.1	1723.8	11.4	1721.2	12.4	1721.2	12.4	100.3	-0.3
LOW VININI 97SF12-128	226	294688	1.6	9.4835	0.4	4.4540	2.3	0.3064	2.3	0.99	1722.7	34.8	1722.5	19.3	1722.1	6.5	1722.1	6.5	100.0	0.0
LOW VININI 97SF12-149	224	158788	1.2	9.4781	0.4	4.5286	1.8	0.3113	1.8	0.98	1747.1	27.4	1736.2	15.2	1723.1	7.0	1723.1	7.0	101.4	-1.4
LOW VININI 97SF12-58	147	178452	0.8	9.4771	0.6	4.4994	1.6	0.3093	1.5	0.93	1737.1	23.3	1730.9	13.7	1723.3	11.0	1723.3	11.0	100.8	-0.8
LOW VININI 97SF12-138	115	192707	1.0	9.4738	0.7	4.4816	2.6	0.3079	2.5	0.96	1730.5	37.4	1727.6	21.4	1724.0	13.8	1724.0	13.8	100.4	-0.4
LOW VININI 97SF12-194	174	369932	2.9	9.4714	0.5	4.4958	2.5	0.3088	2.5	0.98	1734.9	37.6	1730.2	20.9	1724.4	8.8	1724.4	8.8	100.6	-0.6
LOW VININI 97SF12-198	70	68060	1.6	9.4710	0.9	4.5447	2.7	0.3122	2.6	0.94	1751.4	39.6	1739.2	22.8	1724.5	16.6	1724.5	16.6	101.6	-1.6
LOW VININI 97SF12-66	287	207517	1.1	9.4674	0.2	4.4787	1.2	0.3075	1.2	0.98	1728.5	18.3	1727.0	10.2	1725.2	4.2	1725.2	4.2	100.2	-0.2
LOW VININI 97SF12-163	188	134321	1.2	9.4661	0.3	4.4049	2.6	0.3024	2.6	0.99	1703.3	38.7	1713.3	21.6	1725.5	5.5	1725.5	5.5	98.7	1.3
LOW VININI 97SF12-91	84	71940	1.0	9.4616	1.0	4.4819	3.3	0.3076	3.1	0.95	1728.7	47.1	1727.6	27.1	1726.3	18.1	1726.3	18.1	100.1	-0.1
LOW VININI 97SF12-161	212	84543	1.1	9.4575	0.3	4.2385	1.5	0.2907	1.4	0.98	1645.2	20.8	1681.5	12.0	1727.1	4.8	1727.1	4.8	95.3	4.7
LOW VININI 97SF12-13	93	154926	1.0	9.4549	0.3	4.4849	1.5	0.3075	1.5	0.98	1728.6	22.9	1728.2	12.8	1727.6	5.8	1727.6	5.8	100.1	-0.1
LOW VININI 97SF12-141	149	145193	1.4	9.4387	0.6	4.5178	2.0	0.3093	1.9	0.95	1737.1	28.6	1734.2	16.4	1730.8	10.9	1730.8	10.9	100.4	-0.4
LOW VININI 97SF12-100	86	117345	1.7	9.4377	0.7	4.5437	2.5	0.3110	2.5	0.97	1745.7	37.5	1739.0	21.1	1731.0	12.0	1731.0	12.0	100.8	-0.8
LOW VININI 97SF12-R85	92	52081	1.2	9.4334	0.6	4.5009	1.7	0.3079	1.6	0.93	1730.6	24.3	1731.1	14.3	1731.8	11.4	1731.8	11.4	99.9	0.1
LOW VININI 97SF12-3	181	304251	1.3	9.4292	0.5	4.5644	1.6	0.3121	1.5	0.95	1751.3	23.4	1742.8	13.3	1732.6	8.8	1732.6	8.8	101.1	-1.1
LOW VININI 97SF12-80	78	76788	1.4	9.4284	1.0	4.5995	2.2	0.3145	2.0	0.90	1762.9	31.0	1749.2	18.6	1732.8	17.9	1732.8	17.9	101.7	-1.7
LOW VININI 97SF12-9	74	71185	2.3	9.4278	0.9	4.5588	1.7	0.3117	1.5	0.85	1749.1	22.4	1741.8	14.3	1732.9	16.6	1732.9	16.6	100.9	-0.9
LOW VININI 97SF12-164	64	56466	3.3	9.4108	1.1	4.4894	2.1	0.3064	1.8	0.86	1723.0	27.8	1729.0	17.7	1736.2	19.9	1736.2	19.9	99.2	0.8
LOW VININI 97SF12-184	76	55717	2.0	9.4098	0.7	4.5488	2.4	0.3104	2.3	0.95	1742.8	34.7	1739.9	19.9	1736.4	13.5	1736.4	13.5	100.4	-0.4
LOW VININI 97SF12-110	61	8771	1.3	9.3783	1.9	4.4996	5.5	0.3060	5.1	0.94	1721.2	77.6	1730.9	45.4	1742.6	33.9	1742.6	33.9	98.8	1.2
LOW VININI 97SF12-37	221	184461	2.6	9.3718	0.3	4.6291	1.3	0.3146	1.3	0.98	1763.5	20.2	1754.5	11.2	1743.8	5.1	1743.8	5.1	101.1	-1.1
LOW VININI 97SF12-67	99	73291	2.5	9.3703	0.5	4.5933	2.8	0.3122	2.7	0.98	1751.3	41.6	1748.0	23.1	1744.1	9.8	1744.1	9.8	100.4	-0.4
LOW VININI 97SF12-26	163	114168	1.5	9.3689	0.3	4.4190	1.8	0.3003	1.8	0.99	1692.6	26.1	1715.9	14.7	1744.4	5.1	1744.4	5.1	97.0	3.0
LOW VININI 97SF12-73	97	47754	3.2	9.3328	0.6	4.6284	2.6	0.3133	2.5	0.98	1756.9	38.5	1754.4	21.4	1751.5	10.4	1751.5	10.4	100.3	-0.3
LOW VININI 97SF12-86	155	325229	0.8	9.3239	0.3	4.6496	1.2	0.3144	1.1	0.96	1762.4	17.1	1758.2	9.7	1753.2	6.1	1753.2	6.1	100.5	-0.5
LOW VININI 97SF12-97	72	57679	2.1	9.3156	0.9	4.5912	2.5	0.3102	2.3	0.92	1741.7	34.8	1747.7	20.5	1754.8	17.2	1754.8	17.2	99.2	0.8
LOW VININI 97SF12-34	156	229809	1.5	9.2652	0.6	4.8500	2.1	0.3259	2.1	0.97	1818.5	32.6	1793.6	18.0	1764.8	10.1	1764.8	10.1	103.0	-3.0
LOW VININI 97SF12-74	103	80501	2.3	9.2586	0.7	4.7989	1.3	0.3222	1.1	0.84	1800.7	16.7	1784.7	10.6	1766.1	12.4	1766.1	12.4	102.0	-2.0
LOW VININI 97SF12-174	73	81806	2.5	9.2494	1.0	4.6910	1.8	0.3147	1.5	0.84	1763.7	23.5	1765.6	15.2	1767.9	18.0	1767.9	18.0	99.8	0.2
LOW VININI 97SF12-143	132	143079	1.4	9.2473	0.4	4.7128	1.4	0.3161	1.3	0.97	1770.5	20.5	1769.5	11.5	1768.3	6.4	1768.3	6.4	100.1	-0.1
LOW VININI 97SF12-98	277	64839	2.6	9.2271	0.2	4.1950	1.2	0.2807	1.2	0.99	1595.0	16.6	1673.0	9.7	1772.3	2.8	1772.3	2.8	90.0	10.0
LOW VININI 97SF12-39	217	291915	2.7	9.2168	0.4	4.7067	1.4	0.3146	1.4	0.96	1763.4	20.9	1768.4	11.7	1774.3	6.8	1774.3	6.8	99.4	0.6
LOW VININI 97SF12-65	194	243517	2.9	9.2115	0.3	4.8294	1.4	0.3226	1.4	0.98	1802.6	21.7	1790.0	11.8	1775.4	4.8	1775.4	4.8	101.5	-1.5
LOW VININI 97SF12-171	185	165324	2.4	9.1945	0.4	4.8313	1.5	0.3222	1.4	0.97	1800.3	22.5	1790.4	12.4	1778.7	6.6	1778.7	6.6	101.2	-1.2
LOW VININI 97SF12-42	222	370324	3.1	9.1835	0.3	4.8584	2.1	0.3236	2.0	0.99	1807.3	32.1	1795.1	17.3	1780.9	5.6	1780.9	5.6	101.5	-1.5
LOW VININI 97SF12-R84	189	187822	2.1	9.1782	0.3	4.6937	2.7	0.3124	2.7	0.99	1752.7	40.8	1766.1	22.4	1782.0	5.5	1782.0	5.5	98.4	1.6
LOW VININI 97SF12-14	49	70213	1.7	9.1724	1.4	4.7970	2.5	0.3191	2.1	0.83	1785.4	32.6	1784.4	21.2	1783.1	25.8	1783.1	25.8	100.1	-0.1
LOW VININI 97SF12-196	96	128411	1.1	9.1657	0.5	4.8297	1.5	0.3211	1.4	0.94	1794.9	22.7	1790.1	12.9	1784.5	9.4	1784.5	9.4	100.6	-0.6
LOW VININI 97SF12-49	103	30402	1.2	9.1623	0.6	4.4626	1.2	0.2965	1.1	0.89	1674.2	16.4	1724.0	10.3	1785.1	10.2	1785.1	10.2	93.8	6.2
LOW VININI 97SF12-92	169	237871	2.3	9.1543	0.3	4.7847	3.0	0.3177	3.0	0.99	1778.3	47.0	1782.2	25.5	1786.7	5.6	1786.7	5.6	99.5	0.5
LOW VININI 97SF12-124	325	163281	3.2	9.1435	0.3	4.7644	3.1	0.3160	3.1	1.00	1769.9	48.1	1778.6	26.2	1788.9	4.9	1788.9	4.9	98.9	1.1
LOW VININI 97SF12-94	146	167028	1.4	9.1415	0.3	4.8305	3.8	0.3203	3.8	1.00	1791.0	59.4	1790.2	32.1	1789.3	6.1	1789.3	6.1	100.1	-0.1
LOW VININI 97SF12-162	110	357801	2.1	9.1368	0.4	4.7633	1.1	0.3156	1.1	0.95	1768.4	16.6	1778.5	9.5	1790.2	6.5	1790.2	6.5	98.8	1.2
LOW VININI 97SF12-31	209	143390	3.0	9.1325	0.3	4.9242	1.8	0.3262	1.8	0.99	1819.7	28.9	1806.4	15.6	1791.1	5.6	1791.1	5.6	101.6	-1.6
LOW VININI 97SF12-185	146	161711	4.2	9.0933	0.5	4.8171	2.2	0.3177	2.2	0.97	1778.4	33.9	1787.9	18.8	1798.9	9.5	1798.9	9.5	98.9	1.1
LOW VININI 97SF12-133	111	279035	1.8	9.0872	0.7	4.8966	1.1	0.3227	0.9	0.79	1803.0	14.0	1801.7	9.6	1800.1	12.8	1800.1	12.8	100.2	-0.2
LOW VININI 97SF12-52	226	259281	2.8	9.0314	0.3	4.8990	1.4	0.3209	1.3	0.98	1794.1	20.8	1802.1	11.4	1811.3	4.7	1811.3	4.7	99.0	1.0
LOW VININI 97SF12-104	168	279256	1.7	8.9156	0.4	5.0957	1.3	0.3295	1.2	0.96	1836.0	19.6	1835.4	10.9	1834.7	6.7	1834.7	6.7	100.1	-0.1
LOW VININI 97SF12-68	122	95153	3.6	8.9014	0.3	5.1116	1.4	0.3300	1.3	0.97	1838.4	20.9	1838.0	11.5	1837.6	6.3	1837.6	6.3	100.0	0.0
LOW VININI 97SF12-140	52	72302	5.3	8.8933	0.8	5.1292	1.9	0.3308	1.8	0.92	1842.4	28.5	1841.0	16.5	1839.3	14.0	1839.3	14.0	100.2	-0.2
LOW VININI 97SF12-108	78	57012	0.3	8.8916	0.9	5.0023	3.2	0.3226	3.1	0.96	1802.4	48.5	1819.7	27.3	1839.6	16.8	1839.6	16.8	98.0	2.0
LOW VININI 97SF12-114	28	33391	1.5	8.8593	1.7	5.1032	2.6	0.3279	2.0	0.76	1828.2	31.9	1836.6	22.5	1846.2	31.4	1846.2	31.4	99.0	1.0
LOW VININI 97SF12-136	62	76652	2.2	8.8377	0.7	5.1851	2.3	0.3324	2.2	0.96	1849.8	34.7	1850.2	19.2	1850.6	11.9	1850.6	11.9	100.0	0.0
LOW VININI 97SF12-122	114	202841	1.3	8.7940	0.3	5.2586	1.3	0.3354	1.3	0.97	1864.5	20.8	1862.2	11.3	1859.6	5.7	1859.6	5.7	100.3	-0.3
LOW VININI 97SF12-120	112	193366	1.6	8.7042	0.4	5.3783	2.5	0.3395	2.5	0.99	1884.4	40.8	1881.4	21.6	1878.1	6.8	1878.1	6.8	100.3	-0.3
LOW VININI 97SF12-24	61	117159	1.0	7.9951	0.8	6.2269	1.4	0.3611	1.1	0.81	1987.3	19.4	2008.2	12.2	2029.9	14.6	2029.9	14.6	97.9	2.1
LOW VININI 97SF12-195	267	888276	2.2	7.8205	0.2	6.7372	3.8	0.3821	3.8	1.00	2086.2	68.2	2077.5	33.9	2068.9	3.2	2068.9	3.2	100.8	-0.8
LOW VININI 97SF12-186	74	105883	2.0	6.2041	0.5	10.3680	2.6	0.4665	2.6	0.98	2468.3	52.8	2468.2	24.2	2468.1	8.0	2468.1	8.0	100.0	0.0
LOW VININI 97SF12-46	154	157278	1.8	6.1748	0.2	10.5204	1.8	0.4711	1.8	0.99	2488.6	37.5	2481.7	17.0	2476.1	3.7	2476.1	3.7	100.5	-0.5
LOW VININI 97SF12-147	247	296113	2.1	6.1670	0.2	10.4444	2.2	0.4672	2.2	1.00	2471.1	45.6	2475.0	20.7	2478.2	2.7	2478.2	2.7	99.7	0.3
LOW VININI 97SF12-153	126	319555	1.9	6.1530	0.2	10.5374	1.6	0.4702	1.5	0.99	2484.6	31.7	2483.2	14.4	2482.1	3.9	2482.1	3.9	100.1	-0.1
LOW VININI 97SF12-200	148	217710	1.7	6.1294	0.3	10.6930	3.0	0.4754	3.0	1.00	2507.0	61.8	2496.8	27.7	2488.5	4.5	2488.5	4.5	100.7	-0.7
LOW VININI 97SF12-59	159	348263	3.7	6.0045	0.3	11.1262	1.4	0.4845	1.4	0.98	2547.0	29.1	2533.8	13.1	2523.2	4.5	2523.2	4.5	100.9	-0.9
LOW VININI 97SF12-137	108	110111	0.7	5.8495	0.2	11.5969	1.7	0.4920	1.7	1.00	2579.3	36.1	2572.4	16.0	2567.0	2.5	2567.0	2.5	100.5	-0.5
LOW VININI 97SF12-112	59	66397	1.0	5.7248	0.6	11.4255	2.4	0.4744	2.3	0.97	2502.8	48.0	2558.5	22.2	2603.0	9.5	2603.0	9.5	96.2	3.8
LOW VININI 97SF12-188	107	306697	2.2	5.4138	0.4	13.0321	0.8	0.5117	0.7	0.87	2663.9	15.5	2682.0	7.7	2695.6	6.5	2695.6	6.5	98.8	1.2

U-Pb geochronologic anlayses of selected Roberts Mountains allochthon strata

					Isotope ratios						Apparent ages (Ma)									
	U	206Pb	U/Th	206Pb*	±	207Pb*	±	206Pb*	±	error	206Pb*	±	207Pb*	±	206Pb*	±	Best age	±	Conc.	Discord.
	(ppm)	204Pb		207Pb*	(%)	235U*	(%)	238U	(%)	corr.	238U*	(Ma)	235U	(Ma)	207Pb*	(Ma)	(Ma)	(Ma)	(%)	(%)
Sample: lower Vinini Formation. Location: Petes Summit, Toquima Range; 0518089 4337111 (NAD 83 UTM 11T)																				
LOW VININI 97SF12-11	93	158753	2.2	5.2788	0.5	14.2477	2.5	0.5455	2.4	0.98	2806.3	55.2	2766.3	23.5	2737.3	7.9	2737.3	7.9	102.5	-2.5
LOW VININI 97SF12-64	33	72078	0.5	5.2747	0.4	13.8462	2.7	0.5297	2.6	0.99	2740.2	58.7	2739.2	25.2	2738.6	6.1	2738.6	6.1	100.1	-0.1
LOW VININI 97SF12-29	67	218455	1.2	5.1698	1.6	13.8605	4.9	0.5197	4.6	0.94	2697.9	102.3	2740.2	46.6	2771.6	26.6	2771.6	26.6	97.3	2.7
LOW VININI 97SF12-182	49	97648	0.6	4.8298	0.4	16.1139	1.6	0.5645	1.6	0.97	2885.0	36.9	2883.6	15.7	2882.6	6.9	2882.6	6.9	100.1	-0.1
LOW VININI 97SF12-40	139	189158	1.7	4.6013	0.2	17.4251	3.3	0.5815	3.3	1.00	2954.9	77.2	2958.5	31.4	2961.0	3.6	2961.0	3.6	99.8	0.2
LOW VININI 97SF12-99	94	250515	0.9	3.8593	0.2	23.2126	1.4	0.6497	1.4	0.99	3227.1	35.9	3235.9	14.0	3241.3	3.8	3241.3	3.8	99.6	0.4
Sample: upper Vinini Formation. Location: Petes Summit, Toquima Range; 0518089 4337111 (NAD 83 UTM 11T)																				
VININI-97SF-11-52	153	45733	1.5	13.2079	1.2	1.9055	2.1	0.1825	1.7	0.81	1080.8	16.8	1083.0	13.8	1087.5	24.0	1087.5	24.0	99.4	0.6 0.9, 0.7
VININI-97SF-11-191	164	95852	3.0	12.1570	0.8	2.4261	1.6	0.2139	1.4	0.87	1249.6	15.4	1250.4	11.2	1251.7	15.2	1251.7	15.2	99.8	0.2
VININI-97SF-11-137	233	61061	1.5	10.7459	0.5	3.3328	1.2	0.2597	1.1	0.90	1488.6	14.7	1488.8	9.6	1489.1	10.1	1489.1	10.1	100.0	0.0
VININI-97SF-11-40	95	35185	1.8	9.4755	1.0	4.5558	2.3	0.3131	2.1	0.91	1755.9	32.6	1741.2	19.4	1723.6	17.6	1723.6	17.6	101.9	-1.9
VININI-97SF-11-74	196	89887	4.4	9.1612	0.3	4.7560	1.2	0.3160	1.1	0.96	1770.2	17.2	1777.2	9.7	1785.4	5.9	1785.4	5.9	99.2	0.8
VININI-97SF-11-138	208	81623	2.8	9.1314	0.3	4.8870	1.1	0.3237	1.1	0.97	1807.5	17.7	1800.0	9.7	1791.3	4.7	1791.3	4.7	100.9	-0.9
VININI-97SF-11-36	18	7005	1.8	9.1163	3.4	4.9391	10.6	0.3266	10.0	0.95	1821.7	158.6	1809.0	89.3	1794.3	61.8	1794.3	61.8	101.5	-1.5
VININI-97SF-11-29	68	25326	1.1	9.0951	0.6	4.7530	3.1	0.3135	3.1	0.98	1758.1	47.4	1776.6	26.3	1798.5	10.7	1798.5	10.7	97.7	2.3
VININI-97SF-11-93	153	109995	4.3	9.0487	0.2	4.9292	1.5	0.3235	1.4	0.99	1806.8	22.8	1807.3	12.4	1807.8	4.5	1807.8	4.5	99.9	0.1
VININI-97SF-11-192	42	14707	1.3	9.0413	0.7	5.1360	1.4	0.3368	1.2	0.86	1871.2	19.6	1842.1	11.9	1809.3	13.1	1809.3	13.1	103.4	-3.4
VININI-97SF-11-76	15	18239	0.9	9.0405	3.2	5.1142	3.5	0.3353	1.3	0.37	1864.2	20.7	1838.5	29.5	1809.5	58.8	1809.5	58.8	103.0	-3.0
VININI-97SF-11-25	118	29729	7.5	9.0201	0.4	4.8775	1.1	0.3191	1.0	0.90	1785.3	14.9	1798.4	8.9	1813.6	8.2	1813.6	8.2	98.4	1.6
VININI-97SF-11-54	25	23149	0.9	9.0059	2.0	5.1032	2.8	0.3333	2.0	0.72	1854.5	32.8	1836.6	24.0	1816.5	35.5	1816.5	35.5	102.1	-2.1
VININI-97SF-11-56	106	40476	0.8	8.9972	0.6	5.1093	1.6	0.3334	1.5	0.92	1854.8	23.7	1837.7	13.5	1818.2	11.2	1818.2	11.2	102.0	-2.0
VININI-97SF-11-42	39	16785	0.9	8.9801	1.7	5.0146	1.9	0.3266	1.0	0.51	1821.9	15.7	1821.8	16.5	1821.7	30.5	1821.7	30.5	100.0	0.0
VININI-97SF-11-78	115	88956	1.0	8.9787	0.6	4.7961	0.9	0.3123	0.6	0.69	1752.1	9.4	1784.2	7.5	1821.9	11.7	1821.9	11.7	96.2	3.8
VININI-97SF-11-187	182	67811	1.5	8.9739	0.5	5.2032	2.5	0.3386	2.5	0.98	1880.2	40.2	1853.1	21.4	1822.9	9.5	1822.9	9.5	103.1	-3.1
VININI-97SF-11-100	180	57040	0.9	8.9688	0.3	5.0708	1.1	0.3298	1.1	0.97	1837.6	17.6	1831.2	9.6	1824.0	5.2	1824.0	5.2	100.7	-0.7
VININI-97SF-11-157	271	123010	1.0	8.9588	0.2	5.0341	0.8	0.3271	0.8	0.97	1824.3	12.9	1825.1	7.1	1826.0	3.6	1826.0	3.6	99.9	0.1
VININI-97SF-11-67	145	140883	2.1	8.9526	0.5	5.0379	1.6	0.3271	1.5	0.95	1824.4	24.1	1825.7	13.6	1827.2	9.4	1827.2	9.4	99.8	0.2
VININI-97SF-11-164	59	26870	0.7	8.9480	0.9	5.1394	1.2	0.3335	0.9	0.71	1855.5	14.1	1842.6	10.4	1828.2	15.6	1828.2	15.6	101.5	-1.5
VININI-97SF-11-27	59	25440	1.3	8.9476	0.8	4.9817	2.5	0.3233	2.4	0.95	1805.7	37.4	1816.2	21.1	1828.2	14.1	1828.2	14.1	98.8	1.2
VININI-97SF-11-17	81	43137	2.4	8.9467	0.6	5.1746	1.4	0.3358	1.3	0.92	1866.3	20.5	1848.4	11.7	1828.4	10.0	1828.4	10.0	102.1	-2.1
VININI-97SF-11-4	140	20590	2.3	8.9343	0.3	4.7053	2.5	0.3049	2.4	0.99	1715.5	36.9	1768.2	20.7	1830.9	5.8	1830.9	5.8	93.7	6.3
VININI-97SF-11-85	80	53383	0.5	8.9333	0.7	5.1722	1.3	0.3351	1.1	0.85	1863.1	18.3	1848.1	11.4	1831.1	12.9	1831.1	12.9	101.7	-1.7
VININI-97SF-11-190	114	125413	0.9	8.9229	0.6	5.2880	1.2	0.3422	1.1	0.86	1897.3	17.6	1866.9	10.6	1833.3	11.4	1833.3	11.4	103.5	-3.5
VININI-97SF-11-112	132	59165	2.5	8.9211	0.3	5.2343	0.9	0.3387	0.9	0.95	1880.3	14.2	1858.2	7.8	1833.6	5.2	1833.6	5.2	102.5	-2.5
VININI-97SF-11-180	80	115104	1.4	8.9208	0.6	5.1822	1.0	0.3353	0.8	0.81	1864.0	12.7	1849.7	8.2	1833.7	10.3	1833.7	10.3	101.7	-1.7
VININI-97SF-11-182	229	129017	1.7	8.9198	0.2	5.1606	1.6	0.3339	1.6	0.99	1857.0	26.2	1846.1	14.0	1833.9	4.2	1833.9	4.2	101.3	-1.3
VININI-97SF-11-173	96	28135	1.3	8.9184	0.6	4.9813	2.0	0.3222	1.9	0.96	1800.5	29.9	1816.2	16.8	1834.2	10.6	1834.2	10.6	98.2	1.8
VININI-97SF-11-99	36	28260	0.8	8.9162	1.5	5.1436	2.1	0.3326	1.5	0.71	1851.1	23.7	1843.3	17.7	1834.6	26.5	1834.6	26.5	100.9	-0.9
VININI-97SF-11-1	74	25752	1.2	8.9161	0.9	5.2119	3.0	0.3370	2.9	0.96	1872.4	46.7	1854.6	25.6	1834.6	15.8	1834.6	15.8	102.1	-2.1
VININI-97SF-11-34	34	24461	0.9	8.9159	1.6	5.1908	2.4	0.3357	1.8	0.75	1865.8	28.9	1851.1	20.3	1834.7	28.7	1834.7	28.7	101.7	-1.7
VININI-97SF-11-53	37	25202	1.0	8.9154	1.8	5.1984	2.8	0.3361	2.1	0.76	1868.0	34.4	1852.4	23.8	1834.8	33.1	1834.8	33.1	101.8	-1.8
VININI-97SF-11-19	73	29432	1.4	8.9078	0.6	5.1612	1.5	0.3334	1.4	0.91	1855.0	21.8	1846.2	12.6	1836.3	11.0	1836.3	11.0	101.0	-1.0
VININI-97SF-11-96	40	12582	0.6	8.9066	1.1	5.2902	3.3	0.3417	3.1	0.94	1895.0	50.3	1867.3	27.9	1836.6	20.7	1836.6	20.7	103.2	-3.2
VININI-97SF-11-142	36	16147	0.7	8.9061	1.3	5.1591	1.7	0.3332	1.1	0.66	1854.1	18.1	1845.9	14.4	1836.7	22.9	1836.7	22.9	100.9	-0.9
VININI-97SF-11-24	53	39772	1.2	8.9057	1.4	5.1759	1.7	0.3343	1.0	0.59	1859.2	16.0	1848.7	14.3	1836.8	24.7	1836.8	24.7	101.2	-1.2
VININI-97SF-11-44	177	117286	1.1	8.9051	0.5	5.0228	1.0	0.3244	0.9	0.90	1811.2	14.8	1823.2	8.8	1836.9	8.4	1836.9	8.4	98.6	1.4
VININI-97SF-11-59	113	53068	1.7	8.9033	0.6	5.0543	3.3	0.3264	3.2	0.98	1820.8	50.9	1828.5	27.7	1837.2	11.3	1837.2	11.3	99.1	0.9
VININI-97SF-11-95	54	44905	1.6	8.9024	1.0	5.1617	1.9	0.3333	1.7	0.87	1854.2	26.7	1846.3	16.2	1837.4	17.2	1837.4	17.2	100.9	-0.9
VININI-97SF-11-123	49	20002	1.4	8.9014	1.3	5.0465	1.9	0.3258	1.5	0.76	1818.0	23.3	1827.2	16.5	1837.6	23.1	1837.6	23.1	98.9	1.1
VININI-97SF-11-153	95	37674	2.7	8.8976	0.5	5.1286	1.3	0.3310	1.2	0.92	1843.0	19.1	1840.9	11.0	1838.4	9.3	1838.4	9.3	100.3	-0.3
VININI-97SF-11-35	159	68874	1.7	8.8969	0.3	5.2401	1.0	0.3381	0.9	0.96	1877.6	15.1	1859.2	8.3	1838.5	5.1	1838.5	5.1	102.1	-2.1
VININI-97SF-11-3	106	33251	2.1	8.8942	0.4	5.2864	1.0	0.3410	0.9	0.90	1891.5	14.0	1866.7	8.1	1839.1	7.6	1839.1	7.6	102.9	-2.9
VININI-97SF-11-79	95	106846	1.2	8.8942	1.0	5.2908	2.1	0.3413	1.8	0.88	1892.9	30.1	1867.4	17.8	1839.1	17.6	1839.1	17.6	102.9	-2.9
VININI-97SF-11-127	109	25081	1.6	8.8908	0.5	5.1389	1.2	0.3314	1.1	0.91	1845.0	17.1	1842.6	9.9	1839.8	8.7	1839.8	8.7	100.3	-0.3
VININI-97SF-11-105	36	23115	1.0	8.8894	1.7	5.2789	2.1	0.3403	1.2	0.59	1888.3	20.4	1865.5	18.0	1840.1	30.7	1840.1	30.7	102.6	-2.6
VININI-97SF-11-177	139	81084	1.5	8.8892	0.4	5.1166	1.4	0.3299	1.3	0.96	1837.7	21.0	1838.9	11.6	1840.1	7.0	1840.1	7.0	99.9	0.1
VININI-97SF-11-128	53	38166	0.7	8.8878	0.9	5.0888	1.3	0.3280	1.0	0.72	1828.8	15.1	1834.2	11.2	1840.4	16.5	1840.4	16.5	99.4	0.6
VININI-97SF-11-131	82	20315	1.0	8.8834	0.8	5.0425	1.5	0.3249	1.2	0.85	1813.5	19.5	1826.5	12.3	1841.3	13.9	1841.3	13.9	98.5	1.5
VININI-97SF-11-175	162	71238	4.4	8.8832	0.3	5.1096	1.3	0.3292	1.3	0.97	1834.5	20.4	1837.7	11.3	1841.3	6.2	1841.3	6.2	99.6	0.4
VININI-97SF-11-13	36	42978	0.8	8.8832	1.0	5.2113	1.6	0.3358	1.3	0.80	1866.2	20.3	1854.5	13.4	1841.3	17.3	1841.3	17.3	101.3	-1.3
VININI-97SF-11-18	53	36090	0.8	8.8804	1.2	5.2335	2.0	0.3371	1.5	0.78	1872.6	25.2	1858.1	16.9	1841.9	22.4	1841.9	22.4	101.7	-1.7
VININI-97SF-11-141	76	26815	0.8	8.8789	0.6	4.5936	5.0	0.2958	5.0	0.99	1670.5	73.5	1748.1	42.0	1842.2	11.2	1842.2	11.2	90.7	9.3
VININI-97SF-11-145	162	142648	1.4	8.8772	0.3	5.1696	0.9	0.3328	0.9	0.96	1852.1	14.2	1847.6	7.8	1842.6	4.7	1842.6	4.7	100.5	-0.5
VININI-97SF-11-139	50	23064	1.8	8.8730	0.8	5.2889	1.8	0.3404	1.6	0.88	1888.4	25.9	1867.1	15.3	1843.4	15.3	1843.4	15.3	102.4	-2.4
VININI-97SF-11-165	101	66631	1.0	8.8682	0.6	5.2688	1.9	0.3389	1.8	0.95	1881.3	28.9	1863.8	15.9	1844.4	10.3	1844.4	10.3	102.0	-2.0
VININI-97SF-11-169	37	11793	0.3	8.8654	1.1	5.2109	2.1	0.3350	1.7	0.83	1862.8	27.8	1854.4	17.6	1845.0	20.7	1845.0	20.7	101.0	-1.0
VININI-97SF-11-118	130	46679	1.5	8.8642	0.4	5.1212	1.6	0.3292	1.6	0.97	1834.7	25.0	1839.6	13.7	1845.2	6.8	1845.2	6.8	99.4	0.6
VININI-97SF-11-87	37	18389	0.7	8.8622	1.1	5.3125	1.5	0.3415	1.0	0.67	1893.7	16.5	1870.9	12.9	1845.6	20.3	1845.6	20.3	102.6	-2.6
VININI-97SF-11-136	110	43222	1.0	8.8612	0.5	5.1773	1.2	0.3327	1.1	0.90	1851.6	17.0	1848.9	10.0	1845.8	9.4	1845.8	9.4	100.3	-0.3
VININI-97SF-11-159	72	23436	0.7	8.8589	0.6	5.2198	3.0	0.3354	2.9	0.98	1864.4	46.9	1855.9	25.2	1846.3	10.5	1846.3	10.5	101.0	-1.0
VININI-97SF-11-148	66	11108	1.1	8.8502	1.1	5.1988	2.3	0.3337	2.0	0.87	1856.3	32.8	1852.4	19.9	1848.1	20.6	1848.1	20.6	100.4	-0.4
VININI-97SF-11-129	209	133641	2.5	8.8428	0.3	5.0141	1.2	0.3216	1.2	0.97	1797.4	18.2	1821.7	10.1	1849.6	5.1	1849.6	5.1	97.2	2.8
VININI-97SF-11-163	136	65993	1.8	8.8410	0.3	5.2700	1.2	0.3379	1.2	0.97	1876.7	19.6	1864.0	10.6	1849.9	5.5	1849.9	5.5	101.4	-1.4
VININI-97SF-11-6	54	32943	1.1	8.8408	0.9	5.1979	1.6	0.3333	1.3	0.82	1854.3	20.7	1852.3	13.4	1850.0	16.4	1850.0	16.4	100.2	-0.2
VININI-97SF-11-15	48	38933	1.1	8.8233	1.5	5.2740	2.1	0.3375	1.5	0.72	1874.6	24.3	1864.7	17.8	1853.6	26.4	1853.6	26.4	101.1	-1.1
VININI-97SF-11-198	48	52927	1.7	8.8172	1.1	5.4056	1.5	0.3457	1.1	0.70	1913.9	17.5	1885.7	12.9	1854.8	19.3	1854.8	19.3	103.2	-3.2
VININI-97SF-11-20	243	171121	1.2	8.8129	0.3	5.2104	1.1	0.3330	1.0	0.95	1853.1	16.9	1854.3	9.4	1855.7	6.2	1855.7	6.2	99.9	0.1
VININI-97SF-11-51	134	89130	3.5	8.8119	0.6	5.3033	2.2	0.3389	2.2	0.97	1881.6	35.2	1869.4	19.0	1855.9	10.0	1855.9	10.0	101.4	-1.4
VININI-97SF-11-28	116	98444	2.0	8.8116	0.5	5.2560	1.7	0.3359	1.7	0.96	1866.9	26.9	1861.7	14.7	1856.0	8.3	1856.0	8.3	100.6	-0.6
VININI-97SF-11-186	89	70353	2.4	8.8067	0.6	5.2017	1.8	0.3322	1.7	0.93	1849.2	26.7	1852.9	15.1	1857.0	11.5	1857.0	11.5	99.6	0.4
VININI-97SF-11-61	43	24054	1.2	8.8045	0.8	5.1574	1.4	0.3293	1.2	0.84	1835.1	19.0	1845.6	12.0	1857.4	13.9	1857.4	13.9	98.8	1.2
VININI-97SF-11-91	44	40833	0.9	8.8033	1.2	5.2024	1.9	0.3322	1.5	0.79	1848.9	24.3	1853.0	16.4	1857.7	21.5	1857.7	21.5	99.5	0.5
VININI-97SF-11-176	135	59143	0.9	8.7991	0.7	5.0581	1.4	0.3228	1.2	0.87	1803.4	19.3	1829.1	12.0	1858.5	12.7	1858.5	12.7	97.0	3.0

U-Pb geochronologic anlayses of selected Roberts Mountains allochthon strata

						Isotope ratios								Apparent ages (Ma)							
	U	206Pb	U/Th	206Pb*	±	207Pb*	±	206Pb*	±	error	206Pb*	±	207Pb*	±	206Pb*	±	Best age	±	Conc.	Discord.
	(ppm)	204Pb		207Pb*	(%)	235U*	(%)	238U	(%)	corr.	238U*	(Ma)	235U	(Ma)	207Pb*	(Ma)	(Ma)	(Ma)	(%)	(%)
Sample: upper Vinini Formation. Location: Petes Summit, Toquima Range; 0518089 4337111 (NAD 83 UTM 11T)																				
VININI-97SF-11-58	195	96148	0.9	8.7987	0.5	5.1796	1.6	0.3305	1.5	0.94	1840.9	23.5	1849.3	13.2	1858.6	9.3	1858.6	9.3	99.0	1.0
VININI-97SF-11-146	55	40013	1.6	8.7971	0.8	5.2271	1.8	0.3335	1.6	0.89	1855.4	25.3	1857.1	15.0	1858.9	14.5	1858.9	14.5	99.8	0.2
VININI-97SF-11-134	242	301056	2.5	8.7901	0.2	5.2515	0.9	0.3348	0.9	0.97	1861.6	14.4	1861.0	7.9	1860.4	4.2	1860.4	4.2	100.1	-0.1
VININI-97SF-11-167	74	27962	2.8	8.7875	0.4	4.9894	1.3	0.3180	1.2	0.95	1779.9	18.8	1817.5	10.7	1860.9	7.2	1860.9	7.2	95.6	4.4
VININI-97SF-11-132	94	22789	1.2	8.7866	0.6	5.0952	1.7	0.3247	1.6	0.93	1812.6	24.6	1835.3	14.2	1861.1	11.1	1861.1	11.1	97.4	2.6
VININI-97SF-11-8	132	82264	1.6	8.7745	0.6	5.2939	1.0	0.3369	0.9	0.84	1871.7	13.8	1867.9	8.7	1863.6	10.0	1863.6	10.0	100.4	-0.4
VININI-97SF-11-47	44	12818	0.8	8.7729	1.1	5.1821	1.8	0.3297	1.4	0.79	1837.0	22.9	1849.7	15.4	1863.9	19.9	1863.9	19.9	98.6	1.4
VININI-97SF-11-9	112	57066	2.6	8.7339	0.5	5.4446	1.0	0.3449	0.9	0.85	1910.1	14.7	1891.9	8.9	1872.0	9.8	1872.0	9.8	102.0	-2.0
VININI-97SF-11-140	47	18779	0.6	8.7206	1.5	5.4564	2.2	0.3451	1.7	0.74	1911.2	27.3	1893.8	19.0	1874.7	26.7	1874.7	26.7	101.9	-1.9
VININI-97SF-11-10	37	16789	1.2	8.7196	0.8	5.3984	2.2	0.3414	2.0	0.92	1893.4	32.6	1884.6	18.5	1874.9	15.3	1874.9	15.3	101.0	-1.0
VININI-97SF-11-158	106	54672	2.1	8.7155	0.5	5.3007	2.0	0.3351	2.0	0.97	1862.9	32.2	1869.0	17.5	1875.8	8.4	1875.8	8.4	99.3	0.7
VININI-97SF-11-121	220	71623	1.7	8.6691	0.4	5.2383	1.1	0.3294	1.0	0.92	1835.2	16.0	1858.9	9.3	1885.4	7.7	1885.4	7.7	97.3	2.7
VININI-97SF-11-88	88	26408	0.9	8.6669	0.7	5.4691	1.6	0.3438	1.4	0.89	1904.8	23.1	1895.8	13.6	1885.8	13.2	1885.8	13.2	101.0	-1.0
VININI-97SF-11-5	79	24795	1.2	8.6432	0.9	5.5642	1.6	0.3488	1.3	0.83	1928.9	22.4	1910.6	13.9	1890.8	16.3	1890.8	16.3	102.0	-2.0
VININI-97SF-11-144	63	23221	1.0	8.6421	0.7	5.4626	2.9	0.3424	2.8	0.97	1898.1	45.8	1894.7	24.5	1891.0	11.8	1891.0	11.8	100.4	-0.4
VININI-97SF-11-48	96	37594	1.9	8.6322	0.6	5.5456	1.1	0.3472	1.0	0.87	1921.2	16.1	1907.7	9.6	1893.1	10.1	1893.1	10.1	101.5	-1.5
VININI-97SF-11-150	172	95937	1.0	8.6252	0.4	5.5077	1.5	0.3445	1.5	0.96	1908.5	24.1	1901.8	13.0	1894.5	7.6	1894.5	7.6	100.7	-0.7
VININI-97SF-11-124	215	75870	1.6	8.6170	1.0	5.1652	2.5	0.3228	2.3	0.92	1803.4	36.3	1846.9	21.3	1896.2	17.5	1896.2	17.5	95.1	4.9
VININI-97SF-11-149	43	25262	0.9	8.6166	0.8	5.5322	1.5	0.3457	1.3	0.86	1914.2	22.1	1905.6	13.3	1896.3	14.1	1896.3	14.1	100.9	-0.9
VININI-97SF-11-193	200	226678	2.4	8.6105	0.2	5.5836	1.6	0.3487	1.6	0.99	1928.4	26.9	1913.6	14.1	1897.6	4.1	1897.6	4.1	101.6	-1.6
VININI-97SF-11-31	53	27944	0.7	8.6018	1.0	5.6715	2.6	0.3538	2.4	0.92	1952.8	40.2	1927.0	22.4	1899.4	18.4	1899.4	18.4	102.8	-2.8
VININI-97SF-11-32	56	66327	1.5	8.5947	0.8	5.4539	1.5	0.3400	1.3	0.84	1886.5	21.1	1893.4	13.3	1900.9	15.2	1900.9	15.2	99.2	0.8
VININI-97SF-11-133	19	18778	0.7	8.5709	2.8	5.4682	3.3	0.3399	1.8	0.53	1886.3	28.9	1895.6	28.5	1905.9	50.6	1905.9	50.6	99.0	1.0
VININI-97SF-11-2	75	54375	1.1	8.5587	0.6	5.6308	1.2	0.3495	1.0	0.85	1932.3	16.9	1920.8	10.3	1908.4	11.2	1908.4	11.2	101.3	-1.3
VININI-97SF-11-77	49	62223	1.1	8.5346	1.2	5.6287	1.5	0.3484	0.9	0.61	1927.0	15.2	1920.5	12.8	1913.5	21.1	1913.5	21.1	100.7	-0.7
VININI-97SF-11-71	47	80247	1.1	8.5337	1.7	5.6273	4.5	0.3483	4.2	0.93	1926.4	69.4	1920.3	38.9	1913.7	30.6	1913.7	30.6	100.7	-0.7
VININI-97SF-11-86	221	217719	1.7	8.5158	0.2	5.4175	1.8	0.3346	1.8	0.99	1860.6	29.2	1887.6	15.6	1917.4	3.8	1917.4	3.8	97.0	3.0
VININI-97SF-11-57	50	26794	0.6	8.5120	0.9	5.6866	1.6	0.3511	1.4	0.84	1939.7	23.0	1929.3	14.1	1918.2	16.0	1918.2	16.0	101.1	-1.1
VININI-97SF-11-97	37	24331	1.3	8.5046	1.3	5.6365	1.7	0.3477	1.1	0.63	1923.4	18.1	1921.7	14.9	1919.8	24.0	1919.8	24.0	100.2	-0.2
VININI-97SF-11-199	44	24016	2.1	8.4738	1.6	5.8044	2.2	0.3567	1.5	0.69	1966.6	25.7	1947.1	19.1	1926.3	28.7	1926.3	28.7	102.1	-2.1
VININI-97SF-11-41	28	19005	1.1	8.4723	1.4	5.5113	1.7	0.3387	0.9	0.53	1880.2	14.5	1902.4	14.4	1926.6	25.5	1926.6	25.5	97.6	2.4
VININI-97SF-11-156	86	35825	0.9	8.4715	0.4	5.5706	1.6	0.3423	1.6	0.97	1897.6	26.0	1911.6	14.0	1926.8	6.8	1926.8	6.8	98.5	1.5
VININI-97SF-11-197	40	69540	0.6	8.4589	1.3	5.7741	2.0	0.3542	1.5	0.76	1954.8	25.5	1942.5	17.2	1929.5	23.2	1929.5	23.2	101.3	-1.3
VININI-97SF-11-172	536	38226	3.1	8.4583	0.2	5.0091	1.2	0.3073	1.2	0.98	1727.3	18.0	1820.9	10.2	1929.6	3.9	1929.6	3.9	89.5	10.5
VININI-97SF-11-115	82	34522	1.0	8.4560	0.6	5.6348	1.8	0.3456	1.7	0.94	1913.4	28.6	1921.4	15.8	1930.1	10.8	1930.1	10.8	99.1	0.9
VININI-97SF-11-183	54	34688	1.2	8.4553	1.0	5.7332	1.3	0.3516	0.8	0.64	1942.1	14.1	1936.4	11.4	1930.2	18.2	1930.2	18.2	100.6	-0.6
VININI-97SF-11-101	292	164616	0.6	8.4505	0.3	5.7603	1.1	0.3530	1.1	0.97	1949.1	17.9	1940.5	9.5	1931.2	4.5	1931.2	4.5	100.9	-0.9
VININI-97SF-11-166	224	164058	0.6	8.4412	0.3	5.8299	0.9	0.3569	0.8	0.94	1967.5	14.0	1950.9	7.6	1933.2	5.5	1933.2	5.5	101.8	-1.8
VININI-97SF-11-122	94	27302	1.3	8.4402	0.7	5.6000	1.8	0.3428	1.7	0.92	1900.1	27.8	1916.1	15.9	1933.4	13.3	1933.4	13.3	98.3	1.7
VININI-97SF-11-70	42	32447	0.6	8.4369	1.0	5.8650	1.8	0.3589	1.5	0.84	1976.9	25.6	1956.1	15.6	1934.1	17.7	1934.1	17.7	102.2	-2.2
VININI-97SF-11-170	144	47086	0.7	8.4256	0.3	5.7505	1.6	0.3514	1.6	0.98	1941.3	27.0	1939.0	14.2	1936.5	5.5	1936.5	5.5	100.2	-0.2
VININI-97SF-11-11	64	5075	1.2	8.4222	1.1	5.8381	1.7	0.3566	1.3	0.78	1966.1	22.8	1952.1	15.0	1937.2	19.3	1937.2	19.3	101.5	-1.5
VININI-97SF-11-7	134	65089	0.7	8.4214	0.2	5.8099	1.0	0.3549	1.0	0.97	1957.7	16.7	1947.9	8.8	1937.4	4.1	1937.4	4.1	101.0	-1.0
VININI-97SF-11-65	27	8307	0.3	8.4210	2.3	5.8671	2.4	0.3583	0.8	0.33	1974.3	13.7	1956.4	20.9	1937.5	40.6	1937.5	40.6	101.9	-1.9
VININI-97SF-11-81	101	53354	0.4	8.3538	0.6	5.9342	1.0	0.3595	0.8	0.79	1980.0	14.1	1966.3	9.1	1951.8	11.5	1951.8	11.5	101.4	-1.4
VININI-97SF-11-110	130	60871	0.8	8.3056	0.4	5.9535	1.8	0.3586	1.7	0.97	1975.7	29.0	1969.1	15.3	1962.2	7.6	1962.2	7.6	100.7	-0.7
VININI-97SF-11-160	29	11398	1.3	8.2504	1.2	5.9962	1.9	0.3588	1.4	0.77	1976.5	24.3	1975.3	16.1	1974.1	21.0	1974.1	21.0	100.1	-0.1
VININI-97SF-11-14	237	205331	2.3	8.2273	0.5	5.9906	2.9	0.3575	2.8	0.98	1970.1	47.5	1974.5	24.8	1979.0	9.7	1979.0	9.7	99.5	0.5
VININI-97SF-11-38	45	10213	0.8	8.2272	4.2	5.8646	4.7	0.3499	2.1	0.45	1934.3	35.2	1956.0	40.7	1979.1	74.6	1979.1	74.6	97.7	2.3
VININI-97SF-11-114	81	25313	0.5	8.2147	0.5	6.0538	1.1	0.3607	0.9	0.87	1985.4	16.0	1983.6	9.4	1981.8	9.7	1981.8	9.7	100.2	-0.2
VININI-97SF-11-154	61	37663	1.4	8.0477	1.1	6.2700	1.7	0.3660	1.3	0.78	2010.4	22.4	2014.3	14.7	2018.2	18.7	2018.2	18.7	99.6	0.4
VININI-97SF-11-94	266	178919	4.8	7.9887	0.8	6.2291	1.7	0.3609	1.5	0.88	1986.5	26.3	2008.5	15.3	2031.3	14.4	2031.3	14.4	97.8	2.2
VININI-97SF-11-84	62	30123	1.4	7.8706	0.9	6.4274	4.3	0.3669	4.2	0.98	2014.8	73.0	2036.0	37.9	2057.6	15.8	2057.6	15.8	97.9	2.1
VININI-97SF-11-12	79	38142	1.3	7.7992	0.5	6.7935	0.9	0.3843	0.7	0.84	2096.2	12.8	2084.9	7.5	2073.7	8.2	2073.7	8.2	101.1	-1.1
VININI-97SF-11-179	36	25677	1.1	7.7867	1.2	6.8150	2.2	0.3849	1.8	0.84	2099.0	32.8	2087.7	19.3	2076.5	20.6	2076.5	20.6	101.1	-1.1
VININI-97SF-11-30	266	91671	2.0	7.7866	0.3	6.6047	1.9	0.3730	1.8	0.99	2043.5	32.1	2060.0	16.4	2076.5	5.0	2076.5	5.0	98.4	1.6
VININI-97SF-11-50	66	34430	1.2	7.7787	0.8	6.7563	1.3	0.3812	1.0	0.78	2081.7	17.3	2080.0	11.1	2078.3	13.9	2078.3	13.9	100.2	-0.2
VININI-97SF-11-130	57	21363	1.2	7.7763	0.6	6.6440	1.6	0.3747	1.5	0.93	2051.5	26.6	2065.2	14.4	2078.8	10.6	2078.8	10.6	98.7	1.3
VININI-97SF-11-55	61	73812	0.9	7.7734	0.4	6.8380	2.1	0.3855	2.0	0.98	2102.0	36.7	2090.7	18.5	2079.5	7.6	2079.5	7.6	101.1	-1.1
VININI-97SF-11-49	55	46742	1.2	7.7663	1.0	6.7774	2.0	0.3817	1.8	0.88	2084.4	32.1	2082.8	18.1	2081.1	17.1	2081.1	17.1	100.2	-0.2
VININI-97SF-11-178	64	39446	0.2	7.7454	0.5	6.8775	1.2	0.3863	1.1	0.91	2105.8	20.2	2095.8	10.9	2085.9	8.8	2085.9	8.8	101.0	-1.0
VININI-97SF-11-189	52	82298	1.5	7.7452	0.8	7.1892	1.4	0.4038	1.1	0.84	2186.7	21.2	2135.2	12.2	2085.9	13.2	2085.9	13.2	104.8	-4.8
VININI-97SF-11-111	79	64156	0.9	7.7392	0.8	6.7275	1.4	0.3776	1.1	0.80	2065.1	19.4	2076.2	12.1	2087.3	14.5	2087.3	14.5	98.9	1.1
VININI-97SF-11-37	157	556788	1.4	7.7353	0.3	6.8896	1.6	0.3865	1.6	0.99	2106.7	28.4	2097.3	14.2	2088.2	4.8	2088.2	4.8	100.9	-0.9
VININI-97SF-11-23	110	41354	1.3	7.7311	0.5	7.0165	1.4	0.3934	1.3	0.94	2138.7	23.1	2113.5	12.0	2089.1	8.3	2089.1	8.3	102.4	-2.4
VININI-97SF-11-68	162	148352	1.3	7.7270	0.3	6.8519	1.4	0.3840	1.4	0.98	2094.9	24.5	2092.5	12.4	2090.0	5.4	2090.0	5.4	100.2	-0.2
VININI-97SF-11-113	22	11547	0.4	7.7261	1.8	6.9337	3.4	0.3885	2.9	0.85	2116.0	52.3	2103.0	30.2	2090.2	31.3	2090.2	31.3	101.2	-1.2
VININI-97SF-11-151	359	64158	2.4	7.7202	0.3	6.9160	0.8	0.3872	0.8	0.92	2110.0	13.7	2100.7	7.3	2091.6	5.6	2091.6	5.6	100.9	-0.9
VININI-97SF-11-161	108	18748	2.0	7.7163	1.0	6.9724	2.2	0.3902	2.0	0.89	2123.8	35.3	2107.9	19.5	2092.5	17.7	2092.5	17.7	101.5	-1.5
VININI-97SF-11-60	95	39126	1.6	7.7062	0.4	6.9143	1.4	0.3864	1.4	0.96	2106.3	24.3	2100.5	12.4	2094.8	6.6	2094.8	6.6	100.6	-0.6
VININI-97SF-11-181	137	102353	1.5	7.6955	0.4	7.0135	1.2	0.3914	1.1	0.94	2129.5	19.6	2113.1	10.2	2097.2	6.9	2097.2	6.9	101.5	-1.5
VININI-97SF-11-195	368	204826	4.7	7.6876	0.3	6.8982	1.2	0.3846	1.2	0.97	2097.8	21.0	2098.4	10.7	2099.0	5.0	2099.0	5.0	99.9	0.1
VININI-97SF-11-135	96	83737	1.4	7.6812	0.5	6.8667	0.9	0.3825	0.8	0.86	2088.2	13.8	2094.4	7.9	2100.5	7.9	2100.5	7.9	99.4	0.6
VININI-97SF-11-196	110	10732	0.6	7.6723	1.4	6.9802	2.0	0.3884	1.4	0.70	2115.4	25.2	2108.9	17.8	2102.5	25.2	2102.5	25.2	100.6	-0.6
VININI-97SF-11-63	40	38719	1.9	7.6277	0.5	6.9799	1.8	0.3861	1.7	0.96	2104.9	31.4	2108.9	16.1	2112.7	8.7	2112.7	8.7	99.6	0.4
VININI-97SF-11-117	120	34916	1.6	7.5072	0.9	7.3724	1.6	0.4014	1.4	0.85	2175.5	25.6	2157.6	14.6	2140.6	15.0	2140.6	15.0	101.6	-1.6
VININI-97SF-11-184	378	88387	3.0	7.3134	6.5	6.0776	7.0	0.3224	2.4	0.34	1801.3	37.5	1987.0	60.7	2186.3	113.8	2186.3	113.8	82.4	17.6
VININI-97SF-11-107	184	79568	2.0	6.8531	1.8	8.5006	2.7	0.4225	2.1	0.76	2271.9	39.7	2286.0	24.7	2298.6	30.1	2298.6	30.1	98.8	1.2
VININI-97SF-11-33	173	174724	1.3	6.8297	3.5	8.0004	3.6	0.3963	0.6	0.17	2151.9	10.9	2231.1	32.1	2304.5	60.3	2304.5	60.3	93.4	6.6
VININI-97SF-11-125	31	27294	0.9	6.7790	0.9	8.6027	1.8	0.4230	1.5	0.86	2273.9	29.2	2296.8	16.2	2317.3	15.8	2317.3	15.8	98.1	1.9
VININI-97SF-11-162	130	95137	1.3	6.7708	0.5	9.0639	1.5	0.4451	1.5	0.96	2373.4	29.2	2344.5	14.1	2319.4	7.8	2319.4	7.8	102.3	-2.3
VININI-97SF-11-66	51	34600	1.1	6.7670	0.6	8.7344	1.8	0.4287	1.7	0.94	2299.7	33.5	2310.7	16.8	2320.3	11.0	2320.3	11.0	99.1	0.9
VININI-97SF-11-109	70	43594	1.1	6.5193	0.5	8.8693	1.6	0.4194	1.6	0.94	2257.6	29.6	2324.6	15.0	2384.1	9.2	2384.1	9.2	94.7	5.3
VININI-97SF-11-16	98	69578	1.9	6.2437	0.5	10.1161	1.5	0.4581	1.4	0.95	2431.1	28.4	2445.4	13.6	2457.4	7.6	2457.4	7.6	98.9	1.1

U-Pb geochronologic anlayses of selected Roberts Mountains allochthon strata

						Isotope ratios							Apparent ages (Ma)							
	U	206Pb	U/Th	206Pb*	±	207Pb*	±	206Pb*	±	error	206Pb*	±	207Pb*	±	206Pb*	±	Best age	±	Conc.	Discord.
	(ppm)	204Pb		207Pb*	(%)	235U*	(%)	238U	(%)	corr.	238U*	(Ma)	235U	(Ma)	207Pb*	(Ma)	(Ma)	(Ma)	(%)	(%)
Sample: upper Vinini Formation. Location: Petes Summit, Toquima Range; 0518089 4337111 (NAD 83 UTM 11T)																				
VININI-97SF-11-106	33	25913	1.3	6.2191	1.6	9.7716	4.0	0.4408	3.7	0.92	2354.0	72.9	2413.5	37.0	2464.0	26.4	2464.0	26.4	95.5	4.5
VININI-97SF-11-171	67	25273	1.2	6.1697	0.5	10.3846	2.2	0.4647	2.1	0.97	2460.2	43.8	2469.7	20.5	2477.5	9.3	2477.5	9.3	99.3	0.7
VININI-97SF-11-119	302	236598	1.9	5.8782	0.2	11.3351	1.3	0.4832	1.3	0.99	2541.4	26.6	2551.1	12.0	2558.8	3.6	2558.8	3.6	99.3	0.7
VININI-97SF-11-83	39	38140	1.3	5.8084	0.8	11.7178	1.7	0.4936	1.5	0.89	2586.3	32.5	2582.1	16.0	2578.8	12.9	2578.8	12.9	100.3	-0.3
VININI-97SF-11-64	78	56320	1.4	5.7655	1.0	11.4819	2.3	0.4801	2.1	0.90	2527.8	44.2	2563.1	21.9	2591.2	16.9	2591.2	16.9	97.6	2.4
VININI-97SF-11-116	132	68890	2.2	5.7549	0.3	11.5848	0.6	0.4835	0.5	0.83	2542.6	10.5	2571.5	5.6	2594.2	5.5	2594.2	5.5	98.0	2.0
VININI-97SF-11-43	97	90131	1.9	5.7124	0.3	12.3047	1.0	0.5098	0.9	0.94	2655.7	20.3	2627.9	9.3	2606.6	5.5	2606.6	5.5	101.9	-1.9
VININI-97SF-11-80	41	63401	0.7	5.5871	0.6	12.3834	1.4	0.5018	1.3	0.91	2621.5	27.6	2633.9	13.2	2643.5	9.6	2643.5	9.6	99.2	0.8
VININI-97SF-11-92	57	111053	1.3	5.5806	0.3	12.5648	0.9	0.5086	0.8	0.93	2650.5	18.5	2647.6	8.6	2645.4	5.6	2645.4	5.6	100.2	-0.2
VININI-97SF-11-200	60	100513	1.1	5.4764	0.6	13.4425	1.0	0.5339	0.8	0.81	2757.9	18.8	2711.3	9.8	2676.6	10.1	2676.6	10.1	103.0	-3.0
VININI-97SF-11-72	64	54439	0.5	5.4749	0.5	12.9087	1.1	0.5126	1.0	0.89	2667.6	21.7	2673.0	10.5	2677.1	8.3	2677.1	8.3	99.6	0.4
VININI-97SF-11-188	168	80782	1.1	5.4709	0.1	13.2225	1.2	0.5247	1.2	0.99	2718.9	27.3	2695.7	11.7	2678.3	2.4	2678.3	2.4	101.5	-1.5
VININI-97SF-11-69	48	52485	1.5	5.4691	0.4	13.2482	1.7	0.5255	1.7	0.97	2722.5	37.6	2697.5	16.4	2678.8	6.7	2678.8	6.7	101.6	-1.6
VININI-97SF-11-46	165	39003	0.6	5.4482	0.2	12.4556	1.9	0.4922	1.9	1.00	2580.1	40.0	2639.4	17.8	2685.2	3.0	2685.2	3.0	96.1	3.9
VININI-97SF-11-62	177	113543	0.9	5.4240	0.2	13.4588	4.0	0.5294	4.0	1.00	2739.1	88.4	2712.4	37.5	2692.5	2.8	2692.5	2.8	101.7	-1.7
VININI-97SF-11-102	26	21015	0.5	5.4048	0.8	13.3199	1.7	0.5221	1.5	0.90	2708.2	33.8	2702.6	16.1	2698.4	12.4	2698.4	12.4	100.4	-0.4
VININI-97SF-11-174	19	21930	1.2	5.3960	1.0	13.2173	2.3	0.5173	2.1	0.91	2687.6	46.4	2695.3	21.9	2701.1	16.0	2701.1	16.0	99.5	0.5
VININI-97SF-11-108	88	36668	0.6	5.3944	0.3	13.4664	2.3	0.5269	2.3	0.99	2728.2	51.1	2712.9	21.9	2701.6	4.4	2701.6	4.4	101.0	-1.0
VININI-97SF-11-73	130	109070	0.7	5.3937	0.2	12.8656	1.2	0.5033	1.2	0.98	2627.9	25.3	2669.9	11.2	2701.8	3.6	2701.8	3.6	97.3	2.7
VININI-97SF-11-75	112	64953	0.9	5.3782	0.3	13.3490	0.7	0.5207	0.6	0.92	2702.1	14.0	2704.7	6.5	2706.5	4.5	2706.5	4.5	99.8	0.2
VININI-97SF-11-90	79	143842	1.1	5.3658	0.4	13.9583	1.3	0.5432	1.2	0.95	2796.8	27.3	2746.9	12.0	2710.3	6.4	2710.3	6.4	103.2	-3.2
VININI-97SF-11-194	45	40729	0.6	5.3557	0.5	14.1007	2.1	0.5477	2.0	0.97	2815.7	45.8	2756.5	19.6	2713.4	8.0	2713.4	8.0	103.8	-3.8
VININI-97SF-11-22	92	74917	0.8	5.3557	0.2	13.6992	1.0	0.5321	0.9	0.97	2750.4	20.9	2729.1	9.1	2713.4	3.6	2713.4	3.6	101.4	-1.4
VININI-97SF-11-120	41	19469	0.4	5.3465	0.3	13.5105	1.0	0.5239	0.9	0.94	2715.7	19.9	2716.0	9.0	2716.3	5.3	2716.3	5.3	100.0	0.0
VININI-97SF-11-126	38	21471	0.3	5.3380	0.6	13.3728	1.1	0.5177	0.9	0.86	2689.5	20.6	2706.3	10.3	2718.9	9.1	2718.9	9.1	98.9	1.1
VININI-97SF-11-147	30	30860	0.4	5.3048	0.7	13.8093	1.6	0.5313	1.5	0.90	2746.9	32.9	2736.7	15.5	2729.2	11.7	2729.2	11.7	100.7	-0.7
VININI-97SF-11-185	37	19455	1.0	5.3014	0.6	13.6739	1.2	0.5258	1.1	0.88	2723.5	24.1	2727.4	11.7	2730.2	9.7	2730.2	9.7	99.8	0.2
VININI-97SF-11-89	48	38408	1.6	5.2898	0.5	13.9833	0.7	0.5365	0.5	0.73	2768.7	11.9	2748.6	6.8	2733.8	8.1	2733.8	8.1	101.3	-1.3
VININI-97SF-11-152	40	9737	0.8	5.1804	0.6	14.4418	1.3	0.5426	1.1	0.87	2794.4	25.7	2779.2	12.4	2768.2	10.6	2768.2	10.6	100.9	-0.9
VININI-97SF-11-82	82	28437	1.6	5.0348	0.4	11.7699	3.6	0.4298	3.6	0.99	2304.8	70.1	2586.3	34.1	2814.9	6.6	2814.9	6.6	81.9	18.1
VININI-97SF-11-103	40	8209	0.7	5.0250	0.6	15.3149	1.2	0.5581	1.1	0.87	2859.0	24.8	2835.0	11.7	2818.0	9.8	2818.0	9.8	101.5	-1.5
VININI-97SF-11-104	97	65054	3.3	4.9992	2.3	13.6211	3.9	0.4939	3.1	0.80	2587.4	65.8	2723.7	36.7	2826.5	38.2	2826.5	38.2	91.5	8.5
VININI-97SF-11-155	98	118308	0.8	3.2308	0.4	31.5737	2.7	0.7398	2.6	0.99	3570.0	72.3	3537.1	26.3	3518.5	6.3	3518.5	6.3	101.5	-1.5
Sample: Elder Sandstone. Location: Elder Creek, Shoshone Range; 0516196 4460270 (NAD 83 UTM 11T)																				
ELDERSS-143 <>	463	19005	7.1	21.5974	8.6	0.0727	8.9	0.0114	2.5	0.27	73.0	1.8	71.3	6.2	13.4	207.1	73.0	1.8	NA	NA 0.8, 0.8
ELDERSS-29 <>	1260	12089	3.2	18.0411	0.7	0.4201	2.4	0.0550	2.2	0.95	344.9	7.5	356.1	7.1	429.5	16.7	344.9	7.5	NA	NA
ELDERSS-23 <>	256	54686	0.9	14.0057	1.0	1.5854	1.1	0.1610	0.5	0.50	962.6	4.9	964.5	6.8	968.9	19.4	968.9	19.4	99.4	0.6
ELDERSS-197 <>	56	26051	0.7	13.4985	2.7	1.7931	2.8	0.1755	1.0	0.35	1042.6	9.4	1043.0	18.4	1043.7	53.5	1043.7	53.5	99.9	0.1
ELDERSS-74 <>	132	56241	2.0	13.4913	1.3	1.7383	1.8	0.1701	1.2	0.69	1012.6	11.5	1022.8	11.4	1044.8	25.8	1044.8	25.8	96.9	3.1
ELDERSS-22 <>	136	85797	1.1	12.8970	1.3	2.0618	1.4	0.1929	0.5	0.34	1136.8	5.0	1136.2	9.7	1135.0	26.7	1135.0	26.7	100.2	-0.2
ELDERSS-99 <>	50	13222	1.8	11.9004	2.3	2.4903	4.9	0.2149	4.3	0.88	1255.1	49.2	1269.2	35.5	1293.2	45.5	1293.2	45.5	97.0	3.0
ELDERSS-185 <>	222	191878	2.0	11.3531	0.5	2.8591	0.8	0.2354	0.7	0.78	1362.8	8.1	1371.2	6.4	1384.2	10.2	1384.2	10.2	98.5	1.5
ELDERSS-155 <>	74	65602	2.1	11.2670	1.4	2.9634	1.5	0.2422	0.6	0.41	1397.9	7.9	1398.3	11.6	1398.8	26.6	1398.8	26.6	99.9	0.1
ELDERSS-87 <>	187	172967	0.9	10.8788	0.6	3.2648	1.3	0.2576	1.1	0.87	1477.5	14.7	1472.7	9.9	1465.8	11.7	1465.8	11.7	100.8	-0.8
ELDERSS-183 <>	143	136954	1.6	9.9179	0.7	4.0429	1.2	0.2908	0.9	0.80	1645.6	13.7	1642.9	9.6	1639.4	13.0	1639.4	13.0	100.4	-0.4
ELDERSS-184 <>	292	185849	5.2	9.9007	0.4	3.9798	1.3	0.2858	1.2	0.96	1620.4	17.9	1630.1	10.5	1642.6	6.5	1642.6	6.5	98.6	1.4
ELDERSS-145 <>	112	6588	0.7	9.8350	1.4	3.7989	3.2	0.2710	2.9	0.90	1545.7	39.3	1592.5	25.6	1655.0	25.7	1655.0	25.7	93.4	6.6
ELDERSS-109 <>	38	32248	1.3	9.6908	1.7	4.2513	2.1	0.2988	1.2	0.58	1685.3	18.1	1684.0	17.3	1682.3	31.7	1682.3	31.7	100.2	-0.2
ELDERSS-104 <>	614	87858	1.5	9.5047	0.2	3.6418	0.7	0.2510	0.6	0.95	1443.9	8.3	1558.7	5.4	1718.0	3.7	1718.0	3.7	84.0	16.0
ELDERSS-63 <>	337	228687	2.9	9.3265	0.4	4.5882	0.9	0.3104	0.8	0.91	1742.4	12.4	1747.1	7.4	1752.7	6.6	1752.7	6.6	99.4	0.6
ELDERSS-94 <>	325	445712	2.4	9.2080	0.2	4.7777	0.8	0.3191	0.8	0.97	1785.2	12.4	1781.0	6.9	1776.1	3.5	1776.1	3.5	100.5	-0.5
ELDERSS-3 <>	236	224617	2.7	9.1980	0.4	4.8018	0.7	0.3203	0.6	0.85	1791.3	9.5	1785.2	6.0	1778.1	6.8	1778.1	6.8	100.7	-0.7
ELDERSS-89 <>	731	211771	1.4	9.1566	0.2	4.6329	1.2	0.3077	1.2	0.99	1729.2	17.6	1755.2	9.8	1786.3	2.8	1786.3	2.8	96.8	3.2
ELDERSS-199 <>	45	36913	2.6	9.1386	1.7	4.7590	1.7	0.3154	0.5	0.30	1767.3	8.0	1777.7	14.6	1789.9	30.2	1789.9	30.2	98.7	1.3
ELDERSS-133 <>	172	148839	3.8	9.1353	0.4	4.7995	0.6	0.3180	0.5	0.78	1779.9	7.7	1784.8	5.3	1790.5	7.3	1790.5	7.3	99.4	0.6
ELDERSS-121 <>	118	91364	5.7	9.0936	0.5	4.9341	0.9	0.3254	0.8	0.83	1816.1	11.9	1808.1	7.7	1798.8	9.3	1798.8	9.3	101.0	-1.0
ELDERSS-140 <>	29	27025	1.5	9.0508	1.7	5.0503	1.8	0.3315	0.8	0.41	1845.7	12.0	1827.8	15.6	1807.4	30.6	1807.4	30.6	102.1	-2.1
ELDERSS-76 <>	55	75145	1.1	9.0392	1.3	4.9831	1.6	0.3267	0.9	0.55	1822.3	13.9	1816.5	13.4	1809.8	24.1	1809.8	24.1	100.7	-0.7
ELDERSS-56 <>	30	15195	1.2	9.0130	1.9	5.0117	2.1	0.3276	0.9	0.40	1826.8	13.6	1821.3	17.9	1815.0	35.1	1815.0	35.1	100.6	-0.6
ELDERSS-124 <>	48	46919	0.5	8.9844	1.0	4.9864	1.5	0.3249	1.2	0.75	1813.7	18.2	1817.0	13.1	1820.8	18.7	1820.8	18.7	99.6	0.4
ELDERSS-59 <>	63	58702	1.7	8.9743	1.2	5.0024	1.8	0.3256	1.4	0.77	1817.0	22.3	1819.7	15.4	1822.8	20.9	1822.8	20.9	99.7	0.3
ELDERSS-43 <>	35	30933	0.9	8.9694	1.2	5.0392	1.7	0.3278	1.1	0.68	1827.8	17.8	1825.9	14.0	1823.8	22.1	1823.8	22.1	100.2	-0.2
ELDERSS-90 <>	79	52161	0.8	8.9579	0.7	5.1591	1.3	0.3352	1.1	0.83	1863.4	17.4	1845.9	11.0	1826.2	12.9	1826.2	12.9	102.0	-2.0
ELDERSS-47 <>	22	23481	0.4	8.9579	2.8	5.1371	3.1	0.3338	1.2	0.40	1856.5	20.0	1842.3	26.3	1826.2	51.4	1826.2	51.4	101.7	-1.7
ELDERSS-83 <>	85	144312	2.3	8.9418	1.2	5.1432	1.6	0.3335	1.1	0.67	1855.5	17.7	1843.3	13.8	1829.4	21.8	1829.4	21.8	101.4	-1.4
ELDERSS-130 <>	70	73157	1.1	8.9369	0.9	4.9967	1.3	0.3239	0.9	0.73	1808.6	14.9	1818.8	10.9	1830.4	15.8	1830.4	15.8	98.8	1.2
ELDERSS-84 <>	55	56967	1.4	8.9356	0.9	5.2176	1.5	0.3381	1.2	0.81	1877.7	19.1	1855.5	12.4	1830.7	15.5	1830.7	15.5	102.6	-2.6
ELDERSS-142 <>	75	49812	1.9	8.9328	1.2	5.0866	1.4	0.3295	0.7	0.54	1836.2	11.8	1833.9	11.6	1831.2	20.8	1831.2	20.8	100.3	-0.3
ELDERSS-52 <>	30	40737	0.6	8.9307	1.8	5.0567	2.2	0.3275	1.3	0.59	1826.4	20.6	1828.9	18.6	1831.7	32.2	1831.7	32.2	99.7	0.3
ELDERSS-79 <>	110	431235	1.5	8.9280	0.5	5.1096	0.9	0.3309	0.8	0.86	1842.5	12.8	1837.7	7.9	1832.2	8.6	1832.2	8.6	100.6	-0.6
ELDERSS-189 <>	98	83569	1.3	8.9277	1.1	5.1404	1.5	0.3328	1.0	0.69	1852.1	16.1	1842.8	12.3	1832.3	19.1	1832.3	19.1	101.1	-1.1
ELDERSS-129 <>	90	96047	1.7	8.9266	0.6	4.3717	1.8	0.2830	1.7	0.95	1606.6	24.0	1707.0	14.7	1832.5	10.4	1832.5	10.4	87.7	12.3
ELDERSS-173 <>	71	89043	1.3	8.9226	1.0	5.1202	1.2	0.3313	0.7	0.58	1844.9	11.0	1839.5	10.0	1833.3	17.4	1833.3	17.4	100.6	-0.6
ELDERSS-110 <>	82	61362	1.4	8.9205	1.2	5.1439	1.5	0.3328	0.9	0.58	1851.9	13.9	1843.4	12.7	1833.8	22.0	1833.8	22.0	101.0	-1.0
ELDERSS-128 <>	168	209354	1.6	8.9197	0.4	5.1031	1.2	0.3301	1.1	0.94	1839.0	17.4	1836.6	9.8	1833.9	7.2	1833.9	7.2	100.3	-0.3
ELDERSS-187 <>	118	110481	1.7	8.9189	0.7	5.0737	1.0	0.3282	0.7	0.73	1829.6	11.6	1831.7	8.5	1834.1	12.4	1834.1	12.4	99.8	0.2
ELDERSS-194 <>	206	266044	1.6	8.9187	0.4	5.1596	0.7	0.3337	0.6	0.86	1856.5	10.2	1846.0	6.3	1834.1	6.9	1834.1	6.9	101.2	-1.2
ELDERSS-68 <>	76	71756	0.8	8.9159	0.9	5.1197	1.3	0.3311	0.9	0.70	1843.5	14.0	1839.4	10.6	1834.7	16.2	1834.7	16.2	100.5	-0.5
ELDERSS-42 <>	76	156915	1.3	8.9155	0.5	5.1285	0.8	0.3316	0.6	0.78	1846.2	10.3	1840.8	7.0	1834.8	9.4	1834.8	9.4	100.6	-0.6
ELDERSS-36 <>	87	114784	0.7	8.9148	0.5	5.1339	0.8	0.3319	0.6	0.82	1847.8	10.4	1841.7	6.7	1834.9	8.2	1834.9	8.2	100.7	-0.7
ELDERSS-86 <>	121	82963	0.8	8.9142	0.4	5.1282	0.8	0.3316	0.7	0.87	1845.9	11.7	1840.8	7.1	1835.0	7.5	1835.0	7.5	100.6	-0.6
ELDERSS-191 <>	107	68625	1.8	8.9139	0.8	5.2166	1.3	0.3372	1.0	0.79	1873.4	16.4	1855.3	10.8	1835.1	14.0	1835.1	14.0	102.1	-2.1
ELDERSS-96 <>	130	75780	0.8	8.9129	0.5	5.0911	1.1	0.3291	1.0	0.88	1834.0	16.1	1834.6	9.7	1835.3	9.6	1835.3	9.6	99.9	0.1

U-Pb geochronologic anlayses of selected Roberts Mountains allochthon strata

						Isotope ratios							Apparent ages (Ma)							
	U	206Pb	U/Th	206Pb*	±	207Pb*	±	206Pb*	±	error	206Pb*	±	207Pb*	±	206Pb*	±	Best age	±	Conc.	Discord.
	(ppm)	204Pb		207Pb*	(%)	235U*	(%)	238U	(%)	corr.	238U*	(Ma)	235U	(Ma)	207Pb*	(Ma)	(Ma)	(Ma)	(%)	(%)
Sample: Elder Sandstone. Location: Elder Creek, Shoshone Range; 0516196 4460270 (NAD 83 UTM 11T)																				
ELDERSS-49 <>	217	218333	1.5	8.9118	0.4	5.1873	1.2	0.3353	1.1	0.95	1863.9	18.5	1850.5	10.3	1835.5	7.0	1835.5	7.0	101.5	-1.5
ELDERSS-64 <>	91	114121	1.2	8.9110	0.5	5.1990	1.1	0.3360	1.0	0.87	1867.4	16.0	1852.5	9.6	1835.7	9.9	1835.7	9.9	101.7	-1.7
ELDERSS-85 <>	334	120849	2.0	8.9086	0.2	4.7108	2.6	0.3044	2.6	1.00	1713.0	39.6	1769.2	22.1	1836.2	4.5	1836.2	4.5	93.3	6.7
ELDERSS-200 <>	111	83082	1.7	8.9086	0.5	5.1175	1.0	0.3306	0.9	0.88	1841.5	14.1	1839.0	8.5	1836.2	8.5	1836.2	8.5	100.3	-0.3
ELDERSS-88 <>	104	83527	1.1	8.9065	0.6	5.1581	0.8	0.3332	0.5	0.64	1853.8	8.5	1845.7	7.0	1836.6	11.4	1836.6	11.4	100.9	-0.9
ELDERSS-80 <>	76	99241	1.2	8.9050	1.3	5.1131	1.6	0.3302	0.9	0.56	1839.5	14.3	1838.3	13.7	1836.9	24.3	1836.9	24.3	100.1	-0.1
ELDERSS-75 <>	60	59563	1.6	8.9042	0.8	5.1059	1.3	0.3297	1.0	0.79	1837.1	16.7	1837.1	11.2	1837.1	14.5	1837.1	14.5	100.0	0.0
ELDERSS-98 <>	34	21414	0.7	8.9038	2.3	5.1372	2.7	0.3317	1.3	0.50	1846.8	21.6	1842.3	23.0	1837.1	42.6	1837.1	42.6	100.5	-0.5
ELDERSS-45 <>	155	142861	1.7	8.8976	0.5	5.1479	0.8	0.3322	0.6	0.77	1849.1	9.4	1844.1	6.4	1838.4	8.7	1838.4	8.7	100.6	-0.6
ELDERSS-150 <>	76	50979	1.3	8.8973	0.7	5.2407	1.5	0.3382	1.3	0.88	1877.9	21.0	1859.3	12.5	1838.5	12.7	1838.5	12.7	102.1	-2.1
ELDERSS-127 <>	157	120824	1.7	8.8954	0.6	4.5174	2.1	0.2914	2.0	0.96	1648.7	29.0	1734.2	17.2	1838.9	10.4	1838.9	10.4	89.7	10.3
ELDERSS-51 <>	58	56474	1.9	8.8940	0.9	5.1072	1.3	0.3294	0.9	0.70	1835.7	14.1	1837.3	10.7	1839.1	16.3	1839.1	16.3	99.8	0.2
ELDERSS-6 <>	104	179003	1.2	8.8938	0.9	5.0954	1.3	0.3287	1.0	0.73	1832.0	15.4	1835.3	11.2	1839.2	16.2	1839.2	16.2	99.6	0.4
ELDERSS-100 <>	63	44668	3.2	8.8912	1.4	4.4198	1.9	0.2850	1.4	0.71	1616.5	19.8	1716.1	16.1	1839.7	24.6	1839.7	24.6	87.9	12.1
ELDERSS-138 <>	65	71616	1.6	8.8901	1.9	5.1041	2.1	0.3291	0.9	0.43	1834.0	14.6	1836.8	17.9	1839.9	34.5	1839.9	34.5	99.7	0.3
ELDERSS-108 <>	82	66583	1.0	8.8901	0.6	5.1660	1.1	0.3331	0.9	0.83	1853.3	14.5	1847.0	9.3	1839.9	11.1	1839.9	11.1	100.7	-0.7
ELDERSS-70 <>	55	56099	1.0	8.8900	1.0	4.5934	3.2	0.2962	3.0	0.95	1672.3	44.0	1748.1	26.3	1840.0	18.1	1840.0	18.1	90.9	9.1
ELDERSS-44 <>	105	114428	3.5	8.8891	0.7	5.2165	1.4	0.3363	1.2	0.85	1868.9	19.2	1855.3	11.8	1840.1	13.0	1840.1	13.0	101.6	-1.6
ELDERSS-118 <>	145	115477	2.0	8.8889	0.7	5.1279	1.1	0.3306	0.9	0.78	1841.2	14.1	1840.7	9.6	1840.2	12.7	1840.2	12.7	100.1	-0.1
ELDERSS-82 <>	235	480780	1.2	8.8848	0.4	5.1698	0.7	0.3331	0.5	0.76	1853.6	8.2	1847.7	5.7	1841.0	8.0	1841.0	8.0	100.7	-0.7
ELDERSS-25 <>	59	69246	1.4	8.8838	1.6	5.0809	1.8	0.3274	0.7	0.42	1825.6	11.8	1832.9	15.1	1841.2	29.2	1841.2	29.2	99.2	0.8
ELDERSS-144 <>	41	46781	0.8	8.8797	0.8	5.1500	1.1	0.3317	0.8	0.68	1846.5	12.6	1844.4	9.7	1842.0	15.2	1842.0	15.2	100.2	-0.2
ELDERSS-153 <>	63	60767	0.6	8.8721	0.5	5.1636	0.9	0.3323	0.8	0.85	1849.3	12.2	1846.6	7.6	1843.6	8.6	1843.6	8.6	100.3	-0.3
ELDERSS-112 <>	110	198208	2.1	8.8704	0.5	5.1722	1.1	0.3328	1.0	0.90	1851.7	16.5	1848.1	9.7	1843.9	9.1	1843.9	9.1	100.4	-0.4
ELDERSS-78 <>	90	258213	1.5	8.8701	0.6	5.2328	1.6	0.3366	1.4	0.91	1870.5	23.3	1858.0	13.4	1844.0	11.5	1844.0	11.5	101.4	-1.4
ELDERSS-149 <>	43	46516	1.2	8.8698	1.0	5.1303	1.3	0.3300	0.8	0.60	1838.5	12.5	1841.1	11.1	1844.1	19.0	1844.1	19.0	99.7	0.3
ELDERSS-34 <>	115	205282	1.3	8.8686	0.5	5.2001	0.8	0.3345	0.6	0.81	1860.0	10.0	1852.6	6.5	1844.3	8.2	1844.3	8.2	100.9	-0.9
ELDERSS-163 <>	155	114274	2.1	8.8682	0.4	4.6673	3.4	0.3002	3.4	0.99	1692.3	50.6	1761.4	28.7	1844.4	8.0	1844.4	8.0	91.8	8.2
ELDERSS-156 <>	206	425547	1.6	8.8681	0.4	5.2459	0.8	0.3374	0.7	0.87	1874.2	11.5	1860.1	6.9	1844.4	7.2	1844.4	7.2	101.6	-1.6
ELDERSS-28 <>	123	180092	2.1	8.8653	0.4	5.2032	1.8	0.3346	1.8	0.97	1860.4	28.5	1853.1	15.5	1845.0	7.6	1845.0	7.6	100.8	-0.8
ELDERSS-175 <>	81	65325	0.8	8.8650	0.7	5.1849	1.0	0.3334	0.8	0.78	1854.7	13.1	1850.1	8.9	1845.0	11.9	1845.0	11.9	100.5	-0.5
ELDERSS-151 <>	84	65452	1.5	8.8634	0.6	5.1969	0.8	0.3341	0.5	0.66	1858.1	8.4	1852.1	6.7	1845.4	10.8	1845.4	10.8	100.7	-0.7
ELDERSS-111 <>	99	92275	1.6	8.8631	0.6	5.1977	0.9	0.3341	0.7	0.74	1858.3	10.9	1852.2	7.7	1845.4	11.0	1845.4	11.0	100.7	-0.7
ELDERSS-177 <>	118	123861	1.8	8.8628	0.6	5.1150	0.9	0.3288	0.7	0.73	1832.5	10.4	1838.6	7.6	1845.5	10.9	1845.5	10.9	99.3	0.7
ELDERSS-72 <>	91	118382	1.6	8.8602	0.5	5.1936	0.9	0.3337	0.7	0.81	1856.5	11.8	1851.6	7.7	1846.0	9.7	1846.0	9.7	100.6	-0.6
ELDERSS-171 <>	42	53500	1.4	8.8600	1.5	5.2359	1.8	0.3364	1.0	0.57	1869.6	16.4	1858.5	15.1	1846.1	26.4	1846.1	26.4	101.3	-1.3
ELDERSS-162 <>	30	24123	0.9	8.8594	1.4	5.1953	2.4	0.3338	1.9	0.80	1856.9	31.3	1851.8	20.6	1846.2	26.0	1846.2	26.0	100.6	-0.6
ELDERSS-117 <>	143	201862	1.9	8.8593	0.3	5.1883	0.8	0.3334	0.8	0.92	1854.7	12.5	1850.7	7.2	1846.2	5.9	1846.2	5.9	100.5	-0.5
ELDERSS-126 <>	151	358113	1.7	8.8578	0.6	4.9248	1.3	0.3164	1.2	0.90	1772.0	18.2	1806.5	11.0	1846.5	10.5	1846.5	10.5	96.0	4.0
ELDERSS-16 <>	107	217485	1.8	8.8570	0.5	5.2303	0.8	0.3360	0.5	0.70	1867.3	8.6	1857.6	6.5	1846.7	9.7	1846.7	9.7	101.1	-1.1
ELDERSS-101 <>	117	107829	1.6	8.8569	0.4	5.1895	0.6	0.3334	0.4	0.68	1854.6	6.4	1850.9	5.0	1846.7	7.7	1846.7	7.7	100.4	-0.4
ELDERSS-102 <>	223	324482	1.8	8.8534	0.5	5.2102	0.9	0.3345	0.7	0.78	1860.4	11.0	1854.3	7.4	1847.4	9.8	1847.4	9.8	100.7	-0.7
ELDERSS-134 <>	118	101378	1.2	8.8525	0.5	5.1805	0.8	0.3326	0.7	0.80	1851.0	10.8	1849.4	7.1	1847.6	9.0	1847.6	9.0	100.2	-0.2
ELDERSS-165 <>	53	40051	1.3	8.8520	0.8	5.2337	1.1	0.3360	0.7	0.65	1867.4	11.4	1858.1	9.2	1847.7	14.7	1847.7	14.7	101.1	-1.1
ELDERSS-122 <>	199	153850	2.0	8.8479	0.3	5.2277	0.6	0.3355	0.6	0.91	1864.8	8.9	1857.1	5.2	1848.5	4.6	1848.5	4.6	100.9	-0.9
ELDERSS-30 <>	325	25733	3.0	8.8478	0.3	4.2523	3.3	0.2729	3.2	1.00	1555.3	44.8	1684.2	26.7	1848.6	5.4	1848.6	5.4	84.1	15.9
ELDERSS-103 <>	36	24389	1.0	8.8478	2.2	5.2694	2.5	0.3381	1.2	0.49	1877.7	20.0	1863.9	21.2	1848.6	39.1	1848.6	39.1	101.6	-1.6
ELDERSS-18 <>	31	36073	0.7	8.8459	1.3	5.2648	1.8	0.3378	1.3	0.68	1875.9	20.6	1863.2	15.8	1848.9	24.4	1848.9	24.4	101.5	-1.5
ELDERSS-107 <>	69	52402	2.2	8.8459	0.8	5.1842	1.4	0.3326	1.2	0.81	1851.0	18.6	1850.0	12.1	1848.9	14.9	1848.9	14.9	100.1	-0.1
ELDERSS-115 <>	235	306229	1.6	8.8457	0.2	5.2118	0.5	0.3344	0.4	0.90	1859.5	7.1	1854.5	4.2	1849.0	4.0	1849.0	4.0	100.6	-0.6
ELDERSS-33 <>	95	110969	2.0	8.8441	0.9	5.1608	1.5	0.3310	1.2	0.82	1843.4	19.2	1846.2	12.5	1849.3	15.4	1849.3	15.4	99.7	0.3
ELDERSS-13 <>	218	124615	1.7	8.8391	0.3	5.3010	1.5	0.3398	1.5	0.98	1885.9	24.0	1869.0	12.7	1850.3	4.9	1850.3	4.9	101.9	-1.9
ELDERSS-164 <>	298	194707	1.8	8.8355	0.2	5.0537	1.1	0.3238	1.0	0.98	1808.5	16.6	1828.4	9.1	1851.1	3.8	1851.1	3.8	97.7	2.3
ELDERSS-21 <>	30	30954	1.9	8.8344	2.1	5.2980	2.7	0.3395	1.7	0.64	1884.0	27.9	1868.5	22.9	1851.3	37.3	1851.3	37.3	101.8	-1.8
ELDERSS-116 <>	74	209506	0.8	8.8337	0.5	5.2547	1.1	0.3367	1.0	0.91	1870.6	16.5	1861.5	9.5	1851.4	8.3	1851.4	8.3	101.0	-1.0
ELDERSS-167 <>	219	190824	1.2	8.8313	0.3	5.2310	0.5	0.3351	0.4	0.81	1862.8	6.4	1857.7	4.1	1851.9	5.2	1851.9	5.2	100.6	-0.6
ELDERSS-159 <>	284	301976	1.9	8.8299	0.3	5.2690	0.6	0.3374	0.6	0.88	1874.3	9.0	1863.9	5.4	1852.2	5.5	1852.2	5.5	101.2	-1.2
ELDERSS-17 <>	169	50387	1.4	8.8259	0.3	5.1768	1.7	0.3314	1.7	0.98	1845.0	26.9	1848.8	14.6	1853.0	6.3	1853.0	6.3	99.6	0.4
ELDERSS-2 <>	145	196658	1.3	8.8213	0.3	5.1587	0.9	0.3300	0.8	0.93	1838.6	13.5	1845.8	7.7	1854.0	6.1	1854.0	6.1	99.2	0.8
ELDERSS-4 <>	77	68040	0.6	8.8204	1.2	5.2958	1.6	0.3388	1.0	0.65	1880.8	16.7	1868.2	13.5	1854.2	21.7	1854.2	21.7	101.4	-1.4
ELDERSS-179 <>	105	95160	1.3	8.7979	0.4	5.2751	1.0	0.3366	0.8	0.89	1870.3	13.7	1864.8	8.1	1858.8	7.9	1858.8	7.9	100.6	-0.6
ELDERSS-192 <>	121	137449	1.0	8.7979	0.6	5.2408	1.4	0.3344	1.3	0.91	1859.7	20.7	1859.3	12.0	1858.8	10.3	1858.8	10.3	100.1	-0.1
ELDERSS-193 <>	68	77421	1.2	8.7955	1.1	5.1831	1.4	0.3306	0.8	0.60	1841.5	13.1	1849.8	11.7	1859.3	19.9	1859.3	19.9	99.0	1.0
ELDERSS-69 <>	35	60647	1.0	8.7955	1.2	5.2110	1.6	0.3324	1.2	0.71	1850.1	18.8	1854.4	14.0	1859.3	21.0	1859.3	21.0	99.5	0.5
ELDERSS-40 <>	60	53177	0.5	8.7925	0.7	5.2664	1.2	0.3358	0.9	0.79	1866.6	15.2	1863.4	10.1	1859.9	13.0	1859.9	13.0	100.4	-0.4
ELDERSS-15 <>	30	22980	1.1	8.7911	1.6	5.2223	2.1	0.3330	1.3	0.64	1852.8	21.2	1856.3	17.6	1860.2	28.9	1860.2	28.9	99.6	0.4
ELDERSS-198 <>	33	28323	0.7	8.7880	2.2	5.3261	2.4	0.3395	1.1	0.45	1884.1	17.8	1873.1	20.9	1860.8	39.4	1860.8	39.4	101.3	-1.3
ELDERSS-119 <>	65	60912	4.1	8.7851	0.9	5.2899	1.7	0.3371	1.5	0.86	1872.5	23.8	1867.2	14.6	1861.4	16.0	1861.4	16.0	100.6	-0.6
ELDERSS-154 <>	63	118711	1.2	8.7828	1.2	5.2713	1.5	0.3358	0.8	0.54	1866.3	13.0	1864.2	12.6	1861.9	22.3	1861.9	22.3	100.2	-0.2
ELDERSS-139 <>	24	24561	1.2	8.7611	3.6	5.3308	3.8	0.3387	1.2	0.31	1880.5	19.2	1873.8	32.6	1866.3	65.5	1866.3	65.5	100.8	-0.8
ELDERSS-135 <>	125	132820	2.3	8.7496	0.5	5.3347	0.8	0.3385	0.6	0.73	1879.6	9.5	1874.4	6.8	1868.7	9.8	1868.7	9.8	100.6	-0.6
ELDERSS-120 <>	35	8195	0.9	8.7479	3.3	5.2524	3.4	0.3332	0.9	0.27	1854.1	15.1	1861.2	29.1	1869.1	59.1	1869.1	59.1	99.2	0.8
ELDERSS-12 <>	113	202363	1.2	8.7407	0.5	5.3847	1.2	0.3414	1.0	0.89	1893.2	17.2	1882.4	10.1	1870.6	9.5	1870.6	9.5	101.2	-1.2
ELDERSS-31 <>	146	171774	3.3	8.7162	0.4	5.3271	2.7	0.3368	2.7	0.99	1871.1	44.3	1873.2	23.5	1875.6	6.5	1875.6	6.5	99.8	0.2
ELDERSS-14 <>	137	22068	0.8	8.7031	2.2	5.1965	2.7	0.3280	1.5	0.57	1828.7	24.2	1852.0	22.7	1878.3	39.4	1878.3	39.4	97.4	2.6
ELDERSS-181 <>	41	29795	1.7	8.6769	1.0	5.3612	1.4	0.3374	1.0	0.68	1874.1	16.0	1878.7	12.3	1883.8	18.9	1883.8	18.9	99.5	0.5
ELDERSS-141 <>	74	116996	1.5	8.6712	0.8	5.4649	1.2	0.3437	0.9	0.74	1904.4	15.1	1895.1	10.7	1884.9	15.1	1884.9	15.1	101.0	-1.0
ELDERSS-148 <>	32	34824	0.9	8.6183	1.8	5.5477	2.1	0.3468	1.2	0.56	1919.1	19.9	1908.0	18.4	1896.0	31.9	1896.0	31.9	101.2	-1.2
ELDERSS-152 <>	26	42201	1.0	8.6082	2.4	5.4602	2.7	0.3409	1.4	0.50	1891.0	22.3	1894.4	23.6	1898.1	42.9	1898.1	42.9	99.6	0.4
ELDERSS-174 <>	53	38033	1.1	8.6068	2.3	5.4100	2.9	0.3377	1.9	0.63	1875.6	30.2	1886.4	25.3	1898.4	41.2	1898.4	41.2	98.8	1.2
ELDERSS-60 <>	60	59225	0.9	8.5999	1.1	5.6068	1.3	0.3497	0.7	0.55	1933.2	12.2	1917.1	11.5	1899.8	20.0	1899.8	20.0	101.8	-1.8
ELDERSS-158 <>	21	22437	0.8	8.5778	2.6	5.6452	3.2	0.3512	1.7	0.55	1940.3	29.3	1923.0	27.2	1904.4	47.2	1904.4	47.2	101.9	-1.9
ELDERSS-176 <>	78	61265	0.9	8.5441	0.9	5.5466	1.0	0.3437	0.6	0.56	1904.5	9.6	1907.9	8.9	1911.5	15.4	1911.5	15.4	99.6	0.4
ELDERSS-136 <>	61	126244	0.7	8.5394	0.9	5.6082	1.3	0.3473	0.9	0.70	1921.9	15.0	1917.4	11.1	1912.5	16.4	1912.5	16.4	100.5	-0.5

U-Pb geochronologic anlayses of selected Roberts Mountains allochthon strata

						Isotope ratios							Apparent ages (Ma)							
	U	206Pb	U/Th	206Pb*	±	207Pb*	±	206Pb*	±	error	206Pb*	±	207Pb*	±	206Pb*	±	Best age	±	Conc.	Discord.
	(ppm)	204Pb		207Pb*	(%)	235U*	(%)	238U	(%)	corr.	238U*	(Ma)	235U	(Ma)	207Pb*	(Ma)	(Ma)	(Ma)	(%)	(%)
Sample: Elder Sandstone. Location: Elder Creek, Shoshone Range; 0516196 4460270 (NAD 83 UTM 11T)																				
ELDERSS-41 <>	29	35676	0.9	8.5345	1.3	5.6243	1.4	0.3481	0.7	0.46	1925.7	10.9	1919.8	12.2	1913.5	22.5	1913.5	22.5	100.6	-0.6
ELDERSS-92 <>	99	177855	0.7	8.5163	0.7	4.6904	1.6	0.2897	1.5	0.89	1640.1	21.2	1765.5	13.7	1917.3	13.1	1917.3	13.1	85.5	14.5
ELDERSS-180 <>	56	36132	0.7	8.5119	1.1	5.6435	1.2	0.3484	0.5	0.40	1926.9	8.1	1922.8	10.4	1918.3	19.9	1918.3	19.9	100.5	-0.5
ELDERSS-24 <>	112	283830	1.2	8.4649	0.8	5.7724	1.1	0.3544	0.7	0.67	1955.5	12.6	1942.3	9.7	1928.2	15.0	1928.2	15.0	101.4	-1.4
ELDERSS-7 <>	34	45222	0.2	8.4617	1.3	5.7095	1.4	0.3504	0.5	0.37	1936.5	8.9	1932.8	12.5	1928.9	24.0	1928.9	24.0	100.4	-0.4
ELDERSS-8 <>	109	181067	1.7	8.4584	0.7	5.7392	1.1	0.3521	0.8	0.76	1944.5	14.0	1937.3	9.6	1929.6	13.0	1929.6	13.0	100.8	-0.8
ELDERSS-106 <>	42	136724	1.0	8.4175	1.2	5.7160	1.6	0.3490	1.0	0.62	1929.6	16.6	1933.8	13.8	1938.2	22.2	1938.2	22.2	99.6	0.4
ELDERSS-132 <>	90	97520	1.2	8.3935	0.6	5.8141	0.7	0.3539	0.4	0.62	1953.4	7.5	1948.5	6.3	1943.4	10.1	1943.4	10.1	100.5	-0.5
ELDERSS-53 <>	77	19906	1.0	8.2721	2.2	5.9103	2.3	0.3546	0.7	0.32	1956.5	12.4	1962.8	19.9	1969.4	38.7	1969.4	38.7	99.3	0.7
ELDERSS-81 <>	41	44088	0.6	7.8282	1.3	6.7012	1.6	0.3805	1.0	0.58	2078.5	17.0	2072.8	14.5	2067.1	23.6	2067.1	23.6	100.5	-0.5
ELDERSS-66 <>	84	112732	1.0	7.8206	0.7	6.6936	1.6	0.3797	1.5	0.91	2074.7	26.4	2071.8	14.5	2068.9	12.2	2068.9	12.2	100.3	-0.3
ELDERSS-65 <>	37	7116	0.6	7.7917	0.9	6.7475	1.2	0.3813	0.8	0.67	2082.4	14.0	2078.9	10.4	2075.4	15.4	2075.4	15.4	100.3	-0.3
ELDERSS-182 <>	56	82181	1.3	7.7877	1.0	6.7177	1.5	0.3794	1.1	0.73	2073.6	19.4	2075.0	13.2	2076.3	17.8	2076.3	17.8	99.9	0.1
ELDERSS-172 <>	205	286259	2.3	7.7793	0.3	6.8295	0.7	0.3853	0.6	0.91	2101.1	10.7	2089.6	5.8	2078.2	4.7	2078.2	4.7	101.1	-1.1
ELDERSS-57 <>	68	74519	1.4	7.7793	0.6	6.8074	1.2	0.3841	1.0	0.87	2095.3	17.9	2086.7	10.2	2078.2	10.1	2078.2	10.1	100.8	-0.8
ELDERSS-190 <>	42	49227	1.3	7.7765	1.0	6.7742	1.3	0.3821	0.9	0.68	2085.9	15.9	2082.4	11.7	2078.8	17.1	2078.8	17.1	100.3	-0.3
ELDERSS-1 <>	60	45885	1.0	7.7751	0.8	6.7537	1.3	0.3808	1.0	0.76	2080.2	17.6	2079.7	11.4	2079.1	14.7	2079.1	14.7	100.1	-0.1
ELDERSS-188 <>	167	194472	1.5	7.7703	0.3	6.7408	0.7	0.3799	0.6	0.89	2075.7	10.8	2078.0	6.1	2080.2	5.5	2080.2	5.5	99.8	0.2
ELDERSS-93 <>	16	23988	0.5	7.7679	1.7	6.6596	2.0	0.3752	1.0	0.53	2053.8	18.4	2067.3	17.5	2080.7	29.5	2080.7	29.5	98.7	1.3
ELDERSS-37 <>	250	240027	2.3	7.7546	0.2	6.7902	1.0	0.3819	1.0	0.97	2085.1	17.7	2084.4	9.0	2083.8	4.2	2083.8	4.2	100.1	-0.1
ELDERSS-38 <>	55	77482	1.6	7.7546	0.6	6.8097	1.4	0.3830	1.3	0.90	2090.2	23.0	2087.0	12.6	2083.8	10.8	2083.8	10.8	100.3	-0.3
ELDERSS-11 <>	122	84593	2.1	7.7534	0.5	6.7676	1.0	0.3806	0.8	0.85	2078.9	15.0	2081.5	8.8	2084.0	9.2	2084.0	9.2	99.8	0.2
ELDERSS-166 <>	108	187062	1.4	7.7458	0.3	6.8787	0.8	0.3864	0.7	0.90	2106.2	12.7	2095.9	6.9	2085.8	5.9	2085.8	5.9	101.0	-1.0
ELDERSS-157 <>	78	71436	1.6	7.7360	0.9	6.8850	1.1	0.3863	0.6	0.59	2105.6	11.5	2096.7	9.7	2088.0	15.6	2088.0	15.6	100.8	-0.8
ELDERSS-27 <>	114	112866	1.4	7.7357	0.5	6.9254	0.6	0.3885	0.4	0.66	2116.1	7.4	2101.9	5.5	2088.1	8.1	2088.1	8.1	101.3	-1.3
ELDERSS-146 <>	106	79515	0.5	7.7339	0.8	6.7903	1.1	0.3809	0.8	0.68	2080.4	13.8	2084.5	10.1	2088.5	14.6	2088.5	14.6	99.6	0.4
ELDERSS-114 <>	16	20153	0.5	7.7262	3.4	6.8791	3.8	0.3855	1.6	0.41	2101.8	27.9	2096.0	33.4	2090.2	60.3	2090.2	60.3	100.6	-0.6
ELDERSS-178 <>	62	75401	1.4	7.7219	1.0	6.8626	1.4	0.3843	0.9	0.69	2096.5	17.0	2093.8	12.2	2091.2	17.5	2091.2	17.5	100.3	-0.3
ELDERSS-123 <>	87	141464	1.0	7.7107	0.4	7.1694	3.1	0.4009	3.1	0.99	2173.3	57.5	2132.7	28.0	2093.8	6.3	2093.8	6.3	103.8	-3.8
ELDERSS-195 <>	19	35465	0.8	7.6614	2.4	6.8129	2.8	0.3786	1.4	0.50	2069.6	25.1	2087.4	25.0	2105.0	43.0	2105.0	43.0	98.3	1.7
ELDERSS-39 <>	253	624938	1.9	6.9476	0.2	8.3585	1.4	0.4212	1.4	0.99	2265.8	25.9	2270.7	12.4	2275.1	3.6	2275.1	3.6	99.6	0.4
ELDERSS-46 <>	83	74014	1.7	6.7976	0.4	8.7993	1.1	0.4338	1.0	0.91	2322.9	19.2	2317.4	9.9	2312.6	7.7	2312.6	7.7	100.4	-0.4
ELDERSS-54 <>	92	342415	2.0	6.1576	0.4	10.6530	0.8	0.4758	0.7	0.90	2508.7	14.9	2493.3	7.4	2480.8	5.9	2480.8	5.9	101.1	-1.1
ELDERSS-147 <>	238	480675	1.2	6.0331	0.2	10.5102	0.6	0.4599	0.6	0.96	2439.1	12.2	2480.8	5.8	2515.2	3.1	2515.2	3.1	97.0	3.0
ELDERSS-55 <>	86	109099	1.8	5.9692	0.5	11.1532	1.1	0.4829	1.0	0.92	2539.7	22.0	2536.0	10.7	2533.1	7.7	2533.1	7.7	100.3	-0.3
ELDERSS-35 <>	90	69078	1.5	5.9336	0.4	11.3082	1.7	0.4866	1.7	0.98	2556.1	36.0	2548.9	16.3	2543.1	6.2	2543.1	6.2	100.5	-0.5
ELDERSS-5 <>	107	88583	1.5	5.8319	0.5	11.6983	1.4	0.4948	1.3	0.95	2591.4	28.6	2580.6	13.2	2572.0	7.6	2572.0	7.6	100.8	-0.8
ELDERSS-10 <>	94	186588	1.7	5.7951	0.4	11.7280	1.0	0.4929	0.9	0.92	2583.3	19.3	2582.9	9.2	2582.6	6.5	2582.6	6.5	100.0	0.0
ELDERSS-160 <>	99	174317	1.6	5.7770	0.3	11.9143	0.7	0.4992	0.6	0.88	2610.3	13.3	2597.7	6.6	2587.8	5.5	2587.8	5.5	100.9	-0.9
ELDERSS-26 <>	97	233706	1.3	5.7139	0.3	12.1106	1.4	0.5019	1.3	0.98	2621.8	28.9	2613.0	12.9	2606.2	4.8	2606.2	4.8	100.6	-0.6
ELDERSS-62 <>	36	124177	1.3	5.6648	0.6	12.2916	0.9	0.5050	0.6	0.68	2635.2	13.1	2626.9	8.3	2620.5	10.8	2620.5	10.8	100.6	-0.6
ELDERSS-137 <>	29	29832	1.0	5.5998	0.6	12.1245	1.5	0.4924	1.4	0.91	2581.1	29.6	2614.1	14.3	2639.7	10.5	2639.7	10.5	97.8	2.2
ELDERSS-105 <>	111	101319	1.2	5.5549	0.3	12.7736	1.0	0.5146	0.9	0.94	2676.3	20.7	2663.1	9.5	2653.1	5.7	2653.1	5.7	100.9	-0.9
ELDERSS-71 <>	166	205889	0.7	5.4167	0.3	13.3403	0.7	0.5241	0.7	0.92	2716.5	14.9	2704.0	6.9	2694.7	4.8	2694.7	4.8	100.8	-0.8
ELDERSS-170 <>	112	102665	1.8	5.3951	0.4	14.0636	6.4	0.5503	6.4	1.00	2826.4	145.7	2754.0	60.6	2701.3	6.7	2701.3	6.7	104.6	-4.6
ELDERSS-67 <>	37	54762	0.8	5.3887	0.5	13.6905	1.1	0.5351	1.0	0.89	2762.7	22.3	2728.5	10.5	2703.3	8.2	2703.3	8.2	102.2	-2.2
ELDERSS-131 <>	63	363538	1.1	5.3569	0.4	13.4233	0.8	0.5215	0.7	0.87	2705.6	14.5	2709.9	7.1	2713.1	6.2	2713.1	6.2	99.7	0.3
ELDERSS-95 <>	67	132426	0.7	5.3448	0.3	13.5930	0.8	0.5269	0.7	0.92	2728.5	16.2	2721.8	7.5	2716.8	5.0	2716.8	5.0	100.4	-0.4
ELDERSS161 <>	57	27381	0.9	5.3413	0.4	13.7374	0.9	0.5322	0.8	0.89	2750.6	17.6	2731.8	8.4	2717.9	6.7	2717.9	6.7	101.2	-1.2
ELDERSS-77 <>	32	41093	2.2	5.2395	0.7	14.3539	3.8	0.5455	3.7	0.98	2806.3	85.1	2773.4	36.1	2749.5	10.9	2749.5	10.9	102.1	-2.1
ELDERSS-20 <>	78	83592	0.7	5.1814	0.3	14.0466	4.4	0.5279	4.4	1.00	2732.4	98.1	2752.9	41.8	2767.9	4.9	2767.9	4.9	98.7	1.3
ELDERSS-168 <>	93	99897	1.4	5.1657	0.4	14.2307	0.6	0.5332	0.5	0.81	2754.7	11.2	2765.2	5.9	2772.9	6.0	2772.9	6.0	99.3	0.7
ELDERSS-48 <>	35	94709	1.4	4.6421	0.3	17.3120	0.8	0.5828	0.8	0.92	2960.4	18.5	2952.3	8.1	2946.8	5.4	2946.8	5.4	100.5	-0.5
ELDERSS-50 <>	237	302151	1.6	4.6071	0.2	17.1584	2.5	0.5733	2.5	1.00	2921.5	57.6	2943.7	23.6	2959.0	3.6	2959.0	3.6	98.7	1.3
ELDERSS-73 <>	83	156251	1.4	4.5302	0.4	17.9749	1.2	0.5906	1.2	0.95	2991.8	28.2	2988.4	11.9	2986.1	6.4	2986.1	6.4	100.2	-0.2
ELDERSS-196 <>	57	116507	1.1	4.5032	0.2	18.2561	0.8	0.5962	0.7	0.95	3014.7	17.9	3003.3	7.5	2995.7	3.8	2995.7	3.8	100.6	-0.6
Sample: Slaven Chert. Location: Slaven Canyon, Shoshone Range; 0519428 4479302 (NAD 83 UTM 11T)																				
SLAVEN RMA-192	154	105026	0.8	13.5681	0.9	1.7562	1.6	0.1728	1.3	0.80	1027.6	12.0	1029.5	10.2	1033.3	19.1	1033.3	19.1	99.5	0.5 0.9, 0.8
SLAVEN RMA-113	30	26227	1.6	13.3586	4.8	1.8735	5.4	0.1815	2.4	0.45	1075.2	24.1	1071.8	35.9	1064.7	97.6	1064.7	97.6	101.0	-1.0
SLAVEN RMA-3	34	18032	1.5	12.4548	1.6	2.3192	2.8	0.2095	2.3	0.83	1226.1	26.2	1218.2	20.1	1204.1	31.4	1204.1	31.4	101.8	-1.8
SLAVEN RMA-43	174	144184	1.8	10.6361	0.6	3.3175	3.3	0.2559	3.3	0.98	1468.9	43.1	1485.2	26.0	1508.5	11.6	1508.5	11.6	97.4	2.6
SLAVEN RMA-118	122	147670	1.8	10.6334	0.5	3.3990	1.0	0.2621	0.9	0.90	1500.8	12.6	1504.2	8.2	1509.0	8.7	1509.0	8.7	99.5	0.5
SLAVEN RMA-123	107	61595	2.4	9.9185	1.1	4.0364	2.4	0.2904	2.1	0.89	1643.3	30.5	1641.6	19.2	1639.3	19.9	1639.3	19.9	100.2	-0.2
SLAVEN RMA-79	431	451993	4.7	9.8427	0.1	3.9814	1.3	0.2842	1.3	1.00	1612.6	18.8	1630.4	10.7	1653.5	2.1	1653.5	2.1	97.5	2.5
SLAVEN RMA-179	34	25022	0.8	9.4936	1.0	4.4599	2.2	0.3071	1.9	0.89	1726.3	29.1	1723.5	17.9	1720.1	18.2	1720.1	18.2	100.4	-0.4
SLAVEN RMA-172	218	231053	1.6	9.1565	0.4	4.6776	1.8	0.3106	1.7	0.98	1743.9	26.7	1763.3	14.9	1786.3	6.7	1786.3	6.7	97.6	2.4
SLAVEN RMA-185	64	156480	1.0	9.1032	0.8	4.6582	1.4	0.3075	1.1	0.80	1728.6	16.5	1759.8	11.4	1796.9	14.9	1796.9	14.9	96.2	3.8
SLAVEN RMA-27	90	119630	2.0	9.0928	0.5	4.8106	1.2	0.3172	1.1	0.91	1776.3	17.2	1786.8	10.2	1799.0	9.0	1799.0	9.0	98.7	1.3
SLAVEN RMA-14	141	183681	1.7	9.0911	0.3	4.9470	2.9	0.3262	2.8	0.99	1819.9	45.0	1810.3	24.1	1799.3	5.3	1799.3	5.3	101.1	-1.1
SLAVEN RMA-33	176	107162	2.8	9.0767	0.3	4.8216	2.1	0.3174	2.1	0.99	1777.1	32.7	1788.7	18.0	1802.2	6.1	1802.2	6.1	98.6	1.4
SLAVEN RMA-57	27	49096	2.0	9.0395	1.6	4.9069	2.8	0.3217	2.3	0.81	1798.0	35.3	1803.4	23.4	1809.7	29.4	1809.7	29.4	99.4	0.6
SLAVEN RMA-11	44	40346	0.5	8.9868	1.8	5.0309	5.2	0.3279	4.9	0.94	1828.2	78.5	1824.5	44.4	1820.3	32.1	1820.3	32.1	100.4	-0.4
SLAVEN RMA-178	39	70673	0.8	8.9823	2.2	4.9774	3.2	0.3243	2.3	0.72	1810.5	36.4	1815.5	26.9	1821.2	39.9	1821.2	39.9	99.4	0.6
SLAVEN RMA-176	15	12777	1.2	8.9670	2.7	5.0717	3.6	0.3298	2.4	0.66	1837.6	38.6	1831.4	30.9	1824.3	49.5	1824.3	49.5	100.7	-0.7
SLAVEN RMA-17	114	16675	1.3	8.9643	0.6	4.8063	1.5	0.3125	1.3	0.90	1752.9	20.4	1786.0	12.4	1824.9	11.5	1824.9	11.5	96.1	3.9
SLAVEN RMA-129	89	74468	1.4	8.9630	0.5	5.1440	2.3	0.3344	2.2	0.97	1859.6	36.0	1843.4	19.5	1825.1	9.7	1825.1	9.7	101.9	-1.9
SLAVEN RMA-168	47	79798	1.2	8.9628	1.3	4.9680	2.3	0.3229	1.9	0.83	1804.1	30.1	1813.9	19.5	1825.2	23.3	1825.2	23.3	98.8	1.2
SLAVEN RMA-15	159	337505	1.2	8.9608	0.3	5.0565	1.5	0.3286	1.4	0.98	1831.7	23.1	1828.8	12.6	1825.6	5.7	1825.6	5.7	100.3	-0.3
SLAVEN RMA-100	52	53917	2.8	8.9584	0.8	5.1026	3.3	0.3315	3.2	0.97	1845.8	51.3	1836.5	27.9	1826.1	14.2	1826.1	14.2	101.1	-1.1
SLAVEN RMA-167	26	16499	2.0	8.9426	1.9	5.0196	2.8	0.3256	2.1	0.75	1816.8	33.0	1822.6	23.6	1829.3	33.6	1829.3	33.6	99.3	0.7
SLAVEN RMA-78	61	75453	1.4	8.9376	0.7	4.8624	4.9	0.3152	4.9	0.99	1766.2	75.6	1795.8	41.7	1830.3	13.1	1830.3	13.1	96.5	3.5
SLAVEN RMA-180	73	52125	1.3	8.9309	1.0	5.0401	1.2	0.3265	0.7	0.57	1821.2	10.6	1826.1	10.0	1831.6	17.5	1831.6	17.5	99.4	0.6
SLAVEN RMA-152	91	132542	1.2	8.9303	0.8	5.0676	1.7	0.3282	1.5	0.88	1829.8	24.4	1830.7	14.8	1831.8	14.9	1831.8	14.9	99.9	0.1

U-Pb geochronologic anlayses of selected Roberts Mountains allochthon strata

						Isotope ratios							Apparent ages (Ma)							
	U	206Pb	U/Th	206Pb*	±	207Pb*	±	206Pb*	±	error	206Pb*	±	207Pb*	±	206Pb*	±	Best age	±	Conc.	Discord.
	(ppm)	204Pb		207Pb*	(%)	235U*	(%)	238U	(%)	corr.	238U*	(Ma)	235U	(Ma)	207Pb*	(Ma)	(Ma)	(Ma)	(%)	(%)
Sample: Slaven Chert. Location: Slaven Canyon, Shoshone Range; 0519428 4479302 (NAD 83 UTM 11T)																				
SLAVEN RMA-142	117	109625	1.1	8.9285	0.5	5.1101	1.2	0.3309	1.1	0.91	1842.8	17.1	1837.8	10.0	1832.1	9.1	1832.1	9.1	100.6	-0.6
SLAVEN RMA-186	191	58078	1.2	8.9271	0.3	5.0303	1.8	0.3257	1.7	0.99	1817.5	27.5	1824.4	15.0	1832.4	5.5	1832.4	5.5	99.2	0.8
SLAVEN RMA-131	31	61577	1.5	8.9217	1.5	5.0472	2.0	0.3266	1.4	0.69	1821.8	22.1	1827.3	17.1	1833.5	26.4	1833.5	26.4	99.4	0.6
SLAVEN RMA-171	54	61627	1.6	8.9207	1.0	5.2060	2.5	0.3368	2.3	0.91	1871.4	37.0	1853.6	21.3	1833.7	18.8	1833.7	18.8	102.1	-2.1
SLAVEN RMA-12	86	122215	1.4	8.9190	0.9	5.0822	2.4	0.3287	2.3	0.93	1832.3	36.3	1833.1	20.8	1834.0	16.4	1834.0	16.4	99.9	0.1
SLAVEN RMA-22	128	86828	1.1	8.9172	0.5	5.1138	1.5	0.3307	1.4	0.95	1841.9	22.7	1838.4	12.7	1834.4	8.4	1834.4	8.4	100.4	-0.4
SLAVEN RMA-28	55	59183	1.2	8.9161	0.8	4.8488	1.8	0.3136	1.5	0.88	1758.2	23.6	1793.4	14.8	1834.6	15.3	1834.6	15.3	95.8	4.2
SLAVEN RMA-124	125	111124	1.4	8.9146	0.4	4.6678	2.9	0.3018	2.8	0.99	1700.2	42.5	1761.5	24.0	1834.9	7.5	1834.9	7.5	92.7	7.3
SLAVEN RMA-46	76	120714	1.7	8.9144	0.4	4.9994	1.1	0.3232	1.1	0.94	1805.5	17.0	1819.2	9.7	1835.0	7.1	1835.0	7.1	98.4	1.6
SLAVEN RMA-16	44	29740	1.3	8.9117	1.6	5.1475	2.3	0.3327	1.6	0.69	1851.5	25.5	1844.0	19.4	1835.5	29.7	1835.5	29.7	100.9	-0.9
SLAVEN RMA-52	166	172336	1.4	8.9055	0.3	4.9763	2.3	0.3214	2.3	0.99	1796.6	35.4	1815.3	19.3	1836.8	5.9	1836.8	5.9	97.8	2.2
SLAVEN RMA-195	257	205593	1.7	8.9024	0.3	4.8982	2.3	0.3163	2.3	0.99	1771.4	35.4	1801.9	19.4	1837.4	4.6	1837.4	4.6	96.4	3.6
SLAVEN RMA-158	200	131219	1.6	8.9022	0.3	4.9000	2.4	0.3164	2.4	0.99	1772.0	37.0	1802.3	20.3	1837.5	5.7	1837.5	5.7	96.4	3.6
SLAVEN RMA-102	307	167140	2.2	8.9015	0.2	4.9225	1.7	0.3178	1.7	0.99	1779.0	26.1	1806.1	14.3	1837.6	3.1	1837.6	3.1	96.8	3.2
SLAVEN RMA-197	154	109996	1.7	8.9003	0.3	5.0744	1.8	0.3276	1.8	0.99	1826.5	29.0	1831.8	15.6	1837.9	4.9	1837.9	4.9	99.4	0.6
SLAVEN RMA-93	94	114605	1.5	8.9002	0.6	5.0491	2.2	0.3259	2.1	0.97	1818.6	33.4	1827.6	18.5	1837.9	10.0	1837.9	10.0	99.0	1.0
SLAVEN RMA-122	85	169822	1.2	8.8998	0.8	5.0800	1.5	0.3279	1.2	0.86	1828.2	19.8	1832.8	12.4	1837.9	13.7	1837.9	13.7	99.5	0.5
SLAVEN RMA-112	286	239066	4.9	8.8996	0.3	5.1671	0.9	0.3335	0.8	0.95	1855.4	13.5	1847.2	7.5	1838.0	5.2	1838.0	5.2	100.9	-0.9
SLAVEN RMA-193	71	73587	2.5	8.8988	0.9	5.1146	1.3	0.3301	0.9	0.71	1838.8	15.2	1838.5	11.3	1838.2	17.0	1838.2	17.0	100.0	0.0
SLAVEN RMA-127	44	41862	1.0	8.8983	1.0	5.1307	3.0	0.3311	2.9	0.95	1843.8	45.9	1841.2	25.7	1838.3	17.8	1838.3	17.8	100.3	-0.3
SLAVEN RMA-73	67	134699	1.3	8.8980	0.5	5.0011	1.4	0.3227	1.4	0.94	1803.1	21.5	1819.5	12.2	1838.3	8.6	1838.3	8.6	98.1	1.9
SLAVEN RMA-92	68	65527	1.2	8.8968	0.6	5.0815	1.2	0.3279	1.0	0.84	1828.1	15.4	1833.0	9.8	1838.6	11.5	1838.6	11.5	99.4	0.6
SLAVEN RMA-62	124	133404	1.8	8.8942	0.4	5.0354	2.2	0.3248	2.2	0.99	1813.2	34.5	1825.3	18.8	1839.1	6.9	1839.1	6.9	98.6	1.4
SLAVEN RMA-143	65	125684	1.6	8.8936	1.1	5.0114	1.9	0.3232	1.6	0.83	1805.6	24.9	1821.2	16.2	1839.2	19.4	1839.2	19.4	98.2	1.8
SLAVEN RMA-56	66	67339	1.2	8.8925	1.0	4.9855	2.2	0.3215	2.0	0.90	1797.2	31.0	1816.9	18.7	1839.4	17.8	1839.4	17.8	97.7	2.3
SLAVEN RMA-94	122	66177	1.4	8.8912	0.4	5.1196	1.3	0.3301	1.2	0.96	1839.1	19.6	1839.4	10.8	1839.7	6.4	1839.7	6.4	100.0	0.0
SLAVEN RMA-105	79	57645	1.2	8.8888	0.8	4.9791	1.7	0.3210	1.5	0.89	1794.6	23.9	1815.8	14.4	1840.2	13.8	1840.2	13.8	97.5	2.5
SLAVEN RMA-60	182	217075	1.7	8.8886	0.3	4.4069	1.9	0.2841	1.9	0.99	1612.0	26.5	1713.6	15.6	1840.2	5.6	1840.2	5.6	87.6	12.4
SLAVEN RMA-6	56	54293	1.8	8.8874	1.1	5.1284	2.5	0.3306	2.3	0.90	1841.1	36.8	1840.8	21.6	1840.5	19.8	1840.5	19.8	100.0	0.0
SLAVEN RMA-150	138	141996	1.7	8.8862	0.4	5.1879	2.0	0.3344	2.0	0.98	1859.5	31.6	1850.6	17.0	1840.7	7.4	1840.7	7.4	101.0	-1.0
SLAVEN RMA-80	111	181988	2.1	8.8858	0.4	5.0233	0.8	0.3237	0.7	0.87	1807.9	11.6	1823.3	7.1	1840.8	7.5	1840.8	7.5	98.2	1.8
SLAVEN RMA-75	195	141169	1.6	8.8853	0.3	4.7846	3.0	0.3083	3.0	1.00	1732.5	45.4	1782.2	25.2	1840.9	5.3	1840.9	5.3	94.1	5.9
SLAVEN RMA-32	101	93368	1.7	8.8824	0.5	5.1485	2.5	0.3317	2.4	0.98	1846.5	39.2	1844.2	21.2	1841.5	9.4	1841.5	9.4	100.3	-0.3
SLAVEN RMA-31	74	100498	0.4	8.8815	0.9	4.9953	1.8	0.3218	1.6	0.86	1798.4	24.6	1818.5	15.5	1841.7	17.0	1841.7	17.0	97.6	2.4
SLAVEN RMA-121	125	148722	2.3	8.8814	0.3	5.1081	0.8	0.3290	0.8	0.93	1833.7	12.5	1837.5	7.2	1841.7	5.7	1841.7	5.7	99.6	0.4
SLAVEN RMA-151	103	44551	1.6	8.8810	0.5	5.0733	1.5	0.3268	1.5	0.95	1822.7	23.2	1831.6	13.1	1841.8	8.8	1841.8	8.8	99.0	1.0
SLAVEN RMA-98	91	77128	1.4	8.8803	1.0	5.1371	1.7	0.3309	1.4	0.80	1842.6	21.8	1842.3	14.4	1841.9	18.5	1841.9	18.5	100.0	0.0
SLAVEN RMA-87	74	55771	0.7	8.8791	0.6	5.0334	1.3	0.3241	1.1	0.89	1809.9	17.9	1825.0	10.8	1842.2	10.4	1842.2	10.4	98.2	1.8
SLAVEN RMA-96	127	203828	1.3	8.8777	0.5	5.1169	2.2	0.3295	2.1	0.97	1835.8	34.0	1838.9	18.5	1842.5	8.8	1842.5	8.8	99.6	0.4
SLAVEN RMA-42	104	173022	1.3	8.8771	0.4	5.0378	2.3	0.3243	2.2	0.98	1810.9	35.0	1825.7	19.1	1842.6	7.2	1842.6	7.2	98.3	1.7
SLAVEN RMA-188	36	17569	0.8	8.8770	2.3	5.0687	2.5	0.3263	0.9	0.36	1820.6	14.4	1830.9	21.2	1842.6	42.1	1842.6	42.1	98.8	1.2
SLAVEN RMA-8	71	60018	1.4	8.8758	0.7	5.1571	2.1	0.3320	2.0	0.95	1848.0	32.2	1845.6	18.0	1842.8	12.5	1842.8	12.5	100.3	-0.3
SLAVEN RMA-68	180	132934	2.0	8.8757	0.4	5.0572	2.7	0.3255	2.7	0.99	1816.8	42.1	1829.0	22.8	1842.9	7.3	1842.9	7.3	98.6	1.4
SLAVEN RMA-132	86	64621	1.8	8.8710	0.4	5.1180	1.3	0.3293	1.2	0.94	1834.9	19.3	1839.1	10.9	1843.8	7.6	1843.8	7.6	99.5	0.5
SLAVEN RMA-111	39	46488	1.0	8.8684	0.9	5.1458	1.4	0.3310	1.0	0.73	1843.1	15.8	1843.7	11.5	1844.4	16.8	1844.4	16.8	99.9	0.1
SLAVEN RMA-66	103	195797	1.5	8.8678	0.4	5.1058	1.2	0.3284	1.1	0.94	1830.5	17.6	1837.1	10.0	1844.5	7.0	1844.5	7.0	99.2	0.8
SLAVEN RMA-71	70	92108	0.8	8.8673	1.1	4.9940	1.9	0.3212	1.5	0.81	1795.4	23.8	1818.3	15.9	1844.6	20.1	1844.6	20.1	97.3	2.7
SLAVEN RMA-145	26	14743	1.8	8.8662	1.5	5.1792	2.6	0.3330	2.2	0.82	1853.1	34.8	1849.2	22.3	1844.8	26.9	1844.8	26.9	100.4	-0.4
SLAVEN RMA-126	48	35931	1.5	8.8627	0.8	5.1862	2.0	0.3334	1.8	0.92	1854.6	29.1	1850.4	16.7	1845.5	13.9	1845.5	13.9	100.5	-0.5
SLAVEN RMA-53	59	88254	1.0	8.8626	0.6	4.9532	1.1	0.3184	0.9	0.84	1781.8	14.1	1811.4	9.1	1845.5	10.6	1845.5	10.6	96.5	3.5
SLAVEN RMA-108	64	67789	1.3	8.8616	0.5	5.0667	1.5	0.3256	1.4	0.95	1817.2	22.8	1830.6	12.9	1845.7	9.0	1845.7	9.0	98.5	1.5
SLAVEN RMA-140	49	59245	1.3	8.8592	1.8	5.0364	1.9	0.3236	0.5	0.25	1807.3	7.4	1825.5	15.8	1846.2	32.7	1846.2	32.7	97.9	2.1
SLAVEN RMA-13	30	5021	0.8	8.8573	2.4	5.1960	3.2	0.3338	2.2	0.67	1856.7	35.0	1852.0	27.4	1846.6	43.0	1846.6	43.0	100.5	-0.5
SLAVEN RMA-7	75	120099	1.1	8.8572	0.6	5.0739	2.0	0.3259	1.9	0.95	1818.7	29.6	1831.7	16.7	1846.6	11.6	1846.6	11.6	98.5	1.5
SLAVEN RMA-1	38	99655	1.6	8.8524	0.9	5.1692	2.2	0.3319	2.0	0.92	1847.5	32.5	1847.6	18.8	1847.6	16.1	1847.6	16.1	100.0	0.0
SLAVEN RMA-20	41	46129	1.4	8.8468	1.2	5.1637	3.4	0.3313	3.2	0.94	1844.8	50.7	1846.6	28.7	1848.8	21.3	1848.8	21.3	99.8	0.2
SLAVEN RMA-67	63	87611	1.5	8.8434	0.7	5.1530	3.8	0.3305	3.8	0.99	1840.8	60.2	1844.9	32.5	1849.5	11.8	1849.5	11.8	99.5	0.5
SLAVEN RMA-110	34	2047	0.2	8.8338	3.2	5.0183	4.0	0.3215	2.4	0.59	1797.1	37.0	1822.4	33.7	1851.4	57.8	1851.4	57.8	97.1	2.9
SLAVEN RMA-137	76	118710	2.9	8.8315	0.6	5.1669	2.2	0.3309	2.1	0.96	1843.0	33.8	1847.2	18.7	1851.9	11.1	1851.9	11.1	99.5	0.5
SLAVEN RMA-5	82	158869	0.7	8.8289	0.6	4.8605	2.6	0.3112	2.5	0.97	1746.8	38.1	1795.4	21.6	1852.4	11.1	1852.4	11.1	94.3	5.7
SLAVEN RMA-161	122	265126	1.9	8.8287	0.3	5.1298	1.7	0.3285	1.7	0.99	1831.0	26.7	1841.0	14.4	1852.5	4.5	1852.5	4.5	98.8	1.2
SLAVEN RMA-165	32	41040	2.1	8.8256	0.9	5.1418	1.6	0.3291	1.3	0.83	1834.1	20.7	1843.0	13.2	1853.1	15.6	1853.1	15.6	99.0	1.0
SLAVEN RMA-89	98	197230	1.5	8.8246	0.4	5.1017	1.2	0.3265	1.1	0.93	1821.5	18.0	1836.4	10.3	1853.3	7.8	1853.3	7.8	98.3	1.7
SLAVEN RMA-144	275	234933	2.7	8.8227	0.2	5.2211	1.9	0.3341	1.9	0.99	1858.2	31.0	1856.1	16.4	1853.7	3.5	1853.7	3.5	100.2	-0.2
SLAVEN RMA-77	80	63252	1.1	8.8194	0.4	4.9664	5.0	0.3177	4.9	1.00	1778.4	76.9	1813.6	42.0	1854.4	7.6	1854.4	7.6	95.9	4.1
SLAVEN RMA-10	163	112111	1.2	8.8157	0.3	5.1981	2.3	0.3324	2.3	0.99	1849.8	37.3	1852.3	19.9	1855.1	5.4	1855.1	5.4	99.7	0.3
SLAVEN RMA-84	69	58512	0.9	8.8141	0.7	5.0588	1.9	0.3234	1.8	0.93	1806.3	28.4	1829.2	16.5	1855.4	13.3	1855.4	13.3	97.3	2.7
SLAVEN RMA-19	45	52409	2.2	8.8078	0.9	5.2196	2.8	0.3334	2.7	0.95	1855.0	42.9	1855.8	23.9	1856.7	15.7	1856.7	15.7	99.9	0.1
SLAVEN RMA-76	21	47849	0.7	8.8077	1.6	4.9924	1.9	0.3189	1.0	0.53	1784.4	15.7	1818.0	16.2	1856.8	29.4	1856.8	29.4	96.1	3.9
SLAVEN RMA-40	39	54017	0.9	8.8036	1.1	5.1051	2.6	0.3260	2.4	0.91	1818.8	37.5	1837.0	22.2	1857.6	19.9	1857.6	19.9	97.9	2.1
SLAVEN RMA-164	58	63141	0.8	8.8029	0.7	5.1430	1.1	0.3284	0.8	0.75	1830.4	12.6	1843.2	9.0	1857.7	12.5	1857.7	12.5	98.5	1.5
SLAVEN RMA-187	129	152938	2.5	8.7915	0.5	5.2529	1.0	0.3349	0.9	0.89	1862.3	14.9	1861.2	8.8	1860.1	8.6	1860.1	8.6	100.1	-0.1
SLAVEN RMA-49	126	97236	1.5	8.7732	0.6	4.8303	1.3	0.3073	1.1	0.88	1727.7	16.9	1790.2	10.6	1863.9	10.6	1863.9	10.6	92.7	7.3
SLAVEN RMA-55	69	6844	1.4	8.7667	2.1	5.0826	2.7	0.3232	1.7	0.63	1805.2	27.2	1833.2	23.1	1865.2	38.1	1865.2	38.1	96.8	3.2
SLAVEN RMA-147	118	230714	1.0	8.7451	0.3	5.3244	2.0	0.3377	2.0	0.99	1875.6	32.9	1872.8	17.4	1869.6	4.5	1869.6	4.5	100.3	-0.3
SLAVEN RMA-177	138	95928	1.7	8.7432	1.0	4.3943	2.1	0.2787	1.9	0.89	1584.6	26.4	1711.3	17.5	1870.0	17.3	1870.0	17.3	84.7	15.3
SLAVEN RMA-170	37	7708	0.9	8.7321	2.3	5.2182	2.6	0.3305	1.2	0.46	1840.7	18.9	1855.6	21.8	1872.3	40.8	1872.3	40.8	98.3	1.7
SLAVEN RMA-86	97	153204	0.8	8.7234	0.5	5.0737	3.5	0.3210	3.4	0.99	1794.6	53.5	1831.7	29.3	1874.1	9.0	1874.1	9.0	95.8	4.2
SLAVEN RMA-64	48	49594	1.6	8.7209	1.1	5.2270	3.2	0.3306	3.0	0.94	1841.3	47.8	1857.0	27.2	1874.6	20.3	1874.6	20.3	98.2	1.8
SLAVEN RMA-191	113	127651	2.1	8.7090	0.5	5.1174	2.2	0.3232	2.1	0.97	1805.5	33.3	1839.0	18.5	1877.1	9.0	1877.1	9.0	96.2	3.8
SLAVEN RMA-26	55	69205	1.9	8.6586	0.6	5.3727	2.4	0.3374	2.4	0.97	1874.1	38.6	1880.5	21.0	1887.6	11.0	1887.6	11.0	99.3	0.7
SLAVEN RMA-194	84	53342	0.7	8.5842	0.5	5.3893	3.0	0.3355	2.9	0.98	1865.1	47.7	1883.1	25.6	1903.1	9.8	1903.1	9.8	98.0	2.0
SLAVEN RMA-198	45	30166	0.8	8.5710	1.0	5.4964	1.9	0.3417	1.6	0.84	1894.7	26.4	1900.0	16.4	1905.8	18.5	1905.8	18.5	99.4	0.6
SLAVEN RMA-117	99	129735	1.4	8.5369	0.5	5.6504	1.3	0.3498	1.2	0.90	1933.9	19.3	1923.8	11.0	1913.0	9.8	1913.0	9.8	101.1	-1.1

U-Pb geochronologic anlayses of selected Roberts Mountains allochthon strata

						Isotope ratios							Apparent ages (Ma)							
	U	206Pb	U/Th	206Pb*	±	207Pb*	±	206Pb*	±	error	206Pb*	±	207Pb*	±	206Pb*	±	Best age	±	Conc.	Discord.
	(ppm)	204Pb		207Pb*	(%)	235U*	(%)	238U	(%)	corr.	238U*	(Ma)	235U	(Ma)	207Pb*	(Ma)	(Ma)	(Ma)	(%)	(%)
Sample: Slaven Chert. Location: Slaven Canyon, Shoshone Range; 0519428 4479302 (NAD 83 UTM 11T)																				
SLAVEN RMA-47	38	23566	0.5	8.5290	0.6	5.3984	3.4	0.3339	3.3	0.98	1857.4	53.4	1884.6	28.9	1914.7	11.2	1914.7	11.2	97.0	3.0
SLAVEN RMA-125	392	88729	4.1	8.5172	0.2	5.2718	4.6	0.3257	4.6	1.00	1817.3	72.5	1864.3	39.1	1917.1	4.0	1917.1	4.0	94.8	5.2
SLAVEN RMA-174	154	193641	0.4	8.5114	0.4	4.7403	2.2	0.2926	2.2	0.99	1654.6	31.9	1774.4	18.6	1918.4	6.8	1918.4	6.8	86.3	13.7
SLAVEN RMA-138	53	100317	1.5	8.5067	0.9	5.4901	2.5	0.3387	2.4	0.93	1880.5	38.7	1899.0	21.8	1919.4	16.2	1919.4	16.2	98.0	2.0
SLAVEN RMA-37	58	74694	1.0	8.5025	0.9	5.4795	4.5	0.3379	4.4	0.98	1876.6	72.1	1897.4	38.8	1920.2	15.7	1920.2	15.7	97.7	2.3
SLAVEN RMA-25	63	72016	1.0	8.4971	0.5	5.6448	1.7	0.3479	1.7	0.95	1924.4	27.8	1923.0	15.1	1921.4	9.4	1921.4	9.4	100.2	-0.2
SLAVEN RMA-109	45	46541	1.2	8.4793	0.8	5.6046	1.4	0.3447	1.2	0.85	1909.1	20.1	1916.8	12.4	1925.1	13.5	1925.1	13.5	99.2	0.8
SLAVEN RMA-156	89	71249	1.0	8.4691	0.4	5.6200	1.0	0.3452	0.9	0.90	1911.7	14.6	1919.2	8.4	1927.3	7.7	1927.3	7.7	99.2	0.8
SLAVEN RMA-18	130	163380	1.3	8.4610	0.3	5.6023	2.5	0.3438	2.4	0.99	1904.8	40.3	1916.4	21.2	1929.0	5.8	1929.0	5.8	98.7	1.3
SLAVEN RMA-119	64	67698	0.7	8.4166	0.4	5.7846	2.2	0.3531	2.1	0.98	1949.4	35.4	1944.1	18.6	1938.4	8.0	1938.4	8.0	100.6	-0.6
SLAVEN RMA-30	187	167062	1.4	8.4066	0.3	5.6973	1.7	0.3474	1.7	0.98	1922.0	28.4	1931.0	15.0	1940.5	5.9	1940.5	5.9	99.0	1.0
SLAVEN RMA-70	50	66069	0.5	8.3967	1.0	5.6820	1.9	0.3460	1.6	0.84	1915.6	26.3	1928.6	16.2	1942.7	18.2	1942.7	18.2	98.6	1.4
SLAVEN RMA-106	37	49729	1.2	8.3881	0.8	5.5876	1.2	0.3399	0.9	0.74	1886.3	14.5	1914.2	10.4	1944.5	14.6	1944.5	14.6	97.0	3.0
SLAVEN RMA-21	102	137776	1.3	8.3844	0.5	5.8493	3.1	0.3557	3.1	0.99	1961.7	52.2	1953.7	27.1	1945.3	8.9	1945.3	8.9	100.8	-0.8
SLAVEN RMA-81	62	66867	0.5	8.3192	0.5	5.6688	1.1	0.3420	0.9	0.87	1896.5	15.1	1926.6	9.2	1959.2	9.5	1959.2	9.5	96.8	3.2
SLAVEN RMA-163	99	106591	0.8	8.2100	0.7	4.7029	4.2	0.2800	4.1	0.99	1591.5	58.4	1767.8	35.2	1982.8	12.7	1982.8	12.7	80.3	19.7
SLAVEN RMA-134	81	90875	1.9	8.1417	0.6	6.0998	2.7	0.3602	2.6	0.97	1983.1	44.3	1990.2	23.2	1997.6	10.7	1997.6	10.7	99.3	0.7
SLAVEN RMA-104	31	32749	0.9	8.0968	1.6	6.0550	2.5	0.3556	1.9	0.77	1961.1	32.5	1983.8	21.7	2007.5	28.2	2007.5	28.2	97.7	2.3
SLAVEN RMA-72	92	82821	2.2	7.9055	0.6	6.4055	2.0	0.3673	1.9	0.95	2016.5	32.6	2033.0	17.4	2049.8	10.6	2049.8	10.6	98.4	1.6
SLAVEN RMA-91	101	73045	0.9	7.8573	0.4	6.5378	4.8	0.3726	4.8	1.00	2041.5	83.5	2051.0	42.2	2060.6	7.6	2060.6	7.6	99.1	0.9
SLAVEN RMA-59	24	25752	0.9	7.8338	1.5	6.5396	1.9	0.3716	1.2	0.64	2036.7	21.0	2051.2	16.6	2065.9	25.7	2065.9	25.7	98.6	1.4
SLAVEN RMA-107	41	78567	1.3	7.8322	1.3	6.5547	1.5	0.3723	0.8	0.52	2040.4	13.7	2053.3	13.2	2066.2	22.6	2066.2	22.6	98.7	1.3
SLAVEN RMA-39	65	100705	1.2	7.8145	0.7	6.6290	1.6	0.3757	1.4	0.90	2056.2	25.1	2063.2	13.9	2070.2	11.9	2070.2	11.9	99.3	0.7
SLAVEN RMA-45	56	53937	0.8	7.7924	0.7	6.5721	1.5	0.3714	1.4	0.91	2036.1	24.5	2055.6	13.7	2075.2	11.5	2075.2	11.5	98.1	1.9
SLAVEN RMA-183	43	107679	0.8	7.7841	1.1	6.3797	1.9	0.3602	1.5	0.79	1983.0	25.2	2029.5	16.4	2077.1	20.1	2077.1	20.1	95.5	4.5
SLAVEN RMA-135	55	44286	0.5	7.7833	0.9	6.7280	4.3	0.3798	4.1	0.97	2075.3	73.5	2076.3	37.6	2077.3	16.7	2077.3	16.7	99.9	0.1
SLAVEN RMA-157	88	64081	0.7	7.7802	0.4	6.6599	1.2	0.3758	1.2	0.93	2056.6	20.3	2067.3	10.9	2078.0	7.8	2078.0	7.8	99.0	1.0
SLAVEN RMA-141	70	70082	1.0	7.7762	0.6	6.7056	1.1	0.3782	0.9	0.85	2067.8	16.3	2073.4	9.6	2078.9	10.1	2078.9	10.1	99.5	0.5
SLAVEN RMA-196	45	83740	0.7	7.7750	0.7	6.7347	2.4	0.3798	2.3	0.96	2075.2	40.2	2077.2	20.8	2079.1	11.5	2079.1	11.5	99.8	0.2
SLAVEN RMA-24	72	108215	1.6	7.7602	0.6	6.8340	1.8	0.3846	1.7	0.95	2097.9	30.0	2090.1	15.7	2082.5	9.9	2082.5	9.9	100.7	-0.7
SLAVEN RMA-155	47	15484	1.4	7.7568	1.5	6.6005	1.8	0.3713	1.1	0.58	2035.6	18.6	2059.4	16.3	2083.3	26.6	2083.3	26.6	97.7	2.3
SLAVEN RMA-160	30	49020	0.5	7.7557	1.1	6.7514	2.4	0.3798	2.1	0.88	2075.2	37.1	2079.4	21.0	2083.5	20.0	2083.5	20.0	99.6	0.4
SLAVEN RMA-36	79	100177	0.8	7.7496	0.6	6.6402	2.4	0.3732	2.4	0.97	2044.5	41.2	2064.7	21.4	2084.9	10.3	2084.9	10.3	98.1	1.9
SLAVEN RMA-35	88	188835	2.2	7.7466	0.5	6.7425	1.3	0.3788	1.2	0.92	2070.8	20.5	2078.2	11.1	2085.6	8.6	2085.6	8.6	99.3	0.7
SLAVEN RMA-175	49	91812	1.4	7.7109	1.2	6.9796	2.5	0.3903	2.2	0.88	2124.4	39.9	2108.8	22.4	2093.7	21.4	2093.7	21.4	101.5	-1.5
SLAVEN RMA-166	64	84675	0.6	7.6457	0.5	6.9071	0.9	0.3830	0.7	0.84	2090.3	13.1	2099.6	7.8	2108.6	8.4	2108.6	8.4	99.1	0.9
SLAVEN RMA-61	154	57196	1.0	7.2775	0.5	7.3625	3.3	0.3886	3.3	0.99	2116.3	59.4	2156.4	29.8	2194.8	8.9	2194.8	8.9	96.4	3.6
SLAVEN RMA-69	60	23660	0.7	7.0508	1.3	7.9687	2.5	0.4075	2.2	0.86	2203.5	41.1	2227.5	23.0	2249.6	22.2	2249.6	22.2	97.9	2.1
SLAVEN RMA-58	120	178689	2.4	6.9650	0.3	8.1912	1.2	0.4138	1.1	0.96	2232.2	21.3	2252.4	10.6	2270.8	5.4	2270.8	5.4	98.3	1.7
SLAVEN RMA-189	39	42299	0.8	6.8352	1.1	8.7989	1.6	0.4362	1.2	0.74	2333.6	23.1	2317.4	14.5	2303.1	18.4	2303.1	18.4	101.3	-1.3
SLAVEN RMA-83	62	132694	0.7	6.8233	1.0	8.5611	1.2	0.4237	0.7	0.58	2277.1	13.9	2292.4	11.3	2306.1	17.3	2306.1	17.3	98.7	1.3
SLAVEN RMA-181	155	70268	1.0	6.6404	0.5	7.7200	1.7	0.3718	1.6	0.96	2037.9	28.4	2198.9	15.2	2352.7	7.8	2352.7	7.8	86.6	13.4
SLAVEN RMA-159	79	96153	0.9	6.5720	0.6	8.5122	3.9	0.4057	3.9	0.99	2195.4	72.0	2287.2	35.6	2370.3	9.8	2370.3	9.8	92.6	7.4
SLAVEN RMA-95	96	246129	2.6	6.5425	0.5	9.0011	2.1	0.4271	2.0	0.97	2292.7	38.5	2338.1	18.8	2378.0	8.8	2378.0	8.8	96.4	3.6
SLAVEN RMA-88	16	24833	0.8	6.4506	2.1	8.9540	6.7	0.4189	6.3	0.95	2255.5	120.4	2333.3	61.0	2402.1	36.1	2402.1	36.1	93.9	6.1
SLAVEN RMA-54	144	180847	1.2	6.2924	0.3	9.7455	1.5	0.4448	1.4	0.98	2371.9	28.6	2411.0	13.6	2444.2	5.5	2444.2	5.5	97.0	3.0
SLAVEN RMA-23	75	115115	2.2	6.2474	0.6	10.2028	3.2	0.4623	3.1	0.98	2449.7	63.7	2453.3	29.5	2456.4	10.7	2456.4	10.7	99.7	0.3
SLAVEN RMA-50	108	240510	1.6	5.9609	0.4	9.9722	2.2	0.4311	2.1	0.99	2310.8	41.5	2432.2	20.0	2535.4	6.0	2535.4	6.0	91.1	8.9
SLAVEN RMA-41	13	13259	0.4	5.8816	1.6	11.2177	2.8	0.4785	2.3	0.82	2520.8	47.9	2541.4	26.1	2557.8	26.8	2557.8	26.8	98.6	1.4
SLAVEN RMA-29	51	115551	1.4	5.8648	0.6	11.3669	2.1	0.4835	2.0	0.95	2542.5	42.1	2553.7	19.6	2562.6	10.4	2562.6	10.4	99.2	0.8
SLAVEN RMA-90	114	88337	1.6	5.8340	0.5	11.2707	1.0	0.4769	0.9	0.87	2513.7	18.0	2545.8	9.3	2571.4	8.2	2571.4	8.2	97.8	2.2
SLAVEN RMA-153	144	239479	2.4	5.8320	0.1	11.2377	1.4	0.4753	1.4	1.00	2506.9	29.1	2543.1	13.1	2572.0	1.9	2572.0	1.9	97.5	2.5
SLAVEN RMA-169	215	265095	2.9	5.7863	0.4	10.9722	2.5	0.4605	2.4	0.98	2441.6	49.4	2520.8	23.0	2585.2	7.4	2585.2	7.4	94.4	5.6
SLAVEN RMA-190	66	13637	0.5	5.7612	0.5	11.3294	1.0	0.4734	0.9	0.87	2498.4	17.8	2550.6	9.2	2592.4	8.1	2592.4	8.1	96.4	3.6
SLAVEN RMA-103	86	167372	1.0	5.7063	0.4	11.8294	1.6	0.4896	1.6	0.98	2568.8	33.3	2591.0	15.1	2608.4	5.9	2608.4	5.9	98.5	1.5
SLAVEN RMA-136	40	31484	0.9	5.6583	0.6	11.8790	1.7	0.4875	1.6	0.94	2559.8	33.3	2594.9	15.7	2622.4	9.5	2622.4	9.5	97.6	2.4
SLAVEN RMA-85	22	29092	0.6	5.6581	0.6	11.5086	2.0	0.4723	1.9	0.96	2493.5	39.9	2565.3	18.8	2622.5	9.2	2622.5	9.2	95.1	4.9
SLAVEN RMA-199	25	67512	0.8	5.5146	1.2	12.6069	2.1	0.5042	1.7	0.82	2631.9	37.1	2650.7	19.8	2665.1	20.1	2665.1	20.1	98.8	1.2
SLAVEN RMA-101	70	105539	1.4	5.5048	0.3	12.5437	2.5	0.5008	2.4	0.99	2617.3	52.3	2646.0	23.1	2668.1	5.3	2668.1	5.3	98.1	1.9
SLAVEN RMA-48	36	61997	0.6	5.4977	0.6	12.3548	2.3	0.4926	2.2	0.96	2582.0	47.1	2631.7	21.6	2670.2	10.1	2670.2	10.1	96.7	3.3
SLAVEN RMA-74	29	27407	0.5	5.4735	0.6	12.8827	2.4	0.5114	2.3	0.96	2662.6	49.8	2671.1	22.3	2677.5	10.3	2677.5	10.3	99.4	0.6
SLAVEN RMA-38	29	77229	1.4	5.4728	1.0	12.9545	4.1	0.5142	3.9	0.97	2674.5	85.8	2676.4	38.2	2677.7	17.1	2677.7	17.1	99.9	0.1
SLAVEN RMA-146	131	202392	1.3	5.4581	0.2	12.9707	1.6	0.5135	1.6	0.99	2671.4	34.2	2677.5	14.9	2682.2	3.5	2682.2	3.5	99.6	0.4
SLAVEN RMA-2	80	283386	1.0	5.4518	0.2	13.1494	2.1	0.5199	2.1	0.99	2698.9	46.2	2690.4	19.9	2684.1	4.0	2684.1	4.0	100.6	-0.6
SLAVEN RMA-162	259	163237	1.3	5.4472	0.1	12.6083	0.7	0.4981	0.7	0.98	2605.7	15.1	2650.8	6.8	2685.5	2.2	2685.5	2.2	97.0	3.0
SLAVEN RMA-139	51	91593	0.9	5.4448	0.3	12.9172	1.0	0.5101	0.9	0.97	2657.0	20.6	2673.6	9.2	2686.2	4.2	2686.2	4.2	98.9	1.1
SLAVEN RMA-82	58	88826	1.3	5.4443	0.6	12.6903	2.5	0.5011	2.5	0.98	2618.5	53.0	2656.9	23.8	2686.4	9.2	2686.4	9.2	97.5	2.5
SLAVEN RMA-148	96	175608	1.2	5.4241	0.2	13.2252	3.0	0.5203	3.0	1.00	2700.3	66.8	2695.9	28.7	2692.5	3.9	2692.5	3.9	100.3	-0.3
SLAVEN RMA-154	197	307925	0.7	5.4021	0.1	12.8859	1.1	0.5049	1.1	1.00	2634.7	23.8	2671.3	10.4	2699.2	1.8	2699.2	1.8	97.6	2.4
SLAVEN RMA-51	68	94363	0.9	5.3895	0.5	12.9389	2.1	0.5058	2.1	0.97	2638.5	45.0	2675.2	20.1	2703.1	7.9	2703.1	7.9	97.6	2.4
SLAVEN RMA-120	177	408557	1.3	5.3809	0.3	13.3235	2.4	0.5200	2.3	0.99	2699.0	51.7	2702.8	22.3	2705.7	4.2	2705.7	4.2	99.8	0.2
SLAVEN RMA-99	30	31879	0.6	5.3604	0.9	13.6547	4.2	0.5309	4.1	0.97	2745.1	90.9	2726.1	39.5	2712.0	15.4	2712.0	15.4	101.2	-1.2
SLAVEN RMA-182	40	43297	0.6	5.3589	0.7	13.4870	1.5	0.5242	1.3	0.87	2716.9	28.6	2714.4	14.1	2712.5	12.2	2712.5	12.2	100.2	-0.2
SLAVEN RMA-4	95	378889	2.3	5.3030	0.3	13.4241	1.2	0.5163	1.2	0.97	2683.5	26.2	2710.0	11.6	2729.7	4.6	2729.7	4.6	98.3	1.7
SLAVEN RMA-97	60	211522	1.8	5.2929	0.2	13.7308	1.7	0.5271	1.7	0.99	2729.2	37.6	2731.3	16.1	2732.9	3.9	2732.9	3.9	99.9	0.1
SLAVEN RMA-173	43	65339	1.3	5.2610	0.4	14.0268	2.0	0.5352	2.0	0.98	2763.4	44.4	2751.5	19.2	2742.8	7.4	2742.8	7.4	100.7	-0.7
SLAVEN RMA-200	17	33307	0.2	5.1455	1.4	13.8622	2.2	0.5173	1.7	0.78	2687.8	37.5	2740.3	20.8	2779.3	22.6	2779.3	22.6	96.7	3.3
SLAVEN RMA-149	51	195285	1.4	5.1063	0.5	14.5186	2.2	0.5377	2.1	0.97	2773.8	47.9	2784.2	20.8	2791.8	8.9	2791.8	8.9	99.4	0.6
SLAVEN RMA-65	43	115006	1.2	5.0877	0.4	14.4934	1.7	0.5348	1.6	0.97	2761.6	36.5	2782.6	16.0	2797.8	7.0	2797.8	7.0	98.7	1.3
SLAVEN RMA-128	28	61280	0.9	4.9133	0.8	15.4833	1.8	0.5517	1.6	0.89	2832.4	35.7	2845.5	16.7	2854.7	13.1	2854.7	13.1	99.2	0.8
SLAVEN RMA-34	83	135796	1.6	3.9967	0.2	22.0895	1.8	0.6403	1.8	0.99	3190.2	44.8	3187.7	17.4	3186.1	3.4	3186.1	3.4	100.1	-0.1
SLAVEN RMA-44	62	130352	0.8	3.9125	0.3	22.2745	2.9	0.6321	2.9	1.00	3157.7	72.9	3195.8	28.5	3219.7	4.1	3219.7	4.1	98.1	1.9

Notes:
1. Analyses with >10% uncertainty (1-sigma) in 206Pb/238U age are not included.
2. Analyses with >10% uncertainty (1-sigma) in 206Pb/207Pb age are not included, unless 206Pb/238U age is <500 Ma.
3. Best age is determined from 206Pb/238U age for analyses with 206Pb/238U age <1000 Ma and from 206Pb/207Pb age for analyses with 206Pb/238Uage > 1000 Ma.
4. Concordance is based on 206Pb/238U age / 206Pb/207Pb age. Value is not reported for 206Pb/238U ages <500 Ma because of large uncertainty in 206Pb/207Pb age.
5. Discordance is 100% - concordance.
6. Analyses with 206Pb/238U age > 500 Ma and with >20% discordance (<80% concordance) are not included.
7. Analyses with 206Pb/238U age > 500 Ma and with >5% reverse discordance (<105% concordance) are not included.
8. All uncertainties are reported at the 1-sigma level, and include only measurement errors.
9. External (systematic) errors are shown as 206Pb/238U uncertainty, 206Pb/207Pb uncertainty to the right of each sample (in %, at 2-sigma level).
10. Analyses conducted by LA-MC-ICPMS, as described by Gehrels et al. (2008).
11. U concentration and U/Th are calibrated relative to Sri Lanka zircon standard and are accurate to ~20%.
12. Common Pb correction is from measured 204Pb with common Pb composition interpreted from Stacey and Kramers (1975).
13. Uncertainties of 1.5 for 206Pb/204Pb, 0.3 for 207Pb/ 204Pb, and 2.0 for 208Pb/ 204Pb are applied to common Pb composition.
14. U/Pb and 206Pb/207Pb fractionation is calibrated relative to fragments of a large Sri Lanka zircon of 563.5 ± 3.2 Ma (2-sigma).
15. U decay constants and composition as follows: 235U = 9.8485 x 10-10, 238U = 1.55125 x 10-10, 238U/235U = 137.88.
16. Weighted mean and concordia plots determined with Isoplot (Ludwig, 2008).
17. Analytical methods as described by Gehrels and Pecha (2014).

APPENDIX D

Hafnium isotope data of selected Roberts Mountains allochthon strata

Table notes are at the end of the appendix.

	(^{176}Yb + ^{176}Lu) / ^{176}Hf (%)	Volts Hf	^{176}Hf/^{177}Hf	± (1σ)	^{176}Lu/^{177}Hf	^{176}Hf^{177}Hf (T)	E-Hf (0)	E-Hf (0) ± (1σ)	E-Hf (T)	Age (Ma)
Sample: Snow Canyon Formation. Location: Snow Canyon, Independence Mountains; 0579760 4585698 (NAD 83 UTM 11T)										
Snow-CYN-GG2000SPE-9	6.9	5.4	0.281448	0.000016	0.00041	0.281434	-47.3	0.6	-6.6	1826
Snow-CYAN-GG2000SPE-30	7.5	5.3	0.281335	0.000017	0.00044	0.281320	-51.3	0.6	-10.6	1827
Snow-CYAN-GG2000SPE-38	9.2	4.8	0.281420	0.000021	0.00055	0.281401	-48.3	0.7	-7.7	1829
Snow-CYAN-GG2000SPE-27	9.1	4.5	0.281408	0.000020	0.00055	0.281389	-48.7	0.7	-8.1	1832
Snow-CYN-GG2000SPE-14	7.5	5.1	0.281438	0.000021	0.00046	0.281422	-47.6	0.7	-6.9	1832
Snow-CYAN-GG2000SPE-36	14.4	4.0	0.281423	0.000022	0.00084	0.281394	-48.2	0.8	-7.9	1832
Snow-CYAN-GG2000SPE-58	6.8	5.5	0.281443	0.000020	0.00041	0.281429	-47.5	0.7	-6.4	1842
Snow-CYN-GG2000SPE-45	11.1	5.5	0.281453	0.000018	0.00063	0.281431	-47.1	0.6	-6.3	1844
Snow-CYN-GG2000SPE-48	9.0	4.8	0.281478	0.000022	0.00051	0.281460	-46.2	0.8	-5.2	1845
Snow-CYN-GG2000SPE-53L	17.5	4.7	0.281499	0.000022	0.00098	0.281465	-45.5	0.8	-5.1	1845
Snow-CYN-GG2000SPE-53R	7.7	5.0	0.281422	0.000021	0.00045	0.281406	-48.2	0.8	-7.2	1845
Snow-CYAN-GG2000SPE-195	10.9	5.5	0.281532	0.000019	0.00067	0.281509	-44.3	0.7	-3.4	1849
Snow-CYAN-GG2000SPE-181	15.9	4.5	0.281463	0.000020	0.00090	0.281431	-46.7	0.7	-6.1	1849
Snow-CYAN-GG2000SPE-186	6.9	4.5	0.281420	0.000019	0.00040	0.281406	-48.3	0.7	-7.0	1851
Snow-CYAN-GG2000SPE-57	7.0	5.2	0.281444	0.000016	0.00045	0.281428	-47.4	0.6	-6.2	1853
Snow-CYAN-GG2000SPE-190	12.2	4.2	0.281542	0.000025	0.00071	0.281517	-44.0	0.9	-2.9	1857
Snow-CYAN-GG2000SPE-129	2.7	5.1	0.281464	0.000023	0.00024	0.281455	-46.7	0.8	-5.1	1857
Snow-CYN-GG2000SPE-198	9.6	5.1	0.281831	0.000015	0.00060	0.281810	-33.7	0.5	7.8	1870
Snow-CYAN-GG2000SPE-184	6.4	5.2	0.281363	0.000021	0.00039	0.281349	-50.3	0.7	-8.3	1884
Snow-CYAN-GG2000SPE-193	7.0	5.5	0.281426	0.000023	0.00041	0.281411	-48.1	0.8	-6.0	1886
Snow-CYN-GG2000SPE-44	3.9	6.9	0.281616	0.000017	0.00034	0.281604	-41.3	0.6	1.2	1905
Snow-CYN-GG2000SPE-24	7.3	4.8	0.281465	0.000022	0.00043	0.281449	-46.7	0.8	-4.2	1906
Snow-CYN-GG2000SPE-12	3.4	5.7	0.281421	0.000022	0.00026	0.281411	-48.2	0.8	-5.4	1913
Snow-CYN-GG2000SPE-42	9.5	5.8	0.281502	0.000018	0.00055	0.281482	-45.4	0.6	-2.8	1917
Snow-CYAN-GG2000SPE-60	11.9	4.6	0.281362	0.000020	0.00065	0.281338	-50.3	0.7	-7.7	1924
Snow-CYN-GG2000SPE-199	6.7	4.7	0.281457	0.000019	0.00039	0.281443	-47.0	0.7	-4.0	1925
Snow-CYN-GG2000SPE-51	14.9	5.7	0.281261	0.000022	0.00084	0.281230	-53.9	0.8	-11.5	1926
Snow-CYN-GG2000SPE-16	5.8	5.4	0.281410	0.000016	0.00035	0.281397	-48.6	0.6	-5.6	1928
Snow-CYAN-GG2000SPE-137	10.7	4.0	0.281491	0.000020	0.00072	0.281463	-45.8	0.7	-1.2	2016
Snow-CYN-GG2000SPE-55	11.4	4.8	0.281497	0.000020	0.00067	0.281471	-45.5	0.7	0.1	2056
Snow-CYAN-GG2000SPE-180	8.2	5.0	0.281417	0.000021	0.00051	0.281397	-48.4	0.7	-2.6	2058
Snow-CYN-GG2000SPE-174	12.3	5.2	0.281450	0.000015	0.00077	0.281420	-47.2	0.5	-1.5	2070
Snow-CYAN-GG2000SPE-168	7.2	5.1	0.281438	0.000020	0.00045	0.281420	-47.6	0.7	-1.4	2072
Snow-CYN-GG2000SPE-46	8.9	6.4	0.281114	0.000015	0.00051	0.281089	-59.1	0.5	-2.6	2524
Snow-CYN-GG2000SPE-25	19.9	4.6	0.281254	0.000022	0.00120	0.281191	-54.2	0.8	5.0	2695
Snow-CYN-GG2000SPE-13	3.6	5.8	0.281007	0.000019	0.00022	0.280995	-62.9	0.7	-1.8	2704
Snow-CYN-GG2000SPE-41	7.6	5.3	0.281060	0.000015	0.00045	0.281036	-61.0	0.5	-0.3	2705
Snow-CYN-GG2000SPE-165	4.5	4.3	0.281052	0.000025	0.00027	0.281038	-61.3	0.9	0.2	2722
Snow-CYAN-GG2000SPE-34	3.0	5.3	0.280916	0.000022	0.00022	0.280905	-66.1	0.8	-4.4	2728
Snow-CYAN-GG2000SPE-192	8.6	3.5	0.281127	0.000023	0.00049	0.281102	-58.6	0.8	2.6	2731
Snow-CYN-GG2000SPE-26	12.0	5.3	0.281035	0.000019	0.00072	0.280997	-61.9	0.7	-0.9	2739
Snow-CYAN-GG2000SPE-123	5.9	4.7	0.281031	0.000028	0.00038	0.281010	-62.0	1.0	2.0	2843
Sample: McAfee Quartzite. Location:McAfee Creek, Independence Mountains; 0590637 4599583 (NAD 83 UTM 11T)										
MCAFEE-97SF1-GG2000SPE-196	8.5	4.7	0.281278	0.000021	0.00054	0.281260	-53.3	0.7	-13.3	1803
MCAFEE-97SF1-GG2000SPE-138	7.6	4.3	0.281454	0.000020	0.00045	0.281439	-47.1	0.7	-6.7	1815
MCAFEE-97SF1-GG2000SPE-24	5.4	4.8	0.281485	0.000019	0.00034	0.281473	-46.0	0.7	-5.1	1830
MCAFEE-97SF1-GG2000SPE-32	18.5	5.5	0.281386	0.000019	0.00110	0.281347	-49.5	0.7	-9.5	1833
MCAFEE-97SF1-GG2000SPE-29	5.9	5.3	0.281436	0.000018	0.00037	0.281423	-47.7	0.6	-6.8	1834
MCAFEE-97SF1-GG2000SPE-182	10.3	4.1	0.281427	0.000022	0.00062	0.281405	-48.0	0.8	-7.4	1835
MCAFEE-97SF1-GG2000SPE-4	12.4	4.0	0.281818	0.000027	0.00074	0.281792	-34.2	1.0	6.3	1835
MCAFEE-97SF1-GG2000SPE-199	10.6	4.7	0.281401	0.000017	0.00062	0.281380	-48.9	0.6	-8.3	1835
MCAFEE-97SF1-GG2000SPE-1	11.2	4.0	0.281523	0.000021	0.00067	0.281499	-44.6	0.8	-4.0	1837
MCAFEE-97SF1-GG2000SPE-171	7.1	5.1	0.281428	0.000019	0.00044	0.281413	-48.0	0.7	-7.1	1838
MCAFEE-97SF1-GG2000SPE-10	6.2	5.1	0.281439	0.000022	0.00038	0.281426	-47.6	0.8	-6.6	1838
MCAFEE-97SF1-GG2000SPE-2	11.4	4.4	0.281482	0.000027	0.00069	0.281458	-46.1	1.0	-5.3	1844
MCAFEE-97SF1-GG2000SPE-181	5.7	5.2	0.281417	0.000016	0.00035	0.281405	-48.4	0.5	-7.2	1844
MCAFEE-97SF1-GG2000SPE-9	8.2	3.8	0.281498	0.000024	0.00055	0.281479	-45.5	0.8	-4.5	1846
MCAFEE-97SF1-GG2000SPE-7	7.0	4.6	0.281586	0.000024	0.00042	0.281571	-42.4	0.8	-1.3	1846
MCAFEE-97SF1-GG2000SPE-21	9.2	4.6	0.281437	0.000021	0.00056	0.281418	-47.7	0.7	-6.7	1847
MCAFEE-97SF1-GG2000SPE-15	15.7	4.6	0.281415	0.000021	0.00092	0.281383	-48.5	0.7	-7.9	1847
MCAFEE-97SF1-GG2000SPE-179	11.1	4.2	0.281251	0.000020	0.00074	0.281225	-54.2	0.7	-13.5	1849
MCAFEE-97SF1-GG2000SPE-174	7.0	4.4	0.281468	0.000022	0.00042	0.281453	-46.6	0.8	-5.2	1857
MCAFEE-97SF1-GG2000SPE-186	19.0	3.4	0.281450	0.000030	0.00116	0.281409	-47.2	1.1	-6.7	1862
MCAFEE-97SF1-GG2000SPE-188	10.4	5.7	0.281584	0.000019	0.00063	0.281562	-42.5	0.7	-1.2	1863
MCAFEE-97SF1-GG2000SPE-198	6.8	3.8	0.281853	0.000021	0.00040	0.281839	-33.0	0.7	8.7	1866
MCAFEE-97SF1-GG2000SPE-84	9.5	5.9	0.281276	0.000019	0.00056	0.281255	-53.4	0.7	-11.6	1884
MCAFEE-97SF1-GG2000SPE-16	17.4	4.5	0.281507	0.000022	0.00102	0.281470	-45.2	0.8	-3.4	1910

Hafnium isotope data of selected Roberts Mountains allochthon strata

	$(^{176}Yb + ^{176}Lu) / ^{176}Hf$ (%)	Volts Hf	$^{176}Hf/^{177}Hf$	± (1σ)	$^{176}Lu/^{177}Hf$	$^{176}Hf/^{177}Hf$ (T)	E-Hf (0)	E-Hf (0) ± (1σ)	E-Hf (T)	Age (Ma)
Sample: McAfee Quartzite. Location:McAfee Creek, Independence Mountains; 0590637 4599583 (NAD 83 UTM 11T)										
MCAFEE-97SF1-GG2000SPE-197	5.2	5.5	0.281340	0.000020	0.00031	0.281328	-51.1	0.7	-8.3	1913
MCAFEE-97SF1-GG2000SPE-175	5.9	3.7	0.281433	0.000026	0.00037	0.281419	-47.8	0.9	-5.0	1917
MCAFEE-97SF1-GG2000SPE-12	2.0	4.9	0.281366	0.000018	0.00012	0.281362	-50.2	0.6	-7.0	1917
MCAFEE-97SF1-GG2000SPE-176	13.4	4.8	0.281492	0.000022	0.00077	0.281464	-45.7	0.8	-3.4	1918
MCAFEE-97SF1-GG2000SPE-166	6.7	5.6	0.281445	0.000020	0.00040	0.281430	-47.4	0.7	-4.5	1922
MCAFEE-97SF1-GG2000SPE-187	8.0	5.5	0.281353	0.000019	0.00047	0.281335	-50.6	0.7	-7.7	1930
MCAFEE-97SF1-GG2000SPE-20	8.0	4.5	0.281419	0.000024	0.00046	0.281402	-48.3	0.9	-5.3	1933
MCAFEE-97SF1-GG2000SPE-172	3.9	4.9	0.281463	0.000019	0.00023	0.281455	-46.7	0.7	-3.3	1935
MCAFEE-97SF1-GG2000SPE-169	6.4	4.9	0.281483	0.000022	0.00042	0.281467	-46.1	0.8	-2.8	1939
MCAFEE-97SF1-GG2000SPE-17	9.0	5.1	0.281481	0.000026	0.00054	0.281460	-46.1	0.9	-0.1	2070
MCAFEE-97SF1-GG2000SPE-159	7.3	5.8	0.281462	0.000016	0.00048	0.281443	-46.8	0.6	-0.4	2079
MCAFEE-97SF1-GG2000SPE-157	10.1	5.1	0.281479	0.000018	0.00065	0.281453	-46.2	0.6	0.2	2091
MCAFEE-97SF1-GG2000SPE-144	18.4	6.1	0.281458	0.000017	0.00111	0.281414	-46.9	0.6	-1.2	2091
MCAFEE-97SF1-GG2000SPE-161	13.6	5.1	0.281399	0.000019	0.00083	0.281365	-49.0	0.7	-2.8	2095
MCAFEE-97SF1-GG2000SPE-109	7.6	4.6	0.280890	0.000018	0.00046	0.280866	-67.0	0.6	-7.3	2665
MCAFEE-97SF1-GG2000SPE-189	7.1	4.5	0.281061	0.000019	0.00047	0.281036	-61.0	0.7	-0.6	2694
MCAFEE-97SF1-GG2000SPE-5	5.4	4.8	0.280917	0.000028	0.00035	0.280899	-66.1	1.0	-5.4	2697
Sample: lower Vinini Formation. Location: Petes Summit, Toquima Range; 0518089 4337111 (NAD 83 UTM 11T)										
Low-Vinini-97SF12-GG2000SPE-21	15.1	3.0	0.282370	0.000031	0.00092	0.282362	-14.7	1.1	-4.3	476
Low-Vinini-97SF12-GG2000SPE-19	19.8	3.1	0.282504	0.000027	0.00116	0.282493	-10.0	1.0	0.4	483
Low-Vinini-97SF12-GG2000SPE-165	47.6	3.7	0.282535	0.000030	0.00278	0.282510	-8.8	1.1	1.1	486
Low-Vinini-97SF12-GG2000SPE-22	11.9	5.6	0.282469	0.000021	0.00066	0.282463	-11.2	0.8	-0.4	493
Low-Vinini-97SF12-GG2000SPE-20	12.7	5.3	0.282504	0.000017	0.00070	0.282497	-10.0	0.6	0.8	494
Low-Vinini-97SF12-GG2000SPE-176	22.5	4.3	0.282514	0.000020	0.00127	0.282502	-9.6	0.7	1.0	495
Low-Vinini-97SF12-GG2000SPE-190	17.7	4.4	0.282508	0.000019	0.00100	0.282499	-9.8	0.7	0.9	495
Low-Vinini-97SF12-GG2000SPE-10	19.2	5.8	0.281800	0.000016	0.00114	0.281789	-34.8	0.6	-24.2	496
Low-Vinini-97SF12-GG2000SPE-35	28.9	6.1	0.281903	0.000022	0.00178	0.281886	-31.2	0.8	-20.7	497
Low-Vinini-97SF12-GG2000SPE-35	29.9	4.8	0.282567	0.000024	0.00163	0.282552	-7.7	0.9	2.9	497
Low-Vinini-97SF12-GG2000SPE-45	25.5	5.3	0.282253	0.000017	0.00133	0.282225	-18.8	0.6	5.2	1117
Low-Vinini-97SF12-GG2000SPE-2	36.3	4.6	0.282133	0.000023	0.00216	0.282074	-23.1	0.8	6.9	1422
Low-Vinini-97SF12-GG2000SPE-101	18.3	4.5	0.282014	0.000020	0.00105	0.281985	-27.3	0.7	4.0	1433
Low-Vinini-97SF12-GG2000SPE-121	14.0	4.8	0.281986	0.000018	0.00082	0.281963	-28.3	0.7	3.2	1434
Low-Vinini-97SF12-GG2000SPE-27	8.8	4.7	0.282086	0.000022	0.00053	0.282072	-24.7	0.8	7.1	1435
Low-Vinini-97SF12-GG2000SPE-87	15.0	4.8	0.281975	0.000021	0.00085	0.281952	-28.7	0.7	3.0	1444
Low-Vinini-97SF12-GG2000SPE-28	16.1	5.5	0.281936	0.000016	0.00098	0.281905	-30.0	0.6	7.1	1694
Low-Vinini-97SF12-GG2000SPE-172	25.6	4.3	0.281939	0.000026	0.00153	0.281890	-29.9	0.9	6.6	1694
Low-Vinini-97SF12-GG2000SPE-41	12.8	5.3	0.281905	0.000016	0.00083	0.281878	-31.1	0.6	6.5	1708
Low-Vinini-97SF12-GG2000SPE-43	19.6	5.9	0.281827	0.000018	0.00114	0.281790	-33.9	0.6	3.5	1713
Low-Vinini-97SF12-GG2000SPE-23	24.3	5.5	0.281764	0.000022	0.00139	0.281719	-36.1	0.8	1.0	1716
Low-Vinini-97SF12-GG2000SPE-8	12.1	4.6	0.281844	0.000019	0.00071	0.281820	-33.3	0.7	4.6	1717
Low-Vinini-97SF12-GG2000SPE-194	16.8	6.5	0.281822	0.000019	0.00100	0.281789	-34.0	0.7	3.7	1724
Low-Vinini-97SF12-GG2000SPE-3	4.9	4.5	0.281870	0.000020	0.00032	0.281859	-32.4	0.7	6.4	1733
Low-Vinini-97SF12-GG2000SPE-9	11.5	5.0	0.281915	0.000020	0.00067	0.281893	-30.8	0.7	7.5	1733
Low-Vinini-97SF12-GG2000SPE-164	13.3	4.0	0.282002	0.000020	0.00084	0.281975	-27.7	0.7	10.5	1736
Low-Vinini-97SF12-GG2000SPE-37	27.3	4.8	0.282009	0.000023	0.00162	0.281955	-27.4	0.8	10.0	1744
Low-Vinini-97SF12-GG2000SPE-26	6.5	5.3	0.281938	0.000021	0.00039	0.281925	-30.0	0.7	9.0	1744
Low-Vinini-97SF12-GG2000SPE-174	10.7	4.9	0.281843	0.000018	0.00067	0.281820	-33.3	0.6	5.8	1768
Low-Vinini-97SF12-GG2000SPE-39	15.9	5.6	0.281733	0.000016	0.00092	0.281702	-37.2	0.6	1.7	1774
Low-Vinini-97SF12-GG2000SPE-14	4.5	5.6	0.281841	0.000019	0.00027	0.281832	-33.4	0.7	6.6	1783
Low-Vinini-97SF12-GG2000SPE-49	14.3	5.4	0.281675	0.000019	0.00085	0.281646	-39.2	0.7	0.0	1785
Low-Vinini-97SF12-GG2000SPE-200	11.3	5.3	0.281202	0.000020	0.00067	0.281170	-56.0	0.7	-0.6	2489
Sample: upper Vinini Formation. Location: Petes Summit, Toquima Range; 0518089 4337111 (NAD 83 UTM 11T)										
upper VININI-97SF-11-GG2000SPE-138	11.4	5.5	0.281589	0.000022	0.00066	0.281566	-42.3	0.8	-2.7	1791
upper VININI-97SF-11-GG2000SPE-192	7.3	4.2	0.281493	0.000024	0.00044	0.281478	-45.7	0.9	-5.4	1809
upper VININI-97SF-11-GG2000SPE-25	6.4	5.3	0.281319	0.000024	0.00039	0.281306	-51.8	0.8	-11.4	1814
upper VININI-97SF-11-GG2000SPE-187	10.8	5.8	0.281500	0.000021	0.00068	0.281476	-45.4	0.7	-5.2	1823
upper VININI-97SF-11-GG2000SPE-27	9.7	4.6	0.281388	0.000024	0.00058	0.281368	-49.4	0.8	-8.9	1828
upper VININI-97SF-11-GG2000SPE-17	6.3	6.0	0.281504	0.000020	0.00038	0.281491	-45.3	0.7	-4.5	1828
upper VININI-97SF-11-GG2000SPE-4	11.5	4.5	0.281568	0.000021	0.00068	0.281544	-43.0	0.7	-2.6	1831
upper VININI-97SF-11-GG2000SPE-180	13.9	4.1	0.281649	0.000026	0.00090	0.281618	-40.2	0.9	0.1	1834
upper VININI-97SF-11-GG2000SPE-182	11.9	5.3	0.281476	0.000026	0.00069	0.281452	-46.3	0.9	-5.8	1834
upper VININI-97SF-11-GG2000SPE-1	13.2	4.4	0.281570	0.000022	0.00077	0.281544	-43.0	0.8	-2.5	1835
upper VININI-97SF-11-GG2000SPE-19	10.6	4.2	0.281416	0.000020	0.00065	0.281393	-48.4	0.7	-7.8	1836
upper VININI-97SF-11-GG2000SPE-145	7.6	5.9	0.281465	0.000019	0.00046	0.281449	-46.7	0.7	-5.7	1843
upper VININI-97SF-11-GG2000SPE-139	13.8	4.4	0.281767	0.000026	0.00092	0.281735	-36.0	0.9	4.5	1843
upper VININI-97SF-11-GG2000SPE-165	11.2	4.6	0.281518	0.000028	0.00067	0.281495	-44.8	1.0	-4.0	1844
upper VININI-97SF-11-GG2000SPE-169	10.9	3.9	0.281472	0.000022	0.00067	0.281449	-46.4	0.8	-5.6	1845
upper VININI-97SF-11-GG2000SPE-159	15.2	4.4	0.281510	0.000025	0.00090	0.281479	-45.1	0.9	-4.5	1846
upper VININI-97SF-11-GG2000SPE-6	8.7	5.0	0.281424	0.000021	0.00053	0.281405	-48.1	0.8	-7.1	1850
upper VININI-97SF-11-GG2000SPE-15	10.9	4.3	0.281576	0.000019	0.00067	0.281553	-42.7	0.7	-1.7	1854
upper VININI-97SF-11-GG2000SPE-198	15.4	3.2	0.281794	0.000029	0.00094	0.281761	-35.0	1.0	5.7	1855
upper VININI-97SF-11-GG2000SPE-8	4.3	5.6	0.281494	0.000020	0.00027	0.281485	-45.6	0.7	-3.9	1864
upper VININI-97SF-11-GG2000SPE-9	13.0	5.2	0.281844	0.000019	0.00081	0.281815	-33.3	0.7	8.0	1872
upper VININI-97SF-11-GG2000SPE-5	7.5	4.3	0.281495	0.000026	0.00044	0.281479	-45.6	0.9	-3.5	1891

Hafnium isotope data of selected Roberts Mountains allochthon strata

	$(^{176}Yb + ^{176}Lu) / ^{176}Hf$ (%)	Volts Hf	$^{176}Hf/^{177}Hf$	± (1σ)	$^{176}Lu/^{177}Hf$	$^{176}Hf/^{177}Hf$ (T)	E-Hf (0)	E-Hf (0) ± (1σ)	E-Hf (T)	Age (Ma)
Sample: upper Vinini Formation. Location: Petes Summit, Toquima Range; 0518089 4337111 (NAD 83 UTM 11T)										
upper VININI-97SF-11-GG2000SPE-150	8.7	5.2	0.281498	0.000020	0.00054	0.281478	-45.5	0.7	-3.4	1895
upper VININI-97SF-11-GG2000SPE-149	11.7	4.5	0.281463	0.000023	0.00070	0.281438	-46.7	0.8	-4.8	1896
upper VININI-97SF-11-GG2000SPE-133	6.5	5.0	0.281477	0.000018	0.00040	0.281463	-46.2	0.6	-3.7	1906
upper VININI-97SF-11-GG2000SPE-2	8.2	5.0	0.281514	0.000024	0.00049	0.281496	-45.0	0.8	-2.5	1908
upper VININI-97SF-11-GG2000SPE-199	7.8	4.5	0.281562	0.000025	0.00049	0.281544	-43.2	0.9	-0.4	1926
upper VININI-97SF-11-GG2000SPE-197	8.6	4.9	0.281352	0.000023	0.00050	0.281334	-50.7	0.8	-7.8	1929
upper VININI-97SF-11-GG2000SPE-11	5.5	5.2	0.281162	0.000025	0.00034	0.281150	-57.4	0.9	-14.1	1937
upper VININI-97SF-11-GG2000SPE-7	9.0	5.3	0.281354	0.000022	0.00052	0.281335	-50.6	0.8	-7.6	1937
upper VININI-97SF-11-GG2000SPE-160	6.0	5.5	0.281464	0.000014	0.00037	0.281450	-46.7	0.5	-2.6	1974
upper VININI-97SF-11-GG2000SPE-12	10.2	4.8	0.281496	0.000018	0.00065	0.281471	-45.6	0.6	0.4	2074
upper VININI-97SF-11-GG2000SPE-179	7.8	5.1	0.281399	0.000023	0.00046	0.281381	-49.0	0.8	-2.7	2077
upper VININI-97SF-11-GG2000SPE-178	32.6	5.1	0.281508	0.000027	0.00191	0.281432	-45.2	0.9	-0.7	2086
upper VININI-97SF-11-GG2000SPE-189	9.3	5.1	0.281441	0.000020	0.00058	0.281418	-47.5	0.7	-1.2	2086
upper VININI-97SF-11-GG2000SPE-23	11.1	5.2	0.281410	0.000019	0.00067	0.281384	-48.6	0.7	-2.3	2089
upper VININI-97SF-11-GG2000SPE-135	12.1	4.8	0.281414	0.000023	0.00074	0.281384	-48.5	0.8	-2.0	2100
upper VININI-97SF-11-GG2000SPE-125	8.9	4.1	0.281371	0.000022	0.00055	0.281347	-50.0	0.8	1.7	2317
upper VININI-97SF-11-GG2000SPE-200	1.7	4.7	0.281044	0.000023	0.00011	0.281039	-61.6	0.8	-0.9	2677
upper VININI-97SF-11-GG2000SPE-194	9.5	3.9	0.280969	0.000025	0.00057	0.280939	-64.2	0.9	-3.6	2713
upper VININI-97SF-11-GG2000SPE-22	14.4	4.3	0.281085	0.000023	0.00081	0.281043	-60.1	0.8	0.1	2713
Sample: Elder Sandstone. Location: Elder Creek, Shoshone Range; 0516196 4460270 (NAD 83 UTM 11T)										
Elder-SS-GG2000SPE-59	13.0	3.7	0.281720	0.000022	0.00074	0.281695	-37.6	0.8	2.6	1823
Elder-SS-GG2000SPE-43	10.1	4.4	0.281560	0.000020	0.00060	0.281539	-43.3	0.7	-2.9	1824
Elder-SS-GG2000SPE-47	12.2	4.2	0.281403	0.000023	0.00067	0.281380	-48.9	0.8	-8.5	1826
Elder-SS-GG2000SPE-52	15.6	4.0	0.281483	0.000020	0.00087	0.281453	-46.0	0.7	-5.8	1832
Elder-SS-GG2000SPE-42	10.5	4.4	0.281431	0.000020	0.00063	0.281409	-47.9	0.7	-7.3	1835
Elder-SS-GG2000SPE-36	10.8	5.9	0.281460	0.000019	0.00069	0.281436	-46.9	0.7	-6.3	1835
Elder-SS-GG2000SPE-49	8.5	5.2	0.281431	0.000018	0.00049	0.281414	-47.9	0.6	-7.1	1836
Elder-SS-GG2000SPE-64	12.8	4.7	0.281571	0.000022	0.00075	0.281545	-42.9	0.8	-2.4	1836
Elder-SS-GG2000SPE-28	17.1	5.9	0.281385	0.000022	0.00096	0.281352	-49.5	0.8	-9.1	1845
Elder-SS-GG2000SPE-33	13.0	4.0	0.281749	0.000024	0.00077	0.281722	-36.6	0.8	4.1	1846
Elder-SS-GG2000SPE-72	8.5	4.8	0.281562	0.000016	0.00050	0.281544	-43.3	0.6	-2.2	1846
Elder-SS-GG2000SPE-16	7.4	4.5	0.281331	0.000027	0.00050	0.281314	-51.4	1.0	-10.4	1847
Elder-SS-GG2000SPE-101	12.0	4.2	0.281568	0.000020	0.00069	0.281544	-43.0	0.7	-2.2	1847
Elder-SS-GG2000SPE-102	17.8	3.0	0.281592	0.000038	0.00116	0.281551	-42.2	1.3	-1.9	1847
Elder-SS-GG2000SPE-30	37.8	3.9	0.281899	0.000035	0.00202	0.281828	-31.3	1.2	7.9	1849
Elder-SS-GG2000SPE-18	18.6	4.2	0.281581	0.000025	0.00105	0.281544	-42.6	0.9	-2.2	1849
Elder-SS-GG2000SPE-13	13.5	4.7	0.281545	0.000020	0.00077	0.281517	-43.9	0.7	-3.1	1850
Elder-SS-GG2000SPE-17	52.7	4.7	0.281635	0.000036	0.00270	0.281540	-40.7	1.3	-2.2	1853
Elder-SS-GG2000SPE-21	9.1	3.2	0.281590	0.000025	0.00053	0.281571	-42.3	0.9	-0.9	1860
Elder-SS-GG2000SPE-12	12.1	4.3	0.281539	0.000022	0.00076	0.281512	-44.1	0.8	-2.8	1871
Elder-SS-GG2000SPE-141	49.2	3.8	0.281879	0.000031	0.00311	0.281767	-32.0	1.1	6.6	1885
Elder-SS-GG2000SPE-148	10.8	4.0	0.281435	0.000027	0.00059	0.281414	-47.7	0.9	-5.7	1896
Elder-SS-GG2000SPE-148	15.9	3.7	0.281566	0.000025	0.00099	0.281530	-43.1	0.9	-1.6	1896
Elder-SS-GG2000SPE-41	7.2	4.9	0.281383	0.000017	0.00039	0.281368	-49.6	0.6	-6.9	1914
Elder-SS-GG2000SPE-92	10.3	4.5	0.281417	0.000017	0.00055	0.281398	-48.4	0.6	-5.8	1917
Elder-SS-GG2000SPE-66	11.4	5.5	0.281432	0.000020	0.00069	0.281404	-47.9	0.7	-2.0	2069
Elder-SS-GG2000SPE-57	10.7	4.6	0.281486	0.000021	0.00062	0.281461	-45.9	0.7	0.2	2078
Elder-SS-GG2000SPE-37	8.4	5.1	0.281490	0.000019	0.00054	0.281469	-45.8	0.7	0.6	2084
Elder-SS-GG2000SPE-11	7.7	5.4	0.281463	0.000021	0.00051	0.281443	-46.7	0.8	-0.3	2084
Elder-SS-GG2000SPE-27	14.9	5.4	0.281488	0.000020	0.00083	0.281455	-45.9	0.7	0.2	2088
Elder-SS-GG2000SPE-31	6.2	5.3	0.281858	0.000022	0.00036	0.281841	-32.8	0.8	26.0	2606
Elder-SS-GG2000SPE-62	7.1	4.3	0.281216	0.000017	0.00042	0.281195	-55.5	0.6	3.4	2621
Elder-SS-GG2000SPE-95	12.5	4.9	0.280973	0.000021	0.00066	0.280938	-64.1	0.7	-3.5	2717
Sample: Slaven Chert. Location: Slaven Canyon, Shoshone Range; 0519428 4479302 (NAD 83 UTM 11T)										
Slaven-RMA-GG2000SPE-172	44.8	4.3	0.281830	0.000027	0.00259	0.281742	-33.8	0.9	3.4	1786
Slaven-RMA-GG2000SPE-129	12.0	4.9	0.281468	0.000029	0.00069	0.281444	-46.6	1.0	-6.2	1825
Slaven-RMA-GG2000SPE-168	6.7	5.0	0.281442	0.000021	0.00040	0.281428	-47.5	0.8	-6.8	1825
Slaven-RMA-GG2000SPE-15	14.9	4.2	0.281670	0.000022	0.00079	0.281643	-39.4	0.8	0.8	1826
Slaven-RMA-GG2000SPE-100	5.5	3.9	0.281603	0.000029	0.00035	0.281591	-41.8	1.0	-1.0	1826
Slaven-RMA-GG2000SPE-167	9.0	4.0	0.281637	0.000023	0.00055	0.281618	-40.6	0.8	0.0	1829
Slaven-RMA-GG2000SPE-78	10.4	4.9	0.281640	0.000025	0.00065	0.281618	-40.5	0.9	0.0	1830
Slaven-RMA-GG2000SPE-180	7.5	5.2	0.281444	0.000016	0.00045	0.281428	-47.4	0.6	-6.7	1832
Slaven-RMA-GG2000SPE-152	9.2	5.4	0.281491	0.000026	0.00055	0.281472	-45.7	0.9	-5.1	1832
Slaven-RMA-GG2000SPE-142	11.2	5.6	0.281458	0.000027	0.00065	0.281435	-46.9	1.0	-6.4	1832
Slaven-RMA-GG2000SPE-186	10.2	4.8	0.281743	0.000028	0.00058	0.281723	-36.8	1.0	3.8	1832
Slaven-RMA-GG2000SPE-197	15.9	5.3	0.281339	0.000031	0.00089	0.281308	-51.1	1.1	-10.8	1838
Slaven-RMA-GG2000SPE-126	7.9	4.6	0.281476	0.000026	0.00048	0.281459	-46.3	0.9	-5.2	1846
Slaven-RMA-GG2000SPE-53	8.1	5.3	0.281454	0.000027	0.00049	0.281437	-47.1	0.9	-6.0	1846
Slaven-RMA-GG2000SPE-108	11.7	5.3	0.281385	0.000022	0.00068	0.281361	-49.5	0.8	-8.7	1846
Slaven-RMA-GG2000SPE-140	7.6	5.0	0.281458	0.000020	0.00046	0.281442	-46.9	0.7	-5.9	1846
Slaven-RMA-GG2000SPE-13	9.2	4.4	0.281474	0.000023	0.00056	0.281454	-46.4	0.8	-5.4	1847
Slaven-RMA-GG2000SPE-7	14.5	4.5	0.281591	0.000026	0.00086	0.281561	-42.2	0.9	-1.6	1847
Slaven-RMA-GG2000SPE-1	8.0	4.7	0.281530	0.000036	0.00048	0.281514	-44.4	1.3	-3.3	1848
Slaven-RMA-GG2000SPE-20	9.4	4.6	0.281455	0.000027	0.00054	0.281436	-47.0	1.0	-6.0	1849
Slaven-RMA-GG2000SPE-67	10.1	4.6	0.281498	0.000025	0.00061	0.281477	-45.5	0.9	-4.5	1849

Hafnium isotope data of selected Roberts Mountains allochthon strata

	$(^{176}Yb + ^{176}Lu) / ^{176}Hf$ (%)	Volts Hf	$^{176}Hf/^{177}Hf$	± (1σ)	$^{176}Lu/^{177}Hf$	$^{176}Hf/^{177}Hf$ (T)	E-Hf (0)	E-Hf (0) ± (1σ)	E-Hf (T)	Age (Ma)
Sample: Slaven Chert. Location: Slaven Canyon, Shoshone Range; 0519428 4479302 (NAD 83 UTM 11T)										
Slaven-RMA-GG2000SPE-137	4.9	5.1	0.281870	0.000017	0.00030	0.281859	-32.4	0.6	9.1	1852
Slaven-RMA-GG2000SPE-5	17.0	5.1	0.281519	0.000025	0.00102	0.281483	-44.8	0.9	-4.2	1852
Slaven-RMA-GG2000SPE-170	8.6	4.7	0.281522	0.000017	0.00054	0.281503	-44.7	0.6	-3.1	1872
Slaven-RMA-GG2000SPE-86	13.3	4.3	0.281479	0.000024	0.00080	0.281450	-46.2	0.9	-4.9	1874
Slaven-RMA-GG2000SPE-117	7.5	6.8	0.281536	0.000023	0.00047	0.281519	-44.2	0.8	-1.6	1913
Slaven-RMA-GG2000SPE-109	4.6	4.3	0.281358	0.000035	0.00028	0.281347	-50.5	1.2	-7.4	1925
Slaven-RMA-GG2000SPE-156	6.8	4.5	0.281482	0.000024	0.00042	0.281467	-46.1	0.9	-3.1	1927
Slaven-RMA-GG2000SPE-18	7.7	4.8	0.281656	0.000024	0.00047	0.281639	-39.9	0.9	3.0	1929
Slaven-RMA-GG2000SPE-107	13.1	5.3	0.281504	0.000039	0.00077	0.281474	-45.3	1.4	0.4	2066
Slaven-RMA-GG2000SPE-39	13.8	5.7	0.281482	0.000021	0.00083	0.281449	-46.1	0.7	-0.4	2070
Slaven-RMA-GG2000SPE-35	11.2	4.4	0.281547	0.000027	0.00086	0.281513	-43.8	0.9	2.2	2086
Slaven-RMA-GG2000SPE-175	18.2	5.1	0.281436	0.000017	0.00104	0.281395	-47.7	0.6	-1.8	2094
Slaven-RMA-GG2000SPE-90	11.5	5.4	0.281257	0.000021	0.00068	0.281224	-54.0	0.7	3.2	2571
Slaven-RMA-GG2000SPE-153	11.2	5.6	0.281245	0.000028	0.00064	0.281213	-54.5	1.0	2.9	2572
Slaven-RMA-GG2000SPE-48	15.1	5.1	0.280907	0.000033	0.00087	0.280863	-66.4	1.2	-7.3	2670
Slaven-RMA-GG2000SPE-82	8.3	4.2	0.281280	0.000033	0.00055	0.281251	-53.2	1.2	6.9	2686
Slaven-RMA-GG2000SPE-148	22.9	4.2	0.281257	0.000029	0.00135	0.281187	-54.0	1.0	4.8	2692

Notes:

1. Data reduction methodology is from Woodhead et al. (2004)
2. Analytical methods described in detail by Gehrels and Pecha (2014)
3. (176Yb + 176Lu) / 176Hf (%) expresses the proportion of 176 due to 176Yb + 176Lu versus the proportion due to 176Hf, in %.
4. Volts Hf is the sum of voltages of all Hf isotopes.
5. 176Hf/177Hf is the measured 176Hf/177Hf, corrected for fractionation and inferences. Shown with uncertainty expressed at 1-sigma.
6. $^{176}Lu/^{177}Hf$ is the intensity of 176Lu, calculated from the measured instensity of 175Lu and 176Lu/175Lu=0.02653 (from Patchett, 1983), compared to the measured intensity of 177Hf. Fractionation of Lu isotopes is assumed to be the same as fractionation of Yb isotopes.
7. 176Hf/177Hf (T) is the 176Hf/177Hf corrected to the time of crystallization using a decay constant of 1.867e-11 (from Scherer et al., 2001 and Soderland et al., 2004)
8. E-Hf (0) is the present-day epsilon Hf value using 176Hf/177Hf=0.282785 and 176Lu/177Hf=0.0336 (from Bouvier et al., 2008). The uncertainty is expressed at 1-sigma.
9. E-Hf(T) is the epsilon Hf value at time of crystallization. Uncertainty is expressed at 1 sigma.
10. U-Pb ages are based on 206/238 for ages younger than ~1.0 Ga, and on 206/207 for ages older than ~1.0 Ga. This age cutoff may be slightly different for each sample.
11. Isotope ratios as follows:

180/177	1.8866600	Patchett (1983)
179/177	0.7325000	Patchett & Tatsumoto (1980)
178/177	1.4671800	Patchett (1983)
176/177	0.2821600	Patchett (1983)
174/177	0.0087100	Patchett (1983)
176/175	0.0265300	Patchett (1983)
176/171	0.9016910	Vervoort et al. (2004)
173/171	1.1323569	Vervoort et al. (2004)
172/171	1.5317360	Vervoort et al. (2004)

Notes for plots:

1. DM array is from Vervoort and Blichert-Toft (1999), using 176Hf/177Hf=0.283225 and 176Lu/177Hf=0.0383

2. CHUR is from Bouvier et al. (2008), using 176Hf/177Hf=0.282785 and 176Lu/177Hf=0.0336.
3. Hf isotope evolution lines assume an average value of 176Lu/177Hf=0.0115 and a range of 176Lu/177Hf=0.0036 to 176Lu/177Hf=0.0193. Values are from the average and 2-sigma range of values reported by Vervoort and Patchett (1996) and Vervoort et al. (1999).
4. Uncertainties shown at 2-sigma.
5. Uncertainty for EpsilonT is nearly identical for Espsilon 0 because of the very long half-life.

APPENDIX E

U-Pb Geochronologic anlayses of selected Harmony Formation strata

Table notes are at the end of the appendix.

					Isotope ratios								Apparent ages (Ma)							
	U	206Pb	U/Th	206Pb*	±	207Pb*	±	206Pb*	±	error	206Pb*	±	207Pb*	±	206Pb*	±	Best age	±	Conc.	Discor.
	(ppm)	204Pb		207Pb*	(%)	235U*	(%)	238U	(%)	corr.	238U*	(Ma)	235U	(Ma)	207Pb*	(Ma)	(Ma)	(Ma)	(%)	(%)
Sample: LCC #1. Location: Little Cottonwood Canyon, Galena Range; 0490600 4494792 (NAD 83 UTM 11T)																				
LCC1-88-RM15-1	182	39487	2.0	13.2319	0.6	1.9196	1.5	0.1842	1.4	0.93	1090.0	14.4	1087.9	10.3	1083.8	11.6	1083.8	11.6	100.6	-0.6
LCC1-88-RM15-10	116	24982	1.4	12.7615	1.4	2.1130	3.6	0.1959	3.3	0.92	1153.1	34.7	1153.1	24.5	1152.9	27.1	1152.9	27.1	100.0	0.0
LCC1-88-RM15-100	64	17974	1.5	13.1335	1.8	1.9113	2.9	0.1821	2.2	0.77	1078.2	22.0	1085.0	19.3	1098.8	37.0	1098.8	37.0	98.1	1.9
LCC1-88-RM15-102	80	32781	0.7	9.8351	0.8	4.0861	2.6	0.2915	2.5	0.95	1648.8	35.7	1651.5	21.1	1654.9	15.3	1654.9	15.3	99.6	0.4
LCC1-88-RM15-103	58	24276	1.0	9.7648	1.8	4.2505	7.6	0.3010	7.4	0.97	1696.4	110.2	1683.8	62.6	1668.2	33.9	1668.2	33.9	101.7	-1.7
LCC1-88-RM15-104	117	40705	1.7	13.0278	1.1	2.0520	3.9	0.1939	3.8	0.96	1142.4	39.8	1133.0	27.0	1114.9	21.5	1114.9	21.5	102.5	-2.5
LCC1-88-RM15-106	21	5810	1.8	13.0514	5.5	1.9940	5.8	0.1887	2.0	0.34	1114.6	20.1	1113.5	39.2	1111.3	109.0	1111.3	109.0	100.3	-0.3
LCC1-88-RM15-107	261	25120	1.8	4.9085	0.3	13.7127	1.4	0.4882	1.4	0.98	2562.8	29.1	2730.1	13.2	2856.3	4.3	2856.3	4.3	89.7	10.3
LCC1-88-RM15-108	43	9139	0.9	11.6310	2.5	2.8138	3.7	0.2374	2.8	0.75	1373.0	34.3	1359.2	27.8	1337.7	47.4	1337.7	47.4	102.6	-2.6
LCC1-88-RM15-109	174	25420	2.0	13.3269	0.5	1.8943	1.5	0.1831	1.4	0.94	1083.9	13.8	1079.1	9.8	1069.5	10.0	1069.5	10.0	101.3	-1.3
LCC1-88-RM15-110	105	20397	2.0	13.3037	1.2	1.9242	2.2	0.1857	1.9	0.85	1097.8	19.2	1089.5	14.9	1073.0	23.3	1073.0	23.3	102.3	-2.3
LCC1-88-RM15-111	54	15414	1.6	13.3441	2.2	1.8598	3.2	0.1800	2.3	0.72	1067.0	23.1	1066.9	21.4	1066.9	45.2	1066.9	45.2	100.0	0.0
LCC1-88-RM15-112	63	17482	1.4	13.0287	1.6	2.0019	2.8	0.1892	2.2	0.81	1116.9	22.8	1116.2	18.7	1114.8	32.6	1114.8	32.6	100.2	-0.2
LCC1-88-RM15-113	136	55605	2.7	13.2656	1.1	1.8641	3.6	0.1793	3.5	0.96	1063.4	34.2	1068.4	24.1	1078.7	21.2	1078.7	21.2	98.6	1.4
LCC1-88-RM15-114	66	15720	3.0	12.5992	1.5	2.2009	2.5	0.2011	2.0	0.80	1181.3	21.8	1181.3	17.7	1181.4	30.3	1181.4	30.3	100.0	0.0
LCC1-88-RM15-115	282	82238	1.0	12.2627	0.5	2.3171	2.5	0.2061	2.4	0.98	1207.9	26.6	1217.5	17.5	1234.7	10.1	1234.7	10.1	97.8	2.2
LCC1-88-RM15-116	26	9370	1.5	13.5778	8.2	1.8388	8.6	0.1811	2.7	0.32	1072.8	27.0	1059.4	56.9	1031.9	165.9	1031.9	165.9	104.0	-4.0
LCC1-88-RM15-118	155	85081	2.3	9.1392	0.3	4.8430	1.1	0.3210	1.1	0.96	1794.7	16.6	1792.4	9.3	1789.7	5.8	1789.7	5.8	100.3	-0.3
LCC1-88-RM15-119	47	13087	2.1	12.8797	1.6	2.0915	2.7	0.1954	2.2	0.82	1150.4	23.4	1146.0	18.6	1137.7	30.9	1137.7	30.9	101.1	-1.1
LCC1-88-RM15-121	156	80163	1.7	13.2510	1.0	1.9284	1.7	0.1853	1.4	0.81	1096.0	13.9	1091.0	11.3	1080.9	19.6	1080.9	19.6	101.4	-1.4
LCC1-88-RM15-122	37	11074	0.9	13.3704	3.2	1.8838	4.1	0.1827	2.5	0.61	1081.6	24.8	1075.4	27.1	1062.9	65.1	1062.9	65.1	101.8	-1.8
LCC1-88-RM15-123	81	35495	1.2	10.9544	1.0	3.1932	2.1	0.2537	1.8	0.89	1457.5	24.0	1455.5	16.0	1452.6	18.3	1452.6	18.3	100.3	-0.3
LCC1-88-RM15-124	104	41683	1.9	13.0900	1.9	1.9333	3.2	0.1835	2.6	0.80	1086.3	25.8	1092.7	21.5	1105.4	38.3	1105.4	38.3	98.3	1.7
LCC1-88-RM15-125	187	47454	2.2	12.8428	0.6	2.0969	2.8	0.1953	2.7	0.98	1150.1	28.3	1147.8	18.9	1143.4	11.7	1143.4	11.7	100.6	-0.6
LCC1-88-RM15-126	52	10717	2.2	12.8719	2.4	2.0977	3.1	0.1958	1.8	0.61	1152.9	19.5	1148.0	21.0	1138.9	48.3	1138.9	48.3	101.2	-1.2
LCC1-88-RM15-127	57	7411	1.1	15.7953	4.1	1.0083	6.0	0.1155	4.3	0.72	704.7	28.8	708.0	30.5	718.6	88.1	704.7	28.8	98.1	1.9
LCC1-88-RM15-128	60	29628	1.6	8.7847	0.9	5.3318	5.3	0.3397	5.2	0.98	1885.2	85.6	1874.0	45.5	1861.5	16.6	1861.5	16.6	101.3	-1.3
LCC1-88-RM15-129	80	19756	1.4	12.3785	0.9	2.3201	2.1	0.2083	1.8	0.89	1219.7	20.4	1218.5	14.6	1216.2	18.4	1216.2	18.4	100.3	-0.3
LCC1-88-RM15-13	49	9226	0.8	12.5629	7.3	2.0939	8.9	0.1908	5.1	0.57	1125.6	52.3	1146.8	60.9	1187.1	143.8	1187.1	143.8	94.8	5.2
LCC1-88-RM15-130	180	54058	3.1	13.4363	0.7	1.8295	2.1	0.1783	2.0	0.94	1057.6	19.2	1056.1	13.8	1053.0	14.8	1053.0	14.8	100.4	-0.4
LCC1-88-RM15-131	151	89915	3.4	5.3569	0.1	13.4392	2.3	0.5221	2.3	1.00	2708.3	51.7	2711.0	22.1	2713.1	2.4	2713.1	2.4	99.8	0.2
LCC1-88-RM15-133	550	89612	2.6	13.1985	0.2	1.9031	2.4	0.1822	2.3	1.00	1078.8	23.3	1082.2	15.7	1088.9	4.4	1088.9	4.4	99.1	0.9
LCC1-88-RM15-134	78	37895	0.6	13.2022	1.8	1.9115	2.4	0.1830	1.6	0.67	1083.5	16.1	1085.1	16.1	1088.3	36.0	1088.3	36.0	99.6	0.4
LCC1-88-RM15-135	112	63794	1.3	9.2090	0.7	4.7209	1.7	0.3153	1.6	0.91	1766.8	24.3	1771.0	14.5	1775.9	13.3	1775.9	13.3	99.5	0.5
LCC1-88-RM15-136	66	28533	1.5	11.4427	1.4	2.9146	4.5	0.2419	4.3	0.95	1396.5	53.7	1385.7	34.0	1369.1	26.6	1369.1	26.6	102.0	-2.0
LCC1-88-RM15-137	126	20916	0.8	15.9911	2.2	0.9624	2.8	0.1116	1.7	0.60	682.1	10.8	684.5	13.9	692.5	47.6	682.1	10.8	98.5	1.5
LCC1-88-RM15-138	110	25720	1.9	13.2219	2.0	1.8807	2.8	0.1804	1.9	0.70	1068.9	19.2	1074.3	18.5	1085.3	40.0	1085.3	40.0	98.5	1.5
LCC1-88-RM15-139	191	56410	1.8	13.3174	1.2	1.8784	2.6	0.1814	2.3	0.89	1074.8	23.2	1073.5	17.4	1070.9	23.7	1070.9	23.7	100.4	-0.4
LCC1-88-RM15-14	74	16843	1.2	13.3982	0.9	1.8299	1.1	0.1778	0.6	0.58	1055.0	6.3	1056.2	7.2	1058.8	18.0	1058.8	18.0	99.6	0.4
LCC1-88-RM15-140	26	11190	1.0	10.8367	4.5	3.1929	5.2	0.2509	2.6	0.50	1443.3	34.0	1455.4	40.3	1473.1	85.3	1473.1	85.3	98.0	2.0
LCC1-88-RM15-141	69	19484	3.8	12.8033	3.3	2.0729	5.0	0.1925	3.7	0.75	1134.8	38.6	1139.9	34.0	1149.6	65.3	1149.6	65.3	98.7	1.3
LCC1-88-RM15-142	218	38398	2.1	13.5439	0.5	1.7628	1.1	0.1732	1.0	0.88	1029.5	9.2	1031.9	7.1	1036.9	10.7	1036.9	10.7	99.3	0.7
LCC1-88-RM15-143	281	11695	1.1	5.8923	0.2	9.0594	2.2	0.3872	2.2	0.99	2109.6	40.2	2344.0	20.6	2554.8	4.1	2554.8	4.1	82.6	17.4
LCC1-88-RM15-144	47	19464	1.8	12.0248	1.3	2.4874	4.0	0.2169	3.8	0.95	1265.6	43.3	1268.4	28.8	1273.0	24.9	1273.0	24.9	99.4	0.6
LCC1-88-RM15-145	88	68285	1.2	9.8781	0.8	4.0176	2.0	0.2878	1.9	0.92	1630.7	26.7	1637.8	16.4	1646.8	14.6	1646.8	14.6	99.0	1.0
LCC1-88-RM15-146	141	21183	1.1	12.9934	1.5	1.9676	2.5	0.1854	2.0	0.79	1096.5	19.9	1104.5	16.9	1120.2	30.9	1120.2	30.9	97.9	2.1
LCC1-88-RM15-147	283	85348	1.9	10.8200	0.3	3.2770	3.8	0.2572	3.8	1.00	1475.3	49.6	1475.6	29.4	1476.0	6.1	1476.0	6.1	99.9	0.1
LCC1-88-RM15-148	71	29738	2.1	9.7772	0.7	4.1894	2.8	0.2971	2.8	0.97	1676.8	40.7	1672.0	23.3	1665.9	13.1	1665.9	13.1	100.7	-0.7
LCC1-88-RM15-149	54	18147	2.8	13.1826	2.7	1.9368	3.5	0.1852	2.2	0.64	1095.2	22.5	1093.9	23.3	1091.3	53.5	1091.3	53.5	100.4	-0.4
LCC1-88-RM15-15	110	18505	1.0	13.2410	1.0	1.8939	2.3	0.1819	2.1	0.91	1077.2	21.1	1078.9	15.5	1082.5	19.7	1082.5	19.7	99.5	0.5
LCC1-88-RM15-150	178	62900	2.0	13.1520	0.8	1.9555	1.7	0.1865	1.5	0.87	1102.6	14.7	1100.3	11.3	1096.0	16.7	1096.0	16.7	100.6	-0.6
LCC1-88-RM15-151	80	33415	3.2	9.0739	0.4	4.7912	1.6	0.3153	1.6	0.97	1766.8	24.3	1783.4	13.6	1802.8	7.4	1802.8	7.4	98.0	2.0
LCC1-88-RM15-152	167	16190	2.0	13.5991	1.0	1.7027	1.9	0.1679	1.6	0.85	1000.8	14.7	1009.6	11.9	1028.7	19.8	1028.7	19.8	97.3	2.7
LCC1-88-RM15-153	261	144990	1.4	5.9124	0.1	10.9297	1.3	0.4687	1.3	1.00	2477.7	26.2	2517.2	11.9	2549.1	1.9	2549.1	1.9	97.2	2.8
LCC1-88-RM15-154	172	114327	1.2	5.8944	0.2	11.0631	1.2	0.4730	1.2	0.98	2496.5	24.8	2528.5	11.3	2554.2	3.7	2554.2	3.7	97.7	2.3
LCC1-88-RM15-155	201	62533	2.5	12.5935	0.6	2.1525	2.4	0.1966	2.4	0.97	1157.0	24.9	1165.9	16.8	1182.3	11.0	1182.3	11.0	97.9	2.1
LCC1-88-RM15-156	112	30440	1.2	13.2529	1.1	1.8757	1.7	0.1803	1.2	0.74	1068.6	12.2	1072.5	11.2	1080.7	22.9	1080.7	22.9	98.9	1.1
LCC1-88-RM15-157	144	25601	1.8	13.3223	1.3	1.8642	3.6	0.1801	3.5	0.94	1067.6	34.9	1068.5	24.9	1070.2	25.5	1070.2	25.5	99.8	0.2
LCC1-88-RM15-158	53	18414	1.7	11.0492	0.9	3.1503	1.7	0.2525	1.4	0.83	1451.1	17.9	1445.1	12.8	1436.2	17.8	1436.2	17.8	101.0	-1.0
LCC1-88-RM15-159	136	36069	1.4	12.9902	0.4	2.0111	1.8	0.1895	1.8	0.98	1118.5	18.3	1119.3	12.3	1120.7	7.3	1120.7	7.3	99.8	0.2
LCC1-88-RM15-160	107	31296	2.5	9.4831	0.8	4.4954	1.9	0.3092	1.7	0.91	1736.7	26.1	1730.1	15.6	1722.2	14.2	1722.2	14.2	100.8	-0.8
LCC1-88-RM15-162	435	124266	3.0	13.0680	0.2	1.9498	2.6	0.1848	2.6	1.00	1093.1	26.3	1098.4	17.6	1108.8	3.8	1108.8	3.8	98.6	1.4
LCC1-88-RM15-163	90	25964	2.2	11.6814	0.7	2.6996	1.3	0.2287	1.1	0.86	1327.8	13.2	1328.4	9.5	1329.3	12.7	1329.3	12.7	99.9	0.1
LCC1-88-RM15-165	119	47802	1.9	10.8494	0.7	3.2720	2.2	0.2575	2.1	0.95	1476.8	28.2	1474.4	17.4	1470.9	12.7	1470.9	12.7	100.4	-0.4
LCC1-88-RM15-166	102	16358	1.4	11.8226	1.1	2.5528	2.3	0.2189	2.0	0.89	1278.0	23.5	1287.2	16.7	1306.0	20.4	1306.0	20.4	97.7	2.3
LCC1-88-RM15-167	120	21233	2.5	13.5931	1.2	1.7713	3.0	0.1746	2.8	0.92	1037.6	26.9	1035.0	19.8	1029.6	23.9	1029.6	23.9	100.8	-0.8
LCC1-88-RM15-168	107	35975	1.7	13.0386	1.7	2.0355	6.6	0.1925	6.4	0.97	1134.8	66.2	1127.4	44.8	1113.3	33.7	1113.3	33.7	101.9	-1.9
LCC1-88-RM15-169	81	15420	1.4	13.1660	2.4	1.9055	3.7	0.1819	2.8	0.75	1077.6	27.3	1083.0	24.3	1093.9	48.0	1093.9	48.0	98.5	1.5
LCC1-88-RM15-171	123	95269	3.4	12.8175	0.6	2.0684	2.1	0.1923	2.0	0.95	1133.7	20.7	1138.4	14.4	1147.4	12.9	1147.4	12.9	98.8	1.2
LCC1-88-RM15-172	226	74807	2.8	13.1055	0.6	1.9393	2.3	0.1843	2.2	0.97	1090.6	22.1	1094.7	15.2	1103.0	11.1	1103.0	11.1	98.9	1.1
LCC1-88-RM15-174	42	16265	2.3	11.4378	2.6	2.8508	3.5	0.2365	2.3	0.66	1368.4	28.5	1369.0	26.4	1370.0	51.0	1370.0	51.0	99.9	0.1

1.0,0.8

U-Pb Geochronologic anlayses of selected Harmony Formation strata

				Isotope ratios									Apparent ages (Ma)							
	U	206Pb	U/Th	206Pb*	±	207Pb*	±	206Pb*	±	error	206Pb*	±	207Pb*	±	206Pb*	±	Best age	±	Conc.	Discor.
	(ppm)	204Pb		207Pb*	(%)	235U*	(%)	238U	(%)	corr.	238U*	(Ma)	235U	(Ma)	207Pb*	(Ma)	(Ma)	(Ma)	(%)	(%)
Sample: LCC #1. Location: Little Cottonwood Canyon, Galena Range; 0490600 4494792 (NAD 83 UTM 11T)																				
LCC1-88-RM15-175	63	29651	1.2	9.4761	0.9	4.4013	1.6	0.3025	1.3	0.83	1703.6	19.8	1712.6	13.2	1723.5	16.5	1723.5	16.5	98.8	1.2
LCC1-88-RM15-176	101	20426	2.3	13.6745	1.8	1.7360	2.6	0.1722	1.9	0.72	1024.0	17.8	1022.0	16.9	1017.5	36.9	1017.5	36.9	100.6	-0.6
LCC1-88-RM15-177	82	27712	1.6	11.4543	1.0	2.7976	1.8	0.2324	1.5	0.83	1347.1	17.6	1354.9	13.1	1367.2	19.0	1367.2	19.0	98.5	1.5
LCC1-88-RM15-178	61	34230	1.1	5.4765	0.2	12.5121	1.1	0.4970	1.1	0.99	2600.8	23.6	2643.6	10.5	2676.6	2.7	2676.6	2.7	97.2	2.8
LCC1-88-RM15-179	368	111675	3.2	13.5458	0.6	1.7679	1.4	0.1737	1.2	0.90	1032.4	11.9	1033.7	9.0	1036.6	12.0	1036.6	12.0	99.6	0.4
LCC1-88-RM15-18	118	33662	2.5	9.7087	2.1	4.1365	3.4	0.2913	2.6	0.78	1647.9	38.5	1661.6	27.9	1678.9	39.6	1678.9	39.6	98.2	1.8
LCC1-88-RM15-180	38	21982	1.1	5.8935	0.6	11.1761	2.5	0.4777	2.4	0.97	2517.3	50.4	2537.9	23.2	2554.5	9.4	2554.5	9.4	98.5	1.5
LCC1-88-RM15-181	133	18213	6.8	13.6544	1.2	1.6737	1.6	0.1657	1.0	0.64	988.6	9.4	998.6	10.3	1020.5	25.2	1020.5	25.2	96.9	3.1
LCC1-88-RM15-182	123	20752	1.8	11.4074	0.8	2.7904	1.0	0.2309	0.6	0.60	1339.0	7.1	1353.0	7.3	1375.1	15.1	1375.1	15.1	97.4	2.6
LCC1-88-RM15-184	199	15241	0.8	15.5628	5.7	1.0212	6.6	0.1153	3.3	0.50	703.3	22.2	714.5	33.9	750.0	120.6	703.3	22.2	93.8	6.2
LCC1-88-RM15-187	79	13515	2.1	12.4638	5.3	2.0964	6.6	0.1895	4.0	0.61	1118.7	41.3	1147.6	45.7	1202.7	104.2	1202.7	104.2	93.0	7.0
LCC1-88-RM15-188	260	79056	2.5	10.8659	1.1	3.2921	9.6	0.2594	9.5	0.99	1487.0	126.1	1479.2	74.6	1468.0	20.4	1468.0	20.4	101.3	-1.3
LCC1-88-RM15-190	175	26563	3.6	13.5858	1.3	1.6906	1.9	0.1666	1.3	0.71	993.2	12.1	1005.0	11.9	1030.7	26.6	1030.7	26.6	96.4	3.6
LCC1-88-RM15-191	61	10359	0.9	13.2809	2.3	1.8765	4.6	0.1807	4.0	0.87	1071.1	39.1	1072.8	30.3	1076.4	45.8	1076.4	45.8	99.5	0.5
LCC1-88-RM15-192	60	9631	1.6	13.1874	2.4	1.9008	2.5	0.1818	0.9	0.36	1076.8	9.0	1081.4	16.8	1090.6	47.2	1090.6	47.2	98.7	1.3
LCC1-88-RM15-194	76	14378	2.0	13.4397	1.3	1.7998	1.5	0.1754	0.7	0.49	1042.0	7.1	1045.4	9.9	1052.5	26.7	1052.5	26.7	99.0	1.0
LCC1-88-RM15-196	17	1912	1.0	15.2475	9.7	1.2178	10.1	0.1347	3.0	0.30	814.5	23.0	808.8	56.5	793.1	203.4	814.5	23.0	102.7	-2.7
LCC1-88-RM15-197	403	90085	2.2	13.5572	0.6	1.7007	1.0	0.1672	0.8	0.81	996.8	7.4	1008.8	6.4	1034.9	11.8	1034.9	11.8	96.3	3.7
LCC1-88-RM15-198	148	23135	3.2	13.2171	0.5	1.8437	0.9	0.1767	0.8	0.87	1049.1	7.9	1061.2	6.1	1086.1	9.1	1086.1	9.1	96.6	3.4
LCC1-88-RM15-199	59	17899	0.9	11.6051	1.5	2.7199	2.0	0.2289	1.2	0.63	1328.9	15.0	1333.9	14.8	1342.0	29.9	1342.0	29.9	99.0	1.0
LCC1-88-RM15-20	39	5081	1.2	13.1253	9.0	1.9450	9.3	0.1852	2.2	0.23	1095.1	21.7	1096.7	62.2	1100.0	180.4	1100.0	180.4	99.5	0.5
LCC1-88-RM15-200	148	23657	2.2	13.1238	1.2	1.8731	1.3	0.1783	0.4	0.34	1057.6	4.3	1071.6	8.5	1100.3	24.2	1100.3	24.2	96.1	3.9
LCC1-88-RM15-23	91	18831	2.4	12.9891	1.3	2.0260	1.5	0.1909	0.8	0.54	1126.0	8.4	1124.3	10.2	1120.9	25.2	1120.9	25.2	100.5	-0.5
LCC1-88-RM15-24	42	7403	1.3	13.2797	4.7	1.9154	5.0	0.1845	1.7	0.34	1091.4	17.2	1086.4	33.7	1076.6	95.3	1076.6	95.3	101.4	-1.4
LCC1-88-RM15-25	55	13203	2.4	10.9733	1.0	3.1405	2.0	0.2499	1.7	0.87	1438.2	22.4	1442.7	15.4	1449.3	18.8	1449.3	18.8	99.2	0.8
LCC1-88-RM15-26	89	26706	1.6	11.3539	0.6	2.8799	1.4	0.2371	1.3	0.91	1371.8	16.0	1376.7	10.7	1384.1	11.2	1384.1	11.2	99.1	0.9
LCC1-88-RM15-27	102	22046	1.7	13.1343	1.3	1.9085	2.1	0.1818	1.6	0.76	1076.8	15.7	1084.1	13.8	1098.7	27.0	1098.7	27.0	98.0	2.0
LCC1-88-RM15-28	19	10055	1.7	11.6043	4.8	2.8211	5.2	0.2374	2.1	0.41	1373.3	26.1	1361.2	39.0	1342.1	91.9	1342.1	91.9	102.3	-2.3
LCC1-88-RM15-29	60	57004	0.5	9.1391	0.7	4.7518	2.2	0.3150	2.1	0.95	1765.1	32.1	1776.4	18.3	1789.8	12.4	1789.8	12.4	98.6	1.4
LCC1-88-RM15-3	48	11105	1.5	13.0719	1.5	1.9027	1.9	0.1804	1.2	0.64	1069.1	12.0	1082.0	12.7	1108.2	29.3	1108.2	29.3	96.5	3.5
LCC1-88-RM15-30	143	68053	1.2	12.5441	1.1	2.2197	1.6	0.2019	1.1	0.69	1185.8	12.0	1187.3	11.1	1190.1	22.6	1190.1	22.6	99.6	0.4
LCC1-88-RM15-31	151	116521	2.6	13.1671	0.5	1.8492	3.1	0.1766	3.0	0.99	1048.3	29.1	1063.1	20.1	1093.7	10.1	1093.7	10.1	95.9	4.1
LCC1-88-RM15-32	50	26421	2.2	13.1863	1.7	1.8448	1.9	0.1764	0.8	0.41	1047.4	7.4	1061.6	12.4	1090.7	34.4	1090.7	34.4	96.0	4.0
LCC1-88-RM15-33	38	7104	2.1	12.8569	2.2	2.0964	3.2	0.1955	2.4	0.73	1151.0	24.9	1147.6	22.3	1141.2	44.1	1141.2	44.1	100.9	-0.9
LCC1-88-RM15-35	165	18971	2.2	13.5282	1.8	1.7314	4.5	0.1699	4.1	0.92	1011.4	38.3	1020.3	28.7	1039.3	35.8	1039.3	35.8	97.3	2.7
LCC1-88-RM15-36	64	9341	1.2	13.0752	2.0	1.8699	2.4	0.1773	1.3	0.53	1052.3	12.4	1070.5	15.9	1107.7	40.5	1107.7	40.5	95.0	5.0
LCC1-88-RM15-37	196	10062	1.3	10.4089	0.7	3.1725	2.4	0.2395	2.3	0.96	1384.1	28.8	1450.5	18.7	1549.1	13.3	1549.1	13.3	89.3	10.7
LCC1-88-RM15-38	74	16678	1.8	12.2800	1.0	2.3544	1.5	0.2097	1.1	0.74	1227.2	12.6	1228.9	10.9	1231.9	20.4	1231.9	20.4	99.6	0.4
LCC1-88-RM15-39	90	37598	1.0	5.6360	0.2	12.1634	2.5	0.4972	2.5	1.00	2601.7	52.7	2617.1	23.2	2629.0	2.8	2629.0	2.8	99.0	1.0
LCC1-88-RM15-4	108	50468	1.7	13.9283	1.6	1.6172	2.8	0.1634	2.2	0.81	975.5	20.3	976.9	17.3	980.1	32.8	980.1	32.8	99.5	0.5
LCC1-88-RM15-40	98	16382	1.8	13.7643	1.9	1.6827	2.4	0.1680	1.5	0.64	1001.0	14.3	1002.0	15.4	1004.2	37.6	1004.2	37.6	99.7	0.3
LCC1-88-RM15-41	156	29875	2.8	12.6234	1.1	2.1831	2.6	0.1999	2.3	0.90	1174.6	24.8	1175.7	17.8	1177.6	21.8	1177.6	21.8	99.7	0.3
LCC1-88-RM15-42	216	28421	1.0	13.7822	0.7	1.6770	1.7	0.1676	1.6	0.91	999.0	14.5	999.8	11.0	1001.6	14.7	1001.6	14.7	99.7	0.3
LCC1-88-RM15-43	114	11616	1.4	15.9561	2.6	0.9910	3.2	0.1147	1.8	0.57	699.9	12.2	699.2	16.2	697.1	56.0	699.9	12.2	100.4	-0.4
LCC1-88-RM15-44	31	5816	1.8	13.3250	4.1	1.8345	4.4	0.1773	1.6	0.37	1052.2	15.6	1057.9	29.0	1069.8	82.5	1069.8	82.5	98.4	1.6
LCC1-88-RM15-45	62	29519	1.3	11.4422	0.8	2.8240	2.3	0.2344	2.2	0.94	1357.3	26.3	1361.9	17.2	1369.2	15.1	1369.2	15.1	99.1	0.9
LCC1-88-RM15-48	168	44481	1.0	5.9150	0.3	10.6686	2.0	0.4577	1.9	0.99	2429.3	38.9	2494.7	18.1	2548.3	5.4	2548.3	5.4	95.3	4.7
LCC1-88-RM15-5	67	15738	2.0	10.8789	1.2	3.1815	1.6	0.2510	1.0	0.63	1443.8	13.1	1452.7	12.3	1465.7	23.4	1465.7	23.4	98.5	1.5
LCC1-88-RM15-50	39	12815	0.7	12.8052	2.2	2.0687	3.9	0.1921	3.2	0.82	1132.9	33.8	1138.5	27.0	1149.2	44.5	1149.2	44.5	98.6	1.4
LCC1-88-RM15-52	230	54017	1.8	10.8725	0.3	3.1407	1.1	0.2477	1.0	0.95	1426.4	13.3	1442.7	8.4	1466.9	6.4	1466.9	6.4	97.2	2.8
LCC1-88-RM15-53	106	12996	1.8	13.1956	0.9	1.9489	2.5	0.1865	2.3	0.93	1102.5	23.4	1098.1	16.6	1089.3	17.9	1089.3	17.9	101.2	-1.2
LCC1-88-RM15-54	270	74376	1.8	13.1359	0.5	1.9212	1.5	0.1830	1.4	0.93	1083.5	14.4	1088.5	10.3	1098.4	10.9	1098.4	10.9	98.6	1.4
LCC1-88-RM15-55	112	55702	0.9	5.4482	0.4	12.9030	1.6	0.5098	1.6	0.98	2656.0	35.0	2672.6	15.5	2685.2	5.9	2685.2	5.9	98.9	1.1
LCC1-88-RM15-56	172	24013	1.8	13.3746	1.2	1.8350	1.8	0.1780	1.3	0.74	1056.0	13.1	1058.1	12.0	1062.3	24.9	1062.3	24.9	99.4	0.6
LCC1-88-RM15-57	87	15760	1.0	12.4018	1.2	2.2444	1.5	0.2019	0.9	0.62	1185.4	9.9	1195.0	10.5	1212.5	23.1	1212.5	23.1	97.8	2.2
LCC1-88-RM15-58	79	34442	0.9	6.2353	0.4	10.1607	1.0	0.4595	0.9	0.93	2437.3	19.2	2449.5	9.4	2459.6	6.1	2459.6	6.1	99.1	0.9
LCC1-88-RM15-61	131	12920	0.7	16.1662	1.6	0.9391	2.3	0.1101	1.6	0.70	673.4	10.1	672.4	11.1	669.2	34.2	673.4	10.1	100.6	-0.6
LCC1-88-RM15-62	38	6246	1.8	13.2932	5.7	1.9211	6.5	0.1852	3.1	0.48	1095.4	31.1	1088.5	43.4	1074.6	114.8	1074.6	114.8	101.9	-1.9
LCC1-88-RM15-63	152	44519	0.7	11.4132	1.1	2.9192	2.7	0.2416	2.5	0.91	1395.2	31.4	1386.9	20.8	1374.1	21.9	1374.1	21.9	101.5	-1.5
LCC1-88-RM15-64	256	72545	5.7	12.1877	0.3	2.3905	2.0	0.2113	2.0	0.99	1235.8	22.7	1239.8	14.7	1246.7	6.8	1246.7	6.8	99.1	0.9
LCC1-88-RM15-65	164	33920	3.0	13.2223	1.2	1.8991	1.9	0.1821	1.5	0.77	1078.5	14.7	1080.8	12.8	1085.3	24.5	1085.3	24.5	99.4	0.6
LCC1-88-RM15-66	179	101621	0.9	5.3943	0.1	13.1680	1.9	0.5152	1.9	1.00	2678.7	41.4	2691.8	17.8	2701.6	1.6	2701.6	1.6	99.2	0.8
LCC1-88-RM15-67	73	9426	2.1	11.7779	5.2	2.5934	9.8	0.2215	8.3	0.85	1290.0	96.9	1298.8	71.8	1313.4	101.0	1313.4	101.0	98.2	1.8
LCC1-88-RM15-68	106	50327	1.3	5.8719	0.4	11.7657	4.4	0.5011	4.4	1.00	2618.4	94.4	2585.9	41.3	2560.6	7.1	2560.6	7.1	102.3	-2.3
LCC1-88-RM15-69	151	47925	1.8	9.5453	0.4	4.4654	1.3	0.3091	1.2	0.94	1736.4	18.1	1724.6	10.5	1710.2	7.9	1710.2	7.9	101.5	-1.5
LCC1-88-RM15-7	119	15885	1.9	13.1787	1.1	1.9413	2.0	0.1856	1.7	0.83	1097.2	17.2	1095.5	13.7	1091.9	22.5	1091.9	22.5	100.5	-0.5
LCC1-88-RM15-70	99	28141	2.1	12.6201	0.9	2.1755	2.0	0.1991	1.8	0.89	1170.6	19.0	1173.2	13.8	1178.1	17.6	1178.1	17.6	99.4	0.6
LCC1-88-RM15-71	409	71091	2.8	13.0860	0.5	1.9313	1.6	0.1833	1.6	0.95	1085.0	15.6	1092.0	11.0	1106.0	10.4	1106.0	10.4	98.1	1.9
LCC1-88-RM15-72	375	123619	2.1	13.6102	0.5	1.7929	2.2	0.1770	2.2	0.98	1050.4	21.2	1042.9	14.6	1027.1	10.0	1027.1	10.0	102.3	-2.3
LCC1-88-RM15-73	272	13427	1.3	13.2906	0.5	1.7626	4.1	0.1699	4.0	0.99	1011.6	37.7	1031.8	26.3	1075.0	9.7	1075.0	9.7	94.1	5.9
LCC1-88-RM15-74	71	26528	1.8	11.7539	1.4	2.7211	2.1	0.2320	1.6	0.75	1344.8	19.0	1334.2	15.4	1317.3	26.6	1317.3	26.6	102.1	-2.1
LCC1-88-RM15-75	116	45166	1.8	11.5595	0.7	2.8000	1.4	0.2347	1.2	0.87	1359.3	14.6	1355.5	10.2	1349.6	13.0	1349.6	13.0	100.7	-0.7
LCC1-88-RM15-76	32	13634	1.1	11.5165	3.2	2.8439	3.6	0.2375	1.6	0.45	1373.9	19.9	1367.2	26.8	1356.8	61.4	1356.8	61.4	101.3	-1.3
LCC1-88-RM15-77	40	8860	2.8	13.1399	3.0	1.9507	4.3	0.1859	3.0	0.72	1099.2	30.7	1098.7	28.6	1097.8	59.5	1097.8	59.5	100.1	-0.1
LCC1-88-RM15-78	97	44555	1.3	10.8481	0.8	3.2584	1.9	0.2564	1.7	0.91	1471.2	22.8	1471.2	14.8	1471.1	14.7	1471.1	14.7	100.0	0.0
LCC1-88-RM15-79	149	35632	2.1	12.9360	0.9	2.0397	1.6	0.1914	1.4	0.84	1128.8	14.0	1128.9	11.0	1129.0	17.3	1129.0	17.3	100.0	0.0
LCC1-88-RM15-8	53	7166	0.9	13.3689	2.3	1.8487	2.6	0.1792	1.2	0.47	1062.9	11.8	1063.0	17.1	1063.2	46.1	1063.2	46.1	100.0	0.0
LCC1-88-RM15-80	21	3916	1.1	12.7722	5.4	2.1243	5.9	0.1968	2.2	0.38	1158.0	23.6	1156.7	40.5	1154.3	107.7	1154.3	107.7	100.3	-0.3
LCC1-88-RM15-81	152	22615	1.7	15.8273	1.7	0.9808	2.8	0.1126	2.2	0.78	687.7	14.1	694.0	13.9	714.4	36.8	687.7	14.1	96.3	3.7
LCC1-88-RM15-82	81	14143	1.8	13.2432	1.3	1.8859	1.7	0.1811	1.1	0.64	1073.2	10.9	1076.1	11.5	1082.1	26.7	1082.1	26.7	99.2	0.8
LCC1-88-RM15-83	96	10087	1.1	12.9456	1.1	1.9501	1.9	0.1831	1.6	0.82	1083.9	15.6	1098.5	12.8	1127.5	21.9	1127.5	21.9	96.1	3.9
LCC1-88-RM15-85	63	14462	2.0	13.0096	2.2	1.9706	3.4	0.1859	2.6	0.75	1099.3	26.0	1105.5	23.0	1117.7	44.7	1117.7	44.7	98.4	1.6
LCC1-88-RM15-86	161	25555	8.7	12.9386	0.9	2.0167	2.2	0.1892	2.0	0.91	1117.3	20.5	1121.1	14.8	1128.7	17.6	1128.7	17.6	99.0	1.0
LCC1-88-RM15-89	111	40913	1.6	11.6147	1.0	2.7381	2.3	0.2307	2.1	0.91	1337.9	24.8	1338.9	16.9	1340.4	18.6	1340.4	18.6	99.8	0.2
LCC1-88-RM15-9	228	35096	2.3	13.1029	0.7	1.9547	1.4	0.1858	1.2	0.86	1098.3	12.0	1100.1	9.2	1103.4	14.0	1103.4	14.0	99.5	0.5
LCC1-88-RM15-90	35	6011	1.7	11.8358	3.9	2.5661	4.9	0.2203	3.0	0.61	1283.3	35.0	1291.0	36.0	1303.8	75.6	1303.8	75.6	98.4	1.6
LCC1-88-RM15-91	83	50277	1.1	8.1720	0.5	5.9266	2.3	0.3513	2.2	0.97	1940.6	36.9	1965.1	19.6	1991.0	9.0	1991.0	9.0	97.5	2.5
LCC1-88-RM15-93	168	34705	1.1	16.0329	1.4	1.0113	2.4	0.1176	2.0	0.82	716.7	13.7	709.5	12.5	686.9	29.7	716.7	13.7	104.3	-4.3
LCC1-88-RM15-94	24	9708	1.8	9.4126	1.6	4.5496	2.5	0.3106	2.0	0.79	1743.6	30.7	1740.1	21.2	1735.9	28.5	1735.9	28.5	100.4	-0.4
LCC1-88-RM15-95	62	34052	1.4	13.0859	1.8	1.9383	2.8	0.1840	2.2	0.76	1088.6	21.8	1094.4	19.1	1106.0	36.7	1106.0	36.7	98.4	1.6
LCC1-88-RM15-96	51	15464	2.5	12.0572	1.4	2.4835	2.9	0.2172	2.6	0.88	1266.9	29.5	1267.2	21.2	1267.8	27.6	1267.8	27.6	99.9	0.1
LCC1-88-RM15-97	35	6599	1.2	12.7466	3.7	2.0767	4.5	0.1920	2.5	0.56	1132.1	26.4	1141.1	30.9	1158.3	74.0	1158.3	74.0	97.7	2.3
LCC1-88-RM15-98	46	18787	1.9	12.9881	2.4	1.9854	4.2	0.1870	3.5	0.83	1105.2	35.4	1110.6	28.5	1121.0	47.3	1121.0	47.3	98.6	1.4
LCC1-88-RM15-99	89	20789	2.2	12.5914	0.9	2.1484	2.9	0.1962	2.8	0.95	1154.9	29.3	1164.5	20.1	1182.6	17.3	1182.6	17.3	97.7	2.3
LCC2-H971-52	41	11920	1.6	14.3206	2.6	1.5069	3.4	0.1565	2.2	0.63	937.4	18.8	933.2	20.8	923.4	54.3	923.4	54.3	101.5	-1.5 1.4,0.8
LCC2-H971-121	104	19867	1.2	13.7302	1.9	1.7252	2.3	0.1718	1.3	0.57	1022.0	12.5	1017.9	14.9	1009.3	38.6	1009.3	38.6	101.3	-1.3
LCC2-H971-129	131	12849	2.6	13.7020	1.1	1.7971	2.6	0.1786	2.3	0.90	1059.2	22.5	1044.4	16.8	1013.4	23.0	1013.4	23.0	104.5	-4.5
LCC2-H971-151	47	18341	2.0	13.6945	3.5	1.7841	3.9	0.1772	1.7	0.43	1051.7	16.3	1039.7	25.4	1014.5	71.3	1014.5	71.3	103.7	-3.7
LCC2-H971-156	175	83091	2.2	13.6169	1.2	1.7151	2.7	0.1694	2.4	0.90	1008.7	22.4	1014.2	17.1	1026.1	23.3	1026.1	23.3	98.3	1.7
LCC2-H971-91	122	27854	1.6	13.6109	1.4	1.7877	1.9	0.1765	1.3	0.70	1047.7	12.8	1041.0	12.4	1026.9	27.6	1026.9	27.6	102.0	-2.0

U-Pb Geochronologic anlayses of selected Harmony Formation strata

					Isotope ratios							Apparent ages (Ma)							
	U	206Pb	U/Th	206Pb*	±	207Pb*	±	206Pb*	±	error	206Pb*	±	207Pb*	±	206Pb*	±	Best age	±	Conc.	Discor.
	(ppm)	204Pb		207Pb*	(%)	235U*	(%)	238U	(%)	corr.	238U*	(Ma)	235U	(Ma)	207Pb*	(Ma)	(Ma)	(Ma)	(%)	(%)
Sample: LCC #2. Location: Little Cottonwood Canyon, Galena Range; 0490529 4495008 (NAD 83 UTM 11T)																				
LCC2-H971-190	86	33207	2.6	13.5968	2.2	1.7832	2.4	0.1759	1.0	0.40	1044.3	9.2	1039.4	15.3	1029.0	43.5	1029.0	43.5	101.5	-1.5
LCC2-H971-171	178	41260	2.6	13.5919	0.7	1.7176	0.8	0.1693	0.4	0.55	1008.4	4.2	1015.1	5.2	1029.8	13.7	1029.8	13.7	97.9	2.1
LCC2-H971-112	145	30365	2.1	13.5873	0.9	1.8085	1.4	0.1782	1.1	0.77	1057.3	10.5	1048.6	9.1	1030.4	17.9	1030.4	17.9	102.6	-2.6
LCC2-H971-164	266	52049	5.2	13.5422	0.8	1.8047	1.0	0.1773	0.6	0.60	1051.9	6.0	1047.2	6.8	1037.2	16.8	1037.2	16.8	101.4	-1.4
LCC2-H971-53	186	17904	3.0	13.5339	1.0	1.7638	2.1	0.1731	1.9	0.89	1029.3	18.1	1032.2	13.8	1038.4	19.4	1038.4	19.4	99.1	0.9
LCC2-H971-3	46	14370	1.4	13.5002	1.7	1.8748	2.1	0.1836	1.2	0.58	1086.4	12.0	1072.2	13.6	1043.4	33.8	1043.4	33.8	104.1	-4.1
LCC2-H971-170	131	38084	3.2	13.4693	1.1	1.7577	1.3	0.1717	0.6	0.45	1021.5	5.3	1030.0	8.1	1048.1	22.6	1048.1	22.6	97.5	2.5
LCC2-H971-110	87	14944	1.5	13.4665	2.3	1.8405	2.6	0.1798	1.1	0.44	1065.6	10.9	1060.0	16.8	1048.5	46.3	1048.5	46.3	101.6	-1.6
LCC2-H971-30	52	10162	1.9	13.4524	3.6	1.8581	3.8	0.1813	1.0	0.26	1074.0	9.8	1066.3	24.9	1050.6	73.4	1050.6	73.4	102.2	-2.2
LCC2-H971-47	44	10971	1.3	13.4359	3.0	1.8763	5.4	0.1828	4.5	0.83	1082.5	45.0	1072.8	35.8	1053.1	60.0	1053.1	60.0	102.8	-2.8
LCC2-H971-36	77	47568	2.3	13.4221	1.0	1.7914	1.4	0.1744	1.0	0.72	1036.3	9.8	1042.3	9.3	1055.2	20.2	1055.2	20.2	98.2	1.8
LCC2-H971-142	40	6447	1.5	13.3801	4.4	1.9190	4.7	0.1862	1.6	0.34	1100.9	16.2	1087.7	31.5	1061.5	89.2	1061.5	89.2	103.7	-3.7
LCC2-H971-29	47	18130	1.7	13.3653	3.5	1.9071	3.8	0.1849	1.4	0.38	1093.5	14.4	1083.6	25.4	1063.7	71.1	1063.7	71.1	102.8	-2.8
LCC2-H971-104	67	24826	1.6	13.3640	1.1	1.8605	1.6	0.1803	1.2	0.74	1068.8	11.7	1067.2	10.7	1063.9	22.0	1063.9	22.0	100.5	-0.5
LCC2-H971-54	60	10635	1.5	13.3268	2.6	1.9314	3.1	0.1867	1.6	0.52	1103.3	16.1	1092.0	20.5	1069.5	52.8	1069.5	52.8	103.2	-3.2
LCC2-H971-126	87	15592	1.3	13.3173	1.1	1.9681	1.7	0.1901	1.3	0.78	1121.9	13.8	1104.7	11.7	1070.9	22.0	1070.9	22.0	104.8	-4.8
LCC2-H971-192	123	48954	2.1	13.3161	1.4	1.9047	1.8	0.1839	1.0	0.58	1088.5	10.2	1082.7	11.7	1071.1	28.8	1071.1	28.8	101.6	-1.6
LCC2-H971-194	58	19465	0.5	13.3105	2.3	1.9651	2.5	0.1897	1.0	0.38	1119.8	9.8	1103.6	16.7	1072.0	46.1	1072.0	46.1	104.5	-4.5
LCC2-H971-49	42	10820	1.3	13.3055	3.6	1.9371	4.7	0.1869	3.0	0.64	1104.7	30.1	1094.0	31.2	1072.7	72.4	1072.7	72.4	103.0	-3.0
LCC2-H971-179	27	9067	1.7	13.2869	4.2	1.9343	4.4	0.1864	1.3	0.29	1101.9	12.8	1093.0	29.3	1075.5	84.2	1075.5	84.2	102.4	-2.4
LCC2-H971-27	78	51974	2.1	13.2842	1.8	1.8794	2.2	0.1811	1.2	0.55	1072.8	12.0	1073.9	14.6	1075.9	36.9	1075.9	36.9	99.7	0.3
LCC2-H971-187	40	20614	1.7	13.2732	2.5	1.8950	2.8	0.1824	1.1	0.41	1080.2	11.3	1079.3	18.5	1077.6	51.1	1077.6	51.1	100.2	-0.2
LCC2-H971-198	105	35854	1.8	13.2695	1.2	1.9560	1.3	0.1882	0.6	0.44	1111.8	6.0	1100.5	8.9	1078.1	23.8	1078.1	23.8	103.1	-3.1
LCC2-H971-136	128	63659	1.8	13.2618	0.7	1.9287	0.9	0.1855	0.5	0.58	1097.0	5.2	1091.1	5.9	1079.3	14.6	1079.3	14.6	101.6	-1.6
LCC2-H971-5	76	25787	2.6	13.2559	1.4	1.9321	1.9	0.1858	1.2	0.64	1098.3	12.0	1092.3	12.5	1080.2	28.8	1080.2	28.8	101.7	-1.7
LCC2-H971-123	305	34064	1.7	13.2444	0.4	1.9599	3.2	0.1883	3.1	0.99	1112.0	32.0	1101.8	21.2	1081.9	8.3	1081.9	8.3	102.8	-2.8
LCC2-H971-94	208	58594	2.6	13.2117	1.2	1.9120	1.4	0.1832	0.9	0.59	1084.5	8.6	1085.3	9.6	1086.9	23.3	1086.9	23.3	99.8	0.2
LCC2-H971-174	124	65332	2.7	13.2086	1.2	1.9320	1.3	0.1851	0.6	0.43	1094.7	5.6	1092.2	8.6	1087.4	23.1	1087.4	23.1	100.7	-0.7
LCC2-H971-63	62	12395	1.2	13.2056	2.6	1.8740	4.3	0.1795	3.4	0.80	1064.1	33.6	1071.9	28.3	1087.8	51.1	1087.8	51.1	97.8	2.2
LCC2-H971-78	92	27097	2.1	13.2015	1.5	1.9772	1.6	0.1893	0.6	0.35	1117.6	5.7	1107.8	10.8	1088.4	30.0	1088.4	30.0	102.7	-2.7
LCC2-H971-118	399	63096	2.4	13.1933	0.4	1.9784	2.1	0.1893	2.0	0.98	1117.6	20.8	1108.2	14.0	1089.7	8.3	1089.7	8.3	102.6	-2.6
LCC2-H971-173	149	57941	2.9	13.1846	0.6	1.9359	0.9	0.1851	0.6	0.69	1094.9	6.0	1093.6	5.7	1091.0	12.3	1091.0	12.3	100.4	-0.4
LCC2-H971-152	138	32744	1.0	13.1785	1.0	1.9903	1.3	0.1902	0.9	0.66	1122.6	8.9	1112.2	8.9	1091.9	19.7	1091.9	19.7	102.8	-2.8
LCC2-H971-11	81	21721	1.5	13.1705	2.2	1.9401	2.9	0.1853	1.9	0.64	1096.0	18.8	1095.0	19.5	1093.1	44.8	1093.1	44.8	100.3	-0.3
LCC2-H971-188	80	69757	2.1	13.1690	0.9	1.9488	1.1	0.1861	0.7	0.62	1100.4	7.1	1098.0	7.6	1093.4	17.7	1093.4	17.7	100.6	-0.6
LCC2-H971-28	46	15920	1.7	13.1685	2.9	1.9086	3.2	0.1823	1.4	0.44	1079.4	13.8	1084.1	21.1	1093.5	57.1	1093.5	57.1	98.7	1.3
LCC2-H971-39	76	34222	1.5	13.1679	2.5	1.9772	2.7	0.1888	0.9	0.32	1115.0	8.8	1107.8	18.0	1093.6	50.5	1093.6	50.5	102.0	-2.0
LCC2-H971-109	177	71152	1.3	13.1660	1.3	1.9594	2.4	0.1871	2.0	0.84	1105.7	20.3	1101.7	16.0	1093.9	25.5	1093.9	25.5	101.1	-1.1
LCC2-H971-50	99	20812	2.4	13.1587	1.7	1.9024	2.7	0.1816	2.1	0.77	1075.5	20.7	1081.9	18.0	1095.0	34.6	1095.0	34.6	98.2	1.8
LCC2-H971-115	126	53785	4.9	13.1439	1.0	2.0185	1.3	0.1924	0.8	0.64	1134.5	8.8	1121.8	9.0	1097.2	20.3	1097.2	20.3	103.4	-3.4
LCC2-H971-189	41	15819	1.5	13.1414	3.8	2.0038	3.9	0.1910	0.8	0.19	1126.7	7.8	1116.8	26.2	1097.6	76.0	1097.6	76.0	102.7	-2.7
LCC2-H971-34	126	24422	1.3	13.1064	0.7	1.9765	0.9	0.1879	0.6	0.66	1109.9	6.3	1107.5	6.3	1102.9	14.1	1102.9	14.1	100.6	-0.6
LCC2-H971-169	263	74143	2.8	13.1002	1.0	1.9478	1.2	0.1851	0.7	0.55	1094.6	6.7	1097.7	8.1	1103.9	20.1	1103.9	20.1	99.2	0.8
LCC2-H971-193	109	27840	0.9	13.0978	1.5	2.0547	5.5	0.1952	5.3	0.96	1149.4	56.1	1133.9	37.8	1104.2	30.0	1104.2	30.0	104.1	-4.1
LCC2-H971-96	99	33238	1.3	13.0978	2.3	1.9595	2.5	0.1861	0.9	0.37	1100.4	9.4	1101.7	16.8	1104.2	46.3	1104.2	46.3	99.7	0.3
LCC2-H971-20	81	26351	1.8	13.0929	2.0	1.9502	2.2	0.1852	0.9	0.39	1095.2	8.7	1098.5	14.7	1105.0	40.4	1105.0	40.4	99.1	0.9
LCC2-H971-145	52	32807	1.4	13.0912	2.8	1.9521	3.9	0.1853	2.8	0.72	1096.1	28.4	1099.2	26.5	1105.2	55.0	1105.2	55.0	99.2	0.8
LCC2-H971-88	124	56794	1.4	13.0685	1.7	2.0243	2.8	0.1919	2.2	0.79	1131.5	22.5	1123.7	18.7	1108.7	33.8	1108.7	33.8	102.1	-2.1
LCC2-H971-133	30	23246	2.0	13.0556	5.7	1.9206	6.0	0.1819	1.8	0.31	1077.1	18.2	1088.3	40.0	1110.7	113.9	1110.7	113.9	97.0	3.0
LCC2-H971-150	472	21224	16.4	13.0259	0.5	1.9431	1.5	0.1836	1.4	0.94	1086.4	13.7	1096.1	9.7	1115.2	9.5	1115.2	9.5	97.4	2.6
LCC2-H971-51	65	19928	1.2	13.0237	2.2	1.9644	3.4	0.1856	2.6	0.77	1097.2	26.2	1103.4	22.8	1115.5	43.6	1115.5	43.6	98.4	1.6
LCC2-H971-60	111	39042	4.4	12.9972	1.1	2.0359	2.2	0.1919	1.9	0.87	1131.7	20.1	1127.6	15.2	1119.6	22.0	1119.6	22.0	101.1	-1.1
LCC2-H971-9	85	54434	1.0	12.9936	0.9	2.0679	2.0	0.1949	1.8	0.90	1147.8	18.5	1138.3	13.4	1120.2	17.3	1120.2	17.3	102.5	-2.5
LCC2-H971-166	35	13849	1.3	12.9875	4.6	1.9720	4.7	0.1858	1.1	0.23	1098.3	11.2	1106.0	31.8	1121.1	91.6	1121.1	91.6	98.0	2.0
LCC2-H971-131	348	62691	2.5	12.9813	0.4	1.9930	1.6	0.1876	1.6	0.97	1108.6	15.9	1113.1	10.9	1122.1	8.2	1122.1	8.2	98.8	1.2
LCC2-H971-32	48	17721	1.7	12.9746	2.9	2.0110	3.3	0.1892	1.6	0.50	1117.2	16.8	1119.2	22.5	1123.1	57.3	1123.1	57.3	99.5	0.5
LCC2-H971-16	33	11937	1.2	12.9634	5.2	1.9924	5.5	0.1873	1.8	0.32	1106.8	17.9	1112.9	36.9	1124.8	103.1	1124.8	103.1	98.4	1.6
LCC2-H971-134	96	32435	1.6	12.9092	1.4	2.0542	2.1	0.1923	1.5	0.74	1134.0	15.9	1133.7	14.0	1133.1	27.3	1133.1	27.3	100.1	-0.1
LCC2-H971-62	79	56362	1.3	12.8506	2.0	2.0678	3.2	0.1927	2.5	0.79	1136.1	26.1	1138.2	21.8	1142.2	39.2	1142.2	39.2	99.5	0.5
LCC2-H971-149	93	82023	2.3	12.8387	1.0	2.0774	1.2	0.1934	0.7	0.59	1140.0	7.5	1141.4	8.4	1144.0	19.6	1144.0	19.6	99.6	0.4
LCC2-H971-176	45	15508	1.2	12.8287	3.8	2.0770	3.9	0.1933	0.8	0.22	1139.0	8.9	1141.2	26.7	1145.6	75.5	1145.6	75.5	99.4	0.6
LCC2-H971-8	39	12946	0.9	12.8244	2.7	2.1574	3.7	0.2007	2.6	0.69	1178.9	27.7	1167.4	25.8	1146.3	53.5	1146.3	53.5	102.8	-2.8
LCC2-H971-191	39	8170	1.4	12.8231	2.9	2.1211	3.1	0.1973	1.0	0.32	1160.6	10.4	1155.7	21.4	1146.5	58.4	1146.5	58.4	101.2	-1.2
LCC2-H971-101	104	32053	2.0	12.8117	1.7	2.0924	2.4	0.1944	1.6	0.69	1145.3	17.1	1146.3	16.2	1148.2	33.8	1148.2	33.8	99.7	0.3
LCC2-H971-197	84	29763	1.9	12.8024	2.1	2.1929	2.2	0.2036	0.6	0.29	1194.7	6.9	1178.8	15.1	1149.7	41.1	1149.7	41.1	103.9	-3.9
LCC2-H971-72	93	10190	1.5	12.7888	2.8	1.9878	2.9	0.1844	0.5	0.19	1090.8	5.4	1111.4	19.4	1151.8	55.9	1151.8	55.9	94.7	5.3
LCC2-H971-102	24	5005	2.3	12.7842	5.7	1.9946	6.2	0.1849	2.3	0.37	1093.9	22.8	1113.7	41.6	1152.5	113.7	1152.5	113.7	94.9	5.1
LCC2-H971-106	158	104345	1.2	12.7514	0.8	2.0990	1.4	0.1941	1.2	0.84	1143.7	12.5	1148.5	9.8	1157.6	15.5	1157.6	15.5	98.8	1.2
LCC2-H971-6	102	33374	2.6	12.7493	1.7	2.1673	2.7	0.2004	2.0	0.76	1177.5	21.8	1170.6	18.4	1157.9	34.1	1157.9	34.1	101.7	-1.7
LCC2-H971-40	137	44770	2.8	12.7303	1.3	2.1335	1.9	0.1970	1.3	0.72	1159.1	14.2	1159.7	12.8	1160.9	25.5	1160.9	25.5	99.8	0.2
LCC2-H971-148	87	21122	2.3	12.7141	1.7	2.1980	2.2	0.2027	1.4	0.63	1189.7	15.2	1180.4	15.4	1163.4	34.0	1163.4	34.0	102.3	-2.3
LCC2-H971-86	73	17224	1.8	12.7136	3.5	2.1719	3.8	0.2003	1.3	0.35	1176.7	13.9	1172.1	26.1	1163.5	69.9	1163.5	69.9	101.1	-1.1
LCC2-H971-132	65	14315	3.0	12.7032	1.9	2.1657	2.6	0.1995	1.9	0.71	1172.8	20.3	1170.1	18.4	1165.1	36.7	1165.1	36.7	100.7	-0.7
LCC2-H971-33	81	33016	1.3	12.6938	2.3	2.1600	3.8	0.1989	3.0	0.80	1169.2	32.4	1168.3	26.2	1166.6	44.6	1166.6	44.6	100.2	-0.2
LCC2-H971-42	65	25387	1.0	12.6934	1.8	2.1604	2.0	0.1989	0.9	0.45	1169.3	9.6	1168.4	13.9	1166.6	35.5	1166.6	35.5	100.2	-0.2
LCC2-H971-37	439	215857	2.2	12.6804	0.3	2.1794	0.6	0.2004	0.4	0.79	1177.7	4.7	1174.5	3.9	1168.6	6.8	1168.6	6.8	100.8	-0.8
LCC2-H971-57	61	43591	1.2	12.6604	1.6	2.2038	2.8	0.2024	2.3	0.83	1188.0	24.8	1182.2	19.3	1171.8	30.7	1171.8	30.7	101.4	-1.4
LCC2-H971-93	308	63960	3.3	12.6408	0.5	2.2177	1.4	0.2033	1.3	0.93	1193.1	14.3	1186.7	9.9	1174.9	10.3	1174.9	10.3	101.6	-1.6
LCC2-H971-83	221	53315	2.7	12.6360	0.5	2.1883	1.1	0.2005	1.0	0.89	1178.3	10.8	1177.3	7.9	1175.6	10.3	1175.6	10.3	100.2	-0.2
LCC2-H971-43	123	79293	4.8	12.6198	1.1	2.1930	1.3	0.2007	0.8	0.59	1179.2	8.4	1178.8	9.2	1178.2	21.2	1178.2	21.2	100.1	-0.1
LCC2-H971-68	159	33777	2.1	12.5821	1.3	2.2162	1.5	0.2022	0.8	0.55	1187.4	9.1	1186.2	10.7	1184.1	25.2	1184.1	25.2	100.3	-0.3
LCC2-H971-114	108	36835	2.4	12.5513	1.3	2.2283	2.2	0.2028	1.8	0.80	1190.6	19.2	1190.0	15.5	1188.9	26.3	1188.9	26.3	100.1	-0.1
LCC2-H971-125	146	15833	1.1	12.5305	0.7	2.3435	1.4	0.2130	1.2	0.86	1244.7	13.1	1225.6	9.6	1192.2	13.7	1192.2	13.7	104.4	-4.4
LCC2-H971-163	80	12492	1.9	12.4726	1.1	2.3026	1.6	0.2083	1.2	0.73	1219.7	13.3	1213.1	11.6	1201.3	21.8	1201.3	21.8	101.5	-1.5
LCC2-H971-119	110	21336	1.2	12.4369	0.8	2.4010	1.7	0.2166	1.5	0.89	1263.7	17.6	1242.9	12.4	1207.0	15.8	1207.0	15.8	104.7	-4.7
LCC2-H971-127	34	4758	1.1	12.4339	2.6	2.2029	4.3	0.1987	3.5	0.80	1168.1	37.1	1181.9	30.2	1207.5	50.7	1207.5	50.7	96.7	3.3
LCC2-H971-65	87	108350	2.0	12.3822	1.2	2.2286	3.3	0.2001	3.1	0.93	1176.0	33.4	1190.1	23.5	1215.7	24.5	1215.7	24.5	96.7	3.3
LCC2-H971-184	47	16300	1.4	12.3391	2.5	2.3212	2.7	0.2077	0.9	0.32	1216.7	9.5	1218.8	19.0	1222.5	49.9	1222.5	49.9	99.5	0.5
LCC2-H971-98	230	29419	1.8	12.2797	0.5	2.3683	1.3	0.2109	1.2	0.93	1233.7	13.6	1233.1	9.3	1232.0	9.6	1232.0	9.6	100.1	-0.1
LCC2-H971-140	158	72661	1.6	12.2522	0.7	2.4426	1.2	0.2171	0.9	0.77	1266.3	10.3	1255.2	8.3	1236.4	14.4	1236.4	14.4	102.4	-2.4
LCC2-H971-82	166	55508	1.5	12.2289	0.4	2.3574	0.9	0.2091	0.8	0.89	1223.9	8.6	1229.8	6.1	1240.1	7.6	1240.1	7.6	98.7	1.3
LCC2-H971-177	91	18056	2.2	12.1938	1.6	2.4400	1.7	0.2158	0.6	0.33	1259.6	6.6	1254.5	12.5	1245.7	31.9	1245.7	31.9	101.1	-1.1
LCC2-H971-79	41	10348	1.9	12.1516	2.4	2.5204	4.1	0.2221	3.4	0.81	1293.1	39.4	1277.9	30.0	1252.5	46.8	1252.5	46.8	103.2	-3.2
LCC2-H971-26	32	14662	1.4	12.0768	2.4	2.6080	3.3	0.2284	2.3	0.69	1326.3	27.3	1302.9	24.3	1264.6	46.9	1264.6	46.9	104.9	-4.9
LCC2-H971-185	42	20155	1.5	12.0057	4.3	2.6290	4.4	0.2289	1.1	0.25	1328.8	13.2	1308.8	32.3	1276.1	83.0	1276.1	83.0	104.1	-4.1
LCC2-H971-61	275	51367	1.0	12.0000	0.6	2.5350	3.5	0.2206	3.5	0.98	1285.2	40.6	1282.1	25.8	1277.0	12.4	1277.0	12.4	100.6	-0.6
LCC2-H971-64	20	5528	1.6	11.9864	5.2	2.6445	6.6	0.2299	4.1	0.62	1333.9	49.0	1313.1	48.6	1279.2	101.1	1279.2	101.1	104.3	-4.3
LCC2-H971-138	82	62308	2.1	11.9702	1.0	2.6008	2.4	0.2258	2.1	0.90	1312.4	25.0	1300.9	17.2	1281.9	20.3	1281.9	20.3	102.4	-2.4
LCC2-H971-105	79	32448	1.7	11.7787	1.8	2.5137	2.8	0.2147	2.2	0.78	1254.0	24.9	1276.0	20.4	1313.2	34.2	1313.2	34.2	95.5	4.5
LCC2-H971-182	63	19680	1.6	11.7218	1.8	2.7099	1.8	0.2304	0.4	0.24	1336.5	5.4	1331.2	13.6	1322.6	34.4	1322.6	34.4	101.0	-1.0
LCC2-H971-144	92	11891	2.3	11.6761	1.5	2.7542	1.9	0.2332	1.2	0.61	1351.4	14.4	1343.2	14.4	1330.2	29.6	1330.2	29.6	101.6	-1.6

U-Pb Geochronologic anlayses of selected Harmony Formation strata

					Isotope ratios								Apparent ages (Ma)							
	U	206Pb	U/Th	206Pb*	±	207Pb*	±	206Pb*	±	error	206Pb*	±	207Pb*	±	206Pb*	±	Best age	±	Conc.	Discor.
	(ppm)	204Pb		207Pb*	(%)	235U*	(%)	238U	(%)	corr.	238U*	(Ma)	235U	(Ma)	207Pb*	(Ma)	(Ma)	(Ma)	(%)	(%)
Sample: LCC #2. Location: Little Cottonwood Canyon, Galena Range; 0490529 4495008 (NAD 83 UTM 11T)																				
LCC2-H971-157	35	17210	1.6	11.6710	2.9	2.7728	7.2	0.2347	6.6	0.91	1359.1	80.8	1348.2	53.8	1331.0	56.3	1331.0	56.3	102.1	-2.1
LCC2-H971-92	205	72082	2.0	11.6600	0.7	2.7530	2.5	0.2328	2.4	0.96	1349.2	29.1	1342.9	18.5	1332.8	13.3	1332.8	13.3	101.2	-1.2
LCC2-H971-108	270	62133	0.6	11.6444	0.4	2.6780	1.4	0.2262	1.3	0.95	1314.3	15.3	1322.4	10.0	1335.4	8.1	1335.4	8.1	98.4	1.6
LCC2-H971-77	80	7702	1.5	11.6275	1.6	2.7401	1.9	0.2311	1.0	0.53	1340.1	12.2	1339.4	14.1	1338.2	31.0	1338.2	31.0	100.1	-0.1
LCC2-H971-168	45	9799	1.3	11.5702	3.5	2.7431	3.6	0.2302	0.9	0.24	1335.5	10.5	1340.2	26.7	1347.8	67.1	1347.8	67.1	99.1	0.9
LCC2-H971-45	93	23766	1.4	11.5105	1.6	2.7840	2.3	0.2324	1.7	0.73	1347.2	20.6	1351.3	17.3	1357.8	30.2	1357.8	30.2	99.2	0.8
LCC2-H971-44	52	12073	1.1	11.4511	2.2	2.8833	3.4	0.2395	2.6	0.75	1383.9	31.9	1377.6	25.7	1367.7	43.1	1367.7	43.1	101.2	-1.2
LCC2-H971-183	206	76217	2.0	11.4382	0.4	2.8478	0.6	0.2362	0.3	0.60	1367.1	4.1	1368.2	4.2	1369.9	8.6	1369.9	8.6	99.8	0.2
LCC2-H971-89	40	10623	1.6	11.4003	2.3	2.9177	3.1	0.2412	2.0	0.66	1393.2	25.6	1386.5	23.3	1376.3	44.3	1376.3	44.3	101.2	-1.2
LCC2-H971-67	64	14858	0.9	11.3897	2.2	2.8897	2.7	0.2387	1.5	0.55	1380.0	18.1	1379.2	20.1	1378.1	43.0	1378.1	43.0	100.1	-0.1
LCC2-H971-46	59	23260	1.1	11.3786	1.6	2.9337	2.5	0.2421	1.9	0.77	1397.6	24.3	1390.6	19.0	1379.9	30.9	1379.9	30.9	101.3	-1.3
LCC2-H971-160	184	109201	0.8	11.3774	0.4	2.9007	1.4	0.2394	1.4	0.97	1383.3	17.3	1382.1	10.8	1380.1	7.0	1380.1	7.0	100.2	-0.2
LCC2-H971-70	89	33843	1.5	11.3481	1.2	2.9509	2.2	0.2429	1.8	0.82	1401.6	22.4	1395.1	16.4	1385.1	23.5	1385.1	23.5	101.2	-1.2
LCC2-H971-84	39	9464	1.1	11.3361	2.8	3.0313	3.3	0.2492	1.8	0.54	1434.5	23.3	1415.5	25.4	1387.1	53.7	1387.1	53.7	103.4	-3.4
LCC2-H971-141	51	25758	1.6	11.3122	2.2	2.9579	3.1	0.2427	2.1	0.69	1400.6	26.9	1396.9	23.5	1391.2	42.9	1391.2	42.9	100.7	-0.7
LCC2-H971-76	65	12431	1.7	11.2425	1.8	2.9148	2.0	0.2377	0.8	0.42	1374.6	10.5	1385.8	15.2	1403.0	34.9	1403.0	34.9	98.0	2.0
LCC2-H971-116	168	9978	1.1	11.1777	0.9	2.4307	8.7	0.1971	8.7	0.99	1159.5	92.0	1251.7	62.8	1414.1	18.1	1414.1	18.1	82.0	18.0
LCC2-H971-153	87	41598	2.1	11.0639	1.2	3.1719	1.7	0.2545	1.2	0.72	1461.8	15.5	1450.4	12.8	1433.6	22.0	1433.6	22.0	102.0	-2.0
LCC2-H971-122	80	13652	1.5	11.0170	1.5	3.2809	1.9	0.2622	1.2	0.64	1500.8	16.3	1476.5	14.9	1441.7	28.1	1441.7	28.1	104.1	-4.1
LCC2-H971-195	97	44380	1.0	10.9837	0.8	3.2665	1.1	0.2602	0.7	0.64	1490.9	9.2	1473.1	8.3	1447.5	15.6	1447.5	15.6	103.0	-3.0
LCC2-H971-14	111	47690	1.2	10.9320	0.5	3.0728	1.1	0.2436	1.0	0.89	1405.6	12.4	1425.9	8.4	1456.5	9.5	1456.5	9.5	96.5	3.5
LCC2-H971-161	88	17070	1.4	10.9083	0.8	3.2213	1.0	0.2549	0.6	0.60	1463.5	7.9	1462.3	7.8	1460.6	15.2	1460.6	15.2	100.2	-0.2
LCC2-H971-23	96	46175	1.6	10.9063	0.8	3.2803	1.9	0.2595	1.7	0.89	1487.1	22.3	1476.4	14.6	1461.0	16.0	1461.0	16.0	101.8	-1.8
LCC2-H971-143	130	77961	1.7	10.9055	0.6	3.2959	1.2	0.2607	1.1	0.88	1493.4	14.2	1480.1	9.4	1461.1	10.7	1461.1	10.7	102.2	-2.2
LCC2-H971-113	57	12306	1.0	10.9009	2.0	3.2780	2.9	0.2592	2.2	0.74	1485.5	28.9	1475.8	22.8	1461.9	37.1	1461.9	37.1	101.6	-1.6
LCC2-H971-41	126	142999	1.2	10.8593	0.6	3.1741	1.0	0.2500	0.8	0.79	1438.4	10.4	1450.9	7.8	1469.2	11.8	1469.2	11.8	97.9	2.1
LCC2-H971-159	73	15906	1.6	10.8526	1.0	3.3635	2.0	0.2647	1.7	0.86	1514.1	23.3	1495.9	15.6	1470.3	19.2	1470.3	19.2	103.0	-3.0
LCC2-H971-167	81	28751	1.0	10.8242	1.4	3.3273	1.8	0.2612	1.1	0.60	1496.0	14.2	1487.5	13.8	1475.3	26.7	1475.3	26.7	101.4	-1.4
LCC2-H971-100	101	11881	0.8	10.7963	1.1	3.3178	1.2	0.2598	0.5	0.44	1488.8	7.2	1485.2	9.6	1480.2	21.0	1480.2	21.0	100.6	-0.6
LCC2-H971-18	89	106427	1.1	10.7915	0.8	3.3228	1.0	0.2601	0.6	0.58	1490.2	7.6	1486.4	7.7	1481.0	15.2	1481.0	15.2	100.6	-0.6
LCC2-H971-19	59	19979	4.5	10.7875	1.2	3.2623	1.5	0.2552	0.9	0.58	1465.4	11.6	1472.1	11.9	1481.8	23.6	1481.8	23.6	98.9	1.1
LCC2-H971-186	65	38508	1.4	10.7862	1.0	3.2802	1.2	0.2566	0.7	0.57	1472.5	8.9	1476.4	9.1	1482.0	18.2	1482.0	18.2	99.4	0.6
LCC2-H971-58	56	18219	0.7	10.0428	1.4	3.6315	1.9	0.2645	1.3	0.68	1512.9	17.6	1556.5	15.2	1616.1	25.9	1616.1	25.9	93.6	6.4
LCC2-H971-17	25	10457	1.9	10.0253	3.0	3.9859	3.2	0.2898	1.1	0.34	1640.6	16.0	1631.3	26.0	1619.4	56.0	1619.4	56.0	101.3	-1.3
LCC2-H971-21	132	63503	1.2	9.9285	0.5	4.0407	0.9	0.2910	0.7	0.84	1646.4	10.6	1642.4	7.1	1637.4	8.8	1637.4	8.8	100.5	-0.5
LCC2-H971-147	69	45640	1.2	9.8733	1.5	4.1311	1.7	0.2958	0.7	0.42	1670.5	10.2	1660.5	13.6	1647.8	28.0	1647.8	28.0	101.4	-1.4
LCC2-H971-154	72	83931	1.0	9.7673	1.1	4.2565	2.7	0.3015	2.4	0.91	1698.9	36.1	1685.0	21.9	1667.7	20.7	1667.7	20.7	101.9	-1.9
LCC2-H971-175	134	141660	1.1	9.7555	0.5	4.2859	0.7	0.3032	0.6	0.76	1707.4	8.5	1690.7	6.1	1670.0	8.9	1670.0	8.9	102.2	-2.2
LCC2-H971-158	96	20031	2.4	9.6870	1.1	3.6874	3.6	0.2591	3.4	0.95	1485.0	44.8	1568.6	28.5	1683.0	21.2	1683.0	21.2	88.2	11.8
LCC2-H971-97	187	99848	1.0	9.4931	0.6	4.5124	1.4	0.3107	1.3	0.91	1744.0	19.3	1733.3	11.6	1720.2	10.8	1720.2	10.8	101.4	-1.4
LCC2-H971-165	162	53185	1.8	9.4430	0.4	4.5220	0.9	0.3097	0.8	0.87	1739.2	11.7	1735.0	7.3	1729.9	7.9	1729.9	7.9	100.5	-0.5
LCC2-H971-200	85	40615	0.8	9.3222	0.8	4.7533	0.9	0.3214	0.5	0.53	1796.4	7.4	1776.7	7.5	1753.5	13.9	1753.5	13.9	102.4	-2.4
LCC2-H971-178	62	45541	1.3	9.2428	0.9	4.7159	1.1	0.3161	0.7	0.60	1770.8	10.7	1770.1	9.6	1769.2	16.8	1769.2	16.8	100.1	-0.1
LCC2-H971-196	99	39770	1.3	9.1855	0.9	4.8611	1.1	0.3238	0.7	0.58	1808.5	10.5	1795.5	9.6	1780.5	16.9	1780.5	16.9	101.6	-1.6
LCC2-H971-24	9	7316	3.2	9.1557	5.5	4.4735	5.9	0.2971	2.1	0.36	1676.7	31.7	1726.1	49.2	1786.4	100.6	1786.4	100.6	93.9	6.1
LCC2-H971-107	137	78563	1.9	9.1253	0.5	4.8691	1.4	0.3223	1.3	0.93	1800.7	19.9	1796.9	11.5	1792.5	9.3	1792.5	9.3	100.5	-0.5
LCC2-H971-69	299	257960	1.5	9.1183	0.3	4.9123	1.2	0.3249	1.1	0.97	1813.4	18.0	1804.4	9.9	1793.9	5.0	1793.9	5.0	101.1	-1.1
LCC2-H971-71	121	71484	1.5	9.1172	0.4	4.9654	1.3	0.3283	1.2	0.94	1830.3	19.6	1813.5	11.0	1794.1	8.0	1794.1	8.0	102.0	-2.0
LCC2-H971-90	98	41193	1.8	9.1076	0.5	4.8767	1.8	0.3221	1.8	0.96	1800.1	27.9	1798.2	15.5	1796.0	8.9	1796.0	8.9	100.2	-0.2
LCC2-H971-103	62	58780	3.3	9.0980	0.9	4.9045	1.3	0.3236	0.9	0.69	1807.4	14.4	1803.0	11.1	1798.0	17.3	1798.0	17.3	100.5	-0.5
LCC2-H971-66	63	22955	5.0	8.9311	0.9	4.9627	3.6	0.3215	3.5	0.97	1796.8	55.2	1813.0	30.8	1831.6	16.8	1831.6	16.8	98.1	1.9
LCC2-H971-180	120	80808	1.6	8.8415	0.4	5.1031	0.7	0.3272	0.6	0.81	1825.0	8.8	1836.6	5.8	1849.9	7.3	1849.9	7.3	98.7	1.3
LCC2-H971-139	67	53253	2.5	8.8127	1.0	5.2834	1.3	0.3377	0.9	0.66	1875.6	14.4	1866.2	11.3	1855.7	17.9	1855.7	17.9	101.1	-1.1
LCC2-H971-181	63	31214	1.0	8.4793	0.7	5.8869	0.9	0.3620	0.5	0.58	1991.8	9.1	1959.3	7.9	1925.1	13.2	1925.1	13.2	103.5	-3.5
LCC2-H971-56	61	82760	0.9	8.4615	0.7	5.7150	1.6	0.3507	1.5	0.91	1938.1	24.4	1933.6	13.9	1928.9	12.0	1928.9	12.0	100.5	-0.5
LCC2-H971-7	56	28873	0.8	8.3054	0.7	6.0661	1.0	0.3654	0.7	0.72	2007.7	12.2	1985.4	8.5	1962.2	12.1	1962.2	12.1	102.3	-2.3
LCC2-H971-15	185	90270	0.8	7.9925	0.3	6.2685	1.8	0.3634	1.8	0.98	1998.1	30.5	2014.1	15.8	2030.4	6.0	2030.4	6.0	98.4	1.6
LCC2-H971-38	132	154107	0.8	5.7829	0.2	11.8073	0.5	0.4952	0.4	0.92	2593.2	9.4	2589.2	4.5	2586.1	3.0	2586.1	3.0	100.3	-0.3
LCC2-H971-59	78	61154	2.0	5.7376	0.6	12.0464	1.8	0.5013	1.7	0.94	2619.3	36.6	2608.0	17.0	2599.2	10.5	2599.2	10.5	100.8	-0.8
LCC2-H971-99	222	45555	1.8	5.7184	0.2	11.6756	1.8	0.4842	1.8	0.99	2545.7	37.4	2578.7	16.8	2604.8	3.6	2604.8	3.6	97.7	2.3
LCC2-H971-10	107	96440	1.3	5.6589	0.3	12.9224	2.4	0.5304	2.4	0.99	2743.0	54.0	2674.0	22.9	2622.2	4.7	2622.2	4.7	104.6	-4.6
LCC2-H971-137	73	78489	0.7	5.6395	0.2	12.4617	1.0	0.5097	1.0	0.97	2655.4	22.0	2639.8	9.8	2628.0	3.9	2628.0	3.9	101.0	-1.0
LCC2-H971-87	293	33603	0.7	5.5509	0.2	11.9051	1.6	0.4793	1.6	0.99	2524.2	34.0	2597.0	15.4	2654.2	3.3	2654.2	3.3	95.1	4.9
LCC2-H971-13	17	38823	1.8	5.4535	0.8	13.0328	1.2	0.5155	0.8	0.71	2680.0	18.5	2682.0	11.1	2683.6	13.7	2683.6	13.7	99.9	0.1
LCC2-H971-48	102	27759	1.1	5.4456	0.2	11.3973	2.2	0.4501	2.2	0.99	2395.9	43.6	2556.2	20.5	2686.0	4.0	2686.0	4.0	89.2	10.8
LCC2-H971-135	140	89322	1.3	5.4431	0.2	12.4202	1.2	0.4903	1.2	0.99	2572.0	26.3	2636.7	11.7	2686.7	2.8	2686.7	2.8	95.7	4.3
LCC2-H971-55	28	27801	1.4	5.2866	0.6	13.9436	1.4	0.5346	1.2	0.90	2760.9	27.6	2745.9	12.9	2734.9	9.7	2734.9	9.7	101.0	-1.0
LCC2-H971-162	28	23216	0.6	4.5928	0.5	17.5752	0.7	0.5854	0.5	0.71	2970.9	11.7	2966.8	6.7	2964.0	7.9	2964.0	7.9	100.2	-0.2
Sample: LCC #3. Location: Little Cottonwood Canyon, Galena Range; 0490459 4494916 (NAD 83 UTM 11T)																				
LCC3-H973-47	32	21590	1.0	10.7807	1.8	3.1903	1.9	0.2494	0.8	0.41	1435.6	10.3	1454.8	15.0	1482.9	33.5	1482.9	33.5	96.8	3.2 0.8,0.8
LCC3-H973-147	392	10013	0.7	9.5521	2.4	3.5893	9.5	0.2487	9.1	0.97	1431.6	117.4	1547.2	75.2	1708.8	44.7	1708.8	44.7	83.8	16.2
LCC3-H973-190	136	10603	1.6	9.3577	1.2	4.6032	2.5	0.3124	2.2	0.88	1752.6	33.6	1749.9	20.8	1746.6	21.8	1746.6	21.8	100.3	-0.3
LCC3-H973-174	81	31485	2.0	9.3207	1.3	4.0358	8.3	0.2728	8.2	0.99	1555.1	112.8	1641.4	67.3	1753.8	23.3	1753.8	23.3	88.7	11.3
LCC3-H973-3	321	36284	1.9	9.2932	0.4	4.1375	1.2	0.2789	1.2	0.96	1585.7	16.4	1661.7	9.9	1759.3	6.4	1759.3	6.4	90.1	9.9
LCC3-H973-131	192	49311	1.2	9.2698	0.5	4.1518	1.6	0.2791	1.5	0.96	1587.0	21.2	1664.6	12.9	1763.9	8.3	1763.9	8.3	90.0	10.0
LCC3-H973-2	273	13314	0.7	9.2621	0.8	3.8226	4.3	0.2568	4.2	0.98	1473.4	55.6	1597.5	34.6	1765.4	15.3	1765.4	15.3	83.5	16.5
LCC3-H973-73	32	40123	1.1	9.2330	2.8	4.7598	3.4	0.3187	2.0	0.57	1783.5	30.4	1777.8	28.8	1771.1	51.5	1771.1	51.5	100.7	-0.7
LCC3-H973-105	186	10256	1.1	9.2281	0.5	3.8029	2.0	0.2545	1.9	0.96	1461.8	24.6	1593.4	15.7	1772.1	9.5	1772.1	9.5	82.5	17.5
LCC3-H973-160	151	62682	1.3	9.2162	0.6	4.1920	2.9	0.2802	2.8	0.98	1592.4	39.5	1672.5	23.5	1774.4	11.4	1774.4	11.4	89.7	10.3
LCC3-H973-58	78	76263	3.4	9.2131	0.8	4.7378	1.4	0.3166	1.2	0.84	1773.0	18.0	1774.0	11.6	1775.1	13.8	1775.1	13.8	99.9	0.1
LCC3-H973-133	252	303718	2.8	9.2127	0.2	4.3896	1.9	0.2933	1.9	1.00	1658.0	27.1	1710.4	15.4	1775.1	2.9	1775.1	2.9	93.4	6.6
LCC3-H973-179	95	25546	1.1	9.2006	0.6	4.0928	4.9	0.2731	4.8	0.99	1556.6	67.0	1652.9	39.9	1777.5	10.7	1777.5	10.7	87.6	12.4
LCC3-H973-126	61	58412	1.1	9.1929	0.8	4.7349	1.2	0.3157	1.0	0.79	1768.6	15.0	1773.4	10.4	1779.1	13.9	1779.1	13.9	99.4	0.6
LCC3-H973-197	262	17150	2.7	9.1920	0.4	4.4258	0.8	0.2951	0.7	0.86	1666.7	10.7	1717.2	7.0	1779.2	7.8	1779.2	7.8	93.7	6.3
LCC3-H973-18	64	39414	1.7	9.1890	0.8	4.7444	1.5	0.3162	1.2	0.82	1771.1	18.5	1775.1	12.2	1779.8	15.0	1779.8	15.0	99.5	0.5
LCC3-H973-113	139	127968	2.1	9.1866	0.4	4.7672	1.4	0.3176	1.3	0.96	1778.1	20.8	1779.1	11.8	1780.3	7.5	1780.3	7.5	99.9	0.1
LCC3-H973-51	62	77371	1.1	9.1849	0.5	4.7433	0.8	0.3160	0.7	0.83	1770.0	10.3	1774.9	6.7	1780.7	8.2	1780.7	8.2	99.4	0.6
LCC3-H973-200	75	92628	1.8	9.1827	0.7	4.8511	0.9	0.3231	0.6	0.64	1804.8	8.8	1793.8	7.4	1781.1	12.4	1781.1	12.4	101.3	-1.3
LCC3-H973-145	63	139204	2.1	9.1788	1.0	4.7821	1.4	0.3183	1.0	0.70	1781.7	15.5	1781.8	11.9	1781.9	18.3	1781.9	18.3	100.0	0.0
LCC3-H973-35	158	211013	1.4	9.1622	0.6	4.7440	1.0	0.3152	0.8	0.82	1766.4	12.4	1775.0	8.2	1785.2	10.2	1785.2	10.2	99.0	1.0
LCC3-H973-139	221	211204	2.5	9.1594	0.2	4.7793	1.0	0.3175	1.0	0.98	1777.5	15.2	1781.3	8.4	1785.7	4.0	1785.7	4.0	99.5	0.5
LCC3-H973-76	70	76833	1.5	9.1574	0.8	4.8249	1.3	0.3205	1.0	0.79	1791.9	16.3	1789.3	11.2	1786.1	15.0	1786.1	15.0	100.3	-0.3
LCC3-H973-49	80	53488	2.2	9.1556	0.8	4.8199	1.1	0.3201	0.7	0.62	1790.0	10.5	1788.4	9.1	1786.5	15.5	1786.5	15.5	100.2	-0.2
LCC3-H973-26	111	227840	2.0	9.1554	0.5	4.7148	1.0	0.3131	0.9	0.87	1755.8	13.9	1769.9	8.7	1786.5	9.2	1786.5	9.2	98.3	1.7
LCC3-H973-10	186	15847	2.4	9.1541	0.4	4.7865	0.9	0.3178	0.8	0.88	1778.9	11.9	1782.5	7.3	1786.8	7.5	1786.8	7.5	99.6	0.4
LCC3-H973-178	76	64972	1.6	9.1498	0.5	4.8724	0.9	0.3233	0.8	0.84	1806.0	12.4	1797.5	7.9	1787.6	9.2	1787.6	9.2	101.0	-1.0
LCC3-H973-185	140	247408	1.3	9.1467	0.6	4.7878	1.3	0.3176	1.2	0.89	1778.1	18.5	1782.8	11.2	1788.2	11.0	1788.2	11.0	99.4	0.6
LCC3-H973-173	65	39861	1.5	9.1447	1.0	4.8177	1.4	0.3195	0.9	0.65	1787.4	13.8	1788.0	11.4	1788.7	18.8	1788.7	18.8	99.9	0.1
LCC3-H973-186	105	63893	1.0	9.1362	0.7	4.9024	1.7	0.3248	1.6	0.93	1813.3	25.3	1802.7	14.6	1790.3	11.9	1790.3	11.9	101.3	-1.3
LCC3-H973-71	85	127684	1.2	9.1336	0.7	4.5503	1.1	0.3014	0.9	0.78	1698.4	13.3	1740.2	9.5	1790.9	13.0	1790.9	13.0	94.8	5.2

U-Pb Geochronologic anlayses of selected Harmony Formation strata

				Isotope ratios								Apparent ages (Ma)							
	U	206Pb	U/Th	206Pb*	±	207Pb*	±	206Pb*	±	error	206Pb*	±	207Pb*	±	206Pb*	±	Best age	±	Conc.	Discor.
	(ppm)	204Pb		207Pb*	(%)	235U*	(%)	238U	(%)	corr.	238U*	(Ma)	235U	(Ma)	207Pb*	(Ma)	(Ma)	(Ma)	(%)	(%)
Sample: LCC #3. Location: Little Cottonwood Canyon, Galena Range; 0490459 4494916 (NAD 83 UTM 11T)																			
LCC3-H973-34	50	27840	1.2	9.1245	1.2	4.8729	1.7	0.3225	1.1	0.68	1801.8	17.7	1797.6	14.0	1792.7	22.1	1792.7	22.1	100.5	-0.5
LCC3-H973-189	169	234370	2.8	9.1240	0.4	4.8665	0.8	0.3220	0.7	0.90	1799.7	11.4	1796.5	6.8	1792.8	6.5	1792.8	6.5	100.4	-0.4
LCC3-H973-88	213	12678	1.9	9.1215	0.5	4.8784	1.3	0.3227	1.2	0.91	1803.0	18.8	1798.5	11.1	1793.3	9.9	1793.3	9.9	100.5	-0.5
LCC3-H973-8	78	8974	1.6	9.0824	1.6	4.8795	1.9	0.3214	1.1	0.58	1796.7	17.5	1798.7	16.2	1801.1	28.4	1801.1	28.4	99.8	0.2
LCC3-H973-68	213	6033	0.8	9.0793	1.7	4.4766	1.9	0.2948	0.9	0.47	1665.4	13.3	1726.7	15.9	1801.7	30.7	1801.7	30.7	92.4	7.6
LCC3-H973-169	168	4185	1.3	9.0274	1.7	4.6754	2.3	0.3061	1.5	0.65	1721.6	22.0	1762.9	18.8	1812.1	31.2	1812.1	31.2	95.0	5.0
LCC3-H973-171	56	42944	1.5	9.0074	0.7	5.0487	1.3	0.3298	1.2	0.87	1837.5	18.8	1827.5	11.4	1816.2	12.0	1816.2	12.0	101.2	-1.2
LCC3-H973-85	47	59631	0.8	8.9826	1.5	4.2240	2.0	0.2752	1.4	0.67	1567.1	18.8	1678.7	16.5	1821.2	27.0	1821.2	27.0	86.0	14.0
LCC3-H973-25	160	16816	0.7	8.9540	0.2	3.9302	1.1	0.2552	1.1	0.98	1465.4	14.7	1619.9	9.3	1826.9	4.5	1826.9	4.5	80.2	19.8
LCC3-H973-15	46	66150	1.2	8.9303	0.9	5.1461	1.5	0.3333	1.1	0.77	1854.4	18.2	1843.8	12.4	1831.8	16.8	1831.8	16.8	101.2	-1.2
LCC3-H973-78	31	24454	1.0	8.9301	2.0	4.6449	2.4	0.3008	1.4	0.59	1695.5	21.2	1757.4	20.3	1831.8	35.7	1831.8	35.7	92.6	7.4
LCC3-H973-98	109	193277	1.9	8.9186	0.6	5.1220	1.1	0.3313	1.0	0.84	1844.7	15.4	1839.8	9.7	1834.1	11.4	1834.1	11.4	100.6	-0.6
LCC3-H973-23	50	50771	1.0	8.8953	0.8	5.0775	1.2	0.3276	0.9	0.75	1826.6	14.6	1832.4	10.4	1838.9	14.6	1838.9	14.6	99.3	0.7
LCC3-H973-121	294	34843	3.3	8.8865	0.3	5.1481	1.2	0.3318	1.1	0.96	1847.1	18.0	1844.1	10.0	1840.7	6.3	1840.7	6.3	100.3	-0.3
LCC3-H973-192	89	61697	2.0	8.8755	0.7	5.1890	1.5	0.3340	1.3	0.86	1857.8	20.3	1850.8	12.4	1842.9	13.4	1842.9	13.4	100.8	-0.8
LCC3-H973-53	46	54628	0.7	8.8740	1.1	5.2185	1.6	0.3359	1.2	0.72	1866.7	18.6	1855.6	13.6	1843.2	20.0	1843.2	20.0	101.3	-1.3
LCC3-H973-172	90	127628	1.0	8.8735	0.8	5.1778	1.0	0.3332	0.7	0.65	1854.0	10.8	1849.0	8.8	1843.3	14.1	1843.3	14.1	100.6	-0.6
LCC3-H973-124	26	26506	1.1	8.8697	1.5	5.2267	2.0	0.3362	1.3	0.66	1868.5	21.7	1857.0	17.4	1844.1	27.9	1844.1	27.9	101.3	-1.3
LCC3-H973-103	138	42283	0.8	8.8676	0.5	4.7522	0.8	0.3056	0.6	0.73	1719.2	8.5	1776.5	6.5	1844.5	9.6	1844.5	9.6	93.2	6.8
LCC3-H973-167	151	103516	2.1	8.8527	0.4	4.9626	3.1	0.3186	3.1	0.99	1783.0	48.6	1813.0	26.6	1847.6	7.7	1847.6	7.7	96.5	3.5
LCC3-H973-99	95	109548	2.2	8.8442	0.4	4.2848	0.8	0.2748	0.7	0.89	1565.4	10.2	1690.4	6.8	1849.3	6.7	1849.3	6.7	84.6	15.4
LCC3-H973-118	65	70522	1.1	8.8379	1.3	4.6333	2.9	0.2970	2.6	0.89	1676.4	38.1	1755.3	24.2	1850.6	24.1	1850.6	24.1	90.6	9.4
LCC3-H973-195	24	18635	0.4	8.8332	2.5	5.2903	2.9	0.3389	1.5	0.50	1881.5	24.0	1867.3	25.0	1851.5	45.7	1851.5	45.7	101.6	-1.6
LCC3-H973-21	221	15230	1.4	8.8323	1.0	5.2246	2.0	0.3347	1.7	0.87	1861.0	27.7	1856.6	16.8	1851.7	17.6	1851.7	17.6	100.5	-0.5
LCC3-H973-90	23	26557	0.7	8.8306	2.3	5.2522	2.7	0.3364	1.5	0.55	1869.2	24.1	1861.1	23.0	1852.1	40.7	1852.1	40.7	100.9	-0.9
LCC3-H973-117	132	126267	1.9	8.8284	0.6	5.0822	2.4	0.3254	2.3	0.97	1816.1	36.5	1833.1	20.2	1852.5	10.8	1852.5	10.8	98.0	2.0
LCC3-H973-196	74	47358	0.7	8.8258	0.9	5.2517	1.2	0.3362	0.7	0.59	1868.2	11.2	1861.0	9.9	1853.1	16.9	1853.1	16.9	100.8	-0.8
LCC3-H973-59	21	24552	0.8	8.8149	2.0	5.2109	2.4	0.3331	1.4	0.57	1853.6	22.1	1854.4	20.5	1855.3	35.7	1855.3	35.7	99.9	0.1
LCC3-H973-96	73	155037	0.6	8.8105	0.8	5.1881	1.2	0.3315	0.9	0.74	1845.7	13.8	1850.7	9.9	1856.2	14.3	1856.2	14.3	99.4	0.6
LCC3-H973-29	122	6297	1.1	8.8037	1.1	4.3698	2.1	0.2790	1.8	0.84	1586.4	24.9	1706.6	17.4	1857.6	20.7	1857.6	20.7	85.4	14.6
LCC3-H973-170	19	13201	0.4	8.7931	2.1	5.1740	2.5	0.3300	1.4	0.55	1838.2	22.0	1848.4	21.2	1859.8	37.4	1859.8	37.4	98.8	1.2
LCC3-H973-109	96	92474	2.9	8.7868	0.5	5.2893	0.8	0.3371	0.7	0.85	1872.6	11.7	1867.1	7.2	1861.0	8.1	1861.0	8.1	100.6	-0.6
LCC3-H973-44	102	89292	0.7	8.7812	0.4	5.2130	2.4	0.3320	2.3	0.98	1848.1	37.5	1854.7	20.2	1862.2	7.7	1862.2	7.7	99.2	0.8
LCC3-H973-122	48	34121	0.9	8.7758	1.2	5.2352	1.9	0.3332	1.4	0.78	1853.9	23.3	1858.4	15.8	1863.3	21.0	1863.3	21.0	99.5	0.5
LCC3-H973-11	64	55240	1.0	8.7742	0.6	5.3449	1.4	0.3401	1.2	0.89	1887.3	20.3	1876.1	11.9	1863.7	11.4	1863.7	11.4	101.3	-1.3
LCC3-H973-1	111	150846	1.6	8.7396	0.3	5.3061	0.8	0.3363	0.7	0.93	1869.0	11.5	1869.8	6.5	1870.8	5.2	1870.8	5.2	99.9	0.1
LCC3-H973-143	82	88944	1.0	8.7276	0.7	5.4370	1.3	0.3442	1.1	0.83	1906.6	17.9	1890.7	11.2	1873.3	13.0	1873.3	13.0	101.8	-1.8
LCC3-H973-75	98	2315	0.7	8.7122	1.3	4.6252	3.6	0.2923	3.4	0.93	1652.8	49.2	1753.8	30.3	1876.4	23.9	1876.4	23.9	88.1	11.9
LCC3-H973-43	90	101565	0.7	8.6983	1.0	5.2695	1.1	0.3324	0.5	0.45	1850.1	8.0	1863.9	9.3	1879.3	17.5	1879.3	17.5	98.4	1.6
LCC3-H973-95	60	64431	0.8	8.6233	0.8	5.4544	1.1	0.3411	0.8	0.73	1892.1	13.6	1893.4	9.7	1894.9	13.9	1894.9	13.9	99.9	0.1
LCC3-H973-135	82	96248	1.1	8.5990	0.8	5.4886	1.4	0.3423	1.1	0.79	1897.7	18.1	1898.8	11.9	1900.0	15.2	1900.0	15.2	99.9	0.1
LCC3-H973-94	77	21290	1.5	8.5484	3.9	4.9428	5.9	0.3064	4.4	0.75	1723.2	66.7	1809.6	49.6	1910.6	69.4	1910.6	69.4	90.2	9.8
LCC3-H973-22	11	31965	1.4	8.3769	4.3	5.3621	5.1	0.3258	2.7	0.54	1817.9	43.1	1878.8	43.5	1946.9	76.7	1946.9	76.7	93.4	6.6
LCC3-H973-130	31	42475	2.2	8.2877	1.6	5.8864	2.1	0.3538	1.4	0.65	1952.8	22.9	1959.2	18.0	1966.0	28.0	1966.0	28.0	99.3	0.7
LCC3-H973-100	51	86313	0.8	7.8635	0.9	6.6044	1.2	0.3767	0.9	0.71	2060.7	15.2	2059.9	10.8	2059.2	15.3	2059.2	15.3	100.1	-0.1
LCC3-H973-93	14	21093	0.9	7.7030	3.8	7.0521	4.1	0.3940	1.5	0.38	2141.3	27.8	2118.0	36.1	2095.5	66.0	2095.5	66.0	102.2	-2.2
LCC3-H973-110	163	46433	1.2	7.5945	0.8	6.6702	5.2	0.3674	5.2	0.99	2017.1	89.6	2068.7	46.3	2120.4	14.8	2120.4	14.8	95.1	4.9
LCC3-H973-177	65	90579	3.1	7.0633	0.6	7.8378	1.4	0.4015	1.3	0.91	2176.0	24.0	2212.6	12.9	2246.6	10.3	2246.6	10.3	96.9	3.1
LCC3-H973-64	114	117601	1.3	6.8296	0.6	8.3231	4.7	0.4123	4.7	0.99	2225.3	88.2	2266.8	42.8	2304.5	9.5	2304.5	9.5	96.6	3.4
LCC3-H973-193	267	18480	0.8	6.8289	0.5	8.7417	1.7	0.4330	1.7	0.96	2319.0	32.2	2311.4	15.6	2304.7	7.8	2304.7	7.8	100.6	-0.6
LCC3-H973-146	177	271278	1.2	6.7574	0.2	8.7842	1.1	0.4305	1.1	0.98	2308.0	21.1	2315.9	10.1	2322.8	4.0	2322.8	4.0	99.4	0.6
LCC3-H973-129	128	21824	2.1	6.7035	0.5	8.3008	0.8	0.4036	0.7	0.83	2185.4	12.8	2264.4	7.5	2336.5	7.9	2336.5	7.9	93.5	6.5
LCC3-H973-32	84	115203	1.5	6.6598	0.4	8.5447	1.0	0.4127	0.9	0.91	2227.3	17.6	2290.7	9.4	2347.7	7.5	2347.7	7.5	94.9	5.1
LCC3-H973-164	54	56636	1.6	6.5191	0.9	8.9587	1.4	0.4236	1.1	0.76	2276.7	20.3	2333.8	12.8	2384.1	15.5	2384.1	15.5	95.5	4.5
LCC3-H973-46	147	128968	2.4	6.4900	0.6	9.5314	1.9	0.4486	1.8	0.96	2389.2	36.4	2390.6	17.5	2391.7	9.4	2391.7	9.4	99.9	0.1
LCC3-H973-112	9	11638	0.8	6.4276	4.6	9.0945	4.8	0.4240	1.5	0.31	2278.4	28.8	2347.6	44.0	2408.2	77.6	2408.2	77.6	94.6	5.4
LCC3-H973-6	234	33100	2.2	6.3973	1.0	8.1139	5.0	0.3765	4.9	0.98	2059.8	86.0	2243.8	45.1	2416.2	17.2	2416.2	17.2	85.2	14.8
LCC3-H973-198	76	70636	1.6	6.3864	0.4	8.8751	1.2	0.4111	1.2	0.95	2219.9	21.9	2325.2	11.2	2419.1	6.4	2419.1	6.4	91.8	8.2
LCC3-H973-39	128	36121	1.0	6.0947	0.5	9.0409	1.3	0.3996	1.2	0.93	2167.3	21.9	2342.1	11.7	2498.1	8.0	2498.1	8.0	86.8	13.2
LCC3-H973-102	57	152729	1.4	6.0536	0.4	10.9203	0.9	0.4795	0.8	0.88	2524.9	16.1	2516.4	8.2	2509.5	7.1	2509.5	7.1	100.6	-0.6
LCC3-H973-79	50	73860	1.1	6.0251	0.4	11.1569	1.3	0.4875	1.3	0.94	2560.0	26.6	2536.3	12.4	2517.4	7.4	2517.4	7.4	101.7	-1.7
LCC3-H973-12	239	31638	1.8	5.9689	0.3	9.1974	2.3	0.3982	2.3	0.99	2160.6	41.5	2357.9	20.9	2533.1	5.6	2533.1	5.6	85.3	14.7
LCC3-H973-81	119	29318	1.2	5.8945	0.5	11.1638	2.2	0.4773	2.2	0.98	2515.4	45.0	2536.9	20.6	2554.2	7.6	2554.2	7.6	98.5	1.5
LCC3-H973-97	63	91522	1.5	5.8936	0.4	10.9411	2.4	0.4677	2.3	0.99	2473.3	48.2	2518.1	22.2	2554.4	6.8	2554.4	6.8	96.8	3.2
LCC3-H973-137	55	65349	1.8	5.8723	0.6	10.5756	1.2	0.4504	1.0	0.86	2397.1	20.5	2486.6	11.1	2560.5	10.3	2560.5	10.3	93.6	6.4
LCC3-H973-149	74	209967	1.6	5.8271	0.4	11.1117	1.8	0.4696	1.7	0.97	2481.8	35.2	2532.5	16.4	2573.4	7.1	2573.4	7.1	96.4	3.6
LCC3-H973-159	269	89775	2.7	5.8145	1.1	12.2602	4.2	0.5170	4.1	0.96	2686.5	89.9	2624.5	39.9	2577.0	19.1	2577.0	19.1	104.2	-4.2
LCC3-H973-125	37	50521	1.6	5.8005	0.9	11.7918	1.5	0.4961	1.2	0.79	2596.9	25.1	2588.0	13.8	2581.1	15.0	2581.1	15.0	100.6	-0.6
LCC3-H973-191	33	35783	0.3	5.7959	1.3	11.8738	3.1	0.4991	2.8	0.91	2610.0	59.4	2594.5	28.6	2582.4	21.6	2582.4	21.6	101.1	-1.1
LCC3-H973-194	144	106685	1.1	5.7880	0.4	11.3917	1.2	0.4782	1.1	0.92	2519.4	22.3	2555.7	10.8	2584.7	7.4	2584.7	7.4	97.5	2.5
LCC3-H973-176	79	393148	2.2	5.7738	0.3	11.8540	0.7	0.4964	0.7	0.90	2598.3	14.3	2592.9	7.0	2588.8	5.5	2588.8	5.5	100.4	-0.4
LCC3-H973-20	139	66284	1.6	5.7696	0.2	11.1332	0.6	0.4659	0.5	0.92	2465.4	11.1	2534.3	5.5	2590.0	3.9	2590.0	3.9	95.2	4.8
LCC3-H973-7	111	119805	2.0	5.7589	0.2	12.0140	1.3	0.5018	1.3	0.99	2621.5	28.0	2605.5	12.4	2593.1	3.6	2593.1	3.6	101.1	-1.1
LCC3-H973-56	28	41408	0.7	5.7585	1.3	11.7597	1.9	0.4911	1.5	0.75	2575.6	30.8	2585.5	18.2	2593.2	21.7	2593.2	21.7	99.3	0.7
LCC3-H973-136	79	159856	0.9	5.7520	0.3	10.6267	1.7	0.4433	1.7	0.98	2365.5	33.8	2491.0	16.2	2595.1	5.7	2595.1	5.7	91.2	8.8
LCC3-H973-24	76	98298	1.2	5.7449	0.3	11.9347	1.1	0.4973	1.0	0.95	2602.1	22.5	2599.3	10.3	2597.1	5.7	2597.1	5.7	100.2	-0.2
LCC3-H973-54	81	122511	1.8	5.7307	0.3	11.5937	0.9	0.4819	0.8	0.92	2535.4	17.4	2572.2	8.4	2601.3	5.8	2601.3	5.8	97.5	2.5
LCC3-H973-74	74	84396	1.7	5.7087	0.3	12.0479	0.9	0.4988	0.9	0.95	2608.8	18.7	2608.1	8.6	2607.7	4.7	2607.7	4.7	100.0	0.0
LCC3-H973-165	72	121114	0.9	5.6986	0.3	12.1600	0.8	0.5026	0.7	0.93	2624.9	16.0	2616.8	7.5	2610.6	4.8	2610.6	4.8	100.5	-0.5
LCC3-H973-128	127	128511	1.4	5.6981	0.3	10.8371	2.4	0.4479	2.4	0.99	2385.7	47.3	2509.3	22.3	2610.8	5.4	2610.8	5.4	91.4	8.6
LCC3-H973-151	133	310749	2.0	5.6972	0.2	12.2078	0.6	0.5044	0.6	0.95	2632.8	12.3	2620.5	5.6	2611.0	3.2	2611.0	3.2	100.8	-0.8
LCC3-H973-33	106	125142	2.3	5.6924	0.3	12.2216	1.6	0.5046	1.5	0.98	2633.4	32.8	2621.6	14.6	2612.4	5.3	2612.4	5.3	100.8	-0.8
LCC3-H973-45	44	67822	2.0	5.6899	0.4	12.2091	1.3	0.5038	1.3	0.95	2630.2	27.2	2620.6	12.5	2613.2	7.0	2613.2	7.0	100.7	-0.7
LCC3-H973-184	68	114710	1.6	5.6877	0.5	12.1643	1.0	0.5018	0.8	0.85	2621.5	17.7	2617.2	9.1	2613.8	8.6	2613.8	8.6	100.3	-0.3
LCC3-H973-86	129	172200	2.8	5.6874	0.2	12.2072	0.7	0.5035	0.6	0.93	2629.0	13.4	2620.5	6.2	2613.9	3.9	2613.9	3.9	100.6	-0.6
LCC3-H973-82	140	225439	1.6	5.6858	0.2	12.3679	1.6	0.5100	1.6	0.99	2656.7	35.7	2632.7	15.5	2614.3	2.8	2614.3	2.8	101.6	-1.6
LCC3-H973-116	41	99701	1.1	5.6403	0.5	12.2431	1.4	0.5008	1.3	0.93	2617.4	27.6	2623.2	12.9	2627.7	8.4	2627.7	8.4	99.6	0.4
LCC3-H973-52	124	171793	1.6	5.6161	0.3	11.2064	1.2	0.4565	1.1	0.97	2423.9	22.5	2540.5	10.7	2634.9	4.9	2634.9	4.9	92.0	8.0
LCC3-H973-142	48	69443	1.1	5.5891	0.8	12.1669	3.1	0.4932	3.0	0.97	2584.5	64.6	2617.4	29.4	2642.9	12.9	2642.9	12.9	97.8	2.2
LCC3-H973-141	41	39320	1.3	5.5849	0.6	12.2768	1.4	0.4973	1.2	0.89	2602.1	25.8	2625.8	12.7	2644.1	10.3	2644.1	10.3	98.4	1.6
LCC3-H973-31	121	87971	0.8	5.5762	0.6	10.4930	5.0	0.4244	4.9	0.99	2280.2	94.5	2479.3	45.9	2646.7	9.3	2646.7	9.3	86.2	13.8
LCC3-H973-30	134	150848	0.8	5.5592	0.5	11.7765	2.4	0.4748	2.3	0.98	2504.7	48.0	2586.8	22.2	2651.8	8.3	2651.8	8.3	94.5	5.5
LCC3-H973-41	74	64266	0.8	5.5487	0.4	10.3035	2.9	0.4146	2.9	0.99	2236.1	55.2	2462.4	27.3	2654.9	6.5	2654.9	6.5	84.2	15.8
LCC3-H973-161	41	50233	1.0	5.5189	0.7	12.6966	1.2	0.5082	1.0	0.82	2649.0	21.7	2657.4	11.5	2663.8	11.7	2663.8	11.7	99.4	0.6
LCC3-H973-132	64	76822	1.0	5.5186	1.2	12.8451	2.3	0.5141	2.0	0.87	2674.2	44.4	2668.4	22.0	2663.9	19.3	2663.9	19.3	100.4	-0.4
LCC3-H973-89	103	208729	1.8	5.5007	0.2	12.9340	0.8	0.5160	0.8	0.98	2682.2	17.3	2674.9	7.6	2669.3	2.9	2669.3	2.9	100.5	-0.5
LCC3-H973-115	26	60358	0.9	5.4882	0.8	12.9644	1.4	0.5160	1.1	0.81	2682.3	24.6	2677.1	13.0	2673.1	13.3	2673.1	13.3	100.3	-0.3
LCC3-H973-158	81	110652	0.9	5.4845	0.5	12.9844	0.9	0.5165	0.8	0.86	2684.2	17.2	2678.5	8.6	2674.2	7.6	2674.2	7.6	100.4	-0.4
LCC3-H973-112	15	28566	0.6	5.4732	1.3	13.1278	1.8	0.5211	1.3	0.70	2703.9	28.1	2688.9	17.2	2677.6	21.7	2677.6	21.7	101.0	-1.0
LCC3-H973-16	98	143732	1.3	5.4645	0.3	12.9277	1.6	0.5124	1.6	0.99	2666.7	34.9	2674.4	15.3	2680.2	4.3	2680.2	4.3	99.5	0.5

U-Pb Geochronologic anlayses of selected Harmony Formation strata

				Isotope ratios									Apparent ages (Ma)							
	U	206Pb	U/Th	206Pb*	±	207Pb*	±	206Pb*	±	error	206Pb*	±	207Pb*	±	206Pb*	±	Best age	±	Conc.	Discor.
	(ppm)	204Pb		207Pb*	(%)	235U*	(%)	238U	(%)	corr.	238U*	(Ma)	235U	(Ma)	207Pb*	(Ma)	(Ma)	(Ma)	(%)	(%)
Sample: LCC #3. Location: Little Cottonwood Canyon, Galena Range; 0490459 4494916 (NAD 83 UTM 11T)																				
LCC3-H973-108	110	357936	1.6	5.4627	0.2	12.6260	0.5	0.5002	0.5	0.90	2614.8	10.3	2652.2	5.0	2680.8	3.8	2680.8	3.8	97.5	2.5
LCC3-H973-148	209	23237	1.0	5.4598	0.2	13.2400	1.8	0.5243	1.7	0.99	2717.3	38.7	2696.9	16.6	2681.6	3.0	2681.6	3.0	101.3	-1.3
LCC3-H973-127	16	10317	0.7	5.4501	1.4	13.0248	1.7	0.5148	1.0	0.58	2677.3	21.5	2681.5	16.0	2684.6	22.8	2684.6	22.8	99.7	0.3
LCC3-H973-9	24	69676	1.2	5.4384	0.5	12.9251	1.6	0.5098	1.5	0.95	2655.8	32.4	2674.2	14.7	2688.2	7.8	2688.2	7.8	98.8	1.2
LCC3-H973-77	29	78596	0.5	5.4341	0.9	13.1620	1.4	0.5187	1.1	0.78	2693.8	23.9	2691.3	13.2	2689.5	14.6	2689.5	14.6	100.2	-0.2
LCC3-H973-57	24	30729	1.1	5.4259	0.8	13.2228	1.6	0.5203	1.4	0.87	2700.6	30.7	2695.7	15.2	2692.0	13.3	2692.0	13.3	100.3	-0.3
LCC3-H973-27	46	72568	1.5	5.4210	0.6	13.0786	0.9	0.5142	0.7	0.77	2674.6	15.3	2685.3	8.6	2693.4	9.7	2693.4	9.7	99.3	0.7
LCC3-H973-166	79	91251	1.4	5.3881	0.2	12.5344	1.0	0.4898	1.0	0.98	2569.9	20.5	2645.3	9.3	2703.5	3.4	2703.5	3.4	95.1	4.9
LCC3-H973-80	15	13488	0.3	5.3831	1.0	13.2351	3.7	0.5167	3.6	0.96	2685.3	79.0	2696.6	35.3	2705.0	16.7	2705.0	16.7	99.3	0.7
LCC3-H973-37	97	220310	1.4	5.3598	0.3	13.3717	1.0	0.5198	1.0	0.97	2698.3	21.0	2706.3	9.3	2712.2	4.1	2712.2	4.1	99.5	0.5
LCC3-H973-163	177	13382	1.9	5.3594	0.3	13.5407	0.8	0.5263	0.7	0.94	2726.0	16.4	2718.1	7.4	2712.3	4.4	2712.3	4.4	100.5	-0.5
LCC3-H973-157	175	113946	1.0	5.3410	0.1	14.1216	3.0	0.5470	3.0	1.00	2812.8	69.4	2757.9	28.9	2718.0	2.3	2718.0	2.3	103.5	-3.5
LCC3-H973-70	92	142962	0.8	5.3395	0.2	13.5657	0.9	0.5253	0.8	0.97	2721.8	18.4	2719.9	8.1	2718.4	3.7	2718.4	3.7	100.1	-0.1
LCC3-H973-101	35	40920	1.6	5.3386	0.7	14.2757	2.7	0.5527	2.7	0.97	2836.6	60.9	2768.2	26.0	2718.7	11.2	2718.7	11.2	104.3	-4.3
LCC3-H973-83	47	118041	1.2	5.3154	0.5	12.5486	2.4	0.4838	2.3	0.97	2543.6	49.4	2646.4	22.7	2725.9	9.0	2725.9	9.0	93.3	6.7
LCC3-H973-40	81	136102	1.6	5.2966	0.3	13.7024	0.7	0.5264	0.6	0.89	2726.1	13.4	2729.4	6.4	2731.7	5.0	2731.7	5.0	99.8	0.2
LCC3-H973-4	28	92323	1.5	5.2861	0.4	13.6849	1.2	0.5247	1.2	0.95	2718.9	26.1	2728.1	11.7	2735.0	6.2	2735.0	6.2	99.4	0.6
LCC3-H973-87	50	71229	1.6	5.2709	0.6	13.9752	0.8	0.5343	0.5	0.65	2759.3	12.3	2748.0	8.0	2739.7	10.5	2739.7	10.5	100.7	-0.7
LCC3-H973-91	157	147286	3.9	5.2707	0.7	13.7061	4.4	0.5239	4.3	0.99	2715.8	96.2	2729.6	41.6	2739.8	10.8	2739.8	10.8	99.1	0.9
LCC3-H973-187	28	57696	1.1	4.9625	0.5	15.1794	1.2	0.5463	1.1	0.91	2809.9	24.4	2826.6	11.2	2838.5	7.8	2838.5	7.8	99.0	1.0
LCC3-H973-155	55	83128	0.8	4.9602	0.6	15.8261	1.2	0.5693	1.0	0.87	2905.1	23.6	2866.4	11.0	2839.2	9.2	2839.2	9.2	102.3	-2.3
LCC3-H973-140	53	131907	1.6	4.6767	0.3	16.6499	1.4	0.5647	1.4	0.97	2886.2	31.7	2914.9	13.4	2934.8	5.1	2934.8	5.1	98.3	1.7
LCC3-H973-67	8	12793	0.3	4.5888	1.8	17.3004	2.9	0.5758	2.2	0.78	2931.5	52.2	2951.6	27.4	2965.4	29.1	2965.4	29.1	98.9	1.1
LCC3-H973-111	150	129946	0.5	4.0642	0.3	16.8515	1.8	0.4967	1.8	0.98	2599.7	37.5	2926.4	17.1	3159.5	5.5	3159.5	5.5	82.3	17.7
LCC3-H973-92	110	254422	1.0	3.5012	0.4	26.5414	2.1	0.6740	2.1	0.98	3321.2	54.1	3366.7	20.8	3393.9	6.7	3393.9	6.7	97.9	2.1
LCC3-H973-17	108	208359	1.1	2.9199	0.2	35.7474	1.3	0.7570	1.3	0.99	3633.4	35.5	3659.5	12.8	3673.8	3.4	3673.8	3.4	98.9	1.1
Sample: LCC #4. Location: Little Cottonwood Canyon, Galena Range; 0490623 4494977 (NAD 83 UTM 11T)																				
LCC4-88RM13-122	164	63542	1.7	12.7286	1.1	2.1680	3.0	0.2001	2.8	0.93	1176.1	29.6	1170.9	20.5	1161.1	21.2	1161.1	21.2	101.3	-1.3 1.0,0.8
LCC4-88RM13-157	105	49618	1.1	9.5690	0.8	4.0690	3.3	0.2824	3.2	0.97	1603.4	45.3	1648.1	26.8	1705.6	14.2	1705.6	14.2	94.0	6.0
LCC4-88RM13-80	18	7740	0.8	9.4151	3.2	4.6997	4.7	0.3209	3.4	0.73	1794.2	53.3	1767.2	39.3	1735.4	59.2	1735.4	59.2	103.4	-3.4
LCC4-88RM13-52	182	24329	1.6	9.3259	0.5	4.1554	5.5	0.2811	5.5	0.99	1596.7	77.1	1665.3	44.9	1752.8	10.1	1752.8	10.1	91.1	8.9
LCC4-88RM13-38	407	14111	1.5	9.3087	0.2	3.8655	2.5	0.2610	2.5	1.00	1494.8	33.2	1606.5	20.1	1756.2	4.4	1756.2	4.4	85.1	14.9
LCC4-88RM13-46	52	35011	1.1	9.3028	1.1	4.8549	1.6	0.3276	1.1	0.71	1826.6	17.5	1794.5	13.1	1757.4	20.0	1757.4	20.0	103.9	-3.9
LCC4-88RM13-61	482	123777	3.9	9.2839	0.3	3.8328	3.4	0.2581	3.4	1.00	1480.0	45.1	1599.7	27.5	1761.1	4.6	1761.1	4.6	84.0	16.0
LCC4-88RM13-113	375	14040	1.0	9.2818	0.4	4.0430	6.9	0.2722	6.9	1.00	1551.8	95.4	1642.9	56.5	1761.5	7.4	1761.5	7.4	88.1	11.9
LCC4-88RM13-42	92	35125	1.2	9.2576	0.4	4.4184	0.7	0.2967	0.6	0.87	1674.8	9.5	1715.8	6.1	1766.3	6.6	1766.3	6.6	94.8	5.2
LCC4-88RM13-94	355	15842	2.7	9.2495	0.4	4.4413	3.3	0.2979	3.3	0.99	1681.1	48.3	1720.1	27.2	1767.9	7.0	1767.9	7.0	95.1	4.9
LCC4-88RM13-37	205	36400	1.0	9.2397	0.4	4.8706	0.8	0.3264	0.7	0.84	1820.9	10.8	1797.2	6.8	1769.8	8.0	1769.8	8.0	102.9	-2.9
LCC4-88RM13-24	35	23786	1.0	9.2260	1.2	4.7664	1.6	0.3189	1.1	0.70	1784.5	17.8	1779.0	13.8	1772.5	21.5	1772.5	21.5	100.7	-0.7
LCC4-88RM13-54	115	55259	1.1	9.2235	0.6	4.8130	1.1	0.3220	0.9	0.83	1799.3	14.0	1787.2	9.0	1773.0	10.8	1773.0	10.8	101.5	-1.5
LCC4-88RM13-82	211	29672	2.3	9.2191	0.6	4.4530	0.8	0.2977	0.5	0.60	1680.1	6.8	1722.3	6.4	1773.9	11.4	1773.9	11.4	94.7	5.3
LCC4-88RM13-108	38	35099	0.6	9.2177	1.0	4.9242	2.2	0.3292	1.9	0.89	1834.5	30.7	1806.4	18.2	1774.1	17.9	1774.1	17.9	103.4	-3.4
LCC4-88RM13-48	193	14078	0.6	9.2168	0.4	4.3541	1.5	0.2911	1.4	0.96	1646.8	20.4	1703.7	12.1	1774.3	7.5	1774.3	7.5	92.8	7.2
LCC4-88RM13-39	87	31614	1.5	9.2108	0.4	4.8638	1.3	0.3249	1.2	0.95	1813.7	19.5	1796.0	10.9	1775.5	7.4	1775.5	7.4	102.1	-2.1
LCC4-88RM13-86	245	22636	1.3	9.2054	0.4	4.4574	1.1	0.2976	1.0	0.94	1679.3	15.3	1723.1	9.1	1776.6	6.6	1776.6	6.6	94.5	5.5
LCC4-88RM13-177	113	52669	0.7	9.2026	0.6	4.7746	0.8	0.3187	0.6	0.74	1783.3	9.5	1780.4	6.9	1777.1	10.2	1777.1	10.2	100.3	-0.3
LCC4-88RM13-166	76	54241	1.0	9.1977	0.8	4.7655	1.1	0.3179	0.7	0.63	1779.4	10.5	1778.8	8.9	1778.1	15.0	1778.1	15.0	100.1	-0.1
LCC4-88RM13-130	74	30558	1.4	9.1975	0.9	4.9571	1.7	0.3307	1.5	0.86	1841.6	23.6	1812.0	14.4	1778.2	15.7	1778.2	15.7	103.6	-3.6
LCC4-88RM13-71	176	21688	3.2	9.1930	0.3	4.8430	1.6	0.3229	1.6	0.98	1803.9	24.4	1792.4	13.3	1779.0	5.1	1779.0	5.1	101.4	-1.4
LCC4-88RM13-87	85	8108	1.6	9.1924	0.9	4.7628	3.0	0.3175	2.8	0.95	1777.7	44.1	1778.4	25.1	1779.2	16.8	1779.2	16.8	99.9	0.1
LCC4-88RM13-191	301	38477	2.5	9.1912	0.3	4.4010	0.8	0.2934	0.8	0.94	1658.4	11.1	1712.5	6.7	1779.4	4.9	1779.4	4.9	93.2	6.8
LCC4-88RM13-183	197	38098	1.4	9.1882	0.3	4.7635	1.1	0.3174	1.0	0.96	1777.2	16.2	1778.5	9.1	1780.0	5.7	1780.0	5.7	99.8	0.2
LCC4-88RM13-88	100	51613	1.3	9.1867	0.5	4.6549	1.2	0.3101	1.1	0.92	1741.4	16.5	1759.2	9.8	1780.3	8.5	1780.3	8.5	97.8	2.2
LCC4-88RM13-92	178	103161	1.9	9.1865	0.3	4.6888	0.8	0.3124	0.8	0.94	1752.5	11.6	1765.3	6.8	1780.3	5.2	1780.3	5.2	98.4	1.6
LCC4-88RM13-40	111	43024	1.8	9.1860	0.5	4.8141	0.8	0.3207	0.6	0.75	1793.3	9.5	1787.4	6.8	1780.4	9.8	1780.4	9.8	100.7	-0.7
LCC4-88RM13-26	60	60059	3.6	9.1832	0.6	4.9694	1.0	0.3310	0.8	0.81	1843.1	13.5	1814.1	8.8	1781.0	11.1	1781.0	11.1	103.5	-3.5
LCC4-88RM13-147	57	27670	1.8	9.1811	1.2	4.6902	1.5	0.3123	0.8	0.56	1752.1	12.9	1765.5	12.5	1781.4	22.5	1781.4	22.5	98.4	1.6
LCC4-88RM13-167	62	61332	0.8	9.1793	1.1	4.8263	2.1	0.3213	1.7	0.83	1796.1	26.9	1789.5	17.3	1781.8	20.9	1781.8	20.9	100.8	-0.8
LCC4-88RM13-9	48	26030	1.4	9.1774	1.4	4.9560	1.6	0.3299	0.9	0.54	1837.8	14.0	1811.8	13.6	1782.1	24.7	1782.1	24.7	103.1	-3.1
LCC4-88RM13-29	104	50203	1.3	9.1772	0.6	4.9285	1.0	0.3280	0.8	0.83	1828.9	13.4	1807.1	8.6	1782.2	10.4	1782.2	10.4	102.6	-2.6
LCC4-88RM13-50	115	82978	2.3	9.1754	0.4	4.9502	1.1	0.3294	1.1	0.94	1835.6	16.9	1810.9	9.5	1782.5	6.9	1782.5	6.9	103.0	-3.0
LCC4-88RM13-93	189	26727	1.2	9.1731	0.2	4.5879	1.4	0.3052	1.4	0.99	1717.2	21.0	1747.1	11.7	1783.0	3.1	1783.0	3.1	96.3	3.7
LCC4-88RM13-170	151	51498	1.9	9.1723	0.5	4.7733	0.8	0.3175	0.6	0.80	1777.7	9.5	1780.2	6.4	1783.2	8.2	1783.2	8.2	99.7	0.3
LCC4-88RM13-23	88	45825	1.6	9.1711	0.7	4.8244	1.1	0.3209	0.8	0.78	1794.1	12.9	1789.2	8.9	1783.4	12.1	1783.4	12.1	100.6	-0.6
LCC4-88RM13-17	173	159723	2.3	9.1686	0.4	4.8671	0.8	0.3237	0.7	0.89	1807.5	10.9	1796.6	6.6	1783.9	6.6	1783.9	6.6	101.3	-1.3
LCC4-88RM13-197	111	80881	2.2	9.1677	0.8	4.8748	1.3	0.3241	1.0	0.76	1809.9	15.2	1797.9	10.7	1784.1	14.9	1784.1	14.9	101.4	-1.4
LCC4-88RM13-181	226	192290	1.3	9.1655	0.4	4.7293	0.9	0.3144	0.8	0.88	1762.2	11.8	1772.5	7.3	1784.5	7.5	1784.5	7.5	98.8	1.2
LCC4-88RM13-69	122	106540	0.8	9.1646	0.3	4.9681	0.8	0.3302	0.7	0.93	1839.4	11.8	1813.9	6.7	1784.7	5.4	1784.7	5.4	103.1	-3.1
LCC4-88RM13-143	106	35619	2.2	9.1603	0.6	4.8714	1.7	0.3236	1.6	0.94	1807.5	24.7	1797.3	14.1	1785.5	10.6	1785.5	10.6	101.2	-1.2
LCC4-88RM13-96	72	32232	1.5	9.1573	0.8	4.9745	1.5	0.3304	1.3	0.86	1840.2	21.4	1815.0	13.1	1786.1	14.2	1786.1	14.2	103.0	-3.0
LCC4-88RM13-1	212	60639	1.9	9.1542	0.3	4.6258	3.0	0.3071	3.0	0.99	1726.5	45.7	1753.9	25.4	1786.7	6.0	1786.7	6.0	96.6	3.4
LCC4-88RM13-138	79	49191	1.1	9.1539	0.8	4.7775	1.6	0.3172	1.4	0.88	1775.9	22.3	1781.0	13.7	1786.8	13.9	1786.8	13.9	99.4	0.6
LCC4-88RM13-107	52	27916	1.8	9.1511	0.8	5.0050	1.2	0.3322	0.8	0.70	1849.0	13.0	1820.2	9.8	1787.4	15.1	1787.4	15.1	103.4	-3.4
LCC4-88RM13-65	157	245530	1.2	9.1505	0.6	5.0126	1.1	0.3327	0.9	0.84	1851.3	15.1	1821.5	9.4	1787.5	10.9	1787.5	10.9	103.6	-3.6
LCC4-88RM13-100	102	84161	1.7	9.1456	0.8	5.0409	1.7	0.3344	1.5	0.89	1859.5	24.2	1826.2	14.3	1788.5	14.2	1788.5	14.2	104.0	-4.0
LCC4-88RM13-104	134	109695	1.4	9.1389	0.5	4.9811	0.7	0.3302	0.5	0.71	1839.1	7.5	1816.1	5.6	1789.8	8.4	1789.8	8.4	102.8	-2.8
LCC4-88RM13-49	66	23253	1.5	9.1378	1.1	5.0767	1.3	0.3364	0.7	0.55	1869.6	11.9	1832.2	11.4	1790.0	20.5	1790.0	20.5	104.4	-4.4
LCC4-88RM13-64	130	68585	1.4	9.1190	0.9	5.0736	1.7	0.3356	1.4	0.84	1865.3	23.3	1831.7	14.6	1793.8	17.0	1793.8	17.0	104.0	-4.0
LCC4-88RM13-193	36	10898	1.0	9.0656	1.6	4.2246	4.1	0.2778	3.8	0.92	1580.1	53.1	1678.8	33.7	1804.5	28.3	1804.5	28.3	87.6	12.4
LCC4-88RM13-47	155	8545	1.4	8.9976	0.4	5.0282	0.7	0.3281	0.6	0.84	1829.3	9.5	1824.1	6.0	1818.1	6.9	1818.1	6.9	100.6	-0.6
LCC4-88RM13-109	55	60208	1.3	8.9631	1.1	5.1856	1.6	0.3371	1.2	0.75	1872.7	19.4	1850.3	13.5	1825.1	19.1	1825.1	19.1	102.6	-2.6
LCC4-88RM13-111	175	11882	0.6	8.9345	0.5	3.9868	3.9	0.2583	3.9	0.99	1481.4	51.7	1631.5	32.1	1830.9	9.9	1830.9	9.9	80.9	19.1
LCC4-88RM13-55	87	53295	0.5	8.9029	0.5	4.8196	1.4	0.3112	1.3	0.94	1746.6	19.6	1788.3	11.4	1837.3	8.2	1837.3	8.2	95.1	4.9
LCC4-88RM13-153	67	43578	1.3	8.8945	0.9	5.1461	1.0	0.3320	0.5	0.46	1847.9	7.3	1843.7	8.4	1839.0	16.0	1839.0	16.0	100.5	-0.5
LCC4-88RM13-186	128	77443	2.3	8.8909	0.3	5.1342	0.9	0.3311	0.9	0.94	1843.5	13.8	1841.8	7.8	1839.8	5.6	1839.8	5.6	100.2	-0.2
LCC4-88RM13-91	168	89944	2.0	8.8668	0.3	5.3252	1.1	0.3425	1.1	0.96	1898.5	18.1	1872.9	9.7	1844.7	5.5	1844.7	5.5	102.9	-2.9
LCC4-88RM13-68	214	129627	1.9	8.8658	0.2	5.3265	0.8	0.3425	0.8	0.96	1898.7	12.5	1873.1	6.8	1844.9	3.7	1844.9	3.7	102.9	-2.9
LCC4-88RM13-70	85	49600	1.7	8.8512	0.7	5.3087	1.1	0.3408	0.9	0.80	1890.5	14.5	1870.3	9.5	1847.9	12.2	1847.9	12.2	102.3	-2.3
LCC4-88RM13-161	53	33916	2.9	8.8478	1.2	5.3522	2.1	0.3434	1.8	0.84	1903.2	29.5	1877.2	18.2	1848.6	20.9	1848.6	20.9	103.0	-3.0
LCC4-88RM13-155	25	13817	0.5	8.8234	2.2	5.2301	2.6	0.3347	1.5	0.57	1861.1	24.5	1857.5	22.5	1853.5	39.0	1853.5	39.0	100.4	-0.4
LCC4-88RM13-189	127	42630	0.8	8.8128	0.4	5.3223	1.7	0.3402	1.7	0.98	1887.5	27.8	1872.4	14.9	1855.7	7.0	1855.7	7.0	101.7	-1.7
LCC4-88RM13-58	108	43597	1.9	8.8116	0.6	5.3707	1.1	0.3432	1.0	0.86	1902.2	16.1	1880.2	9.7	1856.0	10.4	1856.0	10.4	102.5	-2.5
LCC4-88RM13-139	139	31218	1.6	8.8050	0.6	4.6690	3.4	0.2982	3.3	0.99	1682.2	49.1	1761.7	28.1	1857.3	10.5	1857.3	10.5	90.6	9.4
LCC4-88RM13-35	29	8971	6.0	8.8049	1.9	5.3965	2.6	0.3446	1.7	0.68	1908.8	28.8	1884.3	22.0	1857.3	34.2	1857.3	34.2	102.8	-2.8
LCC4-88RM13-103	236	45187	1.5	8.7880	0.4	5.1289	1.3	0.3269	1.3	0.96	1823.3	20.3	1840.9	11.3	1860.8	6.6	1860.8	6.6	98.0	2.0
LCC4-88RM13-102	264	9472	1.1	8.7754	0.3	4.6532	1.6	0.2962	1.6	0.98	1672.2	22.9	1758.9	13.3	1863.4	6.1	1863.4	6.1	89.7	10.3
LCC4-88RM13-72	169	43438	2.8	8.7747	0.4	5.4703	0.6	0.3481	0.5	0.81	1925.7	8.4	1896.0	5.3	1863.5	6.5	1863.5	6.5	103.3	-3.3
LCC4-88RM13-2	67	54917	3.1	8.7572	0.8	5.3945	1.1	0.3426	0.7	0.67	1899.3	12.2	1884.0	9.5	1867.1	14.7	1867.1	14.7	101.7	-1.7
LCC4-88RM13-152	73	90073	1.3	8.7438	0.5	5.1176	2.8	0.3245	2.7	0.98	1811.9	42.9	1839.0	23.5	1869.9	9.7	1869.9	9.7	96.9	3.1

U-Pb Geochronologic anlayses of selected Harmony Formation strata

				Isotope ratios										Apparent ages (Ma)						
	U	206Pb	U/Th	206Pb*	±	207Pb*	±	206Pb*	±	error	206Pb*	±	207Pb*	±	206Pb*	±	Best age	±	Conc.	Discor.
	(ppm)	204Pb		207Pb*	(%)	235U*	(%)	238U	(%)	corr.	238U*	(Ma)	235U	(Ma)	207Pb*	(Ma)	(Ma)	(Ma)	(%)	(%)
Sample: LCC #4. Location: Little Cottonwood Canyon, Galena Range; 0490623 4494977 (NAD 83 UTM 11T)																				
LCC4-88RM13-74	71	49204	3.7	8.6461	0.5	5.6543	1.0	0.3546	0.8	0.83	1956.4	13.6	1924.4	8.4	1890.2	9.9	1890.2	9.9	103.5	-3.5
LCC4-88RM13-14	18	26282	0.8	8.5246	2.2	5.5974	2.4	0.3461	0.9	0.38	1915.8	14.8	1915.7	20.4	1915.6	39.3	1915.6	39.3	100.0	0.0
LCC4-88RM13-141	42	47070	4.0	8.4410	1.0	5.6362	1.1	0.3450	0.4	0.38	1910.9	6.8	1921.7	9.3	1933.2	17.8	1933.2	17.8	98.8	1.2
LCC4-88RM13-75	101	30628	0.9	7.8383	0.5	6.7180	1.7	0.3819	1.7	0.95	2085.2	29.4	2075.0	15.4	2064.9	9.6	2064.9	9.6	101.0	-1.0
LCC4-88RM13-179	254	23372	1.9	7.8005	2.1	5.5538	2.7	0.3142	1.7	0.64	1761.4	26.5	1909.0	23.3	2073.4	36.8	2073.4	36.8	85.0	15.0
LCC4-88RM13-162	122	75117	1.8	7.7097	0.4	6.9111	0.8	0.3864	0.6	0.84	2106.3	11.6	2100.1	6.8	2094.0	7.4	2094.0	7.4	100.6	-0.6
LCC4-88RM13-178	91	89611	1.6	6.5373	0.8	8.9396	1.8	0.4239	1.6	0.90	2277.9	31.2	2331.9	16.4	2379.4	13.1	2379.4	13.1	95.7	4.3
LCC4-88RM13-13	359	32405	2.5	6.3819	2.4	9.5544	7.4	0.4422	7.0	0.95	2360.6	138.1	2392.8	67.9	2420.3	40.0	2420.3	40.0	97.5	2.5
LCC4-88RM13-120	174	24333	2.1	6.3179	0.8	9.0122	2.4	0.4130	2.2	0.95	2228.4	42.0	2339.2	21.5	2437.4	12.8	2437.4	12.8	91.4	8.6
LCC4-88RM13-43	195	14744	0.7	6.2962	0.7	7.9861	3.2	0.3648	3.1	0.97	2004.8	53.7	2229.7	28.9	2443.2	12.0	2443.2	12.0	82.1	17.9
LCC4-88RM13-133	308	16722	0.8	6.2622	0.3	8.8874	3.0	0.4036	3.0	1.00	2185.8	54.8	2326.5	27.1	2452.3	4.9	2452.3	4.9	89.1	10.9
LCC4-88RM13-9	182	53176	1.4	6.0616	0.2	10.8600	0.7	0.4775	0.6	0.93	2516.2	12.8	2511.2	6.2	2507.2	4.2	2507.2	4.2	100.4	-0.4
LCC4-88RM13-89	21	14830	10.8	6.0487	2.0	10.2875	2.7	0.4513	1.9	0.69	2401.0	37.7	2461.0	25.1	2510.8	32.9	2510.8	32.9	95.6	4.4
LCC4-88RM13-19	191	32279	0.9	5.9507	0.8	10.4933	1.5	0.4529	1.3	0.85	2408.0	25.6	2479.3	13.9	2538.3	13.3	2538.3	13.3	94.9	5.1
LCC4-88RM13-151	64	50122	1.8	5.8893	0.6	11.0957	1.3	0.4739	1.1	0.88	2500.8	23.8	2531.2	12.2	2555.7	10.4	2555.7	10.4	97.9	2.1
LCC4-88RM13-115	205	27165	1.1	5.8676	0.6	10.7859	1.8	0.4590	1.7	0.95	2435.1	35.2	2504.9	17.0	2561.8	9.8	2561.8	9.8	95.1	4.9
LCC4-88RM13-83	55	64497	0.9	5.8622	1.3	11.1763	3.5	0.4752	3.2	0.93	2506.3	66.6	2537.9	32.2	2563.4	21.7	2563.4	21.7	97.8	2.2
LCC4-88RM13-126	235	24306	1.0	5.8168	0.4	10.7707	4.6	0.4544	4.6	1.00	2414.7	92.8	2503.5	43.0	2576.4	6.3	2576.4	6.3	93.7	6.3
LCC4-88RM13-192	132	34846	1.5	5.8127	0.5	10.6774	3.1	0.4501	3.1	0.99	2395.9	61.6	2495.5	29.0	2577.5	8.6	2577.5	8.6	93.0	7.0
LCC4-88RM13-32	264	18331	1.2	5.8076	0.1	11.0938	0.7	0.4673	0.7	0.98	2471.6	13.4	2531.0	6.2	2579.0	2.2	2579.0	2.2	95.8	4.2
LCC4-88RM13-185	126	27904	1.1	5.7988	0.3	9.6784	1.2	0.4070	1.2	0.96	2201.4	21.5	2404.7	11.0	2581.6	5.5	2581.6	5.5	85.3	14.7
LCC4-88RM13-154	61	31979	0.9	5.7977	0.6	11.7012	1.2	0.4920	1.0	0.86	2579.4	22.1	2580.8	11.3	2581.9	10.4	2581.9	10.4	99.9	0.1
LCC4-88RM13-11	23	25181	1.1	5.7835	1.3	11.3457	2.7	0.4759	2.4	0.87	2509.4	48.9	2552.0	25.1	2586.0	21.9	2586.0	21.9	97.0	3.0
LCC4-88RM13-44	188	19921	1.1	5.7819	0.3	11.0826	1.2	0.4647	1.1	0.97	2460.5	23.0	2530.1	10.8	2586.4	4.3	2586.4	4.3	95.1	4.9
LCC4-88RM13-22	120	39399	1.5	5.7811	0.4	11.3616	0.6	0.4764	0.4	0.71	2511.5	8.3	2553.3	5.2	2586.6	6.6	2586.6	6.6	97.1	2.9
LCC4-88RM13-81	146	77202	1.0	5.7584	0.2	11.9238	0.8	0.4980	0.8	0.96	2605.1	16.4	2598.4	7.3	2593.2	2.6	2593.2	2.6	100.5	-0.5
LCC4-88RM13-8	244	27697	1.2	5.7505	0.2	10.7217	1.2	0.4472	1.2	0.99	2382.6	24.2	2499.3	11.5	2595.5	3.4	2595.5	3.4	91.8	8.2
LCC4-88RM13-163	75	101593	2.1	5.7474	0.7	11.9667	1.1	0.4988	0.8	0.76	2608.7	18.1	2601.8	10.4	2596.4	12.0	2596.4	12.0	100.5	-0.5
LCC4-88RM13-73	123	15791	0.8	5.7464	0.3	9.5333	1.2	0.3973	1.1	0.96	2156.7	20.5	2390.8	10.7	2596.7	5.5	2596.7	5.5	83.1	16.9
LCC4-88RM13-199	163	63955	1.0	5.7437	0.2	12.2107	4.8	0.5087	4.7	1.00	2650.9	103.2	2620.7	44.6	2597.5	3.9	2597.5	3.9	102.1	-2.1
LCC4-88RM13-45	112	184197	1.1	5.7055	0.3	12.4651	1.0	0.5158	1.0	0.96	2681.4	21.0	2640.1	9.4	2608.6	4.9	2608.6	4.9	102.8	-2.8
LCC4-88RM13-79	124	68769	1.9	5.6980	0.3	12.2531	1.1	0.5064	1.1	0.97	2641.1	23.9	2624.0	10.6	2610.8	4.5	2610.8	4.5	101.2	-1.2
LCC4-88RM13-57	106	168679	1.9	5.6636	3.8	11.7190	5.4	0.4814	3.8	0.71	2533.2	80.4	2582.2	50.6	2620.9	63.2	2620.9	63.2	96.7	3.3
LCC4-88RM13-149	159	38433	0.9	5.6561	0.2	10.4846	0.7	0.4301	0.7	0.96	2306.2	13.3	2478.6	6.6	2623.1	3.2	2623.1	3.2	87.9	12.1
LCC4-88RM13-7	157	283348	1.4	5.6432	0.2	12.2830	0.5	0.5027	0.5	0.93	2625.5	9.7	2626.3	4.6	2626.9	3.0	2626.9	3.0	99.9	0.1
LCC4-88RM13-90	81	149965	5.2	5.5622	0.3	13.0026	1.2	0.5245	1.2	0.96	2718.4	26.5	2679.8	11.7	2650.9	5.8	2650.9	5.8	102.5	-2.5
LCC4-88RM13-78	80	55216	1.2	5.4866	0.6	13.0765	6.9	0.5204	6.9	1.00	2700.7	152.8	2685.2	65.6	2673.5	9.9	2673.5	9.9	101.0	-1.0
LCC4-88RM13-84	130	12290	1.8	5.4749	0.6	10.9983	5.5	0.4367	5.4	0.99	2335.9	106.8	2523.0	51.1	2677.1	9.8	2677.1	9.8	87.3	12.7
LCC4-88RM13-118	86	120604	1.0	5.4444	0.4	13.7106	1.4	0.5414	1.4	0.97	2789.2	31.0	2729.9	13.4	2686.3	5.8	2686.3	5.8	103.8	-3.8
LCC4-88RM13-172	155	15888	0.8	5.4353	0.3	10.1149	2.1	0.3987	2.0	0.99	2163.2	37.3	2445.3	19.0	2689.1	5.2	2689.1	5.2	80.4	19.6
LCC4-88RM13-16	146	18934	1.0	5.4215	0.3	12.1920	1.6	0.4794	1.6	0.99	2524.6	33.0	2619.3	15.0	2693.3	4.5	2693.3	4.5	93.7	6.3
LCC4-88RM13-60	36	37590	0.4	5.4213	1.2	13.6816	2.8	0.5379	2.6	0.91	2774.8	57.9	2727.9	26.7	2693.4	19.0	2693.4	19.0	103.0	-3.0
LCC4-88RM13-169	103	18603	0.6	5.4158	0.3	10.1913	2.3	0.4003	2.3	0.99	2170.5	42.4	2452.3	21.4	2695.0	4.2	2695.0	4.2	80.5	19.5
LCC4-88RM13-194	72	48567	0.6	5.3970	0.3	13.4750	0.8	0.5275	0.8	0.93	2730.7	17.1	2713.5	7.8	2700.8	5.1	2700.8	5.1	101.1	-1.1
LCC4-88RM13-134	51	51777	2.4	5.2944	0.6	14.1070	1.1	0.5417	1.0	0.87	2790.5	22.6	2756.9	10.9	2732.4	9.4	2732.4	9.4	102.1	-2.1
LCC4-88RM13-136	52	29452	1.5	5.2534	0.4	13.8998	1.0	0.5296	0.9	0.92	2739.7	19.6	2742.9	9.0	2745.2	6.0	2745.2	6.0	99.8	0.2
LCC4-88RM13-127	119	103494	1.8	5.1717	0.3	14.7895	0.9	0.5547	0.9	0.95	2844.8	20.6	2801.8	8.9	2770.9	4.6	2770.9	4.6	102.7	-2.7
LCC4-88RM13-180	29	41080	1.1	5.0667	0.9	14.7251	1.0	0.5411	0.6	0.56	2788.1	13.3	2797.6	10.0	2804.5	14.2	2804.5	14.2	99.4	0.6
LCC4-88RM13-12	88	37914	0.7	4.9035	0.4	13.3720	1.4	0.4756	1.4	0.95	2507.9	28.6	2706.3	13.6	2857.9	7.0	2857.9	7.0	87.8	12.2
LCC4-88RM13-150	114	202774	1.7	4.8374	0.2	15.6955	1.3	0.5507	1.3	0.98	2827.9	29.2	2858.4	12.4	2880.0	4.1	2880.0	4.1	98.2	1.8
Sample: LCC #9. Location: Little Cottonwood Canyon, Galena Range; 0491232 4495602 (NAD 83 UTM 11T)																				
LCC-09HA-76	148	34636	1.6	9.5251	1.1	4.4450	3.5	0.3071	3.3	0.95	1726.3	49.8	1720.8	28.7	1714.0	19.9	1714.0	19.9	100.7	-0.7 0.9,2.1
LCC-09HA-9	253	12741	1.4	9.4099	0.5	3.5777	4.1	0.2442	4.1	0.99	1408.3	51.9	1544.6	32.9	1736.4	10.0	1736.4	10.0	81.1	18.9
LCC-09HA-51	420	7829	5.4	9.3216	0.5	3.9124	4.2	0.2645	4.2	0.99	1512.8	56.7	1616.3	34.3	1753.7	9.6	1753.7	9.6	86.3	13.7
LCC-09HA-65	434	24820	7.2	9.3056	0.4	3.9646	2.8	0.2676	2.7	0.99	1528.5	37.4	1627.0	22.6	1756.8	7.9	1756.8	7.9	87.0	13.0
LCC-09HA-83	333	20660	0.9	9.2859	0.8	3.2367	1.9	0.2180	1.7	0.91	1271.2	19.7	1466.0	14.6	1760.7	14.3	1760.7	14.3	72.2	27.8
LCC-09HA-12	123	31731	2.8	9.2477	0.6	4.8717	1.9	0.3267	1.9	0.96	1822.6	29.4	1797.4	16.3	1768.2	10.2	1768.2	10.2	103.1	-3.1
LCC-09HA-64	105	23048	2.7	9.2140	0.8	4.5717	3.2	0.3055	3.1	0.97	1718.6	47.2	1744.1	27.0	1774.9	15.2	1774.9	15.2	96.8	3.2
LCC-09HA-2	136	23912	1.3	9.2096	1.0	4.5773	1.3	0.3057	0.8	0.63	1719.7	12.1	1745.1	10.6	1775.8	18.0	1775.8	18.0	96.8	3.2
LCC-09HA-6	99	21929	3.2	9.2055	0.8	4.8108	2.0	0.3212	1.9	0.92	1795.5	29.4	1786.8	17.1	1776.6	14.5	1776.6	14.5	101.1	-1.1
LCC-09HA-37	275	31451	1.7	9.2026	0.6	4.2070	1.7	0.2808	1.5	0.93	1595.3	21.8	1675.4	13.6	1777.1	11.2	1777.1	11.2	89.8	10.2
LCC-09HA-63	160	38008	3.9	9.1968	0.8	4.7989	3.7	0.3201	3.6	0.98	1790.2	55.8	1784.7	30.7	1778.3	14.1	1778.3	14.1	100.7	-0.7
LCC-09HA-100	174	35060	3.8	9.1963	0.8	4.8021	2.7	0.3203	2.5	0.95	1791.2	39.6	1785.3	22.3	1778.4	14.6	1778.4	14.6	100.7	-0.7
LCC-09HA-69	210	27577	2.0	9.1881	0.5	3.8581	3.4	0.2571	3.4	0.99	1475.0	44.5	1605.0	27.5	1780.0	9.0	1780.0	9.0	82.9	17.1
LCC-09HA-97	171	34770	2.4	9.1789	0.7	4.2094	3.3	0.2802	3.3	0.98	1592.5	46.1	1675.9	27.3	1781.8	12.2	1781.8	12.2	89.4	10.6
LCC-09HA-14	163	45909	2.7	9.1676	0.9	4.8055	1.7	0.3195	1.4	0.84	1787.4	21.8	1785.9	14.1	1784.1	16.7	1784.1	16.7	100.2	-0.2
LCC-09HA-86	144	34871	1.8	9.1564	1.0	4.3712	3.7	0.2903	3.6	0.96	1642.9	52.1	1706.9	30.8	1786.3	18.1	1786.3	18.1	92.0	8.0
LCC-09HA-68	177	49508	2.6	9.1490	0.8	4.6985	3.2	0.3118	3.1	0.97	1749.4	46.9	1767.0	26.5	1787.8	14.5	1787.8	14.5	97.9	2.1
LCC-09HA-32	134	8924	1.0	9.1353	1.1	3.5113	7.2	0.2326	7.1	0.99	1348.3	86.9	1529.8	57.1	1790.5	19.8	1790.5	19.8	75.3	24.7
LCC-09HA-20	259	60771	7.2	9.1324	0.5	4.8469	2.0	0.3210	1.9	0.96	1794.8	29.4	1793.1	16.5	1791.1	9.9	1791.1	9.9	100.2	-0.2
LCC-09HA-8	135	41137	2.4	9.1244	0.7	4.7974	1.2	0.3175	1.0	0.80	1777.4	14.8	1784.4	10.0	1792.7	13.0	1792.7	13.0	99.1	0.9
LCC-09HA-67	240	40312	2.6	9.1227	0.4	4.8123	3.7	0.3184	3.7	0.99	1781.9	57.3	1787.1	31.2	1793.0	7.9	1793.0	7.9	99.4	0.6
LCC-09HA-38	159	51804	2.8	9.0983	0.7	4.8446	1.8	0.3197	1.7	0.93	1788.2	26.2	1792.7	15.2	1797.9	12.0	1797.9	12.0	99.5	0.5
LCC-09HA-62	147	35077	2.5	9.0982	0.8	4.9761	4.0	0.3284	3.9	0.98	1830.4	61.7	1815.3	33.4	1797.9	14.1	1797.9	14.1	101.8	-1.8
LCC-09HA-74	255	58252	2.9	9.0966	0.4	4.8562	3.6	0.3204	3.6	0.99	1791.6	56.7	1794.7	30.7	1798.2	7.3	1798.2	7.3	99.6	0.4
LCC-09HA-50	151	41121	2.7	9.0960	0.8	4.7624	2.1	0.3142	2.0	0.93	1761.2	30.5	1778.3	17.9	1798.4	14.3	1798.4	14.3	97.9	2.1
LCC-09HA-39	161	41006	2.8	9.0943	0.7	4.6878	2.4	0.3092	2.3	0.96	1736.8	35.4	1765.1	20.3	1798.7	12.5	1798.7	12.5	96.6	3.4
LCC-09HA-79	305	37687	2.6	9.0872	0.6	4.9050	2.0	0.3233	1.9	0.95	1805.7	29.4	1803.1	16.6	1800.1	11.7	1800.1	11.7	100.3	-0.3
LCC-09HA-78	142	46883	3.3	9.0782	0.9	4.8183	4.2	0.3172	4.1	0.98	1776.2	63.8	1788.1	35.3	1801.9	15.7	1801.9	15.7	98.6	1.4
LCC-09HA-31	149	36613	2.9	9.0772	0.5	4.9568	1.9	0.3263	1.8	0.96	1820.6	29.1	1812.0	16.2	1802.1	9.8	1802.1	9.8	101.0	-1.0
LCC-09HA-34	263	48794	2.7	9.0647	0.6	4.8237	3.5	0.3171	3.4	0.99	1775.7	53.2	1789.0	29.3	1804.6	10.6	1804.6	10.6	98.4	1.6
LCC-09HA-81	101	29676	2.8	9.0579	0.9	4.9482	3.5	0.3251	3.4	0.97	1814.5	53.5	1810.5	29.5	1806.0	15.5	1806.0	15.5	100.5	-0.5
LCC-09HA-21	334	7445	0.9	9.0241	0.6	3.5843	1.0	0.2346	0.8	0.81	1358.5	9.8	1546.1	7.8	1812.8	10.5	1812.8	10.5	74.9	25.1
LCC-09HA-22	253	21267	2.9	8.9955	0.5	4.4892	1.6	0.2929	1.5	0.95	1655.9	22.2	1729.0	13.3	1818.6	9.2	1818.6	9.2	91.1	8.9
LCC-09HA-55	161	19954	1.8	8.9232	1.1	4.4645	5.3	0.2889	5.2	0.98	1636.2	75.0	1724.4	44.0	1833.2	20.0	1833.2	20.0	89.3	10.7
LCC-09HA-99	94	32639	3.7	8.9228	2.6	5.0703	3.4	0.3281	2.2	0.63	1829.3	34.5	1831.2	29.0	1833.3	48.0	1833.3	48.0	99.8	0.2
LCC-09HA-44	102	21092	0.5	8.8830	0.8	3.9719	5.1	0.2559	5.1	0.99	1468.8	66.6	1628.5	41.6	1841.4	13.9	1841.4	13.9	79.8	20.2
LCC-09HA-72	344	44212	2.0	8.8368	0.3	4.8399	2.2	0.3102	2.2	0.99	1741.6	33.0	1791.9	18.4	1850.8	5.2	1850.8	5.2	94.1	5.9
LCC-09HA-3	230	67835	1.5	8.8341	0.6	5.2890	1.3	0.3389	1.1	0.88	1881.2	18.7	1867.1	11.1	1851.4	11.2	1851.4	11.2	101.6	-1.6
LCC-09HA-57	178	35738	1.3	8.8275	0.7	4.9752	2.3	0.3185	2.2	0.95	1782.5	34.3	1815.1	19.5	1852.7	12.4	1852.7	12.4	96.2	3.8
LCC-09HA-95	68	20314	2.7	8.7924	0.9	4.9567	2.8	0.3161	2.6	0.94	1770.6	40.7	1812.0	23.6	1859.9	16.8	1859.9	16.8	95.2	4.8
LCC-09HA-58	118	33062	4.9	8.7851	0.9	5.1469	3.4	0.3279	3.2	0.96	1828.4	51.2	1843.9	28.5	1861.4	16.9	1861.4	16.9	98.2	1.8
LCC-09HA-42	51	13055	4.7	8.7806	3.1	5.0789	3.3	0.3234	1.2	0.37	1806.5	19.1	1832.6	27.9	1862.3	55.2	1862.3	55.2	97.0	3.0
LCC-09HA-4	74	20331	1.4	8.7761	1.0	5.3656	1.3	0.3415	0.8	0.63	1894.0	13.9	1879.4	11.5	1863.3	18.9	1863.3	18.9	101.6	-1.6
LCC-09HA-88	125	34269	3.0	8.7704	0.8	5.3127	3.4	0.3379	3.3	0.97	1876.7	54.2	1870.9	29.2	1864.4	14.2	1864.4	14.2	100.7	-0.7
LCC-09HA-85	109	29328	1.3	8.7471	0.6	5.1631	3.9	0.3275	3.8	0.99	1826.5	60.9	1846.6	33.0	1869.2	11.5	1869.2	11.5	97.7	2.3
LCC-09HA-28	134	35439	3.0	8.7431	0.8	5.2393	1.9	0.3322	1.7	0.90	1849.2	28.0	1859.0	16.5	1870.1	15.2	1870.1	15.2	98.9	1.1
LCC-09HA-93	125	36358	4.2	8.7303	0.6	5.3099	5.6	0.3362	5.6	0.99	1868.4	90.6	1870.5	48.0	1872.7	10.9	1872.7	10.9	99.8	0.2
LCC-09HA-45	39	11547	9.3	8.7166	1.6	5.3583	2.9	0.3387	2.4	0.82	1880.6	38.4	1878.2	24.5	1875.5	29.5	1875.5	29.5	100.3	-0.3
LCC-09HA-89	143	42330	3.5	8.6955	0.7	5.3496	2.2	0.3374	2.0	0.95	1874.0	33.2	1876.8	18.4	1879.9	12.2	1879.9	12.2	99.7	0.3
LCC-09HA-84	90	26073	4.3	8.6701	0.9	5.3970	3.7	0.3394	3.6	0.97	1883.6	59.1	1884.4	32.0	1885.2	16.9	1885.2	16.9	99.9	0.1

U-Pb Geochronologic anlayses of selected Harmony Formation strata

				Isotope ratios									Apparent ages (Ma)							
	U	206Pb	U/Th	206Pb*	±	207Pb*	±	206Pb*	±	error	206Pb*	±	207Pb*	±	206Pb*	±	Best age	±	Conc.	Discor.
	(ppm)	204Pb		207Pb*	(%)	235U*	(%)	238U	(%)	corr.	238U*	(Ma)	235U	(Ma)	207Pb*	(Ma)	(Ma)	(Ma)	(%)	(%)
Sample: LCC #9. Location: Little Cottonwood Canyon, Galena Range; 0491232 4495602 (NAD 83 UTM 11T)																				
LCC-09HA-98	101	29345	1.1	8.6433	0.7	5.1826	4.0	0.3249	3.9	0.99	1813.5	61.8	1849.8	33.8	1890.7	11.8	1890.7	11.8	95.9	4.1
LCC-09HA-41	119	27555	2.5	8.5544	1.0	5.7972	4.1	0.3597	3.9	0.97	1980.6	67.1	1946.0	35.1	1909.3	17.5	1909.3	17.5	103.7	-3.7
LCC-09HA-40	90	10988	2.2	8.5298	1.2	4.9018	1.4	0.3032	0.8	0.56	1707.4	11.9	1802.6	11.8	1914.5	20.8	1914.5	20.8	89.2	10.8
LCC-09HA-15	257	52961	1.1	8.4791	0.4	5.6289	2.3	0.3462	2.3	0.98	1916.2	37.6	1920.5	19.9	1925.2	7.9	1925.2	7.9	99.5	0.5
LCC-09HA-80	148	44166	1.3	8.4776	0.9	5.9687	4.3	0.3670	4.2	0.98	2015.2	73.1	1971.3	37.5	1925.5	15.6	1925.5	15.6	104.7	-4.7
LCC-09HA-36	134	52604	2.1	7.0730	0.9	7.6484	2.4	0.3923	2.2	0.93	2133.7	39.9	2190.6	21.3	2244.2	15.4	2244.2	15.4	95.1	4.9
LCC-09HA-82	80	26866	1.2	6.1156	0.9	10.4224	2.4	0.4623	2.2	0.93	2449.6	44.4	2473.0	21.8	2492.3	14.9	2492.3	14.9	98.3	1.7
LCC-09HA-75	221	48289	2.3	5.9916	0.5	10.4072	6.1	0.4522	6.1	1.00	2405.2	122.0	2471.7	56.5	2526.8	8.1	2526.8	8.1	95.2	4.8
LCC-09HA-52	120	43744	3.2	5.7198	0.4	11.7241	3.2	0.4864	3.1	0.99	2554.9	66.0	2582.6	29.6	2604.4	7.3	2604.4	7.3	98.1	1.9
LCC-09HA-54	223	22607	1.4	5.7195	0.4	10.1058	1.4	0.4192	1.3	0.95	2256.9	24.5	2444.5	12.6	2604.5	7.3	2604.5	7.3	86.7	13.3
LCC-09HA-27	195	67476	2.0	5.7069	0.5	11.5631	0.9	0.4786	0.8	0.85	2521.2	16.6	2569.7	8.8	2608.2	8.2	2608.2	8.2	96.7	3.3
LCC-09HA-71	171	65244	3.6	5.6653	0.3	11.8508	3.8	0.4869	3.8	1.00	2557.4	80.0	2592.7	35.6	2620.4	5.1	2620.4	5.1	97.6	2.4
LCC-09HA-19	170	54182	1.3	5.6453	0.3	11.4288	1.9	0.4679	1.9	0.99	2474.5	39.2	2558.8	18.0	2626.2	5.2	2626.2	5.2	94.2	5.8
LCC-09HA-7	128	19736	1.1	5.4432	1.2	8.8708	4.3	0.3502	4.1	0.96	1935.6	69.2	2324.8	39.4	2686.7	20.3	2686.7	20.3	72.0	28.0
LCC-09HA-1	86	40571	1.4	5.3353	0.4	13.8045	1.2	0.5342	1.1	0.94	2759.0	24.4	2736.4	11.0	2719.7	6.8	2719.7	6.8	101.4	-1.4
LCC-09HA-29	105	42749	1.6	2.7331	0.2	34.2676	0.5	0.6793	0.4	0.88	3341.5	11.6	3617.8	5.0	3774.5	3.7	3774.5	3.7	88.5	11.5
Sample: LCC #10. Location: Little Cottonwood Canyon, Galena Range; 0490510 4495682 (NAD 83 UTM 11T)																				
LCC-10-HQ-86	533	33664	4.1	17.0454	1.9	0.7362	3.3	0.0910	2.7	0.82	561.5	14.7	560.2	14.3	554.8	40.9	561.5	14.7	101.2	-1.2 0.9,5.2
LCC-10-HQ-97	115	14748	2.4	14.2236	3.0	1.6021	4.3	0.1653	3.2	0.73	986.0	29.0	971.0	27.2	937.3	60.9	937.3	60.9	105.2	-5.2
LCC-10-HQ-50	103	11260	2.3	13.9139	3.1	1.6653	3.6	0.1681	1.8	0.49	1001.4	16.3	995.4	22.9	982.3	64.0	982.3	64.0	101.9	-1.9
LCC-10-HQ-16	71	6330	2.5	13.8173	4.0	1.6603	4.4	0.1664	1.9	0.43	992.1	17.6	993.5	27.8	996.5	80.3	996.5	80.3	99.6	0.4
LCC-10-HQ-18	98	11792	1.7	13.7737	3.4	1.6939	4.0	0.1692	2.0	0.51	1007.8	18.8	1006.2	25.4	1002.9	69.5	1002.9	69.5	100.5	-0.5
LCC-10-HQ-23	85	10008	2.3	13.6900	4.5	1.6518	4.7	0.1639	1.2	0.27	1088.0	12.5	1064.1	30.8	1015.2	91.1	1015.2	91.1	107.2	-7.2
LCC-10-HQ-89	229	27578	2.6	13.6207	1.0	1.7500	2.0	0.1729	1.7	0.86	1028.0	16.2	1027.2	12.8	1025.5	20.6	1025.5	20.6	100.2	-0.2
LCC-10-HQ-41	267	29787	2.5	13.6083	1.6	1.7548	2.4	0.1732	1.8	0.74	1029.7	16.8	1028.9	15.6	1027.3	33.0	1027.3	33.0	100.2	-0.2
LCC-10-HQ-03	266	35180	5.8	13.6082	1.0	1.7099	2.7	0.1688	2.5	0.92	1005.3	23.4	1012.2	17.4	1027.3	21.0	1027.3	21.0	97.9	2.1
LCC-10-HQ-91	213	24710	2.7	13.5556	1.3	1.7265	3.2	0.1697	2.9	0.91	1010.7	26.8	1018.4	20.3	1035.2	26.8	1035.2	26.8	97.6	2.4
LCC-10-HQ-78	142	17206	2.5	13.5256	1.5	1.9223	1.8	0.1886	0.9	0.52	1113.6	9.7	1088.9	12.1	1039.6	31.1	1039.6	31.1	107.1	-7.1
LCC-10-HQ-54	159	19089	2.2	13.5182	1.5	1.7352	3.2	0.1701	2.8	0.89	1012.8	26.6	1021.7	20.5	1040.8	29.3	1040.8	29.3	97.3	2.7
LCC-10-HQ-40	54	7937	2.1	13.4720	4.8	1.9284	5.3	0.1884	2.2	0.42	1112.8	22.6	1091.0	35.4	1047.7	97.1	1047.7	97.1	106.2	-6.2
LCC-10-HQ-70	268	32089	4.6	13.4414	1.2	1.8429	2.6	0.1797	2.3	0.88	1065.1	22.4	1060.9	17.1	1052.3	24.8	1052.3	24.8	101.2	-1.2
LCC-10-HQ-36	540	56405	5.8	13.4356	0.5	1.8504	1.9	0.1803	1.8	0.97	1068.7	17.8	1063.6	12.3	1053.1	9.4	1053.1	9.4	101.5	-1.5
LCC-10-HQ-22	136	17385	2.0	13.4188	2.1	1.8696	2.3	0.1820	1.0	0.42	1077.6	9.6	1070.4	15.2	1055.7	41.8	1055.7	41.8	102.1	-2.1
LCC-10-HQ-09	147	17896	1.0	13.4116	1.2	1.8614	2.5	0.1811	2.2	0.88	1072.8	21.5	1067.5	16.4	1056.8	23.9	1056.8	23.9	101.5	-1.5
LCC-10-HQ-07	112	11850	2.6	13.3655	2.3	1.8051	3.6	0.1750	2.7	0.76	1039.5	26.3	1047.3	23.5	1063.7	46.9	1063.7	46.9	97.7	2.3
LCC-10-HQ-17	142	8968	2.4	13.3099	2.2	1.8075	3.7	0.1745	2.9	0.79	1036.8	28.1	1048.2	24.2	1072.1	45.2	1072.1	45.2	96.7	3.3
LCC-10-HQ-59	238	28521	2.6	13.2508	1.2	1.8339	4.5	0.1762	4.4	0.97	1046.4	42.2	1057.7	29.8	1081.0	23.7	1081.0	23.7	96.8	3.2
LCC-10-HQ-62	737	33135	2.2	13.1787	0.6	1.9371	2.3	0.1851	2.2	0.97	1095.0	22.6	1094.0	15.5	1091.9	12.1	1091.9	12.1	100.3	-0.3
LCC-10-HQ-48	102	17271	3.8	13.1621	2.6	1.8960	4.7	0.1810	3.9	0.83	1072.4	38.2	1079.7	31.0	1094.5	52.1	1094.5	52.1	98.0	2.0
LCC-10-HQ-100	227	35625	2.6	13.1518	0.7	1.9323	3.6	0.1843	3.5	0.98	1090.5	35.5	1092.3	24.2	1096.0	14.2	1096.0	14.2	99.5	0.5
LCC-10-HQ-69	372	55727	3.1	13.1445	0.8	1.9592	1.9	0.1868	1.7	0.90	1103.9	17.6	1101.6	12.9	1097.1	16.3	1097.1	16.3	100.6	-0.6
LCC-10-HQ-72	57	6928	1.8	13.0709	3.3	1.9685	4.5	0.1866	3.1	0.68	1103.0	31.1	1104.8	30.5	1108.3	66.9	1108.3	66.9	99.5	0.5
LCC-10-HQ-85	53	7430	2.2	13.0444	3.1	1.9572	3.3	0.1852	1.1	0.33	1095.1	11.1	1100.9	22.4	1112.4	62.8	1112.4	62.8	98.4	1.6
LCC-10-HQ-92	152	17089	2.9	12.9702	2.0	1.9394	8.4	0.1824	8.2	0.97	1080.3	81.3	1094.8	56.5	1123.8	40.7	1123.8	40.7	96.1	3.9
LCC-10-HQ-01	502	63910	4.2	12.9025	0.5	2.0630	1.2	0.1930	1.1	0.91	1137.9	11.0	1136.6	7.9	1134.2	9.7	1134.2	9.7	100.3	-0.3
LCC-10-HQ-47	66	9281	1.7	12.9009	3.6	1.9402	4.7	0.1815	3.0	0.64	1075.4	29.6	1095.1	31.5	1134.4	72.2	1134.4	72.2	94.8	5.2
LCC-10-HQ-52	135	18179	2.0	12.8889	1.5	1.9663	3.2	0.1838	2.9	0.89	1087.8	28.5	1104.0	21.6	1136.3	29.2	1136.3	29.2	95.7	4.3
LCC-10-HQ-60	197	21019	2.1	12.8495	1.1	2.0409	5.0	0.1902	4.9	0.98	1122.5	50.5	1129.3	34.2	1142.4	21.9	1142.4	21.9	98.3	1.7
LCC-10-HQ-19	77	10624	2.3	12.8266	3.5	2.1548	3.9	0.2005	1.7	0.43	1177.8	18.3	1166.6	27.3	1145.9	70.4	1145.9	70.4	102.8	-2.8
LCC-10-HQ-27	408	52605	2.9	12.7986	1.0	2.0535	2.7	0.1906	2.5	0.93	1124.7	25.5	1133.5	18.2	1150.3	19.9	1150.3	19.9	97.8	2.2
LCC-10-HQ-95	202	19119	3.2	12.7513	1.4	2.1574	4.6	0.1995	4.4	0.95	1172.7	47.2	1167.4	32.1	1157.6	28.2	1157.6	28.2	101.3	-1.3
LCC-10-HQ-99	156	12799	2.4	12.7107	1.8	2.0534	2.5	0.1893	1.8	0.71	1117.6	18.2	1133.4	17.2	1163.9	35.3	1163.9	35.3	96.0	4.0
LCC-10-HQ-81	58	6789	2.0	12.5958	5.3	1.9239	5.8	0.1758	2.3	0.39	1043.8	21.9	1089.4	38.8	1181.9	105.7	1181.9	105.7	88.3	11.7
LCC-10-HQ-12	31	5853	1.3	12.5897	3.9	1.8793	4.1	0.1716	1.3	0.31	1020.9	12.0	1073.8	27.3	1182.9	77.6	1182.9	77.6	86.3	13.7
LCC-10-HQ-74	299	25331	4.5	12.5829	0.8	2.1592	2.0	0.1970	1.8	0.92	1159.5	19.5	1168.0	13.9	1184.0	15.6	1184.0	15.6	97.9	2.1
LCC-10-HQ-49	89	11192	1.7	12.5555	1.3	2.1926	2.7	0.1997	2.4	0.89	1173.5	25.9	1178.7	19.0	1188.3	24.9	1188.3	24.9	98.8	1.2
LCC-10-HQ-53	646	52673	7.2	12.5166	0.3	2.1934	2.3	0.1991	2.3	0.99	1170.6	24.9	1179.0	16.3	1194.4	5.5	1194.4	5.5	98.0	2.0
LCC-10-HQ-79	355	55885	4.7	12.4253	0.6	2.2987	2.0	0.2072	1.9	0.96	1213.6	21.1	1211.9	14.1	1208.8	11.2	1208.8	11.2	100.4	-0.4
LCC-10-HQ-45	256	8046	0.6	12.3490	1.7	2.1466	1.9	0.1923	0.9	0.47	1133.6	9.2	1164.0	13.1	1220.9	32.8	1220.9	32.8	92.8	7.2
LCC-10-HQ-25	122	19097	2.7	12.3285	1.5	2.3955	2.4	0.2142	1.9	0.79	1251.1	21.7	1241.3	17.3	1224.2	29.2	1224.2	29.2	102.2	-2.2
LCC-10-HQ-34	200	28451	0.7	12.2501	1.1	2.3761	3.0	0.2111	2.8	0.93	1234.7	31.2	1235.4	21.4	1236.7	21.8	1236.7	21.8	99.8	0.2
LCC-10-HQ-38	106	14945	4.0	12.1782	1.3	2.4226	2.6	0.2140	2.3	0.86	1250.0	25.9	1249.3	18.9	1248.2	26.0	1248.2	26.0	100.1	-0.1
LCC-10-HQ-63	141	23338	1.2	11.8766	1.2	2.6290	2.0	0.2265	1.6	0.80	1315.9	18.8	1308.8	14.6	1297.1	23.2	1297.1	23.2	101.4	-1.4
LCC-10-HQ-11	92	14550	1.5	11.7085	1.9	2.6058	3.0	0.2213	2.3	0.78	1288.6	27.3	1302.3	22.0	1324.8	36.5	1324.8	36.5	97.3	2.7
LCC-10-HQ-80	296	42195	2.7	11.6524	0.8	2.7021	1.2	0.2284	0.9	0.72	1325.9	10.3	1329.0	8.9	1334.1	16.3	1334.1	16.3	99.4	0.6
LCC-10-HQ-76	122	20093	2.7	11.4312	2.0	3.0125	4.8	0.2498	4.3	0.91	1437.2	56.0	1410.8	36.5	1371.1	38.8	1371.1	38.8	104.8	-4.8
LCC-10-HQ-35	265	38222	1.4	11.3923	0.5	2.8557	1.6	0.2359	1.6	0.95	1365.6	19.2	1370.3	12.4	1377.6	10.3	1377.6	10.3	99.1	0.9
LCC-10-HQ-94	147	22513	1.1	11.3606	0.9	2.8074	3.9	0.2313	3.8	0.97	1341.4	46.2	1357.5	29.4	1383.0	18.2	1383.0	18.2	97.0	3.0
LCC-10-HQ-30	39	4198	1.8	11.3213	4.5	3.1764	5.9	0.2608	3.8	0.65	1494.0	50.4	1451.4	45.3	1389.6	85.9	1389.6	85.9	107.5	-7.5
LCC-10-HQ-75	83	7400	2.0	11.3032	2.8	2.7597	3.4	0.2262	2.1	0.60	1314.8	24.4	1344.7	25.6	1392.7	52.9	1392.7	52.9	94.4	5.6
LCC-10-HQ-68	160	26048	2.5	11.2871	0.7	2.8020	3.0	0.2294	2.9	0.97	1331.2	34.9	1356.1	22.3	1395.4	13.1	1395.4	13.1	95.4	4.6
LCC-10-HQ-10	227	24851	1.9	11.2862	0.7	2.9022	3.0	0.2376	2.9	0.97	1374.0	35.7	1382.5	22.4	1395.6	13.2	1395.6	13.2	98.5	1.5
LCC-10-HQ-90	92	14614	11.2	11.2664	1.2	2.9494	2.0	0.2410	1.6	0.79	1391.9	19.8	1394.7	15.2	1399.0	23.4	1399.0	23.4	99.5	0.5
LCC-10-HQ-24	81	11028	2.1	11.2302	2.7	2.8661	4.1	0.2334	3.1	0.76	1352.5	38.1	1373.1	31.1	1405.1	51.8	1405.1	51.8	96.3	3.7
LCC-10-HQ-87	37	6211	2.4	11.1803	3.8	2.9936	5.4	0.2427	3.8	0.71	1401.0	48.4	1406.0	41.2	1413.6	72.7	1413.6	72.7	99.1	0.9
LCC-10-HQ-51	102	17734	2.6	10.9534	1.0	3.1876	2.2	0.2532	1.9	0.89	1455.1	25.4	1454.1	16.9	1452.8	19.0	1452.8	19.0	100.2	-0.2
LCC-10-HQ-08	188	23133	2.1	10.9101	0.7	2.9848	1.4	0.2362	1.2	0.87	1366.8	14.5	1403.7	10.3	1460.3	12.9	1460.3	12.9	93.6	6.4
LCC-10-HQ-04	70	10297	1.8	10.9093	2.9	3.2118	3.8	0.2541	2.5	0.66	1459.7	33.3	1460.0	29.7	1460.4	54.5	1460.4	54.5	99.9	0.1
LCC-10-HQ-58	81	14456	1.7	10.8674	2.3	3.0829	2.8	0.2430	1.6	0.57	1402.2	19.9	1428.5	21.3	1467.7	43.3	1467.7	43.3	95.5	4.5
LCC-10-HQ-65	93	13366	2.4	10.8592	2.2	3.2223	2.6	0.2538	1.4	0.53	1457.9	17.7	1462.5	19.9	1469.2	41.3	1469.2	41.3	99.2	0.8
LCC-10-HQ-14	227	20267	2.0	10.8533	0.9	3.1688	1.6	0.2494	1.3	0.84	1435.6	17.0	1449.6	12.2	1470.2	16.4	1470.2	16.4	97.6	2.4
LCC-10-HQ-43	65	10452	2.1	10.8264	1.9	3.2934	2.7	0.2586	2.0	0.71	1482.7	26.0	1479.5	21.4	1474.9	36.6	1474.9	36.6	100.5	-0.5
LCC-10-HQ-71	154	30022	3.1	10.8237	1.1	3.3134	2.0	0.2601	1.7	0.85	1490.4	23.1	1484.2	15.9	1475.4	20.2	1475.4	20.2	101.0	-1.0
LCC-10-HQ-46	217	31947	4.0	10.8196	0.7	2.9180	2.3	0.2290	2.2	0.95	1329.2	26.4	1386.6	17.5	1476.1	13.7	1476.1	13.7	90.0	10.0
LCC-10-HQ-56	138	22937	2.5	10.8175	1.1	3.2390	3.5	0.2541	3.3	0.95	1459.7	43.6	1466.5	27.2	1476.5	20.5	1476.5	20.5	98.9	1.1
LCC-10-HQ-84	138	24160	2.2	10.7987	0.9	3.1403	1.8	0.2459	1.5	0.86	1417.5	19.6	1442.6	13.8	1479.8	17.3	1479.8	17.3	95.8	4.2
LCC-10-HQ-15	96	21948	0.9	10.7939	1.4	3.4263	2.7	0.2682	2.2	0.84	1531.8	30.4	1510.4	20.9	1480.6	27.4	1480.6	27.4	103.5	-3.5
LCC-10-HQ-05	159	22686	1.9	10.7795	1.2	3.2252	2.2	0.2522	1.8	0.83	1449.6	23.6	1463.2	17.1	1483.1	23.6	1483.1	23.6	97.7	2.3
LCC-10-HQ-44	226	39482	2.4	10.7640	0.5	3.2350	2.3	0.2525	2.2	0.98	1451.6	28.7	1465.6	17.6	1485.9	9.3	1485.9	9.3	97.7	2.3
LCC-10-HQ-86	87	7332	2.4	10.7250	3.3	3.3322	3.7	0.2592	1.6	0.45	1485.7	21.8	1488.6	28.6	1492.8	61.8	1492.8	61.8	99.5	0.5
LCC-10-HQ-16	113	22875	1.2	9.8819	1.7	3.9953	2.0	0.2863	1.1	0.54	1623.2	15.3	1633.2	16.0	1646.1	30.8	1646.1	30.8	98.6	1.4
LCC-10-HQ-64	84	19026	2.3	9.8165	1.1	4.0465	1.4	0.2881	0.8	0.61	1632.0	12.0	1643.6	11.1	1658.4	20.0	1658.4	20.0	98.4	1.6
LCC-10-HQ-88	68	16377	1.5	9.8164	1.3	4.2220	1.4	0.3006	0.6	0.45	1694.2	9.5	1678.3	11.7	1658.5	23.7	1658.5	23.7	102.2	-2.2
LCC-10-HQ-42	96	21876	4.1	9.7883	0.8	4.0861	2.2	0.2901	2.0	0.93	1641.9	29.2	1651.5	17.7	1663.8	15.0	1663.8	15.0	98.7	1.3
LCC-10-HQ-21	112	24329	1.9	9.6203	1.2	4.2968	1.9	0.2998	1.4	0.77	1690.3	21.3	1692.7	15.3	1695.7	21.7	1695.7	21.7	99.7	0.3
LCC-10-HQ-26	304	5733	1.3	9.6020	1.0	3.2606	4.0	0.2271	3.9	0.97	1319.1	46.3	1471.7	31.2	1699.2	19.1	1699.2	19.1	77.6	22.4
LCC-10-HQ-77	369	11933	2.7	9.5981	0.5	4.1940	1.5	0.2920	1.4	0.93	1651.3	19.8	1672.9	12.0	1700.0	10.0	1700.0	10.0	97.1	2.9
LCC-10-HQ-37	226	17466	2.0	9.4345	0.7	3.8560	4.5	0.2638	4.4	0.99	1509.5	59.3	1604.5	36.0	1731.6	13.4	1731.6	13.4	87.2	12.8
LCC-10-HQ-96	158	36388	3.2	9.1743	0.9	4.8428	5.6	0.3222	5.5	0.99	1800.6	86.5	1792.4	46.9	1782.8	15.9	1782.8	15.9	101.0	-1.0
LCC-10-HQ-20	160	32186	1.2	9.1026	0.4	4.7609	2.1	0.3143	2.0	0.98	1761.9	31.5	1778.0	17.5	1797.0	7.9	1797.0	7.9	98.0	2.0

U-Pb Geochronologic anlayses of selected Harmony Formation strata

					Isotope ratios								Apparent ages (Ma)							
	U	206Pb	U/Th	206Pb*	±	207Pb*	±	206Pb*	±	error	206Pb*	±	207Pb*	±	206Pb*	±	Best age	±	Conc.	Discor.
	(ppm)	204Pb		207Pb*	(%)	235U*	(%)	238U	(%)	corr.	238U*	(Ma)	235U	(Ma)	207Pb*	(Ma)	(Ma)	(Ma)	(%)	(%)
Sample: LCC #10. Location: Little Cottonwood Canyon, Galena Range; 0490510 4495682 (NAD 83 UTM 11T)																				
LCC-10-HQ-39	462	104227	6.3	9.0721	0.2	4.8298	2.1	0.3178	2.1	0.99	1778.9	32.4	1790.1	17.7	1803.2	4.5	1803.2	4.5	98.7	1.3
LCC-10-HQ-31	201	41402	2.5	9.0634	0.5	4.8497	2.8	0.3188	2.7	0.98	1783.8	42.1	1793.6	23.2	1804.9	9.6	1804.9	9.6	98.8	1.2
LCC-10-HQ-33	463	70528	5.7	9.0388	0.4	4.9429	2.2	0.3240	2.1	0.99	1809.4	33.7	1809.6	18.3	1809.8	6.4	1809.8	6.4	100.0	0.0
LCC-10-HQ-73	246	41028	2.8	8.2894	0.4	5.7968	1.7	0.3485	1.6	0.97	1927.4	27.0	1945.9	14.4	1965.6	6.9	1965.6	6.9	98.1	1.9
LCC-10-HQ-06	82	16380	2.0	7.9671	1.3	6.2991	3.1	0.3640	2.9	0.92	2001.0	49.3	2018.3	27.4	2036.1	22.2	2036.1	22.2	98.3	1.7
LCC-10-HQ-29	72	12111	1.4	6.0141	1.0	10.9695	2.5	0.4785	2.3	0.92	2520.6	47.2	2520.5	23.0	2520.5	16.7	2520.5	16.7	100.0	0.0
LCC-10-HQ-28	82	21363	0.5	5.5824	0.7	11.0392	4.4	0.4470	4.3	0.99	2381.7	86.5	2526.4	41.0	2644.8	12.0	2644.8	12.0	90.1	9.9
LCC-10-HQ-02	29	10551	1.0	5.5316	1.0	12.8852	1.3	0.5169	0.8	0.65	2686.2	18.4	2671.3	12.2	2660.0	16.3	2660.0	16.3	101.0	-1.0
LCC-10-HQ-32	82	25072	2.0	5.4337	0.5	13.0495	7.1	0.5143	7.0	1.00	2674.8	154.4	2683.2	66.7	2689.6	7.9	2689.6	7.9	99.5	0.5
LCC-10-HQ-61	80	28074	2.2	5.4181	0.5	13.6582	1.5	0.5367	1.4	0.94	2769.7	30.9	2726.3	13.8	2694.3	8.2	2694.3	8.2	102.8	-2.8
LCC-10-HQ-93	274	52535	2.3	5.4003	0.2	12.5829	2.6	0.4928	2.6	1.00	2582.9	54.3	2648.9	24.1	2699.8	3.3	2699.8	3.3	95.7	4.3
LCC-10-HQ-82	56	21460	1.8	5.3148	0.5	13.1857	2.3	0.5083	2.2	0.97	2649.2	47.6	2693.0	21.3	2726.1	8.8	2726.1	8.8	97.2	2.8
LCC-10-HQ-83	53	30076	1.3	4.3131	0.6	18.0614	4.0	0.5650	3.9	0.99	2887.2	91.8	2993.0	38.4	3064.9	9.0	3064.9	9.0	94.2	5.8
LCC-10-HQ-67	178	56861	2.8	3.4889	0.6	27.4114	4.5	0.6936	4.4	0.99	3396.4	117.5	3398.3	44.0	3399.4	8.8	3399.4	8.8	99.9	0.1
Sample: Gough's Canyon. Location: Gough's Canyon, Osgood Mountains; 0471723 4556266 (NAD 83 UTM 11T)																				
GC02HA-42	180	22024	3.7	9.6916	1.0	4.2465	3.5	0.2985	3.3	0.96	1683.8	49.5	1683.1	28.6	1682.1	17.6	1682.1	17.6	100.1	-0.1 1.0,5.6
GC02HA-21	111	4729	1.9	9.3243	0.6	4.7832	2.0	0.3235	1.9	0.95	1806.6	30.5	1781.9	17.2	1753.1	11.9	1753.1	11.9	103.1	-3.1
GC02HA-22	191	5928	1.6	9.2697	0.5	4.6201	1.6	0.3106	1.5	0.96	1743.7	23.6	1752.9	13.5	1763.9	8.5	1763.9	8.5	98.9	1.1
GC02HA-83	149	9943	1.8	9.2339	0.8	4.9524	3.2	0.3317	3.1	0.97	1846.4	49.7	1811.2	27.1	1770.9	15.0	1770.9	15.0	104.3	-4.3
GC02HA-41	273	28599	3.1	9.2125	0.5	4.7496	1.9	0.3173	1.8	0.96	1776.7	28.6	1776.0	16.1	1775.2	9.8	1775.2	9.8	100.1	-0.1
GC02HA-04	186	6410	1.0	9.2104	1.3	4.7135	2.1	0.3149	1.7	0.79	1764.6	25.6	1769.6	17.5	1775.6	23.1	1775.6	23.1	99.4	0.6
GC02HA-50	280	11142	2.6	9.1971	1.0	4.6602	2.3	0.3109	2.0	0.89	1744.9	31.1	1760.1	19.0	1778.2	18.5	1778.2	18.5	98.1	1.9
GC02HA-59	222	25328	1.9	9.1962	0.8	4.5972	1.1	0.3066	0.8	0.70	1724.1	11.8	1748.8	9.4	1778.4	14.7	1778.4	14.7	96.9	3.1
GC02HA-38	380	14526	3.4	9.1924	0.5	4.8739	2.1	0.3249	2.0	0.97	1813.8	31.5	1797.7	17.3	1779.2	8.6	1779.2	8.6	101.9	-1.9
GC02HA-36	395	16307	1.8	9.1893	0.4	4.7370	1.5	0.3157	1.5	0.96	1768.7	22.8	1773.8	12.8	1779.8	7.4	1779.8	7.4	99.4	0.6
GC02HA-87	84	3563	1.3	9.1889	3.1	4.8530	3.3	0.3234	1.0	0.32	1806.4	16.2	1794.1	27.5	1779.8	56.4	1779.8	56.4	101.5	-1.5
GC02HA-03	215	8443	2.2	9.1868	0.6	4.6384	1.8	0.3091	1.7	0.94	1736.0	25.2	1756.2	14.7	1780.3	10.9	1780.3	10.9	97.5	2.5
GC02HA-40	209	9131	3.0	9.1682	0.6	4.6954	1.6	0.3122	1.5	0.92	1751.6	22.9	1766.4	13.6	1784.0	11.5	1784.0	11.5	98.2	1.8
GC02HA-74	110	7832	1.6	9.1620	1.2	5.0049	1.6	0.3326	0.9	0.59	1850.8	14.8	1820.1	13.1	1785.2	22.7	1785.2	22.7	103.7	-3.7
GC02HA-31	232	9141	3.6	9.1571	0.8	4.9557	1.8	0.3291	1.6	0.91	1834.1	25.8	1811.8	15.1	1786.2	13.8	1786.2	13.8	102.7	-2.7
GC02HA-86	116	2875	1.6	9.1444	2.8	4.7421	3.0	0.3145	1.1	0.36	1762.8	16.9	1774.7	25.4	1788.7	51.4	1788.7	51.4	98.6	1.4
GC02HA-80	214	9146	1.3	9.1423	1.1	4.9644	1.7	0.3292	1.3	0.75	1834.3	20.3	1813.3	14.3	1789.1	20.2	1789.1	20.2	102.5	-2.5
GC02HA-66	411	21883	7.5	9.1357	1.2	4.7592	1.7	0.3153	1.3	0.74	1766.9	20.0	1777.7	14.6	1790.4	21.3	1790.4	21.3	98.7	1.3
GC02HA-05	295	10089	4.3	9.0887	1.0	4.9368	2.9	0.3254	2.7	0.94	1816.2	43.3	1808.6	24.5	1799.8	17.4	1799.8	17.4	100.9	-0.9
GC02HA-78	126	9078	1.6	9.0579	1.9	5.0199	2.1	0.3298	0.8	0.39	1837.3	12.9	1822.7	17.5	1806.0	34.7	1806.0	34.7	101.7	-1.7
GC02HA-24	41	2700	0.6	9.0514	2.9	5.0190	3.8	0.3295	2.4	0.63	1835.9	38.3	1822.5	32.0	1807.3	53.1	1807.3	53.1	101.6	-1.6
GC02HA-29	207	9232	5.2	9.0227	0.9	4.4142	3.8	0.2889	3.7	0.97	1635.8	53.2	1715.0	31.5	1813.1	16.7	1813.1	16.7	90.2	9.8
GC02HA-49	127	2593	2.5	8.9259	2.0	5.1294	2.6	0.3321	1.6	0.62	1848.4	25.6	1841.0	21.7	1832.6	36.2	1832.6	36.2	100.9	-0.9
GC02HA-30	84	4090	1.3	8.8818	1.1	5.5139	1.7	0.3552	1.2	0.74	1959.3	20.9	1902.8	14.4	1841.6	20.6	1841.6	20.6	106.4	-6.4
GC02HA-34	67	3320	1.1	8.8714	4.0	5.2225	4.6	0.3360	2.3	0.49	1867.5	36.7	1856.3	39.2	1843.7	72.5	1843.7	72.5	101.3	-1.3
GC02HA-32	85	3424	4.0	8.8688	1.8	5.2005	2.0	0.3345	0.8	0.42	1860.2	13.2	1852.7	16.7	1844.3	32.2	1844.3	32.2	100.9	-0.9
GC02HA-25	252	17538	0.7	8.8677	0.4	5.2661	2.3	0.3387	2.3	0.99	1880.3	37.6	1863.4	19.9	1844.5	7.1	1844.5	7.1	101.9	-1.9
GC02HA-37	296	11658	2.2	8.7462	0.3	5.4612	1.1	0.3464	1.1	0.96	1917.5	18.1	1894.5	9.8	1869.4	5.8	1869.4	5.8	102.6	-2.6
GC02HA-54	50	2700	1.5	8.7433	3.9	5.5706	4.8	0.3532	2.8	0.58	1950.1	47.0	1911.6	41.7	1870.0	71.3	1870.0	71.3	104.3	-4.3
GC02HA-44	268	26706	1.0	8.4886	0.4	5.5009	2.7	0.3387	2.6	0.99	1880.2	43.1	1900.7	22.9	1923.2	6.5	1923.2	6.5	97.8	2.2
GC02HA-60	243	16182	2.5	8.4334	0.7	5.5138	1.9	0.3373	1.7	0.93	1873.4	28.0	1902.8	15.9	1934.9	12.2	1934.9	12.2	96.8	3.2
GC02HA-79	164	9446	1.1	8.4078	1.3	5.9164	1.8	0.3608	1.2	0.70	1985.9	21.4	1963.7	15.4	1940.3	22.6	1940.3	22.6	102.3	-2.3
GC02HA-96	66	3300	1.5	8.3992	2.7	5.6281	3.0	0.3428	1.3	0.43	1900.4	21.4	1920.4	26.1	1942.1	48.9	1942.1	48.9	97.8	2.2
GC02HA-93	309	8170	6.8	8.3227	0.6	5.9235	0.9	0.3576	0.7	0.72	1970.6	11.2	1964.7	8.0	1958.5	11.4	1958.5	11.4	100.6	-0.6
GC02HA-57	275	16916	2.0	8.1691	0.3	5.8976	1.8	0.3494	1.7	0.98	1931.8	29.1	1960.9	15.4	1991.7	6.1	1991.7	6.1	97.0	3.0
GC02HA-58	279	49585	3.4	7.9427	0.5	6.2291	2.3	0.3588	2.2	0.98	1976.6	37.8	2008.5	19.9	2041.5	8.4	2041.5	8.4	96.8	3.2
GC02HA-09	98	3933	2.5	7.8541	3.7	6.5310	3.8	0.3720	1.1	0.30	2038.9	19.9	2050.1	33.7	2061.3	64.5	2061.3	64.5	98.9	1.1
GC02HA-75	44	2756	1.2	7.7866	2.2	6.8430	2.4	0.3865	1.0	0.43	2106.3	18.5	2091.3	21.2	2076.5	38.1	2076.5	38.1	101.4	-1.4
GC02HA-56	166	20615	3.8	7.6487	0.5	6.9399	2.0	0.3850	1.9	0.97	2099.5	34.1	2103.8	17.4	2107.9	8.3	2107.9	8.3	99.6	0.4
GC02HA-71	234	11876	1.8	6.9047	0.6	7.9182	2.7	0.3965	2.6	0.97	2153.0	48.4	2221.8	24.6	2285.7	11.1	2285.7	11.1	94.2	5.8
GC02HA-23	77	3873	1.4	6.7989	0.8	8.8660	2.0	0.4372	1.8	0.91	2338.0	35.7	2324.3	18.3	2312.3	14.5	2312.3	14.5	101.1	-1.1
GC02HA-65	319	13747	1.9	6.7455	0.5	9.1299	2.1	0.4467	2.1	0.97	2380.4	41.0	2351.1	19.5	2325.8	9.3	2325.8	9.3	102.3	-2.3
GC02HA-10	83	11919	2.4	6.2438	0.7	10.3625	1.8	0.4693	1.7	0.93	2480.3	35.2	2467.7	17.1	2457.3	11.5	2457.3	11.5	100.9	-0.9
GC02HA-92	94	7299	2.2	6.0910	0.8	10.5739	2.8	0.4671	2.7	0.96	2470.9	54.4	2486.4	25.6	2499.1	12.6	2499.1	12.6	98.9	1.1
GC02HA-81	95	5402	2.6	6.0799	0.6	10.8187	2.3	0.4771	2.2	0.96	2514.4	45.0	2507.7	20.9	2502.2	10.6	2502.2	10.6	100.5	-0.5
GC02HA-99	206	23323	2.5	6.0795	0.5	10.0095	1.5	0.4413	1.4	0.94	2356.7	27.9	2435.7	13.9	2502.3	8.6	2502.3	8.6	94.2	5.8
GC02HA-73	226	22557	3.2	5.9513	0.2	11.3816	1.8	0.4913	1.8	0.99	2576.1	37.3	2554.9	16.5	2538.1	3.6	2538.1	3.6	101.5	-1.5
GC02HA-72	113	10163	2.1	5.8789	1.3	11.1846	2.1	0.4769	1.6	0.77	2513.7	32.8	2538.6	19.1	2558.6	22.0	2558.6	22.0	98.2	1.8
GC02HA-08	61	9325	2.2	5.8269	1.0	11.9896	2.2	0.5067	2.0	0.89	2642.5	42.5	2603.6	20.7	2573.5	16.8	2573.5	16.8	102.7	-2.7
GC02HA-33	106	9571	3.3	5.8026	0.7	11.7815	1.4	0.4958	1.2	0.85	2595.8	25.3	2587.2	13.1	2580.4	12.5	2580.4	12.5	100.6	-0.6
GC02HA-100	118	11436	2.7	5.7907	1.0	11.2824	1.9	0.4738	1.6	0.85	2500.4	32.8	2546.7	17.4	2583.9	16.6	2583.9	16.6	96.8	3.2
GC02HA-48	225	7293	1.5	5.7864	0.3	11.8415	1.9	0.4970	1.9	0.99	2600.7	40.6	2592.0	17.9	2585.1	4.6	2585.1	4.6	100.6	-0.6
GC02HA-43	197	36999	1.5	5.7790	0.3	11.6563	3.4	0.4886	3.4	1.00	2564.4	72.1	2577.2	32.0	2587.2	5.5	2587.2	5.5	99.1	0.9
GC02HA-46	224	11459	2.5	5.7562	0.2	11.7329	2.0	0.4898	2.0	0.99	2569.9	42.3	2583.3	18.8	2593.9	3.6	2593.9	3.6	99.1	0.9
GC02HA-82	235	16776	1.6	5.7435	0.3	11.4951	1.5	0.4788	1.5	0.98	2522.2	30.6	2564.2	13.9	2597.5	4.4	2597.5	4.4	97.1	2.9
GC02HA-97	81	8386	1.7	5.7327	0.7	11.7734	1.8	0.4895	1.7	0.93	2568.6	35.1	2586.5	16.7	2600.7	11.0	2600.7	11.0	98.8	1.2
GC02HA-95	158	23146	2.0	5.7327	0.4	11.7522	2.3	0.4886	2.2	0.98	2564.7	46.7	2584.9	21.1	2600.7	7.4	2600.7	7.4	98.6	1.4
GC02HA-55	222	12542	1.6	5.7104	0.8	11.8765	1.8	0.4919	1.6	0.90	2578.8	34.5	2594.7	16.8	2607.2	12.7	2607.2	12.7	98.9	1.1
GC02HA-02	171	12821	2.8	5.6924	0.4	11.9969	2.2	0.4953	2.2	0.98	2593.5	46.6	2604.2	20.8	2612.4	6.7	2612.4	6.7	99.3	0.7
GC02HA-94	437	57179	1.5	5.6172	0.1	12.7155	1.6	0.5180	1.6	1.00	2690.8	35.0	2658.8	15.0	2634.5	2.4	2634.5	2.4	102.1	-2.1
GC02HA-76	176	17880	2.5	5.5983	0.2	12.7961	2.0	0.5196	1.9	0.99	2697.3	42.8	2664.8	18.4	2640.1	4.1	2640.1	4.1	102.2	-2.2
GC02HA-91	100	11238	1.0	5.5834	0.9	12.8340	1.5	0.5197	1.2	0.79	2697.9	27.1	2667.5	14.6	2644.6	15.6	2644.6	15.6	102.0	-2.0
GC02HA-06	57	7930	1.5	5.5368	0.6	12.5019	1.8	0.5020	1.7	0.93	2622.5	36.4	2642.9	17.0	2658.5	10.7	2658.5	10.7	98.6	1.4
GC02HA-39	53	4564	1.4	5.4567	0.9	12.9699	1.8	0.5133	1.5	0.86	2670.7	33.7	2677.5	17.0	2682.6	15.4	2682.6	15.4	99.6	0.4
GC02HA-01	87	6227	0.7	5.4246	0.5	13.1736	1.7	0.5183	1.6	0.95	2691.9	35.4	2692.2	16.0	2692.3	8.5	2692.3	8.5	100.0	0.0
GC02HA-88	74	3371	1.7	5.2630	1.6	14.3843	2.5	0.5491	2.0	0.77	2821.3	44.7	2775.4	24.0	2742.2	26.3	2742.2	26.3	102.9	-2.9
GC02HA-70	48	12049	1.8	4.5658	0.3	17.7458	2.8	0.5876	2.7	0.99	2979.8	65.6	2976.1	26.6	2973.5	4.5	2973.5	4.5	100.2	-0.2
Sample: Kluncy Canyon. Location: Kluncy Canyon, Sonoma Range; 0447927 4531085 (NAD 83 UTM 11T)																				
KC-01HA-44	38	6703	1.7	9.4807	5.2	4.5278	5.8	0.3113	2.6	0.45	1747.3	40.2	1736.1	48.2	1722.6	94.9	1722.6	94.9	101.4	-1.4 1.1,5.1
KC-01HA-41	19	2836	1.1	9.4213	4.1	4.8016	4.4	0.3281	1.5	0.35	1829.1	24.3	1785.2	36.6	1734.2	74.8	1734.2	74.8	105.5	-5.5
KC-01HA-51	59	5203	1.7	9.2540	1.6	4.7318	3.9	0.3176	3.6	0.91	1777.9	55.8	1772.9	33.1	1767.0	30.0	1767.0	30.0	100.6	-0.6
KC-01HA-99	113	16778	2.6	9.2457	0.7	4.8488	1.7	0.3251	1.5	0.90	1814.8	24.2	1793.4	14.3	1768.6	13.4	1768.6	13.4	102.6	-2.6
KC-01HA-79	145	22777	2.3	9.2243	1.0	4.6224	6.7	0.3092	6.7	0.99	1737.0	101.3	1753.3	56.2	1772.9	18.1	1772.9	18.1	98.0	2.0
KC-01HA-72	72	7174	1.6	9.2090	2.7	4.6835	4.5	0.3128	3.6	0.80	1754.5	56.0	1764.3	38.0	1775.9	49.3	1775.9	49.3	98.8	1.2
KC-01HA-89	391	59645	2.6	9.2026	0.3	4.7930	1.5	0.3199	1.4	0.98	1789.2	22.5	1783.7	12.3	1777.1	5.2	1777.1	5.2	100.7	-0.7
KC-01HA-87	286	22220	3.2	9.1813	0.8	4.8793	2.2	0.3249	2.1	0.94	1813.7	33.0	1798.7	18.8	1781.4	14.3	1781.4	14.3	101.8	-1.8
KC-01HA-52	212	25188	1.5	9.1780	1.2	4.7813	8.4	0.3183	8.3	0.99	1781.3	129.8	1781.6	70.8	1782.0	21.6	1782.0	21.6	100.0	0.0
KC-01HA-11	192	23130	2.9	9.1716	0.6	4.8744	1.7	0.3242	1.6	0.94	1810.4	24.9	1797.8	14.2	1783.3	10.5	1783.3	10.5	101.5	-1.5
KC-01HA-36	44	3242	1.5	9.1716	2.0	4.8495	2.6	0.3226	1.6	0.61	1802.3	24.5	1793.5	21.6	1783.3	37.1	1783.3	37.1	101.1	-1.1
KC-01HA-10	203	21980	2.7	9.1591	0.5	4.6338	5.3	0.3078	5.3	1.00	1729.9	80.5	1755.4	44.5	1785.8	9.4	1785.8	9.4	96.9	3.1
KC-01HA-86	211	21423	2.6	9.1552	0.8	4.8668	2.8	0.3232	2.7	0.96	1805.1	42.3	1796.5	23.7	1786.5	14.7	1786.5	14.7	101.0	-1.0
KC-01HA-8	159	21935	4.6	9.1443	1.0	4.8464	2.1	0.3214	1.8	0.89	1796.6	28.6	1793.0	17.3	1788.7	17.3	1788.7	17.3	100.4	-0.4
KC-01HA-84	219	35192	3.2	9.1380	0.6	4.8374	1.2	0.3206	1.1	0.87	1792.7	16.4	1791.4	10.2	1790.0	10.9	1790.0	10.9	100.1	-0.1
KC-01HA-26	110	18902	2.7	9.1363	1.1	4.9486	2.4	0.3279	2.2	0.89	1828.2	34.5	1810.6	20.5	1790.3	19.8	1790.3	19.8	102.1	-2.1
KC-01HA-9	144	14782	2.8	9.1211	0.7	4.9670	2.3	0.3286	2.2	0.96	1831.5	35.0	1813.7	19.4	1793.4	12.3	1793.4	12.3	102.1	-2.1

U-Pb Geochronologic anlayses of selected Harmony Formation strata

					Isotope ratios							Apparent ages (Ma)								
	U	206Pb	U/Th	206Pb*	±	207Pb*	±	206Pb*	±	error	206Pb*	±	207Pb*	±	206Pb*	±	Best age	±	Conc.	Discor.
	(ppm)	204Pb		207Pb*	(%)	235U*	(%)	238U	(%)	corr.	238U*	(Ma)	235U	(Ma)	207Pb*	(Ma)	(Ma)	(Ma)	(%)	(%)
Sample: Kluncy Canyon. Location: Kluncy Canyon, Sonoma Range; 0447927 4531085 (NAD 83 UTM 11T)																				
KC-01HA-58	275	8605	3.6	9.1126	1.6	5.0105	2.0	0.3311	1.2	0.59	1843.9	19.2	1821.1	17.2	1795.0	29.9	1795.0	29.9	102.7	-2.7
KC-01HA-83	347	29008	4.8	9.1118	0.7	4.8388	2.7	0.3198	2.6	0.97	1788.6	40.3	1791.7	22.4	1795.2	12.3	1795.2	12.3	99.6	0.4
KC-01HA-75	216	18539	2.6	9.1071	0.5	4.6850	2.6	0.3094	2.6	0.98	1738.0	39.2	1764.6	22.0	1796.1	9.3	1796.1	9.3	96.8	3.2
KC-01HA-54	233	33650	3.4	9.1047	0.6	4.8875	3.2	0.3227	3.2	0.98	1803.1	49.7	1800.1	27.1	1796.6	10.9	1796.6	10.9	100.4	-0.4
KC-01HA-64	134	15909	2.1	9.0928	1.2	4.9653	2.8	0.3274	2.6	0.91	1826.0	41.3	1813.4	24.0	1799.0	20.9	1799.0	20.9	101.5	-1.5
KC-01HA-70	161	21867	2.6	9.0902	0.7	4.7747	3.6	0.3148	3.5	0.98	1764.2	54.5	1780.5	30.3	1799.5	13.3	1799.5	13.3	98.0	2.0
KC-01HA-65	230	30728	2.7	9.0895	0.5	4.8404	1.9	0.3191	1.8	0.96	1785.3	27.9	1791.9	15.6	1799.7	8.9	1799.7	8.9	99.2	0.8
KC-01HA-40	140	4153	3.0	9.0807	1.9	4.7520	3.0	0.3130	2.3	0.77	1755.3	35.6	1776.5	25.2	1801.4	34.8	1801.4	34.8	97.4	2.6
KC-01HA-14	93	14909	1.9	9.0442	1.4	4.8985	2.5	0.3213	2.1	0.83	1796.2	32.5	1802.0	21.0	1808.7	25.2	1808.7	25.2	99.3	0.7
KC-01HA-53	44	6338	2.0	9.0434	3.1	5.2445	5.2	0.3440	4.1	0.80	1905.8	68.2	1859.9	44.0	1808.9	56.1	1808.9	56.1	105.4	-5.4
KC-01HA-82	50	7804	1.5	9.0410	1.9	4.8329	2.8	0.3169	2.1	0.74	1774.6	31.8	1790.6	23.4	1809.4	34.1	1809.4	34.1	98.1	1.9
KC-01HA-25	182	30003	1.9	8.9891	0.6	5.0124	2.8	0.3268	2.7	0.97	1822.8	42.5	1821.4	23.3	1819.9	11.5	1819.9	11.5	100.2	-0.2
KC-01HA-21	68	9196	2.1	8.9386	2.3	5.1079	2.9	0.3311	1.8	0.63	1843.9	29.5	1837.4	25.0	1830.1	41.6	1830.1	41.6	100.8	-0.8
KC-01HA-22	125	16390	2.4	8.8965	0.7	5.1538	2.1	0.3325	2.0	0.95	1850.7	32.1	1845.0	17.9	1838.6	12.1	1838.6	12.1	100.7	-0.7
KC-01HA-98	77	7421	1.5	8.8688	1.5	5.3161	3.5	0.3419	3.2	0.90	1896.0	51.8	1871.5	29.9	1844.3	27.3	1844.3	27.3	102.8	-2.8
KC-01HA-2	93	16494	2.0	8.8464	1.0	5.2560	4.9	0.3372	4.8	0.98	1873.3	78.5	1861.7	42.1	1848.8	18.1	1848.8	18.1	101.3	-1.3
KC-01HA-81	176	24766	1.4	8.8407	0.5	5.1616	3.4	0.3310	3.4	0.99	1843.0	54.0	1846.3	29.0	1850.0	8.8	1850.0	8.8	99.6	0.4
KC-01HA-50	90	7938	1.4	8.8105	2.5	4.9939	3.8	0.3191	2.9	0.76	1785.4	45.3	1818.3	32.3	1856.2	44.6	1856.2	44.6	96.2	3.8
KC-01HA-13	85	11911	1.7	8.8012	0.7	5.0604	3.1	0.3230	3.0	0.97	1804.4	47.6	1829.5	26.3	1858.1	12.5	1858.1	12.5	97.1	2.9
KC-01HA-23	65	10563	1.5	8.8007	2.5	5.3122	3.0	0.3391	1.8	0.58	1882.2	28.8	1870.8	25.9	1858.2	44.5	1858.2	44.5	101.3	-1.3
KC-01HA-91	98	16689	2.4	8.7988	0.9	5.1603	2.7	0.3293	2.6	0.94	1835.0	41.3	1846.1	23.3	1858.6	16.4	1858.6	16.4	98.7	1.3
KC-01HA-100	129	21041	1.0	8.7813	0.6	5.3493	2.9	0.3407	2.9	0.98	1890.0	47.0	1876.8	25.1	1862.2	10.6	1862.2	10.6	101.5	-1.5
KC-01HA-59	83	6798	1.0	8.7586	1.9	5.2458	3.1	0.3332	2.5	0.80	1854.0	39.9	1860.1	26.5	1866.9	33.9	1866.9	33.9	99.3	0.7
KC-01HA-38	90	9832	1.7	8.7381	1.3	5.2754	2.0	0.3343	1.5	0.77	1859.3	24.4	1864.9	16.9	1871.1	22.9	1871.1	22.9	99.4	0.6
KC-01HA-12	119	15231	4.2	8.7319	0.5	5.3675	2.6	0.3399	2.6	0.98	1886.3	42.0	1879.7	22.5	1872.4	9.6	1872.4	9.6	100.7	-0.7
KC-01HA-31	46	3676	0.8	8.7268	3.7	4.8900	11.0	0.3095	10.4	0.94	1738.2	157.8	1800.5	93.0	1873.4	66.9	1873.4	66.9	92.8	7.2
KC-01HA-68	274	25158	1.3	8.7238	0.6	5.3636	2.3	0.3394	2.2	0.97	1883.6	36.4	1879.1	19.7	1874.0	10.2	1874.0	10.2	100.5	-0.5
KC-01HA-76	188	27897	3.9	8.6816	0.8	5.4105	3.1	0.3407	3.0	0.97	1889.9	49.7	1886.5	26.8	1882.8	13.5	1882.8	13.5	100.4	-0.4
KC-01HA-71	82	9928	8.3	8.5933	1.3	5.5685	3.2	0.3471	2.9	0.91	1920.5	49.0	1911.2	27.8	1901.2	23.9	1901.2	23.9	101.0	-1.0
KC-01HA-62	113	22320	2.2	8.0749	0.7	6.1937	2.0	0.3627	1.8	0.94	1995.1	31.5	2003.6	17.1	2012.3	11.9	2012.3	11.9	99.1	0.9
KC-01HA-73	68	10109	2.0	7.8293	1.2	6.9818	3.2	0.3965	2.9	0.93	2152.7	53.9	2109.1	28.2	2066.9	21.0	2066.9	21.0	104.2	-4.2
KC-01HA-24	26	5094	2.9	7.8149	1.7	6.6976	3.1	0.3796	2.6	0.84	2074.5	45.7	2072.3	27.2	2070.1	29.6	2070.1	29.6	100.2	-0.2
KC-01HA-17	83	12625	2.1	7.6938	1.4	6.8495	4.2	0.3822	3.9	0.94	2086.6	70.3	2092.2	37.2	2097.6	25.4	2097.6	25.4	99.5	0.5
KC-01HA-30	14	1312	1.3	7.0593	7.4	7.1884	19.1	0.3680	17.6	0.92	2020.2	306.2	2135.1	172.1	2247.6	127.8	2247.6	127.8	89.9	10.1
KC-01HA-3	123	7331	5.5	6.8780	2.0	8.0496	2.7	0.4015	1.8	0.66	2176.2	32.8	2236.6	24.2	2292.4	34.6	2292.4	34.6	94.9	5.1
KC-01HA-96	127	13618	2.0	6.7596	1.1	8.5435	2.5	0.4189	2.2	0.90	2255.3	41.8	2290.6	22.3	2322.2	18.7	2322.2	18.7	97.1	2.9
KC-01HA-78	267	51661	1.8	6.7326	0.2	8.9445	1.5	0.4368	1.5	0.99	2336.1	28.5	2332.4	13.4	2329.1	3.6	2329.1	3.6	100.3	-0.3
KC-01HA-45	251	60558	1.9	6.2858	0.4	10.1048	1.7	0.4607	1.6	0.97	2442.5	33.4	2444.4	15.6	2446.0	6.4	2446.0	6.4	99.9	0.1
KC-01HA-55	140	9484	1.7	6.0935	1.9	9.8619	1.9	0.4358	0.4	0.20	2332.0	7.7	2422.0	17.8	2498.4	31.8	2498.4	31.8	93.3	6.7
KC-01HA-74	60	9214	2.1	6.0751	2.6	9.5158	3.0	0.4193	1.4	0.48	2257.2	26.9	2389.1	27.2	2503.5	43.7	2503.5	43.7	90.2	9.8
KC-01HA-63	163	16817	1.0	6.0376	0.5	10.5597	0.8	0.4624	0.7	0.78	2450.1	13.6	2485.2	7.9	2513.9	8.9	2513.9	8.9	97.5	2.5
KC-01HA-85	121	25241	2.8	5.9454	0.8	11.0774	3.3	0.4777	3.2	0.97	2517.0	66.9	2529.7	30.9	2539.8	14.0	2539.8	14.0	99.1	0.9
KC-01HA-49	100	19971	2.5	5.9404	0.5	10.8804	3.3	0.4688	3.3	0.99	2478.2	67.3	2513.0	30.8	2541.2	9.1	2541.2	9.1	97.5	2.5
KC-01HA-32	334	30296	2.5	5.8880	0.6	10.2796	4.0	0.4390	4.0	0.99	2346.1	78.5	2460.3	37.3	2556.0	9.3	2556.0	9.3	91.8	8.2
KC-01HA-7	82	11402	1.5	5.8747	0.6	10.9716	1.6	0.4675	1.5	0.93	2472.4	30.5	2520.7	14.9	2559.8	9.9	2559.8	9.9	96.6	3.4
KC-01HA-29	64	12628	1.8	5.8439	0.7	11.2944	2.3	0.4787	2.2	0.95	2521.6	45.5	2547.7	21.4	2568.6	12.0	2568.6	12.0	98.2	1.8
KC-01HA-4	143	19840	2.1	5.8312	1.0	11.5201	1.9	0.4872	1.7	0.87	2558.6	35.6	2566.2	18.2	2572.2	16.3	2572.2	16.3	99.5	0.5
KC-01HA-34	109	14938	2.3	5.8018	0.5	11.5137	1.3	0.4845	1.1	0.91	2546.7	24.1	2565.7	11.7	2580.7	8.6	2580.7	8.6	98.7	1.3
KC-01HA-20	104	18504	2.1	5.7796	0.6	11.7755	2.6	0.4936	2.5	0.97	2586.2	52.7	2586.7	23.9	2587.1	10.4	2587.1	10.4	100.0	0.0
KC-01HA-5	54	4926	1.3	5.7611	1.1	11.9310	1.3	0.4985	0.6	0.48	2607.4	13.1	2599.0	11.9	2592.4	18.5	2592.4	18.5	100.6	-0.6
KC-01HA-80	136	32973	3.1	5.7527	0.3	11.8150	2.4	0.4930	2.4	0.99	2583.4	50.4	2589.9	22.3	2594.9	5.3	2594.9	5.3	99.6	0.4
KC-01HA-97	93	12259	2.3	5.7232	0.7	11.9707	1.8	0.4969	1.7	0.92	2600.4	36.5	2602.1	17.3	2603.4	11.8	2603.4	11.8	99.9	0.1
KC-01HA-39	182	36801	2.6	5.6866	0.4	11.9062	2.3	0.4911	2.2	0.99	2575.2	47.1	2597.1	21.1	2614.1	6.2	2614.1	6.2	98.5	1.5
KC-01HA-69	128	34506	1.8	5.6520	0.5	12.7188	1.6	0.5214	1.5	0.94	2705.0	32.9	2659.0	14.9	2624.3	8.9	2624.3	8.9	103.1	-3.1
KC-01HA-60	194	14063	2.4	5.6438	0.8	11.3049	2.2	0.4627	2.0	0.94	2451.6	41.0	2548.6	20.1	2626.7	12.6	2626.7	12.6	93.3	6.7
KC-01HA-92	34	7444	2.1	5.5870	1.4	12.2297	2.2	0.4956	1.6	0.76	2594.7	35.2	2622.2	20.3	2643.5	23.2	2643.5	23.2	98.2	1.8
KC-01HA-67	452	30818	13.3	5.5470	0.4	11.9660	1.3	0.4814	1.3	0.94	2533.4	26.4	2601.7	12.5	2655.4	7.4	2655.4	7.4	95.4	4.6
KC-01HA-35	206	12779	2.0	5.5372	1.0	11.6499	1.4	0.4679	1.0	0.69	2474.2	20.1	2576.7	13.2	2658.3	16.9	2658.3	16.9	93.1	6.9
KC-01HA-6	69	12234	1.5	5.4933	0.6	13.7187	2.4	0.5466	2.3	0.97	2810.9	52.5	2730.5	22.5	2671.5	9.5	2671.5	9.5	105.2	-5.2
KC-01HA-90	37	4929	1.0	5.4874	1.7	12.7009	2.3	0.5055	1.5	0.66	2637.3	33.4	2657.7	21.9	2673.3	28.8	2673.3	28.8	98.7	1.3
KC-01HA-57	220	14614	5.3	5.4816	1.6	12.6518	2.8	0.5030	2.2	0.82	2626.6	48.5	2654.1	25.9	2675.1	26.3	2675.1	26.3	98.2	1.8
KC-01HA-94	81	16825	1.4	5.4663	0.7	12.5159	1.4	0.4962	1.2	0.87	2597.4	25.4	2643.9	12.8	2679.7	11.0	2679.7	11.0	96.9	3.1
KC-01HA-56	251	16457	3.8	5.4663	0.5	12.8917	2.9	0.5111	2.9	0.98	2661.3	62.3	2671.8	27.4	2679.7	8.5	2679.7	8.5	99.3	0.7
KC-01HA-18	49	13287	1.8	5.4601	0.7	13.3320	1.8	0.5280	1.6	0.91	2732.8	36.4	2703.4	16.9	2681.5	12.1	2681.5	12.1	101.9	-1.9
KC-01HA-46	74	9854	2.3	5.4516	0.8	12.9301	3.5	0.5112	3.4	0.97	2661.9	74.6	2674.6	33.2	2684.1	13.7	2684.1	13.7	99.2	0.8
KC-01HA-93	51	13454	2.9	5.4315	1.1	13.0855	2.3	0.5155	2.0	0.87	2680.0	44.3	2685.8	21.9	2690.2	18.9	2690.2	18.9	99.6	0.4
KC-01HA-27	75	20690	1.3	5.4270	0.6	13.1469	1.9	0.5175	1.8	0.95	2688.4	38.8	2690.3	17.6	2691.6	10.0	2691.6	10.0	99.9	0.1
KC-01HA-88	13	3073	2.5	5.4238	2.3	13.5067	2.7	0.5313	1.6	0.57	2747.0	35.2	2715.8	26.0	2692.6	37.2	2692.6	37.2	102.0	-2.0
KC-01HA-42	114	25542	1.7	5.4168	0.2	13.2061	1.2	0.5188	1.2	0.98	2694.2	25.4	2694.5	11.1	2694.7	4.0	2694.7	4.0	100.0	0.0
KC-01HA-95	55	5897	1.4	5.3812	3.8	12.6595	4.6	0.4941	2.5	0.55	2588.3	53.2	2654.7	42.9	2705.6	62.8	2705.6	62.8	95.7	4.3
KC-01HA-61	114	14641	1.3	5.3732	0.3	12.8622	2.7	0.5012	2.7	0.99	2619.1	58.0	2669.6	25.6	2708.1	5.1	2708.1	5.1	96.7	3.3
KC-01HA-15	63	14184	1.9	5.3680	0.7	12.8292	3.4	0.4995	3.3	0.98	2611.5	70.6	2667.2	31.7	2709.7	11.8	2709.7	11.8	96.4	3.6
KC-01HA-47	53	5652	1.0	5.3609	2.3	13.1674	3.8	0.5120	3.0	0.79	2665.0	66.3	2691.7	36.1	2711.8	38.4	2711.8	38.4	98.3	1.7
KC-01HA-43	51	13677	2.6	5.2566	0.6	13.4089	2.2	0.5112	2.1	0.97	2661.8	45.6	2708.9	20.4	2744.2	9.2	2744.2	9.2	97.0	3.0
KC-01HA-1	92	31677	2.6	3.8433	1.5	23.8622	2.9	0.6651	2.5	0.86	3287.1	63.2	3262.8	27.8	3247.9	23.0	3247.9	23.0	101.2	-1.2
Sample: Harmony Canyon. Location: Harmony Canyon, Sonoma Range; 0446225 4533064 (NAD 83 UTM 11T)																				
HARMCYN-172	126	96945	0.8	11.1506	0.7	2.7255	2.3	0.2204	2.2	0.95	1284.1	25.8	1335.4	17.2	1418.7	13.4	1418.7	13.4	90.5	9.5 1.1,0.8
HARMCYN-132	349	38525	1.0	9.4036	0.3	3.6524	4.7	0.2491	4.6	1.00	1433.8	59.6	1561.0	37.1	1737.6	6.1	1737.6	6.1	82.5	17.5
HARMCYN-142	253	30062	1.2	9.3413	0.4	3.8821	8.1	0.2630	8.1	1.00	1505.2	108.9	1610.0	65.7	1749.8	7.6	1749.8	7.6	86.0	14.0
HARMCYN-141	257	65390	1.4	9.3321	0.3	3.9937	1.9	0.2703	1.9	0.99	1542.3	26.4	1632.9	15.8	1751.6	5.0	1751.6	5.0	88.1	11.9
HARMCYN-126	243	316519	1.4	9.2770	0.7	4.0674	3.7	0.2737	3.6	0.98	1559.4	49.5	1647.8	29.8	1762.4	13.6	1762.4	13.6	88.5	11.5
HARMCYN-154	151	21743	0.8	9.2564	0.8	4.3429	2.7	0.2916	2.6	0.95	1649.3	37.7	1701.5	22.4	1766.5	15.1	1766.5	15.1	93.4	6.6
HARMCYN-143	191	21049	0.8	9.2223	0.5	4.1895	1.8	0.2802	1.7	0.96	1592.5	24.3	1672.0	14.7	1773.2	8.7	1773.2	8.7	89.8	10.2
HARMCYN-188	83	55811	1.5	9.2162	0.6	4.7708	1.8	0.3189	1.7	0.94	1784.3	25.7	1779.8	14.7	1774.5	10.8	1774.5	10.8	100.6	-0.6
HARMCYN-191	366	99962	2.0	9.2102	0.4	4.6848	1.0	0.3129	1.0	0.93	1755.2	14.8	1764.5	8.7	1775.6	7.2	1775.6	7.2	98.8	1.2
HARMCYN-189	234	251686	1.3	9.2088	0.4	4.5858	1.0	0.3063	1.0	0.92	1722.4	14.5	1746.7	8.7	1775.9	7.3	1775.9	7.3	97.0	3.0
HARMCYN-146	127	184644	1.6	9.2081	0.6	4.8169	0.9	0.3217	0.7	0.77	1798.0	11.3	1787.8	7.8	1776.0	10.7	1776.0	10.7	101.2	-1.2
HARMCYN-134	49	61076	1.8	9.2055	1.2	4.9236	1.8	0.3287	1.4	0.76	1832.2	22.1	1806.3	15.3	1776.6	21.4	1776.6	21.4	103.1	-3.1
HARMCYN-133	34	35931	0.6	9.2004	2.0	4.8150	2.5	0.3213	1.4	0.58	1796.0	22.4	1787.5	20.8	1777.6	36.8	1777.6	36.8	101.0	-1.0
HARMCYN-185	198	363348	1.8	9.1870	0.3	4.8128	0.6	0.3207	0.5	0.87	1793.1	8.6	1787.1	5.3	1780.2	5.6	1780.2	5.6	100.7	-0.7
HARMCYN-180	176	284453	2.0	9.1849	0.2	4.7531	1.0	0.3166	1.0	0.97	1773.3	14.7	1776.7	8.2	1780.6	4.4	1780.6	4.4	99.6	0.4
HARMCYN-108	53	44351	1.6	9.1816	1.0	4.7623	1.5	0.3171	1.2	0.76	1775.7	18.2	1778.3	12.9	1781.3	18.2	1781.3	18.2	99.7	0.3
HARMCYN-156	103	100321	2.6	9.1795	0.6	4.8513	1.2	0.3230	1.1	0.86	1804.3	16.5	1793.8	10.3	1781.7	11.5	1781.7	11.5	101.3	-1.3
HARMCYN-129	136	84192	2.1	9.1705	0.5	4.8427	0.9	0.3221	0.7	0.83	1799.9	11.5	1792.3	7.4	1783.5	8.9	1783.5	8.9	100.9	-0.9
HARMCYN-175	164	202544	1.8	9.1560	0.5	4.9024	5.6	0.3255	5.6	1.00	1816.7	88.8	1802.7	47.5	1786.4	9.0	1786.4	9.0	101.7	-1.7
HARMCYN-184	175	107693	2.8	9.1533	0.5	4.8448	0.9	0.3216	0.8	0.82	1797.7	12.1	1792.7	7.9	1786.9	9.9	1786.9	9.9	100.6	-0.6
HARMCYN-178	123	91161	1.7	9.1531	0.8	4.8117	1.3	0.3194	1.0	0.78	1786.9	16.3	1786.9	11.2	1787.0	15.0	1787.0	15.0	100.0	0.0
HARMCYN-179	83	50131	1.1	9.1462	0.5	4.9342	2.0	0.3273	1.9	0.96	1825.3	30.6	1808.1	16.9	1788.3	9.8	1788.3	9.8	102.1	-2.1
HARMCYN-169	122	84853	1.4	9.1455	0.7	4.7787	2.0	0.3170	1.9	0.94	1774.9	29.3	1781.2	16.9	1788.5	12.8	1788.5	12.8	99.2	0.8
HARMCYN-151	153	65270	1.7	9.1443	0.6	4.8410	1.0	0.3211	0.8	0.77	1794.9	12.0	1792.1	8.4	1788.7	11.7	1788.7	11.7	100.3	-0.3
HARMCYN-192	90	72514	1.7	9.1424	0.9	4.8171	1.7	0.3194	1.5	0.86	1786.8	23.1	1787.9	14.5	1789.1	16.2	1789.1	16.2	99.9	0.1
HARMCYN-147	66	62285	1.8	9.1402	1.3	4.8055	1.6	0.3186	0.9	0.58	1782.7	14.6	1785.9	13.5	1789.5	23.9	1789.5	23.9	99.6	0.4
HARMCYN-190	112	217491	1.9	9.1297	0.9	4.8737	1.2	0.3227	0.8	0.67	1803.0	12.6	1797.7	10.0	1791.6	16.0	1791.6	16.0	100.6	-0.6

U-Pb Geochronologic anlayses of selected Harmony Formation strata

					Isotope ratios							Apparent ages (Ma)							
	U	206Pb	U/Th	206Pb*	±	207Pb*	±	206Pb*	±	error	206Pb*	±	207Pb*	±	206Pb*	±	Best age	±	Conc.	Discor.
	(ppm)	204Pb		207Pb*	(%)	235U*	(%)	238U	(%)	corr.	238U*	(Ma)	235U	(Ma)	207Pb*	(Ma)	(Ma)	(Ma)	(%)	(%)
Sample: Harmony Canyon. Location: Harmony Canyon, Sonoma Range; 0446225 4533064 (NAD 83 UTM 11T)																				
HARMCYN-173	81	64547	1.4	9.0451	1.0	4.9068	2.0	0.3219	1.7	0.85	1799.0	26.5	1803.4	16.7	1808.6	18.7	1808.6	18.7	99.5	0.5
HARMCYN-118	72	59144	0.6	8.9847	1.3	4.4771	1.6	0.2917	0.9	0.56	1650.2	12.9	1726.7	13.2	1820.7	23.9	1820.7	23.9	90.6	9.4
HARMCYN-187	493	23339	1.1	8.9561	1.6	4.6868	10.1	0.3044	10.0	0.99	1713.3	150.2	1764.9	84.9	1826.5	29.5	1826.5	29.5	93.8	6.2
HARMCYN-176	82	133891	2.3	8.9548	0.9	5.1573	1.5	0.3349	1.3	0.83	1862.3	20.9	1845.6	13.2	1826.8	15.5	1826.8	15.5	101.9	-1.9
HARMCYN-182	47	45093	1.6	8.9446	1.5	5.1745	1.7	0.3357	0.7	0.45	1865.9	12.0	1848.4	14.1	1828.9	26.8	1828.9	26.8	102.0	-2.0
HARMCYN-117	287	20420	1.0	8.9305	0.5	4.5776	2.5	0.2965	2.5	0.98	1673.9	36.1	1745.2	20.8	1831.7	8.2	1831.7	8.2	91.4	8.6
HARMCYN-115	14	13377	7.5	8.9232	6.3	5.2074	6.7	0.3370	2.3	0.35	1872.3	38.1	1853.8	57.3	1833.2	114.3	1833.2	114.3	102.1	-2.1
HARMCYN-158	90	60528	0.7	8.8897	0.8	5.0439	1.3	0.3252	1.0	0.78	1815.1	15.6	1826.7	10.7	1840.0	14.4	1840.0	14.4	98.6	1.4
HARMCYN-121	203	211768	1.0	8.8792	0.4	5.1684	1.0	0.3328	0.9	0.91	1852.1	14.7	1847.4	8.6	1842.1	7.7	1842.1	7.7	100.5	-0.5
HARMCYN-130	37	27557	1.0	8.8550	2.0	5.1723	2.6	0.3322	1.6	0.62	1848.9	26.2	1848.1	22.2	1847.1	37.0	1847.1	37.0	100.1	-0.1
HARMCYN-137	51	31839	0.7	8.8464	1.9	5.1543	2.4	0.3307	1.6	0.64	1841.8	25.0	1845.1	20.8	1848.8	34.0	1848.8	34.0	99.6	0.4
HARMCYN-111	86	56745	1.7	8.8402	0.6	4.9564	1.2	0.3178	1.0	0.86	1778.9	15.8	1811.9	10.0	1850.1	11.0	1850.1	11.0	96.1	3.9
HARMCYN-164	52	58492	0.8	8.8219	0.7	5.2391	1.5	0.3352	1.3	0.88	1863.6	21.1	1859.0	12.6	1853.9	12.5	1853.9	12.5	100.5	-0.5
HARMCYN-112	78	98840	1.2	8.7919	0.7	5.3315	1.2	0.3400	1.0	0.82	1886.5	16.5	1873.9	10.6	1860.0	12.9	1860.0	12.9	101.4	-1.4
HARMCYN-193	43	41359	2.9	8.7909	2.2	5.3392	2.4	0.3404	1.1	0.44	1888.7	17.7	1875.2	20.9	1860.2	39.6	1860.2	39.6	101.5	-1.5
HARMCYN-120	41	51447	4.8	8.7878	1.0	5.2794	1.3	0.3365	0.9	0.69	1869.7	15.2	1865.5	11.5	1860.8	17.5	1860.8	17.5	100.5	-0.5
HARMCYN-128	87	115310	2.3	8.7655	0.8	5.3966	1.5	0.3431	1.3	0.85	1901.5	21.4	1884.3	13.2	1865.4	14.8	1865.4	14.8	101.9	-1.9
HARMCYN-195	33	26072	0.6	8.7549	1.6	5.2798	2.0	0.3353	1.2	0.60	1863.8	19.3	1865.6	17.1	1867.6	29.0	1867.6	29.0	99.8	0.2
HARMCYN-107	82	6663	0.7	8.7279	1.0	5.3070	1.9	0.3359	1.6	0.85	1867.1	25.5	1870.0	15.9	1873.2	17.9	1873.2	17.9	99.7	0.3
HARMCYN-105	60	49141	3.0	8.7169	1.1	5.2934	1.4	0.3347	0.9	0.66	1860.9	15.2	1867.8	12.2	1875.5	19.3	1875.5	19.3	99.2	0.8
HARMCYN-196	100	69057	2.3	8.7002	0.8	5.4696	3.3	0.3451	3.2	0.97	1911.3	52.5	1895.8	28.0	1878.9	13.6	1878.9	13.6	101.7	-1.7
HARMCYN-167	297	33372	1.0	8.6609	0.2	4.8954	4.9	0.3075	4.9	1.00	1728.4	74.7	1801.5	41.6	1887.1	4.2	1887.1	4.2	91.6	8.4
HARMCYN-136	75	95166	1.5	8.6508	0.7	5.3715	1.1	0.3370	0.9	0.77	1872.3	14.2	1880.3	9.7	1889.2	12.9	1889.2	12.9	99.1	0.9
HARMCYN-181	180	115527	1.4	8.6480	0.7	5.5423	1.9	0.3476	1.7	0.92	1923.2	28.6	1907.2	16.1	1889.8	13.0	1889.8	13.0	101.8	-1.8
HARMCYN-139	99	147553	1.4	8.3920	0.9	5.8193	1.3	0.3542	0.9	0.68	1954.6	14.6	1949.3	11.0	1943.7	16.8	1943.7	16.8	100.6	-0.6
HARMCYN-198	85	76588	0.5	8.0926	0.6	5.1398	1.8	0.3017	1.8	0.95	1699.6	26.2	1842.7	15.6	2008.4	9.9	2008.4	9.9	84.6	15.4
HARMCYN-165	46	49055	0.5	7.9194	1.3	6.2079	3.6	0.3566	3.3	0.94	1965.8	56.6	2005.6	31.2	2046.7	22.2	2046.7	22.2	96.0	4.0
HARMCYN-150	201	81591	1.4	7.8572	0.4	6.5688	2.8	0.3743	2.8	0.99	2049.7	49.4	2055.2	25.1	2060.6	7.5	2060.6	7.5	99.5	0.5
HARMCYN-186	318	36857	1.4	6.7597	2.1	8.5031	6.8	0.4169	6.4	0.95	2246.3	122.0	2286.3	61.7	2322.2	36.8	2322.2	36.8	96.7	3.3
HARMCYN-135	113	120030	4.4	6.2586	0.4	10.0896	1.2	0.4580	1.1	0.93	2430.6	22.9	2443.0	11.2	2453.3	7.3	2453.3	7.3	99.1	0.9
HARMCYN-140	209	125235	1.2	5.9303	0.6	10.8912	1.7	0.4684	1.6	0.92	2476.7	32.0	2513.9	15.7	2544.0	10.9	2544.0	10.9	97.4	2.6
HARMCYN-116	228	167271	5.4	5.9151	0.2	10.3768	1.7	0.4452	1.7	0.99	2373.7	34.2	2469.0	16.1	2548.3	4.0	2548.3	4.0	93.1	6.9
HARMCYN-170	177	239606	1.4	5.9088	0.7	11.7548	6.9	0.5037	6.8	0.99	2629.9	147.9	2585.1	64.5	2550.1	12.0	2550.1	12.0	103.1	-3.1
HARMCYN-123	173	220842	1.2	5.8039	0.4	11.4463	1.0	0.4818	1.0	0.93	2535.2	20.3	2560.2	9.7	2580.1	6.3	2580.1	6.3	98.3	1.7
HARMCYN-174	158	35611	1.2	5.7229	0.3	11.1290	1.5	0.4619	1.5	0.98	2448.0	29.9	2534.0	13.9	2603.5	4.8	2603.5	4.8	94.0	6.0
HARMCYN-171	39	76755	2.4	5.7197	0.7	12.1651	1.4	0.5046	1.2	0.87	2633.7	26.9	2617.2	13.5	2604.5	11.9	2604.5	11.9	101.1	-1.1
HARMCYN-162	142	117727	1.2	5.6944	0.6	12.1023	3.1	0.4998	3.0	0.98	2613.0	64.5	2612.4	28.6	2611.8	9.2	2611.8	9.2	100.0	0.0
HARMCYN-157	129	50997	1.2	5.5851	0.3	11.5307	1.3	0.4671	1.2	0.97	2470.7	25.2	2567.1	11.8	2644.0	4.7	2644.0	4.7	93.4	6.6
HARMCYN-152	136	167553	1.1	5.5473	0.3	12.3552	2.2	0.4971	2.2	0.99	2601.2	47.6	2631.8	21.1	2655.3	5.6	2655.3	5.6	98.0	2.0
HARMCYN-119	157	17539	0.7	5.5072	0.2	9.8822	3.3	0.3947	3.3	1.00	2144.7	60.9	2423.8	30.9	2667.3	4.0	2667.3	4.0	80.4	19.6
HARMCYN-145	91	149908	1.1	5.5068	0.4	12.6627	1.0	0.5057	0.9	0.93	2638.4	19.8	2654.9	9.3	2667.5	6.0	2667.5	6.0	98.9	1.1
HARMCYN-101	130	110380	0.9	5.4106	0.6	12.8200	4.4	0.5031	4.4	0.99	2627.0	95.3	2666.5	41.9	2696.6	9.2	2696.6	9.2	97.4	2.6
HARMCYN-120	91	116123	1.6	5.4033	0.6	13.2790	1.1	0.5204	0.9	0.86	2700.8	20.9	2699.7	10.4	2698.9	9.2	2698.9	9.2	100.1	-0.1
HARMCYN-104	146	186503	1.7	5.3696	0.2	13.6173	1.5	0.5303	1.5	0.99	2742.8	32.9	2723.5	14.1	2709.2	3.4	2709.2	3.4	101.2	-1.2
HARMCYN-124	115	227017	2.2	5.2858	0.3	14.1244	1.9	0.5415	1.9	0.99	2789.6	42.7	2758.1	18.1	2735.1	4.5	2735.1	4.5	102.0	-2.0
Sample: Elbow Canyon. Location: Elbow Canyon, Sonoma Range; 0441026 4514450 (NAD 83 UTM 11T)																				
ELBOW CYN-148	89	22814	1.2	14.3469	2.6	1.3210	2.8	0.1375	1.1	0.41	830.2	8.9	854.9	16.3	919.6	53.1	830.2	8.9	90.3	9.7
ELBOW CYN-69	157	208587	2.6	9.5321	0.3	4.4292	0.8	0.3062	0.8	0.92	1722.0	11.7	1717.8	7.0	1712.7	6.1	1712.7	6.1	100.5	-0.5
ELBOW CYN-119	43	23669	3.1	9.4623	1.8	4.6104	2.0	0.3164	0.9	0.46	1772.1	14.3	1751.2	16.9	1726.2	33.0	1726.2	33.0	102.7	-2.7
ELBOW CYN-139	20	16811	1.0	9.3961	2.9	4.7135	3.2	0.3212	1.2	0.39	1795.6	19.5	1769.6	26.7	1739.1	53.8	1739.1	53.8	103.3	-3.3
ELBOW CYN-174	27	9333	1.1	9.3256	2.3	4.6852	2.4	0.3169	0.7	0.29	1774.5	10.8	1764.6	20.4	1752.9	42.8	1752.9	42.8	101.2	-1.2
ELBOW CYN-196	30	12192	1.1	9.2960	1.7	4.7607	2.3	0.3210	1.5	0.66	1794.5	23.8	1778.0	19.4	1758.7	31.9	1758.7	31.9	102.0	-2.0
ELBOW CYN-178	181	120477	0.8	9.2607	0.3	4.7015	0.9	0.3158	0.9	0.95	1769.1	13.2	1767.5	7.5	1765.6	5.1	1765.6	5.1	100.2	-0.2
ELBOW CYN-12	43	31712	1.2	9.2590	1.0	4.7849	1.4	0.3213	1.0	0.72	1796.2	15.4	1782.3	11.5	1766.0	17.5	1766.0	17.5	101.7	-1.7
ELBOW CYN-188	39	17222	1.2	9.2390	1.1	4.7613	1.5	0.3190	0.9	0.63	1785.1	14.6	1778.1	12.4	1769.9	20.9	1769.9	20.9	100.9	-0.9
ELBOW CYN-175	22	11965	1.1	9.2332	3.4	4.7465	3.6	0.3179	1.3	0.37	1779.2	21.0	1775.5	30.4	1771.1	61.5	1771.1	61.5	100.5	-0.5
ELBOW CYN-102	57	19865	1.2	9.2213	0.7	4.7645	1.1	0.3186	0.9	0.79	1783.1	13.6	1778.7	9.2	1773.4	12.1	1773.4	12.1	100.5	-0.5
ELBOW CYN-137	79	35461	1.1	9.2186	0.5	4.8185	0.7	0.3222	0.5	0.72	1800.3	7.9	1788.1	5.9	1774.0	8.8	1774.0	8.8	101.5	-1.5
ELBOW CYN-105	58	39254	1.2	9.2139	1.1	4.8865	1.4	0.3265	1.0	0.67	1821.6	15.2	1799.9	12.0	1774.9	19.3	1774.9	19.3	102.6	-2.6
ELBOW CYN-106	89	123777	1.5	9.2106	0.8	4.8319	1.2	0.3228	0.9	0.76	1803.3	14.9	1790.5	10.5	1775.5	14.9	1775.5	14.9	101.6	-1.6
ELBOW CYN-88	37	25863	1.0	9.2094	0.8	4.9700	5.0	0.3320	5.0	0.99	1847.9	79.7	1814.2	42.5	1775.8	14.3	1775.8	14.3	104.1	-4.1
ELBOW CYN-109	94	71561	1.5	9.2089	0.5	4.8216	0.8	0.3220	0.6	0.80	1799.6	9.9	1788.7	6.6	1775.9	8.7	1775.9	8.7	101.3	-1.3
ELBOW CYN-94	92	77797	1.4	9.2080	0.5	4.8241	1.3	0.3222	1.2	0.92	1800.3	19.4	1789.1	11.3	1776.1	9.6	1776.1	9.6	101.4	-1.4
ELBOW CYN-74	260	188765	2.5	9.2070	0.3	4.8189	0.7	0.3218	0.6	0.90	1798.4	9.6	1788.2	5.7	1776.3	5.4	1776.3	5.4	101.2	-1.2
ELBOW CYN-135	74	63063	1.5	9.2064	0.6	4.8037	1.2	0.3208	1.1	0.87	1793.4	16.7	1785.6	10.3	1776.4	10.9	1776.4	10.9	101.0	-1.0
ELBOW CYN-66	133	113283	1.4	9.2038	0.3	4.8555	0.9	0.3241	0.8	0.92	1809.8	12.6	1794.6	7.3	1776.9	6.1	1776.9	6.1	101.9	-1.9
ELBOW CYN-10	42	49636	1.5	9.2020	1.6	4.7753	1.8	0.3187	0.9	0.50	1783.4	13.9	1780.6	15.1	1777.3	28.4	1777.3	28.4	100.3	-0.3
ELBOW CYN-42	120	52394	2.2	9.2015	0.3	4.7452	0.9	0.3167	0.8	0.94	1773.5	13.0	1775.3	7.5	1777.4	5.5	1777.4	5.5	99.8	0.2
ELBOW CYN-195	86	109784	0.5	9.1995	0.7	4.8679	1.1	0.3248	0.9	0.78	1813.1	13.5	1796.7	9.2	1777.8	12.5	1777.8	12.5	102.0	-2.0
ELBOW CYN-108	52	42056	1.4	9.1943	1.1	4.8480	1.4	0.3233	0.9	0.64	1805.7	14.6	1793.3	12.1	1778.8	20.2	1778.8	20.2	101.5	-1.5
ELBOW CYN-186	81	64388	1.6	9.1940	0.6	4.7758	1.2	0.3185	1.0	0.87	1782.2	15.6	1780.7	9.7	1778.8	10.4	1778.8	10.4	100.2	-0.2
ELBOW CYN-169	27	15552	0.5	9.1920	1.0	4.8401	1.3	0.3227	0.8	0.61	1802.8	12.3	1791.9	10.8	1779.2	18.6	1779.2	18.6	101.3	-1.3
ELBOW CYN-45	169	50857	1.3	9.1892	0.3	4.7361	0.8	0.3156	0.7	0.94	1768.4	11.4	1773.6	6.6	1779.8	5.0	1779.8	5.0	99.4	0.6
ELBOW CYN-130	105	33822	1.6	9.1883	0.6	4.8370	0.9	0.3223	0.7	0.76	1801.2	10.8	1791.4	7.5	1780.0	10.5	1780.0	10.5	101.2	-1.2
ELBOW CYN-39	36	25885	1.0	9.1871	1.3	4.7392	2.2	0.3158	1.7	0.81	1769.1	27.0	1774.2	18.0	1780.2	23.0	1780.2	23.0	99.4	0.6
ELBOW CYN-198	225	24096	1.8	9.1855	0.3	4.6919	1.4	0.3126	1.3	0.98	1753.4	20.7	1765.8	11.5	1780.5	5.3	1780.5	5.3	98.5	1.5
ELBOW CYN-183	120	50030	2.1	9.1819	0.5	4.8803	0.8	0.3250	0.6	0.82	1814.1	10.2	1798.9	6.7	1781.3	8.3	1781.3	8.3	101.8	-1.8
ELBOW CYN-71	299	174686	3.5	9.1818	0.2	4.7897	0.9	0.3190	0.8	0.98	1784.6	13.1	1783.1	7.2	1781.3	2.9	1781.3	2.9	100.2	-0.2
ELBOW CYN-163	82	47852	0.9	9.1806	0.8	4.7759	1.1	0.3180	0.7	0.63	1780.0	10.4	1780.7	8.9	1781.5	15.0	1781.5	15.0	99.9	0.1
ELBOW CYN-170	100	51842	1.2	9.1792	0.8	4.7452	0.9	0.3159	0.5	0.58	1769.7	8.3	1775.3	7.8	1781.8	13.8	1781.8	13.8	99.3	0.7
ELBOW CYN-99	56	42740	1.7	9.1783	0.7	4.8300	0.9	0.3215	0.6	0.62	1797.1	8.9	1790.1	7.7	1782.0	13.0	1782.0	13.0	100.9	-0.9
ELBOW CYN-100	133	11518	1.7	9.1776	0.6	4.6435	0.9	0.3091	0.6	0.68	1736.2	9.0	1757.1	7.3	1782.1	11.7	1782.1	11.7	97.4	2.6
ELBOW CYN-52	167	103098	2.0	9.1773	0.4	4.7884	0.7	0.3187	0.7	0.88	1783.4	10.2	1782.9	6.2	1782.2	6.4	1782.2	6.4	100.1	-0.1
ELBOW CYN-111	154	71951	2.6	9.1766	0.3	4.8786	0.6	0.3247	0.5	0.82	1812.6	7.7	1798.6	5.0	1782.3	6.3	1782.3	6.3	101.7	-1.7
ELBOW CYN-47	57	43974	1.3	9.1762	0.6	4.8140	1.1	0.3204	0.8	0.79	1791.6	13.1	1787.4	8.9	1782.4	11.8	1782.4	11.8	100.5	-0.5
ELBOW CYN-103	212	54502	1.7	9.1760	0.4	4.8304	0.7	0.3215	0.6	0.84	1796.9	9.2	1790.2	5.9	1782.4	6.9	1782.4	6.9	100.8	-0.8
ELBOW CYN-68	80	101936	1.5	9.1757	0.7	4.8497	1.3	0.3227	1.1	0.84	1803.1	17.1	1793.6	10.9	1782.5	12.6	1782.5	12.6	101.2	-1.2
ELBOW CYN-73	72	96463	1.6	9.1754	0.9	4.8796	1.1	0.3247	0.7	0.61	1812.7	10.7	1798.7	9.3	1782.5	16.0	1782.5	16.0	101.7	-1.7
ELBOW CYN-2	428	58396	4.2	9.1754	0.2	4.5011	0.6	0.2995	0.6	0.97	1689.0	8.4	1731.2	4.9	1782.5	2.8	1782.5	2.8	94.8	5.2
ELBOW CYN-22	58	39914	1.4	9.1748	0.6	4.7746	1.4	0.3177	1.3	0.90	1778.5	20.2	1780.4	12.1	1782.7	11.2	1782.7	11.2	99.8	0.2
ELBOW CYN-54	70	44670	1.1	9.1738	0.7	4.7590	1.0	0.3166	0.7	0.68	1773.3	10.7	1777.7	8.5	1782.9	13.6	1782.9	13.6	99.5	0.5
ELBOW CYN-113	222	158119	2.4	9.1714	0.2	4.8681	1.0	0.3238	1.0	0.98	1808.3	15.1	1796.7	8.3	1783.3	3.6	1783.3	3.6	101.4	-1.4
ELBOW CYN-76	90	80470	1.4	9.1712	0.5	4.8986	1.0	0.3258	0.9	0.88	1818.2	14.4	1802.0	8.7	1783.4	8.9	1783.4	8.9	102.0	-2.0
ELBOW CYN-101	205	34505	2.3	9.1706	0.3	4.6918	2.7	0.3121	2.7	0.99	1750.8	41.2	1765.8	22.6	1783.5	5.1	1783.5	5.1	98.2	1.8
ELBOW CYN-185	52	20718	1.0	9.1704	1.7	4.8385	2.1	0.3218	1.2	0.57	1798.5	18.5	1791.6	17.4	1783.5	31.1	1783.5	31.1	100.8	-0.8
ELBOW CYN-162	42	33297	0.9	9.1680	1.7	4.7880	1.8	0.3184	0.4	0.22	1781.7	6.2	1782.8	15.0	1784.0	31.8	1784.0	31.8	99.9	0.1
ELBOW CYN-46	130	96131	2.0	9.1679	0.5	4.8115	0.9	0.3199	0.8	0.87	1789.3	12.6	1786.9	7.8	1784.0	8.4	1784.0	8.4	100.3	-0.3
ELBOW CYN-151	167	170958	2.0	9.1613	0.4	4.8170	0.9	0.3201	0.8	0.91	1790.0	12.8	1787.9	7.6	1785.3	6.9	1785.3	6.9	100.3	-0.3
ELBOW CYN-86	148	115164	2.2	9.1606	0.4	4.8267	0.6	0.3207	0.5	0.77	1793.0	7.5	1789.6	5.2	1785.5	7.2	1785.5	7.2	100.4	-0.4
ELBOW CYN-182	159	113469	2.0	9.1590	0.3	4.8057	0.8	0.3192	0.7	0.91	1786.0	11.0	1785.9	6.5	1785.8	6.0	1785.8	6.0	100.0	0.0
ELBOW CYN-181	104	50628	3.1	9.1589	0.5	4.7850	0.9	0.3178	0.7	0.81	1779.2	11.5	1782.3	7.7	1785.8	9.9	1785.8	9.9	99.6	0.4
ELBOW CYN-31	182	98574	2.0	9.1584	0.4	4.6937	1.8	0.3118	1.7	0.97	1749.4	26.2	1766.1	14.8	1785.9	8.1	1785.9	8.1	98.0	2.0

1.0,0.8

U-Pb Geochronologic anlayses of selected Harmony Formation strata

				Isotope ratios									Apparent ages (Ma)							
	U	206Pb	U/Th	206Pb*	±	207Pb*	±	206Pb*	±	error	206Pb*	±	207Pb*	±	206Pb*	±	Best age	±	Conc.	Discor.
	(ppm)	204Pb		207Pb*	(%)	235U*	(%)	238U	(%)	corr.	238U*	(Ma)	235U	(Ma)	207Pb*	(Ma)	(Ma)	(Ma)	(%)	(%)
Sample: Elbow Canyon. Location: Elbow Canyon, Sonoma Range; 0441026 4514450 (NAD 83 UTM 11T)																				
ELBOW CYN-56	66	77524	1.5	9.1581	0.6	4.8612	1.2	0.3229	1.1	0.86	1803.8	16.7	1795.5	10.4	1786.0	11.7	1786.0	11.7	101.0	-1.0
ELBOW CYN-173	176	183336	2.4	9.1568	0.3	4.8159	1.2	0.3198	1.1	0.97	1788.9	17.7	1787.7	9.8	1786.2	4.9	1786.2	4.9	100.1	-0.1
ELBOW CYN-160	175	128010	2.3	9.1561	0.2	4.8401	1.1	0.3214	1.1	0.98	1796.6	16.6	1791.9	9.1	1786.4	3.7	1786.4	3.7	100.6	-0.6
ELBOW CYN-140	153	53615	1.5	9.1558	0.3	4.7972	0.9	0.3186	0.8	0.92	1782.7	12.6	1784.4	7.4	1786.4	6.1	1786.4	6.1	99.8	0.2
ELBOW CYN-171	59	19384	1.7	9.1534	1.0	4.8175	1.3	0.3198	0.8	0.64	1788.8	12.8	1788.0	10.7	1786.9	17.7	1786.9	17.7	100.1	-0.1
ELBOW CYN-127	115	118431	1.4	9.1527	0.5	4.8313	1.1	0.3207	0.9	0.86	1793.2	14.2	1790.4	8.9	1787.1	9.9	1787.1	9.9	100.3	-0.3
ELBOW CYN-145	179	96716	2.3	9.1521	0.4	4.8789	1.5	0.3238	1.4	0.96	1808.5	22.7	1798.6	12.7	1787.2	8.0	1787.2	8.0	101.2	-1.2
ELBOW CYN-138	225	89705	4.9	9.1516	0.2	4.8132	0.8	0.3195	0.7	0.98	1787.1	11.5	1787.2	6.3	1787.3	3.0	1787.3	3.0	100.0	0.0
ELBOW CYN-92	27	28066	1.2	9.1510	2.2	4.8249	2.4	0.3202	1.0	0.41	1790.8	15.7	1789.3	20.6	1787.4	40.7	1787.4	40.7	100.2	-0.2
ELBOW CYN-115	122	128374	2.1	9.1478	0.4	4.9398	1.2	0.3277	1.2	0.94	1827.4	18.5	1809.1	10.4	1788.0	7.7	1788.0	7.7	102.2	-2.2
ELBOW CYN-159	177	262841	2.3	9.1464	0.3	4.8343	0.7	0.3207	0.6	0.90	1793.1	9.8	1790.9	5.9	1788.3	5.5	1788.3	5.5	100.3	-0.3
ELBOW CYN-11	109	98857	1.9	9.1462	0.7	4.8397	1.1	0.3210	0.9	0.78	1794.8	13.4	1791.8	9.2	1788.3	12.5	1788.3	12.5	100.4	-0.4
ELBOW CYN-187	34	13360	1.5	9.1409	1.7	4.7836	2.2	0.3171	1.4	0.63	1775.7	21.9	1782.0	18.8	1789.4	31.7	1789.4	31.7	99.2	0.8
ELBOW CYN-7	79	34518	1.4	9.1383	0.8	4.7960	1.3	0.3179	1.0	0.78	1779.3	15.9	1784.2	11.0	1789.9	14.8	1789.9	14.8	99.4	0.6
ELBOW CYN-9	216	98059	3.1	9.1371	0.2	4.8668	0.6	0.3225	0.6	0.94	1802.0	9.2	1796.5	5.2	1790.2	3.7	1790.2	3.7	100.7	-0.7
ELBOW CYN-36	42	35071	1.1	9.1356	0.9	4.9205	1.3	0.3260	0.9	0.72	1819.1	14.8	1805.8	10.9	1790.5	16.3	1790.5	16.3	101.6	-1.6
ELBOW CYN-129	83	89980	2.1	9.1307	0.5	4.8906	0.9	0.3239	0.7	0.81	1808.6	11.7	1800.6	7.7	1791.4	9.9	1791.4	9.9	101.0	-1.0
ELBOW CYN-4	235	26864	1.7	9.1294	0.3	4.7066	1.1	0.3116	1.0	0.96	1748.7	15.9	1768.4	9.1	1791.7	5.7	1791.7	5.7	97.6	2.4
ELBOW CYN-57	47	42256	1.5	9.1276	1.1	4.8895	1.2	0.3237	0.5	0.41	1807.7	8.1	1800.4	10.5	1792.0	20.6	1792.0	20.6	100.9	-0.9
ELBOW CYN-89	146	96978	1.6	9.1247	0.4	4.9209	1.3	0.3257	1.2	0.94	1817.3	18.9	1805.9	10.7	1792.6	7.7	1792.6	7.7	101.4	-1.4
ELBOW CYN-18	75	46576	1.3	9.1243	0.6	4.9373	2.0	0.3267	1.9	0.96	1822.5	29.6	1808.7	16.5	1792.7	10.5	1792.7	10.5	101.7	-1.7
ELBOW CYN-149	152	50766	2.0	9.1235	0.4	4.8226	0.7	0.3191	0.6	0.85	1785.4	8.9	1788.8	5.7	1792.9	6.5	1792.9	6.5	99.6	0.4
ELBOW CYN-26	130	64192	1.7	9.1195	0.4	4.7901	0.8	0.3168	0.7	0.83	1774.2	10.2	1783.2	6.7	1793.7	8.0	1793.7	8.0	98.9	1.1
ELBOW CYN-116	258	88002	2.1	9.1115	0.3	4.7728	3.1	0.3154	3.1	1.00	1767.2	47.5	1780.1	25.9	1795.3	5.4	1795.3	5.4	98.4	1.6
ELBOW CYN-35	36	24854	1.0	9.1092	2.7	4.7612	3.4	0.3146	2.1	0.62	1763.1	32.7	1778.1	28.7	1795.7	48.9	1795.7	48.9	98.2	1.8
ELBOW CYN-21	91	45798	1.3	9.1076	0.6	4.9416	1.2	0.3264	1.0	0.85	1821.0	16.3	1809.4	10.2	1796.1	11.7	1796.1	11.7	101.4	-1.4
ELBOW CYN-60	99	45879	1.3	9.0920	0.7	4.9341	2.0	0.3254	1.9	0.93	1815.9	29.4	1808.1	16.8	1799.2	13.2	1799.2	13.2	100.9	-0.9
ELBOW CYN-117	48	20522	1.4	9.0902	1.2	4.9389	1.8	0.3256	1.3	0.72	1817.1	20.0	1808.9	14.9	1799.5	22.4	1799.5	22.4	101.0	-1.0
ELBOW CYN-114	32	20996	0.7	9.0789	2.7	4.9317	2.8	0.3247	0.6	0.23	1812.8	10.2	1807.7	23.5	1801.8	49.3	1801.8	49.3	100.6	-0.6
ELBOW CYN-8	35	19066	1.3	9.0764	1.3	4.8761	2.4	0.3210	2.0	0.83	1794.5	30.8	1798.1	19.9	1802.3	23.8	1802.3	23.8	99.6	0.4
ELBOW CYN-156	35	35442	0.8	8.9642	0.8	5.1288	1.7	0.3334	1.5	0.88	1855.1	24.7	1840.9	14.9	1824.9	15.2	1824.9	15.2	101.7	-1.7
ELBOW CYN-70	39	58387	1.2	8.9633	1.0	5.0427	1.2	0.3278	0.7	0.56	1827.8	11.0	1826.5	10.4	1825.1	18.3	1825.1	18.3	100.1	-0.1
ELBOW CYN-161	39	17851	1.9	8.9598	0.8	5.1006	1.3	0.3314	1.0	0.78	1845.4	16.7	1836.2	11.3	1825.8	15.0	1825.8	15.0	101.1	-1.1
ELBOW CYN-131	78	17379	0.7	8.9595	0.7	5.0244	1.0	0.3265	0.7	0.72	1821.4	11.4	1823.4	8.4	1825.8	12.5	1825.8	12.5	99.8	0.2
ELBOW CYN-91	20	11265	0.5	8.9469	2.6	5.1775	3.4	0.3360	2.2	0.65	1867.2	35.8	1848.9	29.1	1828.4	47.3	1828.4	47.3	102.1	-2.1
ELBOW CYN-146	28	15319	0.5	8.9435	1.5	5.1336	2.1	0.3330	1.5	0.70	1852.8	23.4	1841.7	17.6	1829.1	26.7	1829.1	26.7	101.3	-1.3
ELBOW CYN-189	132	171375	1.4	8.9344	0.6	5.1645	0.9	0.3347	0.7	0.77	1860.9	11.5	1846.8	7.9	1830.9	10.7	1830.9	10.7	101.6	-1.6
ELBOW CYN-133	150	101588	1.0	8.9102	0.4	5.1409	0.7	0.3322	0.6	0.83	1849.1	9.9	1842.9	6.4	1835.8	7.6	1835.8	7.6	100.7	-0.7
ELBOW CYN-55	80	49058	1.2	8.9028	0.7	4.6322	2.2	0.2991	2.1	0.95	1686.8	30.5	1755.1	18.2	1837.3	12.8	1837.3	12.8	91.8	8.2
ELBOW CYN-53	94	96656	1.0	8.8562	0.7	5.1558	0.8	0.3312	0.5	0.61	1844.0	8.2	1845.3	7.1	1846.8	11.9	1846.8	11.9	99.8	0.2
ELBOW CYN-199	24	28099	1.8	8.8400	1.4	5.1422	1.8	0.3297	1.1	0.61	1836.8	17.3	1843.1	15.1	1850.2	25.4	1850.2	25.4	99.3	0.7
ELBOW CYN-155	224	164060	5.8	8.8303	0.5	5.1976	0.7	0.3329	0.4	0.68	1852.3	7.2	1852.2	5.6	1852.1	8.6	1852.1	8.6	100.0	0.0
ELBOW CYN-29	127	87734	1.6	8.8257	0.4	5.2005	0.6	0.3329	0.4	0.70	1852.4	6.5	1852.7	4.9	1853.1	7.4	1853.1	7.4	100.0	0.0
ELBOW CYN-32	70	60139	2.2	8.8243	0.6	5.1749	1.0	0.3312	0.9	0.84	1844.2	13.9	1848.5	8.8	1853.4	10.2	1853.4	10.2	99.5	0.5
ELBOW CYN-176	155	155674	1.5	8.8178	0.3	5.2335	0.9	0.3347	0.8	0.93	1861.1	13.2	1858.1	7.5	1854.7	5.9	1854.7	5.9	100.3	-0.3
ELBOW CYN-167	74	56348	2.7	8.8114	0.7	5.2063	1.1	0.3327	0.9	0.79	1851.5	14.5	1853.6	9.7	1856.0	12.7	1856.0	12.7	99.8	0.2
ELBOW CYN-23	50	30383	1.3	8.8044	1.1	5.2331	1.4	0.3342	0.9	0.65	1858.5	15.0	1858.0	12.2	1857.4	19.6	1857.4	19.6	100.1	-0.1
ELBOW CYN-184	95	119541	0.9	8.8031	0.5	5.2208	1.3	0.3333	1.3	0.93	1854.5	20.2	1856.0	11.5	1857.7	8.9	1857.7	8.9	99.8	0.2
ELBOW CYN-165	202	311502	8.9	8.7980	0.3	5.2149	0.6	0.3328	0.5	0.86	1851.7	8.8	1855.0	5.4	1858.8	5.9	1858.8	5.9	99.6	0.4
ELBOW CYN-118	253	76721	2.4	8.7957	0.2	5.2218	0.5	0.3331	0.5	0.95	1853.5	7.9	1856.2	4.4	1859.2	3.0	1859.2	3.0	99.7	0.3
ELBOW CYN-65	95	100687	3.8	8.7886	0.4	5.3255	0.8	0.3395	0.7	0.86	1884.0	11.3	1873.0	6.9	1860.7	7.5	1860.7	7.5	101.3	-1.3
ELBOW CYN-158	50	80414	1.3	8.7808	1.3	5.2337	1.6	0.3333	0.9	0.58	1854.4	14.7	1858.1	13.5	1862.3	23.3	1862.3	23.3	99.6	0.4
ELBOW CYN-132	138	279886	2.4	8.7679	0.2	5.3257	1.0	0.3387	1.0	0.98	1880.3	16.7	1873.0	8.9	1864.9	3.8	1864.9	3.8	100.8	-0.8
ELBOW CYN-164	42	8567	0.6	8.7674	1.3	5.2413	1.6	0.3333	0.9	0.58	1854.3	14.8	1859.4	13.4	1865.0	23.0	1865.0	23.0	99.4	0.6
ELBOW CYN-123	18	15282	2.5	8.7647	1.6	5.3473	2.4	0.3399	1.8	0.74	1886.3	29.3	1876.5	20.7	1865.6	29.4	1865.6	29.4	101.1	-1.1
ELBOW CYN-67	93	42284	1.9	8.7592	0.4	5.1911	4.4	0.3298	4.3	0.99	1837.3	69.4	1851.2	37.2	1866.7	8.1	1866.7	8.1	98.4	1.6
ELBOW CYN-194	224	252747	2.2	8.7580	0.3	5.4068	0.8	0.3434	0.7	0.93	1903.2	12.1	1885.9	6.8	1867.0	5.3	1867.0	5.3	101.9	-1.9
ELBOW CYN-85	47	86571	0.7	8.7502	1.1	5.3033	1.3	0.3366	0.7	0.51	1870.1	10.6	1869.4	11.0	1868.6	20.1	1868.6	20.1	100.1	-0.1
ELBOW CYN-1	64	24840	1.2	8.7421	1.1	5.3655	1.7	0.3402	1.3	0.77	1887.6	20.9	1879.4	14.2	1870.3	19.3	1870.3	19.3	100.9	-0.9
ELBOW CYN-93	77	42872	1.1	8.7406	0.7	5.4191	2.5	0.3435	2.4	0.96	1903.6	39.5	1887.9	21.4	1870.6	12.5	1870.6	12.5	101.8	-1.8
ELBOW CYN-27	197	10348	0.9	8.6293	0.5	4.7531	3.7	0.2975	3.6	0.99	1678.8	53.6	1776.7	30.8	1893.7	9.5	1893.7	9.5	88.7	11.3
ELBOW CYN-34	25	50310	0.7	7.8911	2.3	6.8566	3.7	0.3924	2.9	0.79	2134.0	53.4	2093.1	32.9	2053.0	40.0	2053.0	40.0	103.9	-3.9
ELBOW CYN-33	50	36070	1.2	7.7799	1.3	6.6942	1.6	0.3777	0.9	0.55	2065.6	15.1	2071.9	13.9	2078.0	23.2	2078.0	23.2	99.4	0.6
ELBOW CYN-177	48	55142	1.2	6.8439	0.9	8.1154	1.9	0.4028	1.7	0.89	2182.0	32.2	2244.0	17.6	2301.0	15.0	2301.0	15.0	94.8	5.2
ELBOW CYN-112	59	135521	1.2	6.3246	0.4	10.1392	1.1	0.4651	1.0	0.93	2462.0	20.7	2447.6	10.1	2435.6	6.8	2435.6	6.8	101.1	-1.1
ELBOW CYN-124	127	105561	1.2	6.2895	0.2	10.2691	0.8	0.4684	0.7	0.97	2476.7	15.1	2459.3	7.0	2445.0	3.3	2445.0	3.3	101.3	-1.3
ELBOW CYN-59	163	206773	2.4	6.2524	0.2	10.2954	0.7	0.4669	0.7	0.97	2469.8	14.8	2461.7	6.9	2455.0	2.9	2455.0	2.9	100.6	-0.6
ELBOW CYN-172	70	78059	2.4	6.2321	0.6	9.8764	1.1	0.4464	1.0	0.85	2379.3	19.0	2423.3	10.3	2460.5	10.0	2460.5	10.0	96.7	3.3
ELBOW CYN-83	93	109042	2.8	6.1025	0.4	10.6684	1.5	0.4722	1.4	0.96	2493.1	29.4	2494.7	13.7	2495.9	6.7	2495.9	6.7	99.9	0.1
ELBOW CYN-14	157	23162	1.8	6.0947	0.2	10.4937	0.7	0.4639	0.7	0.96	2456.6	13.3	2479.4	6.3	2498.1	3.1	2498.1	3.1	98.3	1.7
ELBOW CYN-147	95	48548	1.1	6.0724	0.1	9.8283	0.9	0.4328	0.9	0.99	2318.5	16.8	2418.8	8.1	2504.3	2.5	2504.3	2.5	92.6	7.4
ELBOW CYN-193	80	101939	0.5	6.0455	0.2	10.9869	0.7	0.4817	0.7	0.94	2534.8	13.9	2522.0	6.6	2511.7	4.1	2511.7	4.1	100.9	-0.9
ELBOW CYN-166	122	184102	1.9	6.0197	0.3	10.9375	0.9	0.4775	0.8	0.93	2516.5	16.7	2517.8	8.0	2518.9	5.1	2518.9	5.1	99.9	0.1
ELBOW CYN-104	57	127803	2.1	5.9102	0.8	11.3776	2.0	0.4877	1.9	0.92	2560.7	39.7	2554.6	19.0	2549.7	13.0	2549.7	13.0	100.4	-0.4
ELBOW CYN-180	88	142967	1.7	5.8776	0.9	11.3185	3.3	0.4825	3.2	0.96	2538.1	66.8	2549.7	31.0	2559.0	15.8	2559.0	15.8	99.2	0.8
ELBOW CYN-98	107	175347	1.3	5.8519	0.3	11.6309	0.7	0.4936	0.6	0.92	2586.4	13.4	2575.2	6.4	2566.3	4.4	2566.3	4.4	100.8	-0.8
ELBOW CYN-41	105	22009	1.5	5.8491	2.0	9.6333	6.5	0.4087	6.2	0.95	2208.8	116.1	2400.4	60.0	2567.1	32.9	2567.1	32.9	86.0	14.0
ELBOW CYN-61	71	30877	2.1	5.8439	0.3	11.7624	0.7	0.4985	0.7	0.91	2607.5	14.4	2585.7	6.9	2568.6	5.2	2568.6	5.2	101.5	-1.5
ELBOW CYN-6	256	213608	3.6	5.8077	0.1	11.6767	0.8	0.4918	0.8	0.99	2578.6	16.3	2578.8	7.3	2579.0	1.9	2579.0	1.9	100.0	0.0
ELBOW CYN-95	30	26720	1.2	5.8029	0.7	11.9158	1.8	0.5015	1.7	0.93	2620.2	37.0	2597.8	17.3	2580.4	11.3	2580.4	11.3	101.5	-1.5
ELBOW CYN-122	100	242893	1.4	5.7859	0.3	11.9207	1.8	0.5002	1.7	0.99	2614.8	37.3	2598.2	16.5	2585.3	4.7	2585.3	4.7	101.1	-1.1
ELBOW CYN-141	125	155602	1.1	5.7827	0.2	11.7917	1.0	0.4945	0.9	0.98	2590.3	20.2	2588.0	9.1	2586.2	3.5	2586.2	3.5	100.2	-0.2
ELBOW CYN-87	165	46590	1.2	5.7733	0.2	11.2829	1.2	0.4724	1.1	0.98	2494.2	23.5	2546.8	10.8	2588.9	3.7	2588.9	3.7	96.3	3.7
ELBOW CYN-16	52	59434	1.0	5.7714	0.4	11.8572	0.8	0.4963	0.7	0.85	2598.0	15.0	2593.2	7.7	2589.5	7.3	2589.5	7.3	100.3	-0.3
ELBOW CYN-190	156	87107	1.5	5.7630	0.2	11.2374	0.8	0.4697	0.8	0.98	2482.2	16.9	2543.0	7.8	2591.9	2.7	2591.9	2.7	95.8	4.2
ELBOW CYN-64	75	128520	2.5	5.7490	0.4	12.2629	1.2	0.5113	1.1	0.95	2662.2	24.4	2624.7	11.0	2595.9	5.8	2595.9	5.8	102.6	-2.6
ELBOW CYN-48	124	195222	2.4	5.7408	0.3	11.9358	0.7	0.4970	0.6	0.87	2600.7	12.6	2599.4	6.3	2598.3	5.5	2598.3	5.5	100.1	-0.1
ELBOW CYN-107	151	126046	2.0	5.7366	0.2	12.1065	0.8	0.5037	0.8	0.98	2629.7	16.9	2612.7	7.5	2599.5	2.9	2599.5	2.9	101.2	-1.2
ELBOW CYN-154	178	259440	2.5	5.7321	0.1	11.8304	1.3	0.4918	1.3	0.99	2578.6	26.7	2591.1	11.8	2600.8	2.4	2600.8	2.4	99.1	0.9
ELBOW CYN-144	119	217931	1.6	5.7191	0.3	12.0820	1.0	0.5011	0.9	0.94	2618.7	19.5	2610.8	9.0	2604.6	5.5	2604.6	5.5	100.5	-0.5
ELBOW CYN-136	99	118990	1.6	5.6963	0.2	12.1308	0.8	0.5012	0.8	0.95	2618.8	16.9	2614.6	7.7	2611.3	4.1	2611.3	4.1	100.3	-0.3
ELBOW CYN-19	103	302632	2.0	5.6941	0.3	12.0350	0.8	0.4970	0.8	0.93	2601.0	16.7	2607.1	7.8	2611.9	5.0	2611.9	5.0	99.6	0.4
ELBOW CYN-142	134	170359	2.1	5.6902	0.2	12.1897	0.9	0.5031	0.8	0.97	2626.9	18.1	2619.1	8.1	2613.1	3.4	2613.1	3.4	100.5	-0.5
ELBOW CYN-58	64	106838	1.9	5.6887	0.3	12.3036	1.3	0.5076	1.3	0.98	2646.5	28.7	2627.8	12.6	2613.5	4.4	2613.5	4.4	101.3	-1.3
ELBOW CYN-125	108	85424	0.8	5.6820	0.2	12.2357	0.8	0.5042	0.8	0.97	2631.9	17.1	2622.7	7.6	2615.5	3.2	2615.5	3.2	100.6	-0.6
ELBOW CYN-40	55	36306	1.0	5.6654	0.5	11.9152	1.0	0.4896	0.9	0.84	2568.9	18.1	2597.8	9.5	2620.4	9.1	2620.4	9.1	98.0	2.0
ELBOW CYN-17	86	69707	2.0	5.6453	0.3	12.1406	0.9	0.4971	0.9	0.94	2601.2	18.5	2615.3	8.6	2626.2	5.2	2626.2	5.2	99.0	1.0
ELBOW CYN-37	129	21341	1.0	5.6197	0.5	10.6262	1.2	0.4331	1.1	0.90	2319.7	20.5	2491.0	10.9	2633.8	8.6	2633.8	8.6	88.1	11.9
ELBOW CYN-84	38	95295	1.5	5.5750	0.4	12.6830	1.0	0.5128	0.9	0.91	2668.7	19.1	2656.4	9.0	2647.0	6.5	2647.0	6.5	100.8	-0.8
ELBOW CYN-49	182	100863	1.8	5.5026	0.2	10.9326	1.7	0.4363	1.7	0.99	2334.1	33.1	2517.4	15.9	2668.7	3.8	2668.7	3.8	87.5	12.5
ELBOW CYN-121	83	18363	0.8	5.4836	0.2	12.8950	5.9	0.5128	5.9	1.00	2668.8	128.9	2672.0	55.7	2674.5	4.1	2674.5	4.1	99.8	0.2
ELBOW CYN-79	48	47725	1.4	5.4722	0.3	13.3726	0.9	0.5307	0.9	0.95	2744.5	20.1	2706.3	8.9	2677.9	4.6	2677.9	4.6	102.5	-2.5
ELBOW CYN-50	172	18920	1.4	5.4647	0.1	12.4888	1.0	0.4950	1.0	0.99	2592.2	21.5	2641.9	9.6	2680.2	2.5	2680.2	2.5	96.7	3.3
ELBOW CYN-179	75	56851	1.2	5.4589	0.5	13.0061	0.8	0.5149	0.7	0.83	2677.6	15.3	2680.1	7.9	2681.9	7.7	2681.9	7.7	99.8	0.2

U-Pb Geochronologic anlayses of selected Harmony Formation strata

				Isotope ratios								Apparent ages (Ma)							
	U	206Pb	U/Th	206Pb*	±	207Pb*	±	206Pb*	±	error	206Pb*	±	207Pb*	±	206Pb*	±	Best age	±	Conc.	Discor.
	(ppm)	204Pb		207Pb*	(%)	235U*	(%)	238U	(%)	corr.	238U*	(Ma)	235U	(Ma)	207Pb*	(Ma)	(Ma)	(Ma)	(%)	(%)
Sample: Elbow Canyon. Location: Elbow Canyon, Sonoma Range; 0441026 4514450 (NAD 83 UTM 11T)																			
ELBOW CYN-56	66	77524	1.5	9.1581	0.6	4.8612	1.2	0.3229	1.1	0.86	1803.8	16.7	1795.5	10.4	1786.0	11.7	1786.0	11.7	101.0	-1.0
ELBOW CYN-173	176	183336	2.4	9.1568	0.3	4.8159	1.2	0.3198	1.1	0.97	1788.9	17.7	1787.7	9.8	1786.2	4.9	1786.2	4.9	100.1	-0.1
ELBOW CYN-160	175	128010	2.3	9.1561	0.2	4.8401	1.1	0.3214	1.1	0.98	1796.6	16.6	1791.9	9.1	1786.4	3.7	1786.4	3.7	100.6	-0.6
ELBOW CYN-140	153	53615	1.5	9.1558	0.3	4.7972	0.9	0.3186	0.8	0.92	1782.7	12.6	1784.4	7.4	1786.4	6.1	1786.4	6.1	99.8	0.2
ELBOW CYN-171	59	19384	1.7	9.1534	1.0	4.8175	1.3	0.3198	0.8	0.64	1788.8	12.8	1788.0	10.7	1786.9	17.7	1786.9	17.7	100.1	-0.1
ELBOW CYN-127	115	118431	1.4	9.1527	0.5	4.8313	1.1	0.3207	0.9	0.86	1793.2	14.2	1790.4	8.9	1787.1	9.9	1787.1	9.9	100.3	-0.3
ELBOW CYN-145	179	96716	2.3	9.1521	0.4	4.8789	1.5	0.3238	1.4	0.96	1808.5	22.7	1798.6	12.7	1787.2	8.0	1787.2	8.0	101.2	-1.2
ELBOW CYN-138	225	89705	4.9	9.1516	0.2	4.8132	0.8	0.3195	0.7	0.98	1787.1	11.5	1787.2	6.3	1787.3	3.0	1787.3	3.0	100.0	0.0
ELBOW CYN-92	27	28066	1.2	9.1510	2.2	4.8249	2.4	0.3202	1.0	0.41	1790.8	15.7	1789.3	20.6	1787.4	40.7	1787.4	40.7	100.2	-0.2
ELBOW CYN-115	122	128374	2.1	9.1478	0.4	4.9398	1.2	0.3277	1.2	0.94	1827.4	18.5	1809.1	10.4	1788.0	7.7	1788.0	7.7	102.2	-2.2
ELBOW CYN-159	177	262841	2.3	9.1464	0.3	4.8343	0.7	0.3207	0.6	0.90	1793.1	9.8	1790.9	5.9	1788.3	5.5	1788.3	5.5	100.3	-0.3
ELBOW CYN-11	109	98857	1.9	9.1462	0.7	4.8397	1.1	0.3210	0.9	0.78	1794.8	13.4	1791.8	9.2	1788.3	12.5	1788.3	12.5	100.4	-0.4
ELBOW CYN-187	34	13360	1.5	9.1409	1.7	4.7836	2.2	0.3171	1.4	0.63	1775.7	21.9	1782.0	18.8	1789.4	31.7	1789.4	31.7	99.2	0.8
ELBOW CYN-7	79	34518	1.4	9.1383	0.8	4.7960	1.3	0.3179	1.0	0.78	1779.3	15.9	1784.2	11.0	1789.9	14.8	1789.9	14.8	99.4	0.6
ELBOW CYN-9	216	98059	3.1	9.1371	0.2	4.8668	0.6	0.3225	0.6	0.94	1802.0	9.2	1796.5	5.2	1790.2	3.7	1790.2	3.7	100.7	-0.7
ELBOW CYN-36	42	35071	1.1	9.1356	0.9	4.9205	1.3	0.3260	0.9	0.72	1819.1	14.8	1805.8	10.9	1790.5	16.3	1790.5	16.3	101.6	-1.6
ELBOW CYN-129	83	89980	2.1	9.1307	0.5	4.8906	0.9	0.3239	0.7	0.81	1808.6	11.7	1800.6	7.7	1791.4	9.9	1791.4	9.9	101.0	-1.0
ELBOW CYN-4	235	26864	1.7	9.1294	0.3	4.7066	1.1	0.3116	1.0	0.96	1748.7	15.9	1768.4	9.1	1791.7	5.7	1791.7	5.7	97.6	2.4
ELBOW CYN-57	47	42256	1.5	9.1276	1.1	4.8895	1.2	0.3237	0.5	0.41	1807.7	8.1	1800.4	10.5	1792.0	20.6	1792.0	20.6	100.9	-0.9
ELBOW CYN-89	146	96978	1.6	9.1247	0.4	4.9209	1.3	0.3257	1.2	0.94	1817.3	18.9	1805.9	10.7	1792.6	7.7	1792.6	7.7	101.4	-1.4
ELBOW CYN-18	75	46576	1.3	9.1243	0.6	4.9373	2.0	0.3267	1.9	0.96	1822.5	29.6	1808.7	16.5	1792.7	10.5	1792.7	10.5	101.7	-1.7
ELBOW CYN-149	152	50766	2.0	9.1235	0.4	4.8226	0.7	0.3191	0.6	0.85	1785.4	8.9	1788.8	5.7	1792.9	6.5	1792.9	6.5	99.6	0.4
ELBOW CYN-26	130	64192	1.7	9.1195	0.4	4.7901	0.8	0.3168	0.7	0.83	1774.2	10.2	1783.2	6.7	1793.7	8.0	1793.7	8.0	98.9	1.1
ELBOW CYN-116	258	88002	2.1	9.1115	0.3	4.7728	3.1	0.3154	3.1	1.00	1767.2	47.5	1780.1	25.9	1795.3	5.4	1795.3	5.4	98.4	1.6
ELBOW CYN-35	36	24854	1.0	9.1092	2.7	4.7612	3.4	0.3146	2.1	0.62	1763.1	32.7	1778.1	28.7	1795.7	48.9	1795.7	48.9	98.2	1.8
ELBOW CYN-21	91	45798	1.3	9.1076	0.6	4.9416	1.2	0.3264	1.0	0.85	1821.0	16.3	1809.4	10.2	1796.1	11.7	1796.1	11.7	101.4	-1.4
ELBOW CYN-60	99	45879	1.3	9.0920	0.7	4.9341	2.0	0.3254	1.9	0.93	1815.9	29.4	1808.1	16.8	1799.2	13.2	1799.2	13.2	100.9	-0.9
ELBOW CYN-117	48	20522	1.4	9.0902	1.2	4.9389	1.8	0.3256	1.3	0.72	1817.1	20.0	1808.9	14.9	1799.5	22.4	1799.5	22.4	101.0	-1.0
ELBOW CYN-114	32	20996	0.7	9.0789	2.7	4.9317	2.8	0.3247	0.6	0.23	1812.8	10.2	1807.7	23.5	1801.8	49.3	1801.8	49.3	100.6	-0.6
ELBOW CYN-8	35	19066	1.3	9.0764	1.3	4.8761	2.4	0.3210	2.0	0.83	1794.5	30.8	1798.1	19.9	1802.3	23.8	1802.3	23.8	99.6	0.4
ELBOW CYN-156	35	35442	0.8	8.9642	0.8	5.1288	1.7	0.3334	1.5	0.88	1855.1	24.7	1840.9	14.9	1824.9	15.2	1824.9	15.2	101.7	-1.7
ELBOW CYN-70	39	58387	1.2	8.9633	1.0	5.0427	1.2	0.3278	0.7	0.56	1827.8	11.0	1826.5	10.4	1825.1	18.3	1825.1	18.3	100.1	-0.1
ELBOW CYN-161	39	17851	1.9	8.9598	0.8	5.1006	1.3	0.3314	1.0	0.78	1845.4	16.7	1836.2	11.3	1825.8	15.0	1825.8	15.0	101.1	-1.1
ELBOW CYN-131	78	17379	0.7	8.9595	0.7	5.0244	1.0	0.3265	0.7	0.72	1821.4	11.4	1823.4	8.4	1825.8	12.5	1825.8	12.5	99.8	0.2
ELBOW CYN-91	20	11265	0.5	8.9469	2.6	5.1775	3.4	0.3360	2.2	0.65	1867.2	35.8	1848.9	29.1	1828.4	47.3	1828.4	47.3	102.1	-2.1
ELBOW CYN-146	28	15319	0.5	8.9435	1.5	5.1336	2.1	0.3330	1.5	0.70	1852.8	23.4	1841.7	17.6	1829.1	26.7	1829.1	26.7	101.3	-1.3
ELBOW CYN-189	132	171375	1.4	8.9344	0.6	5.1645	0.9	0.3347	0.7	0.77	1860.9	11.5	1846.8	7.9	1830.9	10.7	1830.9	10.7	101.6	-1.6
ELBOW CYN-133	150	101588	1.0	8.9102	0.4	5.1409	0.7	0.3322	0.6	0.83	1849.1	9.9	1842.9	6.4	1835.8	7.6	1835.8	7.6	100.7	-0.7
ELBOW CYN-55	80	49058	1.2	8.9028	0.7	4.6322	2.2	0.2991	2.1	0.95	1686.8	30.5	1755.1	18.2	1837.3	12.8	1837.3	12.8	91.8	8.2
ELBOW CYN-53	94	96656	1.0	8.8562	0.7	5.1558	0.8	0.3312	0.5	0.61	1844.0	8.2	1845.3	7.1	1846.8	11.9	1846.8	11.9	99.8	0.2
ELBOW CYN-199	24	28099	1.8	8.8400	1.4	5.1422	1.8	0.3297	1.1	0.61	1836.8	17.3	1843.1	15.1	1850.2	25.4	1850.2	25.4	99.3	0.7
ELBOW CYN-155	224	164060	5.8	8.8303	0.5	5.1976	0.7	0.3329	0.4	0.68	1852.3	7.2	1852.2	5.6	1852.1	8.6	1852.1	8.6	100.0	0.0
ELBOW CYN-29	127	87734	1.6	8.8257	0.4	5.2005	0.6	0.3329	0.4	0.70	1852.4	6.5	1852.7	4.9	1853.1	7.4	1853.1	7.4	100.0	0.0
ELBOW CYN-32	70	60139	2.2	8.8243	0.6	5.1749	1.0	0.3312	0.9	0.84	1844.2	13.9	1848.5	8.8	1853.4	10.2	1853.4	10.2	99.5	0.5
ELBOW CYN-176	155	155674	1.5	8.8178	0.3	5.2335	0.9	0.3347	0.8	0.93	1861.1	13.2	1858.1	7.5	1854.7	5.9	1854.7	5.9	100.3	-0.3
ELBOW CYN-167	74	56348	2.7	8.8114	0.7	5.2063	1.1	0.3327	0.9	0.79	1851.5	14.5	1853.6	9.7	1856.0	12.7	1856.0	12.7	99.8	0.2
ELBOW CYN-23	50	30383	1.3	8.8044	1.1	5.2331	1.4	0.3342	0.9	0.65	1858.5	15.0	1858.0	12.2	1857.4	19.6	1857.4	19.6	100.1	-0.1
ELBOW CYN-184	95	119541	0.9	8.8031	0.5	5.2208	1.3	0.3333	1.3	0.93	1854.5	20.2	1856.0	11.5	1857.7	8.9	1857.7	8.9	99.8	0.2
ELBOW CYN-165	202	311502	8.9	8.7980	0.3	5.2149	0.6	0.3328	0.5	0.86	1851.7	8.8	1855.0	5.4	1858.8	5.9	1858.8	5.9	99.6	0.4
ELBOW CYN-118	253	76721	2.4	8.7957	0.2	5.2218	0.5	0.3331	0.5	0.95	1853.5	7.9	1856.2	4.4	1859.2	3.0	1859.2	3.0	99.7	0.3
ELBOW CYN-65	95	100687	3.8	8.7886	0.4	5.3255	0.8	0.3395	0.7	0.86	1884.0	11.3	1873.0	6.9	1860.7	7.5	1860.7	7.5	101.3	-1.3
ELBOW CYN-158	50	80414	1.3	8.7808	1.3	5.2337	1.6	0.3333	0.9	0.58	1854.4	14.7	1858.1	13.5	1862.3	23.3	1862.3	23.3	99.6	0.4
ELBOW CYN-132	138	279886	2.4	8.7679	0.2	5.3257	1.0	0.3387	1.0	0.98	1880.3	16.7	1873.0	8.9	1864.9	3.8	1864.9	3.8	100.8	-0.8
ELBOW CYN-164	42	8567	0.6	8.7674	1.3	5.2413	1.6	0.3333	0.9	0.58	1854.3	14.8	1859.4	13.4	1865.0	23.0	1865.0	23.0	99.4	0.6
ELBOW CYN-123	18	15282	2.5	8.7647	1.6	5.3473	2.4	0.3399	1.8	0.74	1886.3	29.3	1876.5	20.7	1865.6	29.4	1865.6	29.4	101.1	-1.1
ELBOW CYN-67	93	42284	1.9	8.7592	0.4	5.1911	4.4	0.3298	4.3	0.99	1837.3	69.4	1851.2	37.2	1866.7	8.1	1866.7	8.1	98.4	1.6
ELBOW CYN-194	224	252747	2.2	8.7580	0.3	5.4068	0.8	0.3434	0.7	0.93	1903.2	12.1	1885.9	6.8	1867.0	5.3	1867.0	5.3	101.9	-1.9
ELBOW CYN-85	47	86571	0.7	8.7502	1.1	5.3033	1.3	0.3366	0.7	0.51	1870.1	10.6	1869.4	11.0	1868.6	20.1	1868.6	20.1	100.1	-0.1
ELBOW CYN-1	64	24840	1.2	8.7421	1.1	5.3655	1.7	0.3402	1.3	0.77	1887.6	20.9	1879.4	14.2	1870.3	19.3	1870.3	19.3	100.9	-0.9
ELBOW CYN-93	77	42872	1.1	8.7406	0.7	5.4191	2.5	0.3435	2.4	0.96	1903.6	39.5	1887.9	21.4	1870.6	12.5	1870.6	12.5	101.8	-1.8
ELBOW CYN-27	197	10348	0.9	8.6293	0.5	4.7531	3.7	0.2975	3.6	0.99	1678.8	53.6	1776.7	30.8	1893.7	9.5	1893.7	9.5	88.7	11.3
ELBOW CYN-34	25	50310	0.7	7.8911	2.3	6.8566	3.7	0.3924	2.9	0.79	2134.0	53.4	2093.1	32.9	2053.0	40.0	2053.0	40.0	103.9	-3.9
ELBOW CYN-33	50	36070	1.2	7.7799	1.3	6.6942	1.6	0.3777	0.9	0.55	2065.6	15.1	2071.9	13.9	2078.0	23.2	2078.0	23.2	99.4	0.6
ELBOW CYN-177	48	55142	1.2	6.8439	0.9	8.1154	1.9	0.4028	1.7	0.89	2182.0	32.2	2244.0	17.6	2301.0	15.0	2301.0	15.0	94.8	5.2
ELBOW CYN-112	59	135521	1.2	6.3246	0.4	10.1392	1.1	0.4651	1.0	0.93	2462.0	20.7	2447.6	10.1	2435.6	6.8	2435.6	6.8	101.1	-1.1
ELBOW CYN-124	127	105561	1.2	6.2895	0.2	10.2691	0.8	0.4684	0.7	0.97	2476.7	15.1	2459.3	7.0	2445.0	3.3	2445.0	3.3	101.3	-1.3
ELBOW CYN-59	163	206773	2.4	6.2524	0.2	10.2954	0.7	0.4669	0.7	0.97	2469.8	14.8	2461.7	6.9	2455.0	2.9	2455.0	2.9	100.6	-0.6
ELBOW CYN-172	70	78059	2.4	6.2321	0.6	9.8764	1.1	0.4464	1.0	0.85	2379.3	19.0	2423.3	10.3	2460.5	10.0	2460.5	10.0	96.7	3.3
ELBOW CYN-83	93	109042	2.8	6.1025	0.4	10.6684	1.5	0.4722	1.4	0.96	2493.1	29.4	2494.7	13.7	2495.9	6.7	2495.9	6.7	99.9	0.1
ELBOW CYN-14	157	23162	1.8	6.0947	0.2	10.4937	0.7	0.4639	0.7	0.96	2456.6	13.3	2479.4	6.3	2498.1	3.1	2498.1	3.1	98.3	1.7
ELBOW CYN-147	95	48548	1.1	6.0724	0.1	9.8283	0.9	0.4328	0.9	0.99	2318.5	16.8	2418.8	8.1	2504.3	2.5	2504.3	2.5	92.6	7.4
ELBOW CYN-193	80	101939	0.5	6.0455	0.2	10.9869	0.7	0.4817	0.7	0.94	2534.8	13.9	2522.0	6.6	2511.7	4.1	2511.7	4.1	100.9	-0.9
ELBOW CYN-166	122	184102	1.9	6.0197	0.3	10.9375	0.9	0.4775	0.8	0.93	2516.5	16.7	2517.8	8.0	2518.9	5.1	2518.9	5.1	99.9	0.1
ELBOW CYN-104	57	127803	2.1	5.9102	0.8	11.3776	2.0	0.4877	1.9	0.92	2560.7	39.7	2554.6	19.0	2549.7	13.0	2549.7	13.0	100.4	-0.4
ELBOW CYN-180	88	142967	1.7	5.8776	0.9	11.3185	3.3	0.4825	3.2	0.96	2538.1	66.8	2549.7	31.0	2559.0	15.8	2559.0	15.8	99.2	0.8
ELBOW CYN-98	107	175347	1.3	5.8519	0.3	11.6309	0.7	0.4936	0.6	0.92	2586.4	13.4	2575.2	6.4	2566.3	4.4	2566.3	4.4	100.8	-0.8
ELBOW CYN-41	105	22009	1.5	5.8491	2.0	9.6333	6.5	0.4087	6.2	0.95	2208.8	116.1	2400.4	60.0	2567.1	32.9	2567.1	32.9	86.0	14.0
ELBOW CYN-61	71	30877	2.1	5.8439	0.3	11.7624	0.7	0.4985	0.7	0.91	2607.5	14.4	2585.7	6.9	2568.6	5.2	2568.6	5.2	101.5	-1.5
ELBOW CYN-6	256	213608	3.6	5.8077	0.1	11.6767	0.8	0.4918	0.8	0.99	2578.6	16.3	2578.8	7.3	2579.0	1.9	2579.0	1.9	100.0	0.0
ELBOW CYN-95	30	26720	1.2	5.8029	0.7	11.9158	1.8	0.5015	1.7	0.93	2620.2	37.0	2597.8	17.3	2580.4	11.3	2580.4	11.3	101.5	-1.5
ELBOW CYN-122	100	242893	1.4	5.7859	0.3	11.9207	1.8	0.5002	1.7	0.99	2614.8	37.3	2598.2	16.5	2585.3	4.7	2585.3	4.7	101.1	-1.1
ELBOW CYN-141	125	155602	1.1	5.7827	0.2	11.7917	1.0	0.4945	0.9	0.98	2590.3	20.2	2588.0	9.1	2586.2	3.5	2586.2	3.5	100.2	-0.2
ELBOW CYN-87	165	46590	1.2	5.7733	0.2	11.2829	1.2	0.4724	1.1	0.98	2494.2	23.5	2546.8	10.8	2588.9	3.7	2588.9	3.7	96.3	3.7
ELBOW CYN-16	52	59434	1.0	5.7714	0.4	11.8572	0.8	0.4963	0.7	0.85	2598.0	15.0	2593.2	7.7	2589.5	7.3	2589.5	7.3	100.3	-0.3
ELBOW CYN-190	156	87107	1.5	5.7630	0.2	11.2374	0.8	0.4697	0.8	0.98	2482.2	16.9	2543.0	7.8	2591.9	2.7	2591.9	2.7	95.8	4.2
ELBOW CYN-64	75	128520	2.5	5.7490	0.4	12.2629	1.2	0.5113	1.1	0.95	2662.2	24.4	2624.7	11.0	2595.9	5.8	2595.9	5.8	102.6	-2.6
ELBOW CYN-48	124	195222	2.4	5.7408	0.3	11.9358	0.7	0.4970	0.6	0.87	2600.7	12.6	2599.4	6.3	2598.3	5.5	2598.3	5.5	100.1	-0.1
ELBOW CYN-107	151	126046	2.0	5.7366	0.2	12.1065	0.8	0.5037	0.8	0.98	2629.7	16.9	2612.7	7.5	2599.5	2.9	2599.5	2.9	101.2	-1.2
ELBOW CYN-154	178	259440	2.5	5.7321	0.1	11.8304	1.3	0.4918	1.3	0.99	2578.6	26.7	2591.1	11.8	2600.8	2.4	2600.8	2.4	99.1	0.9
ELBOW CYN-144	119	217931	1.6	5.7191	0.3	12.0820	1.0	0.5011	0.9	0.94	2618.7	19.5	2610.8	9.0	2604.6	5.5	2604.6	5.5	100.5	-0.5
ELBOW CYN-136	99	118990	1.6	5.6963	0.2	12.1308	0.8	0.5012	0.8	0.95	2618.8	16.9	2614.6	7.7	2611.3	4.1	2611.3	4.1	100.3	-0.3
ELBOW CYN-19	103	302632	2.0	5.6941	0.3	12.0350	0.8	0.4970	0.8	0.93	2601.0	16.7	2607.1	7.8	2611.9	5.0	2611.9	5.0	99.6	0.4
ELBOW CYN-142	134	170359	2.1	5.6902	0.2	12.1897	0.9	0.5031	0.8	0.97	2626.9	18.1	2619.1	8.1	2613.1	3.4	2613.1	3.4	100.5	-0.5
ELBOW CYN-58	64	106838	1.9	5.6887	0.3	12.3036	1.3	0.5076	1.3	0.98	2646.5	28.7	2627.8	12.6	2613.5	4.4	2613.5	4.4	101.3	-1.3
ELBOW CYN-125	108	85424	0.8	5.6820	0.2	12.2357	0.8	0.5042	0.8	0.97	2631.9	17.1	2622.7	7.6	2615.5	3.2	2615.5	3.2	100.6	-0.6
ELBOW CYN-40	55	36306	1.0	5.6654	0.5	11.9152	1.0	0.4896	0.9	0.84	2568.9	18.1	2597.8	9.5	2620.4	9.1	2620.4	9.1	98.0	2.0
ELBOW CYN-17	86	69707	2.0	5.6453	0.3	12.1406	0.9	0.4971	0.9	0.94	2601.2	18.5	2615.3	8.6	2626.2	5.2	2626.2	5.2	99.0	1.0
ELBOW CYN-37	129	21341	1.0	5.6197	0.5	10.6262	1.2	0.4331	1.1	0.90	2319.7	20.5	2491.0	10.9	2633.8	8.6	2633.8	8.6	88.1	11.9
ELBOW CYN-84	38	95295	1.5	5.5750	0.4	12.6830	1.0	0.5128	0.9	0.91	2668.7	19.1	2656.4	9.0	2647.0	6.5	2647.0	6.5	100.8	-0.8
ELBOW CYN-49	182	100863	1.8	5.5026	0.2	10.9326	1.7	0.4363	1.7	0.99	2334.1	33.1	2517.4	15.9	2668.7	3.8	2668.7	3.8	87.5	12.5
ELBOW CYN-121	83	18363	0.8	5.4836	0.2	12.8950	5.9	0.5128	5.9	1.00	2668.8	128.9	2672.0	55.7	2674.5	4.1	2674.5	4.1	99.8	0.2
ELBOW CYN-79	48	47725	1.4	5.4722	0.3	13.3726	0.9	0.5307	0.9	0.95	2744.5	20.1	2706.3	8.9	2677.9	4.6	2677.9	4.6	102.5	-2.5
ELBOW CYN-50	172	18920	1.4	5.4647	0.1	12.4888	1.0	0.4950	1.0	0.99	2592.2	21.5	2641.9	9.6	2680.2	2.5	2680.2	2.5	96.7	3.3
ELBOW CYN-179	75	56851	1.2	5.4589	0.5	13.0061	0.8	0.5149	0.7	0.83	2677.6	15.3	2680.1	7.9	2681.9	7.7	2681.9	7.7	99.8	0.2

U-Pb Geochronologic anlayses of selected Harmony Formation strata

				Isotope ratios								Apparent ages (Ma)							
	U	206Pb	U/Th	206Pb*	±	207Pb*	±	206Pb*	±	error	206Pb*	±	207Pb*	±	206Pb*	±	Best age	±	Conc.	Discor.
	(ppm)	204Pb		207Pb*	(%)	235U*	(%)	238U	(%)	corr.	238U*	(Ma)	235U	(Ma)	207Pb*	(Ma)	(Ma)	(Ma)	(%)	(%)
Sample: Elbow Canyon. Location: Elbow Canyon, Sonoma Range; 0441026 4514450 (NAD 83 UTM 11T)																				
ELBOW CYN-72	79	100089	0.9	5.4353	0.3	13.2192	0.5	0.5211	0.4	0.83	2703.9	9.7	2695.4	4.9	2689.1	4.8	2689.1	4.8	100.6	-0.6
ELBOW CYN-96	20	39801	0.8	5.4294	0.7	13.2444	1.3	0.5215	1.1	0.85	2705.7	25.2	2697.2	12.7	2690.9	11.8	2690.9	11.8	100.6	-0.6
ELBOW CYN-134	15	40812	0.8	5.4250	1.1	13.3400	1.5	0.5249	1.0	0.68	2719.8	22.1	2704.0	13.9	2692.2	17.9	2692.2	17.9	101.0	-1.0
ELBOW CYN-97	21	26060	1.7	5.3978	1.1	13.4605	1.4	0.5270	0.8	0.62	2728.6	18.6	2712.5	12.8	2700.5	17.5	2700.5	17.5	101.0	-1.0
ELBOW CYN-152	29	27819	2.8	5.3969	2.7	14.0342	3.1	0.5493	1.6	0.52	2822.4	36.9	2752.0	29.7	2700.8	44.3	2700.8	44.3	104.5	-4.5
ELBOW CYN-38	13	34636	0.7	5.3923	1.9	13.2394	2.2	0.5178	1.2	0.52	2689.7	25.5	2696.9	21.1	2702.2	31.6	2702.2	31.6	99.5	0.5
ELBOW CYN-30	132	322942	0.8	5.3881	0.2	13.2659	0.8	0.5184	0.7	0.98	2692.4	16.2	2698.8	7.1	2703.5	2.6	2703.5	2.6	99.6	0.4
ELBOW CYN-13	21	43739	0.9	5.3684	1.6	12.8093	2.3	0.4987	1.7	0.72	2608.4	35.6	2665.7	21.7	2709.5	26.2	2709.5	26.2	96.3	3.7
ELBOW CYN-28	22	42263	1.2	5.3488	1.4	13.8035	2.3	0.5355	1.9	0.81	2764.5	42.4	2736.3	22.1	2715.6	22.8	2715.6	22.8	101.8	-1.8
ELBOW CYN-191	19	33098	1.0	5.3417	0.6	13.5470	1.3	0.5248	1.2	0.91	2719.7	26.9	2718.6	12.7	2717.8	9.3	2717.8	9.3	100.1	-0.1
ELBOW CYN-150	108	127157	0.8	5.3248	0.1	13.5966	0.8	0.5251	0.8	0.99	2720.7	18.4	2722.0	7.9	2723.0	2.0	2723.0	2.0	99.9	0.1
ELBOW CYN-82	152	20635	0.6	5.1931	0.2	13.9427	0.9	0.5251	0.8	0.96	2720.9	18.5	2745.8	8.2	2764.2	4.0	2764.2	4.0	98.4	1.6
ELBOW CYN-3	130	313414	0.8	4.9648	0.2	15.5384	0.5	0.5595	0.5	0.95	2864.6	11.9	2848.6	5.2	2837.7	2.7	2837.7	2.7	100.9	-0.9
ELBOW CYN-153	12	19658	1.3	4.9147	1.2	15.4135	1.3	0.5494	0.6	0.49	2822.7	14.8	2841.1	12.6	2854.2	18.7	2854.2	18.7	98.9	1.1
ELBOW CYN-126	72	26451	1.2	4.8616	0.5	14.9380	2.0	0.5267	1.9	0.97	2727.6	42.8	2811.3	18.8	2871.9	7.4	2871.9	7.4	95.0	5.0
ELBOW CYN-80	85	97530	1.0	4.7964	0.2	16.2022	3.6	0.5636	3.6	1.00	2881.6	84.2	2888.8	34.7	2893.8	3.6	2893.8	3.6	99.6	0.4
ELBOW CYN-75	100	119046	0.8	4.6187	0.2	17.1784	0.7	0.5754	0.6	0.95	2930.1	14.9	2944.8	6.4	2954.9	3.5	2954.9	3.5	99.2	0.8
ELBOW CYN-157	27	30847	1.5	3.7066	0.4	24.7610	1.0	0.6657	0.9	0.91	3289.1	24.1	3298.8	10.0	3304.8	6.7	3304.8	6.7	99.5	0.5

Notes:

1. Analyses with >10% uncertainty (1-sigma) in 206Pb/238U age are not included.
2. Analyses with >10% uncertainty (1-sigma) in 206Pb/207Pb age are not included, unless 206Pb/238U age is <500 Ma.
3. Best age is determined from 206Pb/238U age for analyses with 206Pb/238U age <1000 Ma and from 206Pb/207Pb age for analyses with 206Pb/238Uage > 1000 Ma.
4. Concordance is based on 206Pb/238U age / 206Pb/207Pb age. Value is not reported for 206Pb/238U ages <500 Ma because of large uncertainty in 206Pb/207Pb age.
5. Discordance is 100% - concordance.
6. Analyses with 206Pb/238U age > 500 Ma and with >20% discordance (<80% concordance) are not included.
7. Analyses with 206Pb/238U age > 500 Ma and with >5% reverse discordance (<105% concordance) are not included.
8. All uncertainties are reported at the 1-sigma level, and include only measurement errors.
9. External (systematic) errors are shown as 206Pb/238U uncertainty, 206Pb/207Pb uncertainty to the right of each sample (in %, at 2-sigma level).
10. Analyses conducted by LA-MC-ICPMS, as described by Gehrels et al. (2008).
11. U concentration and U/Th are calibrated relative to Sri Lanka zircon standard and are accurate to ~20%.
12. Common Pb correction is from measured 204Pb with common Pb composition interpreted from Stacey and Kramers (1975).
13. Uncertainties of 1.5 for 206Pb/204Pb, 0.3 for 207Pb/ 204Pb, and 2.0 for 208Pb/ 204Pb are applied to common Pb composition.
14. U/Pb and 206Pb/207Pb fractionation is calibrated relative to fragments of a large Sri Lanka zircon of 563.5 ± 3.2 Ma (2-sigma).
15. U decay constants and composition as follows: 235U = 9.8485 x 10-10, 238U = 1.55125 x 10-10, 238U/235U = 137.88.
16. Weighted mean and concordia plots determined with Isoplot (Ludwig, 2008).
17. Analytical methods as described by Gehrels and Pecha (2014).

APPENDIX F

Hafnium isotope data of selected Harmony Formation strata

Table notes are at the end of the appendix.

	(^{176}Yb + ^{176}Lu) / ^{176}Hf (%)	Volts Hf	^{176}Hf/^{177}Hf	± (1s)	^{176}Lu/^{177}Hf	^{176}Hf/^{177}Hf (T)	E-Hf (0)	E-Hf (0) ± (1s)	E-Hf (T)	Age (Ma)
Sample: LCC #1. Location: Little Cottonwood Canyon, Galena Range; 0490600 4494792 (NAD 83 UTM 11T)										
LCC1-88-RM15-61	15.3	4.1	0.282381	0.000037	0.00081	0.282371	-14.3	1.3	0.4	673
LCC1-88-RM15-137	13.1	3.9	0.282213	0.000037	0.00074	0.282204	-20.2	1.3	-5.3	682
LCC1-88-RM15-127	7.6	4.2	0.282300	0.000026	0.00043	0.282294	-17.2	0.9	-1.6	705
LCC1-88-RM15-93	7.8	4.3	0.282392	0.000031	0.00044	0.282386	-13.9	1.1	1.9	717
LCC1-88-RM15-152	12.2	5.7	0.282285	0.000029	0.00072	0.282271	-17.7	1.0	4.9	1029
LCC1-88-RM15-190	6.7	5.3	0.282195	0.000025	0.00040	0.282187	-20.9	0.9	1.9	1031
LCC1-88-RM15-130	9.0	6.1	0.282255	0.000027	0.00053	0.282245	-18.7	0.9	4.5	1053
LCC1-88-RM15-157	17.4	5.3	0.282280	0.000026	0.00104	0.282259	-17.9	0.9	5.4	1070
LCC1-88-RM15-139	13.8	6.1	0.282308	0.000030	0.00079	0.282292	-16.9	1.1	6.6	1071
LCC1-88-RM15-110	9.0	5.4	0.282308	0.000020	0.00051	0.282298	-16.9	0.7	6.8	1073
LCC1-88-RM15-62	11.3	4.8	0.282303	0.000027	0.00069	0.282289	-17.0	0.9	6.6	1075
LCC1-88-RM15-133	42.4	7.2	0.282361	0.000029	0.00265	0.282306	-15.0	1.0	7.5	1089
LCC1-88-RM15-192	16.2	5.2	0.282387	0.000032	0.00093	0.282368	-14.1	1.1	9.7	1091
LCC1-88-RM15-32	9.1	5.2	0.282311	0.000039	0.00053	0.282300	-16.7	1.4	7.3	1091
LCC1-88-RM15-149	16.0	4.7	0.282378	0.000036	0.00084	0.282361	-14.4	1.3	9.5	1091
LCC1-88-RM15-7	17.1	5.7	0.282326	0.000028	0.00102	0.282305	-16.2	1.0	7.5	1092
LCC1-88-RM15-95	23.8	4.8	0.282291	0.000031	0.00134	0.282263	-17.5	1.1	6.3	1106
LCC1-88-RM15-36	8.0	5.8	0.282358	0.000033	0.00049	0.282347	-15.1	1.2	9.4	1108
LCC1-88-RM15-3	20.8	4.2	0.282321	0.000034	0.00119	0.282296	-16.4	1.2	7.6	1108
LCC1-88-RM15-162	14.4	6.7	0.282299	0.000022	0.00081	0.282282	-17.2	0.8	7.1	1109
LCC1-88-RM15-86	5.9	4.8	0.282367	0.000030	0.00045	0.282357	-14.8	1.1	10.2	1129
LCC1-88-RM15-79	19.2	4.9	0.282194	0.000024	0.00108	0.282171	-20.9	0.9	3.6	1129
LCC1-88-RM15-10	14.1	5.0	0.282225	0.000026	0.00086	0.282206	-19.8	0.9	5.4	1153
LCC1-88-RM15-80	9.6	2.8	0.282166	0.000032	0.00060	0.282153	-21.9	1.1	3.6	1154
LCC1-88-RM15-13	18.4	4.7	0.282283	0.000028	0.00109	0.282258	-17.8	1.0	8.0	1187
LCC1-88-RM15-30	8.9	5.9	0.282159	0.000022	0.00056	0.282146	-22.1	0.8	4.1	1190
LCC1-88-RM15-57	11.5	5.0	0.282272	0.000032	0.00072	0.282256	-18.1	1.1	8.5	1213
LCC1-88-RM15-67	40.1	3.1	0.282289	0.000040	0.00196	0.282240	-17.6	1.4	10.3	1313
LCC1-88-RM15-75	10.2	5.8	0.282142	0.000020	0.00058	0.282128	-22.7	0.7	7.1	1350
LCC1-88-RM15-45	17.9	5.1	0.282211	0.000028	0.00105	0.282184	-20.3	1.0	9.5	1369
LCC1-88-RM15-174	14.5	4.3	0.282177	0.000026	0.00090	0.282154	-21.5	0.9	8.5	1370
LCC1-88-RM15-188	14.7	6.2	0.282015	0.000023	0.00087	0.281990	-27.2	0.8	4.9	1468
LCC1-88-RM15-165	11.7	5.6	0.282036	0.000024	0.00073	0.282015	-26.5	0.8	5.9	1471
LCC1-88-RM15-103	12.1	5.0	0.281911	0.000019	0.00078	0.281887	-30.9	0.7	5.8	1668
LCC1-88-RM15-175	9.5	3.2	0.282344	0.000027	0.00057	0.282325	-15.6	0.9	22.7	1724
LCC1-88-RM15-94	19.2	4.5	0.282006	0.000029	0.00112	0.281969	-27.5	1.0	10.3	1736
LCC1-88-RM15-153	11.7	5.4	0.280939	0.000027	0.00076	0.280902	-65.3	1.0	-8.7	2549
Sample: LCC #2. Location: Little Cottonwood Canyon, Galena Range; 0490529 4495008 (NAD 83 UTM 11T)										
LCC2-H971-121	13.7	4.7	0.282352	0.000021	0.00076	0.282337	-15.3	0.7	6.8	1009
LCC2-H971-91	12.4	5.6	0.282246	0.000022	0.00072	0.282232	-19.0	0.8	3.5	1027
LCC2-H971-39	22.1	3.9	0.282344	0.000023	0.00128	0.282319	-15.6	0.8	6.8	1040
LCC2-H971-3	8.5	4.3	0.282266	0.000021	0.00050	0.282257	-18.3	0.7	4.7	1044
LCC2-H971-36	7.9	4.4	0.282338	0.000023	0.00046	0.282329	-15.8	0.8	7.5	1055
LCC2-H971-29	13.3	4.1	0.282296	0.000025	0.00077	0.282280	-17.3	0.9	6.0	1064
LCC2-H971-49	23.8	3.7	0.282353	0.000026	0.00138	0.282325	-15.3	0.9	7.8	1073
LCC2-H971-27	12.4	4.1	0.282343	0.000028	0.00071	0.282329	-15.6	1.0	8.0	1076
LCC2-H971-63	22.5	4.0	0.282260	0.000027	0.00128	0.282234	-18.6	0.9	4.9	1088
LCC2-H971-28	15.9	4.2	0.282291	0.000023	0.00089	0.282273	-17.5	0.8	6.4	1093
LCC2-H971-34	10.9	4.7	0.282352	0.000022	0.00067	0.282338	-15.3	0.8	8.9	1103
LCC2-H971-20	14.6	5.2	0.282201	0.000018	0.00085	0.282183	-20.7	0.6	3.5	1105
LCC2-H971-51	17.4	4.6	0.282296	0.000024	0.00095	0.282276	-17.3	0.8	7.0	1116
LCC2-H971-131	17.3	6.4	0.282340	0.000016	0.00097	0.282320	-15.7	0.6	8.7	1122
LCC2-H971-134	19.4	4.7	0.282351	0.000022	0.00113	0.282327	-15.3	0.8	9.2	1133
LCC2-H971-8	17.7	4.7	0.282138	0.000022	0.00106	0.282115	-22.9	0.8	2.0	1146
LCC2-H971-72	19.6	5.4	0.282292	0.000017	0.00122	0.282265	-17.4	0.6	7.5	1152
LCC2-H971-33	26.2	4.1	0.282186	0.000026	0.00151	0.282152	-21.2	0.9	3.6	1157
LCC2-H971-6	26.8	5.5	0.282248	0.000019	0.00164	0.282213	-19.0	0.7	5.7	1158
LCC2-H971-42	31.5	4.0	0.282262	0.000026	0.00181	0.282222	-18.5	0.9	6.3	1167
LCC2-H971-37	40.1	3.0	0.282266	0.000032	0.00199	0.282222	-18.4	1.1	6.3	1169
LCC2-H971-68	10.0	5.8	0.282121	0.000017	0.00057	0.282109	-23.5	0.6	2.6	1184
LCC2-H971-65	15.3	5.2	0.282277	0.000021	0.00094	0.282255	-18.0	0.7	8.6	1216
LCC2-H971-98	62.7	3.3	0.282377	0.000033	0.00333	0.282300	-14.4	1.2	10.5	1233
LCC2-H971-79	5.3	4.5	0.282241	0.000019	0.00033	0.282233	-19.2	0.7	8.6	1253
LCC2-H971-26	5.2	4.5	0.282116	0.000018	0.00032	0.282108	-23.7	0.6	4.5	1265
LCC2-H971-92	29.3	4.9	0.282251	0.000025	0.00154	0.282213	-18.9	0.9	9.7	1333
LCC2-H971-77	18.5	4.3	0.282150	0.000022	0.00104	0.282124	-22.4	0.8	6.7	1338
LCC2-H971-44	23.3	4.3	0.282094	0.000024	0.00150	0.282055	-24.5	0.8	4.9	1368
LCC2-H971-67	28.6	3.9	0.282176	0.000025	0.00169	0.282132	-21.5	0.9	7.9	1378
LCC2-H971-70	23.4	4.3	0.282215	0.000023	0.00129	0.282181	-20.2	0.8	9.8	1385
LCC2-H971-84	14.3	5.1	0.282194	0.000019	0.00090	0.282171	-20.9	0.7	9.5	1387
LCC2-H971-14	18.1	4.9	0.282107	0.000025	0.00110	0.282076	-24.0	0.9	7.7	1456
LCC2-H971-23	10.7	4.9	0.282121	0.000022	0.00072	0.282101	-23.5	0.8	8.7	1461
LCC2-H971-41	16.4	4.7	0.282127	0.000020	0.00097	0.282100	-23.3	0.7	8.8	1469
LCC2-H971-19	43.4	5.6	0.282109	0.000019	0.00256	0.282037	-23.9	0.7	6.9	1482
LCC2-H971-24	13.2	4.8	0.281328	0.000020	0.00093	0.281296	-51.5	0.7	-12.4	1786
LCC2-H971-69	19.4	4.9	0.281902	0.000019	0.00119	0.281861	-31.2	0.7	7.8	1794
LCC2-H971-48	7.9	4.8	0.281207	0.000021	0.00051	0.281180	-55.8	0.7	4.4	2687

Hafnium isotope data of selected Harmony Formation strata

	$(^{176}Yb + ^{176}Lu) / ^{176}Hf$ (%)	Volts Hf	$^{176}Hf/^{177}Hf$	± (1s)	$^{176}Lu/^{177}Hf$	$^{176}Hf/^{177}Hf$ (T)	E-Hf (0)	E-Hf (0) ± (1s)	E-Hf (T)	Age (Ma)
Sample: LCC #3. Location: Little Cottonwood Canyon, Galena Range; 0490459 4494916 (NAD 83 UTM 11T)										
LCC3-H973-1	8.3	5.4	0.281539	0.000017	0.00055	0.281519	-44.1	0.6	-2.5	1871
LCC3-H973-2	38.9	4.2	0.281556	0.000029	0.00242	0.281474	-43.5	1.0	-6.6	1765
LCC3-H973-4	8.4	5.0	0.281215	0.000018	0.00055	0.281186	-55.5	0.6	5.7	2735
LCC3-H973-49	11.3	5.2	0.281586	0.000018	0.00062	0.281565	-42.4	0.6	-2.9	1786
LCC3-H973-58	18.2	4.3	0.281943	0.000022	0.00107	0.281907	-29.8	0.8	9.0	1775
LCC3-H973-90	10.4	4.4	0.281500	0.000024	0.00062	0.281478	-45.4	0.8	-4.4	1852
LCC3-H973-86	6.7	5.0	0.281209	0.000020	0.00040	0.281188	-55.7	0.7	3.0	2614
LCC3-H973-88	18.1	5.2	0.281230	0.000019	0.00111	0.281192	-55.0	0.7	-15.9	1793
LCC3-H973-115	15.8	3.6	0.281227	0.000022	0.00097	0.281177	-55.1	0.8	4.0	2673
LCC3-H973-37	8.0	5.3	0.280842	0.000016	0.00048	0.280817	-68.7	0.6	-7.9	2712
LCC3-H973-33	10.1	5.1	0.281244	0.000017	0.00060	0.281214	-54.5	0.6	3.9	2612
LCC3-H973-34	9.6	5.1	0.281281	0.000018	0.00058	0.281261	-53.2	0.6	-13.5	1793
LCC3-H973-27	11.0	4.2	0.281158	0.000021	0.00068	0.281123	-57.5	0.7	2.5	2693
LCC3-H973-26	17.6	2.3	0.281784	0.000047	0.00116	0.281745	-35.4	1.7	3.5	1787
LCC3-H973-30	29.2	4.4	0.281078	0.000025	0.00164	0.280995	-60.4	0.9	-3.0	2652
LCC3-H973-9	2.8	5.0	0.281089	0.000019	0.00020	0.281079	-60.0	0.7	0.8	2688
LCC3-H973-8	8.9	5.0	0.281568	0.000017	0.00057	0.281549	-43.0	0.6	-3.1	1801
LCC3-H973-7	9.6	6.1	0.281182	0.000016	0.00053	0.281155	-56.7	0.6	1.3	2593
LCC3-H973-10	11.3	5.9	0.281623	0.000018	0.00074	0.281598	-41.1	0.7	-1.7	1787
LCC3-H973-11	8.3	4.8	0.281506	0.000019	0.00051	0.281488	-45.2	0.7	-3.8	1864
LCC3-H973-53	12.3	4.0	0.281520	0.000022	0.00089	0.281489	-44.7	0.8	-4.2	1843
LCC3-H973-15	7.7	4.8	0.281526	0.000016	0.00050	0.281509	-44.5	0.6	-3.8	1832
LCC3-H973-21	11.8	5.2	0.281775	0.000016	0.00069	0.281750	-35.7	0.6	5.2	1852
LCC3-H973-20	10.8	4.9	0.281251	0.000016	0.00064	0.281219	-54.3	0.6	3.5	2590
LCC3-H973-25	9.7	5.7	0.281082	0.000014	0.00056	0.281063	-60.2	0.5	-19.8	1827
LCC3-H973-70	11.6	5.1	0.281149	0.000017	0.00070	0.281112	-57.9	0.6	2.7	2718
LCC3-H973-71	15.1	4.8	0.281630	0.000020	0.00085	0.281601	-40.8	0.7	-1.5	1791
LCC3-H973-73	13.1	3.8	0.281554	0.000021	0.00079	0.281527	-43.5	0.7	-4.5	1771
LCC3-H973-74	13.9	4.5	0.281227	0.000021	0.00084	0.281186	-55.1	0.8	2.7	2608
LCC3-H973-96	24.4	4.4	0.281501	0.000021	0.00142	0.281451	-45.4	0.7	-5.3	1856
Sample: LCC #4. Location: Little Cottonwood Canyon, Galena Range; 0490623 4494977 (NAD 83 UTM 11T)										
LCC4-88RMA13-1	11.1	5.0	0.281525	0.000022	0.00063	0.281503	-44.6	0.8	-5.0	1787
LCC4-88RMA13-2	18.4	4.2	0.281891	0.000021	0.00112	0.281851	-31.6	0.7	9.2	1867
LCC4-88RMA13-22	13.5	4.6	0.281213	0.000020	0.00079	0.281174	-55.6	0.7	1.8	2587
LCC4-88RMA13-23	7.6	4.8	0.281680	0.000023	0.00043	0.281666	-39.1	0.8	0.7	1783
LCC4-88RMA13-24	8.0	4.3	0.281378	0.000019	0.00046	0.281362	-49.8	0.7	-10.4	1773
LCC4-88RMA13-152	7.5	4.2	0.281844	0.000021	0.00045	0.281828	-33.3	0.7	8.4	1870
LCC4-88RMA13-11	4.2	4.5	0.281024	0.000021	0.00023	0.281013	-62.3	0.7	-3.9	2586
LCC4-88RMA13-16	9.3	4.4	0.281166	0.000020	0.00060	0.281135	-57.2	0.7	3.0	2693
LCC4-88RMA13-17	8.5	5.1	0.281788	0.000020	0.00049	0.281771	-35.3	0.7	4.4	1784
LCC4-88RMA13-189	13.3	4.4	0.281448	0.000022	0.00068	0.281424	-47.3	0.8	-6.3	1856
LCC4-88RMA13-48	19.5	4.8	0.281793	0.000020	0.00107	0.281757	-35.1	0.7	3.7	1774
LCC4-88RMA13-44	13.4	4.5	0.281247	0.000018	0.00069	0.281213	-54.4	0.6	3.2	2586
LCC4-88RMA13-42	8.7	2.9	0.281210	0.000035	0.00056	0.281192	-55.7	1.2	-16.6	1766
LCC4-88RMA13-126	14.9	0.4	0.281312	0.000062	0.00102	0.281262	-52.1	2.2	4.7	2576
LCC4-88RMA13-35	1.8	4.6	0.281824	0.000022	0.00013	0.281819	-34.0	0.8	7.8	1857
LCC4-88RMA13-37	13.8	5.5	0.281269	0.000018	0.00080	0.281242	-53.6	0.6	-14.7	1770
LCC4-88RMA13-38	28.5	5.1	0.281778	0.000020	0.00149	0.281728	-35.6	0.7	2.2	1756
LCC4-88RMA13-39	9.2	4.7	0.281510	0.000020	0.00052	0.281493	-45.1	0.7	-5.7	1776
LCC4-88RMA13-181	18.1	5.5	0.281676	0.000020	0.00102	0.281641	-39.2	0.7	-0.2	1785
LCC4-88RMA13-177	13.6	4.1	0.281541	0.000020	0.00077	0.281515	-44.0	0.7	-4.9	1777
LCC4-88RMA13-109	9.5	5.0	0.281609	0.000018	0.00065	0.281587	-41.6	0.6	-1.2	1825
LCC4-88RMA13-170	11.2	4.4	0.281659	0.000023	0.00066	0.281636	-39.8	0.8	-0.4	1783
LCC4-88RMA13-192	10.1	4.2	0.281207	0.000022	0.00067	0.281174	-55.8	0.8	1.6	2578
LCC4-88RMA13-111	18.8	4.4	0.281560	0.000022	0.00113	0.281521	-43.3	0.8	-3.4	1831
LCC4-88RMA13-118	11.2	5.2	0.281221	0.000017	0.00069	0.281186	-55.3	0.6	4.6	2686
LCC4-88RMA13-126	20.2	4.3	0.281189	0.000022	0.00115	0.281133	-56.4	0.8	0.1	2576
LCC4-88RMA13-197	9.9	4.6	0.281677	0.000020	0.00056	0.281658	-39.2	0.7	0.4	1784
Sample: LCC #9. Location: Little Cottonwood Canyon, Galena Range; 0491232 4495602 (NAD 83 UTM 11T)										
1312-LCC-09HA-9	14.3	5.2	0.281550	0.000024	0.00078	0.281525	-43.7	0.8	-5.4	1736
1312-LCC-09HA-51	19.6	5.6	0.281600	0.000018	0.00113	0.281562	-41.9	0.6	-3.7	1754
1312-LCC-09HA-12	10.1	5.1	0.281544	0.000020	0.00060	0.281524	-43.9	0.7	-4.7	1768
1312-LCC-09HA-37	9.7	4.6	0.281399	0.000022	0.00057	0.281380	-49.0	0.8	-9.8	1771
1312-LCC-09HA-2	12.6	5.1	0.281527	0.000024	0.00074	0.281502	-44.5	0.8	-5.3	1776
1312-LCC-09HA-14	9.3	5.3	0.281552	0.000018	0.00055	0.281533	-43.6	0.6	-4.0	1784
1312-LCC-09HA-20	16.7	6.1	0.281604	0.000016	0.00098	0.281571	-41.8	0.6	-2.5	1791
1312-LCC-09HA-8	10.9	5.0	0.281567	0.000016	0.00065	0.281545	-43.1	0.6	-3.4	1793
1312-LCC-09HA-38	8.7	5.5	0.281600	0.000021	0.00052	0.281582	-41.9	0.8	-2.0	1798
1312-LCC-09HA-50	13.2	5.2	0.281576	0.000019	0.00076	0.281550	-42.7	0.7	-3.1	1798
1312-LCC-09HA-31	10.1	5.0	0.281553	0.000018	0.00064	0.281531	-43.6	0.6	-3.7	1802
1312-LCC-09HA-34	10.5	3.3	0.281579	0.000028	0.00065	0.281556	-42.7	1.0	-2.7	1805
1312-LCC-09HA-55	19.4	4.2	0.281828	0.000029	0.00107	0.281791	-33.9	1.0	6.2	1833
1312-LCC-09HA-44	13.5	4.3	0.281438	0.000020	0.00081	0.281410	-47.6	0.7	-7.1	1841
1312-LCC-09HA-3	16.4	5.1	0.281828	0.000022	0.00097	0.281793	-33.9	0.8	6.7	1851
1312-LCC-09HA-42	14.3	4.6	0.281942	0.000019	0.00096	0.281908	-29.8	0.7	11.1	1862
1312-LCC-09HA-4	14.8	4.2	0.281451	0.000025	0.00091	0.281418	-47.2	0.9	-6.3	1863
1312-LCC-09HA-28	5.4	4.7	0.281834	0.000021	0.00034	0.281822	-33.6	0.7	8.2	1870
1312-LCC-09HA-84	11.0	5.1	0.281862	0.000022	0.00072	0.281836	-32.6	0.8	9.0	1885
1312-LCC-09HA-89	5.9	5.1	0.281875	0.000023	0.00036	0.281862	-32.2	0.8	10.3	1898
1312-LCC-09HA-82	3.8	2.7	0.281187	0.000027	0.00025	0.281175	-56.5	1.0	-0.3	2492
1312-LCC-09HA-71	8.1	5.4	0.281232	0.000016	0.00049	0.281207	-54.9	0.6	3.8	2620
1312-LCC-09HA-19	28.4	3.6	0.281313	0.000030	0.00164	0.281230	-52.1	1.1	4.8	2626
1312-LCC-09HA-1	11.1	4.9	0.281039	0.000020	0.00067	0.281004	-61.8	0.7	-1.1	2720

Hafnium isotope data of selected Harmony Formation strata

	$(^{176}Yb + ^{176}Lu) / ^{176}Hf$ (%)	Volts Hf	$^{176}Hf/^{177}Hf$	± (1s)	$^{176}Lu/^{177}Hf$	$^{176}Hf/^{177}Hf$ (T)	E-Hf (0)	E-Hf (0) ± (1s)	E-Hf (T)	Age (Ma)
Sample: LCC #10. Location: Little Cottonwood Canyon, Galena Range; 0490510 4495682 (NAD 83 UTM 11T)										
LCC-10HQ-7	13.1	5.7	0.282309	0.000020	0.00080	0.282293	-16.8	0.7	6.4	1064
LCC-10HQ-8	29.9	3.3	0.282055	0.000026	0.00185	0.282004	-25.8	0.9	5.2	1460
LCC-10HQ-9	32.6	2.6	0.282360	0.000031	0.00202	0.282320	-15.0	1.1	7.2	1057
LCC-10HQ-10	16.6	2.7	0.282160	0.000038	0.00107	0.282132	-22.1	1.3	8.3	1396
LCC-10HQ-12	14.3	2.6	0.282325	0.000030	0.00085	0.282306	-16.3	1.0	9.6	1183
LCC-10HQ-11	35.5	2.6	0.282188	0.000027	0.00211	0.282135	-21.1	1.0	6.8	1325
LCC-10HQ-90	9.5	4.1	0.282171	0.000021	0.00072	0.282152	-21.7	0.7	9.1	1399
LCC-10HQ-86	12.7	0.4	0.282394	0.000083	0.00115	0.282361	-13.8	2.9	18.7	1493
LCC-10HQ-45	19.9	3.8	0.282013	0.000027	0.00120	0.281986	-27.3	1.0	-0.9	1221
LCC-10HQ-99	15.3	2.6	0.282252	0.000029	0.00087	0.282232	-18.9	1.0	6.6	1164
LCC-10HQ-100	18.2	3.2	0.282278	0.000031	0.00108	0.282256	-17.9	1.1	5.9	1097
LCC-10HQ-96	10.2	2.9	0.281761	0.000023	0.00063	0.281741	-36.2	0.8	2.1	1729
LCC-10HQ-95	21.2	2.8	0.282253	0.000032	0.00130	0.282224	-18.8	1.1	6.1	1158
LCC-10HQ-93	11.3	3.2	0.281040	0.000024	0.00069	0.281005	-61.7	0.8	-1.5	2700
LCC-10HQ-16	16.4	1.2	0.282849	0.000098	0.00400	0.282774	2.3	3.5	22.0	996
LCC-10HQ-17	20.4	4.4	0.281904	0.000025	0.00128	0.281878	-31.2	0.9	-8.1	1072
LCC-10HQ-18	13.5	5.3	0.282292	0.000021	0.00080	0.282277	-17.4	0.8	4.5	1003
LCC-10HQ-19	16.3	3.2	0.282387	0.000027	0.00093	0.282367	-14.1	1.0	10.9	1146
LCC-10HQ-20	6.7	3.0	0.281528	0.000023	0.00044	0.281513	-44.4	0.8	-4.5	1797
LCC-10HQ-79	20.5	5.7	0.282277	0.000018	0.00116	0.282250	-18.0	0.6	8.2	1209
LCC-10HQ-77	23.7	3.4	0.281867	0.000024	0.00136	0.281823	-32.5	0.9	4.3	1700
LCC-10HQ-39	9.9	6.4	0.281794	0.000019	0.00063	0.281772	-35.1	0.7	4.9	1803
LCC-10HQ-1	16.6	3.6	0.282336	0.000024	0.00098	0.282315	-15.9	0.8	8.8	1134
LCC-10HQ-2	9.9	2.2	0.281206	0.000032	0.00065	0.281173	-55.8	1.1	3.5	2660
LCC-10HQ-3	6.2	4.6	0.282332	0.000022	0.00044	0.282324	-16.0	0.8	6.7	1027
LCC-10HQ-4	12.2	5.3	0.281949	0.000019	0.00078	0.281928	-29.6	0.7	2.5	1460
LCC-10HQ-5	22.0	0.6	0.282171	0.000091	0.00157	0.282127	-21.7	3.2	10.1	1483
Sample: Harmony Canyon. Location: Harmony Canyon, Sonoma Range; 0446225 4533064 (NAD 83 UTM 11T)										
HARM-CYN-143	16.4	5.4	0.281662	0.000027	0.00089	0.281633	-39.7	1.0	-1.3	1750
HARM-CYN-126	38.8	5.4	0.281693	0.000028	0.00210	0.281623	-38.6	1.0	-1.4	1762
HARM-CYN-17	9.1	3.7	0.281588	0.000037	0.00059	0.281568	-42.3	1.3	-3.0	1773
HARM-CYN-19	16.6	3.0	0.281565	0.000039	0.00098	0.281532	-43.2	1.4	-4.3	1775
HARM-CYN-146	11.4	5.2	0.281580	0.000033	0.00069	0.281557	-42.6	1.2	-3.4	1776
HARM-CYN-134	7.3	5.0	0.281592	0.000026	0.00044	0.281577	-42.2	0.9	-2.6	1777
HARM-CYN-94	14.1	4.7	0.281449	0.000028	0.00087	0.281420	-47.2	1.0	-8.2	1778
HARM-CYN-129	14.4	5.0	0.281737	0.000034	0.00093	0.281706	-37.1	1.2	2.1	1784
HARM-CYN-59	8.4	5.3	0.281591	0.000026	0.00050	0.281574	-42.2	0.9	-2.6	1785
HARM-CYN-32	13.1	5.2	0.281607	0.000030	0.00077	0.281581	-41.6	1.1	-2.3	1785
HARM-CYN-46	8.5	5.9	0.281554	0.000025	0.00049	0.281538	-43.5	0.9	-3.8	1788
HARM-CYN-58	12.4	4.8	0.281522	0.000030	0.00072	0.281498	-44.6	1.1	-5.2	1788
HARM-CYN-89	9.7	4.6	0.281580	0.000034	0.00064	0.281559	-42.6	1.2	-3.0	1788
HARM-CYN-169	11.9	4.5	0.281500	0.000029	0.00072	0.281475	-45.5	1.0	-6.0	1788
HARM-CYN-78	10.7	5.8	0.281764	0.000026	0.00067	0.281741	-36.1	0.9	4.1	1818
HARM-CYN-187	20.0	5.9	0.281518	0.000034	0.00124	0.281475	-44.8	1.2	-5.1	1827
HARM-CYN-117	49.9	4.2	0.281923	0.000037	0.00275	0.281827	-30.5	1.3	7.5	1832
HARM-CYN-115	7.1	4.7	0.281872	0.000020	0.00048	0.281856	-32.3	0.7	8.5	1833
HARM-CYN-121	3.6	4.4	0.281070	0.000028	0.00026	0.281061	-60.6	1.0	-19.5	1842
HARM-CYN-130	5.3	2.8	0.281553	0.000043	0.00037	0.281540	-43.6	1.5	-2.3	1847
HARM-CYN-35	11.5	2.9	0.281824	0.000035	0.00069	0.281800	-34.0	1.2	6.9	1849
HARM-CYN-111	9.0	4.5	0.281855	0.000027	0.00051	0.281837	-32.9	1.0	8.3	1850
HARM-CYN-68	17.1	4.6	0.281512	0.000029	0.00102	0.281476	-45.0	1.0	-4.5	1850
HARM-CYN-64	12.8	5.1	0.281460	0.000025	0.00078	0.281432	-46.9	0.9	-5.7	1867
HARM-CYN-195	11.0	3.9	0.281456	0.000034	0.00069	0.281431	-47.0	1.2	-5.7	1868
HARM-CYN-62	15.6	4.4	0.281815	0.000027	0.00104	0.281778	-34.3	0.9	6.6	1868
HARM-CYN-107	20.9	4.8	0.281574	0.000024	0.00126	0.281529	-42.8	0.8	-2.1	1873
HARM-CYN-105	14.6	2.5	0.281891	0.000034	0.00094	0.281858	-31.6	1.2	9.6	1875
HARM-CYN-135	5.8	6.0	0.281182	0.000026	0.00033	0.281167	-56.7	0.9	-1.5	2453
HARM-CYN-11	13.1	2.8	0.281184	0.000039	0.00077	0.281146	-56.6	1.4	0.9	2591
HARM-CYN-162	22.1	5.0	0.281243	0.000039	0.00143	0.281171	-54.5	1.4	2.3	2612
HARM-CYN-37	14.2	3.0	0.281162	0.000037	0.00087	0.281117	-57.4	1.3	0.9	2634
HARM-CYN-72	10.2	4.1	0.281259	0.000029	0.00076	0.281221	-54.0	1.0	4.6	2634
HARM-CYN-157	14.2	5.7	0.281703	0.000033	0.00085	0.281660	-38.3	1.2	20.5	2644
Sample: Elbow Canyon. Location: Elbow Canyon, Sonoma Range; 0441026 4514450 (NAD 83 UTM 11T)										
Elbow-CYN-74	9.2	5.0	0.281512	0.000021	0.00053	0.281494	-45.0	0.7	-5.6	1776
Elbow-CYN-66	15.1	4.9	0.281664	0.000019	0.00085	0.281636	-39.6	0.7	-0.6	1777
Elbow-CYN-42	8.6	5.3	0.281542	0.000024	0.00049	0.281525	-44.0	0.9	-4.5	1777
Elbow-CYN-195	6.4	3.7	0.281438	0.000027	0.00035	0.281426	-47.6	1.0	-8.0	1778
Elbow-CYN-45	10.0	5.5	0.281386	0.000026	0.00057	0.281366	-49.5	0.9	-10.1	1780
Elbow-CYN-163	19.1	4.4	0.281522	0.000029	0.00102	0.281487	-44.7	1.0	-5.7	1782
Elbow-CYN-170	13.4	4.8	0.281538	0.000036	0.00076	0.281512	-44.1	1.3	-4.8	1782
Elbow-CYN-76	39.5	6.0	0.281676	0.000040	0.00161	0.281621	-39.2	1.4	-0.9	1783
Elbow-CYN-162	8.5	4.7	0.281408	0.000025	0.00049	0.281392	-48.7	0.9	-9.1	1784
Elbow-CYN-182	16.2	5.2	0.281651	0.000018	0.00092	0.281620	-40.1	0.6	-0.9	1786
Elbow-CYN-160	8.7	5.1	0.281563	0.000021	0.00048	0.281547	-43.2	0.7	-3.5	1786
Elbow-CYN-171	9.5	4.3	0.281595	0.000026	0.00061	0.281574	-42.1	0.9	-2.5	1787
Elbow-CYN-127	11.4	4.8	0.281570	0.000018	0.00063	0.281549	-43.0	0.6	-3.4	1787
Elbow-CYN-92	7.7	4.4	0.281379	0.000019	0.00046	0.281364	-49.7	0.7	-10.0	1787
Elbow-CYN-115	10.9	5.0	0.281633	0.000019	0.00063	0.281612	-40.7	0.7	-1.2	1788
Elbow-CYN-159	9.8	5.4	0.281585	0.000017	0.00057	0.281565	-42.5	0.6	-2.8	1788
Elbow-CYN-187	6.3	5.4	0.281372	0.000018	0.00038	0.281360	-50.0	0.6	-10.1	1789
Elbow-CYN-129	7.4	5.4	0.281525	0.000022	0.00043	0.281510	-44.6	0.8	-4.7	1791
Elbow-CYN-116	10.6	5.2	0.281749	0.000020	0.00060	0.281729	-36.6	0.7	3.2	1795
Elbow-CYN-70	6.0	4.0	0.281370	0.000030	0.00036	0.281358	-50.0	1.1	-9.3	1825
Elbow-CYN-133	11.5	5.0	0.281774	0.000025	0.00069	0.281750	-35.7	0.9	4.9	1836

Hafnium isotope data of selected Harmony Formation strata

	$(^{176}Yb + ^{176}Lu) / ^{176}Hf$ (%)	Volts Hf	$^{176}Hf/^{177}Hf$	± (1s)	$^{176}Lu/^{177}Hf$	$^{176}Hf/^{177}Hf$ (T)	E-Hf (0)	E-Hf (0) ± (1s)	E-Hf (T)	Age (Ma)
Sample: Elbow Canyon. Location: Elbow Canyon, Sonoma Range; 0441026 4514450 (NAD 83 UTM 11T)										
Elbow-CYN-53	12.7	4.5	0.281584	0.000016	0.00075	0.281557	-42.5	0.6	-1.7	1847
Elbow-CYN-23	4.7	3.9	0.281357	0.000030	0.00030	0.281347	-50.5	1.1	-9.0	1857
Elbow-CYN-132	7.4	4.8	0.281823	0.000023	0.00045	0.281807	-34.0	0.8	7.6	1865
Elbow-CYN-67	3.6	4.0	0.281577	0.000027	0.00021	0.281569	-42.7	1.0	-0.9	1867
Elbow-CYN-93	10.9	5.0	0.281504	0.000019	0.00067	0.281480	-45.3	0.7	-3.9	1871
Elbow-CYN-112	7.5	4.7	0.281389	0.000017	0.00044	0.281369	-49.4	0.6	5.2	2436
Elbow-CYN-141	11.0	5.3	0.281135	0.000023	0.00065	0.281103	-58.3	0.8	-0.7	2586
Elbow-CYN-87	24.4	4.6	0.281237	0.000020	0.00118	0.281178	-54.7	0.7	2.0	2589
Elbow-CYN-190	24.4	4.5	0.281249	0.000020	0.00130	0.281185	-54.3	0.7	2.3	2592
Elbow-CYN-19	7.2	5.2	0.281195	0.000033	0.00042	0.281174	-56.2	1.2	2.4	2612
Elbow-CYN-58	11.6	3.9	0.281272	0.000020	0.00068	0.281238	-53.5	0.7	4.7	2614
Elbow-CYN-37	10.7	4.2	0.281237	0.000025	0.00064	0.281205	-54.7	0.9	4.0	2634
Elbow-CYN-79	13.5	4.0	0.281163	0.000016	0.00080	0.281121	-57.4	0.6	2.1	2678
Elbow-CYN-96	3.1	5.2	0.280906	0.000025	0.00017	0.280897	-66.4	0.9	-5.6	2691
Elbow-CYN-134	6.0	4.1	0.281033	0.000022	0.00037	0.281013	-62.0	0.8	-1.4	2692
Elbow-CYN-28	8.2	4.0	0.281082	0.000021	0.00053	0.281055	-60.2	0.7	0.6	2716
Elbow-CYN-191	8.1	4.5	0.281178	0.000022	0.00047	0.281154	-56.8	0.8	4.2	2718

Notes:

1. Data reduction methodology is from Woodhead et al. (2004)
2. Analytical methods described in detail by Gehrels and Pecha (2014)
3. (176Yb + 176Lu) / 176Hf (%) expresses the proportion of 176 due to 176Yb + 176Lu versus the proportion due to 176Hf, in %.
4. Volts Hf is the sum of voltages of all Hf isotopes.
5. 176Hf/177Hf is the measured 176Hf/177Hf, corrected for fractionation and inferences. Shown with uncertainty expressed at 1-sigma.
6. $^{176}Lu/^{177}Hf$ is the intensity of 176Lu, calculated from the measured instensity of 175Lu and 176Lu/175Lu=0.02653 (from Patchett, 1983), compared to the measured intensity of 177Hf. Fractionation of Lu isotopes is assumed to be the same as fractionation of Yb isotopes.
7. 176Hf/177Hf (T) is the 176Hf/177Hf corrected to the time of crystallization using a decay constant of 1.867e-11 (from Scherer et al., 2001 and Soderland et al., 2004)
8. E-Hf (0) is the present-day epsilon Hf value using 176Hf/177Hf=0.282785 and 176Lu/177Hf=0.0336 (from Bouvier et al., 2008). The uncertainty is expressed at 1-sigma.
9. E-Hf(T) is the epsilon Hf value at time of crystallization. Uncertainty is expressed at 1 sigma.
10. U-Pb ages are based on 206/238 for ages younger than ~1.0 Ga, and on 206/207 for ages older than ~1.0 Ga. This age cutoff may be slightly different for each sample.
11. Isotope ratios as follows:

180/177	1.8866600	Patchett (1983)
179/177	0.7325000	Patchett & Tatsumoto (1980)
178/177	1.4671800	Patchett (1983)
176/177	0.2821600	Patchett (1983)
174/177	0.0087100	Patchett (1983)
176/175	0.0265300	Patchett (1983)
176/171	0.9016910	Vervoort et al. (2004)
173/171	1.1323569	Vervoort et al. (2004)
172/171	1.5317360	Vervoort et al. (2004)

Notes for plots:

1. DM array is from Vervoort and Blichert-Toft (1999), using 176Hf/177Hf=0.283225 and 176Lu/177Hf=0.0383

2. CHUR is from Bouvier et al. (2008), using 176Hf/177Hf=0.282785 and 176Lu/177Hf=0.0336.
3. Hf isotope evolution lines assume an average value of 176Lu/177Hf=0.0115 and a range of 176Lu/177Hf=0.0036 to 176Lu/177Hf=0.0193. Values are from the average and 2-sigma range of values reported by Vervoort and Patchett (1996) and Vervoort et al. (1999).
4. Uncertainties shown at 2-sigma.
5. Uncertainty for EpsilonT is nearly identical for Espsilon 0 because of the very long half-life.

Appendix References Cited

Bouvier, A., Vervoort, J., and Patchett, J., 2008, The Lu-Hf and Sm-Nd isotopic composiiton of CHUR: Consraints from unequilibrated chondrites and implications for the bulk composition of terrestrial planets: Earth and Planetary Science Letters: v. 273, p. 48-57.

Gehrels, G.E., 2012, Detrital zircon U-Pb geochronology: Current methods and new opportunities, in Busby, C., and Azor, A., eds., Recent Advances in Tectonics of Sedimentary Basins: Hoboken, New Jersey, Blackwell Publishing.

Gehrels, G.E., and Pecha, M., 2014, Detrital zircon U-Pb geochronology and Hf isotope geochemistry of Paleozoic and Triassic passive margin strata of western North America: Geosphere, v. 10, p. 49-65.

Gehrels, G.E., Valencia, V.A., and Ruiz, J., 2008, Enhanced precision, accuracy, efficiency, and spatial resolution of U-Pb ages by laser ablation-multicollector-inductively coupled plasma-mass spectrometry: Geochemistry, Geophysics, Geosystems, v.9, p. 1-13.

Ludwig, K.R., 2003, Isoplot 3.0, Berkeley Geochronology Center.

Ludwig, K., 2008, Isoplot 3.6: Berkeley Geochronology Center Special Publication 4, 77 p.

Patchett, P.J., 1983, Importance of the Lu-Hf isotopic system in studies of planetary chronology and chemical evolution: Geochimica et Cosmochimica Acta, v. 47, p. 81-91.Scherer, E., Munker, C., and Mezger, K., 2001, Calibrating the Lu-Hf clock: Science, v. 293, p. 683–686.

Patchett, P.J., and Tatsumoto, M., 1980, A routine high-precision method for Lu-Hf isotope geochemistry and chronology: Contributions to Mineralogy and Petrology, v. 75, 263-267.

Scherer, E., Munker, C., and Mezger, K., 2001, Calibrating the Lu-Hf clock: Science, v. 293, p. 683–686,

Söderlund, U., Patchett, P.J., Vervoort, J.D., and Isachsen, C.E., 2004, The 176Lu decay constant determined by Lu-Hf and U-Pb isotope systematics of Precambrian mafic intrusions: Earth and Planetary Science Letters, v. 219, p. 311-324.

Stacey, J.S., and Kramers, J.D., 1975, Approximation of terrestrial lead isotope evolution by a two stage model: Earth and Planetary Science Letters, v. 26, p. 207-221.

Vervoort, J.D., and Patchett, P.J., 1996, Behavior of hafnium and neodymium isotopes in the crust: Constraints from crustally derived granites: Geochimica et Cosmochimica Acta, v. 60, p. 3717–3733.

Vervoort, J.D., and Blichert-Toft, J., 1999, Evolution of the depleted mantle: Hf isotope evidence from juvenile rocks through time: Geochimica et Cosmochimica Acta, v. 63, p. 533–556.

Vervoort, J.D., Patchett, P.J., Blichert-Toft, J., and Albarede, F., 1999, Relationships between Lu-Hf and Sm-Nd isotopic systems in the global sedimentary system: Earth and Planetary Science Letters, v. 168, p. 79–99.

Vervoort, J.D., Patchett, P.J., Soderlund, U., and Baker, M., 2004, Isotopic composition of Yb and the determination of Lu concentrations and Lu/Hf ratios by isotope dilution using MC-ICPMS: Geochemistry Geophysics Geosystems, v. 5, Q11002.

Woodhead, J.D., and Hergt, J.M., 2004, A preliminary appraisal of seven natural zircon reference materials for in situ Hf isotope determination: Geostandards and Geoanalytical Research, v. 29 (2), p. 183-195.

Woodhead, J., Hergt, J., Shelley, M., Eggins, S., and Kemp, R., 2004, Zircon Hf-isotope analysis with an excimer laser, depth profiling, ablation of complex geometries, and concomitant age estimation: Chemical Geology, v. 209, p. 121-135.